ISSN 1007-9327 (print)
ISSN 2219-2840 (online)

World Journal of *Gastroenterology*

World J Gastroenterol 2022 July 14; 28(26): 3008-3281

Published by Baishideng Publishing Group Inc

World Journal of Gastroenterology

Contents

Weekly Volume 28 Number 26 July 14, 2022

REVIEW

MINIREVIEWS

ORIGINAL ARTICLE

Basic Study

Contents

Contents

ABOUT COVER

Editorial Board Member of *World Journal of Gastroenterology*, Koichi Suda, MD, PhD, FACS, Professor and Head, Divisions of GI and HPB Surgery, Department of Surgery, Fujita Health University, Rm C908, 1-98 Dengakugakubo, Kutsukake, Toyoake, Aichi 470-1192, Japan. ko-suda@fujita-hu.ac.jp

AIMS AND SCOPE

The primary aim of *World Journal of Gastroenterology* (*WJG*, *World J Gastroenterol*) is to provide scholars and readers from various fields of gastroenterology and hepatology with a platform to publish high-quality basic and clinical research articles and communicate their research findings online. *WJG* mainly publishes articles reporting research results and findings obtained in the field of gastroenterology and hepatology and covering a wide range of topics including gastroenterology, hepatology, gastrointestinal endoscopy, gastrointestinal surgery, gastrointestinal oncology, and pediatric gastroenterology.

INDEXING/ABSTRACTING

The *WJG* is now abstracted and indexed in Science Citation Index Expanded (SCIE, also known as SciSearch®), Current Contents/Clinical Medicine, Journal Citation Reports, Index Medicus, MEDLINE, PubMed, PubMed Central, Scopus, Reference Citation Analysis, China National Knowledge Infrastructure, China Science and Technology Journal Database, and Superstar Journals Database. The 2022 edition of Journal Citation Reports® cites the 2021 impact factor (IF) for *WJG* as 5.374; IF without journal self cites: 5.187; 5-year IF: 5.715; Journal Citation Indicator: 0.84; Ranking: 31 among 93 journals in gastroenterology and hepatology; and Quartile category: Q2. The *WJG*'s CiteScore for 2021 is 8.1 and Scopus CiteScore rank 2021: Gastroenterology is 18/149.

RESPONSIBLE EDITORS FOR THIS ISSUE

Production Editor: *Hua-Ge Yu*; **Production Department Director:** *Xu Guo*; **Editorial Office Director:** *Jia-Ru Fan*.

NAME OF JOURNAL
World Journal of Gastroenterology

ISSN
ISSN 1007-9327 (print) ISSN 2219-2840 (online)

LAUNCH DATE
October 1, 1995

FREQUENCY
Weekly

EDITORS-IN-CHIEF
Andrzej S Tarnawski

EDITORIAL BOARD MEMBERS
http://www.wjgnet.com/1007-9327/editorialboard.htm

PUBLICATION DATE
July 14, 2022

INSTRUCTIONS TO AUTHORS
https://www.wjgnet.com/bpg/gerinfo/204

GUIDELINES FOR ETHICS DOCUMENTS
https://www.wjgnet.com/bpg/GerInfo/287

GUIDELINES FOR NON-NATIVE SPEAKERS OF ENGLISH
https://www.wjgnet.com/bpg/gerinfo/240

PUBLICATION ETHICS
https://www.wjgnet.com/bpg/GerInfo/288

PUBLICATION MISCONDUCT
https://www.wjgnet.com/bpg/gerinfo/208

ARTICLE PROCESSING CHARGE
https://www.wjgnet.com/bpg/gerinfo/242

STEPS FOR SUBMITTING MANUSCRIPTS
https://www.wjgnet.com/bpg/GerInfo/239

ONLINE SUBMISSION
https://www.f6publishing.com

World Journal of Gastroenterology

Submit a Manuscript: https://www.f6publishing.com

World J Gastroenterol 2022 July 14; 28(26): 3008-3026

DOI: 10.3748/wjg.v28.i26.3008

ISSN 1007-9327 (print) ISSN 2219-2840 (online)

REVIEW

Advances in the imaging of gastroenteropancreatic neuroendocrine neoplasms

Anupama Ramachandran, Kumble Seetharama Madhusudhan

Specialty type: Radiology, nuclear medicine and medical imaging

Provenance and peer review: Invited article; Externally peer reviewed.

Peer-review model: Single blind

Peer-review report's scientific quality classification

Grade A (Excellent): A
Grade B (Very good): B
Grade C (Good): C, C
Grade D (Fair): 0
Grade E (Poor): 0

P-Reviewer: Cerwenka H, Austria; Wang WQ, China

Received: October 11, 2021
Peer-review started: October 11, 2021
First decision: November 15, 2021
Revised: November 30, 2021
Accepted: June 19, 2022
Article in press: June 19, 2022
Published online: July 14, 2022

Anupama Ramachandran, Kumble Seetharama Madhusudhan, Department of Radiodiagnosis and Interventional Radiology, All India Institute of Medical Sciences, New Delhi 110029, India

Corresponding author: Kumble Seetharama Madhusudhan, MD, Additional Professor, Department of Radiodiagnosis and Interventional Radiology, All India Institute of Medical Sciences, Ansari Nagar, New Delhi 110029, India. drmadhuks@gmail.com

Abstract

Gastroenteropancreatic neuroendocrine neoplasms comprise a heterogeneous group of tumors that differ in their pathogenesis, hormonal syndromes produced, biological behavior and consequently, in their requirement for and/or response to specific chemotherapeutic agents and molecular targeted therapies. Various imaging techniques are available for functional and morphological evaluation of these neoplasms and the selection of investigations performed in each patient should be customized to the clinical question. Also, with the increased availability of cross sectional imaging, these neoplasms are increasingly being detected incidentally in routine radiology practice. This article is a review of the various imaging modalities currently used in the evaluation of neuroendocrine neoplasms, along with a discussion of the role of advanced imaging techniques and a glimpse into the newer imaging horizons, mostly in the research stage.

Key Words: Neuroendocrine tumor; Gastroenteropancreatic; Intravoxel incoherent motion; Diffusion weighted imaging; Perfusion imaging; Dual energy computed tomography

Core Tip: The prognosis of gastroenteropancreatic neuroendocrine neoplasms (GEPNENs) depends on the stage of the disease and tumor grade. Traditional imaging techniques like multiphase contrast-enhanced computed tomography perform well at disease staging. For tumor grading, histopathological examination, with determination of number of mitoses and Ki-67 index is considered optimal. Advances in imaging techniques have enabled detection of smaller neuroendocrine neoplasms (< 2 cm). By analysing functional information like diffusion, perfusion and tumor heterogeneity, quantitative imaging is currently focused on noninvasive prediction of the grade of GEPNENs preoperatively.

Citation: Ramachandran A, Madhusudhan KS. Advances in the imaging of gastroenteropancreatic neuroendocrine neoplasms. *World J Gastroenterol* 2022; 28(26): 3008-3026
URL: https://www.wjgnet.com/1007-9327/full/v28/i26/3008.htm
DOI: https://dx.doi.org/10.3748/wjg.v28.i26.3008

INTRODUCTION

Gastroenteropancreatic neuroendocrine neoplasms (GEPNENs) are a rare and heterogeneous group of tumors that originate from the gastrointestinal and pancreatic neuroendocrine cells[1,2]. They may be benign or malignant and may or may not secrete hormones. Use of the previous terminology - carcinoid tumor - is no longer encouraged. The gastrointestinal tract (GIT), having the highest density of neuroendocrine cells in the body, is the most common site of involvement of neuroendocrine neoplasms (NENs), comprising nearly 60% of all NENs[3]. Pancreatic NENs (PNENs) account for about 7% of all GEPNENs [4]. Most PNENs are sporadic. However, association with four familial syndromes (in up to 25%) is well described: multiple endocrine neoplasia type I, von Hippel Lindau syndrome, neurofibromatosis type I and tuberous sclerosis[5,6].

Classification based on histological differentiation and grade is desirable as it provides insight into tumor biology, clinical course and helps in planning management. In 2019, the 5th edition of the World Health Organization (WHO) classification of tumors series published the latest NEN classification (Table 1)[7]. The latest WHO classification recognizes that well-differentiated NENs may be high grade, but they are distinct from the poorly differentiated neuroendocrine carcinomas (NECs). Most GEPNENs are well-differentiated and slowly growing. Grade 3 NENs are most common in the pancreas, but can occur throughout the GIT[7]. Given the differences in prognosis, tumor grade is the most important factor determining the treatment of GEPNENs. The treatment of GEPNENs depends on grade, differentiation, site of origin, and stage of tumor, and the opinion about the best treatment strategy is evolving. Surgical resection remains the cornerstone and is the only curative treatment. For patients with small (< 2 cm), low-grade NENs, decisions on surgery *vs* active surveillance need to be individualized based on tumor size, morphology (homogeneous, well circumscribed tumor < 1 cm correlate with low malignant potential) and patient characteristics like age and presence of comorbidities[8].

The commonly used imaging modalities include ultrasonography (US), computed tomography (CT), magnetic resonance imaging (MRI) and positron emission tomography (PET)-CT. Imaging is primarily aimed at accurate detection, characterization and staging of these neoplasms and also at assessment of response to treatment. Sensitivity of common imaging modalities used in the evaluation of GEPNENs are summarized in Table 2.

Improvements and advances in the imaging techniques have mainly focused on the noninvasive prediction of the grade of the NENs. The European Neuroendocrine Tumor Society (ENETS) has also recommended that preoperative assessment of the grade of the NENs is essential for prognosis prediction and management planning[9]. In addition, with the improvements in the imaging technologies, the detection rates of small NENs have significantly improved, with many often being detected incidentally.

US

Transabdominal ultrasonography (USG) often is the commonest initial modality used for patients with gastrointestinal symptoms. It has value in the detection of liver metastases (sensitivity reaching 85%-90%). PNENs in general appear as hypoechoic masses with a hyperechoic halo on USG[10].

However, transabdominal USG has limitations. It has a poor sensitivity (13%-27%) for the detection of GEPNENs[11]. The technique is dependent on the experience of the operator. Presence of bowel gas and increased subcutaneous fat can obscure adequate visualization.

The advent of harmonic imaging, pulse inversion sequence, low mechanical index techniques and ultrasound contrast agents (UCAs) has enabled routine application of contrast-enhanced ultrasound (CEUS) to overcome the limitations of conventional B mode USG. The inherent advantage of CEUS is its ability to assess tumor-enhancement patterns in real time during transabdominal USG[12]. The enhancement patterns are described during arterial, portal venous and late phases. UCAs are gas microbubbles stabilized by a shell, the composition of which varies depending on the type of contrast agent. UCAs are blood pool agents and increase the back scatter of US, enhancing the echogenicity of flowing blood[12]. Harmonic imaging detects harmonic signals from the microbubbles and CEUS specific US modes filter signals from the background tissue, thereby showing even very slow blood flow without Doppler related artifacts. UCAs, unlike CT and MRI contrast agents, are excreted by the lungs and hence can be used safely in patients with deranged renal function.

Table 1 World Health Organization Classification and grading criteria for neuroendocrine neoplasms of the gastrointestinal tract and hepatopancreatobiliary organs (7)

Terminology	Differentiation	Grade	Mitoses/2 mm^2	Ki-67 index
NEN grade 1	Well differentiated	Low	< 2	< 3%
NEN grade 2		Intermediate	2-20	3%-20%
NEN grade 3		High	> 20	> 20%
SCNEC	Poorly differentiated	High[1]	> 20	> 20%
LCNEC			> 20	> 20%
MiNEN	Well or poorly differentiated	Variable	Variable	Variable

[1]Poorly differentiated neuroendocrine carcinomas are not formally graded, but are considered high-grade by definition.
LCNEC: Large cell neuroendocrine carcinoma; MiNEN: Mixed neuroendocrine non-neuroendocrine neoplasm; NEN: Neuroendocrine neoplasm; SCNEC: Small-cell neuroendocrine carcinoma.

Table 2 Sensitivity of common imaging modalities used in the evaluation of gastroenteropancreatic neuroendocrine neoplasms

Imaging modality	Sensitivity
Transabdominal USG	13%-27% for GEPNEN
Contrast enhanced ultrasound	99% in detecting liver metastases
Endoscopic ultrasonography	82%-93% for PNEN
CECT	63%-82% for PNEN
CE MRI	79% for PNEN
DWI	83% for liver metastases

USG: Ultrasonography; GEPNEN: Gastroenteropancreatic neuroendocrine neoplasms; CECT: Contrast enhanced computed tomography; CE MRI: Contrast-enhanced magnetic resonance imaging; DWI: Diffusion-weighted imaging.

The differential perfusion on CEUS has been shown to identify and diagnose pancreatic tumors. Pancreatic adenocarcinomas are in general hypovascular, while NENs are hypervascular. Takeda *et al* [13] found three patterns of hyperenhancement of PNENs and found that CEUS was useful in the differentiation of PNENs from pancreatic adenocarcinomas. Malagò *et al*[14] also showed that the enhancement patterns of nonfunctioning PNENs on CEUS (hyper-, iso- or hypovascular) correlated well with Ki-67 index and CEUS improved the detection of hepatic metastases. Hypervascular lesions had lower Ki-67 index. Another study showed that the enhancement patterns of NENs on CEUS correlated significantly with CT enhancement pattern and histological Ki-67 index and CEUS was a good predictor of response of tumors to somatostatin analogues[15].

Elastography

Elastography is an advancement in USG that enables real-time measurement of tissue stiffness along with display in colors superimposed on the grey scale images[16]. In general, elastography helps with the differentiation of benign and malignant lesions based on stiffness, as malignant lesions are usually hard. Only a few studies have reported the usefulness of transabdominal shear wave elastography (SWE) in the evaluation of pancreatic tumors. Park *et al*[17] showed that elastography can differentiate benign and malignant solid pancreatic lesions based on the difference in the shear wave velocity values (relative stiffness) between the tumor and the normal parenchyma. An early study by Uchida *et al*[18] found that NENs were homogeneous and soft on elastography, comparable to the normal pancreas. They also reported that a combination of elastography and B mode USG, improved the diagnostic accuracy to 90%, from 70%-80 % when B mode USG was used alone. However, if the visualization on the baseline B mode USG is suboptimal, the results of CEUS and elastography are also often unsatisfactory. These limitations have been overcome by the use of endoscopic ultrasound (EUS).

EUS

EUS is considered the most accurate test for the diagnosis of pancreatic masses[19]. EUS uses higher frequency (7.5-12 MHz) probes, placed in proximity to the area of interest and hence performs better at detection of tumors < 2 cm for which CT and MRI have poor sensitivity[20]. Overall, EUS has a sensitivity of 82%-93% and a specificity of 92%-95% for localizing PNENs. EUS is particularly useful in the detection of benign insulinomas that lack somatostatin receptors and consequently are not detected on somatostatin receptor scintigraphy/single photon emission computed tomography (SPECT)/PET [21]. EUS also plays an important role in the detection of functional pancreatic and extrapancreatic (duodenal) gastrinomas[22]; both of which generally have a small size (average 1 cm) at diagnosis. The additional benefit of EUS is its ability to guide accurate tissue sampling *via* fine needle aspiration and core biopsy[23]. CEUS can also be performed through EUS with the use of second generation UCAs (*e.g*, Sonovue), which produce harmonic signals at low acoustic powers. A recent study showed that the time intensity curve analysis during CEUS showed high diagnostic accuracy in grading PNENs, and could differentiate grade 1/2 tumors from grade 3 tumors/carcinomas[24].

EUS elastography

EUS elastography of the pancreas has been shown to be a promising imaging technique in several studies[25-27]. However, a prospective study by Hirche *et al*[28] including 70 patients with undifferentiated pancreatic masses showed an overall lower sensitivity (41%), specificity (53%) and accuracy (45%) for the detection of malignancy. One of the early studies evaluating conventional strain elastography for pancreatic lesions showed significant strain difference between benign and malignant masses[29]. The major utility of EUS elastography is in increasing the yield of sampling by aiding better tumor targeting, especially in the background of pancreatic parenchymal fibrosis[30]. SWE EUS is a recent development and studies evaluating its utility in the pancreas are just emerging[31,32]. A recent comparative study suggested that conventional strain elastography was superior to SWE in the characterization of pancreatic lesions[33].

CT

CT is the cornerstone and the most commonly performed imaging modality for the diagnosis and preoperative staging of GEPNEN. Standard CT scan has low sensitivity (~60%) for the detection of GIT NENs[34]. Dynamic dual-phase protocol, which includes the arterial and portal venous phases, is recommended in patients with suspected NEN[35,36] (Figure 1). For PNEN, the late arterial phase acquired at 40-45 s (pancreatic phase) suits best. For detection of small bowel NENs, CT enterography (oral administration of neutral contrast agent like mannitol for bowel distension) or CT enteroclysis (administration of neutral contrast *via* nasojejunal tube) is required. CT enteroclysis combines the advantages of enteroclysis with imaging capabilities of multidetector computed tomography (MDCT). Study by Kamaoui *et al*[37] showed that CT enteroclysis had 100% sensitivity and 96.2% specificity for the detection of small bowel NEN. A comparative study from Mayo Clinic found that CT enterography was better than capsule endoscopy in detecting small bowel tumors, with a sensitivity of up to 93%[38]. This ability of CT enterography to detect small bowel tumors remains high (sensitivity of 88%) even in the presence of gastrointestinal bleeding[39].

The characteristic imaging feature on CT scan suggesting the diagnosis of NENs is their intense enhancement in the late arterial phase, owing to the hypervascular nature of the tumor. The arterial phase also helps in outlining the relationship of the tumor with the adjacent arteries. Using the maximum intensity projection technique, virtual angiographic images can be obtained. Volume rendering techniques applied to the arterial phase provide easily explainable images to the surgeon. Portal venous phase helps to draw the relationship of the tumor with major veins, especially the splenic vein and the superior mesenteric vein for PNENs. Dual-phase imaging is also crucial for the evaluation of hepatic metastases. The classic liver metastases from NEN, being hypervascular, are most evident on the arterial phase images. About 6%-15% of NEN liver metastases are appreciated only in the arterial phase[40,41]. However up to 16% are hypovascular and show delayed enhancement[40].

One of the early studies suggested that the size of the tumor is an important prognostic factor, with tumors < 1 cm showing lesser incidence of liver metastasis (20%–30%) compared to those with > 1 cm (> 40% risk)[42]. Studies have shown that up to 42% of PNENs may not show arterial phase hyperenhancement[43,44]. Such arterial phase hypoenhancing tumors were associated with a significantly lower 5-year survival (54%) compared to the lesions which were isoenhancing (89%) or hyperenhancing (93%) [45]. Rodallec *et al*[46] found that tumor enhancement on CT scan correlated with microvascular density (MVD) evaluated on histology and that hypoenhancing PNENs correlated with poorly differentiated tumors and a decrease in overall survival rate. These studies showed that the CT enhancement characteristics of NENs have a prognostic value. Gallotti *et al*[6] found that incidentally detected PNENs, size > 3 cm, complex enhancement pattern and, presence of calcification, vascular invasion, main pancreatic duct dilatation, and peripancreatic lymph nodes were associated with nonbenign tumors and required

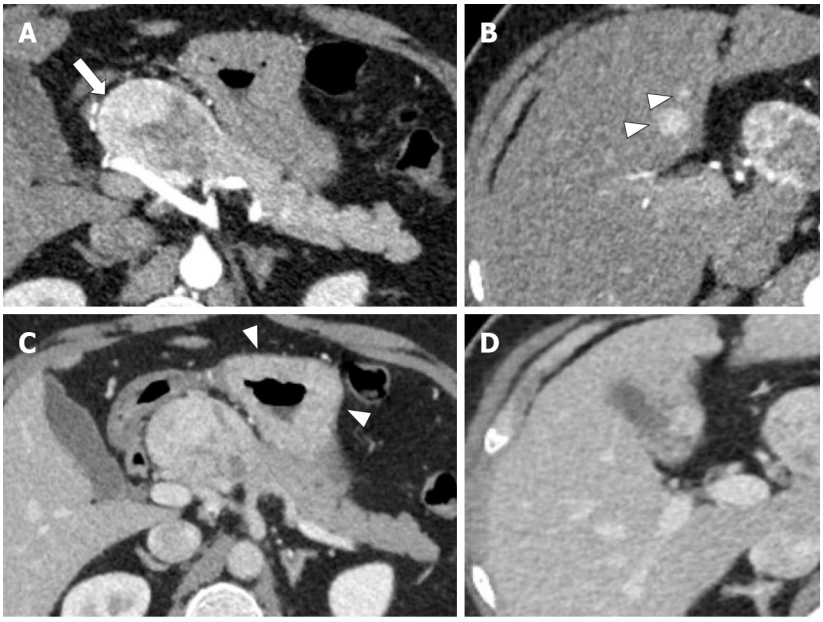

DOI: 10.3748/wjg.v28.i26.3008

Figure 1 49-year-old man with epigastric pain and raised serum gastrin levels. A and B: Axial contrast enhanced pancreatic phase computed tomography (CT) images show a well-defined hyperenhancing mass (arrow in A) in the head and neck of pancreas, abutting the proper hepatic artery along with two hyperenhancing focal lesions in the liver (arrowheads in B), indicating hepatic metastases; C and D: Axial portal venous phase CT images show retention of contrast in the lesions in both locations. Thickened gastric mucosal folds is also noted (arrowheads in C).

more aggressive course of management.

The role of various CT quantitative parameters based on enhancement of the NEN in the arterial or pancreatic and the venous phases has been evaluated in the prediction of tumor grade. Kim *et al*[47] found that portal enhancement ratio (HU value of the tumor divided by the HU value of pancreatic parenchyma on portal phase images) had the best odds ratio (49.6) and a cutoff value of < 1.1 had a sensitivity of 92% and specificity of 81% in differentiating grade 3 PNENs from grade 1 and 2. This high sensitivity and specificity of portal enhancement ratio in differentiating neuroendocrine carcinomas from well-differentiated NENs was also confirmed by another study[48]. Yamada *et al*[49] showed that corrected true enhancement values in the pancreatic phase had a sensitivity of 92%, specificity of 84% and area under the curve of 0.897 in the differentiation of grade 1 from grade 2 PNENs. D'Onofrio *et al* [50] showed that various tumor enhancement parameters (tumor permeability ratios, tumor parenchyma ratios, tumor arterial ratio and tumor venous ratio) were significantly different between grade 1 and grade 3 and between grade 2 and grade 3 PNENs. However, these values could not differentiate grade 1 from grade 2 tumors.

Dual-energy CT

Dual-energy CT (DECT) is an advancement in CT, which allows acquisition of images at two energy levels, with lower energy being 80-100 kVp and higher being 140 kVp. Using DECT, material decomposition of images and generation of iodine maps, virtual noncontrast images, and monochromatic images at different energy levels is possible (Figures 2 and 3). Monoenergetic images at low keV (55 keV) in the pancreatic phase of DECT show improved image contrast for evaluation of pancreatic masses[51]. Monochromatic spectral images improve the sensitivity of detection of NENs like insulinomas, particularly the hypovascular and isoattenuating tumors and the sensitivity is comparable to MRI[52]. One study showed that iodine uptake obtained from DECT is useful in the differentiation of hepatocellular carcinoma from liver metastases arising from NENs, with the former showing significantly higher iodine uptake (3.8 ± 1.2 *vs* 2.3 ± 0.6)[53]. This iodine uptake parameter on DECT may also be used in assessing the response to treatment of NENs.

Perfusion CT

Perfusion CT is a technique that measures the dynamic changes in the attenuation of the tissues after contrast administration. It allows quantitative measurement of tissue perfusion, thereby assisting in the assessment of tumor viability and biological behavior[54]. The commonly used quantitative parameters of perfusion CT in oncoimaging are blood flow, blood volume, vascular permeability-surface area product and mean transit time (Figures 4 and 5). These parameters serve as imaging biomarkers of tumor angiogenesis, which is ideally assessed histologically by calculating the MVD[55]. NENs are among the tumors with significant angiogenesis. Unlike majority of the cancers, where increased tumor

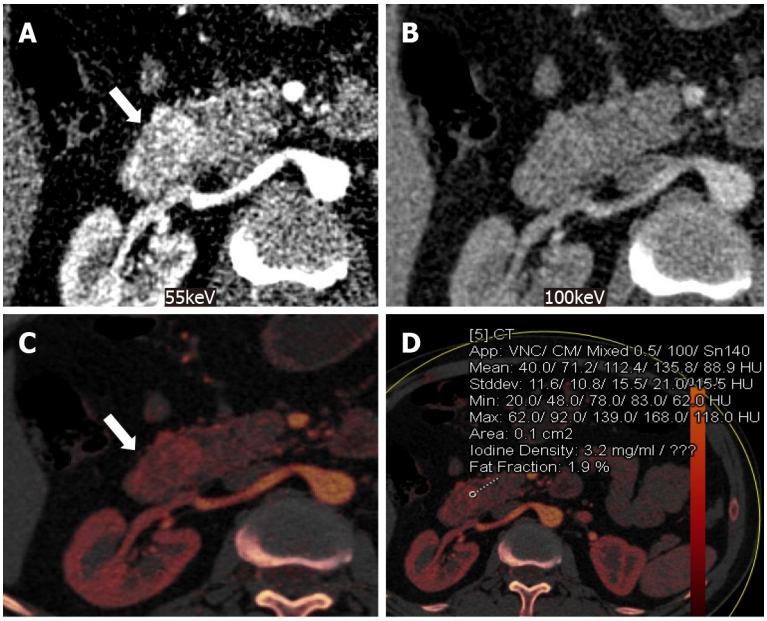

DOI: 10.3748/wjg.v28.i26.3008

Figure 2 Dual-energy computed tomography images of a 46-year-old man presenting with melena. A: Axial monochromatic computed tomography (CT) image at 55 keV in pancreatic phase shows a hyperenhancing well-defined mass (arrow) arising from the duodenal wall; B: Enhancement of the same lesion (arrow) appears subtle on the axial 100 keV monochromatic CT image; C and D: Iodine overlay maps show bright areas (arrow) suggesting contrast uptake (C), with iodine concentration of 3.2 mg/mL in areas of uptake (D). Iodine concentration of normal pancreas was 0.5 mg/mL.

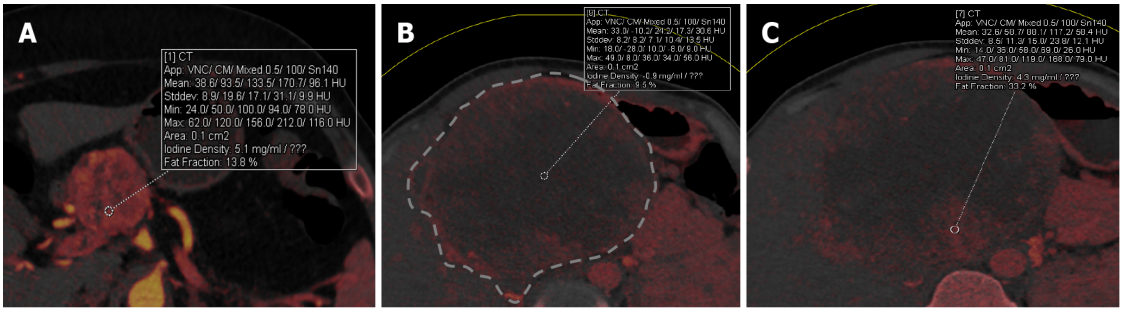

DOI: 10.3748/wjg.v28.i26.3008

Figure 3 Dual-energy computed tomography in grading the pancreatic neuroendocrine neoplasms. A: Iodine overlay dual-energy computed tomography (CT) map of a 40-year-old woman with low-grade (grade 2) pancreatic neuroendocrine neoplasms (PNEN) in head of pancreas shows hyperenhancement of the tumor with an iodine concentration of 5.1 mg/mL; B and C: Iodine overlay dual energy CT maps of a 29-year-old man with grade 3 PNEN (outlined in B) shows large hypoenhancing areas with low iodine concentration (0.9 mg/mL) and peripheral bright areas with iodine concentration of 4.3 mg/mL (C). Measuring iodine concentration helps in objectively assessing the grade of the tumor.

vascularity is associated with aggressive behavior, higher microvascular density in NENs is associated with a low tumor grade[54]. Low MVD was found to be an unfavorable prognostic factor for PNENs in several studies despite the presence of other favorable conventional histoprognostic factors, and call for a more aggressive treatment approach[56-58]. A study by d'Assignies *et al*[59] on 36 patients with PNENs found a significant correlation between MVD and blood flow assessed by using perfusion CT. In their study, the authors found that tumors that are small (< 2 cm), benign (grade 1), with a proliferation index of ≤ 2%, and without histological signs of microvascular involvement had a significantly higher blood flow. Volume perfusion CT has been shown to improve the detection of pancreatic insulinomas, particularly the ones which have transient hyperenhancement (comprising 30% cases)[60,61]. A recent study demonstrated that addition of low dose perfusion CT to contrast enhanced CT improved the detection rate of PNENs from 83.6% to 89.1% and found that blood flow parameters were significantly different between grade 1 and grade 2 tumors[62].

Perfusion CT has also been shown to have a role in monitoring response to treatment with antiangiogenic drugs. Few studies have shown that the perfusion parameters of PNENs and liver metastases decrease as early as 48 h after treatment with anti-angiogenic drugs and perfusion CT offers a significant role in an early noninvasive assessment[63,64]. A major limitation of perfusion CT is the higher radiation dose, resulting in an additional dose of approximately 7 mSv[65].

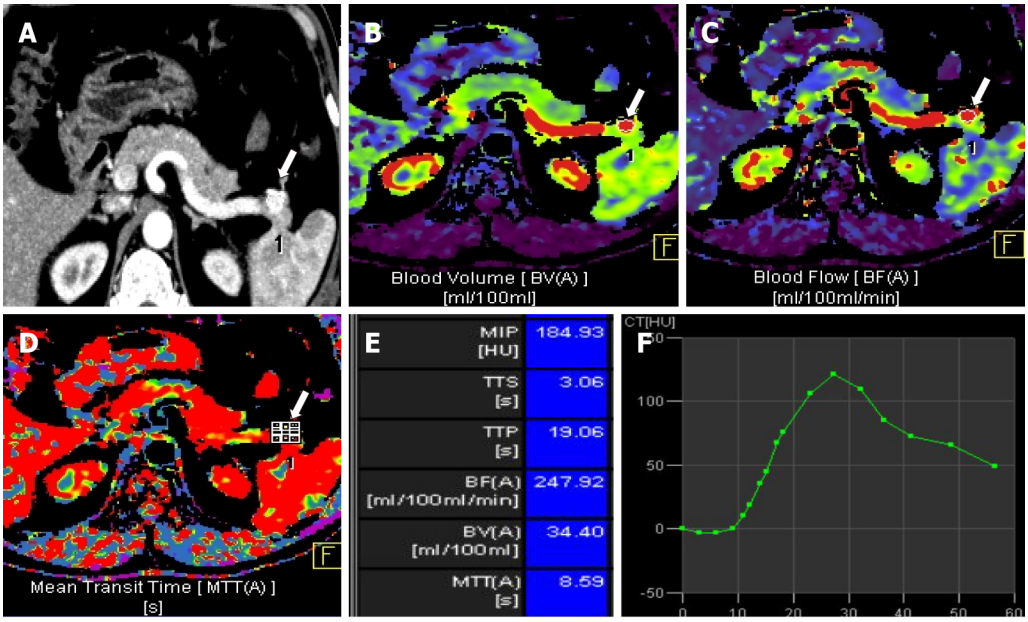

DOI: 10.3748/wjg.v28.i26.3008

Figure 4 Volume perfusion computed tomography images of a 56-year-old man with recurrent hyperinsulinemic hypoglycemia. A: Axial pancreatic phase computed tomography image shows a hyperenhancing lesion in the pancreatic tail (arrow); B-D: Color-coded parametric maps for blood volume (B), blood flow (C) and mean transit time (D) of the tumor (arrow) and normal pancreatic tissue; E: Chart shows mean value of each perfusion parameter of the tumor. Blood flow in the tumor was higher (247 mL/100 mL/min) compared to normal pancreatic parenchyma (72 mL/100 mL/min); F: Time attenuation curve shows dynamic enhancement pattern of the tumor corresponding to transient hyperenhancement. Histopathology after enucleation proved the tumor to be grade 1 insulinoma.

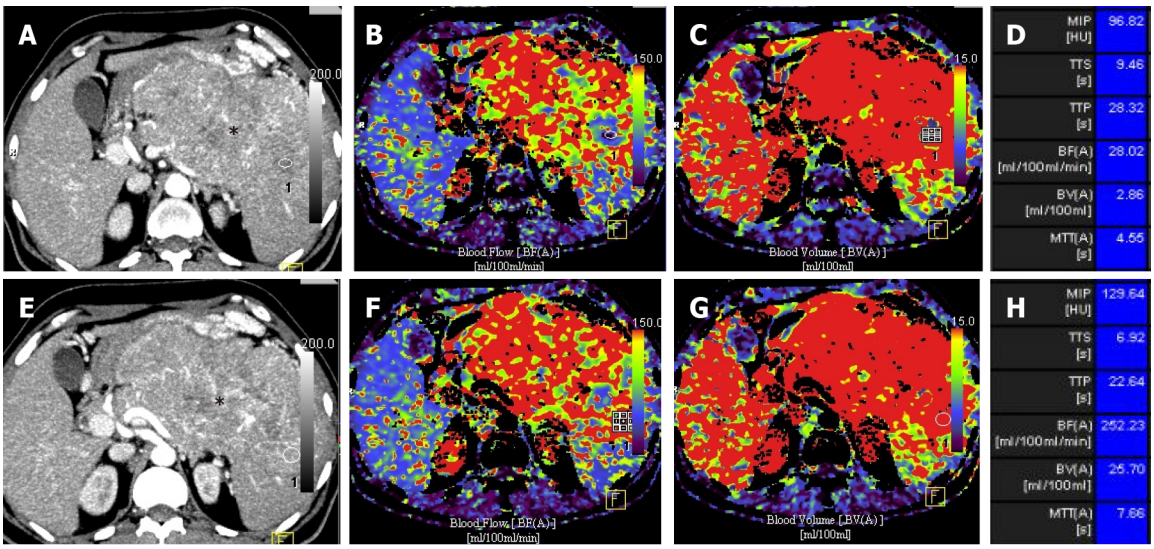

DOI: 10.3748/wjg.v28.i26.3008

Figure 5 Volume perfusion computed tomography images of a 67-year-old man with a large grade 3 neuroendocrine neoplasm involving body and tail of pancreas. A and B: Axial arterial phase computed tomography images with circular regions of interest placed at two different locations in the lesion (*); C-H: Parametric maps for blood flow (C and D) and blood volume (E and F) with mean value of each perfusion parameter (G and H) are shown. Lower values of mean blood flow, mean blood volume and mean transit time are features of high grade neuroendocrine neoplasm.

MRI

MRI is best performed as a problem-solving tool when CT scan findings are equivocal or negative, and is aimed at acquiring images of the lesion and organ with better soft tissue contrast. For instance, MRI has shown better sensitivity for the detection of liver metastases compared to CT and somatostatin receptor scintigraphy[66]. The absence of exposure to ionizing radiation makes MRI the apt modality for screening young individuals suspected of having NEN and those with syndromic association who require multiple follow up imaging[67]. Most NENs are hypointense on T1-weighted and hyperintense on T2-weighted images[10]. Contrast enhancement pattern and morphologic appearances are similar to

that seen in CT scan (Figure 6). For the detection of PNENs, the sensitivity of MRI ranges from 85% to 100% and specificity from 75% to 100%[68].

Diffusion-weighted imaging

Diffusion-weighted imaging (DWI) is a widely used technique in clinical imaging as it reflects the microscopic environment of the neoplasm including tumor cellularity and extracellular matrix. The application of DWI in oncology is mainly in tumor detection and assessing response to chemotherapy and radiotherapy. Wang *et al*[69] demonstrated that the apparent diffusion coefficient (ADC) values of PNEN correlated well with Ki-67 labelling index, thus indicating that DWI has a prognostic value (Figure 6). Another study showed that the ADC values were significantly different between benign and non-benign PNENs (1.48×10^{-3} mm^2/s *vs* 1.04×10^{-3} mm^2/s, respectively)[70]. Lotfalizadeh *et al*[71] showed that DWI has the additional value in identification of high grade tumors (grade 3) and can accurately differentiate grade 3 from grade 1/2 tumors (AUROC-0.96). The ADC values showed an inverse relation with the grade of the tumor.

Another major utility of DWI is in the detection and characterization of liver metastases. Several studies have shown that DWI is more sensitive for the detection of liver metastases than T2-weighted and multiphase gadolinium-enhanced MRI, especially for smaller lesions[72-74]. Besa *et al*[75] showed that the ADC of liver metastases from NEN weakly and significantly correlated negatively with tumor grade and Ki-67 and that the mean ADC and the minimum ADC values were significantly different between the three grades (1.6, 1.35 and 0.9×10^3 mm^2/s and 0.84, 0.5 and 0.27×10^3 mm^2/s for grades 1, 2 and 3, respectively). DWI is hence recommended in routine MRI abdomen protocol for the detection of liver metastases from NEN.

Histogram analysis of the ADC of the whole tumor has also been shown to predict tumor grade and aggressiveness. Pereira *et al*[76] found that whole tumor histogram analysis of the ADC, including the skewness and kurtosis can reliably differentiate grade 1 from grade 2/3 tumors. Another study also showed that this histogram analysis of ADC was useful in predicting tumor grade, vascular invasion and metastasis (node, liver) in PNENs and that $ADC_{entropy}$ and $ADC_{kurtosis}$ were the best markers in identifying tumor aggressiveness[77].

DWI is also useful in predicting and assessing response to various medical treatments for NENs. A recent study by Le Bihan *et al*[78] showed that the change in the ADC values of liver metastases from NENs after transarterial radioembolization was significantly different between the partial response and progressive disease groups, thus concluding that ADC can be used as an additional marker for treatment response evaluation.

While DWI investigates diffusion of water molecules in tissues, it does not detect perfusion of blood. Intravoxel incoherent motion (IVIM) DWI detects translational motion of water molecules in a voxel and can simultaneously quantify their diffusion and microcirculation in tissue capillary network[79]. IVIM images are quantified by ADC, which integrates the effects of both diffusion and perfusion. IVIM therefore enables evaluation of tissue perfusion without the requirement of a contrast agent. The quantitative parameters in IVIM include the pure diffusion coefficient (D_{slow}), which reflects the diffusion of water molecules, the pseudodiffusion coefficient (D_{fast}), which reflects the diffusion movement of capillary microcirculation perfusion, and the perfusion fraction (f), which represents the volume ratio between the perfusion effect of local microcirculation and the overall molecular diffusion (Figures 7 and 8). IVIM-DWI is a useful method to assess true tumor cellularity of PNEN, represented by tissue diffusion, as increased microcirculation of hypervascular PNENs may cause the pseudodiffusion effect and thus leads to the overestimation of ADC values[79]. Hwang *et al*[80] observed that IVIM DWI can differentiate grade 1 from grade 2 or 3 PNENs. They found that pure diffusion coefficient is a better marker of tumor cellularity than ADC, and was significantly higher in grade 1 PNENs, thereby enabling prediction of tumor grade on imaging. A recent study showed that D_{slow} and D_{fast} parameters help in the differentiation of high grade PNENs from pancreatic adenocarcinoma with high diagnostic accuracy (0.460 *vs* 0.579×10^3 mm^2/s and 13.361 *vs* 4.985×10^3 mm^2/s, respectively)[81].

Diffusion kurtosis imaging

Diffusion kurtosis imaging (DKI) is a new rapidly advancing MRI technique based on the concept that water molecules in biological environment have non Gaussian properties. This is in contrast to standard DWI that calculates ADC using monoexponential analysis, assuming that diffusion of water in tissues follows Gaussian behavior[82]. At higher b values (> 1000 s/mm^2), due to the barriers encountered by water molecules in tissues, there is deviation from Gaussian distribution. The deviation when quantified, in fact represents the tissue microenvironment. Two quantitative parameters, diffusion coefficient (D) and kurtosis (K), representing deviation from Gaussian distribution, can be extracted from DKI. DKI thus provides a more accurate model of diffusion and quantifies tissue heterogeneity, and irregularity of cellular microstructure by capturing non Gaussian diffusion parameters (Figure 9)[82,83]. A drawback which hampers its use in routine practice is the long acquisition time due to scan acquisition at multiple b values. There are studies showing application of DKI for the assessment of the pancreas[84,85]. Shi *et al*[83] found that the radiomics model of DKI and T2 weighted imaging could improve the diagnostic accuracy for PNENs.

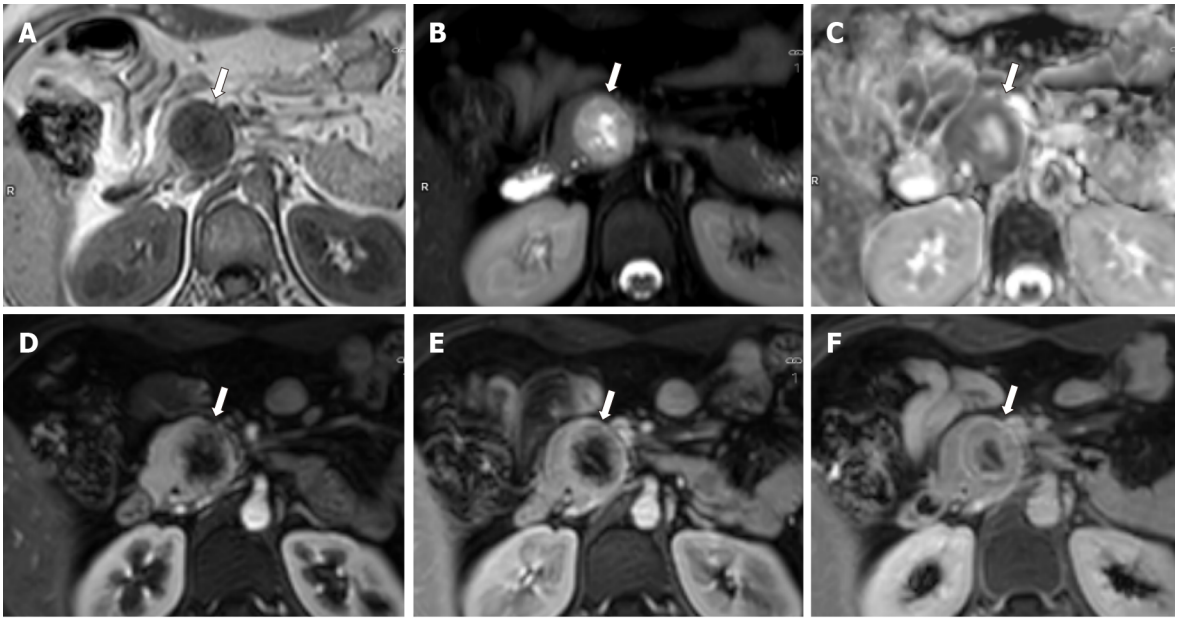

DOI: 10.3748/wjg.v28.i26.3008

Figure 6 Magnetic resonance images of a 24-year-old woman with multiple endocrine neoplasia-type 1 syndrome and pancreatic neuroendocrine neoplasm. A-C: Axial magnetic resonance images through the head of pancreas show a round heterogeneous mass (arrow) which appears hypointense on T1-weighted image (A), hyperintense on T2-weighted image with central cystic / necrotic change (B) and shows peripheral hypointensity on apparent diffusion coefficient (ADC) image (C) suggesting diffusion restriction along the periphery (ADC = 0.93 × 10^3 mm^2/s); D-F: Axial dynamic contrast enhanced T1-weighted images show hyperenhancement of the tumor along the periphery in pancreatic phase (D), with contrast retention in venous (E) and delayed (F) phase images. The patient also had bilateral inferior parathyroid and left superior parathyroid adenomas.

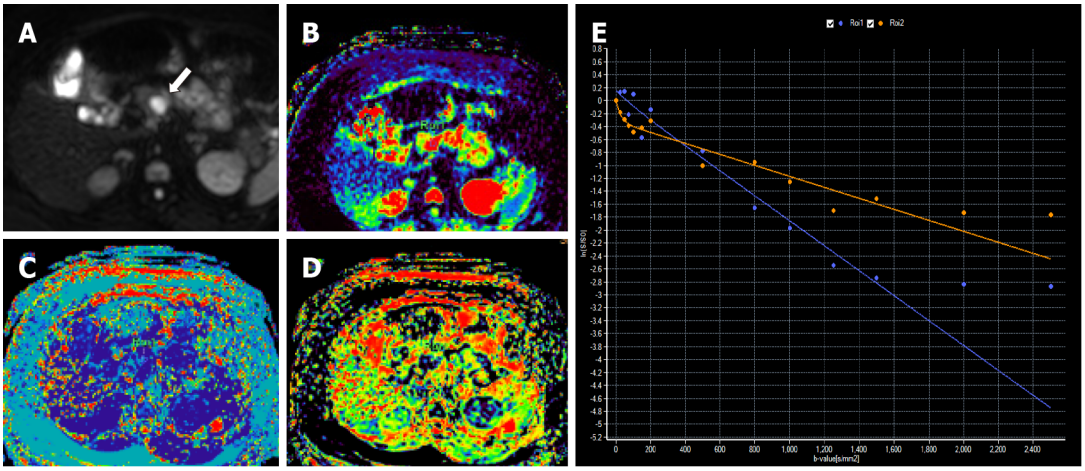

DOI: 10.3748/wjg.v28.i26.3008

Figure 7 Intravoxel incoherent motion diffusion-weighted imaging in a 46-year-old woman with proven grade 1 pancreatic neuroendocrine neoplasm. A: Axial diffusion weighted image (b = 800 s/mm^2) shows a small pancreatic lesion with diffusion restriction (arrow); B: Color-coded diffusion map shows true diffusion coefficient, D = 2.33 × 10^3 mm^2/s; C: Color-coded perfusion map shows pseudodiffusion coefficient, D∗ = 5.37 × 10^3 mm^2/s); D: Color-coded perfusion fraction map shows a value, f = 3.2%; E: Signal decay curve of the tumor (purple) shows fall in signal at lower b values with plateau at higher b values. In comparison, normal pancreas (orange) shows lesser diffusion restriction than the tumor.

MR elastography

MR elastography (MRE) is a phase-contrast-based MRI technique for the evaluation of mechanical tissue properties noninvasively, *e.g.,* tissue stiffness. MRE of pancreas is at an early stage. Recent studies have used MRE to differentiate healthy from pathological pancreatic tissue[86]. The normal pancreatic stiffness in adults measured by MRE is 1.1–1.21 kPa[86]. Shi *et al*[87] used MRE for the characterization of solid pancreatic masses. They found that malignant masses had significantly higher stiffness (3.27 kPa) than benign masses (1.96 kPa). PNENs had a median stiffness of 2.32 kPa. They also suggested that stiffness ratio (ratio of stiffness of mass to normal parenchyma) may perform better in the differentiation of benign from malignant pancreatic masses.

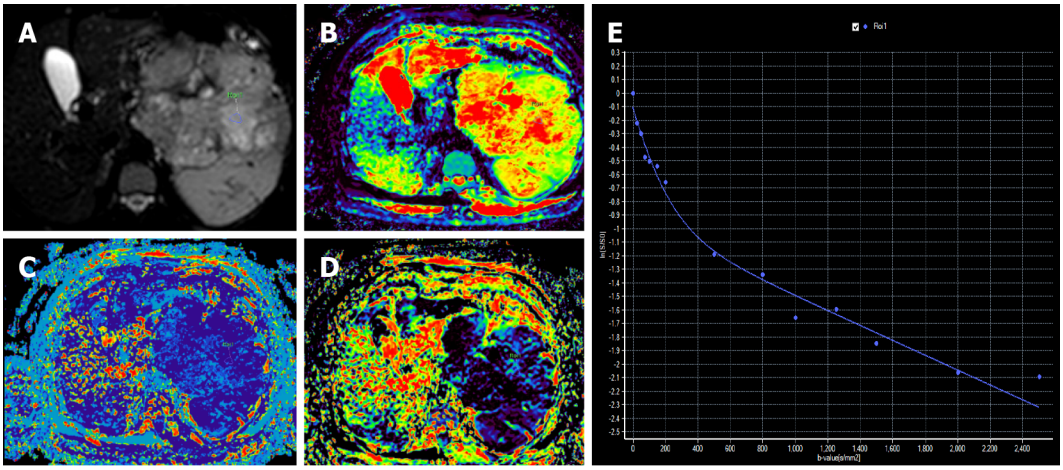

DOI: 10.3748/wjg.v28.i26.3008

Figure 8 Intravoxel incoherent motion diffusion-weighted imaging in a 67-year-old man with grade 3 pancreatic neuroendocrine neoplasm. A: Axial diffusion weighted image (b = 200 s/mm^2) with circular region of interest in the tumor; B: Color-coded diffusion map shows true diffusion coefficient, D = 0.84 × 10^3 mm^2/s; C: Color-coded perfusion map shows pseudodiffusion coefficient, D∗ = 5.01 × 10^3 mm^2/s); D: Color-coded perfusion fraction map shows a value, f = 4.5%; E: Signal decay curve shows steeper decay at low b values and continued fall at higher b values [in comparison to grade 1 pancreatic neuroendocrine neoplasm (PNEN) (Figure 7), true diffusion coefficient is lower in grade 3 PNENs].

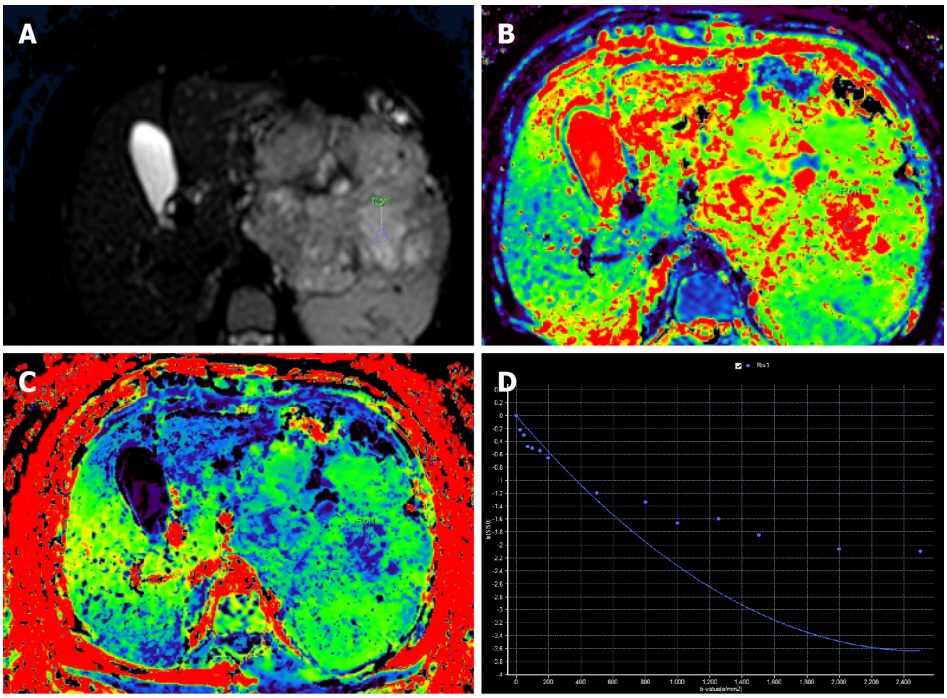

DOI: 10.3748/wjg.v28.i26.3008

Figure 9 Diffusion kurtosis of the lesion same as in Figure 8. A: Axial diffusion-weighted image (b = 200 s/mm^2) with region of interest marked; B: Diffusion map (D = 3 × 10^3 mm^2/s); C: Kurtosis map (k = 0.40); D: Signal decay curve shows non-Gaussian diffusion.

MRI perfusion

MRI perfusion techniques for the assessment of tumor perfusion have the major advantage that they lack adverse effects of radiation compared to the radiation-intensive CT perfusion. T1-weighted dynamic contrast enhanced (DCE) MRI is the technique applied in the evaluation of tumors in the abdomen[88]. This provides both semiquantitative and quantitative information on the microvascular perfusion of the tissue. The semiquantitative analysis is based on the time-signal intensity curve and the quantitative analysis is based on the Tofts two-compartment pharmacokinetic model (intravascular and extravascular-extracellular compartments) with the parameters evaluated being Ktrans (volume transfer constant, wash in), Kep (reverse efflux rate constant, wash out) and Ve (extravascular extracellular space volume fraction)[89]. This technique has shown promising results in the evaluation of PNENs. A study by Donati *et al*[90] showed that Ktrans and Kep values were higher in NENs (2.709 ± 0.110/min; 5.957 ±

0.371/min) compared to other focal lesions and healthy pancreatic parenchyma. This in fact reflects the wash in (Ktrans) and wash out (Kep) of the contrast agent from the hypervascular NENs. Also, well differentiated and poorly differentiated NENs showed different perfusion characteristics. In the study by Kim *et al*[91], Ktrans value of NENs were significantly higher than that of neuroendocrine carcinomas (0.339 ± 0.187/min *vs* 0.077 ± 0.036/min). Ductal adenocarcinomas being hypovascular, show significantly lower average values of Ktrans and Kep[90-92]. The role of DCE MRI in the evaluation of response to systemic chemotherapy and targeted molecular therapy by assessing the changes in the values of MRI perfusion parameters reflecting good or poor response to treatment is a direction for future studies.

PET CT AND PET MRI

Hybrid anatomical and functional imaging using PET/CT is a valuable tool in the current practice of grading and management of NENs. In general, in dual tracer PET/CT (somatostatin receptor imaging with Ga^{68} DOTATATE/TOC/NOC PET/CT and glucose metabolism with FDG PET/CT), low-grade tumors, which express somatostatin receptors, bind to somatostatin analog, but not to FDG[93]. In contrast, poorly differentiated GEPNENs with high Ki-67 index would be negative on somatostatin PET/CT but FDG avid[94]. Zhang *et al*[95] suggested that dual tracer PET /CT may be used as an alternative to tissue sampling, as it reflects both cellular somatostatin receptor expression and glucose metabolism. The authors also found a positive correlation between SUVmax (standardized uptake value) and Ki-67 index with respect to FDG PET/CT and negative correlation with respect to Ga^{68} DOTATATE PET/CT. However, low-grade insulinomas show low expression of somatostatin receptors in contrast to other secreting and nonsecreting NENs and are frequently not detected on Ga^{68} DOTATATE PET/CT[96]. Since virtually all benign insulinomas express glucagon-like peptide 1 (GLP-1) receptors (incretin receptors), these receptors can be targeted by PET/CT for preoperative localization of occult benign insulinomas. GLP-1R PET/CT had higher sensitivity than MRI and SPECT/CT for localization of benign insulinomas in a study by Antwi *et al*[97]. Glucose dependent insulinotropic polypeptide receptor (GIPR) is another incretin receptor overexpressed in GEPNENs. It is a potential target for imaging the small percentage (~10%) of GEPNENs which do not express SSTR and GLP1R, as confirmed by studies in animal models[98].

With technical advances, simultaneous PET and MRI acquisition in an integrated scanner is now possible. The first study in 2013 by Beiderwellen *et al*[99] showed that every lesion detected on PET/CT was identified on PET/MRI. Hope *et al*[100] evaluated hepatic lesions in patients with NENs using Ga^{68} DOTATOC PET/CT and PET/MRI and found that there was a strong correlation between SUVmax obtained in PET/CT and PET/MRI. However, due to the high cost, the routine use of PET/MRI is limited.

RADIOMICS, TEXTURE ANALYSIS AND MACHINE LEARNING

Radiomics is the process of conversion of digital biomedical images to mineable data and the subsequent analysis of this data[101]. Texture analysis is an imaging technique under the wider arena of radiomics, that extracts, analyzes and interprets quantitative imaging features, and enables objective assessment of tumor heterogeneity beyond what is possible to human eyes[102]. In statistical-based model of texture analysis, from each voxel in a region of interest, various first order (*e.g.*, first-order entropy, kurtosis, skewness, standard deviation, mean intensity) and second order (*e.g.*, contrast, uniformity, second order entropy, *etc.*), or higher order features are extracted and analyzed using post processing software. As mentioned previously, tumor grade is an important prognostic factor of NENs and their prediction noninvasively is valuable.

CT radiomics is increasingly finding its place in the grading of NENs. Canellas *et al*[103], evaluating PNENs on CT scan, found that tumors with high entropy (a texture parameter reflecting tissue heterogeneity) values had 3.7 times higher odds of being aggressive (grades 2 and 3). In this study, entropy was a better predictor of tumor grade than the size of the lesion. Choi *et al*[104] found that lower kurtosis, lower sphericity and higher skewness correlated to grade 2 or 3 PNENs. A study on 3D texture analysis of PNENs in 100 patients showed that kurtosis was significantly different between all the three grades and entropy could differentiate grade 1 from grade 3 and grade 2 from grade 3, but not grade 1 from grade 2 tumors[50]. These results of CT texture analysis were confirmed in other recent studies [105,106] thus emphasizing its role in the prediction of tumor grade.

MRI radiomics also help in characterizing PNENs. MRI texture analysis was found to be useful in differentiating nonfunctioning PNEN from solid pseudopapillary neoplasm in a study by Li *et al*[107]. Nonlinear discriminant analysis was found to have the lowest misclassification rate of all the types of analyses performed in their study. Shindo *et al*[108] studied ADC histogram for differentiation of pancreatic adenocarcinoma from PNENs. In their study, ADC entropy had the highest area under the curve (AUC) for differentiating adenocarcinoma from NEN. De Robertis *et al*[77] found that ADC

Table 3 Summary of important research studies on imaging of gastroenteropancreatic neuroendocrine neoplasms

	Ref.	Number (*n*)	Modality	Results	Conclusion
Ultrasonography	Takada *et al* [25], 2019	30	Contrast-enhanced harmonic EUS	Three parameters in TIC showed high diagnostic accuracy: Echo intensity change - 87%; Rate of enhancement - 87%; Enhancement ratio for node/pancreatic parenchyma - 88.5%	Contrast-enhanced EUS and TIC analysis show high diagnostic accuracy for grading of PNEN
CT	Worhunsky *et al*[45], 2014	118	APCT	5-year overall survival: Hypoenhancing - 54%; Isoenhancing - 89%; Hyperenhancin - 93%. On multivariate analysis only hypoenhancement (HR 2.32, P = 0.02) was independently associated with survival	Hypoenhancement of PNEN on APCT (22% of well-differentiated PNEN) was an independent predictor of poor outcome
	Rodallec *et al*[46], 2006	37	Dual-phase contrast-enhanced CT	Poorly differentiated NEC: Hypoattenuating - 71%; Isoattenuating or weakly hyperattenuating - 29%; Well-differentiated NECmoderately or strongly hyperattenuating - 53%. Poor enhancement at pancreatic phase and less vascularized tumors were associated with decreased survival rate	Enhancement of PNEN at CT correlated with microscopic tumor vascularity. Low-enhancing PNEN correlated with poor differentiation and lower overall survival
	Park *et al* [48], 2020	69	Dynamic CT	NEC (compared to well-differentiated NEN): Significantly higher frequencies of main pancreatic ductal dilatation, bile duct dilatation, vascular invasion; Significantly lower conspicuity of interface between tumor and parenchyma, AER and PER. PER < 0.8 showed 94.1% sensitivity, 88.5% specificity for differentiation of NEC from well-differentiated NEN. On combining 3 significant CT features, the sensitivity and specificity for diagnosing NEC were 88.2% and 88.5% respectively	Tumor parenchyma enhancement ratio in portal phase is useful to distinguish NECs from well differentiated NENs. Combining qualitative and quantitative CT features aid in achieving good diagnostic accuracy in differentiation between NEC and well-differentiated NEN
	d'Assignies *et al*[59], 2009	36	MDCT perfusion	Tumor blood flow and intratumoral MVD showed high correlation (r = 0.620, P < 0.001). Blood flow was significantly higher in: Grade 1 than grade 2/3 tumors; Tumors with proliferation index ≤ 2% (P = 0.005); Tumors without histological signs of microscopic vascular involvement (P = 0.008). Mean transit time was longer in tumors with lymph node (P = 0.02) or liver (P = 0.05) metastasis	Perfusion CT is feasible in patients with pancreatic NENs and reflects MVD. Perfusion CT measurements correlated with histoprognostic factors, such as proliferation index and WHO grading
MRI	Canellas *et al*[103], 2018	80	MRI	MRI features associated with aggressive tumors: Size > 2 cm (OR = 4.8); T2 non-bright lesions (OR = 4.6); Presence of pancreatic ductal dilatation (OR = 4.9); Diffusion restriction (OR = 4.9)	MRI can assess aggressiveness of PNEN and identify patients at risk for early disease progression after surgical resection
	d'Assignies *et al*[74], 2013	59	MRI	DWI (71%-71.6%) was more sensitive than T2 weighted images (55.6%) and dynamic CEMRI (47.5%-48.1%). Combination of these sequences improved detection of liver metastases. Specificity of each sequence was comparable (89%-100%)	DWI is more sensitive for detection and characterization of liver metastases from NENs than T2-weighted and dynamic gadolinium-enhanced MRI
Radiomics, texture analysis and machine learning	Canellas *et al*[103], 2018	101	CECT with texture analysis	CT features predictive of a more aggressive tumor: Size > 2 cm (OR = 3.3); Vascular involvement (OR = 25.2); Pancreatic ductal dilatation (OR = 6); Lymphadenopathy (OR = 6.8); Entropy (OR = 3.7); Differences (P < 0.05) in progression free survival were found for: Grade 1 *vs* grade 2 *vs* grade 3 tumors; PNEN with vascular involvement; Tumors with entropy values > 4.65	CT texture analysis and CT features are predictive of aggressiveness and can be used to identify patients at risk of early disease progression after surgical resection
	De Robertis *et al*[77], 2018	42	MRI and histogram analysis	ADC entropy is significantly higher in grade 2/3 tumors (sensitivity: 83.3%, specificity: 61.1%). ADC kurtosis is higher in PNENs with vascular involvement, nodal and hepatic metastases (sensitivity: 85.7%, specificity: 74.3%)	Whole tumor ADC histogram analysis can predict aggressiveness in PNENs. ADC entropy and ADC kurtosis are the most accurate parameters for identification of PNEN with malignant behavior
	Luo *et al* [112], 2020	93	CECT with application of a CNN based DL algorithm	AUC = 0.81 of arterial phase in validation set was significantly higher than those of venous (AUC = 0.57, P = 0.03) and arterial/venous phase (AUC = 0.70, P = 0.03) in predicting the pathological grading of PNENs. The AUC and accuracy of DL algorithm for diagnosing grade 3 PNEN were 0.80% and 79.1%. There was significant difference in OS and PFS between the predicted G1/2 and G3 groups	The CNN-based DL method showed a relatively robust performance in predicting pathological grading of PNENs from CECT images
	Gao *et al*	96	CEMRI with	The average accuracy of the five trained CNNs	With the help of GAN, the CNN

	[114], 2019	application of deep learning algorithm on images	ranged between 79.08% and 82.35%, and the range of micro- average AUC was between 0.8825 and 0.8932. The average accuracy and micro-average AUC of the averaged CNN were 81.05% and 0.8847 respectively	showed the potential to predict the grades of PNENs on CEMRI

EUS: Enhanced ultrasonography; TIC: Time-signal intensity curve; APCT: Arterial phase computed tomography; ADC: Apparent diffusion coefficient; CECT: Contrast enhanced computed tomography; CEMRI: Contrast enhanced magnetic resonance imaging; CNN: Convolutional neural network; DWI: Diffusion weighted imaging; NEC: Neuroendocrine carcinoma; NEN: Neuroendocrine neoplasm; AER: Annual equivalent ratio; PER: Portal enhancement ratio; MVD: Microvascular density; WHO: World Health Organization; MDCT: Multidetector row computed tomography; OS: Overall survival; PFS: Progression free survival; AUC: Area under the curve; PNEN: Pancreatic neuroendocrine neoplasm; GAN: Generative Adversarial Network.

histogram analysis of DWI, using radiomics, could predict aggressiveness of PNENs. They found high ADC kurtosis values in tumors with vascular invasion (AUC of 0.763 for a cut off value of 4.13) and distant metastases (AUC of 0.820 for a cut off of 3.642)[77]. The future prospects of radiomics are in the direction of development of a robust predictive model combining qualitative and quantitative imaging parameters.

Machine learning is increasingly being used in medicine and has various applications including detection of disease, classification of images, identifying treatment and monitoring adherence to therapy [109,110]. The standard radiomics analysis on CT or MRI requires marking of the tumor margins for analysis. However, deep learning using convolutional neural network (CNN) performs analysis automatically and provides better results[111]. A few recent preliminary studies have shown the promising role of deep learning using CNN in the prediction of grade of PNEN and survival using contrast enhanced CT[112-114]. Clinical trials for translation of these imaging techniques into clinical practice and validation for routine use are ongoing.

In short, the quantitative parameters derived from imaging, relevant for prognostication of GEPNENs include tumor size, enhancement ratios derived from HU values, iodine uptake on DECT, entropy on CT texture analysis, tumor blood flow, tumor blood volume, and mean transit time on perfusion CT, ADC and ADC histogram analysis of DWI, true and pseudodiffusion coefficients and perfusion fraction on IVIM DWI, Ktrans and Kep on perfusion MRI and SUVmax on dual tracer PET/CT. A combination of qualitative features and quantitative factors with the newer functional imaging techniques enables better tumor classification based on their prognosis. A summary of important studies on advanced imaging in GEPNENs is shown in Table 3.

CONCLUSION

With the recent advances in CT, MRI, USG and hybrid imaging techniques like PET/CT and PET/MRI using dual tracers, smaller pancreatic and bowel NENs are now being increasingly detected and staged. In addition to tumor detection and staging, their non-invasive grading, prognostication and monitoring response to treatment are shown to be feasible and reliable with the emerging studies using quantitative imaging techniques like CT and MR perfusion studies, DWI, IVIM and texture analysis with radiomics. Standardization of these techniques with more large scale studies would be an important future prospect. These advances in imaging will help in making the right treatment choice, contributing to an overall improvement in patient outcome.

FOOTNOTES

Author contributions: Ramachandran A contributed to initial draft and revision; Madhusudhan KS contributed to review of draft and revision.

Conflict-of-interest statement: No conflict of interests.

Country/Territory of origin: India

ORCID number: Anupama Ramachandran 0000-0002-5808-6076; Kumble Seetharama Madhusudhan 0000-0001-8806-2625.

Corresponding Author's Membership in Professional Societies: Indian Radiological and Imaging Association, No.

501LM/D-285A.

S-Editor: Zhang H
L-Editor: Kerr C
P-Editor: Zhang H

REFERENCES

1 **Lawrence B**, Gustafsson BI, Chan A, Svejda B, Kidd M, Modlin IM. The epidemiology of gastroenteropancreatic neuroendocrine tumors. *Endocrinol Metab Clin North Am* 2011; **40**: 1-18, vii [PMID: 21349409 DOI: 10.1016/j.ecl.2010.12.005]
2 **Turaga KK**, Kvols LK. Recent progress in the understanding, diagnosis, and treatment of gastroenteropancreatic neuroendocrine tumors. *CA Cancer J Clin* 2011; **61**: 113-132 [PMID: 21388967 DOI: 10.3322/caac.20097]
3 **Modlin IM**, Lye KD, Kidd M. A 5-decade analysis of 13,715 carcinoid tumors. *Cancer* 2003; **97**: 934-959 [PMID: 12569593 DOI: 10.1002/cncr.11105]
4 **Sahani DV**, Bonaffini PA, Fernández-Del Castillo C, Blake MA. Gastroenteropancreatic neuroendocrine tumors: role of imaging in diagnosis and management. *Radiology* 2013; **266**: 38-61 [PMID: 23264526 DOI: 10.1148/radiol.12112512]
5 **Toumpanakis CG**, Caplin ME. Molecular genetics of gastroenteropancreatic neuroendocrine tumors. *Am J Gastroenterol* 2008; **103**: 729-732 [PMID: 18341492 DOI: 10.1111/j.1572-0241.2007.01777.x]
6 **Gallotti A**, Johnston RP, Bonaffini PA, Ingkakul T, Deshpande V, Fernández-del Castillo C, Sahani DV. Incidental neuroendocrine tumors of the pancreas: MDCT findings and features of malignancy. *AJR Am J Roentgenol* 2013; **200**: 355-362 [PMID: 23345357 DOI: 10.2214/AJR.11.8037]
7 **Nagtegaal ID**, Odze RD, Klimstra D, Paradis V, Rugge M, Schirmacher P, Washington KM, Carneiro F, Cree IA; WHO Classification of Tumours Editorial Board. The 2019 WHO classification of tumours of the digestive system. *Histopathology* 2020; **76**: 182-188 [PMID: 31433515 DOI: 10.1111/his.13975]
8 **Kunz PL**, Reidy-Lagunes D, Anthony LB, Bertino EM, Brendtro K, Chan JA, Chen H, Jensen RT, Kim MK, Klimstra DS, Kulke MH, Liu EH, Metz DC, Phan AT, Sippel RS, Strosberg JR, Yao JC; North American Neuroendocrine Tumor Society. Consensus guidelines for the management and treatment of neuroendocrine tumors. *Pancreas* 2013; **42**: 557-577 [PMID: 23591432 DOI: 10.1097/MPA.0b013e31828e34a4]
9 **Falconi M**, Eriksson B, Kaltsas G, Bartsch DK, Capdevila J, Caplin M, Kos-Kudla B, Kwekkeboom D, Rindi G, Klöppel G, Reed N, Kianmanesh R, Jensen RT; Vienna Consensus Conference participants. ENETS Consensus Guidelines Update for the Management of Patients with Functional Pancreatic Neuroendocrine Tumors and Non-Functional Pancreatic Neuroendocrine Tumors. *Neuroendocrinology* 2016; **103**: 153-171 [PMID: 26742109 DOI: 10.1159/000443171]
10 **Tan EH**, Tan CH. Imaging of gastroenteropancreatic neuroendocrine tumors. *World J Clin Oncol* 2011; **2**: 28-43 [PMID: 21603312 DOI: 10.5306/wjco.v2.i1.28]
11 **Modlin IM**, Oberg K, Chung DC, Jensen RT, de Herder WW, Thakker RV, Caplin M, Delle Fave G, Kaltsas GA, Krenning EP, Moss SF, Nilsson O, Rindi G, Salazar R, Ruszniewski P, Sundin A. Gastroenteropancreatic neuroendocrine tumours. *Lancet Oncol* 2008; **9**: 61-72 [PMID: 18177818 DOI: 10.1016/S1470-2045(07)70410-2]
12 **Giovannini M**. Contrast-enhanced and 3-dimensional endoscopic ultrasonography. *Gastroenterol Clin North Am* 2010; **39**: 845-858 [PMID: 21093759 DOI: 10.1016/j.gtc.2010.08.027]
13 **Takeda K**, Goto H, Hirooka Y, Itoh A, Hashimoto S, Niwa K, Hayakawa T. Contrast-enhanced transabdominal ultrasonography in the diagnosis of pancreatic mass lesions. *Acta Radiol* 2003; **44**: 103-106 [PMID: 12631008]
14 **Malagò R**, D'Onofrio M, Zamboni GA, Faccioli N, Falconi M, Boninsegna L, Mucelli RP. Contrast-enhanced sonography of nonfunctioning pancreatic neuroendocrine tumors. *AJR Am J Roentgenol* 2009; **192**: 424-430 [PMID: 19155405 DOI: 10.2214/AJR.07.4043]
15 **Del Prete M**, Di Sarno A, Modica R, Lassandro F, Giorgio A, Bianco A, Muto M, Gasperi M, Del Prete F, Colao A, Montesarchio V, Faggiano A; ENETS Centre of Excellence Multidisciplinary Group for Neuroendocrine Tumors in Naples (Italy). Role of contrast-enhanced ultrasound to define prognosis and predict response to biotherapy in pancreatic neuroendocrine tumors. *J Endocrinol Invest* 2017; **40**: 1373-1380 [PMID: 28667452 DOI: 10.1007/s40618-017-0723-x]
16 **Giovannini M**, Hookey LC, Bories E, Pesenti C, Monges G, Delpero JR. Endoscopic ultrasound elastography: the first step towards virtual biopsy? *Endoscopy* 2006; **38**: 344-348 [PMID: 16680632 DOI: 10.1055/s-2006-925158]
17 **Park MK**, Jo J, Kwon H, Cho JH, Oh JY, Noh MH, Nam KJ. Usefulness of acoustic radiation force impulse elastography in the differential diagnosis of benign and malignant solid pancreatic lesions. *Ultrasonography* 2014; **33**: 26-33 [PMID: 24936492 DOI: 10.14366/usg.13017]
18 **Uchida H**, Hirooka Y, Itoh A, Kawashima H, Hara K, Nonogaki K, Kasugai T, Ohno E, Ohmiya N, Niwa Y, Katano Y, Ishigami M, Goto H. Feasibility of tissue elastography using transcutaneous ultrasonography for the diagnosis of pancreatic diseases. *Pancreas* 2009; **38**: 17-22 [PMID: 18695627 DOI: 10.1097/MPA.0b013e318184db78]
19 **Hunt GC**, Faigel DO. Assessment of EUS for diagnosing, staging, and determining resectability of pancreatic cancer: a review. *Gastrointest Endosc* 2002; **55**: 232-237 [PMID: 11818928 DOI: 10.1067/mge.2002.121342]
20 **Legmann P**, Vignaux O, Dousset B, Baraza AJ, Palazzo L, Dumontier I, Coste J, Louvel A, Roseau G, Couturier D, Bonnin A. Pancreatic tumors: comparison of dual-phase helical CT and endoscopic sonography. *AJR Am J Roentgenol* 1998; **170**: 1315-1322 [PMID: 9574609 DOI: 10.2214/ajr.170.5.9574609]
21 **Rösch T**, Lightdale CJ, Botet JF, Boyce GA, Sivak MV Jr, Yasuda K, Heyder N, Palazzo L, Dancygier H, Schusdziarra V. Localization of pancreatic endocrine tumors by endoscopic ultrasonography. *N Engl J Med* 1992; **326**: 1721-1726 [PMID: 1317506 DOI: 10.1056/NEJM199206253262601]
22 **Kim MK**. Endoscopic ultrasound in gastroenteropancreatic neuroendocrine tumors. *Gut Liver* 2012; **6**: 405-410 [PMID:

23170141 DOI: 10.5009/gnl.2012.6.4.405]

23 **Anderson MA**, Carpenter S, Thompson NW, Nostrant TT, Elta GH, Scheiman JM. Endoscopic ultrasound is highly accurate and directs management in patients with neuroendocrine tumors of the pancreas. *Am J Gastroenterol* 2000; **95**: 2271-2277 [PMID: 11007228 DOI: 10.1111/j.1572-0241.2000.02480.x]

24 **Guo J**, Sahai AV, Teoh A, Arcidiacono PG, Larghi A, Saftoiu A, Siddiqui AA, Arturo Arias BL, Jenssen C, Adler DG, Lakhtakia S, Seo DW, Itokawa F, Giovannini M, Mishra G, Sabbagh L, Irisawa A, Iglesias-Garcia J, Poley JW, Vila JJ, Jesse L, Kubota K, Kalaitzakis E, Kida M, El-Nady M, Mukai SU, Ogura T, Fusaroli P, Vilmann P, Rai P, Nguyen NQ, Ponnudurai R, Achanta CR, Baron TH, Yasuda I, Wang HP, Hu J, Duan B, Bhutani MS, Sun S. An international, multi-institution survey on performing EUS-FNA and fine needle biopsy. *Endosc Ultrasound* 2020; **9**: 319-328 [PMID: 32883921 DOI: 10.4103/eus.eus_56_20]

25 **Takada S**, Kato H, Saragai Y, Muro S, Uchida D, Tomoda T, Matsumoto K, Horiguchi S, Tanaka N, Okada H. Contrast-enhanced harmonic endoscopic ultrasound using time-intensity curve analysis predicts pathological grade of pancreatic neuroendocrine neoplasm. *J Med Ultrason (2001)* 2019; **46**: 449-458 [PMID: 31377939 DOI: 10.1007/s10396-019-00967-x]

26 **Janssen J**, Schlörer E, Greiner L. EUS elastography of the pancreas: feasibility and pattern description of the normal pancreas, chronic pancreatitis, and focal pancreatic lesions. *Gastrointest Endosc* 2007; **65**: 971-978 [PMID: 17531630 DOI: 10.1016/j.gie.2006.12.057]

27 **Săftoiu A**, Vilmann P, Gorunescu F, Gheonea DI, Gorunescu M, Ciurea T, Popescu GL, Iordache A, Hassan H, Iordache S. Neural network analysis of dynamic sequences of EUS elastography used for the differential diagnosis of chronic pancreatitis and pancreatic cancer. *Gastrointest Endosc* 2008; **68**: 1086-1094 [PMID: 18656186 DOI: 10.1016/j.gie.2008.04.031]

28 **Hirche TO**, Ignee A, Barreiros AP, Schreiber-Dietrich D, Jungblut S, Ott M, Hirche H, Dietrich CF. Indications and limitations of endoscopic ultrasound elastography for evaluation of focal pancreatic lesions. *Endoscopy* 2008; **40**: 910-917 [PMID: 19009483 DOI: 10.1055/s-2008-1077726]

29 **Havre RF**, Ødegaard S, Gilja OH, Nesje LB. Characterization of solid focal pancreatic lesions using endoscopic ultrasonography with real-time elastography. *Scand J Gastroenterol* 2014; **49**: 742-751 [PMID: 24713038 DOI: 10.3109/00365521.2014.905627]

30 **Micames CG**, Gress FG. EUS elastography: a step ahead? *Gastrointest Endosc* 2007; **65**: 979-981 [PMID: 17531631 DOI: 10.1016/j.gie.2007.02.059]

31 **Ohno E**, Hirooka Y, Kawashima H, Ishikawa T. Feasibility of EUS-guided shear-wave measurement: A preliminary clinical study. *Endosc Ultrasound* 2019; **8**: 215-216 [PMID: 30924448 DOI: 10.4103/eus.eus_6_19]

32 **Yamashita Y**, Tanioka K, Kawaji Y, Tamura T, Nuta J, Hatamaru K, Itonaga M, Yoshida T, Ida Y, Maekita T, Iguchi M, Kitano M. Utility of Elastography with Endoscopic Ultrasonography Shear-Wave Measurement for Diagnosing Chronic Pancreatitis. *Gut Liver* 2020; **14**: 659-664 [PMID: 31722469 DOI: 10.5009/gnl19170]

33 **Ohno E**, Kawashima H, Ishikawa T, Iida T, Suzuki H, Uetsuki K, Yashika J, Yamada K, Yoshikawa M, Gibo N, Aoki T, Kataoka K, Mori H, Yamamura T, Furukawa K, Nakamura M, Hirooka Y, Fujishiro M. Diagnostic performance of endoscopic ultrasonography-guided elastography for solid pancreatic lesions: Shear-wave measurements versus strain elastography with histogram analysis. *Dig Endosc* 2021; **33**: 629-638 [PMID: 32662150 DOI: 10.1111/den.13791]

34 **Manguso N**, Gangi A, Johnson J, Harit A, Nissen N, Jamil L, Lo S, Wachsman A, Hendifar A, Amersi F. The role of pre-operative imaging and double balloon enteroscopy in the surgical management of small bowel neuroendocrine tumors: Is it necessary? *J Surg Oncol* 2018; **117**: 207-212 [PMID: 28940412 DOI: 10.1002/jso.24825]

35 **Malla S**, Kumar P, Madhusudhan KS. Radiology of the neuroendocrine neoplasms of the gastrointestinal tract: a comprehensive review. *Abdom Radiol (NY)* 2021; **46**: 919-935 [PMID: 32960304 DOI: 10.1007/s00261-020-02773-3]

36 **Bonekamp D**, Raman SP, Horton KM, Fishman EK. Role of computed tomography angiography in detection and staging of small bowel carcinoid tumors. *World J Radiol* 2015; **7**: 220-235 [PMID: 26435774 DOI: 10.4329/wjr.v7.i9.220]

37 **Kamaoui I**, De-Luca V, Ficarelli S, Mennesson N, Lombard-Bohas C, Pilleul F. Value of CT enteroclysis in suspected small-bowel carcinoid tumors. *AJR Am J Roentgenol* 2010; **194**: 629-633 [PMID: 20173138 DOI: 10.2214/AJR.09.2760]

38 **Hakim FA**, Alexander JA, Huprich JE, Grover M, Enders FT. CT-enterography may identify small bowel tumors not detected by capsule endoscopy: eight years experience at Mayo Clinic Rochester. *Dig Dis Sci* 2011; **56**: 2914-2919 [PMID: 21735085 DOI: 10.1007/s10620-011-1773-0]

39 **Huprich JE**, Fletcher JG, Fidler JL, Alexander JA, Guimarães LS, Siddiki HA, McCollough CH. Prospective blinded comparison of wireless capsule endoscopy and multiphase CT enterography in obscure gastrointestinal bleeding. *Radiology* 2011; **260**: 744-751 [PMID: 21642417 DOI: 10.1148/radiol.11110143]

40 **Dromain C**, de Baere T, Baudin E, Galline J, Ducreux M, Boige V, Duvillard P, Laplanche A, Caillet H, Lasser P, Schlumberger M, Sigal R. MR imaging of hepatic metastases caused by neuroendocrine tumors: comparing four techniques. *AJR Am J Roentgenol* 2003; **180**: 121-128 [PMID: 12490490 DOI: 10.2214/ajr.180.1.1800121]

41 **Paulson EK**, McDermott VG, Keogan MT, DeLong DM, Frederick MG, Nelson RC. Carcinoid metastases to the liver: role of triple-phase helical CT. *Radiology* 1998; **206**: 143-150 [PMID: 9423664 DOI: 10.1148/radiology.206.1.9423664]

42 **Horton KM**, Kamel I, Hofmann L, Fishman EK. Carcinoid tumors of the small bowel: a multitechnique imaging approach. *AJR Am J Roentgenol* 2004; **182**: 559-567 [PMID: 14975946 DOI: 10.2214/ajr.182.3.1820559]

43 **Manfredi R**, Bonatti M, Mantovani W, Graziani R, Segala D, Capelli P, Butturini G, Mucelli RP. Non-hyperfunctioning neuroendocrine tumours of the pancreas: MR imaging appearance and correlation with their biological behaviour. *Eur Radiol* 2013; **23**: 3029-3039 [PMID: 23793519 DOI: 10.1007/s00330-013-2929-4]

44 **Humphrey PE**, Alessandrino F, Bellizzi AM, Mortele KJ. Non-hyperfunctioning pancreatic endocrine tumors: multimodality imaging features with histopathological correlation. *Abdom Imaging* 2015; **40**: 2398-2410 [PMID: 25989932 DOI: 10.1007/s00261-015-0458-0]

45 **Worhunsky DJ**, Krampitz GW, Poullos PD, Visser BC, Kunz PL, Fisher GA, Norton JA, Poultsides GA. Pancreatic neuroendocrine tumours: hypoenhancement on arterial phase computed tomography predicts biological aggressiveness. *HPB (Oxford)* 2014; **16**: 304-311 [PMID: 23991643 DOI: 10.1111/hpb.12139]

46 **Rodallec M**, Vilgrain V, Couvelard A, Rufat P, O'Toole D, Barrau V, Sauvanet A, Ruszniewski P, Menu Y. Endocrine pancreatic tumours and helical CT: contrast enhancement is correlated with microvascular density, histoprognostic factors and survival. *Pancreatology* 2006; **6**: 77-85 [PMID: 16327283 DOI: 10.1159/000090026]

47 **Kim DW**, Kim HJ, Kim KW, Byun JH, Song KB, Kim JH, Hong SM. Neuroendocrine neoplasms of the pancreas at dynamic enhanced CT: comparison between grade 3 neuroendocrine carcinoma and grade 1/2 neuroendocrine tumour. *Eur Radiol* 2015; **25**: 1375-1383 [PMID: 25465713 DOI: 10.1007/s00330-014-3532-z]

48 **Park HJ**, Kim HJ, Kim KW, Kim SY, Choi SH, You MW, Hwang HS, Hong SM. Comparison between neuroendocrine carcinomas and well-differentiated neuroendocrine tumors of the pancreas using dynamic enhanced CT. *Eur Radiol* 2020; **30**: 4772-4782 [PMID: 32346794 DOI: 10.1007/s00330-020-06867-w]

49 **Yamada S**, Fujii T, Suzuki K, Inokawa Y, Kanda M, Nakayama G, Sugimoto H, Koike M, Nomoto S, Fujiwara M, Nakao A, Kodera Y. Preoperative Identification of a Prognostic Factor for Pancreatic Neuroendocrine Tumors Using Multiphase Contrast-Enhanced Computed Tomography. *Pancreas* 2016; **45**: 198-203 [PMID: 26390421 DOI: 10.1097/MPA.0000000000000443]

50 **D'Onofrio M**, Ciaravino V, Cardobi N, De Robertis R, Cingarlini S, Landoni L, Capelli P, Bassi C, Scarpa A. CT Enhancement and 3D Texture Analysis of Pancreatic Neuroendocrine Neoplasms. *Sci Rep* 2019; **9**: 2176 [PMID: 30778137 DOI: 10.1038/s41598-018-38459-6]

51 **Hardie AD**, Picard MM, Camp ER, Perry JD, Suranyi P, De Cecco CN, Schoepf UJ, Wichmann JL. Application of an Advanced Image-Based Virtual Monoenergetic Reconstruction of Dual Source Dual-Energy CT Data at Low keV Increases Image Quality for Routine Pancreas Imaging. *J Comput Assist Tomogr* 2015; **39**: 716-720 [PMID: 26196343 DOI: 10.1097/RCT.0000000000000276]

52 **Lin XZ**, Wu ZY, Tao R, Guo Y, Li JY, Zhang J, Chen KM. Dual energy spectral CT imaging of insulinoma-Value in preoperative diagnosis compared with conventional multi-detector CT. *Eur J Radiol* 2012; **81**: 2487-2494 [PMID: 22153746 DOI: 10.1016/j.ejrad.2011.10.028]

53 **Kaltenbach B**, Wichmann JL, Pfeifer S, Albrecht MH, Booz C, Lenga L, Hammerstingl R, D'Angelo T, Vogl TJ, Martin SS. Iodine quantification to distinguish hepatic neuroendocrine tumor metastasis from hepatocellular carcinoma at dual-source dual-energy liver CT. *Eur J Radiol* 2018; **105**: 20-24 [PMID: 30017280 DOI: 10.1016/j.ejrad.2018.05.019]

54 **Kambadakone AR**, Sahani DV. Body perfusion CT: technique, clinical applications, and advances. *Radiol Clin North Am* 2009; **47**: 161-178 [PMID: 19195541 DOI: 10.1016/j.rcl.2008.11.003]

55 **Sinitsyn V**. Analysis and Interpretation of Perfusion CT in Oncology: Type of Cancer Matters. *Radiology* 2019; **292**: 636-637 [PMID: 31287775 DOI: 10.1148/radiol.2019191265]

56 **Marion-Audibert AM**, Barel C, Gouysse G, Dumortier J, Pilleul F, Pourreyron C, Hervieu V, Poncet G, Lombard-Bohas C, Chayvialle JA, Partensky C, Scoazec JY. Low microvessel density is an unfavorable histoprognostic factor in pancreatic endocrine tumors. *Gastroenterology* 2003; **125**: 1094-1104 [PMID: 14517793 DOI: 10.1016/s0016-5085(03)01198-3]

57 **Couvelard A**, O'Toole D, Turley H, Leek R, Sauvanet A, Degott C, Ruszniewski P, Belghiti J, Harris AL, Gatter K, Pezzella F. Microvascular density and hypoxia-inducible factor pathway in pancreatic endocrine tumours: negative correlation of microvascular density and VEGF expression with tumour progression. *Br J Cancer* 2005; **92**: 94-101 [PMID: 15558070 DOI: 10.1038/sj.bjc.6602245]

58 **Takahashi Y**, Akishima-Fukasawa Y, Kobayashi N, Sano T, Kosuge T, Nimura Y, Kanai Y, Hiraoka N. Prognostic value of tumor architecture, tumor-associated vascular characteristics, and expression of angiogenic molecules in pancreatic endocrine tumors. *Clin Cancer Res* 2007; **13**: 187-196 [PMID: 17200354 DOI: 10.1158/1078-0432.CCR-06-1408]

59 **d'Assignies G**, Couvelard A, Bahrami S, Vullierme MP, Hammel P, Hentic O, Sauvanet A, Bedossa P, Ruszniewski P, Vilgrain V. Pancreatic endocrine tumors: tumor blood flow assessed with perfusion CT reflects angiogenesis and correlates with prognostic factors. *Radiology* 2009; **250**: 407-416 [PMID: 19095784 DOI: 10.1148/radiol.2501080291]

60 **Zhu L**, Wu WM, Xue HD, Liu W, Wang X, Sun H, Li P, Zhao YP, Jin ZY. Sporadic insulinomas on volume perfusion CT: dynamic enhancement patterns and timing of optimal tumour-parenchyma contrast. *Eur Radiol* 2017; **27**: 3491-3498 [PMID: 28108839 DOI: 10.1007/s00330-016-4709-4]

61 **Zhu L**, Xue H, Sun H, Wang X, Wu W, Jin Z, Zhao Y. Insulinoma Detection With MDCT: Is There a Role for Whole-Pancreas Perfusion? *AJR Am J Roentgenol* 2017; **208**: 306-314 [PMID: 27929662 DOI: 10.2214/AJR.16.16351]

62 **Wan Y**, Hao H, Meng S, Li Z, Yu F, Meng Chi, Chao Q, Gao J. Application of low dose pancreas perfusion CT combined with enhancement scanning in diagnosis of pancreatic neuroendocrine tumors. *Pancreatology* 2021; **21**: 240-245 [PMID: 33191144 DOI: 10.1016/j.pan.2020.10.046]

63 **Ng CS**, Charnsangavej C, Wei W, Yao JC. Perfusion CT findings in patients with metastatic carcinoid tumors undergoing bevacizumab and interferon therapy. *AJR Am J Roentgenol* 2011; **196**: 569-576 [PMID: 21343498 DOI: 10.2214/AJR.10.4455]

64 **Ng CS**, Wei W, Duran C, Ghosh P, Anderson EF, Chandler AG, Yao JC. CT perfusion in normal liver and liver metastases from neuroendocrine tumors treated with targeted antivascular agents. *Abdom Radiol (NY)* 2018; **43**: 1661-1669 [PMID: 29075824 DOI: 10.1007/s00261-017-1367-1]

65 **Ketelsen D**, Horger M, Buchgeister M, Fenchel M, Thomas C, Boehringer N, Schulze M, Tsiflikas I, Claussen CD, Heuschmid M. Estimation of radiation exposure of 128-slice 4D-perfusion CT for the assessment of tumor vascularity. *Korean J Radiol* 2010; **11**: 547-552 [PMID: 20808699 DOI: 10.3348/kjr.2010.11.5.547]

66 **Dromain C**, de Baere T, Lumbroso J, Caillet H, Laplanche A, Boige V, Ducreux M, Duvillard P, Elias D, Schlumberger M, Sigal R, Baudin E. Detection of liver metastases from endocrine tumors: a prospective comparison of somatostatin receptor scintigraphy, computed tomography, and magnetic resonance imaging. *J Clin Oncol* 2005; **23**: 70-78 [PMID: 15625361 DOI: 10.1200/JCO.2005.01.013]

67 **Waldmann J**, Fendrich V, Habbe N, Bartsch DK, Slater EP, Kann PH, Rothmund M, Langer P. Screening of patients with multiple endocrine neoplasia type 1 (MEN-1): a critical analysis of its value. *World J Surg* 2009; **33**: 1208-1218 [PMID: 19350320 DOI: 10.1007/s00268-009-9983-8]

68 **Sundin A**, Vullierme MP, Kaltsas G, Plöckinger U; Mallorca Consensus Conference participants; European

Neuroendocrine Tumor Society. ENETS Consensus Guidelines for the Standards of Care in Neuroendocrine Tumors: radiological examinations. *Neuroendocrinology* 2009; **90**: 167-183 [PMID: 19077417 DOI: 10.1159/000184855]

69 **Wang Y**, Chen ZE, Yaghmai V, Nikolaidis P, McCarthy RJ, Merrick L, Miller FH. Diffusion-weighted MR imaging in pancreatic endocrine tumors correlated with histopathologic characteristics. *J Magn Reson Imaging* 2011; **33**: 1071-1079 [PMID: 21509863 DOI: 10.1002/jmri.22541]

70 **Jang KM**, Kim SH, Lee SJ, Choi D. The value of gadoxetic acid-enhanced and diffusion-weighted MRI for prediction of grading of pancreatic neuroendocrine tumors. *Acta Radiol* 2014; **55**: 140-148 [PMID: 23897307 DOI: 10.1177/0284185113494982]

71 **Lotfalizadeh E**, Ronot M, Wagner M, Cros J, Couvelard A, Vullierme MP, Allaham W, Hentic O, Ruzniewski P, Vilgrain V. Prediction of pancreatic neuroendocrine tumour grade with MR imaging features: added value of diffusion-weighted imaging. *Eur Radiol* 2017; **27**: 1748-1759 [PMID: 27543074 DOI: 10.1007/s00330-016-4539-4]

72 **Parikh T**, Drew SJ, Lee VS, Wong S, Hecht EM, Babb JS, Taouli B. Focal liver lesion detection and characterization with diffusion-weighted MR imaging: comparison with standard breath-hold T2-weighted imaging. *Radiology* 2008; **246**: 812-822 [PMID: 18223123 DOI: 10.1148/radiol.2463070432]

73 **Soyer P**, Boudiaf M, Placé V, Sirol M, Pautrat K, Vignaud A, Staub F, Tiah D, Hamzi L, Duchat F, Fargeaudou Y, Pocard M. Preoperative detection of hepatic metastases: comparison of diffusion-weighted, T2-weighted fast spin echo and gadolinium-enhanced MR imaging using surgical and histopathologic findings as standard of reference. *Eur J Radiol* 2011; **80**: 245-252 [PMID: 20650588 DOI: 10.1016/j.ejrad.2010.06.027]

74 **d'Assignies G**, Fina P, Bruno O, Vullierme MP, Tubach F, Paradis V, Sauvanet A, Ruszniewski P, Vilgrain V. High sensitivity of diffusion-weighted MR imaging for the detection of liver metastases from neuroendocrine tumors: comparison with T2-weighted and dynamic gadolinium-enhanced MR imaging. *Radiology* 2013; **268**: 390-399 [PMID: 23533288 DOI: 10.1148/radiol.13121628]

75 **Besa C**, Ward S, Cui Y, Jajamovich G, Kim M, Taouli B. Neuroendocrine liver metastases: Value of apparent diffusion coefficient and enhancement ratios for characterization of histopathologic grade. *J Magn Reson Imaging* 2016; **44**: 1432-1441 [PMID: 27227756 DOI: 10.1002/jmri.25320]

76 **Pereira JA**, Rosado E, Bali M, Metens T, Chao SL. Pancreatic neuroendocrine tumors: correlation between histogram analysis of apparent diffusion coefficient maps and tumor grade. *Abdom Imaging* 2015; **40**: 3122-3128 [PMID: 26280127 DOI: 10.1007/s00261-015-0524-7]

77 **De Robertis R**, Maris B, Cardobi N, Tinazzi Martini P, Gobbo S, Capelli P, Ortolani S, Cingarlini S, Paiella S, Landoni L, Butturini G, Regi P, Scarpa A, Tortora G, D'Onofrio M. Can histogram analysis of MR images predict aggressiveness in pancreatic neuroendocrine tumors? *Eur Radiol* 2018; **28**: 2582-2591 [PMID: 29352378 DOI: 10.1007/s00330-017-5236-7]

78 **Le Bihan D**, Breton E, Lallemand D, Grenier P, Cabanis E, Laval-Jeantet M. MR imaging of intravoxel incoherent motions: application to diffusion and perfusion in neurologic disorders. *Radiology* 1986; **161**: 401-407 [PMID: 3763909 DOI: 10.1148/radiology.161.2.3763909]

79 **Katharina Ingenerf M**, Karim H, Fink N, Ilhan H, Ricke J, Treitl KM, Schmid-Tannwald C. Apparent diffusion coefficients (ADC) in response assessment of transarterial radioembolization (TARE) for liver metastases of neuroendocrine tumors (NET): a feasibility study. *Acta Radiol* 2021; 2841851211024004 [PMID: 34225464 DOI: 10.1177/02841851211024004]

80 **Hwang EJ**, Lee JM, Yoon JH, Kim JH, Han JK, Choi BI, Lee KB, Jang JY, Kim SW, Nickel MD, Kiefer B. Intravoxel incoherent motion diffusion-weighted imaging of pancreatic neuroendocrine tumors: prediction of the histologic grade using pure diffusion coefficient and tumor size. *Invest Radiol* 2014; **49**: 396-402 [PMID: 24500090 DOI: 10.1097/RLI.0000000000000028]

81 **Ma W**, Wei M, Han Z, Tang Y, Pan Q, Zhang G, Ren J, Huan Y, Li N. The added value of intravoxel incoherent motion diffusion weighted imaging parameters in differentiating high-grade pancreatic neuroendocrine neoplasms from pancreatic ductal adenocarcinoma. *Oncol Lett* 2019; **18**: 5448-5458 [PMID: 31612053 DOI: 10.3892/ol.2019.10863]

82 **Rosenkrantz AB**, Padhani AR, Chenevert TL, Koh DM, De Keyzer F, Taouli B, Le Bihan D. Body diffusion kurtosis imaging: Basic principles, applications, and considerations for clinical practice. *J Magn Reson Imaging* 2015; **42**: 1190-1202 [PMID: 26119267 DOI: 10.1002/jmri.24985]

83 **Shi YJ**, Zhu HT, Liu YL, Wei YY, Qin XB, Zhang XY, Li XT, Sun YS. Radiomics Analysis Based on Diffusion Kurtosis Imaging and T2 Weighted Imaging for Differentiation of Pancreatic Neuroendocrine Tumors From Solid Pseudopapillary Tumors. *Front Oncol* 2020; **10**: 1624 [PMID: 32974201 DOI: 10.3389/fonc.2020.01624]

84 **Kartalis N**, Manikis GC, Loizou L, Albiin N, Zöllner FG, Del Chiaro M, Marias K, Papanikolaou N. Diffusion-weighted MR imaging of pancreatic cancer: A comparison of mono-exponential, bi-exponential and non-Gaussian kurtosis models. *Eur J Radiol Open* 2016; **3**: 79-85 [PMID: 27957518 DOI: 10.1016/j.ejro.2016.04.002]

85 **Pasicz K**, Podgórska J, Jasieniak J, Fabiszewska E, Skrzyński W, Anysz-Grodzicka A, Cieszanowski A, Kukołowicz P, Grabska I. Optimal b-values for diffusion kurtosis imaging of the liver and pancreas in MR examinations. *Phys Med* 2019; **66**: 119-123 [PMID: 31600671 DOI: 10.1016/j.ejmp.2019.09.238]

86 **Steinkohl E**, Bertoli D, Hansen TM, Olesen SS, Drewes AM, Frøkjær JB. Practical and clinical applications of pancreatic magnetic resonance elastography: a systematic review. *Abdom Radiol (NY)* 2021; **46**: 4744-4764 [PMID: 34076721 DOI: 10.1007/s00261-021-03143-3]

87 **Shi Y**, Gao F, Li Y, Tao S, Yu B, Liu Z, Liu Y, Glaser KJ, Ehman RL, Guo Q. Differentiation of benign and malignant solid pancreatic masses using magnetic resonance elastography with spin-echo echo planar imaging and three-dimensional inversion reconstruction: a prospective study. *Eur Radiol* 2018; **28**: 936-945 [PMID: 28986646 DOI: 10.1007/s00330-017-5062-y]

88 **Madhuranthakam AJ**, Yuan Q, Pedrosa I. Quantitative Methods in Abdominal MRI: Perfusion Imaging. *Top Magn Reson Imaging* 2017; **26**: 251-258 [PMID: 29176470 DOI: 10.1097/RMR.0000000000000145]

89 **Tofts PS**, Brix G, Buckley DL, Evelhoch JL, Henderson E, Knopp MV, Larsson HB, Lee TY, Mayr NA, Parker GJ, Port RE, Taylor J, Weisskoff RM. Estimating kinetic parameters from dynamic contrast-enhanced T(1)-weighted MRI of a

diffusable tracer: standardized quantities and symbols. *J Magn Reson Imaging* 1999; **10**: 223-232 [PMID: 10508281 DOI: 10.1002/(sici)1522-2586(199909)10:3<223::aid-jmri2>3.0.co;2-s]

90 **Donati F**, Boraschi P, Cervelli R, Pacciardi F, Lombardo C, Boggi U, Falaschi F, Caramella D. 3 T MR perfusion of solid pancreatic lesions using dynamic contrast-enhanced DISCO sequence: Usefulness of qualitative and quantitative analyses in a pilot study. *Magn Reson Imaging* 2019; **59**: 105-113 [PMID: 30878601 DOI: 10.1016/j.mri.2019.03.001]

91 **Kim JH**, Lee JM, Park JH, Kim SC, Joo I, Han JK, Choi BI. Solid pancreatic lesions: characterization by using timing bolus dynamic contrast-enhanced MR imaging assessment--a preliminary study. *Radiology* 2013; **266**: 185-196 [PMID: 23192779 DOI: 10.1148/radiol.12120111]

92 **Huh J**, Choi Y, Woo DC, Seo N, Kim B, Lee CK, Kim IS, Nickel D, Kim KW. Feasibility of test-bolus DCE-MRI using CAIPIRINHA-VIBE for the evaluation of pancreatic malignancies. *Eur Radiol* 2016; **26**: 3949-3956 [PMID: 26809293 DOI: 10.1007/s00330-016-4209-6]

93 **Basu B**, Basu S. Correlating and Combining Genomic and Proteomic Assessment with In Vivo Molecular Functional Imaging: Will This Be the Future Roadmap for Personalized Cancer Management? *Cancer Biother Radiopharm* 2016; **31**: 75-84 [PMID: 27093341 DOI: 10.1089/cbr.2015.1922]

94 **Binderup T**, Knigge U, Loft A, Federspiel B, Kjaer A. 18F-fluorodeoxyglucose positron emission tomography predicts survival of patients with neuroendocrine tumors. *Clin Cancer Res* 2010; **16**: 978-985 [PMID: 20103666 DOI: 10.1158/1078-0432.CCR-09-1759]

95 **Zhang P**, Yu J, Li J, Shen L, Li N, Zhu H, Zhai S, Zhang Y, Yang Z, Lu M. Clinical and Prognostic Value of PET/CT Imaging with Combination of ^{68}Ga-DOTATATE and ^{18}F-FDG in Gastroenteropancreatic Neuroendocrine Neoplasms. *Contrast Media Mol Imaging* 2018; **2018**: 2340389 [PMID: 29681780 DOI: 10.1155/2018/2340389]

96 **Reubi JC**, Waser B. Concomitant expression of several peptide receptors in neuroendocrine tumours: molecular basis for in vivo multireceptor tumour targeting. *Eur J Nucl Med Mol Imaging* 2003; **30**: 781-793 [PMID: 12707737 DOI: 10.1007/s00259-003-1184-3]

97 **Antwi K**, Fani M, Heye T, Nicolas G, Rottenburger C, Kaul F, Merkle E, Zech CJ, Boll D, Vogt DR, Gloor B, Christ E, Wild D. Comparison of glucagon-like peptide-1 receptor (GLP-1R) PET/CT, SPECT/CT and 3T MRI for the localisation of occult insulinomas: evaluation of diagnostic accuracy in a prospective crossover imaging study. *Eur J Nucl Med Mol Imaging* 2018; **45**: 2318-2327 [PMID: 30054698 DOI: 10.1007/s00259-018-4101-5]

98 **Regazzo D**, Barbot M, Scaroni C, Albiger N, Occhi G. The pathogenic role of the GIP/GIPR axis in human endocrine tumors: emerging clinical mechanisms beyond diabetes. *Rev Endocr Metab Disord* 2020; **21**: 165-183 [PMID: 31933128 DOI: 10.1007/s11154-019-09536-6]

99 **Beiderwellen KJ**, Poeppel TD, Hartung-Knemeyer V, Buchbender C, Kuehl H, Bockisch A, Lauenstein TC. Simultaneous 68Ga-DOTATOC PET/MRI in patients with gastroenteropancreatic neuroendocrine tumors: initial results. *Invest Radiol* 2013; **48**: 273-279 [PMID: 23493121 DOI: 10.1097/RLI.0b013e3182871a7f]

100 **Hope TA**, Pampaloni MH, Nakakura E, VanBrocklin H, Slater J, Jivan S, Aparici CM, Yee J, Bergsland E. Simultaneous (68)Ga-DOTA-TOC PET/MRI with gadoxetate disodium in patients with neuroendocrine tumor. *Abdom Imaging* 2015; **40**: 1432-1440 [PMID: 25820755 DOI: 10.1007/s00261-015-0409-9]

101 **Gillies RJ**, Kinahan PE, Hricak H. Radiomics: Images Are More than Pictures, They Are Data. *Radiology* 2016; **278**: 563-577 [PMID: 26579733 DOI: 10.1148/radiol.2015151169]

102 **Lubner MG**, Smith AD, Sandrasegaran K, Sahani DV, Pickhardt PJ. CT Texture Analysis: Definitions, Applications, Biologic Correlates, and Challenges. *Radiographics* 2017; **37**: 1483-1503 [PMID: 28898189 DOI: 10.1148/rg.2017170056]

103 **Canellas R**, Burk KS, Parakh A, Sahani DV. Prediction of Pancreatic Neuroendocrine Tumor Grade Based on CT Features and Texture Analysis. *AJR Am J Roentgenol* 2018; **210**: 341-346 [PMID: 29140113 DOI: 10.2214/AJR.17.18417]

104 **Choi TW**, Kim JH, Yu MH, Park SJ, Han JK. Pancreatic neuroendocrine tumor: prediction of the tumor grade using CT findings and computerized texture analysis. *Acta Radiol* 2018; **59**: 383-392 [PMID: 28766979 DOI: 10.1177/0284185117725367]

105 **Guo C**, Zhuge X, Wang Z, Wang Q, Sun K, Feng Z, Chen X. Textural analysis on contrast-enhanced CT in pancreatic neuroendocrine neoplasms: association with WHO grade. *Abdom Radiol (NY)* 2019; **44**: 576-585 [PMID: 30182253 DOI: 10.1007/s00261-018-1763-1]

106 **Reinert CP**, Baumgartner K, Hepp T, Bitzer M, Horger M. Complementary role of computed tomography texture analysis for differentiation of pancreatic ductal adenocarcinoma from pancreatic neuroendocrine tumors in the portal-venous enhancement phase. *Abdom Radiol (NY)* 2020; **45**: 750-758 [PMID: 31953587 DOI: 10.1007/s00261-020-02406-9]

107 **Li X**, Zhu H, Qian X, Chen N, Lin X. MRI Texture Analysis for Differentiating Nonfunctional Pancreatic Neuroendocrine Neoplasms From Solid Pseudopapillary Neoplasms of the Pancreas. *Acad Radiol* 2020; **27**: 815-823 [PMID: 31444110 DOI: 10.1016/j.acra.2019.07.012]

108 **Shindo T**, Fukukura Y, Umanodan T, Takumi K, Hakamada H, Nakajo M, Umanodan A, Ideue J, Kamimura K, Yoshiura T. Histogram Analysis of Apparent Diffusion Coefficient in Differentiating Pancreatic Adenocarcinoma and Neuroendocrine Tumor. *Medicine (Baltimore)* 2016; **95**: e2574 [PMID: 26825900 DOI: 10.1097/MD.0000000000002574]

109 **Jordan MI**, Mitchell TM. Machine learning: Trends, perspectives, and prospects. *Science* 2015; **349**: 255-260 [PMID: 26185243 DOI: 10.1126/science.aaa8415]

110 **Briganti G**, Le Moine O. Artificial Intelligence in Medicine: Today and Tomorrow. *Front Med (Lausanne)* 2020; **7**: 27 [PMID: 32118012 DOI: 10.3389/fmed.2020.00027]

111 **Yasaka K**, Akai H, Abe O, Kiryu S. Deep Learning with Convolutional Neural Network for Differentiation of Liver Masses at Dynamic Contrast-enhanced CT: A Preliminary Study. *Radiology* 2018; **286**: 887-896 [PMID: 29059036 DOI: 10.1148/radiol.2017170706]

112 **Luo Y**, Chen X, Chen J, Song C, Shen J, Xiao H, Chen M, Li ZP, Huang B, Feng ST. Preoperative Prediction of Pancreatic Neuroendocrine Neoplasms Grading Based on Enhanced Computed Tomography Imaging: Validation of Deep Learning with a Convolutional Neural Network. *Neuroendocrinology* 2020; **110**: 338-350 [PMID: 31525737 DOI:

10.1159/000503291]

113 **Zhou RQ**, Ji HC, Liu Q, Zhu CY, Liu R. Leveraging machine learning techniques for predicting pancreatic neuroendocrine tumor grades using biochemical and tumor markers. *World J Clin Cases* 2019; **7**: 1611-1622 [PMID: 31367620 DOI: 10.12998/wjcc.v7.i13.1611]

114 **Gao X**, Wang X. Deep learning for World Health Organization grades of pancreatic neuroendocrine tumors on contrast-enhanced magnetic resonance images: a preliminary study. *Int J Comput Assist Radiol Surg* 2019; **14**: 1981-1991 [PMID: 31555998 DOI: 10.1007/s11548-019-02070-5]

World Journal of Gastroenterology

Submit a Manuscript: https://www.f6publishing.com

World J Gastroenterol 2022 July 14; 28(26): 3027-3046

DOI: 10.3748/wjg.v28.i26.3027

ISSN 1007-9327 (print) ISSN 2219-2840 (online)

REVIEW

Tumor microenvironment involvement in colorectal cancer progression *via* Wnt/β-catenin pathway: Providing understanding of the complex mechanisms of chemoresistance

María Belén Novoa Díaz, María Julia Martín, Claudia Gentili

Specialty type: Gastroenterology and hepatology

Provenance and peer review: Invited article; Externally peer reviewed.

Peer-review model: Single blind

Peer-review report's scientific quality classification

Grade A (Excellent): 0
Grade B (Very good): B, B, B, B
Grade C (Good): C
Grade D (Fair): 0
Grade E (Poor): 0

P-Reviewer: Koustas E, Greece; Pan JS, China; Rahimi-Movaghar E, Iran; Scurtu RR, Romania; Ying HQ, China

Received: December 21, 2021
Peer-review started: December 21, 2021
First decision: March 10, 2022
Revised: April 29, 2022
Accepted: June 20, 2022
Article in press: June 20, 2022
Published online: July 14, 2022

María Belén Novoa Díaz, María Julia Martín, Claudia Gentili, Departamento de Biología, Bioquímica y Farmacia, Universidad Nacional del Sur (UNS)-INBIOSUR (CONICET-UNS), Bahía Blanca 8000, Argentina

María Julia Martín, Departamento de Química, Universidad Nacional del Sur (UNS)-INQUISUR (CONICET-UNS), Bahía Blanca 8000, Argentina

Corresponding author: María Julia Martín, PhD, Research Assistant, Departamento de Biología, Bioquímica y Farmacia, Universidad Nacional del Sur (UNS)-INBIOSUR (CONICET-UNS), San Juan 670, Bahía Blanca 8000, Argentina. julia.martin@uns.edu.ar

Abstract

Colorectal cancer (CRC) continues to be one of the main causes of death from cancer because patients progress unfavorably due to resistance to current therapies. Dysregulation of the Wnt/β-catenin pathway plays a fundamental role in the genesis and progression of several types of cancer, including CRC. In many subtypes of CRC, hyperactivation of the β-catenin pathway is associated with mutations of the *adenomatous polyposis coli* gene. However, it can also be associated with other causes. In recent years, studies of the tumor microenvironment (TME) have demonstrated its importance in the development and progression of CRC. In this tumor nest, several cell types, structures, and biomolecules interact with neoplastic cells to pave the way for the spread of the disease. Cross-communications between tumor cells and the TME are then established primarily through paracrine factors, which trigger the activation of numerous signaling pathways. Crucial advances in the field of oncology have been made in the last decade. This Minireview aims to actualize what is known about the central role of the Wnt/β-catenin pathway in CRC chemoresistance and aggressiveness, focusing on cross-communication between CRC cells and the TME. Through this analysis, our main objective was to increase the understanding of this complex disease considering a more global context. Since many treatments for advanced CRC fail due to mechanisms involving chemoresistance, the data here exposed and analyzed are of great interest for the development of novel and effective therapies.

Key Words: Colorectal cancer; β-catenin pathway; Tumor stroma; Tumor microenvironment factors; Cancer progression; Drug resistance

Core Tip: Currently, there is a high probability of failure in treatments for the advanced stages of colorectal cancer (CRC). For this reason, it is necessary to obtain a better understanding of CRC biology in a more global context for the future design of novel therapeutic approaches. The effects of the Wnt/β-catenin signaling pathway and the tumor microenvironment (TME) on the progression and chemoresistance of this disease were separately described in several review articles. Therefore, herein we comprehensively analyze the complex mechanisms of CRC chemoresistance triggered by TME factors that impact Wnt/β-catenin signaling.

Citation: Novoa Díaz MB, Martín MJ, Gentili C. Tumor microenvironment involvement in colorectal cancer progression *via* Wnt/β-catenin pathway: Providing understanding of the complex mechanisms of chemoresistance. *World J Gastroenterol* 2022; 28(26): 3027-3046
URL: https://www.wjgnet.com/1007-9327/full/v28/i26/3027.htm
DOI: https://dx.doi.org/10.3748/wjg.v28.i26.3027

INTRODUCTION

Colorectal cancer (CRC) is the third most frequent malignant disease worldwide in both men and women[1,2]. Data provided by the World Cancer Research Fund International indicate that CRC incidence is growing, and the prevalence of this pathology is expected to increase by 60% in the next 15 years[3]. Among all cancer-induced deaths, the ones associated with CRC reach values of 8%-9%[4,5]. These statistics rely mainly on the fact that 20% of patients show metastasis (stage IV) at the time of diagnosis and the overall survival in these patients is low due to failure in the treatments[5,6]. To improve the response of these patients to therapy, it is necessary to expand the knowledge about the mechanisms that play a critical role in the development, progression and chemoresistance of CRC.

In 2015, Guinney *et al*[7] proposed a classification of colorectal tumors based on four consensus molecular subtypes (CMSs). Groups were defined according to certain parameters such as clinical, genetic and molecular characteristics (Figure 1): The CMS1 group, also designated microsatellite instability immune, is characterized by high microsatellite instability and immune response. The canonical subtype (CMS2) represents 37% of cases and presents hyperactivation of the Wnt and Myc signaling pathways. The CMS3 (metabolic subtype) is characterized by a marked dysregulation of metabolic pathways. Finally, the CMS4 (mesenchymal subtype) group exhibits hyperactivation of the transforming growth factor-β (TGF-β) pathway and a marked switch from the epithelial to mesenchymal transition (EMT)[7,8]. Remarkably, 90% of CRC cases present with aberrant activation of the canonical Wnt/β-catenin signaling pathway[9-11]. This pathway is strictly regulated in physiological conditions and modulates fetal development and homeostasis in adult tissues[11]. Briefly, in the absence of Wnt ligand, β-catenin is continuously phosphorylated in the cytoplasm by a destruction complex comprised of adenomatous polyposis coli (APC), axis inhibition protein (Axin), glycogen synthase kinase 3 (GSK3), and casein kinase 1. Once phosphorylated, β-catenin is ubiquitinated and degraded by the proteasome. When Wnt ligand binds to its receptor, the destruction of β-catenin stops, so this protein accumulates in the cytosol and then translocates to the nucleus. Finally, β-catenin binds to transcription factors from the T-cell factor/lymphoid enhancer factor (TCF/LEF) family and promotes the transcription of several genes[12]. There are several published research as well as review articles on the involvement of the Wnt/β-catenin pathway in CRC development, progression, and chemoresistance[10,13,14]. Furthermore, this pathway became an unquestionable target for novel therapies for CRC. Despite this, to date, there are no approved treatments or clinical trials for CRC based on targeting the Wnt/β-catenin pathway[15].

As extensively described in the open literature, hyperactivation of the Wnt/β-catenin pathway in CRC is directly associated with intrinsic causes such as mutations in the *APC* gene. This results in the nuclear accumulation of β-catenin and the induction of Wnt target genes that promote tumor progression[16]. In this contribution, we intend to analyze how Wnt/β-catenin aberrant activation can be induced or exacerbated by external causes.

In the last decade, the tumor microenvironment (TME) or tumor stroma has become relevant in the progression of CRC[17]. The TME is a niche composed of the extracellular matrix (ECM), a great variety of modified stromal cells and aberrant vasculature[9]. Intercellular communications between the tumor cells and the TME are mainly established through paracrine signaling[9,18]. These communications and factors are extrinsic and may directly affect CRC progression through the Wnt/β-catenin pathway. In this way, a wide range of novel therapeutic targets appears, expanding the possibilities of achieving effective treatments for CRC.

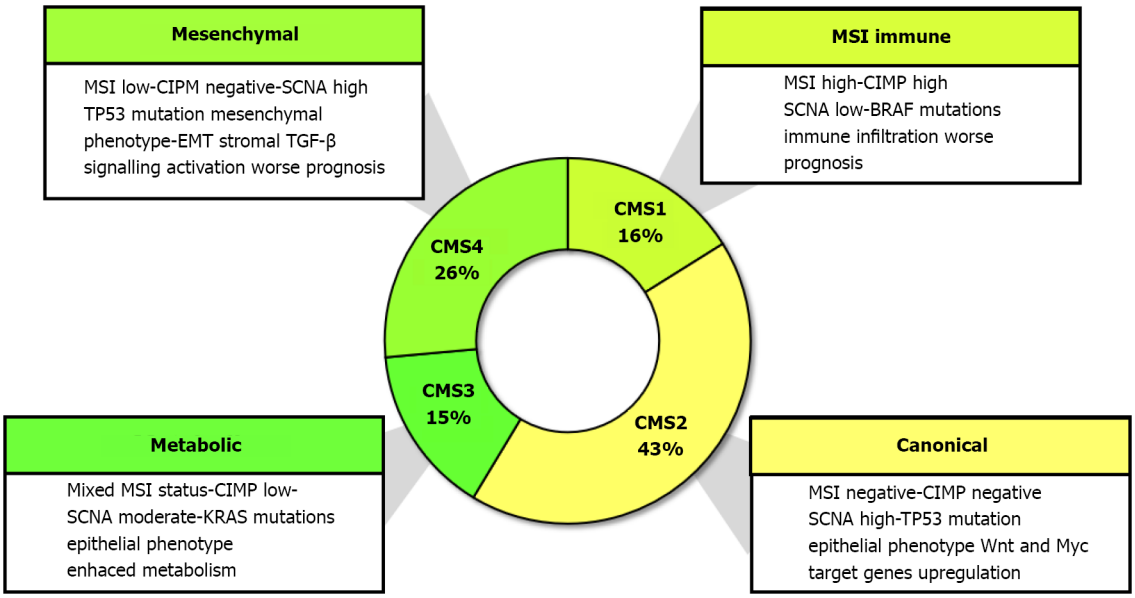

DOI: 10.3748/wjg.v28.i26.3027

Figure 1 Consensus molecular subtypes classification for colorectal tumors. BRAF: B-Raf proto-oncogene; CIMP: CpG island methylator phenotype; CNAs: Copy number alterations; EMT: Epithelial to mesenchymal transition; KRAS: Kirsten rat sarcoma 2 viral oncogene homolog; MSI: Microsatellite instability; TGF-β: Transforming growth factor-β; TP53: Tumor protein 53.

This work analyzed the available literature regarding the biomolecules associated with the TME that can modulate the Wnt/β-catenin signaling pathway in CRC cells, which allows a better understanding of the biological causes of the high morbidity and mortality of this pathology in a global context. Although antecedents of this particular analysis are registered in 2008[19], the enormous amount of information collected in recent years results in the emergence of new biomolecules, structures, and even processes related to the TME and the CRC cells that were previously unknown or unrelated. The comprehension of this information enables countless new possibilities for the development of new therapies for CRC.

DYNAMICS ESTABLISHED BETWEEN THE TME AND CRC CELLS

During CRC genesis, the TME and its associated signaling play a key role in tumor fate, since they facilitate the proliferation, invasion, metastasis, and chemoresistance processes. Specifically, the TME is composed of ECM proteins, mesenchymal stem cells, fibroblasts, cancer-associated fibroblasts (CAFs), endothelial cells (ECs), and tumor-infiltrating immune cells, with the last group comprising tumor-associated macrophages (TAMs), tumor-associated neutrophils, natural killer (NK) cells, regulatory T cells, myeloid-derived suppressor cells, and cytotoxic T lymphocytes (also known as CD8+ T cells), among others[5,20].

The TME cells and neoplastic cells continuously secrete and internalize factors that modulate the CRC development and contribute to the maintenance of the tumor ecosystem. These extracellular signals are schematized in Figure 2 and involve soluble proteins, insoluble proteins from the ECM, or compounds of variable nature loaded in vesicles[21]. Table 1 compiles the biomolecules well described in the literature that can be secreted by the TME cells and that allow communication with CRC cells. Some of these factors can travel freely through the tumor stroma space, whereas others are transported through membrane-bound vesicles known as extracellular vesicles (EVs)[22,23]. The EVs structure includes a lipid bilayer composed mainly of ceramide, cholesterol, sphingomyelin, phosphoglycerides, glycosphingolipids, phosphatidyl serine, phosphatidylethanolamine, mannose, N-linked glycans, polylactosamine, and sialic acid[22]. In recent years, EVs have acquired relevance as biological mediators in the communication between the TME and tumor cells. Concerning EVs related to CRC, their loads are considered prognostic factors or indicative of response to therapies. Recent studies have shown that EVs can carry large amounts of biomolecules from the TME cells to cancer cells and vice versa. Usual cargoes include cytokines/chemokines, angiogenic factors, ECM remodeling factors, and nucleic acids such as microRNAs (miRs), long non-coding RNAs (lncRNAs), and circular RNAs (cRNAs)[24-27]. Fluids from CRC patients such as plasma, saliva, and urine contain large amounts of secreted EVs. These molecules can stimulate or inhibit the expression of oncogenes and oncoproteins, thus affecting the phenotype of the neoplastic cells or altering the secretory profile of the TME cells[22,25,28]. Unlike cytokines and growth factors that act in the nearby cells, the EVs can influence both the primary colorectal tumor and

Table 1 Factors secreted by the tumor microenvironment and their role in colorectal cancer progression

Released/secreted components	Source, TME cell	Known effects in CRC	Ref.
Growth factors			
TGF-β	CAFs; TIICs[1]; MSCs[1]	Proliferation on tumor and stromal cells in late stages of tumorigenesis. EMT program and CSC-like traits. Metastasis, vasculogenesis and angiogenesis	[5,21,136]
BMPs	CAFs	Anti-tumor activity. Or pro-tumor activity, induce CSCs phenotype, EMT program and chemoresistance. Differentiation of colon CSCs	[5,137,138]
HGF	CAFs; TIICs; MSCs[1]	Invasion, metastasis and stemness	[21,54,139,140]
VEGF	ECs; CAFs; TIICs	Angiogenesis, invasiveness, metastasis	[104,140,141]
FGF	CAFs; MSCs	CAFs profiles. Tumor growth and metastasis	[142,143]
PDGF	CAFs	Tumor growth and metastasis	[144]
TNF-α	TIICs	Proliferation. Growth arrest and cancer cell death, angiogenesis and metastasis	[141,145]
Cytokines			
IL-1	TIICs	Angiogenesis and metastasis	[141,146]
IL-2	TIICs	Anti-tumor activity	[1,147]
IL-6	TIICs; MSCs; CAFs	Proliferation, angiogenesis and metastasis	[1,141]
IL-8	TIICs; MSCs	Tumor growth, angiogenesis and chemoresistance	[1,148]
IL-17	CAFs; TIICs	Anti-tumor or pro-tumor activity. Invasion and self-renewal of CSCs	[1,104,149]
IL-18	TIICs	Anti-tumor activity	[150]
IL-22	TIICs	Proliferation, invasion and stemness	[1,104]
IL-33	ECs; TIICs	Anti-tumor activity Suppresses tumorigenesis. Or pro-tumor activity. Angiogenesis and metastasis. Tumor growth through immunosuppressive microenvironment favoring	[1,104,151]
CCL2	TIICs; MCS	Tumor progression	[152]
CCL5	TIICs	Tumor progression. Acts on tumor cells and TAMs	[153]
CCL7	CAFs	Proliferation, invasion, and migration	[154]
CXCL12	CAFs; MSCs	Proliferation and invasion	[142,155]
PTHrP	Undefined TME cells	Proliferation, invasion, angiogenesis, migration and chemoresistance	[34,35,66,156,157]
Osteopontin	TIICs	Metastasis, stemness and chemoresistance	[85]
Prostaglandins			
PGs (like PGE2)	CAFs; TIICs; MSCs	Resistance to apoptosis, increased proliferation, angiogenesis and metastasis	[21,32]
Signaling pathways ligands			
NOTCH ligands (Jagged-1; Jagged-2; DLL4)	ECs	CSCs phenotype, EMT program and metastasis	[104,158]
WNT ligands (Wnt2, Wnt5)	CAFs	Invasion, metastasis and angiogenesis	[44,45,54]
Enzymes			
Serine proteinases (like MMPs)	TAMs; TANs	Invasion and angiogenesis	[140,145]
Immunosuppressive enzymes (like iNOS)	TIICs	Tumor progression. Inhibitory effect on the immune system, apoptosis of immune cells	[39]
Receptors			
TLRs	CAFs, ECs	Inflammatory-mediated tumorigenesis	[41,43]
RNA molecules			

miR-92a-3p	CAFs	CSCs phenotype, EMT program and chemoresistance	[24]
lncRNA H19	CAFs	Stemness and chemoresistance	[25]
miR-155	MSCs[1]	Migration	[21,159]
miR-375	MSCs[1]	Chemoresistance	[21,160]
cRNA	CAFs	Tumor progression or anti-tumor activity	[26,27]

[1]Factor's actions demonstrated for colorectal cancer (CRC). Their source from the tumor microenvironment (TME) has been identified for other types of cancer, but not for CRC. BMP: Bone morphogenetic CAFs: Cancer-associated fibroblasts; CCL: C-C motif chemokine ligand; cRNA: Circular RNA; CSCs: Cancer stem cells; CXCL: C-X-C motif chemokine ligand; ECs: Endothelial cells; EMT: Epithelial to mesenchymal transition; FGF: Fibroblast growth factor; HGF: Hepatocyte growth factor; IL: Interleukin; iNOS: Inducible nitric oxide synthase; lncRNA: Long non-coding RNA; miR: MicroRNA; MMPs: Matrix metalloproteinases; MSCs: Mesenchymal stem cells; PDGF: Platelet-derived growth factor; PGs: Prostaglandins; PTHrP: Parathyroid Hormone-related Peptide; TAMs: Tumor-associated macrophages; TANs: Tumor-associated neutrophils; TGF-β: Transforming growth factor-β; TIICs: Tumor-infiltrating immune cells; TLRs: Toll-like receptors; TNF-α: Tumor necrosis factor-α; VEGF: Vascular endothelial growth factor.

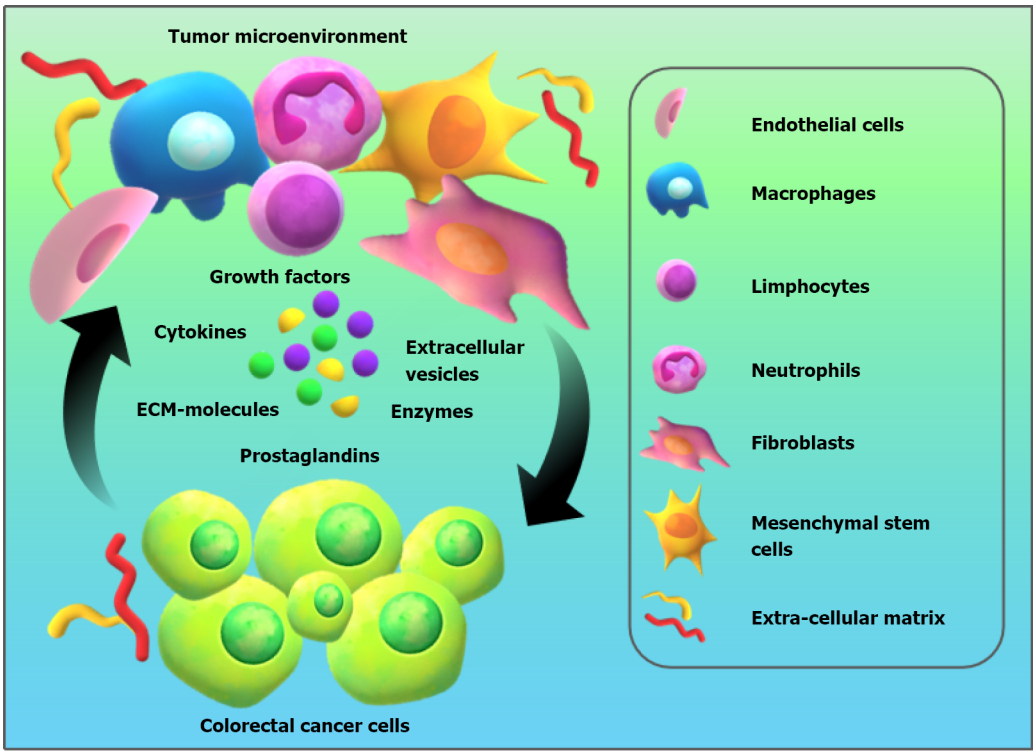

DOI: 10.3748/wjg.v28.i26.3027

Figure 2 Extracellular signal molecules secreted by the tumor microenvironment and neoplastic cells. The traffic of soluble and insoluble factors allows crosstalk between tumor cells and their environment modulating colorectal cancer development and progression.

metastatic niche remotely[22,29]. For instance, analysis of the plasma from CRC patients revealed that EVs are directly linked to the establishment of liver proinflammatory phenotype and liver metastasis, with this effect mediated by the modulation of macrophages by EVs[30]. The correlation between CD8+ T cell activation and high EVs concentrations in plasma has also been demonstrated, thus showing the role of EVs in the modulation of the immune response in CRC[31]. In conclusion, EVs have become a new source of therapeutic targets for CRC[22].

On the other hand, the soluble molecules that are directly secreted to the biological fluids exert their actions locally and participate in the communication between the tumor and the microenvironment. These factors are prostaglandins, cytokines, and other paracrine factors, which have distinctive modes of action. Prostaglandins and cytokines act especially as immunomodulators, by promoting or inhibiting the progression of CRC[1,32,33]. Growth factors such as TGF-β, vascular endothelial growth factor (VEGF), and EGF promote the transformation and development of neoplastic cells by inducing proliferation, invasion, and migration responses and also by affecting the TME[21]. In previous works *in vitro* using two CRC cell lines with different grades of aggressiveness, we demonstrated that parathyroid hormone-related peptide (PTHrP) acts as a paracrine factor by inducing the survival, proliferation, migration, cell cycle progression, angiogenesis, and EMT program. Moreover, our *in vivo* studies in CRC

tumor xenografts revealed that the intratumor administration of PTHrP modulates the expression of several tumorigenic markers, which are involved in the same cell responses observed *in vitro*[5,34-37].

Other proteins with different functions were studied in relation to CRC and the TME. In recent years, it has been reported that both neoplastic cells and TME cells can synthesize and secrete enzymes that participate in tumorigenesis. Muñoz-Galván *et al*[38] demonstrated that phospholipase D2 (PLD2) enzyme is overexpressed and secreted by CRC cells. PLD2 in the extracellular space modulates the phenotype and secretory profile of CAFs, thus contributing to promote stemness in tumor cells[38]. Other enzymes such as nitric oxide synthase are capable of inducing immunomodulatory effects[39]. Moreover, enzymes present in the TME, such as metalloproteases, enable the invasion and migration of cancer cells[39]. These enzymes act mainly by altering the structure and function of the ECM, thus allowing the activation of other factors that amplify the pro-tumor signals[40]. Receptor proteins such as Toll-like receptors (TLRs) play a fundamental role in maintaining epithelial barrier homeostasis in the gut and mediating inflammatory and immune responses[41]. TLRs are also expressed in fibroblasts and ECs in the TME and in CRC cells. The dysregulation in TLR pathways is associated with inflammation-driven carcinogenesis[42]. In response to this evidence, currently, there are clinical trials that include TLRs agonists for the treatment of CRC (www.clinicaltrials.gov)[41,43].

The abovementioned factors generally exert their effects by modulating several signaling pathways in the tumor[1,44-46]. In accordance with the focus of this contribution, in the next sections, we further discuss which of these biomolecules participate in aberrant activation of the β-catenin signaling pathway in CRC, and how these findings have provided new opportunities for the development of more efficient therapies.

TME FACTORS AND CONDITIONS THAT MODULATE THE WNT/β-CATENIN PATHWAY IN CRC

It is clear that the signaling triggered by factors that mediate the communication between TME and CRC cells is of great importance. Since Wnt/β-catenin is involved in most of the processes related to CRC genesis and progression[8,47], in this section we focus on the factors from the TME able to modulate this pathway. Figure 3 schematizes the complex interrelationships between the TME and CRC cells that lead to the activation of β-catenin and the consequent effects on disease progression.

Other β-catenin regulation, independently of the destruction complex actions described in the introduction section, involves phosphorylation by other kinases in different amino acids, such as Ser-552 and Ser-675, resulting in the stabilization and nuclear accumulation of this protein[48]. Mutations in the gene that encodes the β-catenin protein (*CTNNB1* gene) will produce structural alterations and its consequent hyperactivation and nuclear accumulation, events directly associated with CRC genesis and progression[7,49]. Voorneveld and collaborators[50] demonstrated that nuclear β-catenin is found predominantly in cells at the invasive front of CRC tumors. Other investigations have proven that the signals that exacerbate aberrant β-catenin function independently of others than those produced by the tumor can come from the TME[44,51].

Activation of the Wnt pathway by TME factors was initially studied a decade ago. Vermeulen and colleagues showed that CAF-derived hepatocyte growth factor (HGF) activates Wnt/β-catenin signaling and subsequently the clonogenicity in cancer stem cells (CSCs) isolated from CRC patients that were transiently transfected with TCF/LEF luciferase reporter vector. Moreover, HGF restored the CSC phenotype in more differentiated tumor cells both *in vitro* and *in vivo*[52]. Essex and collaborators recently replicated these studies, emphasizing the relevance of this pathway and the interaction of tumor cells with their stroma, and in the promotion and development of CRC[53]. As stated in Table 1, various Wnt ligands are secreted mostly by CAFs[44,45,54,55]. A recent study confirmed that Wnt2 acts in an autocrine manner, generating morphogenetic changes in fibroblasts and contributing to the invasive and metastatic capacity of CRC-derived cells[44]. *In vitro* experiments revealed that the treatment of DLD1 and HCT116 cells (both derived from CRC) with conditioned medium obtained from CAFs transfected with small interfering RNA targeting Wnt2, significantly decreased cell invasion and migration[45]. It is of clinical relevance that these ligands are overexpressed in the tumor stroma of CRC patients[45,53]. Moreover, the aberrant expression of Wnt ligand is correlated with a worse prognosis [44]. EVs play a key role in activating Wnt signaling in CRC. On the one hand, EVs can transport mutant β-catenin and activate the Wnt signaling pathway in the recipient cells, thus promoting CRC progression[56]. Regarding the effects of EVs on TME cells, Hu and colleagues demonstrated *in vitro* that fibroblast-derived exosomes (one type of EVs) promote the tumor growth of CSCs upon treatment with 5-fluorouracil (5-FU) or oxaliplatin (OXA)[57]. Further investigations of the same group in subcutaneous xenografts achieved through HT-29 CRC-derived cells and fibroblast co-implantation demonstrated that stromal fibroblasts can secrete exosomes loaded with Wnt ligands. Once these exosomes interact with differentiated CRC cells, Wnt ligands induce the phenotypic reversion of CRC cells to CSCs, which includes features such as the expression of CSCs markers and elevated Wnt activity [57].

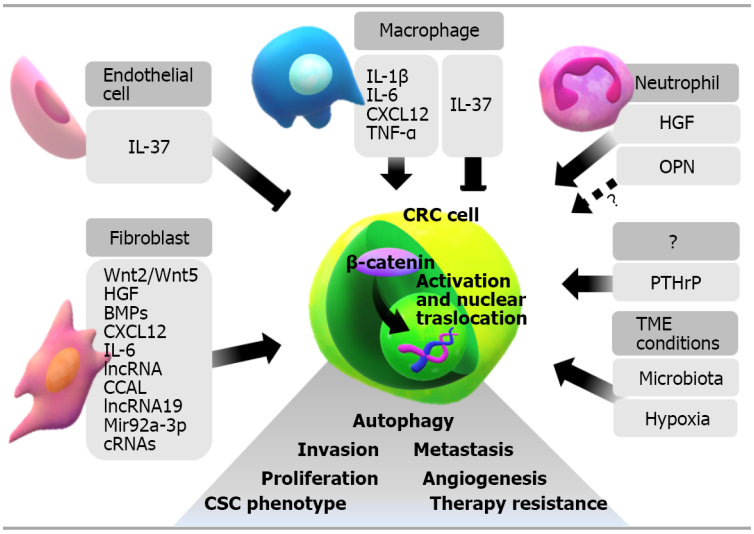

DOI: 10.3748/wjg.v28.i26.3027

Figure 3 Influence of tumor microenvironment-derived factors in the activation of β-catenin pathways. Several cytokines, growth factors, and small nuclei acid molecules secreted by stromal cells induce aberrantly activation of β-catenin and its nuclear translocation in colorectal cancer (CRC) cells promoting events associated with an aggressive phenotype of the tumor cells. Il-37 represses the expression of β-catenin and its transcriptional activity. Osteopontin is statistically associated with the expression of β-catenin in CRC and is known to induce its activation in other types of cancer. More studies are necessary to confirm positive feedback between the secretion of this tumor microenvironment (TME) factor and β-catenin signaling pathways in CRC. In addition to these factors, the microbiota and the hypoxia in the TME, also participate in the modulation of β-catenin activation. This figure is original for this work. BMP: Bone morphogenic protein; CCAL: Colorectal cancer-associated lncRNA; cRNA: Circular RNA; CXCL: C-X-C motif chemokine ligand; HGF: Hepatocyte growth factor; IL: Interleukin; lncRNA: Long non-coding RNA; OPN: Osteopontin; PTHrP: Parathyroid Hormone-related Peptide; TNF-α: Tumor necrosis factor-α; Wnt: Wingless protein.

Hypoxia is a prevalent condition in the solid tumor TME, which involves oxygen pressures of less than 5-10 mmHg. The hypoxic TME can deeply influence CRC, and these effects may be mediated by β-catenin. For instance, it was found *in vitro* that Wnt/β-catenin signaling is responsible for the hypoxia-induced self-renewal of colorectal stem cells[58]. Furthermore, Huang and collaborators observed that hypoxic CRC cells can secrete exosomes enriched with Wnt4 Ligands. These exosomes can activate β-catenin signaling in normoxic CRC cells and stimulate prometastatic behaviors such as cell migration and invasion[59]. In another work, the authors demonstrated that Wnt4-loaded exosomes secreted by the tumor cells promoted angiogenesis through the proliferation and migration of ECs. These effects were induced in conditions of hypoxia and mediated by the activation of Wnt/β-catenin signaling[60].

Autophagy is a physiological process through which normal cells degrade intracellular components to maintain cellular homeostasis. It is postulated as an alternative to cell death when the apoptotic machinery fails and is associated with both CRC and the TME, with controversial findings[61-63]. TME hypoxia induces autophagy and also activates several tumor escape mechanisms[62]. Some of the molecular mechanisms involved in the modulation of autophagy are phosphoinositide 3-kinases (PI3K)/protein kinase B (also known as Akt)/mammalian target of rapamycin, TGF-β, Notch, and Wnt/β-catenin signaling[63]. According to evidence, autophagy induced in the early stages of tumor development prevents the infiltration of immune cells as well as tumor cell death. Autophagy can also promote tumor progression in the advanced stages of the disease[63]. On the other hand, it has been reported that the relationship between autophagy and increased lymphocytic infiltration in the TME is mediated by the autophagy-related protein Vps34 in CRC. The modulation of this autophagy-related protein would improve the efficacy of immunotherapies[64]. However, it is still necessary to conduct additional studies on the interrelationship between the Wnt/β-catenin signaling pathway and autophagy, and which TME factors can mediate these events in CRC.

Because about 90% of patients with CRC present with mutations in genes associated with the Wnt pathway[65], more efforts have been made to identify other molecules with the ability to regulate β-catenin. In line with this evidence, our research group also reported interesting results regarding the participation of PTHrP in the activation of signaling pathways associated with β-catenin. Our published data showed that the exposition of cells derived from colorectal adenocarcinoma, to exogenous PTHrP increases β-catenin expression and upregulates cyclin D1 and c-Myc oncogenes with the concomitant cell proliferation induction[66]. Regarding the role of this cytokine in the TME, we demonstrated *in vitro* that tumor conditioned media from PTHrP-exposed CRC cells promotes pro-angiogenic characteristics in the stromal EC line HMEC-1 through VEGF modulation[35]. In addition, we recently found that PTHrP modulates the protein expression and secretion from the HMEC-1 cells of secreted protein acidic and cysteine-rich, a TME factor involved in the EMT program. This event promotes molecular and morphological changes associated with EMT in cells derived from CRC[36]. In this context, we believe that cross-communication may be initially established through overexpression and secretion of PTHrP

by the tumor, which in turn affects the behavior of neoplastic cells and TME cells inducing the subsequent release from them of this cytokine and other factors. More studies are needed to elucidate which stromal cells can secrete PTHrP and participate in the modulation of the β-catenin pathway. Several authors have also described the relationship between PTHrP and activation of the β-catenin signaling pathway in other types of cancer. In prostate cancer-derived cells, PTHrP downregulates the Wnt inhibitor, DKK1, promoting aberrant activation of this pathway[67]. Other research has shown that PTHrP modulates activation of the canonical Wnt/β-catenin signaling in the mammary mesenchyme [68]. Moreover, Johnson and collaborators reported that Wnt activation promotes PTHrP expression in breast and lung tumor cells[69].

Tumor small and long non-coding RNAs are other factors transported by EVs, which are also involved in the modulation of β-catenin signaling. Colorectal cancer-associated lncRNA (CCAL) and H19 (lncRNA19) expressed by CAFs are capable of stimulating aberrant activation of β-catenin in tumor cells[9,25]. Besides, the overexpression of miR-103 and miR-107 has been detected in the plasma and tumor tissue of patients with CRC[70]. In HCT116 and HT29 cell lines, miR-103/107 overexpression enhanced β-catenin activity and its nuclear translocation. These molecules act by inhibiting Axin2, a negative regulator of the Wnt/β-catenin pathway, and in this way, β-catenin is stabilized and its activation is prolonged[70]. Another study showed that miR-92a-3p secreted by CAFs, induces β-catenin nuclear translocation and the expression of target genes related to stemness, the EMT program, and chemoresistance in the human CRC cell lines SW480, SW620, and LOVO. Moreover, the high expression of exosomal miR-92a-3p in serum predicts metastasis and chemotherapy resistance in CRC patients[24]. The overexpression of miR-100, miR-125b, miR-27a, miR-135, and MIR100HG in CRC tumors modulates the canonical Wnt pathway, promoting events such as proliferation and invasion[71,72].

In the last decade, research on small non-coding RNA molecules has focused on cRNAs. Increasing studies have shown that these molecules intervene in the development and progression of various types of tumors including CRC[73]. Results obtained by Zhang *et al*[73] show that circAGFG1 activates the Wnt/β-catenin pathway in SW480 and HCT116 cells promoting the transcription of the CTNNB1 gene. Two years earlier, Fang and his group revealed that circ_100290 promotes CRC progression through activation of the Wnt/β-catenin pathway[74]. Other cRNAs involved in the activation of this signaling pathway in CRC are Hsa_circ_0005075[75], circMTO1[76] and Circ-PRKDC[72]. On the other hand, cRNAs such as circPRKDC and cirITCH act by inhibiting the activity of the β-catenin pathway[77,78]. The action of most of these molecules is mediated by miRNAs[26,79].

HGF and its receptor RTK Met are associated with β-catenin-related pathways in CRC cells, promoting a CSC phenotype, metastasis, and drug resistance[46,51,80,81]. Other factors including tumor necrosis factor-α (TNF-α) also stimulate the main regulatory mechanism of β-catenin activation in CRC cells. Wei and colleagues demonstrated that under TNF-α action, the CSCs derived from the HT29 cell line increase the survival rate and their invasive capacity *via* the Wnt pathway. These actions are mediated by the modulation of β-catenin related proteins expression, such as c-Myc, cyclin D1, E-cadherin, and vimentin, which are cell cycle regulators associated with the stimulation of cell proliferation and/or the progress of the EMT program[82]. Molecules released from tumor cells including PLD2, modify the secretome of CAFs by promoting the release of the following factors: Macrophage migration inhibitory factor (MIF), HGF, and CCL2. The results shown in this article confirm that the treatment of CRC-derived cells (HCT116 and LS180) with these three factors induces the activation of the Wnt/β-catenin signaling pathway. The authors of this work observed a reduction of β-catenin phosphorylation together with an increase in its total expression after treatment with CCL2, HGF, and MIF, as well as a decrease and an increase in the expression of Axin1 and c-Myc, respectively, consistent with Wnt activation. This research also demonstrated that gene transcription induced by the Wnt signaling pathway correlates with high expression of PLD2 and CAFs-derived factors in CRC patients [38].

Osteopontin (OPN) is another factor that plays an important role in the regulatory mechanism of β-catenin. It is a glycoprotein synthesized by a great variety of cells and is overexpressed in CRC. This protein is capable of activating β-catenin *via* Akt and subsequently GSK3β, or by recruiting and activating mitogen-activated protein kinase (MAPK)[83,84]. Youssef and Osman analyzed tumor samples and found an association between the expression of nuclear OPN/β-catenin and markers related to poor prognosis in CRC[85]. In the last decade, an association has also been established between OPN expression and the activation and nuclear translocation of β-catenin in other types of cancer[83,84]. Recent research has shown that this protein is a target gene of the Wnt pathway[86] and in these cases, positive feedback from the system can be generated. Based on the evidence analyzed in the previous lines, positive feedback is highly probable between OPN secretion and the modulation of the Wnt/β-catenin pathway in CRC.

Other cytokines and growth factors released by the TME cells promote activation of the canonical Wnt pathway in cells derived from human CRC[87]. Bone morphogenetic proteins (BMPs) are cytokines closely linked to angiogenesis, EMT program, and induction of CSCs[88]. Voorneveld and colleagues transfected HCT116, HT29, LS174T, RKO, and SW480 cells with the BMPR2 plasmid, increasing BMP signaling. Hyperactivation of this pathway only downregulated Wnt signaling in HCT116 and LS174T cells, both were SMAD4-positive and had wild type p53. In the remaining cell lines, the Wnt pathway was activated by BMP signaling. This work demonstrated that modulation of Wnt/β-catenin signaling

by the BMP pathway is dependent on SMAD4 and p53 status[5,50]. Regarding the role of interleukins (ILs), neoplastic cells promote the release of IL-1β, mainly from TME macrophages. In HCT116 cells, this cytokine induces β-catenin activation and consequently the expression of target genes, through nuclear factor kappa B (NF-KB)/Akt signaling pathway[87,89]. IL-6 secreted by TME cells induces activation of the Wnt/β-catenin pathway through the signal transducer and activator of transcription 3/extracellular signal-related kinase (ERK) pathway favoring the promotion of the aggressive phenotype of SW48 cells [90]. Chemokines such as C-X-C Motif Chemokine Ligand 12 (CXCL12) are overexpressed in CRC. Song *et al*[91] showed that the increased expression of this cytokine and its receptor (CXCR4) in tumor cells induces activation of the canonical Wnt pathway, possibly mediating the processes of proliferation, survival, and invasion[91]. However, not all cytokines act by promoting aberrant activation of the Wnt pathway. IL-37 mainly expressed by TAMs[92] has been observed to inhibit the proliferation, migration, and CSC phenotype by directly repressing the expression of β-catenin and consequently its translocation to the nucleus[49].

Bacteria, fungi, and viruses constitute the microbiota residing within the gastrointestinal tract. However, the gut microbiota and their metabolites can be altered in the TME and directly influence CRC progression[93,94]. Various bacteria have been implicated in these processes by modulating the β-catenin pathway. *Fusobacterium nucleatum* is a CRC inductor and suppressor of NK cell activity[93,95] Recently, it was reported that *F. nucleatum* can stimulate annexin A1 protein, specifically expressed in CRC cells. Then annexin A1 can induce β-catenin nuclear accumulation and finally the exacerbation of CRC cell proliferation[96]. On the opposite side, as extensively analyzed by Li *et al*[93] in their review article, other bacteria could be beneficial for CRC treatment or its prevention. For example, *Lactobacillus* and *Clostridium butyricum* are probiotics that have inhibitory effects on CRC progression *via* modulation of the β-catenin pathway[93]. This background shows that the complex interrelations between tumor cells and their microenvironment (including the microbiota) involve the participation of one of the most outstanding signaling pathways in the promotion and development of CRC, the β-catenin pathway. Therefore, it is important to consider these phenomena in the development of new treatments that focus on inhibiting or silencing the activators/exacerbators of this pathway.

ROLE OF β-CATENIN AND THE TME IN THE CHEMORESISTANCE OF CRC

Among the most used chemotherapeutic drugs, approved as first- and second-line adjuvants in CRC, are 5-FU, irinotecan (CPT-11), OXA, capecitabine, and leucovorin[97,98]. Depending on the CRC subtype, these drugs are also used in combination with monoclonal antibodies, such as bevacizumab or cetuximab[5]. On certain occasions, signs of a poor prognosis appear. Therefore, neoadjuvant or adjuvant chemotherapy must be implemented[99]. Despite this, patients with advanced grades of metastatic disease continue to lag far behind in successful treatment. One of the main causes of failure in treatment is the chemoresistance observed in about half of patients with CRC[99,100]. In this regard, the cell responses that mediate drug resistance are associated with hypoxic conditions, autophagy, induction of the CSC phenotype, and the EMT program[101,102]. At the molecular level, the development of drug-resistant tumors involves alterations of Wnt/β-catenin among other important signaling pathways such as Hedgehog and Notch. It also includes disturbances in the expression of anti-apoptotic proteins, the overexpression of drug transporters of the ATP-binding cassette (ABC) family, increased aldehyde dehydrogenase 1 enzyme activity and also the release of factors from the TME[99,103]. Regarding the Wnt pathway, its aberrant activation involves induction of the CSC phenotype, the EMT program, the expression of proteins from the ABC family and factors from the TME, all of these events being related to drug resistance[99]. Furthermore, various biological mediators released by stromal cells are capable of inducing chemoresistance through the Wnt/β-catenin pathway in tumor cells[9,25,104]. In this regard, *in vitro* studies made by Hu and colleagues revealed that miR-92a-3p secreted from CAFs activates the Wnt/β-catenin signaling, decreasing the sensitivity to the combination of 5-FU/OXA in SW480, SW620, and Lovo CRC-derived cells[24]. Moreover, *in vivo* studies have demonstrated that exosomes secreted by fibroblasts can load Wnt ligands, thus promoting CSC features and resistance to 5-FU or OXA. On the contrary, the inhibition of Wnt release reverted the observed effects[57]. CAFs are capable of inducing drug resistance by transferring small nucleic acid molecules such as H19 or CCAL lncRNA and activating β-catenin in neighboring cells[25]. H19 lncRNA can also trigger autophagy *via* SIRT1 and consequently induce resistance to 5-FU in CRC cells[105]. Other miRNAs such as miR-27[106], miR-103, and miR-107 decrease the sensitivity of HCT116 cells to 5-FU and OXA, through hyperactivation of the β-catenin pathway[9]. Zhou and colleagues reported that the inhibition of the Wnt/β-catenin signaling pathway by the overexpression of miR-506 decreases the chemoresistance response of HCT116 cells to OXA. The mechanism that explains this effect is that the gene and protein expression of the transporter of the ABC family and multidrug resistance protein 1/P-glycoprotein are blocked[107]. Several cRNAs are also involved in the acquisition of drug resistance by CRC cells through modulation of the β-catenin axis. For instance, circ-PRKDC participates in the development of chemoresistance to 5-FU in SW620 and SW480 cell lines by regulation of miR-375 and the Wnt/β-catenin pathway[77]. These molecules constitute a novel target for the development of

alternative therapies for CRC, given their role in the communication between tumor cells and the TME and their participation in the regulation of Wnt/β-catenin[26,108].

Macrophages also play a crucial role in the development of resistance to drugs. IL-1β released by TAMs activates the canonical Wnt pathway through NF-κB/Akt and subsequently induces the expression of genes associated with chemoresistance. This has been observed in several cell lines derived from CRC such as HCT116, Hke-3, SW480, and RKO[109,110].

In our laboratory, we previously reported that PTHrP, acting as a cytokine, induces chemoresistance to CPT-11 through ERK MAPK and Akt pathways in the CRC cell lines Caco-2 and HCT116[34]. Moreover, as described in previous sections, we also registered nuclear β-catenin nuclear-increased expression after PTHrP treatment in CRC cells[37]. In view of these data, we hypothesize that this protein also participates in the resistance to CPT-11. This is our current research focus.

Growth factors are also involved in the therapy resistance mediated by β-catenin. Activation of the c-MET pathway through HGF signaling is related to drug resistance in many types of tumors[111]. Several works have already shown that HGF is associated with both Met and β-catenin pathways[52,54]. Studies published by Woo and collaborators showed that this factor is related to resistance to CPT-11 in CRC cells[112]. Since the HGF/Met axis plays an important role in CRC, molecules such as inhibitors, neutralizing antibodies, and antagonists of this pathway have been designed. To date, pre-clinical trials have failed and demonstrated poor efficacy[111,113]. One of the possible causes of the resistance of CRC cells to HGF pathway inhibitors is the activation of the Wnt/β-catenin signaling pathway[113]. All of these data highlight the need for consideration of the mitogenic pathways and paracrine factors released by both the tumor and the TME as targets to revert the chemoresistance.

Li *et al*[114] made a relevant contribution in the field of basic sciences related to CRC therapy and TME cells. They observed that the pharmacological treatment of CAFs inhibits their recruitment and increases the sensitivity of tumor cells to OXA[114]. Chemotherapy combined with treatments that inhibit CAFs recruitment and/or their activity may represent a novel method for the improvement of tumor response to chemotherapy[114]. This area of research is practically vacant and needs to be further explored since other unknown factors derived from TME may be able to stimulate the nuclear translocation of β-catenin and modulate the events related to the chemoresistance of CRC cells.

THE TME AND β-CATENIN PATHWAY: FUTURE PERSPECTIVES FOR CRC MANAGEMENT

In the last decade, therapeutic inhibition of the β-catenin pathway has been considered an invaluable tool for developing new therapy regimens for patients with CRC[115-117]. Despite this, as previously stated, there are still no approved drugs for the treatment of CRC or clinical trials based on the targeting of this signaling pathway[15,117]. For these reasons, comprehension of the regulatory mechanisms of the Wnt/β-catenin signaling pathway will not only expand the knowledge about the pathogenesis and evolution of CRC but also improve the treatment with the implementation of new targeted therapies. Many small molecules with β-catenin inhibitory effects have been developed such as tankyrase inhibitors (TNKSi), R-spondin inhibitors, and porcupine enzyme inhibitors. tankyrases (TNKSs) favor Wnt signaling by inducing Axin degradation. Therefore, TNKSi including XAV939 (XAV), JW55, NVP-TNKS656, and GOO7-LK are effective approaches for inhibiting this pathway in the preclinical stage of validation[118,119]. Moon and collaborators recently discovered that β-catenin expression influences the response of CRC-derived cells to MEK inhibitors, and that TNKSi allows the resistance to this treatment to be exceeded in CRC cell lines with mutant KRAS and PI3K. These results demonstrate the possible efficacy of combined treatments with inhibitors of MEK and β-catenin signaling pathways. However, this kind of therapeutic strategy is not yet in the clinical trial phase[118], and there is even controversy on the implementation of this type of scheme[116]. Drugs that disable enzymes related to Wnt secretion are another possibility to inhibit the Wnt/β-catenin. These compounds are denominated IWP-2, LGK974, or ETC-159 and inhibit porcupine enzyme actions. Some R-spondin inhibitors, such as OMP-131R10 (rosmantuzumab), are also currently under investigation for the treatment of CRC. When this ligand binds to the receptor leucine rich repeat containing G protein-coupled receptor 4 (LGR4) or LGR5, it enhances Wnt signaling, so blocking this point would consequently decrease the transcriptional activity of β-catenin[119].

One of the therapeutic targets that is being studied for CRC treatment is the use of antibodies or small molecules for the inhibition of Wnt ligands, like OMP-54F28, OMP-18R5, and OTSA101[116]; the disruption of the transcriptional activity of β-catenin using small molecules that prevent the binding of this protein with the nuclear transcription factors TCF and LEF, such as LF3 and 2,4-diamino-quinazoline; or pharmacological drugs that stimulate β-catenin proteasomal degradation as MSAB[119,120].

In addition to the hyper-activating mutations affecting the β-catenin pathway in CRC, as previously mentioned, cross-communication through paracrine signals between tumor cells and TME cells amplify these effects. The Wnt/β-catenin pathway is key for immune cells differentiation and functioning[120], the aberrant activation of this signaling alters the activation and downregulation of the immune

response, especially related to dendritic cells (DCs) and T cells[119]. In the TME, the β-catenin pathway-dependent production of cytokines, such as IL-10, by DCs has been shown to induce immune tolerance through CD4+ and CD8+ T cells[121]. Moreover, it was reported that β-catenin signaling is activated in tumors with an inflammatory microenvironment, immune evasion and poor infiltration of CD8+ T cells [119,122,123]. In CRC, this immune response is favored by the activation of β-catenin, Myc, and RAS[7, 124,125]. Currently known mechanisms that mediate immune exclusion and evasion through the Wnt/β-catenin pathway are: Modulating the production and release of cytokines from DCs and consequently diminishing CD8+ T cells infiltration; stimulating the production and release of soluble factors like Snail and IL-1β from tumor cells and TAMs, respectively; and increasing regulatory T cells survival, which are also effective inhibitors of CD8+ T cells[120,126]. To date, there are some inhibitors related to the immune response that are approved for clinical use, one of them is programmed death-1[127]. However, although immunomodulation can be effective in the treatment of CRC, resistance often occurs. Given that several of these drugs target CD8+ T cells, one of the explanations for the failure of these therapies may be the hyperactivation of the β-catenin pathway in the TME[128]. From this point of view, the current research focuses on the importance of the development of anticancer therapies that target the Wnt/β-catenin pathway as a checkpoint to improve the efficacy of immunotherapies, mainly by restoring T-cell infiltration[119,120,122].

In previous sections, we described the role of several TME-derived factors that activates the β-catenin signaling pathway. Currently, clinical research is aimed at blocking or inhibiting the effects of these molecules on CRC. In our laboratory, we have found that the selective inhibition of the HGF receptor, the RTK Met, suppresses β-catenin phosphorylation at domains that favor its nuclear translocation induced by PTHrP. Concerning this, Rimassa and his research group[129] explored in a clinical phase II study the effect of an oral selective Met inhibitor (tivantinib) and found that, in combination with another drug, at least 10% of patients with CRC respond better to the therapy. This drug is a possible emerging treatment that is already in phase III study in other types of tumors[130]. Another drug that inhibits the activity of the Met receptor by inducing the degradation of β-catenin is celecoxib[116]. However, recent evidence indicates that the combined treatment of celecoxib with the usual chemotherapy did not improve overall survival or progression-free time in patients with CRC[131].

On the other hand, a large number of clinical trials have been developed using cytokine-based immunotherapy for CRC. Different drugs targeting IL, prostaglandins, CXCL, TNF-α and TGF-β superfamily factors are in clinical trials. Although it has not yet been proven that they generate an effect as monotherapy or in combined treatments with commonly used drugs, future expectations are very optimistic[132,133].

Employing non-coding RNA such as miRNAs or cRNAs is a promising solution to overcome CRC drug resistance. It has been seen that miR505, miR199a/b and miR320 decreased sensitivity to cisplatin and OXA by modulating the activity of the Wnt/β-catenin pathway. Others, such as miR30-5p, favor chemosensitivity in CRC cells[134]. In this work, we have also described the role of TME-derived cRNAs in activating the β-catenin signaling pathway and its influence on CRC development and progression. Nevertheless, there is still a lot to explore about its potential role in future therapies for CRC. In this regard, recent research indicates that knockdown circ-PRKDC decreases the resistance of CRC-derived cells to 5-FU by modulating the Wnt/β-catenin pathway[77]. These results could postulate a new strategy to deal with multidrug resistance in CRC. Additionally, Viralippurath and collaborators propose that gene therapy could be aimed at silencing these oncogenic cRNAs or increasing the effects of those molecules that act as tumor suppressors[26]. Despite these findings, to date, there are no available therapies that use these small molecules to evade the strategies of tumor cells against chemotherapeutic drugs. More studies are needed regarding the role of non-coding RNAs in CRC chemoresistance as well as for the development of delivery strategies for these molecules in new targeted therapies. Figure 4 schematizes current studies related to the disruption of the interrelationships between TME and CRC cells that trigger β-catenin activation and are involved in treatment failure.

As previously mentioned, autophagy is a mechanism associated with chemoresistance in CRC[105]. Recent investigations aim to find drugs that help reverse the autophagy process and overcome chemoresistance in CRC[135]. According to Pérez-Plasencia *et al*[62], the involvement of Wnt/β-catenin signaling in the regulation of autophagy was demonstrated in several types of cancer, such as leukemia, hepatocarcinoma, squamous cell carcinoma, lung cancer and prostate cancer[62]. However, it is just a matter of time before the relationship between these two pathways in CRC will be considered crucial for future pharmacological treatments. In their work, the authors postulate several therapeutic approaches based on drugs that are capable of simultaneously disrupting components of β-catenin and autophagy pathways[61].

From what we have analyzed in this work, it is important to highlight that concerning CRC, the achievement of successful future therapies will involve the use of combined pharmacological compounds that inhibit not only the canonical β-catenin signaling pathway but also the TME- derived signaling.

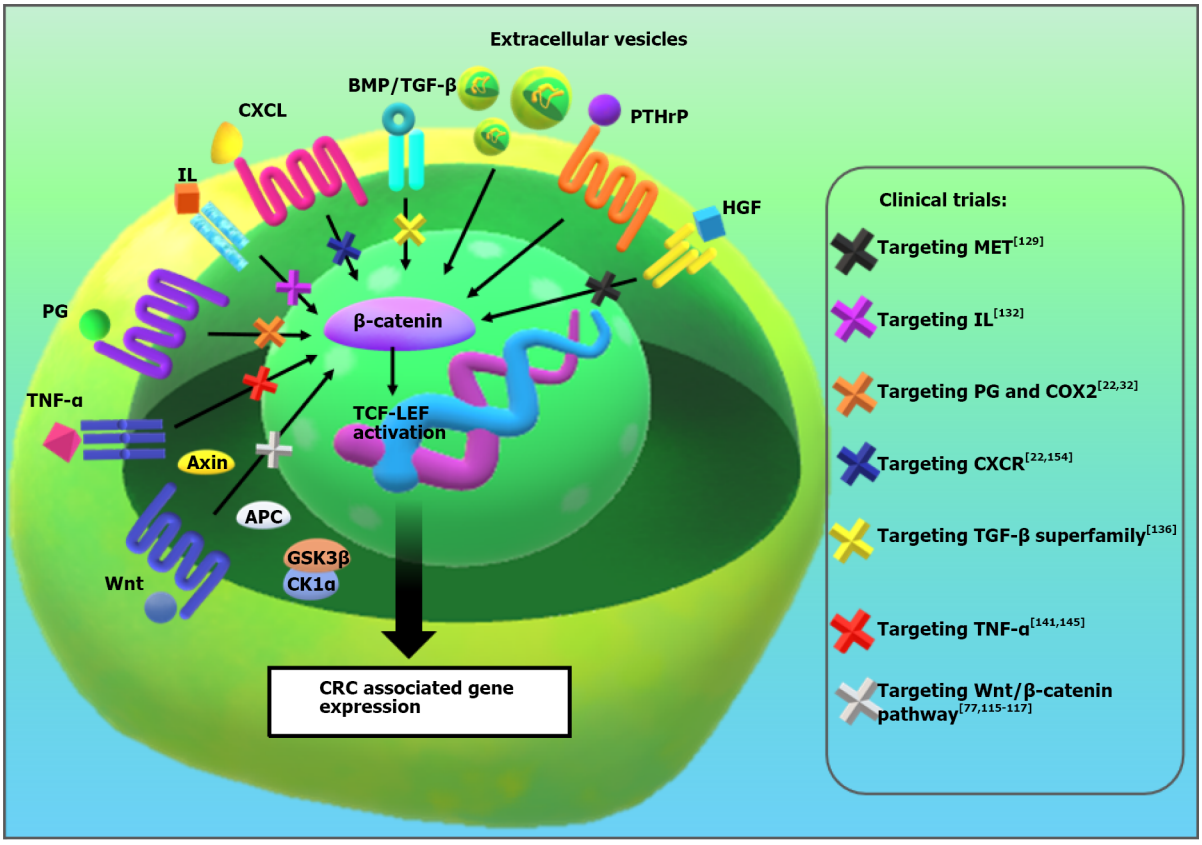

DOI: 10.3748/wjg.v28.i26.3027

Figure 4 Pharmacological targeting of the tumor microenvironment factors involved in the activation of β-catenin signaling in colorectal cancer. Several therapeutic strategies to block or inhibit the induction of the β-catenin pathway by tumor microenvironment factors in colorectal cancer (CRC) are currently under clinical study. This figure is original for this work. APC: Adenomatous polyposis coli; BMP: Bone morphogenic protein; CK1α: Casein kinase 1 alpha; CXCL: C-X-C motif chemokine ligand; GSK3β: Glycogen Synthase Kinase 3 Beta; HGF: Hepatocyte growth factor; IL: Interleukin; PTHrP: Parathyroid Hormone-related Peptide; PG: prostaglandin; TCF/LEF: T-cell factor/lymphoid enhancer factor; TGF-β: Transforming growth factor-beta; TNF-α: Tumor necrosis factor-α; Wnt: Wingless protein.

CONCLUSION

The cells of the TME are mainly responsible for triggering the mechanisms that determine a worse prognosis of cancer disease. These cells and the biological mediators released in the neoplastic context regulate the expression of ligands and modulate the activity of pro-tumor signaling pathways. TME cells control the fate of the tumor cells through permanent bidirectional communication. It is known that a considerable proportion of CRC patients evolve unfavorably due to chemoresistance. To improve CRC therapies, it is necessary to expand the knowledge about the mechanisms that play a critical role in the development, progression and chemoresistance of CRC.

Given that the factors associated with the TME activate the β-catenin signaling pathway, it will be possible in the future to improve the response of CRC patients to treatment. This goal could be achieved through new therapeutic interventions based on interrupting the crosstalk between the stroma and the tumor that control the β-catenin pathway activation. From the exhaustive search of the bibliography made by the authors of this work, it is concluded that there are multiple vacant areas in the research related to chemoresistance induced by cells from the tumor environment. Even to date, new types of biomarkers are continuously identified and related to a worse prognosis and aggressiveness of CRC. For this reason, it is imperative to strengthen *in vitro* and preclinical studies to support clinical trials in order to achieve novel therapeutic approaches considering the background of each patient and personalized medicine.

ACKNOWLEDGEMENTS

The authors would like to thank Antonela Rossi Bertone for her helpful advice. Being a teacher of English graduated from Instituto Superior Juan XXIII (from Bahia Blanca city, Argentina) and currently working at San Cayetano school (in the same city), she revised the paper and made useful comments as

regards the spelling, grammar and punctuation of this manuscript. MBND and MJM thanks CONICET for the fellowships.

FOOTNOTES

Author contributions: Novoa Díaz MB, Martín MJ, and Gentili C contributed to the conceptualization, methodology, investigation, formal analysis, and visualization, wrote the original draft, and edited the manuscript; Gentili C obtained the resources and oversaw the project administration and funding acquisition.

Supported by Agencia Nacional de Promoción Científica y Tecnológica, No. PICT-2013-1441; Consejo Nacional de Investigaciones Científicas y Técnicas, No. PIP11220150100350; Instituto Nacional del Cáncer Asistencia Financiera II, RESOL 493/14, No. 2002-4395-14-1; Instituto Nacional del Cáncer Asistencia Financiera III-2016-2017, RESOL-2016-1006-E-APN-MS, No. 2002-3862-16-1; and Universidad Nacional del Sur (PGI), Argentina, No. 24/B230 and No. 24/B303.

Conflict-of-interest statement: All the authors report no relevant conflicts of interest for this article.

Country/Territory of origin: Argentina

ORCID number: María Belén Novoa Díaz 0000-0002-6684-4076; María Julia Martín 0000-0001-5046-7686; Claudia Gentili 0000-0002-9957-7824.

S-Editor: Fan JR
L-Editor: Filipodia
P-Editor: Fan JR

REFERENCES

1 **Li J**, Huang L, Zhao H, Yan Y, Lu J. The Role of Interleukins in Colorectal Cancer. *Int J Biol Sci* 2020; **16**: 2323-2339 [PMID: 32760201 DOI: 10.7150/ijbs.46651]
2 **Siegel RL**, Miller KD, Jemal A. Cancer statistics, 2020. *CA Cancer J Clin* 2020; **70**: 7-30 [PMID: 31912902 DOI: 10.3322/caac.21590]
3 Erratum: Global cancer statistics 2018: GLOBOCAN estimates of incidence and mortality worldwide for 36 cancers in 185 countries. *CA Cancer J Clin* 2020; **70**: 313 [PMID: 32767693 DOI: 10.3322/caac.21609]
4 **Siegel RL**, Miller KD, Fedewa SA, Ahnen DJ, Meester RGS, Barzi A, Jemal A. Colorectal cancer statistics, 2017. *CA Cancer J Clin* 2017; **67**: 177-193 [PMID: 28248415 DOI: 10.3322/caac.21395]
5 **Villalba M**, Evans SR, Vidal-Vanaclocha F, Calvo A. Role of TGF-β in metastatic colon cancer: it is finally time for targeted therapy. *Cell Tissue Res* 2017; **370**: 29-39 [PMID: 28560691 DOI: 10.1007/s00441-017-2633-9]
6 **Martín MJ**, Gentili C, Lassalle V. In vitro Biological Tests as the First Tools To Validate Magnetic Nanotheranostics for Colorectal Cancer Models. *ChemMedChem* 2020; **15**: 1003-1017 [PMID: 32365271 DOI: 10.1002/cmdc.202000119]
7 **Guinney J**, Dienstmann R, Wang X, de Reyniès A, Schlicker A, Soneson C, Marisa L, Roepman P, Nyamundanda G, Angelino P, Bot BM, Morris JS, Simon IM, Gerster S, Fessler E, De Sousa E Melo F, Missiaglia E, Ramay H, Barras D, Homicsko K, Maru D, Manyam GC, Broom B, Boige V, Perez-Villamil B, Laderas T, Salazar R, Gray JW, Hanahan D, Tabernero J, Bernards R, Friend SH, Laurent-Puig P, Medema JP, Sadanandam A, Wessels L, Delorenzi M, Kopetz S, Vermeulen L, Tejpar S. The consensus molecular subtypes of colorectal cancer. *Nat Med* 2015; **21**: 1350-1356 [PMID: 26457759 DOI: 10.1038/nm.3967]
8 **Stastna M**, Janeckova L, Hrckulak D, Kriz V, Korinek V. Human Colorectal Cancer from the Perspective of Mouse Models. *Genes (Basel)* 2019; **10** [PMID: 31614493 DOI: 10.3390/genes10100788]
9 **Yuan S**, Tao F, Zhang X, Zhang Y, Sun X, Wu D. Role of Wnt/*β*-Catenin Signaling in the Chemoresistance Modulation of Colorectal Cancer. *Biomed Res Int* 2020; **2020**: 9390878 [PMID: 32258160 DOI: 10.1155/2020/9390878]
10 **Flores-Hernández E**, Velázquez DM, Castañeda-Patlán MC, Fuentes-García G, Fonseca-Camarillo G, Yamamoto-Furusho JK, Romero-Avila MT, García-Sáinz JA, Robles-Flores M. Canonical and non-canonical Wnt signaling are simultaneously activated by Wnts in colon cancer cells. *Cell Signal* 2020; **72**: 109636 [PMID: 32283254 DOI: 10.1016/j.cellsig.2020.109636]
11 **Bian J**, Dannappel M, Wan C, Firestein R. Transcriptional Regulation of Wnt/β-Catenin Pathway in Colorectal Cancer. *Cells* 2020; **9** [PMID: 32961708 DOI: 10.3390/cells9092125]
12 **Anthony CC**, Robbins DJ, Ahmed Y, Lee E. Nuclear Regulation of Wnt/β-Catenin Signaling: It's a Complex Situation. *Genes (Basel)* 2020; **11** [PMID: 32759724 DOI: 10.3390/genes11080886]

13 **Chatterjee A**, Paul S, Bisht B, Bhattacharya S, Sivasubramaniam S, Paul MK. Advances in targeting the WNT/β-catenin signaling pathway in cancer. *Drug Discov Today* 2022; **27**: 82-101 [PMID: 34252612 DOI: 10.1016/j.drudis.2021.07.007]

14 **Voloshanenko O**, Schwartz U, Kranz D, Rauscher B, Linnebacher M, Augustin I, Boutros M. β-catenin-independent regulation of Wnt target genes by RoR2 and ATF2/ATF4 in colon cancer cells. *Sci Rep* 2018; **8**: 3178 [PMID: 29453334 DOI: 10.1038/s41598-018-20641-5]

15 **Disoma C**, Zhou Y, Li S, Peng J, Xia Z. Wnt/β-catenin signaling in colorectal cancer: Is therapeutic targeting even possible? *Biochimie* 2022; **195**: 39-53 [PMID: 35066101 DOI: 10.1016/j.biochi.2022.01.009]

16 **Krishnamurthy N**, Kurzrock R. Targeting the Wnt/beta-catenin pathway in cancer: Update on effectors and inhibitors. *Cancer Treat Rev* 2018; **62**: 50-60 [PMID: 29169144 DOI: 10.1016/j.ctrv.2017.11.002]

17 **Li J**, Chen D, Shen M. Tumor Microenvironment Shapes Colorectal Cancer Progression, Metastasis, and Treatment Responses. *Front Med (Lausanne)* 2022; **9**: 869010 [PMID: 35402443 DOI: 10.3389/fmed.2022.869010]

18 **van Pelt GW**, Sandberg TP, Morreau H, Gelderblom H, van Krieken JHJM, Tollenaar RAEM, Mesker WE. The tumour-stroma ratio in colon cancer: the biological role and its prognostic impact. *Histopathology* 2018; **73**: 197-206 [PMID: 29457843 DOI: 10.1111/his.13489]

19 **Huang D**, Du X. Crosstalk between tumor cells and microenvironment *via* Wnt pathway in colorectal cancer dissemination. *World J Gastroenterol* 2008; **14**: 1823-1827 [PMID: 18350618 DOI: 10.3748/wjg.14.1823]

20 **Sandberg TP**, Stuart MPME, Oosting J, Tollenaar RAEM, Sier CFM, Mesker WE. Increased expression of cancer-associated fibroblast markers at the invasive front and its association with tumor-stroma ratio in colorectal cancer. *BMC Cancer* 2019; **19**: 284 [PMID: 30922247 DOI: 10.1186/s12885-019-5462-2]

21 **Laplagne C**, Domagala M, Le Naour A, Quemerais C, Hamel D, Fournié JJ, Couderc B, Bousquet C, Ferrand A, Poupot M. Latest Advances in Targeting the Tumor Microenvironment for Tumor Suppression. *Int J Mol Sci* 2019; **20** [PMID: 31547627 DOI: 10.3390/ijms20194719]

22 **Siveen KS**, Raza A, Ahmed EI, Khan AQ, Prabhu KS, Kuttikrishnan S, Mateo JM, Zayed H, Rasul K, Azizi F, Dermime S, Steinhoff M, Uddin S. The Role of Extracellular Vesicles as Modulators of the Tumor Microenvironment, Metastasis and Drug Resistance in Colorectal Cancer. *Cancers (Basel)* 2019; **11** [PMID: 31146452 DOI: 10.3390/cancers11060746]

23 **Gonda A**, Kabagwira J, Senthil GN, Wall NR. Internalization of Exosomes through Receptor-Mediated Endocytosis. *Mol Cancer Res* 2019; **17**: 337-347 [PMID: 30487244 DOI: 10.1158/1541-7786.MCR-18-0891]

24 **Hu JL**, Wang W, Lan XL, Zeng ZC, Liang YS, Yan YR, Song FY, Wang FF, Zhu XH, Liao WJ, Liao WT, Ding YQ, Liang L. CAFs secreted exosomes promote metastasis and chemotherapy resistance by enhancing cell stemness and epithelial-mesenchymal transition in colorectal cancer. *Mol Cancer* 2019; **18**: 91 [PMID: 31064356 DOI: 10.1186/s12943-019-1019-x]

25 **Ren J**, Ding L, Zhang D, Shi G, Xu Q, Shen S, Wang Y, Wang T, Hou Y. Carcinoma-associated fibroblasts promote the stemness and chemoresistance of colorectal cancer by transferring exosomal lncRNA H19. *Theranostics* 2018; **8**: 3932-3948 [PMID: 30083271 DOI: 10.7150/thno.25541]

26 **Viralippurath Ashraf J**, Sasidharan Nair V, Saleh R, Elkord E. Role of circular RNAs in colorectal tumor microenvironment. *Biomed Pharmacother* 2021; **137**: 111351 [PMID: 33550046 DOI: 10.1016/j.biopha.2021.111351]

27 **Gu C**, Lu H, Qian Z. Matrine reduces the secretion of exosomal circSLC7A6 from cancer-associated fibroblast to inhibit tumorigenesis of colorectal cancer by regulating CXCR5. *Biochem Biophys Res Commun* 2020; **527**: 638-645 [PMID: 32423804 DOI: 10.1016/j.bbrc.2020.04.142]

28 **Herrera M**, Llorens C, Rodríguez M, Herrera A, Ramos R, Gil B, Candia A, Larriba MJ, Garre P, Earl J, Rodríguez-Garrote M, Caldés T, Bonilla F, Carrato A, García-Barberán V, Peña C. Differential distribution and enrichment of non-coding RNAs in exosomes from normal and Cancer-associated fibroblasts in colorectal cancer. *Mol Cancer* 2018; **17**: 114 [PMID: 30075793 DOI: 10.1186/s12943-018-0863-4]

29 **Wortzel I**, Dror S, Kenific CM, Lyden D. Exosome-Mediated Metastasis: Communication from a Distance. *Dev Cell* 2019; **49**: 347-360 [PMID: 31063754 DOI: 10.1016/j.devcel.2019.04.011]

30 **Shao Y**, Chen T, Zheng X, Yang S, Xu K, Chen X, Xu F, Wang L, Shen Y, Wang T, Zhang M, Hu W, Ye C, Yu X, Shao J, Zheng S. Colorectal cancer-derived small extracellular vesicles establish an inflammatory premetastatic niche in liver metastasis. *Carcinogenesis* 2018; **39**: 1368-1379 [PMID: 30184100 DOI: 10.1093/carcin/bgy115]

31 **Abu N**, Othman N, Ab Razak NS, Bakarurraini NAAR, Nasir SN, Soh JEC, Mazlan L, Azman ZAM, Jamal R. Extracellular Vesicles Derived From Colorectal Cancer Affects CD8 T Cells: An Analysis Based on Body Mass Index. *Front Cell Dev Biol* 2020; **8**: 564648 [PMID: 33324632 DOI: 10.3389/fcell.2020.564648]

32 **Karpisheh V**, Nikkhoo A, Hojjat-Farsangi M, Namdar A, Azizi G, Ghalamfarsa G, Sabz G, Yousefi M, Yousefi B, Jadidi-Niaragh F. Prostaglandin E2 as a potent therapeutic target for treatment of colon cancer. *Prostaglandins Other Lipid Mediat* 2019; **144**: 106338 [PMID: 31100474 DOI: 10.1016/j.prostaglandins.2019.106338]

33 **Landskron G**, De la Fuente López M, Dubois-Camacho K, Díaz-Jiménez D, Orellana-Serradell O, Romero D, Sepúlveda SA, Salazar C, Parada-Venegas D, Quera R, Simian D, González MJ, López-Köstner F, Kronberg U, Abedrapo M, Gallegos I, Contreras HR, Peña C, Díaz-Araya G, Roa JC, Hermoso MA. Interleukin 33/ST2 Axis Components Are Associated to Desmoplasia, a Metastasis-Related Factor in Colorectal Cancer. *Front Immunol* 2019; **10**: 1394 [PMID: 31281317 DOI: 10.3389/fimmu.2019.01394]

34 **Martín MJ**, Gigola G, Zwenger A, Carriquiriborde M, Gentil F, Gentili C. Potential therapeutic targets for growth arrest of colorectal cancer cells exposed to PTHrP. *Mol Cell Endocrinol* 2018; **478**: 32-44 [PMID: 30009852 DOI: 10.1016/j.mce.2018.07.005]

35 **Calvo N**, Carriere P, Martín MJ, Gigola G, Gentili C. PTHrP treatment of colon cancer cells promotes tumor associated-angiogenesis by the effect of VEGF. *Mol Cell Endocrinol* 2019; **483**: 50-63 [PMID: 30639585 DOI: 10.1016/j.mce.2019.01.005]

36 **Carriere P**, Calvo N, Novoa Díaz MB, Lopez-Moncada F, Herrera A, Torres MJ, Alonso E, Gandini NA, Gigola G, Contreras HR, Gentili C. Role of SPARC in the epithelial-mesenchymal transition induced by PTHrP in human colon cancer cells. *Mol Cell Endocrinol* 2021; **530**: 111253 [PMID: 33781836 DOI: 10.1016/j.mce.2021.111253]

37 **Novoa Díaz MB**, Carriere PM, Martín MJ, Calvo N, Gentili C. Involvement of parathyroid hormone-related peptide in the

aggressive phenotype of colorectal cancer cells. *World J Gastroenterol* 2021; **27**: 7025-7040 [PMID: 34887626 DOI: 10.3748/wjg.v27.i41.7025]

38 **Muñoz-Galván S**, Lucena-Cacace A, Perez M, Otero-Albiol D, Gomez-Cambronero J, Carnero A. Tumor cell-secreted PLD increases tumor stemness by senescence-mediated communication with microenvironment. *Oncogene* 2019; **38**: 1309-1323 [PMID: 30305726 DOI: 10.1038/s41388-018-0527-2]

39 **Molinier-Frenkel V**, Castellano F. Immunosuppressive enzymes in the tumor microenvironment. *FEBS Lett* 2017; **591**: 3135-3157 [PMID: 28792588 DOI: 10.1002/1873-3468.12784]

40 **Cox TR**. The matrix in cancer. *Nat Rev Cancer* 2021; **21**: 217-238 [PMID: 33589810 DOI: 10.1038/s41568-020-00329-7]

41 **Sameer AS**, Nissar S. Toll-Like Receptors (TLRs): Structure, Functions, Signaling, and Role of Their Polymorphisms in Colorectal Cancer Susceptibility. *Biomed Res Int* 2021; **2021**: 1157023 [PMID: 34552981 DOI: 10.1155/2021/1157023]

42 **Angrini M**, Varthaman A, Cremer I. Toll-Like Receptors (TLRs) in the Tumor Microenvironment (TME): A Dragon-Like Weapon in a Non-fantasy Game of Thrones. *Adv Exp Med Biol* 2020; **1263**: 145-173 [PMID: 32588327 DOI: 10.1007/978-3-030-44518-8_9]

43 **Kamal Y**, Schmit SL, Frost HR, Amos CI. The tumor microenvironment of colorectal cancer metastases: opportunities in cancer immunotherapy. *Immunotherapy* 2020; **12**: 1083-1100 [PMID: 32787587 DOI: 10.2217/imt-2020-0026]

44 **Unterleuthner D**, Neuhold P, Schwarz K, Janker L, Neuditschko B, Nivarthi H, Crncec I, Kramer N, Unger C, Hengstschläger M, Eferl R, Moriggl R, Sommergruber W, Gerner C, Dolznig H. Cancer-associated fibroblast-derived WNT2 increases tumor angiogenesis in colon cancer. *Angiogenesis* 2020; **23**: 159-177 [PMID: 31667643 DOI: 10.1007/s10456-019-09688-8]

45 **Aizawa T**, Karasawa H, Funayama R, Shirota M, Suzuki T, Maeda S, Suzuki H, Yamamura A, Naitoh T, Nakayama K, Unno M. Cancer-associated fibroblasts secrete Wnt2 to promote cancer progression in colorectal cancer. *Cancer Med* 2019; **8**: 6370-6382 [PMID: 31468733 DOI: 10.1002/cam4.2523]

46 **Matsumoto K**, Umitsu M, De Silva DM, Roy A, Bottaro DP. Hepatocyte growth factor/MET in cancer progression and biomarker discovery. *Cancer Sci* 2017; **108**: 296-307 [PMID: 28064454 DOI: 10.1111/cas.13156]

47 **Goïta AA**, Guenot D. Colorectal Cancer: The Contribution of CXCL12 and Its Receptors CXCR4 and CXCR7. *Cancers (Basel)* 2022; **14** [PMID: 35406582 DOI: 10.3390/cancers14071810]

48 **Martín MJ**, Calvo N, de Boland AR, Gentili C. Molecular mechanisms associated with PTHrP-induced proliferation of colon cancer cells. *J Cell Biochem* 2014; **115**: 2133-2145 [PMID: 25053227 DOI: 10.1002/jcb.24890]

49 **Amable G**, Martínez-León E, Picco ME, Di Siervi N, Davio C, Rozengurt E, Rey O. Metformin inhibits β-catenin phosphorylation on Ser-552 through an AMPK/PI3K/Akt pathway in colorectal cancer cells. *Int J Biochem Cell Biol* 2019; **112**: 88-94 [PMID: 31082618 DOI: 10.1016/j.biocel.2019.05.004]

50 **Yan X**, Zhao J, Zhang R. Interleukin-37 mediates the antitumor activity in colon cancer through β-catenin suppression. *Oncotarget* 2017; **8**: 49064-49075 [PMID: 28467774 DOI: 10.18632/oncotarget.17093]

51 **Voorneveld PW**, Kodach LL, Jacobs RJ, van Noesel CJ, Peppelenbosch MP, Korkmaz KS, Molendijk I, Dekker E, Morreau H, van Pelt GW, Tollenaar RA, Mesker W, Hawinkels LJ, Paauwe M, Verspaget HW, Geraets DT, Hommes DW, Offerhaus GJ, van den Brink GR, Ten Dijke P, Hardwick JC. The BMP pathway either enhances or inhibits the Wnt pathway depending on the SMAD4 and p53 status in CRC. *Br J Cancer* 2015; **112**: 122-130 [PMID: 25393365 DOI: 10.1038/bjc.2014.560]

52 **Essex A**, Pineda J, Acharya G, Xin H, Evans J; Reproducibility Project: Cancer Biology. Replication Study: Wnt activity defines colon cancer stem cells and is regulated by the microenvironment. *Elife* 2019; **8** [PMID: 31215867 DOI: 10.7554/eLife.45426]

53 **Vermeulen L**, De Sousa E Melo F, van der Heijden M, Cameron K, de Jong JH, Borovski T, Tuynman JB, Todaro M, Merz C, Rodermond H, Sprick MR, Kemper K, Richel DJ, Stassi G, Medema JP. Wnt activity defines colon cancer stem cells and is regulated by the microenvironment. *Nat Cell Biol* 2010; **12**: 468-476 [PMID: 20418870 DOI: 10.1038/ncb2048]

54 **Zhang L**, Jiang X, Li Y, Fan Q, Li H, Jin L, Li L, Jin Y, Zhang T, Mao Y, Hua D. Clinical Correlation of Wnt2 and COL8A1 With Colon Adenocarcinoma Prognosis. *Front Oncol* 2020; **10**: 1504 [PMID: 32983993 DOI: 10.3389/fonc.2020.01504]

55 **Koliaraki V**, Pallangyo CK, Greten FR, Kollias G. Mesenchymal Cells in Colon Cancer. *Gastroenterology* 2017; **152**: 964-979 [PMID: 28111227 DOI: 10.1053/j.gastro.2016.11.049]

56 **Kalra H**, Gangoda L, Fonseka P, Chitti SV, Liem M, Keerthikumar S, Samuel M, Boukouris S, Al Saffar H, Collins C, Adda CG, Ang CS, Mathivanan S. Extracellular vesicles containing oncogenic mutant β-catenin activate Wnt signalling pathway in the recipient cells. *J Extracell Vesicles* 2019; **8**: 1690217 [PMID: 31819794 DOI: 10.1080/20013078.2019.1690217]

57 **Hu Y**, Yan C, Mu L, Huang K, Li X, Tao D, Wu Y, Qin J. Fibroblast-Derived Exosomes Contribute to Chemoresistance through Priming Cancer Stem Cells in Colorectal Cancer. *PLoS One* 2015; **10**: e0125625 [PMID: 25938772 DOI: 10.1371/journal.pone.0125625]

58 **Hu YB**, Yan C, Mu L, Mi YL, Zhao H, Hu H, Li XL, Tao DD, Wu YQ, Gong JP, Qin JC. Exosomal Wnt-induced dedifferentiation of colorectal cancer cells contributes to chemotherapy resistance. *Oncogene* 2019; **38**: 1951-1965 [PMID: 30390075 DOI: 10.1038/s41388-018-0557-9]

59 **Dong HJ**, Jang GB, Lee HY, Park SR, Kim JY, Nam JS, Hong IS. The Wnt/β-catenin signaling/Id2 cascade mediates the effects of hypoxia on the hierarchy of colorectal-cancer stem cells. *Sci Rep* 2016; **6**: 22966 [PMID: 26965643 DOI: 10.1038/srep22966]

60 **Huang Z**, Yang M, Li Y, Yang F, Feng Y. Exosomes Derived from Hypoxic Colorectal Cancer Cells Transfer Wnt4 to Normoxic Cells to Elicit a Prometastatic Phenotype. *Int J Biol Sci* 2018; **14**: 2094-2102 [PMID: 30585272 DOI: 10.7150/ijbs.28288]

61 **Huang Z**, Feng Y. Exosomes Derived From Hypoxic Colorectal Cancer Cells Promote Angiogenesis Through Wnt4-Induced β-Catenin Signaling in Endothelial Cells. *Oncol Res* 2017; **25**: 651-661 [PMID: 27712599 DOI: 10.3727/096504016X14752792816791]

62 **Pérez-Plasencia C**, López-Urrutia E, García-Castillo V, Trujano-Camacho S, López-Camarillo C, Campos-Parra AD. Interplay Between Autophagy and Wnt/β-Catenin Signaling in Cancer: Therapeutic Potential Through Drug Repositioning. *Front Oncol* 2020; **10**: 1037 [PMID: 33014767 DOI: 10.3389/fonc.2020.01037]

63 **Janji B**, Berchem G, Chouaib S. Targeting Autophagy in the Tumor Microenvironment: New Challenges and Opportunities for Regulating Tumor Immunity. *Front Immunol* 2018; **9**: 887 [PMID: 29922284 DOI: 10.3389/fimmu.2018.00887]

64 **Pandurangan AK**, Divya T, Kumar K, Dineshbabu V, Velavan B, Sudhandiran G. Colorectal carcinogenesis: Insights into the cell death and signal transduction pathways: A review. *World J Gastrointest Oncol* 2018; **10**: 244-259 [PMID: 30254720 DOI: 10.4251/wjgo.v10.i9.244]

65 **Janji B**, Hasmim M, Parpal S, Berchem G, Noman MZ. Firing up the cold tumors by targeting Vps34. *Oncoimmunology* 2020; **9**: 1809936 [PMID: 32939326 DOI: 10.1080/2162402X.2020.1809936]

66 **Rahmani F**, Avan A, Hashemy SI, Hassanian SM. Role of Wnt/β-catenin signaling regulatory microRNAs in the pathogenesis of colorectal cancer. *J Cell Physiol* 2018; **233**: 811-817 [PMID: 28266708 DOI: 10.1002/jcp.25897]

67 **Zhang H**, Yu C, Dai J, Keller JM, Hua A, Sottnik JL, Shelley G, Hall CL, Park SI, Yao Z, Zhang J, McCauley LK, Keller ET. Parathyroid hormone-related protein inhibits DKK1 expression through c-Jun-mediated inhibition of β-catenin activation of the DKK1 promoter in prostate cancer. *Oncogene* 2014; **33**: 2464-2477 [PMID: 23752183 DOI: 10.1038/onc.2013.203]

68 **Hiremath M**, Dann P, Fischer J, Butterworth D, Boras-Granic K, Hens J, Van Houten J, Shi W, Wysolmerski J. Parathyroid hormone-related protein activates Wnt signaling to specify the embryonic mammary mesenchyme. *Development* 2012; **139**: 4239-4249 [PMID: 23034629 DOI: 10.1242/dev.080671]

69 **Johnson RW**, Merkel AR, Page JM, Ruppender NS, Guelcher SA, Sterling JA. Wnt signaling induces gene expression of factors associated with bone destruction in lung and breast cancer. *Clin Exp Metastasis* 2014; **31**: 945-959 [PMID: 25359619 DOI: 10.1007/s10585-014-9682-1]

70 **Chen HY**, Lang YD, Lin HN, Liu YR, Liao CC, Nana AW, Yen Y, Chen RH. miR-103/107 prolong Wnt/β-catenin signaling and colorectal cancer stemness by targeting Axin2. *Sci Rep* 2019; **9**: 9687 [PMID: 31273221 DOI: 10.1038/s41598-019-41053-z]

71 **Ba S**, Xuan Y, Long ZW, Chen HY, Zheng SS. MicroRNA-27a Promotes the Proliferation and Invasiveness of Colon Cancer Cells by Targeting SFRP1 through the Wnt/β-Catenin Signaling Pathway. *Cell Physiol Biochem* 2017; **42**: 1920-1933 [PMID: 28772260 DOI: 10.1159/000479610]

72 **Chu J**, Fang X, Sun Z, Gai L, Dai W, Li H, Yan X, Du J, Zhang L, Zhao L, Xu D, Yan S. Non-Coding RNAs Regulate the Resistance to Anti-EGFR Therapy in Colorectal Cancer. *Front Oncol* 2021; **11**: 801319 [PMID: 35111681 DOI: 10.3389/fonc.2021.801319]

73 **Zhang L**, Dong X, Yan B, Yu W, Shan L. CircAGFG1 drives metastasis and stemness in colorectal cancer by modulating YY1/CTNNB1. *Cell Death Dis* 2020; **11**: 542 [PMID: 32681092 DOI: 10.1038/s41419-020-2707-6]

74 **Fang G**, Ye BL, Hu BR, Ruan XJ, Shi YX. CircRNA_100290 promotes colorectal cancer progression through miR-516b-induced downregulation of FZD4 expression and Wnt/β-catenin signaling. *Biochem Biophys Res Commun* 2018; **504**: 184-189 [PMID: 30173892 DOI: 10.1016/j.bbrc.2018.08.152]

75 **Jin YD**, Ren YR, Gao YX, Zhang L, Ding Z. Hsa_circ_0005075 predicts a poor prognosis and acts as an oncogene in colorectal cancer *via* activating Wnt/β-catenin pathway. *Eur Rev Med Pharmacol Sci* 2019; **23**: 3311-3319 [PMID: 31081084 DOI: 10.26355/eurrev_201904_17693]

76 **Ge Z**, Li LF, Wang CY, Wang Y, Ma WL. CircMTO1 inhibits cell proliferation and invasion by regulating Wnt/β-catenin signaling pathway in colorectal cancer. *Eur Rev Med Pharmacol Sci* 2018; **22**: 8203-8209 [PMID: 30556859 DOI: 10.26355/eurrev_201812_16513]

77 **Chen H**, Pei L, Xie P, Guo G. Circ-PRKDC Contributes to 5-Fluorouracil Resistance of Colorectal Cancer Cells by Regulating miR-375/FOXM1 Axis and Wnt/β-Catenin Pathway. *Onco Targets Ther* 2020; **13**: 5939-5953 [PMID: 32606803 DOI: 10.2147/OTT.S253468]

78 **Su K**, Yi Q, Dai X, Liu O. Circular RNA ITCH: An Emerging Multifunctional Regulator. *Biomolecules* 2022; **12** [PMID: 35327551 DOI: 10.3390/biom12030359]

79 **Geng Y**, Zheng X, Hu W, Wang Q, Xu Y, He W, Wu C, Zhu D, Jiang J. Hsa_circ_0009361 acts as the sponge of miR-582 to suppress colorectal cancer progression by regulating APC2 expression. *Clin Sci (Lond)* 2019; **133**: 1197-1213 [PMID: 31109967 DOI: 10.1042/CS20190286]

80 **Wang J**, Du Y, Liu X, Cho WC, Yang Y. MicroRNAs as Regulator of Signaling Networks in Metastatic Colon Cancer. *Biomed Res Int* 2015; **2015**: 823620 [PMID: 26064956 DOI: 10.1155/2015/823620]

81 **Tomida C**, Yamagishi N, Nagano H, Uchida T, Ohno A, Hirasaka K, Nikawa T, Teshima-Kondo S. VEGF pathway-targeting drugs induce evasive adaptation by activation of neuropilin-1/cMet in colon cancer cells. *Int J Oncol* 2018; **52**: 1350-1362 [PMID: 29532881 DOI: 10.3892/ijo.2018.4291]

82 **Wei X**, Li X, Kong F, Ma L, Sui Y, Chen D, Xu F. [TNF-α activates Wnt signaling pathway to promote the invasion of human colon cancer stem cells]. *Xi Bao Yu Fen Zi Mian Yi Xue Za Zhi* 2018; **34**: 982-988 [PMID: 30591106]

83 **Zheng Y**, Zhou C, Yu XX, Wu C, Jia HL, Gao XM, Yang JM, Wang CQ, Luo Q, Zhu Y, Zhang Y, Wei JW, Sheng YY, Dong QZ, Qin LX. Osteopontin promotes metastasis of intrahepatic cholangiocarcinoma through recruiting MAPK1 and mediating Ser675 phosphorylation of β-Catenin. *Cell Death Dis* 2018; **9**: 179 [PMID: 29415992 DOI: 10.1038/s41419-017-0226-x]

84 **Yi J**, Liu Y, Zhang L, Fang C. Secreted phosphoprotein-1 accelerates the progression of human colorectal cancer through activating β-catenin signaling. *Oncol Lett* 2021; **21**: 372 [PMID: 33777196 DOI: 10.3892/ol.2021.12633]

85 **Youssef NS**, Osman WM. Relationship between osteopontin and β-catenin immunohistochemical expression and prognostic parameters of colorectal carcinoma. *Int J Clin Exp Pathol* 2015; **8**: 1503-1514 [PMID: 25973035]

86 **Ishigamori R**, Komiya M, Takasu S, Mutoh M, Imai T, Takahashi M. Osteopontin Deficiency Suppresses Intestinal Tumor Development in Apc-Deficient Min Mice. *Int J Mol Sci* 2017; **18** [PMID: 28505114 DOI: 10.3390/ijms18051058]

87 **Kaler P**, Augenlicht L, Klampfer L. Macrophage-derived IL-1beta stimulates Wnt signaling and growth of colon cancer

cells: a crosstalk interrupted by vitamin D3. *Oncogene* 2009; **28**: 3892-3902 [PMID: 19701245 DOI: 10.1038/onc.2009.247]

88 **Bach DH**, Park HJ, Lee SK. The Dual Role of Bone Morphogenetic Proteins in Cancer. *Mol Ther Oncolytics* 2018; **8**: 1-13 [PMID: 29234727 DOI: 10.1016/j.omto.2017.10.002]

89 **Kaler P**, Galea V, Augenlicht L, Klampfer L. Tumor associated macrophages protect colon cancer cells from TRAIL-induced apoptosis through IL-1beta-dependent stabilization of Snail in tumor cells. *PLoS One* 2010; **5**: e11700 [PMID: 20661477 DOI: 10.1371/journal.pone.0011700]

90 **Gao S**, Hu J, Wu X, Liang Z. PMA treated THP-1-derived-IL-6 promotes EMT of SW48 through STAT3/ERK-dependent activation of Wnt/β-catenin signaling pathway. *Biomed Pharmacother* 2018; **108**: 618-624 [PMID: 30243096 DOI: 10.1016/j.biopha.2018.09.067]

91 **Song ZY**, Gao ZH, Chu JH, Han XZ, Qu XJ. Downregulation of the CXCR4/CXCL12 axis blocks the activation of the Wnt/β-catenin pathway in human colon cancer cells. *Biomed Pharmacother* 2015; **71**: 46-52 [PMID: 25960214 DOI: 10.1016/j.biopha.2015.01.020]

92 **La Fleur L**, Botling J, He F, Pelicano C, Zhou C, He C, Palano G, Mezheyeuski A, Micke P, Ravetch JV, Karlsson MCI, Sarhan D. Targeting MARCO and IL37R on Immunosuppressive Macrophages in Lung Cancer Blocks Regulatory T Cells and Supports Cytotoxic Lymphocyte Function. *Cancer Res* 2021; **81**: 956-967 [PMID: 33293426 DOI: 10.1158/0008-5472.CAN-20-1885]

93 **Li J**, Zhang AH, Wu FF, Wang XJ. Alterations in the Gut Microbiota and Their Metabolites in Colorectal Cancer: Recent Progress and Future Prospects. *Front Oncol* 2022; **12**: 841552 [PMID: 35223525 DOI: 10.3389/fonc.2022.841552]

94 **Yachida S**, Mizutani S, Shiroma H, Shiba S, Nakajima T, Sakamoto T, Watanabe H, Masuda K, Nishimoto Y, Kubo M, Hosoda F, Rokutan H, Matsumoto M, Takamaru H, Yamada M, Matsuda T, Iwasaki M, Yamaji T, Yachida T, Soga T, Kurokawa K, Toyoda A, Ogura Y, Hayashi T, Hatakeyama M, Nakagama H, Saito Y, Fukuda S, Shibata T, Yamada T. Metagenomic and metabolomic analyses reveal distinct stage-specific phenotypes of the gut microbiota in colorectal cancer. *Nat Med* 2019; **25**: 968-976 [PMID: 31171880 DOI: 10.1038/s41591-019-0458-7]

95 **Kim YJ**, Kim BK, Park SJ, Kim JH. Impact of *Fusobacterium nucleatum* in the gastrointestinal tract on natural killer cells. *World J Gastroenterol* 2021; **27**: 4879-4889 [PMID: 34447232 DOI: 10.3748/wjg.v27.i29.4879]

96 **Rubinstein MR**, Baik JE, Lagana SM, Han RP, Raab WJ, Sahoo D, Dalerba P, Wang TC, Han YW. *Fusobacterium nucleatum* promotes colorectal cancer by inducing Wnt/β-catenin modulator Annexin A1. *EMBO Rep* 2019; **20** [PMID: 30833345 DOI: 10.15252/embr.201847638]

97 **Parsons S**, Maldonado EB, Prasad V. Comparison of Drugs Used for Adjuvant and Metastatic Therapy of Colon, Breast, and Non-Small Cell Lung Cancers. *JAMA Netw Open* 2020; **3**: e202488 [PMID: 32275321 DOI: 10.1001/jamanetworkopen.2020.2488]

98 **Chang CL**, Yuan KS, Wu ATH, Wu SY. Adjuvant Therapy for High-Risk Stage II or III Colon Adenocarcinoma: A Propensity Score-Matched, Nationwide, Population-Based Cohort Study. *Cancers (Basel)* 2019; **11** [PMID: 31842371 DOI: 10.3390/cancers11122003]

99 **Hu T**, Li Z, Gao CY, Cho CH. Mechanisms of drug resistance in colon cancer and its therapeutic strategies. *World J Gastroenterol* 2016; **22**: 6876-6889 [PMID: 27570424 DOI: 10.3748/wjg.v22.i30.6876]

100 **Meyers BM**, Cosby R, Quereshy F, Jonker D. Adjuvant Chemotherapy for Stage II and III Colon Cancer Following Complete Resection: A Cancer Care Ontario Systematic Review. *Clin Oncol (R Coll Radiol)* 2017; **29**: 459-465 [PMID: 28341242 DOI: 10.1016/j.clon.2017.03.001]

101 **Shibue T**, Weinberg RA. EMT, CSCs, and drug resistance: the mechanistic link and clinical implications. *Nat Rev Clin Oncol* 2017; **14**: 611-629 [PMID: 28397828 DOI: 10.1038/nrclinonc.2017.44]

102 **Erin N**, Grahovac J, Brozovic A, Efferth T. Tumor microenvironment and epithelial mesenchymal transition as targets to overcome tumor multidrug resistance. *Drug Resist Updat* 2020; **53**: 100715 [PMID: 32679188 DOI: 10.1016/j.drup.2020.100715]

103 **Gupta R**, Bhatt LK, Johnston TP, Prabhavalkar KS. Colon cancer stem cells: Potential target for the treatment of colorectal cancer. *Cancer Biol Ther* 2019; **20**: 1068-1082 [PMID: 31050577 DOI: 10.1080/15384047.2019.1599660]

104 **Tauriello DV**, Calon A, Lonardo E, Batlle E. Determinants of metastatic competency in colorectal cancer. *Mol Oncol* 2017; **11**: 97-119 [PMID: 28085225 DOI: 10.1002/1878-0261.12018]

105 **Wang M**, Han D, Yuan Z, Hu H, Zhao Z, Yang R, Jin Y, Zou C, Chen Y, Wang G, Gao X, Wang X. Long non-coding RNA H19 confers 5-Fu resistance in colorectal cancer by promoting SIRT1-mediated autophagy. *Cell Death Dis* 2018; **9**: 1149 [PMID: 30451820 DOI: 10.1038/s41419-018-1187-4]

106 **Barisciano G**, Colangelo T, Rosato V, Muccillo L, Taddei ML, Ippolito L, Chiarugi P, Galgani M, Bruzzaniti S, Matarese G, Fassan M, Agostini M, Bergamo F, Pucciarelli S, Carbone A, Mazzoccoli G, Colantuoni V, Bianchi F, Sabatino L. miR-27a is a master regulator of metabolic reprogramming and chemoresistance in colorectal cancer. *Br J Cancer* 2020; **122**: 1354-1366 [PMID: 32132656 DOI: 10.1038/s41416-020-0773-2]

107 **Zhou H**, Lin C, Zhang Y, Zhang X, Zhang C, Zhang P, Xie X, Ren Z. miR-506 enhances the sensitivity of human colorectal cancer cells to oxaliplatin by suppressing MDR1/P-gp expression. *Cell Prolif* 2017; **50** [PMID: 28217977 DOI: 10.1111/cpr.12341]

108 **Zhang Q**, Wang W, Zhou Q, Chen C, Yuan W, Liu J, Li X, Sun Z. Roles of circRNAs in the tumour microenvironment. *Mol Cancer* 2020; **19**: 14 [PMID: 31973726 DOI: 10.1186/s12943-019-1125-9]

109 **Kaler P**, Godasi BN, Augenlicht L, Klampfer L. The NF-κB/AKT-dependent Induction of Wnt Signaling in Colon Cancer Cells by Macrophages and IL-1β. *Cancer Microenviron* 2009; **2**: 69-80 [PMID: 19779850 DOI: 10.1007/s12307-009-0030-y]

110 **Yoshida GJ**. Regulation of heterogeneous cancer-associated fibroblasts: the molecular pathology of activated signaling pathways. *J Exp Clin Cancer Res* 2020; **39**: 112 [PMID: 32546182 DOI: 10.1186/s13046-020-01611-0]

111 **Kim KH**, Kim H. Progress of antibody-based inhibitors of the HGF-cMET axis in cancer therapy. *Exp Mol Med* 2017; **49**: e307 [PMID: 28336955 DOI: 10.1038/emm.2017.17]

112 **Hwang K**, Yoon JH, Lee JH, Lee S. Recent Advances in Monoclonal Antibody Therapy for Colorectal Cancers.

Biomedicines 2021; **9** [PMID: 33466394 DOI: 10.3390/biomedicines9010039]

113 **Huang X**, Li E, Shen H, Wang X, Tang T, Zhang X, Xu J, Tang Z, Guo C, Bai X, Liang T. Targeting the HGF/MET Axis in Cancer Therapy: Challenges in Resistance and Opportunities for Improvement. *Front Cell Dev Biol* 2020; **8**: 152 [PMID: 32435640 DOI: 10.3389/fcell.2020.00152]

114 **Li M**, Li M, Yin T, Shi H, Wen Y, Zhang B, Chen M, Xu G, Ren K, Wei Y. Targeting of cancerassociated fibroblasts enhances the efficacy of cancer chemotherapy by regulating the tumor microenvironment. *Mol Med Rep* 2016; **13**: 2476-2484 [PMID: 26846566 DOI: 10.3892/mmr.2016.4868]

115 **Novellasdemunt L**, Antas P, Li VS. Targeting Wnt signaling in colorectal cancer. A Review in the Theme: Cell Signaling: Proteins, Pathways and Mechanisms. *Am J Physiol Cell Physiol* 2015; **309**: C511-C521 [PMID: 26289750 DOI: 10.1152/ajpcell.00117.2015]

116 **Shang S**, Hua F, Hu ZW. The regulation of β-catenin activity and function in cancer: therapeutic opportunities. *Oncotarget* 2017; **8**: 33972-33989 [PMID: 28430641 DOI: 10.18632/oncotarget.15687]

117 **de Assis JV**, Coutinho LA, Oyeyemi IT, Oyeyemi OT, Grenfell RFEQ. Diagnostic and therapeutic biomarkers in colorectal cancer: a review. *Am J Cancer Res* 2022; **12**: 661-680 [PMID: 35261794]

118 **Moon JH**, Hong SW, Kim JE, Shin JS, Kim JS, Jung SA, Ha SH, Lee S, Kim J, Lee DH, Park YS, Kim DM, Park SS, Hong JK, Kim DY, Kim EH, Jung J, Kim MJ, Kim SM, Deming DA, Kim K, Kim TW, Jin DH. Targeting β-catenin overcomes MEK inhibition resistance in colon cancer with KRAS and PIK3CA mutations. *Br J Cancer* 2019; **120**: 941-951 [PMID: 30944457 DOI: 10.1038/s41416-019-0434-5]

119 **Haseeb M**, Pirzada RH, Ain QU, Choi S. Wnt Signaling in the Regulation of Immune Cell and Cancer Therapeutics. *Cells* 2019; **8** [PMID: 31684152 DOI: 10.3390/cells8111380]

120 **Li X**, Xiang Y, Li F, Yin C, Li B, Ke X. WNT/β-Catenin Signaling Pathway Regulating T Cell-Inflammation in the Tumor Microenvironment. *Front Immunol* 2019; **10**: 2293 [PMID: 31616443 DOI: 10.3389/fimmu.2019.02293]

121 **Hong Y**, Manoharan I, Suryawanshi A, Majumdar T, Angus-Hill ML, Koni PA, Manicassamy B, Mellor AL, Munn DH, Manicassamy S. β-catenin promotes regulatory T-cell responses in tumors by inducing vitamin A metabolism in dendritic cells. *Cancer Res* 2015; **75**: 656-665 [PMID: 25568183 DOI: 10.1158/0008-5472.CAN-14-2377]

122 **Luke JJ**, Bao R, Sweis RF, Spranger S, Gajewski TF. WNT/β-catenin Pathway Activation Correlates with Immune Exclusion across Human Cancers. *Clin Cancer Res* 2019; **25**: 3074-3083 [PMID: 30635339 DOI: 10.1158/1078-0432.CCR-18-1942]

123 **Spranger S**, Bao R, Gajewski TF. Melanoma-intrinsic β-catenin signalling prevents anti-tumour immunity. *Nature* 2015; **523**: 231-235 [PMID: 25970248 DOI: 10.1038/nature14404]

124 **Lal N**, White BS, Goussous G, Pickles O, Mason MJ, Beggs AD, Taniere P, Willcox BE, Guinney J, Middleton GW. KRAS Mutation and Consensus Molecular Subtypes 2 and 3 Are Independently Associated with Reduced Immune Infiltration and Reactivity in Colorectal Cancer. *Clin Cancer Res* 2018; **24**: 224-233 [PMID: 29061646 DOI: 10.1158/1078-0432.CCR-17-1090]

125 **Grasso CS**, Giannakis M, Wells DK, Hamada T, Mu XJ, Quist M, Nowak JA, Nishihara R, Qian ZR, Inamura K, Morikawa T, Nosho K, Abril-Rodriguez G, Connolly C, Escuin-Ordinas H, Geybels MS, Grady WM, Hsu L, Hu-Lieskovan S, Huyghe JR, Kim YJ, Krystofinski P, Leiserson MDM, Montoya DJ, Nadel BB, Pellegrini M, Pritchard CC, Puig-Saus C, Quist EH, Raphael BJ, Salipante SJ, Shin DS, Shinbrot E, Shirts B, Shukla S, Stanford JL, Sun W, Tsoi J, Upfill-Brown A, Wheeler DA, Wu CJ, Yu M, Zaidi SH, Zaretsky JM, Gabriel SB, Lander ES, Garraway LA, Hudson TJ, Fuchs CS, Ribas A, Ogino S, Peters U. Genetic Mechanisms of Immune Evasion in Colorectal Cancer. *Cancer Discov* 2018; **8**: 730-749 [PMID: 29510987 DOI: 10.1158/2159-8290.CD-17-1327]

126 **Pai SG**, Carneiro BA, Mota JM, Costa R, Leite CA, Barroso-Sousa R, Kaplan JB, Chae YK, Giles FJ. Wnt/beta-catenin pathway: modulating anticancer immune response. *J Hematol Oncol* 2017; **10**: 101 [PMID: 28476164 DOI: 10.1186/s13045-017-0471-6]

127 **Payandeh Z**, Khalili S, Somi MH, Mard-Soltani M, Baghbanzadeh A, Hajiasgharzadeh K, Samadi N, Baradaran B. PD-1/PD-L1-dependent immune response in colorectal cancer. *J Cell Physiol* 2020; **235**: 5461-5475 [PMID: 31960962 DOI: 10.1002/jcp.29494]

128 **Spranger S**, Dai D, Horton B, Gajewski TF. Tumor-Residing Batf3 Dendritic Cells Are Required for Effector T Cell Trafficking and Adoptive T Cell Therapy. *Cancer Cell* 2017; **31**: 711-723.e4 [PMID: 28486109 DOI: 10.1016/j.ccell.2017.04.003]

129 **Rimassa L**, Bozzarelli S, Pietrantonio F, Cordio S, Lonardi S, Toppo L, Zaniboni A, Bordonaro R, Di Bartolomeo M, Tomasello G, Dadduzio V, Tronconi MC, Piombo C, Giordano L, Gloghini A, Di Tommaso L, Santoro A. Phase II Study of Tivantinib and Cetuximab in Patients With KRAS Wild-type Metastatic Colorectal Cancer With Acquired Resistance to EGFR Inhibitors and Emergence of MET Overexpression: Lesson Learned for Future Trials With EGFR/MET Dual Inhibition. *Clin Colorectal Cancer* 2019; **18**: 125-132.e2 [PMID: 30846365 DOI: 10.1016/j.clcc.2019.02.004]

130 **Wu ZX**, Yang Y, Teng QX, Wang JQ, Lei ZN, Lusvarghi S, Ambudkar SV, Yang DH, Chen ZS. Tivantinib, A c-Met Inhibitor in Clinical Trials, Is Susceptible to ABCG2-Mediated Drug Resistance. *Cancers (Basel)* 2020; **12** [PMID: 31940916 DOI: 10.3390/cancers12010186]

131 **Meyerhardt JA**, Shi Q, Fuchs CS, Meyer J, Niedzwiecki D, Zemla T, Kumthekar P, Guthrie KA, Couture F, Kuebler P, Bendell JC, Kumar P, Lewis D, Tan B, Bertagnolli M, Grothey A, Hochster HS, Goldberg RM, Venook A, Blanke C, O'Reilly EM, Shields AF. Effect of Celecoxib *vs* Placebo Added to Standard Adjuvant Therapy on Disease-Free Survival Among Patients With Stage III Colon Cancer: The CALGB/SWOG 80702 (Alliance) Randomized Clinical Trial. *JAMA* 2021; **325**: 1277-1286 [PMID: 33821899 DOI: 10.1001/jama.2021.2454]

132 **Turano M**, Cammarota F, Duraturo F, Izzo P, De Rosa M. A Potential Role of IL-6/IL-6R in the Development and Management of Colon Cancer. *Membranes (Basel)* 2021; **11** [PMID: 33923292 DOI: 10.3390/membranes11050312]

133 **Zhao H**, Wu L, Yan G, Chen Y, Zhou M, Wu Y, Li Y. Inflammation and tumor progression: signaling pathways and targeted intervention. *Signal Transduct Target Ther* 2021; **6**: 263 [PMID: 34248142 DOI: 10.1038/s41392-021-00658-5]

134 **Vaghari-Tabari M**, Majidinia M, Moein S, Qujeq D, Asemi Z, Alemi F, Mohamadzadeh R, Targhazeh N, Safa A, Yousefi B. MicroRNAs and colorectal cancer chemoresistance: New solution for old problem. *Life Sci* 2020; **259**: 118255

[PMID: 32818543 DOI: 10.1016/j.lfs.2020.118255]

135 **Azwar S**, Seow HF, Abdullah M, Faisal Jabar M, Mohtarrudin N. Recent Updates on Mechanisms of Resistance to 5-Fluorouracil and Reversal Strategies in Colon Cancer Treatment. *Biology (Basel)* 2021; **10** [PMID: 34571731 DOI: 10.3390/biology10090854]

136 **van Meeteren LA**, Thorikay M, Bergqvist S, Pardali E, Stampino CG, Hu-Lowe D, Goumans MJ, ten Dijke P. Anti-human activin receptor-like kinase 1 (ALK1) antibody attenuates bone morphogenetic protein 9 (BMP9)-induced ALK1 signaling and interferes with endothelial cell sprouting. *J Biol Chem* 2012; **287**: 18551-18561 [PMID: 22493445 DOI: 10.1074/jbc.M111.338103]

137 **Panda PK**, Naik PP, Praharaj PP, Meher BR, Gupta PK, Verma RS, Maiti TK, Shanmugam MK, Chinnathambi A, Alharbi SA, Sethi G, Agarwal R, Bhutia SK. Abrus agglutinin stimulates BMP-2-dependent differentiation through autophagic degradation of β-catenin in colon cancer stem cells. *Mol Carcinog* 2018; **57**: 664-677 [PMID: 29457276 DOI: 10.1002/mc.22791]

138 **Kim BR**, Oh SC, Lee DH, Kim JL, Lee SY, Kang MH, Lee SI, Kang S, Joung SY, Min BW. BMP-2 induces motility and invasiveness by promoting colon cancer stemness through STAT3 activation. *Tumour Biol* 2015; **36**: 9475-9486 [PMID: 26124007 DOI: 10.1007/s13277-015-3681-y]

139 **Todaro M**, Gaggianesi M, Catalano V, Benfante A, Iovino F, Biffoni M, Apuzzo T, Sperduti I, Volpe S, Cocorullo G, Gulotta G, Dieli F, De Maria R, Stassi G. CD44v6 is a marker of constitutive and reprogrammed cancer stem cells driving colon cancer metastasis. *Cell Stem Cell* 2014; **14**: 342-356 [PMID: 24607406 DOI: 10.1016/j.stem.2014.01.009]

140 **Mizuno R**, Kawada K, Itatani Y, Ogawa R, Kiyasu Y, Sakai Y. The Role of Tumor-Associated Neutrophils in Colorectal Cancer. *Int J Mol Sci* 2019; **20** [PMID: 30691207 DOI: 10.3390/ijms20030529]

141 **Yahaya MAF**, Lila MAM, Ismail S, Zainol M, Afizan NARNM. Tumour-Associated Macrophages (TAMs) in Colon Cancer and How to Reeducate Them. *J Immunol Res* 2019; **2019**: 2368249 [PMID: 30931335 DOI: 10.1155/2019/2368249]

142 **Wang S**, Miao Z, Yang Q, Wang Y, Zhang J. The Dynamic Roles of Mesenchymal Stem Cells in Colon Cancer. *Can J Gastroenterol Hepatol* 2018; **2018**: 7628763 [PMID: 30533404 DOI: 10.1155/2018/7628763]

143 **Yu Z**, Lou L, Zhao Y. Fibroblast growth factor 18 promotes the growth, migration and invasion of MDAMB231 cells. *Oncol Rep* 2018; **40**: 704-714 [PMID: 29901199 DOI: 10.3892/or.2018.6482]

144 **Gonzalez-Zubeldia I**, Dotor J, Redrado M, Bleau AM, Manrique I, de Aberasturi AL, Villalba M, Calvo A. Co-migration of colon cancer cells and CAFs induced by TGFβ$_1$ enhances liver metastasis. *Cell Tissue Res* 2015; **359**: 829-839 [PMID: 25557989 DOI: 10.1007/s00441-014-2075-6]

145 **Vinnakota K**, Zhang Y, Selvanesan BC, Topi G, Salim T, Sand-Dejmek J, Jönsson G, Sjölander A. M2-like macrophages induce colon cancer cell invasion *via* matrix metalloproteinases. *J Cell Physiol* 2017; **232**: 3468-3480 [PMID: 28098359 DOI: 10.1002/jcp.25808]

146 **Wu D**, Ding Y, Wang T, Cui P, Huang L, Min Z, Xu M. Significance of Tumor-Infiltrating Immune Cells in the Prognosis of Colon Cancer. *Onco Targets Ther* 2020; **13**: 4581-4589 [PMID: 32547088 DOI: 10.2147/OTT.S250416]

147 **Silva DA**, Yu S, Ulge UY, Spangler JB, Jude KM, Labão-Almeida C, Ali LR, Quijano-Rubio A, Ruterbusch M, Leung I, Biary T, Crowley SJ, Marcos E, Walkey CD, Weitzner BD, Pardo-Avila F, Castellanos J, Carter L, Stewart L, Riddell SR, Pepper M, Bernardes GJL, Dougan M, Garcia KC, Baker D. De novo design of potent and selective mimics of IL-2 and IL-15. *Nature* 2019; **565**: 186-191 [PMID: 30626941 DOI: 10.1038/s41586-018-0830-7]

148 **Fisher RC**, Bellamkonda K, Alex Molina L, Xiang S, Liska D, Sarvestani SK, Chakrabarti S, Berg A, Jorgensen ML, Hatala D, Chen S, Aiello A, Appelman HD, Scott EW, Huang EH. Disrupting Inflammation-Associated CXCL8-CXCR1 Signaling Inhibits Tumorigenicity Initiated by Sporadic- and Colitis-Colon Cancer Stem Cells. *Neoplasia* 2019; **21**: 269-281 [PMID: 30738331 DOI: 10.1016/j.neo.2018.12.007]

149 **Wang X**, Yang L, Huang F, Zhang Q, Liu S, Ma L, You Z. Inflammatory cytokines IL-17 and TNF-α up-regulate PD-L1 expression in human prostate and colon cancer cells. *Immunol Lett* 2017; **184**: 7-14 [PMID: 28223102 DOI: 10.1016/j.imlet.2017.02.006]

150 **Feng X**, Zhang Z, Sun P, Song G, Wang L, Sun Z, Yuan N, Wang Q, Lun L. Interleukin-18 Is a Prognostic Marker and Plays a Tumor Suppressive Role in Colon Cancer. *Dis Markers* 2020; **2020**: 6439614 [PMID: 33294056 DOI: 10.1155/2020/6439614]

151 **Pastille E**, Wasmer MH, Adamczyk A, Vu VP, Mager LF, Phuong NNT, Palmieri V, Simillion C, Hansen W, Kasper S, Schuler M, Muggli B, McCoy KD, Buer J, Zlobec I, Westendorf AM, Krebs P. The IL-33/ST2 pathway shapes the regulatory T cell phenotype to promote intestinal cancer. *Mucosal Immunol* 2019; **12**: 990-1003 [PMID: 31165767 DOI: 10.1038/s41385-019-0176-y]

152 **De la Fuente López M**, Landskron G, Parada D, Dubois-Camacho K, Simian D, Martinez M, Romero D, Roa JC, Chahuán I, Gutiérrez R, Lopez-K F, Alvarez K, Kronberg U, López S, Sanguinetti A, Moreno N, Abedrapo M, González MJ, Quera R, Hermoso-R MA. The relationship between chemokines CCL2, CCL3, and CCL4 with the tumor microenvironment and tumor-associated macrophage markers in colorectal cancer. *Tumour Biol* 2018; **40**: 1010428318810059 [PMID: 30419802 DOI: 10.1177/1010428318810059]

153 **Halama N**, Zoernig I, Berthel A, Kahlert C, Klupp F, Suarez-Carmona M, Suetterlin T, Brand K, Krauss J, Lasitschka F, Lerchl T, Luckner-Minden C, Ulrich A, Koch M, Weitz J, Schneider M, Buechler MW, Zitvogel L, Herrmann T, Benner A, Kunz C, Luecke S, Springfeld C, Grabe N, Falk CS, Jaeger D. Tumoral Immune Cell Exploitation in Colorectal Cancer Metastases Can Be Targeted Effectively by Anti-CCR5 Therapy in Cancer Patients. *Cancer Cell* 2016; **29**: 587-601 [PMID: 27070705 DOI: 10.1016/j.ccell.2016.03.005]

154 **Noh GT**, Kwon J, Kim J, Park M, Choi DW, Cho KA, Woo SY, Oh BY, Lee KY, Lee RA. Verification of the role of exosomal microRNA in colorectal tumorigenesis using human colorectal cancer cell lines. *PLoS One* 2020; **15**: e0242057 [PMID: 33175885 DOI: 10.1371/journal.pone.0242057]

155 **Ma J**, Sun X, Wang Y, Chen B, Qian L. Fibroblast-derived CXCL12 regulates PTEN expression and is associated with the proliferation and invasion of colon cancer cells *via* PI3k/Akt signaling. *Cell Commun Signal* 2019; **17**: 119 [PMID: 31500630 DOI: 10.1186/s12964-019-0432-5]

156 **Calvo N**, Martín MJ, de Boland AR, Gentili C. Involvement of ERK1/2, p38 MAPK, and PI3K/Akt signaling pathways in the regulation of cell cycle progression by PTHrP in colon adenocarcinoma cells. *Biochem Cell Biol* 2014; **92**: 305-315 [PMID: 25051885 DOI: 10.1139/bcb-2013-0106]

157 **Calvo N**, Carriere P, Martin MJ, Gentili C. RSK activation *via* ERK modulates human colon cancer cells response to PTHrP. *J Mol Endocrinol* 2017; **59**: 13-27 [PMID: 28385776 DOI: 10.1530/JME-16-0216]

158 **Meurette O**, Mehlen P. Notch Signaling in the Tumor Microenvironment. *Cancer Cell* 2018; **34**: 536-548 [PMID: 30146333 DOI: 10.1016/j.ccell.2018.07.009]

159 **Al-Haidari A**, Algaber A, Madhi R, Syk I, Thorlacius H. MiR-155-5p controls colon cancer cell migration *via* post-transcriptional regulation of Human Antigen R (HuR). *Cancer Lett* 2018; **421**: 145-151 [PMID: 29471005 DOI: 10.1016/j.canlet.2018.02.026]

160 **Mussnich P**, Rosa R, Bianco R, Fusco A, D'Angelo D. MiR-199a-5p and miR-375 affect colon cancer cell sensitivity to cetuximab by targeting PHLPP1. *Expert Opin Ther Targets* 2015; **19**: 1017-1026 [PMID: 26107137 DOI: 10.1517/14728222.2015.1057569]

World Journal of Gastroenterology

Submit a Manuscript: https://www.f6publishing.com

World J Gastroenterol 2022 July 14; 28(26): 3047-3062

DOI: 10.3748/wjg.v28.i26.3047

ISSN 1007-9327 (print) ISSN 2219-2840 (online)

REVIEW

Role of baicalin as a potential therapeutic agent in hepatobiliary and gastrointestinal disorders: A review

Risha Ganguly, Ashutosh Gupta, Abhay K Pandey

Specialty type: Gastroenterology and hepatology

Provenance and peer review: Invited article; Externally peer reviewed.

Peer-review model: Single blind

Peer-review report's scientific quality classification
Grade A (Excellent): 0
Grade B (Very good): B
Grade C (Good): C
Grade D (Fair): 0
Grade E (Poor): 0

P-Reviewer: Sitkin S, Russia; Wan XH, China
A-Editor: Ribeiro IB, Brazil

Received: January 16, 2022
Peer-review started: January 16, 2022
First decision: March 8, 2022
Revised: March 21, 2022
Accepted: May 21, 2022
Article in press: May 21 2022
Published online: July 14, 2022

Risha Ganguly, Ashutosh Gupta, Abhay K Pandey, Department of Biochemistry, University of Allahabad, Allahabad (Prayagraj) 211002, Uttar Pradesh, India

Corresponding author: Abhay K Pandey, PhD, Full Professor, Department of Biochemistry, University of Allahabad, Faculty of Science, Katra, Allahabad (Prayagraj) 211002, Uttar Pradesh, India. akpandey23@rediffmail.com

Abstract

Baicalin is a natural bioactive compound derived from *Scutellaria baicalensis*, which is extensively used in traditional Chinese medicine. A literature survey demonstrated the broad spectrum of health benefits of baicalin such as antioxidant, anticancer, anti-inflammatory, antimicrobial, cardio-protective, hepatoprotective, renal protective, and neuroprotective properties. Baicalin is hydrolyzed to its metabolite baicalein by the action of gut microbiota, which is further reconverted to baicalin *via* phase 2 metabolism in the liver. Many studies have suggested that baicalin exhibits therapeutic potential against several types of hepatic disorders including hepatic fibrosis, xenobiotic-induced liver injury, fatty liver disease, viral hepatitis, cholestasis, ulcerative colitis, hepatocellular and colorectal cancer. During *in vitro* and *in vivo* examinations, it has been observed that baicalin showed a protective role against liver and gut-associated abnormalities by modifying several signaling pathways such as nuclear factor-kappa B, transforming growth factor beta 1/SMAD3, sirtuin 1, p38/mitogen-activated protein kinase/Janus kinase, and calcium/calmodulin-dependent protein kinase kinaseβ/adenosine monophosphate-activated protein kinase/acetyl-coenzyme A carboxylase pathways. Furthermore, baicalin also regulates the expression of fibrotic genes such as smooth muscle actin, connective tissue growth factor, β-catenin, and inflammatory cytokines such as interferon gamma, interleukin-6 (IL-6), tumor necrosis factor-alpha, and IL-1β, and attenuates the production of apoptotic proteins such as caspase-3, caspase-9 and B-cell lymphoma 2. However, due to its low solubility and poor bioavailability, widespread therapeutic applications of baicalin still remain a challenge. This review summarized the hepatic and gastrointestinal protective attributes of baicalin with an emphasis on the molecular mechanisms that regulate the interaction of baicalin with the gut microbiota.

Key Words: Baicalin; Biotransformation; Gut microbiota; Hepatobiliary and gastrointestinal disorders; Signaling pathways

Core Tip: Baicalin possesses therapeutic efficacy against hepatic and gastrointestinal diseases including hepatic fibrosis, xenobiotic-induced liver injury, fatty liver disease, viral hepatitis, cholestasis, ulcerative colitis, hepatocellular and colorectal cancer. The drug action is mediated through its interaction with the gut microbiota, modulation of several signaling pathways, and inflammatory factors. The limitations of low solubility, permeability, and bioavailability pose challenges in the therapeutic applications. The different modes of drug delivery used in the transport of baicalin for ready absorption have paved the way for its use as a pharmacological agent against hepato-intestinal disorders.

Citation: Ganguly R, Gupta A, Pandey AK. Role of baicalin as a potential therapeutic agent in hepatobiliary and gastrointestinal disorders: A review. *World J Gastroenterol* 2022; 28(26): 3047-3062
URL: https://www.wjgnet.com/1007-9327/full/v28/i26/3047.htm
DOI: https://dx.doi.org/10.3748/wjg.v28.i26.3047

INTRODUCTION

The liver is the largest and central digestive organ in the body, which plays a vital role in several physiological processes including growth, nutrition, immunity, and metabolism of xenobiotics[1-3]. The hepatobiliary system mainly consists of the liver, and intra-hepatic and extra-hepatic bile ducts including the gall bladder. The liver in association with the intestine plays an essential role in digestion with the help of digestive enzymes, which facilitate the breakdown of larger biomolecules into simpler forms such as monosaccharides, amino acids, fatty acids, and glycerol. The intestinal microbiota also interacts with bile and other digestive juices, aiding the process of digestion. The complex network of molecular pathways and signal molecules that are involved in the functioning of the hepatobiliary system are also part of the immune cascade[4-6]. Therefore, any disruption in the gastrointestinal (GI) tract or gut microbiota results in the generation of an inflammatory response. Hepatic disorders such as fibrosis, viral hepatitis, non-alcoholic fatty liver, cirrhosis, cholestasis, and hepatocellular carcinoma (HCC) can be identified by alteration in the levels of inflammatory cytokines such as tumor necrosis factor-alpha (TNF-α), interleukin-6 (IL-6), IL-1β, and nuclear factor-kappa B (NF-κB)[7,8]. Researchers in the past two decades have found numerous natural compounds, which have the ability to interact with the gut microbiome and aid in the treatment of diseases of the hepatobiliary system[9,10]. Natural products and their derivatives form a group of compounds known as secondary metabolites produced by the plants. Several such metabolites such as silymarin, ellagic acid, phyllanthin, rutin, and glycyrrhizin have been used to treat hepatic fibrosis, viral hepatitis, fatty liver disease, and cirrhosis[11,12].

Baicalin (5, 6-dihydroxy-7-O-glucuronide) is a flavonoid isolated predominantly from the roots of *Scutellaria baicalensis* (*S. baicalensis*), a Chinese medicinal herb that belongs to the family Lamiaceae and is widely known as Chinese skullcap[13]. The roots of *S. baicalensis* also contain several other significant bioactive molecules such as baicalein and wogonin[14]. Numerous *in vitro* and *in vivo* studies have indicated different pharmacological properties of baicalin, which include anti-oxidative, antiviral, anti-inflammatory, cardioprotective, hepatoprotective, neuroprotective, and pro-apoptotic properties. These biological activities can be attributed to the ability of baicalin to target multiple pathways and bind with several signaling molecules[15-18]. In addition, baicalin possesses anti-obese, antidyslipidemia, and pro-apoptotic effects, which help to improve hepatic function after injury, alleviate liver diseases due to alcohol abuse, and promote apoptosis of proliferating hepatocytes[19].

In the last two decades, there has been growing interest and research on the hepatoprotective and anticancer properties of baicalin indicated by the increasing number of publications on PubMed. In recent years (2017 to present), there has been a remarkable rise in the number of research and review articles on the biological potential of baicalin as shown in Figure 1. This review gives an account of the therapeutic effects of baicalin exerted on the hepatobiliary system and the mitigation of GI and liver-associated disorders. The use of baicalin alone or in combination with drugs in several *in vitro* and *in vivo* experiments in the last two decades, impact of baicalin on the gut microbiota, its interaction with molecules and receptors at different molecular pathways, and the range of doses at which baicalin has shown maximum activity have also been discussed.

SOURCES OF BAICALIN

Baicalin is the most abundant and important bioactive ingredient obtained from the roots of the

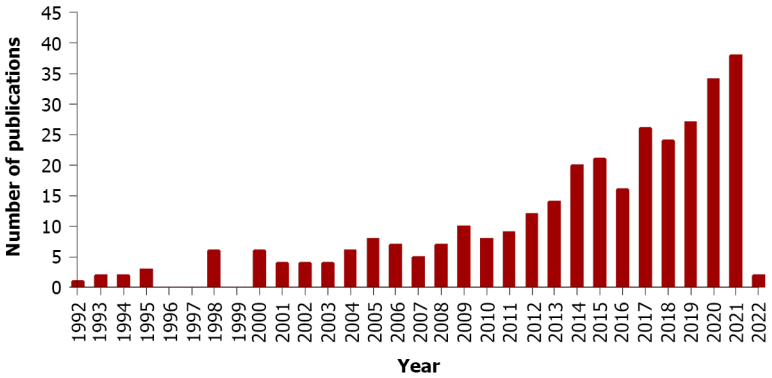

DOI: 10.3748/wjg.v28.i26.3047

Figure 1 Increasing trend of publications on "hepatoprotective and anticancer properties of baicalin" indexed by PubMed.

medicinal plant *S. baicalensis*[20]. The roots of *S. baicalensis* possess baicalin in the range of 8% to 15%. Baicalin is also the main component of other species of *Scutellaria* such as *S. rivularia*, *S. galericulata*, and *S. lateriflora*[21,22]. Baicalin, chrysin, and its glucoside derivatives have also been obtained from various other parts of the popular Asian medicinal plant *Oroxylum indicum*, belonging to the family Bignoniaceae[23]. Baicalin, and its aglycone baicalein, are gaining increasing importance in the pharmaceutical, food, and cosmetics industries due to their remarkable biological properties. Baicalin and baicalein, in particular, have shown anti-inflammatory effects and the potential to ameliorate mitochondrial dysfunction[24], and combination strategies with baicalin or baicalein as chemotherapy adjuncts have been shown to be effective in various cancers and associated signaling pathways[25]. Due to growing interest in the properties of baicalin as a potential therapeutic agent, many studies in last few years have focused on developing appropriate techniques for the identification and quantification of baicalin in raw drug formulations including simple thin layer chromatography, and different modifications of the sophisticated technique of high-performance liquid chromatography[26,27].

CHEMISTRY AND BIOAVAILABILITY

Baicalin is a flavone glycoside (molecular mass = 446.4 g/moL; melting point = 202-205 °C), which is hydrolyzed to its aglycone baicalein in the stomach after ingestion. Baicalin is hydrolyzed to baicalein immediately after administration with the help of β-glucuronidase from gut bacteria. Baicalein is reconverted to baicalin in the systemic circulation by uridine 5'-diphospho(UDP)-glucuronosyltransferase-glucuronosyl transferase *via* phase 2 metabolism[21]. It is noteworthy that the circulating baicalin in the system is not the parent molecule but the conjugated metabolite of baicalein. Circulating baicalin returns to the GI system primarily by bile excretion in the form of glucuronides. The bile excretion of baicalin is mainly mediated by the multidrug resistance (MDR) protein 2 transporter. When baicalin and baicalein are given orally, the conjugated metabolites actually contribute to the *in vivo* effect because the glucuronide/sulfate of baicalin circulates predominantly in plasma[25]. Baicalin is moderately absorbed in the stomach and poorly absorbed in the small and large intestines (Figure 2).

PHARMACOKINETICS OF BAICALIN IN THE GI SYSTEM

The pharmacokinetic profile of baicalin in the GI system involves hydrolysis, enterohepatic recycling, carrier-mediated transport, and complex routes of metabolism with the interaction of gut microbiota. Baicalin administration is safe and endurable, and no evidence of liver or kidney toxicity has been recorded. The main obstacles to the clinical use of baicalin are its low water solubility (approximately 67.0 μg/mL) and bioavailability. Several nano-techniques such as solid nanocrystals, nanoemulsions, and lipid-based solid nanoparticles have been used to improve baicalin lysis, thus improving bioavailability[28-30]. Incomplete absorption in the GI system has emerged as the main barrier to bioavailability [31]. MDR protein 2 is the most important transporter of baicalin, which mediates bile outflow to hepatocytes[32]. In fact, biliary excretion of baicalin in rats with MDR protein 2 deficiency is significantly reduced with a significant increase in plasma baicalin levels[33]. Baicalin is also capable of crossing the blood-brain barrier and may be protective against a variety of neurodegenerative diseases [34,35].

β-glucuronidase and UDP-glucuronosyltransferase are important metabolic enzymes involved in the *in vivo* transformation of baicalin. In fact, five bile metabolites have been identified in rat liver after

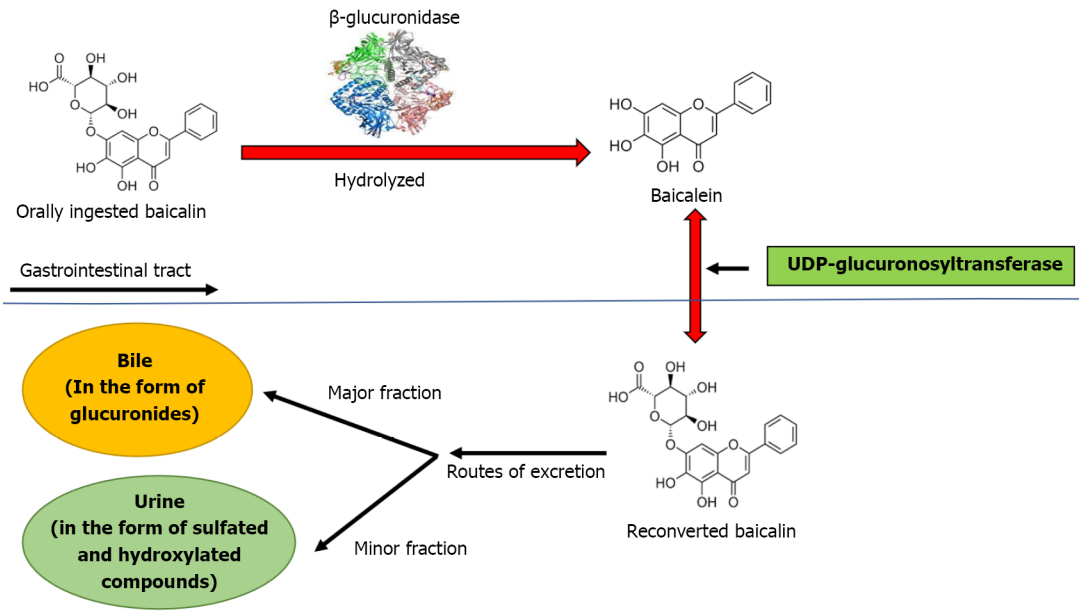

DOI: 10.3748/wjg.v28.i26.3047

Figure 2 Biotransformation of baicalin after oral ingestion. Orally administered baicalin is hydrolyzed to baicalein by β-glucuronidase. Further, baicalein is reconverted to baicalin by uridine 5'-diphospho-glucuronosyltransferase in intestine. The major part of baicalin excretion takes place *via* the biliary route in the form of glucuronides, and a small fraction of baicalin is excreted *via* urine in the form of sulfated and hydroxylated compounds. UDP: Uridine 5'-diphospho.

baicalin administration. The main metabolites include baicalein 6,7diβ-glucopyranuloside and 6oβ-glucopyranuronosyl baicalein-7 sulfate. These conjugated metabolites are hydrolyzed to baicalein in the GI tract by β-glucuronidase/sulfatase. Thirty-two baicalin metabolites have been reported in plasma, urine, and other rat tissues using more efficient approaches[36,37]. In terms of tissue distribution, liver and kidney contain most of the metabolites, indicating that these are the major sites of baicalin metabolism. Baicalin undergoes multiple chemical transformations *in vivo* including hydrolysis, methylation, hydroxylation, methoxylation, glucuronide conjugates, sulfate conjugates, and their combined reactions[37]. The pharmacokinetics of baicalin may help to understand its therapeutic implications in the liver. As a result of enterohepatic circulation, baicalin remains particularly concentrated in the liver and is thus beneficial in the treatment of hepatic anomalies. Baicalein also plays a crucial role in the treatment of hepatic diseases, indicating that the mechanism of baicalin's emphasis on liver-associated disorders may include the ameliorative effects of the metabolites as well. The major part of baicalin excretion takes place *via* the biliary route in the form of glucuronides, and a small fraction of baicalin is excreted *via* urine in the form of sulfated and hydroxylated compounds[38,39].

AMELIORATING EFFECTS OF BAICALIN AGAINST HEPATIC AND COLORECTAL DISEASES

Fatty liver syndrome

Fatty liver syndrome (FLS) occurs due to excess accumulation of non-esterified fatty acids in the hepatocytes. FLS accounts for approximately one-fourth of all liver-related anomalies in the world[40]. FLS causes several hepatic anomalies such as non-alcoholic fatty liver disease, non-alcoholic steatohepatitis (NASH), and advanced FLS may also lead to cirrhosis and ultimately hepatic failure[17,41]. Due to its antioxidant and hepatoprotective potential, baicalin is effective against FLS and associated diseases. Baicalin improves lipid metabolism and suppresses hepatic lipid production by inhibiting the calcium/calmodulin-dependent protein kinase kinase-β/adenosine monophosphate-activated protein kinase (AMPK)/acetyl-coenzyme A (CoA) carboxylase pathway[42,43]. Additionally, baicalin binds directly to carnitine palmitoyl-transferase-1α (CPT-1α) and promotes the influx of lipid into mitochondria, where it is oxidized[44]. Baicalin also downregulates lipid-producing genes such as fatty acid synthase (FASN), peroxisome proliferator-activated receptor-α (PPAR-α), and sterol regulatory element-binding protein-1c (SREBP-1c) to inhibit lipid accumulation in the liver[42,45]. Baicalin (200 mg/kg) has been found to reduce the expression of TNF-α, monocyte chemoattractant protein (MCP-1) and IL-1β, downregulate caspase-3 to alleviate NASH induced by a methionine- and choline-deficient (MCD) diet. In addition, treatment with baicalin can partially lessen the accumulation of lipids induced by the MCD diet in the liver by modulating the expression of SREBP-1c, FASN, PPAR-α, and CPT-1α

[46]. Moreover, baicalin (50 mg/kg) also reduces the synthesis of inflammatory cytokines including TNF-α, IL-6, and IL-1β, and suppresses the Toll-like receptor 4 (TLR-4) signaling pathways in MCD diet fed mice to inhibit fat accumulation in liver. Thus, baicalin also acts as an anti-inflammatory compound in the attenuation of non-alcoholic FLS[47]. In a study of high-fat diet induced FLS, it was found that baicalin (25-100 mg/kg) exerted a substantial ameliorating effect on FLS by activating the expression of hepatic PPAR-γ receptors[48]. In addition, baicalin (5 g/kg) also alleviates FLS by reducing the levels of serum hepatic enzymes such as aspartate aminotransferase (AST) and alanine aminotransferase (ALT), and inflammatory mediators such as TNF-α and MCP-1. Moreover, baicalin also inhibited the phosphorylation of Janus kinase (JNK), and suppressed the production of inflammatory enzyme cyclooxygenase-2 and pro-oxidative enzyme CYP-2E1 in the liver of a mouse model[49]. In another study of orotic acid-induced FLS, baicalin (12.5-50 mg/kg) downregulated SREBP-1c and upregulated AMPK to reduce the toxic effects of free fatty acids, subsequently inhibiting fat accumulation in the liver [45]. In an *in vitro* study of palmitic acid-induced FLS in AML-12 hepatocytes, baicalin (6.25-25 μM) alleviated FLS by reducing endoplasmic reticulum stress and suppression of the thioredoxin-interacting protein/Nod-like receptor protein 3 pathway[50].

Liver injury

The liver is the most important organ for the metabolism and elimination of toxins from the human body. Normal liver function can be deterred with excessive hepatic injuries, which occur due to a variety of factors including alcohol intake, chemical contaminants, hepatocellular ischemia, and drug damage[50,51]. Liver damage is a complex process that can manifest extensive hepatocellular apoptosis [52]. Baicalin (120 mg/kg) has been shown to alleviate alcohol-induced liver injury in a rat model *via* the reduced expression of inflammatory cytokines such as TNF-α, IL-6 and IL-1β and enhances the activity of antioxidant enzymes such as superoxide dismutase (SOD) and glutathione peroxidase (GSH-Px), which is further regulated by blocking the sonic-hedgehog signaling pathway[19]. Similarly, baicalin (30 mg/kg) has been shown to produce anti-inflammatory effects by downregulating the expression of IL-17 in a rat model with acetaminophen-induced liver injury[53]. Baicalin (80 and 200 mg/kg) activates heme oxygenase-1 *via* the nuclear respiratory factor (NRF)-2 antioxidant pathway and inhibits the activity of reactive oxygen species (ROS) generating enzymes in a liver injury model. Baicalin plays an important role in blocking the combination of NRF-2 and Kelch-like ECH-associated protein 1 (Keap-1) that causes phosphorylation of NRF-2, thus reversing liver damage[54,55]. Furthermore, baicalin (60 mg/kg) also downregulates extracellular signal-regulated kinase (ERK) in acetaminophen-induced liver injury[56]. In addition, baicalin (100 mg/kg) downregulates caspase-3 and caspase-9 and also increases the expression of the anti-apoptotic protein B-cell lymphoma 2 (Bcl-2). This helps to significantly reduce NG-nitro-L-arginine methyl ester-induced liver injury in rats[57].

The therapeutic effect of baicalin on reducing liver damage *via* the apoptotic pathway has also been demonstrated *via in vitro* experiments (Table 1). Baicalin at 100 μmol/L regulates apoptotic proteins such as caspase-3, caspase-9, and Bcl-2 associated X (Bax), and has a considerable therapeutic impact on the hypoxic model of L02 human hepatocytes[58]. Another *in vitro* study with L02 hepatocytes and acetaldehyde-treated HepG2 cells were used to identify the adverse effects of baicalin (20-100 mmol/L) on progression of the epithelial-mesenchymal transition (EMT) in the liver, which is an indicator of liver fibrosis and inflammation. This study demonstrated that baicalin considerably suppressed the progression of EMT by downregulating the transforming growth factor-β (TGF-β)/Smad signaling pathway, thus ameliorating liver damage[59]. Studies have shown that baicalin (60 μM) can repair liver injury in nanosecond pulse electric field (ns-PEF)-induced damage to L02 hepatocytes by stabilizing mitochondrial transmembrane potential and prevent excess ROS production[60]. Furthermore, baicalin (5 and 25 μM) can suppress the oxidation and nitrification of the hemin/nitrite/hydrogen peroxide system and protect HepG2 cells by inhibiting lipid peroxidation and GSH depletion[61]. Another study emphasized that baicalin administration (74 mg/kg) can restore the metabolism of amino acids to normal, improve the tricarboxylic acid cycle and ameliorate acute lipopolysaccharide (LPS)-induced sepsis in mice model[62].

Liver fibrosis

Liver fibrosis occurs due to excess deposition of extracellular matrix proteins and collagen. It is characterized by hepatic tissue degeneration, inflammatory cell infiltration and hepatic cell necrosis[63,64]. It has also been confirmed that activation of hepatic stellate cells (HSCs) plays a central role in liver fibrosis[65]. In the absence of appropriate treatment, advanced liver fibrosis causes chronic hepatitis subsequently leading to liver cancer or cirrhosis[66,67]. In a recent study, it was shown that baicalin (200 mg/kg) decreased the expression of fibrotic genes such as α-smooth muscle actin (SMA) and connective tissue growth factor and inflammatory cytokines such as TNF-α, macrophage inflammatory protein-1α (MIP-1α), IL-1β, MIP-2, thereby effectively suppressing liver fibrosis induced by bile duct ligation (BDL) in mice. In addition, an *in vitro* study also showed the efficacy of baicalin in reducing the activation of HSCs and downregulating the expression of SMA, fibronectin, tissue inhibitor of metalloproteinase-1 (TIMP1) protein andcollagen-1[68]. Similarly, baicalin (150 μM) reduced microRNA (miR)-3595 expression and increased the activity of the enzyme long-chain fatty acid CoA ligase 4, significantly inhibiting the activity of HSCs leading to a reduction in fibrosis in HSCT6 hepatocyte cell lines caused

Table 1 *In vitro* hepatoprotective effects of baicalin on different cell lines

Disease/type of study	Cell line	Dose	Mechanism/target pathways	Ref.
Palmitic acid-induced fatty liver	AML-12 hepatocytes	6.25-25 μM	ER stress↓; TXNIP/NLRP-3 pathway ↓	[50]
Hypoxic liver injury	L02 human hepatocytes	100 μmol/L	Caspase-3, caspase-9, and Bax↓	[58]
Acetaldehyde induced EMT	HepG2 cells	20-100 mmol/L	TGF-β/Smad pathway↓	[59]
ns-PEF induced liver injury	L02 hepatocytes	60 μM	MTP stabilization, ROS↓	[60]
Hemin-nitrite-H_2O_2 induced liver injury	HepG2 cells	5 μM and 25 μM	Lipid peroxidation↓; GSH depletion↓	[61]
PDGF-BB induced fibrosis	HSCT6 hepatocytes	150 μM	miR-3595↓; ACSL-4↑	[69]
BDL-induced fibrosis	HSCs	67.5-270 μM	Wnt pathway↓; PPAR-γ↓	[70]
LPS-induced hepatitis	L20, THLE cell lines	25-100 μM	TUG-1↑; p38-MAPK↓; JNK pathway↓	[82]
Viral hepatitis	HuH7, HepG2 cells	75 μg/mL	NF-κB pathway↓	[83]
	pHBV1.2HepG2 cells	10 μM	HNF-4α/HNF-1α↓	[84]
	HepG2.2.15 cells	10 μg/kg	HBsAg, HBeAg↓	[85]
	PBMCs	50-200 mg/mL	Mitochondrial pathway↑; Caspase 3↑	[87]
HCC	HepG2-HCC	100 μmol/L	ER-mediated TF-6↑; S-2P protein↑	[94]
	SMMC7721-HCC cells	160 μM	CD47↓	[95]
	SMMC7721, HepG2-HCC cells	40 μM	STAT3, IFN-γ↓; Block PDL-1/PD-1 pathway	[96,97]

ACSL-4: Long chain fatty acid CoA ligase 4; AML: Alpha mouse liver; BDL: Bile duct ligation; EMT: Epithelial-mesenchymal transition; ER: Endoplasmic reticulum; GSH: Reduced glutathione; HCC: Hepatocellular carcinoma; HSCs: Hepatic stellate cells; LPS: Lipopolysaccharide; MAPK: Mitogen-activated protein kinase; MTP: Mitochondrial transmembrane potential; NLRP-3: Nod-like receptor protein 3; nsPEF: Nanosecond-pulse electric field; PBMCs: Peripheral blood mononuclear cells; PDGF-BB: Platelet-derived growth factor BB; PPAR-γ: Peroxisome proliferator-activated receptor-γ; ROS: Reactive oxygen species; THLE: Transformed human liver epithelial; TUG-1: Taurine upregulated-1; TXNIP: Thioredoxin-interacting protein.

by platelet-derived growth factor BB[69]. Moreover, baicalin (67.5-270 μM) helps in the reduction of BDL-induced activity of HSCs by inhibiting PPAR-γ *via* Wnt signaling, leading to alleviation of liver fibrosis[70]. Baicalin (100 mg/kg) attenuated carbon tetrachloride-induced hepatic fibrosis in mice by regulating the rise in TGF-β1, hydroxyproline, type III collagen, and hyaluronic acid laminin (Table 2). In addition, baicalin also attenuates liver fibrosis by suppressing the activity of antioxidant enzymes SOD and GSH-Px[71]. Similarly, baicalin (25-100 mg/kg) evidently reduces the level of PPAR-γ, suppresses the activity of HSCs, and downregulates the expression of TGF-β1, causing inhibition of hepatic fibrosis[72].

Cholestasis

Cholestasis is a condition that occurs due to the obstruction or complete blockage of bile secretion through the intrahepatic or extrahepatic bile ducts[73]. Consequently, there is excess accumulation of conjugated bilirubin, bile salts, and cholesterol in the liver, which leads to hepatic injury and damage to the human body[74]. Baicalin plays an important role at several stages to mitigate cholestasis and related hepatic damage. Baicalin specifically targets nuclear factor-erythroid factor 2-related factor 2 (NRF-2) in reversing cholestasis. Recent studies in a mouse model indicate that the interaction of baicalin (50 mg/kg) with NRF-2, inflammatory cytokines, and oxidative stress regulatory elements forms the central pathway of reducing cholestasis induced hepatic damage. Baicalin is capable of activating SMA, TIMP1, and collagen, resulting in amelioration of liver fibrosis due to BDL-induced cholestasis[68]. Another pharmacokinetic study in a rat model indicated that administration of baicalin (50-200 mg/kg) has therapeutic potential for cholestasis. It significantly increases bile excretion rates, which lead to a decline in serum levels of total bile acids as well as hepatic enzymes such as AST, ALT, and alkaline phosphatase in 17α-ethinyl estradiol-induced cholestasis[75,76]. In estrogen-induced cholestasis, it has been shown that baicalin targets NF-κB and inhibits the expression of inflammatory markers such as TNF-α, IL-6, and IL-1β, thereby increasing the activity of hepatic bile acid-metabolizing enzymes. Reports have also shown that baicalin alleviates 17α-ethinyl estradiol-induced cholestasis in mice by suppressing the expression of multidrug resistance protein 2 and bile salt export pump genes *via* the sirtuin 1/nuclear hepatic receptor 1α (HNF-1α)/farnesoid X receptor (FXR) pathway[77].

Table 2 *In vivo* protective effects of baicalin on various hepatobiliary and colorectal disorders

Disease/type of study	Dose	Mechanism/target pathway	Ref.
MCD induced NASH	200 mg/kg	TNF-α, MCP-1, IL-1β↓; Caspase-3↓; SREBP-1c, FASN, PPAR-α, CPT-1α↓	[46]
	50 mg/kg	TNF-α, IL-6, IL-1β↓; TLR-4 pathway↓	[47]
High fat diet induced non- alcoholic FLS	25-100 mg/kg	PPAR-γ receptors↑	[48]
	5 g/kg	AST, ALT↓; TNF-α, MCP-1↓; JNK-P↓; COX-2, CYP-2E1↓	[49]
Orotic acid induced FLS	12.5-50 mg/kg	SREBP-1c↓; AMPK↑	[45]
Alcohol-induced liver injury	120 mg/kg	TNF-α, IL-6, IL-1β↓; SOD, GSH-Px↑; Block sonic-hedgehog pathway	[19]
	200 mg/kg	HO-1, NRF-2 pathway↑	[54]
Acetaminophen-induced liver injury	30 mg/kg	IL-17↓	[53]
	80 mg/kg	NRF-2, Keap-1↓	[55]
	60 mg/kg	ERK↓	[56]
NG-nitro-L-arginine methyl ester induced liver injury	100 mg/kg	Caspases-3 and 9↓; Bcl-2↑	[57]
LPS-induced sepsis	74 mg/kg	Amino acid metabolism↑; TCA cycle↑	[62]
BDL-induced liver fibrosis	200 mg/kg	SMA, CTGF↓; TNF-α, MIP-1α, IL-1β, MIP-2↓	[68]
CCl_4-induced fibrosis	100 mg/kg	TGF-β1, hydroxyproline, type III collagen, hyaluronic acid laminin↑; SOD, GSH-Px↓	[71]
	25-100 mg/kg	PPAR-γ↓; TGF-β1↓	[72]
17α- ethinyl estradiol-induced cholestasis	50-200 mg/kg	TBA, AST, ALT, ALP↓; TNF-α, IL-6 and IL-1β↓	[75,76]
		Sirt1/HNF-1α/FXR pathway↓	[77]
Hepatitis B in young duck model	10 μg/kg	HBsAg, HBeAg↓; HNF-4α/HNF-1α↓	[85]
Hepatitis in male BALB/c mouse model	100-200 mg/kg	TNF-α, IL-6 and IFN-γ↓	[86]
Hepatitis in male Sprague-Dawley rat model	0.5-5.0 mg/kg	ALT, AST↓	[86]
HCC	50 mg/kg	RelB/p52 pathway↑	[93]
CRC in mice	100, 200 mg/kg	TGF-β/Smad pathway↓	[100]
TNBS-induced UC	30-90 mg/kg	IL-1β, TNF-α↓; Caspase 9, Bcl-2↓; IKK/IKB/NF-κB pathway↓	[107]
	5-20 mg	IL-1β, TNF-α, IL-6↓; TLR4/NF-κB pathway↓	[108]
	30-120 mg/kg	Catalase, GSH-PX, SOD↑; Bcl-2↑; MDA↓; TGF-β, Bax↓	[109]
HTHE-induced UC	100 mg/kg	NF-κB, MAPK pathways↓	[110]
DSS-induced UC	50-150 mg/kg	MPO, NO↓; IL-1β, TNF-α and IL-6↑	[111]
	100 mg/kg	TLR-4/NF-κB-p65/IL-6 pathway↓; TNF-α, IL-6, IL-13↓	[112]
TNBS-induced UC	10 mg/kg	MIF, MCP-1, MIP-3a↓	[113]
	20-100mg/kg	Maintain Th17/Treg balance	[114]

ALP: Alkaline phosphatase; ALT: Alanine transaminase; AST: Aspartate transaminase; AMPK; AMP-activated protein kinase; Bcl-2: B-cell lymphoma 2; CCL_4: Carbon tetrachloride; COX-2: Cyclooxygenase-2; CPT-1α: Carnitine palmitoyl-transferase-1α; CRC: Colorectal cancer; CTGF: Connective tissue growth factor; CYP-2E1: Cytochrome P450 2E1; DSS: Dextran sulfate sodium; ERK: Extracellular signal-regulated kinase; FASN: Fatty acid synthase; FLS: Fatty liver syndrome; FXR: Farnesoid X receptor; GSH-Px: Glutathione peroxidase; HBsAg: Hepatitis B surface antigen; HBeAg: Hepatitis B e antigen; HNF: hepatic nuclear factor; HO-1: Heme oxygenase 1; HTHE: High temperature and humid environment; IL-1: Interleukin-1; JNK: c-Jun N-terminal kinase; Keap-1: Kelch-like ECH-associated protein 1; MCD: Methionine- and choline-deficient; MCP-1: Monocyte chemoattractant protein-1; MIP-1α: Macrophage inflammatory protein-1 alpha; NASH: Non-alcoholic steatohepatitis; NF-κB: Nuclear factor-kappa B; NRF2: Nuclear factor-erythroid factor 2-related factor 2; PPAR-γ: Peroxisome proliferator-activated receptor-γ; Sirt: Sirtuin; SMA: Smooth muscle actin; SOD: Superoxide dismutase; SREBP: Sterol

regulatory element-binding protein; TBA: Total bile acid; TCA: Tricarboxylic acid cycle; Th17: T helper 17 cells; TLR-4: Toll-like receptor 4; TNBS: 2,4,6-trinitrobenzenesulfonic acid; TNF-α: Tumor necrosis factor-alpha; Treg: Regulatory T cells; UC: Ulcerative colitis.

Hepatitis

Hepatitis caused by hepatitis A virus (HAV), hepatitis B virus (HBV), and other viral hepatitis are prevalent infectious diseases worldwide[78,79]. Liver-specific proteins and immune complex hypersensitivity have multiple roles in hepatitis[80]. Subsequent studies have proven that baicalin plays a key role in the attenuation of hepatitis by lowering the levels of hepatitis B surface antigen (HBsAg), viral antigen protein hepatitis B e-antigen (HBeAg), and hepatitis B virus (HBV)-DNA, and regulating oxidative stress, inflammation, and apoptosis in hepatic cells[80,81]. It has been found that baicalin (25-100 μM) significantly increases *taurine upregulated 1* gene expression to suppress inflammation and apoptosis by downregulating the p38-mitogen activated protein kinase (MAPK) and JNK signaling pathways in L20 and transformed human liver epithelial cell lines to thwart LPS-induced hepatitis[82]. Another recent study showed that baicalin (75 μg/mL) significantly suppressed HBV replication and inflammation by downregulating the NF-κB signaling pathway in HepG2 and HuH7 cells[83]. Furthermore, it has also been confirmed that baicalin (10 μM) strongly suppresses the transcription of HBV by downregulating the liver-specific HNF-4α/HNF-1α axis in pHBV1.2 HepG2 cells[84]. In another experiment, baicalin (10 μg/kg) significantly reduced HBsAg and HBeAg levels in HepG2 cells, wild-type HBV cells, and young duck models infected with HBV by downregulating the HNF-4α/HNF-1α axis[85]. In addition, baicalin pre-treatment (100-200 mg/kg) attenuated elevated levels of plasma cytokines such as TNF-α, IL-6, and interferon-γ (IFN-γ) in male BALB/c mouse models, resulting in alleviation of hepatocyte necrosis and apoptosis[86]. Similarly in an *in vivo* study, pre-treatment with baicalin (0.5-5.0 mg/kg) considerably reduced serum levels of ALT and AST and lowered hepatic oxidative stress in a male Sprague-Dawley rat model[86]. Another study demonstrated the pro-oxidant properties of baicalin (50-200 mg/mL) by upregulating the mitochondrial signaling pathway in human peripheral blood mononuclear cells, thereby inducing the activation of caspase-3 and apoptosis[87]. Furthermore, baicalin has often been co-administered with other bioactive flavonoids in combination studies, to yield better results at prevention of hepatitis. For instance, combination of the alkaloid oxymatrine (1 g/L) with baicalin showed more efficacy against HBV than oxymatrine alone[88]. Below 31.50 μg/mL, the baicalin-phospholipid complex exhibits direct anti-duck HAV-1 activity by preventing the adsorption, replication, and release of duck HAV-1 and indirectly by promoting immunity in ducklings[89]. Baicalin (20 μg/mL) regulates the immunomodulatory effects and anti-HAV-1 reproduction by reducing the adsorption and release of HAV-1 in duck-suppressed embryonic hepatocytes[90].

HCC

HCC ranks sixth amongst the most common malignant tumors worldwide, and is the fourth highest cause of mortality due to malignancies[91]. The present modes of treatment for HCC include radiation therapy, local resection therapy, surgery, and liver transplantation. However, these treatments typically cause several side effects and have adverse consequences[91,92]. Several studies have reported that baicalin can effectively ameliorate HCC by indirectly inducing autophagy in liver tumor cells. Studies have revealed that baicalin (50 mg/kg) promotes the polarization of tumor-related macrophages into M1-like macrophages, subsequently increasing autophagy in cancerous cells to make them non-proliferating. Additionally, baicalin mediated anti-cancer effects may also be closely associated with activation of the RelB/p52 signaling pathway[93]. Similarly, baicalin (100 μmol/L) promotes apoptosis in HepG2-HCC cells by activating the ER-mediated TF-6 signaling cascade combined with S-2P protein [94]. Moreover, baicalin (160 μM) suppresses cluster of differentiation 47 and activates apoptosis and autophagy in SMMC7721-HCC cells[95]. Although nsPEFs have been developed as a new mode of treatment for cancer, they also result in the elimination of normal hepatocytes. Therefore, a study was designed combining nsPEF and baicalin for the treatment of HCC, which revealed that baicalin suppresses the proliferation of HCC cells, and protects normal liver cells by increasing mitochondrial membrane potential and reducing ROS production[59]. In recent times, cancer immunotherapy has emerged as a significant line of treatment for HCC. Baicalin (40 μM) is capable of reducing the activity of signal transducer and activator of transcription 3 protein and IFN-γ, thereby blocking the programmed death-ligand 1/programmed cell death protein 1 pathway. This increases the sensitivity of the immune system to hepatic cancerous cells and thus further activates T cells against hepatic cancer cells[96,97]. Based on several *in vitro* and *in vivo* studies, the protective effect of baicalin on many hepatic disorders is summarized in Tables 1 and 2.

Colorectal cancer

Colorectal cancer (CRC) is also a common malignant tumor worldwide, and is primarily due to genetic inheritance, colon polyps, and ulcerative colitis (UC)[98,99]. Baicalin, due to its pro-apoptotic properties, results in the killing of CRC cells. Researchers have used the human colon cancer cell line (HCT-166)

and transplanted colon tumors into mice to conduct simultaneous *in vivo* and *in vitro* experiments to examine the antitumor mechanism of baicalin (100 and 200 mg/kg). Baicalin induces apoptosis in colon tumors by inhibiting the cells at the G1 stage and arresting EMT protein expression by blocking the TGF-β/Smad pathway[100]. Baicalin (40 mmol/L) promotes Dickkopf protein expression, suppresses the expression of proteins β-catenin and c-Myc, and inhibits miR-217 expression, thereby leading to the apoptosis of HCT-166 cancer cells by inhibition of the Wnt signaling pathway[101]. Another similar study demonstrated that apoptosis of HT-29 colon cancer cells was induced by baicalin (50-200 μM) *via* inhibition of c-Myc expression and regulation of the miR-10a, miR-23a, miR-31, miR-151a, and miR-205 mechanism[14]. Similarly, it has been reported that the antioxidant properties of baicalin (40 μM) increase progesterone expression in the intestine and leads to the apoptosis of HCT-116 colon cancer cells by activating the Ras/Raf/MEK/ERK pathways[102]. Reports have also shown that the antitumor activity of baicalin can be further enhanced by glycosidase pre-treatment[103]. Several studies have revealed that the development of CRC is closely associated with genetic mutations. In a study on colon cancer cells SW-480, baicalin (50-400 μg/mL) inhibited the expression of the transcription factor SP-1, leading to the apoptosis of cancer cells[104].

Inflammatory bowel disease

Inflammatory bowel disease (IBD) is a collective term that refers to the chronic inflammation of GI tract. The two major types of IBD are Crohn's disease (CD) and UC. CD and UC are nonspecific chronic IBDs that cause inflammation and ulcers on the inner lining of the large intestine[105-107]. Baicalin plays an important role in the treatment of IBD, as it is capable of suppressing oxidative stress, immune regulation, and its anti-inflammatory properties. In addition, baicalin is capable of regulating NF-κB activation, which modulates both autophagic and inflammatory processes in intestinal epithelial cells, subsequently leading to enhancement in paracellular permeability. Baicalin alleviates dextran sulfate sodium (DSS)-induced UC by modulating the polarization of M1 macrophages to the M2 phenotype [107]. Dose-dependent administration of baicalin (30-90 mg/kg) has been found to largely downregulate the inflammatory cytokines IL-1β and TNF-α, and apoptotic genes Bcl-2 and caspase-9 in the colon tissue of rats affected by 2,4,6-trinitrobenzenesulfonic acid (TNBS)-induced UC. In addition, baicalin also inhibits the inhibitory κB (IKB) kinase (IKK)/IKB/NF-κB signaling pathway, leading to the alleviation of IBD[107,108]. Likewise, in another study, rats with TNBS-induced UC were given baicalin (5-20 mg) which resulted in the downregulation of inflammatory factors TNF-α, IL-6 and IL-1β in rat intestine and inhibition of the TLR4/NF-κB signaling pathway, leading to alleviation of UC[109]. Furthermore, baicalin (30-120 mg/kg) has also been effective in the treatment of TNBS-induced UC by promoting antioxidant enzymes such as catalase, SOD and GSH-PX, and reducing malondialdehyde (MDA). Baicalin also suppresses the regulation of apoptosis by upregulating Bcl-2 and downregulating TGF-β and Bax[110]. In a UC model generated by high temperature and humid environment, baicalin (100 mg/kg) significantly reduced the serum levels of IL-6, IL-1β, and IL-17, and inhibited SOD, GSH-PX, and MDA. That study attributed the anti-inflammatory effect of baicalin to suppression of the NF-κB and MAPK pathways[111]. In an *in vivo* study, baicalin (50-150 mg/kg) reduced myeloperoxidase activity, nitric oxide content, and elevated IL-1β, TNF-α and IL-6 levels in the colon of DSS-induced UC rats[112]. Another study revealed that baicalin (100 mg/kg) attenuated DSS-induced UC by blocking the TLR-4/NF-κB-p65/IL-6 signaling pathway and suppressing TNF-α, IL-6, and IL-13 mRNA expression [113]. Furthermore, baicalin (10 mg/kg) downregulated the expression of macrophage migration inhibitory factor, MCP-1 and MIP-3a in the colon tissue of TNBS-induced UC rat model[114]. Several reports have suggested the association of T helper 16 cell (Th17)/regulatory T cell (Treg) equilibrium with UC. Baicalin (20-100 mg/kg) regulates the Th17/Treg balance by inhibiting the rise in ROS and MDA, whereas simultaneously reducing GSH and SOD levels and regulating the expression of Th17-related factors IL-6 and IL-17 in TNBS-induced UC rats[115,116]. In a clinical study of UC patients, baicalin promoted the production of immune cells like CD4+ and CD29+ and induced immunomodulation to alleviate UC[117] (Figure 3).

INTERACTION OF BAICALIN WITH THE INTESTINAL MICROBIOTA

In the past decade, the intestinal microbiota has become an emerging aspect of research for the evaluation of several diseases. Besides playing an important role in the metabolism and breakdown of biomolecules into simpler molecules like fatty acids, amino acids, vitamins and bile salts, the gut microbiota is also capable of interacting with the host and affect the functioning of various organs including the liver and kidney to regulate homeostasis and disease development[5,118]. Baicalin, a flavonoid, exerts many therapeutic effects by modulating gut microbiota homeostasis. Intake of high fat diet causes imbalance of the gut microbiota, leading to several metabolic syndromes. Baicalin administered (200 mg/kg/d) to mice with high fat diet induced metabolic syndrome led to an increase in short-chain fatty acid (SCFA)-producing gut bacteria, thereby effectively reducing the metabolic syndrome in mice[119]. Baicalin also reduces damage to the intestinal barrier caused due to hypertension. A study reported that baicalin (100 mg/kg) significantly increased the number of SCFA-

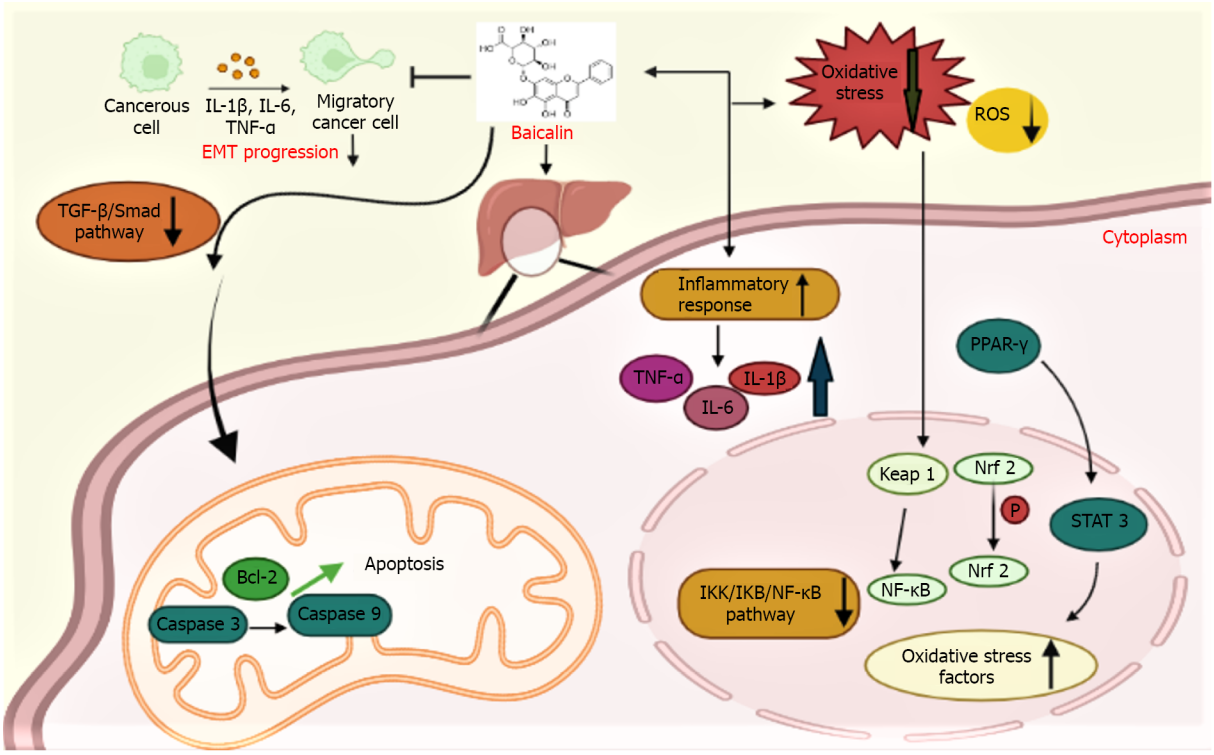

DOI: 10.3748/wjg.v28.i26.3047

Figure 3 Mechanism of baicalin action against hepatobiliary diseases. Baicalin downregulated peroxisome proliferator-activated receptor-α and activated the nuclear respiratory factor-2 antioxidant pathway to reduce oxidative stress in the hepatocytes. Baicalin suppressed epithelial-mesenchymal transition progression by downregulating the transforming growth factor-β/Smad pathway, inhibited the inhibitory κB (IKB) kinase/IKB/nuclear factor-kappa B pathway, reduced the elevated levels of inflammatory factors such as tumor necrosis factor-α, interleukin-6 (IL-6) and IL-1β, and attenuated the apoptotic proteins caspase-3, caspase-9, B-cell lymphoma 2, which led to the alleviation of liver diseases. ROS: Reactive oxygen species; STAT: Signal transducer and activator of transcription; PPAR-γ: Peroxisome proliferator-activated receptor-γ; IL: Interleukin; Nrf2: Nuclear respiratory factor-2; TGF-β: Transforming growth factor-β; NF-κB: Nuclear factor-kappa B; TNF-α: Tumor necrosis factor-alpha; Bcl-2: B-cell lymphoma 2; EMT: Epithelial-mesenchymal transition; IKK: Inhibitory κB kinase; IKB: Inhibitory κB.

producing bacteria and altered the intestinal microflora, leading to a reduction in damage of the intestinal barrier in rats caused by hypertension[120]. Another study revealed that baicalin (25-100 mg/kg) helped increase SCFA-producing bacteria such as *Eubacterium* spp, *Subdoligranulum* spp, and *Butyricimonas* spp, thereby ameliorating TNBS-induced UC[114]. In some cases, the gut microbiome can also downregulate the therapeutic efficacy of baicalin[121]. The gut microbiota regulates hepatobiliary homeostasis *via* the gut-hepatic axis, and although it can regulate baicalin activity, baicalin can also modulate the gut microbiota[122]. Consequently, baicalin has the potential to exert a therapeutic role in liver and gut diseases by modulating FXR and TGR5-mediated crosstalk involving bile acids associated with the gut microbiome.

DRUG DELIVERY, CLINICAL TRIAL, AND FUTURE PROSPECTS

The clinical application of baicalin in pharmacology has been challenging, due to its low solubility and bioavailability. In the last decade, many researchers have designed novel delivery strategies for baicalin that include phospholipid complex, liposomes, solid baicalin nanocrystals, and micelle formation[123]. The dissolution and solubility of baicalin is considerably enhanced when administered in combination with other molecules in complex form. For instance, baicalin has exhibited improved oral bioavailability, distribution, targeting, and therapeutic efficacy when combined with polyethylene glycol and folic acid in the form of liposomes. β-Cyclodextrin complex has also been used as an effective formulation to facilitate the effective delivery of baicalin with wide range of therapeutic outcomes[123, 124]. Moreover, baicalin is commonly used as adjuvant therapy for hepatitis. In a clinical study, single dose baicalin (500 mg/kg) in combination with cyclosporin A was found to be safe and well tolerated in adult human subjects without any severe adverse effects[125]. However, the co-administration of baicalin with other herbal formulations or drugs might impede baicalin's *in vivo* actions and consequently its efficacy. Therefore, it is important to thoroughly study the clinically approved doses of baicalin which can be administered in combination with other compounds that help to improve the absorption and effectiveness of baicalin.

CONCLUSION

GI disorders have emerged as the leading cause of mortality in the recent years across the world. Baicalin, a major flavone obtained from *S. baicalensis*, exerts protective effect against hepatobiliary and colorectal disorders by modulating signaling pathways. Further, novel delivery strategies that are used in the transport of baicalin for ready absorption including phospholipid complex, liposomes, solid baicalin nanocrystals, and β-cyclodextrin complex have paved way for its widespread use as a pharmacological alternative in hepatic and GI disorders.

ACKNOWLEDGEMENTS

All of the authors acknowledge DST-FIST and UGC-SAP facilities of the Department of Biochemistry, University of Allahabad, Prayagraj, India.

FOOTNOTES

Author contributions: Ganguly R performed the literature review and wrote the manuscript; Ganguly R and Gupta A made the tables and figures; Pandey AK conceptualized the idea, critically reviewed and revised the manuscript; All authors have read and approved the final manuscript.

Supported by University Grants Commission, New Delhi, India in The Form of UGC-Junior and Senior Research Fellowships.

Conflict-of-interest statement: All the authors report no relevant conflicts of interest for this article.

Country/Territory of origin: India

ORCID number: Risha Ganguly 0000-0002-6190-8923; Ashutosh Gupta 0000-0002-6547-6312; Abhay K Pandey 0000-0002-4774-3085.

S-Editor: Fan JR
L-Editor: Filipodia
P-Editor: Fan JR

REFERENCES

1 **Gupta A**, Pandey AK. Aceclofenac-induced hepatotoxicity: An ameliorative effect of *Terminalia bellirica* fruit and ellagic acid. *World J Hepatol* 2020; **12**: 949-964 [PMID: 33312421 DOI: 10.4254/wjh.v12.i11.949]
2 **Sharma UK**, Kumar R, Ganguly R, Gupta A, Pandey AK. Cinnamaldehyde, an active component of cinnamon provides protection against food color induced oxidative stress and hepatotoxicity in albino wistar rats. *Vegetos* 2018; **31**: 123-129 [DOI: 10.5958/2229-4473.2018.00063.0]
3 **Gupta A**, Kumar R, Ganguly R, Singh AK, Rana HK, Pandey AK. Antioxidant, anti-inflammatory and hepatoprotective activities of *Terminalia bellirica* and its bioactive component ellagic acid against diclofenac induced oxidative stress and hepatotoxicity. *Toxicol Rep* 2021; **8**: 44-52 [PMID: 33391996 DOI: 10.1016/j.toxrep.2020.12.010]
4 **Björkholm B**, Bok CM, Lundin A, Rafter J, Hibberd ML, Pettersson S. Intestinal microbiota regulate xenobiotic metabolism in the liver. *PLoS One* 2009; **4**: e6958 [PMID: 19742318 DOI: 10.1371/journal.pone.0006958]
5 **Kumar S**, Kumar R, Dwivedi A, Pandey AK. In vitro antioxidant, antibacterial, and cytotoxic activity and in vivo effect of *Syngonium podophyllum* and *Eichhornia crassipes* leaf extracts on isoniazid induced oxidative stress and hepatic markers. *Biomed Res Int* 2014; **2014**: 459452 [PMID: 25162013 DOI: 10.1155/2014/459452]
6 **Hu Q**, Zhang W, Wu Z, Tian X, Xiang J, Li L, Li Z, Peng X, Wei S, Ma X, Zhao Y. Baicalin and the liver-gut system: Pharmacological bases explaining its therapeutic effects. *Pharmacol Res* 2021; **165**: 105444 [PMID: 33493657 DOI: 10.1016/j.phrs.2021.105444]
7 **Xiong F**, Guan YS. Cautiously using natural medicine to treat liver problems. *World J Gastroenterol* 2017; **23**: 3388-3395 [PMID: 28596675 DOI: 10.3748/wjg.v23.i19.3388]
8 **Rajaratnam M**, Prystupa A, Lachowska-Kotowska P, Załuska W, Filip R. Herbal medicine for treatment and prevention of liver diseases. *J Pre Clin Clin Res* 2014; **8**: 55-60

9 **Kumar Singh A**, Cabral C, Kumar R, Ganguly R, Kumar Rana H, Gupta A, Rosaria Lauro M, Carbone C, Reis F, Pandey AK. Beneficial Effects of Dietary Polyphenols on Gut Microbiota and Strategies to Improve Delivery Efficiency. *Nutrients* 2019; **11**: 2216 [PMID: 31540270 DOI: 10.3390/nu11092216]

10 **Sharma UK**, Kumar R, Gupta A, Ganguly R, Singh AK, Ojha AK, Pandey AK. Ameliorating efficacy of eugenol against metanil yellow induced toxicity in albino Wistar rats. *Food Chem Toxicol* 2019; **126**: 34-40 [PMID: 30738991 DOI: 10.1016/j.fct.2019.01.032]

11 **Sharma AK**, Kumar S, Chashoo G, Saxena AK, Pandey AK. Cell cycle inhibitory activity of *Piper longum* against A549 cell line and its protective effect against metal-induced toxicity in rats. *Indian J Biochem Biophys* 2014; **51**: 358-364 [PMID: 25630105]

12 **Sharma UK**, Sharma AK, Gupta A, Kumar R, Pandey A, Pandey AK. Pharmacological activities of cinnamaldehyde and eugenol: antioxidant, cytotoxic and anti-leishmanial studies. *Cell Mol Biol (Noisy-le-grand)* 2017; **63**: 73-78 [PMID: 28968213 DOI: 10.14715/cmb/2017.63.6.15]

13 **Waisundara VY**, Hsu A, Tan BK, Huang D. Baicalin reduces mitochondrial damage in streptozotocin-induced diabetic Wistar rats. *Diabetes Metab Res Rev* 2009; **25**: 671-677 [PMID: 19688721 DOI: 10.1002/dmrr.1005]

14 **Tao Y**, Zhan S, Wang Y, Zhou G, Liang H, Chen X, Shen H. Baicalin, the major component of traditional Chinese medicine *Scutellaria baicalensis* induces colon cancer cell apoptosis through inhibition of oncomiRNAs. *Sci Rep* 2018; **8**: 14477 [PMID: 30262902 DOI: 10.1038/s41598-018-32734-2]

15 **Zheng WX**, Wang F, Cao XL, Pan HY, Liu XY, Hu XM, Sun YY. Baicalin protects PC-12 cells from oxidative stress induced by hydrogen peroxide *via* anti-apoptotic effects. *Brain Inj* 2014; **28**: 227-234 [PMID: 24456060 DOI: 10.3109/02699052.2013.860469]

16 **Chen H**, Xu Y, Wang J, Zhao W, Ruan H. Baicalin ameliorates isoproterenol-induced acute myocardial infarction through iNOS, inflammation and oxidative stress in rat. *Int J Clin Exp Pathol* 2015; **8**: 10139-10147 [PMID: 26617721]

17 **Zhong X**, Liu H. Baicalin attenuates diet induced nonalcoholic steatohepatitis by inhibiting inflammation and oxidative stress *via* suppressing JNK signaling pathways. *Biomed Pharmacother* 2018; **98**: 111-117 [PMID: 29247950 DOI: 10.1016/j.biopha.2017.12.026]

18 **Lei K**, Shen Y, He Y, Zhang L, Zhang J, Tong W, Xu Y, Jin L. Baicalin represses C/EBP*β* *via* its antioxidative effect in Parkinson's Disease. *Oxid Med Cell Longev* 2020; **2020**: 8951907 [PMID: 32566108 DOI: 10.1155/2020/8951907]

19 **Wang H**, Zhang Y, Bai R, Wang M, Du S. Baicalin attenuates alcoholic liver injury through modulation of hepatic oxidative stress, inflammation and sonic hedgehog pathway in rats. *Cell Physiol Biochem* 2016; **39**: 1129-1140 [PMID: 27576501 DOI: 10.1159/000447820]

20 **Li-Weber M**. New therapeutic aspects of flavones: the anticancer properties of *Scutellaria* and its main active constituents wogonin, baicalein and baicalin. *Cancer Treat Rev* 2009; **35**: 57-68 [PMID: 19004559 DOI: 10.1016/j.ctrv.2008.09.005]

21 **Noh K**, Kang Y, Nepal MR, Jeong KS, Oh DG, Kang MJ, Lee S, Kang W, Jeong HG, Jeong TC. Role of Intestinal Microbiota in Baicalin-Induced Drug Interaction and its pharmacokinetics. *Molecules* 2016; **21**: 337 [PMID: 26978333 DOI: 10.3390/molecules21030337]

22 **Sowndhararajan K**, Deepa P, Kim M, Park SJ, Kim S. Neuroprotective and cognitive enhancement potentials of baicalin: a review. *Brain Sci* 2018; **8** [PMID: 29891783 DOI: 10.3390/brainsci8060104]

23 **Dinda B**, SilSarma I, Dinda M, Rudrapaul P. *Oroxylum indicum* (L.) Kurz, an important Asian traditional medicine: from traditional uses to scientific data for its commercial exploitation. *J Ethnopharmacol* 2015; **161**: 255-278 [PMID: 25543018 DOI: 10.1016/j.jep.2014.12.027]

24 **Mu X**, He G, Cheng Y, Li X, Xu B, Du G. Baicalein exerts neuroprotective effects in 6-hydroxydopamine-induced experimental parkinsonism in vivo and in vitro. *Pharmacol Biochem Behav* 2009; **92**: 642-648 [PMID: 19327378 DOI: 10.1016/j.pbb.2009.03.008]

25 **Chen H**, Gao Y, Wu J, Chen Y, Chen B, Hu J, Zhou J. Exploring therapeutic potentials of baicalin and its aglycone baicalein for hematological malignancies. *Cancer Lett* 2014; **354**: 5-11 [PMID: 25128647 DOI: 10.1016/j.canlet.2014.08.003]

26 **Lin M**, Tsai MJ, Wen KC. Supercritical fluid extraction of flavonoids from *Scutellariae* Radix. *J Chromatogr A* 1999; **830**: 387-395 [DOI: 10.1016/S0021-9673(98)00906-6]

27 **Yang R**, Zeng HJ, Wang QW, Guo C, Li JJ, Qu LB. Simultaneous determination of eight active components in Chinese medicine 'JiangYaBiFeng' tablet by HPLC coupled with diode array detection. *J Pharm Biomed Anal* 2011; **55**: 552-556 [PMID: 21376498 DOI: 10.1016/j.jpba.2011.01.021]

28 **Taiming L**, Xuehua J. Investigation of the absorption mechanisms of baicalin and baicalein in rats. *J Pharm Sci* 2006; **95**: 1326-1333 [PMID: 16628739 DOI: 10.1002/jps.20593]

29 **Hao J**, Wang F, Wang X, Zhang D, Bi Y, Gao Y, Zhao X, Zhang Q. Development and optimization of baicalin-loaded solid lipid nanoparticles prepared by coacervation method using central composite design. *Eur J Pharm Sci* 2012; **47**: 497-505 [PMID: 22820033 DOI: 10.1016/j.ejps.2012.07.006]

30 **Zhao L**, Wei Y, Huang Y, He B, Zhou Y, Fu J. Nanoemulsion improves the oral bioavailability of baicalin in rats: in vitro and in vivo evaluation. *Int J Nanomedicine* 2013; **8**: 3769-3779 [PMID: 24124365 DOI: 10.2147/IJN.S51578]

31 **Moore OA**, Gao Y, Chen AY, Brittain R, Chen YC. The extraction, anticancer effect, bioavailability, and nanotechnology of baicalin. *J Nutr Med Diet Care* 2016; **2** [PMID: 27790646 DOI: 10.23937/2572-3278.1510011]

32 **Kalapos-Kovács B**, Magda B, Jani M, Fekete Z, Szabó PT, Antal I, Krajcsi P, Klebovich I. Multiple ABC transporters efflux baicalin. *Phytother Res* 2015; **29**: 1987-1990 [PMID: 26400418 DOI: 10.1002/ptr.5477]

33 **Akao T**, Sato K, Hanada M. Hepatic contribution to a marked increase in the plasma concentration of baicalin after oral administration of its aglycone, baicalein, in multidrug resistance-associated protein 2-deficient rat. *Biol Pharm Bull* 2009; **32**: 2079-2082 [PMID: 19952434 DOI: 10.1248/bpb.32.2079]

34 **Tang Y**, Zhu H, Zhang Y, Huang C. Determination of human plasma protein binding of baicalin by ultrafiltration and high-performance liquid chromatography. *Biomed Chromatogr* 2006; **20**: 1116-1119 [PMID: 16708379 DOI: 10.1002/bmc.655]

35 **Liang W**, Huang X, Chen W. The effects of baicalin and baicalein on cerebral ischemia: a review. *Aging Dis* 2017; **8**:

850-867 [PMID: 29344420 DOI: 10.14336/AD.2017.0829]

36 **Abe K**, Inoue O, Yumioka E. Biliary excretion of metabolites of baicalin and baicalein in rats. *Chem Pharm Bull (Tokyo)* 1990; **38**: 209-211 [PMID: 2337942 DOI: 10.1248/CPB.38.208]

37 **Zhang J**, Cai W, Zhou Y, Liu Y, Wu X, Li Y, Lu J, Qiao Y. Profiling and identification of the metabolites of baicalin and study on their tissue distribution in rats by ultra-high-performance liquid chromatography with linear ion trap-Orbitrap mass spectrometer. *J Chromatogr B Analyt Technol Biomed Life Sci* 2015; **985**: 91-102 [PMID: 25661005 DOI: 10.1016/j.jchromb.2015.01.018]

38 **Lai CC**, Huang PH, Yang AH, Chiang SC, Tang CY, Tseng KW, Huang CH. Baicalein reduces liver injury induced by myocardial ischemia and reperfusion. *Am J Chin Med* 2016; **44**: 531-550 [PMID: 27109160 DOI: 10.1142/S0192415X16500294]

39 **Dong Y**, Xing Y, Sun J, Sun W, Xu Y, Quan C. Baicalein alleviates liver oxidative stress and apoptosis induced by high-level glucose through the activation of the PERK/Nrf2 signaling pathway. *Molecules* 2020; **25** [PMID: 32019168 DOI: 10.3390/molecules25030599]

40 **Akuta N**, Kawamura Y, Suzuki F, Saitoh S, Arase Y, Fujiyama S, Sezaki H, Hosaka T, Kobayashi M, Suzuki Y, Ikeda K, Kumada H. Analysis of association between circulating miR-122 and histopathological features of nonalcoholic fatty liver disease in patients free of hepatocellular carcinoma. *BMC Gastroenterol* 2016; **16**: 141 [PMID: 27955628 DOI: 10.1186/s12876-016-0557-6]

41 **Xi Y**, Wu M, Li H, Dong S, Luo E, Gu M, Shen X, Jiang Y, Liu Y, Liu H. Baicalin attenuates high fat diet-induced obesity and liver dysfunction: dose-response and potential role of CaMKKβ/AMPK/ACC pathway. *Cell Physiol Biochem* 2015; **35**: 2349-2359 [PMID: 25896320 DOI: 10.1159/000374037]

42 **Guo HX**, Liu DH, Ma Y, Liu JF, Wang Y, Du ZY, Wang X, Shen JK, Peng HL. Long-term baicalin administration ameliorates metabolic disorders and hepatic steatosis in rats given a high-fat diet. *Acta Pharmacol Sin* 2009; **30**: 1505-1512 [PMID: 19890358 DOI: 10.1038/aps.2009.150]

43 **Ma Y**, Yang F, Wang Y, Du Z, Liu D, Guo H, Shen J, Peng H. CaMKKβ is involved in AMP-activated protein kinase activation by baicalin in LKB1 deficient cell lines. *PLoS One* 2012; **7**: e47900 [PMID: 23110126 DOI: 10.1371/journal.pone.0047900]

44 **Dai J**, Liang K, Zhao S, Jia W, Liu Y, Wu H, Lv J, Cao C, Chen T, Zhuang S, Hou X, Zhou S, Zhang X, Chen XW, Huang Y, Xiao RP, Wang YL, Luo T, Xiao J, Wang C. Chemoproteomics reveals baicalin activates hepatic CPT1 to ameliorate diet-induced obesity and hepatic steatosis. *Proc Natl Acad Sci U S A* 2018; **115**: E5896-E5905 [PMID: 29891721 DOI: 10.1073/pnas.1801745115]

45 **Chen Q**, Liu M, Yu H, Li J, Wang S, Zhang Y, Qiu F, Wang T. *Scutellaria baicalensis* regulates FFA metabolism to ameliorate NAFLD through the AMPK-mediated SREBP signaling pathway. *J Nat Med* 2018; **72**: 655-666 [PMID: 29542003 DOI: 10.1007/s11418-018-1199-5]

46 **Zhang J**, Zhang H, Deng X, Zhang N, Liu B, Xin S, Li G, Xu K. Baicalin attenuates non-alcoholic steatohepatitis by suppressing key regulators of lipid metabolism, inflammation and fibrosis in mice. *Life Sci* 2018; **192**: 46-54 [PMID: 29158052 DOI: 10.1016/j.lfs.2017.11.027]

47 **Liu J**, Yuan Y, Gong X, Zhang L, Zhou Q, Wu S, Zhang X, Hu J, Kuang G, Yin X, Wan J. Baicalin and its nanoliposomes ameliorates nonalcoholic fatty liver disease *via* suppression of TLR4 signaling cascade in mice. *Int Immunopharmacol* 2020; **80**: 106208 [PMID: 31955065 DOI: 10.1016/j.intimp.2020.106208]

48 **Zhao W**, Liu L, Wang Y, Mao T, Li J. Effects of a combination of puerarin, baicalin and berberine on the expression of proliferator-activated receptor-γ and insulin receptor in a rat model of nonalcoholic fatty liver disease. *Exp Ther Med* 2016; **11**: 183-190 [PMID: 26889237 DOI: 10.3892/etm.2015.2846]

49 **Zhang J**, Zhang H, Deng X, Zhang Y, Xu K. Baicalin protects AML-12 cells from lipotoxicity *via* the suppression of ER stress and TXNIP/NLRP3 inflammasome activation. *Chem Biol Interact* 2017; **278**: 189-196 [PMID: 29031535 DOI: 10.1016/j.cbi.2017.10.010]

50 **Zhang HY**, Wang HL, Zhong GY, Zhu JX. Molecular mechanism and research progress on pharmacology of traditional Chinese medicine in liver injury. *Pharm Biol* 2018; **56**: 594-611 [PMID: 31070528 DOI: 10.1080/13880209.2018.1517185]

51 **Real M**, Barnhill MS, Higley C, Rosenberg J, Lewis JH. Drug-induced liver injury: highlights of the recent literature. *Drug Saf* 2019; **42**: 365-387 [PMID: 30343418 DOI: 10.1007/s40264-018-0743-2]

52 **Brenner C**, Galluzzi L, Kepp O, Kroemer G. Decoding cell death signals in liver inflammation. *J Hepatol* 2013; **59**: 583-594 [PMID: 23567086 DOI: 10.1016/j.jhep.2013.03.033]

53 **Liao CC**, Day YJ, Lee HC, Liou JT, Chou AH, Liu FC. Baicalin attenuates IL-17-mediated acetaminophen-induced liver injury in a mouse model. *PLoS One* 2016; **11**: e0166856 [PMID: 27855209 DOI: 10.1371/journal.pone.0166856]

54 **He P**, Wu Y, Shun J, Liang Y, Cheng M, Wang Y. Baicalin ameliorates liver injury induced by chronic plus binge ethanol feeding by modulating oxidative stress and inflammation *via* CYP2E1 and NRF2 in mice. *Oxid Med Cell Longev* 2017; **2017**: 4820414 [PMID: 28951767 DOI: 10.1155/2017/4820414]

55 **Shi L**, Hao Z, Zhang S, Wei M, Lu B, Wang Z, Ji L. Baicalein and baicalin alleviate acetaminophen-induced liver injury by activating Nrf2 antioxidative pathway: The involvement of ERK1/2 and PKC. *Biochem Pharmacol* 2018; **150**: 9-23 [PMID: 29338970 DOI: 10.1016/j.bcp.2018.01.026]

56 **Liao CC**, Day YJ, Lee HC, Liou JT, Chou AH, Liu FC. ERK signaling pathway plays a key role in baicalin protection against acetaminophen-induced liver injury. *Am J Chin Med* 2017; **45**: 105-121 [PMID: 28081632 DOI: 10.1142/S0192415X17500082]

57 **Wang Y**, Jia Y, Yang X, Liang B, Gao H, Yang T. A potential role of Baicalin to inhibit apoptosis and protect against acute liver and kidney injury in rat preeclampsia model. *Biomed Pharmacother* 2018; **108**: 1546-1552 [PMID: 30372856 DOI: 10.1016/j.biopha.2018.09.107]

58 **Liu F**, Zhang J, Qian J, Wu G, Ma Z. Baicalin attenuates liver hypoxia/reoxygenation injury by inducing autophagy. *Exp Ther Med* 2018; **16**: 657-664 [PMID: 30116320 DOI: 10.3892/etm.2018.6284]

59 **Wu T**, Liu T, Xing L, Ji G. Baicalin and puerarin reverse epithelial-mesenchymal transition *via* the TGF-β1/Smad3

pathway *in vitro*. *Exp Ther Med* 2018; **16**: 1968-1974 [PMID: 30186426 DOI: 10.3892/etm.2018.6400]

60 **Wang Y**, Yin S, Zhou Y, Zhou W, Chen T, Wu Q, Zhou L, Zheng S. Dual-function of Baicalin in nsPEFs-treated hepatocytes and hepatocellular carcinoma cells for different death pathway and mitochondrial response. *Int J Med Sci* 2019; **16**: 1271-1282 [PMID: 31588193 DOI: 10.7150/ijms.34876]

61 **Zhao Y**, Li H, Gao Z, Gong Y, Xu H. Effects of flavonoids extracted from *Scutellaria baicalensis* Georgi on hemin-nitrite-H2O2 induced liver injury. *Eur J Pharmacol* 2006; **536**: 192-199 [PMID: 16574098 DOI: 10.1016/j.ejphar.2006.02.045]

62 **Liao S**, Li P, Wang J, Zhang Q, Xu D, Yang M, Kong L. Protection of baicalin against lipopolysaccharide induced liver and kidney injuries based on ^{1}H NMR metabolomic profiling. *Toxicol Res (Camb)* 2016; **5**: 1148-1159 [PMID: 30090421 DOI: 10.1039/c6tx00082g]

63 **Seki E**, Brenner DA. Recent advancement of molecular mechanisms of liver fibrosis. *J Hepatobiliary Pancreat Sci* 2015; **22**: 512-518 [PMID: 25869468 DOI: 10.1002/jhbp.245]

64 **Klingenberg M**, Groß M, Goyal A, Polycarpou-Schwarz M, Miersch T, Ernst AS, Leupold J, Patil N, Warnken U, Allgayer H, Longerich T, Schirmacher P, Boutros M, Diederichs S. The long noncoding RNA cancer susceptibility 9 and RNA binding protein heterogeneous nuclear ribonucleoprotein L form a complex and coregulate genes linked to AKT signaling. *Hepatology* 2018; **68**: 1817-1832 [PMID: 29790588 DOI: 10.1002/hep.30102]

65 **Dawood RM**, El-Meguid MA, Salum GM, El Awady MK. Key players of hepatic fibrosis. *J Interferon Cytokine Res* 2020; **40**: 472-489 [PMID: 32845785 DOI: 10.1089/jir.2020.0059]

66 **Lin L**, Zhou F, Shen S, Zhang T. Fighting liver fibrosis with naturally occurring antioxidants. *Planta Med* 2018; **84**: 1318-1333 [PMID: 30312974 DOI: 10.1055/a-0757-0008]

67 **Zhao Z**, Lin CY, Cheng K. siRNA- and miRNA-based therapeutics for liver fibrosis. *Transl Res* 2019; **214**: 17-29 [PMID: 31476281 DOI: 10.1016/j.trsl.2019.07.007]

68 **Shen K**, Feng X, Pan H, Zhang F, Xie H, Zheng S. Baicalin ameliorates experimental liver cholestasis in mice by modulation of oxidative stress, inflammation, and NRF2 transcription factor. *Oxid Med Cell Longev* 2017; **2017**: 6169128 [PMID: 28757911 DOI: 10.1155/2017/6169128]

69 **Wu X**, Zhi F, Lun W, Deng Q, Zhang W. Baicalin inhibits PDGF-BB-induced hepatic stellate cell proliferation, apoptosis, invasion, migration and activation *via* the miR-3595/ACSL4 axis. *Int J Mol Med* 2018; **41**: 1992-2002 [PMID: 29393361 DOI: 10.3892/ijmm.2018.3427]

70 **Yang MD**, Chiang YM, Higashiyama R, Asahina K, Mann DA, Mann J, Wang CC, Tsukamoto H. Rosmarinic acid and baicalin epigenetically derepress peroxisomal proliferator-activated receptor γ in hepatic stellate cells for their antifibrotic effect. *Hepatology* 2012; **55**: 1271-1281 [PMID: 22095555 DOI: 10.1002/hep.24792]

71 **Wei XL**, Fang RT, Yang YH, Bi XY, Ren GX, Luo AL, Zhao M, Zang WJ. Protective effects of extracts from Pomegranate peels and seeds on liver fibrosis induced by carbon tetrachloride in rats. *BMC Complement Altern Med* 2015; **15**: 389 [PMID: 26508316 DOI: 10.1186/s12906-015-0916-9]

72 **Qiao H**, Han H, Hong D, Ren Z, Chen Y, Zhou C. Protective effects of baicalin on carbon tetrachloride induced liver injury by activating PPARγ and inhibiting TGFβ1. *Pharm Biol* 2011; **49**: 38-45 [PMID: 20687787 DOI: 10.3109/13880209.2010.493179]

73 **de Vries E**, Bolier R, Goet J, Parés A, Verbeek J, de Vree M, Drenth J, van Erpecum K, van Nieuwkerk K, van der Heide F, Mostafavi N, Helder J, Ponsioen C, Oude Elferink R, van Buuren H, Beuers U; Netherlands association for the study of the liver-cholestasis working group. Fibrates for Itch (FITCH) in fibrosing cholangiopathies: a double-blind, randomized, placebo-controlled trial. *Gastroenterology* 2021; **160**: 734-743.e6 [PMID: 33031833 DOI: 10.1053/j.gastro.2020.10.001]

74 **Salas-Silva S**, Simoni-Nieves A, Razori MV, López-Ramirez J, Barrera-Chimal J, Lazzarini R, Bello O, Souza V, Miranda-Labra RU, Gutiérrez-Ruiz MC, Gomez-Quiroz LE, Roma MG, Bucio-Ortiz L. HGF induces protective effects in α-naphthylisothiocyanate-induced intrahepatic cholestasis by counteracting oxidative stress. *Biochem Pharmacol* 2020; **174**: 113812 [PMID: 31954718 DOI: 10.1016/j.bcp.2020.113812]

75 **Zhang CL**, Xu YJ, Xiang D, Yang JY, Lei K, Liu D. Pharmacokinetic characteristics of baicalin in rats with 17α-ethynyl-estradiol-induced intrahepatic cholestasis. *Curr Med Sci* 2018; **38**: 167-173 [PMID: 30074167 DOI: 10.1007/s11596-018-1861-x]

76 **Gupta A**, Kumar R, Bhattacharyya P, Bishayee A, Pandey AK. *Terminalia bellirica* (Gaertn.) roxb. (Bahera) in health and disease: A systematic and comprehensive review. *Phytomedicine* 2020; **77**: 153278 [PMID: 32781393 DOI: 10.1016/j.phymed.2020.153278]

77 **Yang J**, Xiang D, He W, Liu Y, Lan L, Li G, Jiang C, Ren X, Liu D, Zhang C. Baicalin protects against 17α-ethinylestradiol-induced cholestasis *via* the sirtuin1/hepatic nuclear receptor-1α/farnesoid X receptor pathway. *Front Pharmacol* 2019; **10**: 1685 [PMID: 32116682 DOI: 10.3389/fphar.2019.01685]

78 **Lanini S**, Ustianowski A, Pisapia R, Zumla A, Ippolito G. Viral hepatitis: etiology, epidemiology, transmission, diagnostics, treatment, and prevention. *Infect Dis Clin North Am* 2019; **33**: 1045-1062 [PMID: 31668190 DOI: 10.1016/j.idc.2019.08.004]

79 **Suzuki K**, Suda G, Yamamoto Y, Furuya K, Baba M, Nakamura A, Miyoshi H, Kimura M, Maehara O, Yamada R, Kitagataya T, Yamamoto K, Shigesawa T, Ohara M, Kawagishi N, Nakai M, Sho T, Natsuizaka M, Morikawa K, Ogawa K, Ohnishi S, Sakamoto N; NORTE Study Group. Tenofovir-disoproxil-fumarate modulates lipid metabolism *via* hepatic CD36/PPAR-alpha activation in hepatitis B virus infection. *J Gastroenterol* 2021; **56**: 168-180 [PMID: 33211179 DOI: 10.1007/s00535-020-01750-3]

80 **Lim HK**, Jeffrey GP, Ramm GA, Soekmadji C. Pathogenesis of viral hepatitis-induced chronic liver disease: role of extracellular vesicles. *Front Cell Infect Microbiol* 2020; **10**: 587628 [PMID: 33240824 DOI: 10.3389/fcimb.2020.587628]

81 **Robertson BH**. Viral hepatitis and primates: historical and molecular analysis of human and nonhuman primate hepatitis A, B, and the GB-related viruses. *J Viral Hepat* 2001; **8**: 233-242 [PMID: 11454173 DOI: 10.1046/j.1365-2893.2001.00295.x]

82 **Huang Y**, Sun M, Yang X, Ma A, Ma Y, Zhao A. Baicalin relieves inflammation stimulated by lipopolysaccharide *via* upregulating TUG1 in liver cells. *J Physiol Biochem* 2019; **75**: 463-473 [PMID: 31396818 DOI:

10.1007/s13105-019-00698-0]
83 **Pollicino T**, Musolino C, Irrera N, Bitto A, Lombardo D, Timmoneri M, Minutoli L, Raimondo G, Squadrito G, Squadrito F, Altavilla D. Flavocoxid exerts a potent antiviral effect against hepatitis B virus. *Inflamm Res* 2018; **67**: 89-103 [PMID: 29018874 DOI: 10.1007/s00011-017-1099-2]
84 **Xia C**, Tang W, Geng P, Zhu H, Zhou W, Huang H, Zhou P, Shi X. Baicalin down-regulating hepatitis B virus transcription depends on the liver-specific HNF4α-HNF1α axis. *Toxicol Appl Pharmacol* 2020; **403**: 115131 [PMID: 32687838 DOI: 10.1016/j.taap.2020.115131]
85 **Huang H**, Zhou W, Zhu H, Zhou P, Shi X. Baicalin benefits the anti-HBV therapy *via* inhibiting HBV viral RNAs. *Toxicol Appl Pharmacol* 2017; **323**: 36-43 [PMID: 28322895 DOI: 10.1016/j.taap.2017.03.016]
86 **Hwang JM**, Tseng TH, Tsai YY, Lee HJ, Chou FP, Wang CJ, Chu CY. Protective effects of baicalein on tert-butyl hydroperoxide-induced hepatic toxicity in rat hepatocytes. *J Biomed Sci* 2005; **12**: 389-397 [PMID: 15917992 DOI: 10.1007/s11373-005-1572-8]
87 **Ueda S**, Nakamura H, Masutani H, Sasada T, Takabayashi A, Yamaoka Y, Yodoi J. Baicalin induces apoptosis *via* mitochondrial pathway as prooxidant. *Mol Immunol* 2002; **38**: 781-791 [PMID: 11841838 DOI: 10.1016/s0161-5890(01)00115-8]
88 **Cheng Y**, Ping J, Xu HD, Fu HJ, Zhou ZH. Synergistic effect of a novel oxymatrine-baicalin combination against hepatitis B virus replication, alpha smooth muscle actin expression and type I collagen synthesis in vitro. *World J Gastroenterol* 2006; **12**: 5153-5159 [PMID: 16937525 DOI: 10.3748/wjg.v12.i32.5153]
89 **Wan JY**, Gong X, Zhang L, Li HZ, Zhou YF, Zhou QX. Protective effect of baicalin against lipopolysaccharide/D-galactosamine-induced liver injury in mice by up-regulation of heme oxygenase-1. *Eur J Pharmacol* 2008; **587**: 302-308 [PMID: 18420187 DOI: 10.1016/j.ejphar.2008.02.081]
90 **Chen Y**, Zeng L, Yang J, Wang Y, Yao F, Wu Y, Wang D, Hu Y, Liu J. Anti-DHAV-1 reproduction and immuno-regulatory effects of a flavonoid prescription on duck virus hepatitis. *Pharm Biol* 2017; **55**: 1545-1552 [PMID: 28385083 DOI: 10.1080/13880209.2017.1309554]
91 **Singh AK**, Kumar R, Pandey AK. Hepatocellular carcinoma: causes, mechanism of progression and biomarkers. *Curr Chem Genom Transl Med* 2018; **12**: 9-26 [PMID: 30069430 DOI: 10.2174/2213988501812010009]
92 **Su L**, Zhou T, Zhang Z, Zhang X, Zhi X, Li C, Wang Q, Jia C, Shi W, Yue Y, Gao Y, Cheng B. Optimal staging system for predicting the prognosis of patients with hepatocellular carcinoma in China: a retrospective study. *BMC Cancer* 2016; **16**: 424 [PMID: 27387757 DOI: 10.1186/s12885-016-2420-0]
93 **Tan HY**, Wang N, Man K, Tsao SW, Che CM, Feng Y. Autophagy-induced RelB/p52 activation mediates tumour-associated macrophage repolarisation and suppression of hepatocellular carcinoma by natural compound baicalin. *Cell Death Dis* 2015; **6**: e1942 [PMID: 26492375 DOI: 10.1038/cddis.2015.271]
94 **Yu Z**, Luo X, Wang C, Ye J, Liu S, Xie L, Wang F, Bao J. Baicalin promoted site-2 protease and not site-1 protease in endoplasmic reticulum stress-induced apoptosis of human hepatocellular carcinoma cells. *FEBS Open Bio* 2016; **6**: 1093-1101 [PMID: 27833850 DOI: 10.1002/2211-5463.12130]
95 **Zhang X**, Tang X, Liu H, Li L, Hou Q, Gao J. Autophagy induced by baicalin involves downregulation of CD147 in SMMC-7721 cells in vitro. *Oncol Rep* 2012; **27**: 1128-1134 [PMID: 22200845 DOI: 10.3892/or.2011.1599]
96 **Giraud J**, Chalopin D, Blanc JF, Saleh M. Hepatocellular carcinoma immune landscape and the potential of immunotherapies. *Front Immunol* 2021; **12**: 655697 [PMID: 33815418 DOI: 10.3389/fimmu.2021.655697]
97 **Gupta A**, Singh AK, Kumar R, Ganguly R, Rana HK, Pandey PK, Sethi G, Bishayee A, Pandey AK. Corilagin in cancer: a critical evaluation of anticancer activities and molecular mechanisms. *Molecules* 2019; **24** [PMID: 31546767 DOI: 10.3390/molecules24183399]
98 **Kurilova I**, Bendet A, Petre EN, Boas FE, Kaye E, Gonen M, Covey A, Brody LA, Brown KT, Kemeny NE, Yarmohammadi H, Ziv E, D'Angelica MI, Kingham TP, Cercek A, Solomon SB, Beets-Tan RGH, Sofocleous CT. Factors associated with local tumor control and complications after thermal ablation of colorectal cancer liver metastases: a 15-year retrospective cohort study. *Clin Colorectal Cancer* 2021; **20**: e82-e95 [PMID: 33246789 DOI: 10.1016/j.clcc.2020.09.005]
99 **Singh AK**, Bishayee A, Pandey AK. Targeting histone deacetylases with natural and synthetic agents: an emerging anticancer strategy. *Nutrients* 2018; **10** [PMID: 29882797 DOI: 10.3390/nu10060731]
100 **Yang B**, Bai H, Sa Y, Zhu P, Liu P. Inhibiting EMT, stemness and cell cycle involved in baicalin-induced growth inhibition and apoptosis in colorectal cancer cells. *J Cancer* 2020; **11**: 2303-2317 [PMID: 32127957 DOI: 10.7150/jca.37242]
101 **Jia Y**, Chen L, Guo S, Li Y. Baicalin induced colon cancer cells apoptosis through miR-217/DKK1-mediated inhibition of Wnt signaling pathway. *Mol Biol Rep* 2019; **46**: 1693-1700 [PMID: 30737617 DOI: 10.1007/s11033-019-04618-9]
102 **Wang Z**, Ma L, Su M, Zhou Y, Mao K, Li C, Peng G, Zhou C, Shen B, Dou J. Baicalin induces cellular senescence in human colon cancer cells *via* upregulation of DEPP and the activation of Ras/Raf/MEK/ERK signaling. *Cell Death Dis* 2018; **9**: 217 [PMID: 29440765 DOI: 10.1038/s41419-017-0223-0]
103 **Yu C**, Zhang Z, Zhang H, Zhen Z, Calway T, Wang Y, Yuan CS, Wang CZ. Pretreatment of baicalin and wogonoside with glycoside hydrolase: a promising approach to enhance anticancer potential. *Oncol Rep* 2013; **30**: 2411-2418 [PMID: 24026776 DOI: 10.3892/or.2013.2726]
104 **Ma W**, Liu X, Du W. Baicalin induces apoptosis in SW480 cells through downregulation of the SP1 transcription factor. *Anticancer Drugs* 2019; **30**: 153-158 [PMID: 30362980 DOI: 10.1097/CAD.0000000000000708]
105 **Neurath MF**, Leppkes M. Resolution of ulcerative colitis. *Semin Immunopathol* 2019; **41**: 747-756 [PMID: 31278430 DOI: 10.1007/s00281-019-00751-6]
106 **Ungaro R**, Mehandru S, Allen PB, Peyrin-Biroulet L, Colombel JF. Ulcerative colitis. *Lancet* 2017; **389**: 1756-1770 [PMID: 27914657 DOI: 10.1016/S0140-6736(16)32126-2]
107 **Rizzo V**, Ferlazzo N, Currò M, Isola G, Matarese M, Bertuccio MP, Caccamo D, Matarese G, Ientile R. Baicalin-induced autophagy preserved LPS-stimulated intestinal cells from inflammation and alterations of paracellular permeability. *Int J Mol Sci* 2021; **22** [PMID: 33652555 DOI: 10.3390/ijms22052315]

108 **Shen J**, Cheng J, Zhu S, Zhao J, Ye Q, Xu Y, Dong H, Zheng X. Regulating effect of baicalin on IKK/IKB/NF-kB signaling pathway and apoptosis-related proteins in rats with ulcerative colitis. *Int Immunopharmacol* 2019; **73**: 193-200 [PMID: 31103874 DOI: 10.1016/j.intimp.2019.04.052]

109 **Cui L**, Feng L, Zhang ZH, Jia XB. The anti-inflammation effect of baicalin on experimental colitis through inhibiting TLR4/NF-κB pathway activation. *Int Immunopharmacol* 2014; **23**: 294-303 [PMID: 25239813 DOI: 10.1016/j.intimp.2014.09.005]

110 **Yao J**, Cao X, Zhang R, Li YX, Xu ZL, Zhang DG, Wang LS, Wang JY. Protective effect of baicalin against experimental colitis *via* suppression of oxidant stress and apoptosis. *Pharmacogn Mag* 2016; **12**: 225-234 [PMID: 27601854 DOI: 10.4103/0973-1296.186342]

111 **Liang S**, Deng X, Lei L, Zheng Y, Ai J, Chen L, Xiong H, Mei Z, Cheng YC, Ren Y. The comparative study of the therapeutic effects and mechanism of baicalin, baicalein, and their combination on ulcerative colitis rat. *Front Pharmacol* 2019; **10**: 1466 [PMID: 31920656 DOI: 10.3389/fphar.2019.01466]

112 **Zhang CL**, Zhang S, He WX, Lu JL, Xu YJ, Yang JY, Liu D. Baicalin may alleviate inflammatory infiltration in dextran sodium sulfate-induced chronic ulcerative colitis *via* inhibiting IL-33 expression. *Life Sci* 2017; **186**: 125-132 [PMID: 28802904 DOI: 10.1016/j.lfs.2017.08.010]

113 **Feng J**, Guo C, Zhu Y, Pang L, Yang Z, Zou Y, Zheng X. Baicalin down regulates the expression of TLR4 and NFkB-p65 in colon tissue in mice with colitis induced by dextran sulfate sodium. *Int J Clin Exp Med* 2014; **7**: 4063-4072 [PMID: 25550915]

114 **Dai SX**, Zou Y, Feng YL, Liu HB, Zheng XB. Baicalin down-regulates the expression of macrophage migration inhibitory factor (MIF) effectively for rats with ulcerative colitis. *Phytother Res* 2012; **26**: 498-504 [PMID: 21887805 DOI: 10.1002/ptr.3581]

115 **Zhu L**, Xu LZ, Zhao S, Shen ZF, Shen H, Zhan LB. Protective effect of baicalin on the regulation of Treg/Th17 balance, gut microbiota and short-chain fatty acids in rats with ulcerative colitis. *Appl Microbiol Biotechnol* 2020; **104**: 5449-5460 [PMID: 32322944 DOI: 10.1007/s00253-020-10527-w]

116 **Zou Y**, Dai SX, Chi HG, Li T, He ZW, Wang J, Ye CG, Huang GL, Zhao B, Li WY, Wan Z, Feng JS, Zheng XB. Baicalin attenuates TNBS-induced colitis in rats by modulating the Th17/Treg paradigm. *Arch Pharm Res* 2015; **38**: 1873-1887 [PMID: 25269538 DOI: 10.1007/s12272-014-0486-2]

117 **Yu FY**, Huang SG, Zhang HY, Ye H, Chi HG, Zou Y, Lv RX, Zheng XB. Effects of baicalin in CD4 + CD29 + T cell subsets of ulcerative colitis patients. *World J Gastroenterol* 2014; **20**: 15299-15309 [PMID: 25386078 DOI: 10.3748/wjg.v20.i41.15299]

118 **Feng W**, Ao H, Peng C, Yan D. Gut microbiota, a new frontier to understand traditional Chinese medicines. *Pharmacol Res* 2019; **142**: 176-191 [PMID: 30818043 DOI: 10.1016/j.phrs.2019.02.024]

119 **Ju M**, Liu Y, Li M, Cheng M, Zhang Y, Deng G, Kang X, Liu H. Baicalin improves intestinal microecology and abnormal metabolism induced by high-fat diet. *Eur J Pharmacol* 2019; **857**: 172457 [PMID: 31202804 DOI: 10.1016/j.ejphar.2019.172457]

120 **Wu D**, Ding L, Tang X, Wang W, Chen Y, Zhang T. Baicalin protects against hypertension-associated intestinal barrier impairment in part through enhanced microbial production of short-chain fatty acids. *Front Pharmacol* 2019; **10**: 1271 [PMID: 31719823 DOI: 10.3389/fphar.2019.01271]

121 **Dey P**. Gut microbiota in phytopharmacology: A comprehensive overview of concepts, reciprocal interactions, biotransformations and mode of actions. *Pharmacol Res* 2019; **147**: 104367 [PMID: 31344423 DOI: 10.1016/j.phrs.2019.104367]

122 **Chopyk DM**, Grakoui A. Contribution of the intestinal microbiome and gut barrier to hepatic disorders. *Gastroenterology* 2020; **159**: 849-863 [PMID: 32569766 DOI: 10.1053/j.gastro.2020.04.077]

123 **Ganguly R**, Kumar R, Pandey AK. Baicalin provides protection against fluoxetine-induced hepatotoxicity by modulation of oxidative stress and inflammation. *World J Hepatol* 2022; **14**: 729-743 [DOI: 10.4254/wjh.v14.i4.729]

124 **Li J**, Jiang Q, Deng P, Chen Q, Yu M, Shang J, Li W. The formation of a host-guest inclusion complex system between β-cyclodextrin and baicalin and its dissolution characteristics. *J Pharm Pharmacol* 2017; **69**: 663-674 [PMID: 28299800 DOI: 10.1111/jphp.12708]

125 **Ibrahim A**, Nasr M, El-Sherbiny IM. Baicalin as an emerging magical nutraceutical molecule: Emphasis on pharmacological properties and advances in pharmaceutical delivery. *J Drug Deliv Sci Technol* 2022; **70**: 1773-2247 [DOI: 10.1016/j.jddst.2022.103269]

World Journal of Gastroenterology

Submit a Manuscript: https://www.f6publishing.com

World J Gastroenterol 2022 July 14; 28(26): 3063-3070

DOI: 10.3748/wjg.v28.i26.3063

ISSN 1007-9327 (print) ISSN 2219-2840 (online)

MINIREVIEWS

Alterations of autophagic and innate immune responses by the Crohn's disease-associated *ATG16L1* mutation

Natsuki Okai, Tomohiro Watanabe, Kosuke Minaga, Ken Kamata, Hajime Honjo, Masatoshi Kudo

Specialty type: Immunology

Provenance and peer review: Invited article; Externally peer reviewed.

Peer-review model: Single blind

Peer-review report's scientific quality classification

Grade A (Excellent): 0
Grade B (Very good): B, B
Grade C (Good): 0
Grade D (Fair): 0
Grade E (Poor): 0

P-Reviewer: Huang X, China; Kaczmarek-Ryś M

Received: January 10, 2022
Peer-review started: January 10, 2022
First decision: April 16, 2022
Revised: April 21, 2022
Accepted: June 16, 2022
Article in press: June 16, 2022
Published online: July 14, 2022

Natsuki Okai, Tomohiro Watanabe, Kosuke Minaga, Ken Kamata, Hajime Honjo, Masatoshi Kudo, Department of Gastroenterology and Hepatology, Kindai University Faculty of Medicine, Osaka-Sayama 589-8511, Osaka, Japan

Corresponding author: Tomohiro Watanabe, MD, PhD, Associate Professor, Department of Gastroenterology and Hepatology, Kindai University Faculty of Medicine, 377-2 Ohno-Higashi, Osaka-Sayama 589-8511, Osaka, Japan. tomohiro@med.kindai.ac.jp

Abstract

Crohn's disease (CD) is driven by the loss of tolerance to intestinal microbiota and excessive production of pro-inflammatory cytokines. These pro-inflammatory cytokines are produced by macrophages and dendritic cells (DCs) upon sensing the intestinal microbiota by the pattern recognition receptors (PRRs). Impaired activation of PRR-mediated signaling pathways is associated with chronic gastrointestinal inflammation, as shown by the fact that loss-of-function mutations in the nucleotide-binding oligomerization domain 2 gene increase the risk of CD development. Autophagy is an intracellular degradation process, during which cytoplasmic nutrients and intracellular pathogens are digested. Given that impaired reaction to intestinal microbiota alters signaling pathways mediated by PRRs, it is likely that dysfunction of the autophagic machinery is involved in the development of CD. Indeed, the loss-of-function mutation T300A in the autophagy related 16 like 1 (ATG16L1) protein, a critical regulator of autophagy, increases susceptibility to CD. Recent studies have provided evidence that ATG16L1 is involved not only in autophagy, but also in PRR-mediated signaling pathways. ATG16L1 negatively regulates pro-inflammatory cytokine responses of macrophages and DCs after these cells sense the intestinal microbiota by PRRs. Here, we discuss the molecular mechanisms underlying the development of CD in the T300A *ATG16L1* mutation by focusing on PRR-mediated signaling pathways.

Key Words: ATG16L1; Crohn's disease; Autophagy; Innate immunity; Cytokine; Pattern recognition receptors

Core Tip: The loss-of-function mutation T300A in autophagy related 16 like 1 (*ATG16L1*) increases the risk of Crohn's disease (CD). ATG16L1 is a multifunctional protein involved in autophagy and innate immunity. The CD-associated *ATG16L1* mutation T300A leads to overgrowth of intestinal microbiota and enhanced pro-inflammatory cytokine responses, which disrupt intestinal immune homeostasis. In this minireview article, we have summarized the immunopathogenesis of CD in the presence of *ATG16L1* mutation.

Citation: Okai N, Watanabe T, Minaga K, Kamata K, Honjo H, Kudo M. Alterations of autophagic and innate immune responses by the Crohn's disease-associated *ATG16L1* mutation. *World J Gastroenterol* 2022; 28(26): 3063-3070

URL: https://www.wjgnet.com/1007-9327/full/v28/i26/3063.htm

DOI: https://dx.doi.org/10.3748/wjg.v28.i26.3063

INTRODUCTION

Pro-inflammatory cytokines, such as tumor necrosis factor (TNF)-α, interleukin (IL)-6, IL-12, and IL-23, underlie the immunopathogenesis of Crohn's disease (CD), as evidenced by the clinical efficacy of targeting these cytokines for the treatment of patients[1,2]. These colitogenic cytokines are produced by macrophages and dendritic cells (DCs) upon sensing the intestinal microbiota by the pattern recognition receptors (PRRs), which are classified into Toll-like receptors (TLRs), nucleotide-binding oligomerization domain (NOD)-like receptors (NLRs), and retinoic acid-inducible gene I (RIG-I)-like receptors (RLRs)[3-6]. Thus, excessive pro-inflammatory cytokine responses caused by PRR activation play critical roles in the development of CD. This notion is fully supported by the identification of loss-of-function mutations in *NOD2* as one of the strongest risk factors for CD. NOD2 is an intracellular PRR that senses muramyl dipeptide (MDP) derived from bacterial cell wall components and negatively regulates TLR-mediated pro-inflammatory cytokine responses[5,6].

Autophagy refers to the process during which cytoplasmic components and intracellular pathogens are delivered to the lysosome for degradation in the form of double-membrane-bound autophagosomes [7]. The autophagy related 16 like 1 (ATG16L1) protein plays an indispensable role in the initiation and completion of the autophagic process. In addition to its role in autophagy, ATG16L1 has been shown to be involved in PRR-mediated innate immunity. ATG16L1 negatively regulates pro-inflammatory and type I interferon (IFN-I) responses mediated by TLRs, NLRs, and RLRs[8]. More importantly, the loss-of-function mutation T300A in *ATG16L1* has been identified as a risk factor for CD in parallel with mutations in *NOD2*[6]. In this minireview article, we summarize the molecular mechanisms by which the T300A mutation in *ATG16L1* predisposes the host to CD development by focusing on the regulatory role of ATG16L1 in PRR-mediated signaling pathways.

INDUCTION OF AUTOPHAGY BY ATG16L1

ATG16L1 is an indispensable molecule for autophagic responses (Table 1). The autophagy process includes vesicle nucleation, vesicle elongation, vesicle completion, fusion with lysosome, degradation, and recycling[9]. Autophagy dysfunction is associated with neurodegenerative diseases, microbial infections, and aging[7]. Although autophagy has been identified as the primary cell response to the lack of nutrients, recent studies have highlighted the importance of autophagy in microbial infection and immune responses[9]. The autophagy process is negatively regulated by growth factors, which activate the mechanistic target of rapamycin (mTOR) and the phosphoinositide 3-kinase (PI3K)-AKT pathways[7,9]. On the contrary, nutrient starvation or rapamycin treatment promotes the autophagic process through the inhibition of mTOR. Thus, the PI3K–AKT–mTOR pathway negatively regulates autophagic process. On the molecular level, mTOR activation controls the initiation of autophagy by suppressing the activation of the primary initiation complex of autophagy, called Unc-51 Like autophagy activating kinase 1 (ULK1) complex, composed of ULK1/2, ATG101, ATG13, and RB1CC1/FIP200[9]. The formed ULK1 complex translocates to the site of the second complex, called the PI3K complex[9]. The latter PI3K complex recruits a number of ATG proteins to promote elongation and expansion of the autophagosome.

Two ubiquitin-like conjugation systems, the ATG5–ATG12–ATG16L1 conjugation system and the microtubule-associated protein 1 Light chain 3 (LC3) conjugation system, play important roles in the elongation and expansion of the autophagosome[7,9]. The conjugation of the membrane lipid phosphatidylethanolamine with the soluble form of LC3 and formation of the ATG5–ATG12–ATG16L1 complex is necessary for the maturation of autophagosomes[7,9,10]. Matured autophagosomes are fused with lysosomes for the degradation of cellular materials. Vesicles containing ATG16L1 are necessary for

Table 1 Physiological functions of autophagy related 16 like 1

Function	Cell type	Ref.
Positive regulation		
Autophagy	ECs, DCs, macrophages	[9,10]
Regulatory T cell responses	DCs	[22]
Negative regulation		
IFN-I production by RLRs	MEFs	[11,12]
IFN-I production by TLR3 and TLR4	Macrophages	[13]
IL-1β production by TLR4	Macrophages	[16,17,19]
IL-6 and IL-12 production by TLR2	DCs	[27]

EC: Epithelial cell; DC: Dendritic cell; IFN-I: Type I interferon; RLR: Retinoic acid-inducible gene I-like receptors; MEF: Mouse embryonic fibroblast; TLR: Toll-like receptor; IL: Interleukin.

membrane trafficking and autophagosome formation[7,9,10]. Thus, ATG16L1 is an essential protein for the induction and completion of autophagic responses.

ATG16L1 AND INNATE IMMUNITY

ATG16L1 has been shown to attenuate proinflammatory cytokine responses in innate immunity (Table 1)[8]. RLRs, including RIG-I and melanoma differentiation-associated gene 5 (MDA5), are sensors for RNA viruses[3]. IFN-I, which is produced after viral RNA is sensed by RLRs, plays a protective role in host defense[3]. Mouse embryonic fibroblasts deficient in ATG5 displayed enhanced production of IFN-I after exposure to vesicular stomatitis virus due to enhanced activation of IFN regulatory factor 3 [11]. Enhanced production of IFN-I is associated with reduced viral load[11]. ATG16L1 is involved in the regulation of IFN-I mediated by RLRs. Two mitochondrial proteins, NLRX1 and its binding partner, Tu translation elongation factor, interact with ATG5, ATG12, and ATG16L1, and suppress RLR-induced IFN-I production and thereby promoting autophagy[12]. In addition, ATG16L1 has been shown to regulate IFN-I production by interacting with TLR3 and TLR4[13]. Samie *et al*[13] have provided evidence that macrophages deficient in ATG16L1 produced large amounts of IFN-I after stimulation with TLR3 and TLR4 Ligands (Figure 1). Mechanistically, the loss of ATG16L1 resulted in the accumulation of the toll-IL-1 receptor domain-containing adaptor inducing IFN-β protein (TRIF), leading to the excessive activation of TLR3- and TLR4-mediated signaling pathways. Interestingly, macrophages isolated from individuals bearing the CD-associated ATG16L1 T300A variant also exhibited enhanced IFN-I production upon stimulation with TLR3 and TLR4 Ligands[13]. Thus, ATG16L1 functions as a negative regulator of IFN-I production induced by TLR activation. Excessive activation of IFN-I signaling caused by ATG16L1 deficiency may protect against microbial infection. In fact, ATG16L1 hypomorphic mice displayed enhanced IFN-I signaling upon challenge with *Citrobacter rodentium*, which conferred protection from enteric pathogen infection[14]. This protection was mediated by mitochondrial antiviral signaling (MAVS) and stimulator of interferon genes (STING) proteins, because mice with hypomorphic ATG16L1 expression and deficient in MAVS or STING were not protected from the *C. rodentium* infection. Similarly, the clearance of *Salmonella typhimurium* from the intestine was augmented in mice with myeloid cell-specific ATG16L1 deficiency in an IFN-I-dependent manner[13]. IL-22 is a barrier protective cytokine that stimulates antimicrobial responses in the intestine[15]. IL-22 induces STING-dependent IFN-I signaling, which is augmented in the absence of ATG16L1[15]. Such enhanced IFN-I signaling promotes TNF-α production, leading to ileal inflammation, suggesting that ATG16L1 deficiency mediates pro-inflammatory TNF-α responses through cooperative interaction between IL-22 and IFN-I[15]. Taken together, these studies suggest that ATG16L1 dampens IFN-I production mediated by RLRs and TLRs. In turn, the lack of negative regulation of IFN-I signaling owing to the absence of ATG16L1 or the presence of ATG16L1 T300A variant mediates protection from microbial infection in the gastrointestinal tract in an IFN-I-dependent manner.

In addition to attenuating IFN-I production, ATG16L1 also suppresses IL-1β production by macrophages[16,17]. Macrophages expressing ATG16L1 that lacks the coiled-coil domain produced large amounts of IL-1β upon stimulation with lipopolysaccharide (LPS) (Figure 1)[17]. Pro-IL-1β is processed into the mature form of IL-1β by caspase-1[18]. Accumulation of TRIF is involved in enhanced IFN-I production in the absence of *ATG16L1* or presence of the *ATG16L1* T300A mutation[13]. Similarly, TRIF-dependent activation of caspase-1 leads to increased production of IL-1β in macrophages lacking ATG16L1[17]. In a murine model of urinary tract infection, ATG16L1 deficiency promoted clearance of

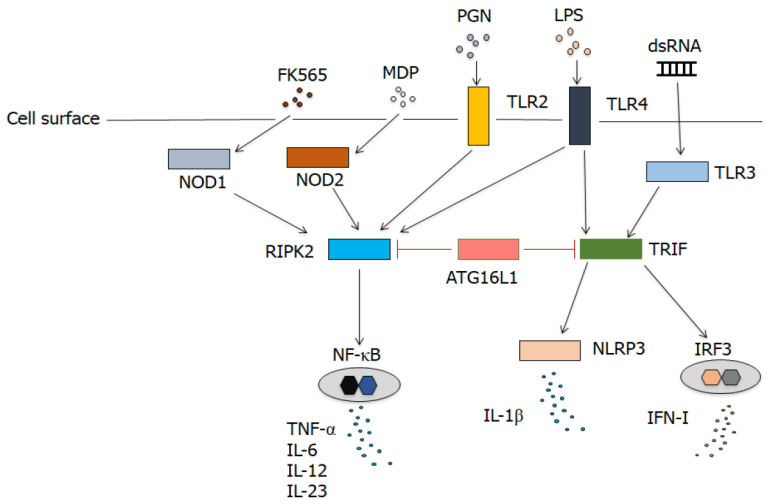

DOI: 10.3748/wjg.v28.i26.3063

Figure 1 Negative effect of autophagy related 16 like 1 on pattern recognition receptor signaling pathways. Autophagy related 16 like 1 (ATG16L1) negatively regulates pro-inflammatory and type I interferon (IFN-I) responses by toll-like receptors (TLRs) and nucleotide-binding oligomerization domain (NOD)-like receptors (NLRs). Production of pro-inflammatory cytokines such as tumor necrosis factor (TNF)-α, interleukin (IL)-6, IL-12, and IL-23 mediated by TLRs is suppressed by ATG16L1 through the inhibition of activation of receptor-interacting serine/threonine-protein kinase 2 and nuclear factor-kB. Production of IL-1β and IFN-I mediated by TLRs is suppressed by ATG16L1 through the inhibition of toll-IL-1 receptor domain-containing adaptor inducing IFN-β, NOD-, LRR-, and pyrin domain-containing protein 3, and interferon regulatory factor 3. MDP: Muramyl dipeptide; PGN: Peptidoglycan; TLR: Toll-like receptor; LPS: Lipopolysaccharide; NOD: Nucleotide-binding oligomerization domain; RIPK2: Receptor-interacting serine/threonine-protein kinase 2; ATG16L1: Autophagy related 16 like 1; IL: Interleukin; IFN: Interferon; TRIF: Toll-IL-1 receptor domain-containing adaptor inducing IFN-β protein; NF-κB: Nuclear factor-κB; NLRP3: NOD-, LRR-, and pyrin domain-containing protein 3; IRF3: Interferon regulatory factor 3; TNF: Tumor necrosis factor.

uropathogenic *Escherichia coli* through excessive production of IL-1β[19]. Thus, ATG16L1 negatively regulates pro-inflammatory pathways mediated not only by IFN-I, but also by IL-1β.

Regulatory T cells (Tregs) expressing forkhead box P3 (FOXP3) are a specialized T cell population that is indispensable for the establishment and maintenance of immunological self-tolerance[20]. Impaired activation of Tregs leads to the development of autoimmune disorders. *Bacteroides fragilis* (*B. fragilis*) has been considered to stimulate beneficial immunoregulatory functions through induction of Tregs[21]. Chu *et al*[22] provided evidence that ATG16L1 expressed in DCs was required for the induction of Tregs expressing FOXP3 upon exposure to outer membrane vesicles (OMVs) of *B. fragilis*. Oral administration of OMVs from *B. fragilis* protected wild-type mice from experimental colitis[22], and this effect was accompanied by increased proportions of Tregs expressing FOXP3 and IL-10. Such protective effect of oral administration of OMVs was not seen in mice with DC-specific ATG16L1 deficiency. Thus, ATG16L1 is involved in the maintenance of immune homeostasis through induction of Tregs expressing FOXP3.

Mutations in *NOD2* are the strongest risk factor for the development of CD[5,6]. MDP, a bacterial component derived from intestinal bacteria, is a prototypical NOD2 ligand[23,24]. Activation of NOD2 by MDP induces autophagy in macrophages, DCs, and fibroblasts, but not in cells harboring CD-associated *NOD2* mutations[25]. Physical interaction between NOD2 and ATG16L1 is induced by the stimulation with MDP[25,26]. Thus, MDP activation of NOD2 mediates bactericidal effects in an ATG16L1-dependent manner, and the presence of CD-associated *NOD2* mutations promotes overgrowth of intestinal bacteria, leading to excessive production of pro-inflammatory cytokines.

Receptor-interacting serine/threonine-protein kinase 2 (RIPK2) is a signaling molecule downstream of NOD2 and TLRs[23,24]. It remains unclear whether ATG16L1 binds to RIPK2 after activation of NOD2. In this regard, we confirmed that ATG16L1 binds to the kinase domain of RIPK2 in overexpression studies[26,27]. In human DCs, ATG16L1 interacted with RIPK2 after the stimulation with MDP and this interaction suppressed NF-κB-dependent proinflammatory responses mediated by TLRs[26,27]. Transfection of intact *ATG16L1*, but not of *ATG16L1* with the T300A mutation, reduced TLR2-mediated NF-κB activation in human embryonic kidney cells. In the physiological setting, NF-κB activation, as assessed by the degradation of IκBα and expression of phospho-IκBα, was markedly suppressed in human DCs stimulated with TLR2 and NOD2 ligands as compared to the effect of stimulation with a TLR2 ligand alone[26,27]. Furthermore, knockdown of *ATG16L1* by its specific siRNA increased IL-6 and IL-12p40 production by human DCs upon exposure to TLR2 and NOD2 ligands as compared to the levels of those cytokines in cells transfected with control siRNA[26,27]. These studies strongly suggest that ATG16L1 functions as a negative regulator of TLR2-mediated pro-inflammatory cytokine responses (Figure 1).

NF-κB activation mediated by TLRs and NOD2 is tightly regulated by Lys (K63)- linked polyubiquitination of RIPK2[23,24,27,28]. As for the molecular mechanisms accounting for the suppression of TLR2-mediated NF-κB activation and pro-inflammatory cytokine production, ATG16L1 has been shown to inhibit polyubiquitination of RIPK2[26,28]. NOD2 activation by MDP also inhibited polyubiquitination of RIPK2 through the induction of interferon regulatory factor 4 (IRF4)[23,24]. Overexpression studies revealed that ATG16L1 and IRF4 act cooperatively to suppress K63-linked polyubiquitination of RIPK2 [27]. Given that physical interaction between RIPK2 and IRF4 or ATG16L1 is induced after NOD2 activation by MDP, it is likely that NOD2 downregulates TLR-mediated proinflammatory cytokine responses through binding of ATG16L1 and IRF4 to RIPK2. This idea is fully supported by the fact that RIPK2 expression level is markedly elevated in the colonic mucosa of patients with CD and ulcerative colitis (UC), and it corelates with the levels of pro-inflammatory cytokines, such as TNF-α and IL-6[29]. Furthermore, the percentages of lamina propria DCs expressing ATG16L1 and IRF4 in the colon inversely correlate with the expression levels of TNF-α and IL-6[27]. Collectively, these studies support the idea that ATG16L1 acts in concert with NOD2 to suppress excessive pro-inflammatory cytokine responses mediated by TLRs and thereby maintains intestinal homeostasis.

ATG16L1 AND CD

The polymorphism Thr300Ala (or T300A) in the coding region of the *ATG16L1* gene confers increased risk for the development of CD[6,10,16]. This polymorphism is a loss-of-function mutation, which affects the induction of autophagy against invading bacteria and is associated with gut bacterial overgrowth and pro-inflammatory cytokine responses[6,10,16]. Recent studies have successfully elucidated some of the molecular mechanisms accounting for the development of CD in the presence of the ATG16L1 T300A variant. Given that ATG16L1 is constitutively expressed in epithelial cells, especially Paneth cells and myeloid cells, these studies have highlighted the importance of ATG16L1-mediated signaling pathways in innate immune cells for the immunopathogenesis of CD[17,25,28,30,31].

Paneth cells are localized at the base of the crypts in the ileum, and they contribute to the maintenance of intestinal homeostasis through the secretion of antimicrobial peptides (AMPs) and inhibition of intestinal bacterial overgrowth[32]. Mice with hypomorphic expression of ATG16L1 and ATG16L1 T300A-knockin (KI) mice exhibit increased proportions of Paneth cells with abnormal phenotypes, as assessed by lysozyme localization and granule morphology[30-32]. Moreover, Paneth cells from patients with CD carrying ATG16L1 T300A have unusual granule morphology and accumulation of AMPs, with both having been observed also in mice deficient in ATG16L1 or expressing ATG16L1 T300A[32]. Furthermore, defective function of Paneth cells in the absence of ATG16L1 or the presence of the *ATG16L1* T300A mutation led to higher susceptibility to TNF-α-mediated necroptosis and accumulation of the endoplasmic reticulum stress sensor IRE1a, indicating that necroptosis and endoplasmic reticulum stress are involved in the pathogenesis of CD[33]. Thus, the ileal mucosa of patients and mice bearing ATG16L1 T300A is characterized by the defective function of Paneth cells, which results in the overgrowth of intestinal bacteria. This notion is supported by the fact that CD patients bearing the *ATG16L1* T300A mutation display impaired clearance of pathogenic bacteria in the ileal mucosa[34]. It is well established that CD occurs as a result of the interplay between genetic susceptibility and environmental factors. Cigarette smoking is a risk factor for developing CD[35]. Interestingly, cigarette smoking has been suggested to amplify effects of the *ATG16L1* T300A mutation, triggering Paneth cell defects, thereby causing chronic intestinal inflammation[31].

Pro-inflammatory cytokine responses play an important role in the development of CD[1]. The *ATG16L1* T300A mutation has been shown to enhance pro-inflammatory cytokine responses in the intestine. Mice lacking ATG16L1 in hematopoietic cells were susceptible to dextran sodium sulfate (DSS)-induced colitis[17]. Aggravated DSS-induced colitis in mice lacking ATG16L1 was alleviated by blocking IL-1β-mediated signaling pathways[17]. Furthermore, macrophages lacking ATG16L1 produced more IL-1β upon stimulation with LPS[17]. As for the molecular mechanisms accounting for enhanced production of IL-1β in the absence of ATG16L1, Saitoh *et al*[17] showed that ATG16L1 deficiency resulted in increased production of this cytokine through the TRIF-dependent activation of caspase-1. Thus, ATG16L1 deficiency predisposed mice to DSS-induced colitis by activating IL-1β-mediated signaling pathways. In line with these data obtained in mice lacking ATG16L1 in hematopoietic cells, ATG16L1 T300A-KI mice displayed enhanced production of IL-1β upon exposure to LPS[16]. These studies, which utilized ATG16L1-deficient and ATG16L1 T300A-KI mice, support the idea that intact ATG16L1-medaited signaling pathways limit pro-inflammatory cytokine responses triggered by activation of TLRs. In this regard, we and others have reported that ATG16L1 negatively regulates pro-inflammatory cytokine responses mediated by RIPK2, a downstream signaling molecule of TLRs and NLRs[27,28]. Binding of ATG16L1 to the kinase domain of RIPK2 inhibits polyubiquitination of RIPK2, followed by suppression of NF-κB activation[27,28]. These studies strongly suggest that ATG16L1 activation maintains intestinal homeostasis and attenuates reactions against microbiota by inhibiting TLR-mediated pro-inflammatory cytokine responses in macrophages and DCs. Strong support for this idea also comes from the observations that colonic pro-inflammatory cytokine

expression inversely correlates with the percentage of CD11c$^+$ DCs expressing ATG16L1 in patients with CD and that induction of remission is accompanied by accumulation of CD11c$^+$ DCs expressing ATG16L1 in the gastrointestinal tract of patients with CD[27].

ATG16L1 negatively regulates IFN-I responses mediated by RLRs and TLRs[11-14]. Isolated macrophages from patients with CD bearing the *ATG16L1* T300A mutation produced more IFN-I upon stimulation with TLR3 and TLR4 ligands than macrophages from patients with intact ATG16L1[13,36]. Excessive production of IFN-I is involved in the immunopathogenesis of CD and UC. Expression levels of the IFN-stimulated genes was shown to be higher in the inflamed colonic mucosa of patients with CD or UC than in healthy controls[13]. Moreover, expression levels of IFN-stimulated genes rapidly declined in response to infliximab treatment. Although the presence of the *ATG16L1* T300A variant is associated with colitogenic IFN-I responses, the enhanced production of IFN-I may improve survival of patients with colorectal cancer[36].

Similar to the molecular mechanisms of chronic inflammation in the presence of CD-associated mutations in *NOD2*, the *ATG16L1* T300A mutation promotes the development of CD by causing impaired production of AMPs in Paneth cells and excessive secretion of TLR-mediated pro-inflammatory cytokines by macrophages and DCs. MDP activation of NOD2 induces robust production of AMPs from Paneth cells, thereby preventing bacterial overgrowth in the intestine[5]. Paneth cells deficient in NOD2 or bearing CD-associated *NOD2* mutations fail to produce AMPs[5]. With regard to the pro-inflammatory cytokine responses, activation of intact NOD2 by MDP negatively regulates the production of TLR-mediated pro-inflammatory cytokines through the induction of IRF4[23,24]. In the absence of intact *NOD2* or the presence of CD-associated *NOD2* mutations, pro-inflammatory cytokine responses by DCs are markedly enhanced upon exposure to TLR ligands derived from the intestinal microbiota[5]. Thus, impaired function of Paneth cells and excessive pro-inflammatory cytokine responses by TLRs underlie the immunopathogenesis of CD in the presence of *ATG16L1* and *NOD2* mutations.

CONCLUSION

The autophagic protein ATG16L1 plays an indispensable role in the maintenance of intestinal homeostasis. The *ATG16L1* T300A mutation confers an increased risk for the development of CD as it is associated with increased bacterial burden and excessive pro-inflammatory cytokine responses in the gastrointestinal tract. Elucidation of the molecular mechanisms by which the *ATG16L1* T300A variant leads to the development of CD has provided new insights into the immunopathogenesis of CD induced by impaired induction of autophagy.

ACKNOWLEDGEMENTS

We appreciate Ms. Yukiko Ueno for her secretarial support.

FOOTNOTES

Author contributions: Okai N and Watanabe T drafted the manuscript; Watanabe T, Minaga K, Kamata K, Honjo H, and Kudo M revised the manuscript; OKai N, Watanabe T, Minaga K, Kamata K, Honjo H and Kudo M have read and approved the final manuscript.

Conflict-of-interest statement: The authors declare that they have no conflicts of interest to disclose.

Country/Territory of origin: Japan

ORCID number: Natsuki Okai 0000-0002-3167-4927; Tomohiro Watanabe 0000-0001-7781-6305; Kosuke Minaga 0000-0001-5407-7925; Ken Kamata 0000-0003-1568-0769; Hajime Honjo 0000-0002-0888-3384; Masatoshi Kudo 0000-0002-4102-3474.

Corresponding Author's Membership in Professional Societies: The Japanese Society of Gastroenterology, No. 34410.

S-Editor: Ma YJ
L-Editor: A

P-Editor: Ma YJ

REFERENCES

1 **Strober W**, Fuss IJ. Proinflammatory cytokines in the pathogenesis of inflammatory bowel diseases. *Gastroenterology* 2011; **140**: 1756-1767 [PMID: 21530742 DOI: 10.1053/j.gastro.2011.02.016]

2 **Neurath MF**. Current and emerging therapeutic targets for IBD. *Nat Rev Gastroenterol Hepatol* 2017; **14**: 269-278 [PMID: 28144028 DOI: 10.1038/nrgastro.2016.208]

3 **Kawai T**, Akira S. Toll-like receptor and RIG-I-like receptor signaling. *Ann N Y Acad Sci* 2008; **1143**: 1-20 [PMID: 19076341 DOI: 10.1196/annals.1443.020]

4 **Takeda K**, Akira S. Toll-like receptors in innate immunity. *Int Immunol* 2005; **17**: 1-14 [PMID: 15585605 DOI: 10.1093/intimm/dxh186]

5 **Strober W**, Asano N, Fuss I, Kitani A, Watanabe T. Cellular and molecular mechanisms underlying NOD2 risk-associated polymorphisms in Crohn's disease. *Immunol Rev* 2014; **260**: 249-260 [PMID: 24942694 DOI: 10.1111/imr.12193]

6 **Cho JH**. The genetics and immunopathogenesis of inflammatory bowel disease. *Nat Rev Immunol* 2008; **8**: 458-466 [PMID: 18500230 DOI: 10.1038/nri2340]

7 **Klionsky DJ**, Petroni G, Amaravadi RK, Baehrecke EH, Ballabio A, Boya P, Bravo-San Pedro JM, Cadwell K, Cecconi F, Choi AMK, Choi ME, Chu CT, Codogno P, Colombo MI, Cuervo AM, Deretic V, Dikic I, Elazar Z, Eskelinen EL, Fimia GM, Gewirtz DA, Green DR, Hansen M, Jäättelä M, Johansen T, Juhász G, Karantza V, Kraft C, Kroemer G, Ktistakis NT, Kumar S, Lopez-Otin C, Macleod KF, Madeo F, Martinez J, Meléndez A, Mizushima N, Münz C, Penninger JM, Perera RM, Piacentini M, Reggiori F, Rubinsztein DC, Ryan KM, Sadoshima J, Santambrogio L, Scorrano L, Simon HU, Simon AK, Simonsen A, Stolz A, Tavernarakis N, Tooze SA, Yoshimori T, Yuan J, Yue Z, Zhong Q, Galluzzi L, Pietrocola F. Autophagy in major human diseases. *EMBO J* 2021; **40**: e108863 [PMID: 34459017 DOI: 10.15252/embj.2021108863]

8 **Hamaoui D**, Subtil A. ATG16L1 functions in cell homeostasis beyond autophagy. *FEBS J* 2022; **289**: 1779-1800 [PMID: 33752267 DOI: 10.1111/febs.15833]

9 **Kabat AM**, Pott J, Maloy KJ. The Mucosal Immune System and Its Regulation by Autophagy. *Front Immunol* 2016; **7**: 240 [PMID: 27446072 DOI: 10.3389/fimmu.2016.00240]

10 **Salem M**, Ammitzboell M, Nys K, Seidelin JB, Nielsen OH. ATG16L1: A multifunctional susceptibility factor in Crohn disease. *Autophagy* 2015; **11**: 585-594 [PMID: 25906181 DOI: 10.1080/15548627.2015.1017187]

11 **Jounai N**, Takeshita F, Kobiyama K, Sawano A, Miyawaki A, Xin KQ, Ishii KJ, Kawai T, Akira S, Suzuki K, Okuda K. The Atg5 Atg12 conjugate associates with innate antiviral immune responses. *Proc Natl Acad Sci U S A* 2007; **104**: 14050-14055 [PMID: 17709747 DOI: 10.1073/pnas.0704014104]

12 **Lei Y**, Wen H, Yu Y, Taxman DJ, Zhang L, Widman DG, Swanson KV, Wen KW, Damania B, Moore CB, Giguère PM, Siderovski DP, Hiscott J, Razani B, Semenkovich CF, Chen X, Ting JP. The mitochondrial proteins NLRX1 and TUFM form a complex that regulates type I interferon and autophagy. *Immunity* 2012; **36**: 933-946 [PMID: 22749352 DOI: 10.1016/j.immuni.2012.03.025]

13 **Samie M**, Lim J, Verschueren E, Baughman JM, Peng I, Wong A, Kwon Y, Senbabaoglu Y, Hackney JA, Keir M, Mckenzie B, Kirkpatrick DS, van Lookeren Campagne M, Murthy A. Selective autophagy of the adaptor TRIF regulates innate inflammatory signaling. *Nat Immunol* 2018; **19**: 246-254 [PMID: 29358708 DOI: 10.1038/s41590-017-0042-6]

14 **Martin PK**, Marchiando A, Xu R, Rudensky E, Yeung F, Schuster SL, Kernbauer E, Cadwell K. Autophagy proteins suppress protective type I interferon signalling in response to the murine gut microbiota. *Nat Microbiol* 2018; **3**: 1131-1141 [PMID: 30202015 DOI: 10.1038/s41564-018-0229-0]

15 **Aden K**, Tran F, Ito G, Sheibani-Tezerji R, Lipinski S, Kuiper JW, Tschurtschenthaler M, Saveljeva S, Bhattacharyya J, Häsler R, Bartsch K, Luzius A, Jentzsch M, Falk-Paulsen M, Stengel ST, Welz L, Schwarzer R, Rabe B, Barchet W, Krautwald S, Hartmann G, Pasparakis M, Blumberg RS, Schreiber S, Kaser A, Rosenstiel P. ATG16L1 orchestrates interleukin-22 signaling in the intestinal epithelium *via* cGAS-STING. *J Exp Med* 2018; **215**: 2868-2886 [PMID: 30254094 DOI: 10.1084/jem.20171029]

16 **Lassen KG**, Kuballa P, Conway KL, Patel KK, Becker CE, Peloquin JM, Villablanca EJ, Norman JM, Liu TC, Heath RJ, Becker ML, Fagbami L, Horn H, Mercer J, Yilmaz OH, Jaffe JD, Shamji AF, Bhan AK, Carr SA, Daly MJ, Virgin HW, Schreiber SL, Stappenbeck TS, Xavier RJ. Atg16L1 T300A variant decreases selective autophagy resulting in altered cytokine signaling and decreased antibacterial defense. *Proc Natl Acad Sci U S A* 2014; **111**: 7741-7746 [PMID: 24821797 DOI: 10.1073/pnas.1407001111]

17 **Saitoh T**, Fujita N, Jang MH, Uematsu S, Yang BG, Satoh T, Omori H, Noda T, Yamamoto N, Komatsu M, Tanaka K, Kawai T, Tsujimura T, Takeuchi O, Yoshimori T, Akira S. Loss of the autophagy protein Atg16L1 enhances endotoxin-induced IL-1beta production. *Nature* 2008; **456**: 264-268 [PMID: 18849965 DOI: 10.1038/nature07383]

18 **Place DE**, Kanneganti TD. Recent advances in inflammasome biology. *Curr Opin Immunol* 2018; **50**: 32-38 [PMID: 29128729 DOI: 10.1016/j.coi.2017.10.011]

19 **Symington JW**, Wang C, Twentyman J, Owusu-Boaitey N, Schwendener R, Núñez G, Schilling JD, Mysorekar IU. ATG16L1 deficiency in macrophages drives clearance of uropathogenic E. coli in an IL-1β-dependent manner. *Mucosal Immunol* 2015; **8**: 1388-1399 [PMID: 25669147 DOI: 10.1038/mi.2015.7]

20 **Kitagawa Y**, Sakaguchi S. Molecular control of regulatory T cell development and function. *Curr Opin Immunol* 2017; **49**: 64-70 [PMID: 29065384 DOI: 10.1016/j.coi.2017.10.002]

21 **Caruso R**, Lo BC, Núñez G. Host-microbiota interactions in inflammatory bowel disease. *Nat Rev Immunol* 2020; **20**: 411-426 [PMID: 32005980 DOI: 10.1038/s41577-019-0268-7]

22 **Chu H**, Khosravi A, Kusumawardhani IP, Kwon AH, Vasconcelos AC, Cunha LD, Mayer AE, Shen Y, Wu WL, Kambal A, Targan SR, Xavier RJ, Ernst PB, Green DR, McGovern DP, Virgin HW, Mazmanian SK. Gene-microbiota interactions

contribute to the pathogenesis of inflammatory bowel disease. *Science* 2016; **352**: 1116-1120 [PMID: 27230380 DOI: 10.1126/science.aad9948]

23 **Watanabe T**, Asano N, Murray PJ, Ozato K, Tailor P, Fuss IJ, Kitani A, Strober W. Muramyl dipeptide activation of nucleotide-binding oligomerization domain 2 protects mice from experimental colitis. *J Clin Invest* 2008; **118**: 545-559 [PMID: 18188453 DOI: 10.1172/JCI33145]

24 **Watanabe T**, Asano N, Meng G, Yamashita K, Arai Y, Sakurai T, Kudo M, Fuss IJ, Kitani A, Shimosegawa T, Chiba T, Strober W. NOD2 downregulates colonic inflammation by IRF4-mediated inhibition of K63-linked polyubiquitination of RICK and TRAF6. *Mucosal Immunol* 2014; **7**: 1312-1325 [PMID: 24670424 DOI: 10.1038/mi.2014.19]

25 **Cooney R**, Baker J, Brain O, Danis B, Pichulik T, Allan P, Ferguson DJ, Campbell BJ, Jewell D, Simmons A. NOD2 stimulation induces autophagy in dendritic cells influencing bacterial handling and antigen presentation. *Nat Med* 2010; **16**: 90-97 [PMID: 19966812 DOI: 10.1038/nm.2069]

26 **Honjo H**, Watanabe T, Kamata K, Minaga K, Kudo M. RIPK2 as a New Therapeutic Target in Inflammatory Bowel Diseases. *Front Pharmacol* 2021; **12**: 650403 [PMID: 33935757 DOI: 10.3389/fphar.2021.650403]

27 **Honjo H**, Watanabe T, Arai Y, Kamata K, Minaga K, Komeda Y, Yamashita K, Kudo M. ATG16L1 negatively regulates RICK/RIP2-mediated innate immune responses. *Int Immunol* 2021; **33**: 91-105 [PMID: 32909611 DOI: 10.1093/intimm/dxaa062]

28 **Sorbara MT**, Ellison LK, Ramjeet M, Travassos LH, Jones NL, Girardin SE, Philpott DJ. The protein ATG16L1 suppresses inflammatory cytokines induced by the intracellular sensors Nod1 and Nod2 in an autophagy-independent manner. *Immunity* 2013; **39**: 858-873 [PMID: 24238340 DOI: 10.1016/j.immuni.2013.10.013]

29 **Watanabe T**, Minaga K, Kamata K, Sakurai T, Komeda Y, Nagai T, Kitani A, Tajima M, Fuss IJ, Kudo M, Strober W. RICK/RIP2 is a NOD2-independent nodal point of gut inflammation. *Int Immunol* 2019; **31**: 669-683 [PMID: 31132297 DOI: 10.1093/intimm/dxz045]

30 **Cadwell K**, Liu JY, Brown SL, Miyoshi H, Loh J, Lennerz JK, Kishi C, Kc W, Carrero JA, Hunt S, Stone CD, Brunt EM, Xavier RJ, Sleckman BP, Li E, Mizushima N, Stappenbeck TS, Virgin HW 4th. A key role for autophagy and the autophagy gene Atg16l1 in mouse and human intestinal Paneth cells. *Nature* 2008; **456**: 259-263 [PMID: 18849966 DOI: 10.1038/nature07416]

31 **Liu TC**, Kern JT, VanDussen KL, Xiong S, Kaiko GE, Wilen CB, Rajala MW, Caruso R, Holtzman MJ, Gao F, McGovern DP, Nunez G, Head RD, Stappenbeck TS. Interaction between smoking and ATG16L1T300A triggers Paneth cell defects in Crohn's disease. *J Clin Invest* 2018; **128**: 5110-5122 [PMID: 30137026 DOI: 10.1172/JCI120453]

32 **Stappenbeck TS**, McGovern DPB. Paneth Cell Alterations in the Development and Phenotype of Crohn's Disease. *Gastroenterology* 2017; **152**: 322-326 [PMID: 27729212 DOI: 10.1053/j.gastro.2016.10.003]

33 **Tschurtschenthaler M**, Adolph TE, Ashcroft JW, Niederreiter L, Bharti R, Saveljeva S, Bhattacharyya J, Flak MB, Shih DQ, Fuhler GM, Parkes M, Kohno K, Iwawaki T, Janneke van der Woude C, Harding HP, Smith AM, Peppelenbosch MP, Targan SR, Ron D, Rosenstiel P, Blumberg RS, Kaser A. Defective ATG16L1-mediated removal of IRE1α drives Crohn's disease-like ileitis. *J Exp Med* 2017; **214**: 401-422 [PMID: 28082357 DOI: 10.1084/jem.20160791]

34 **Sadaghian Sadabad M**, Regeling A, de Goffau MC, Blokzijl T, Weersma RK, Penders J, Faber KN, Harmsen HJ, Dijkstra G. The ATG16L1-T300A allele impairs clearance of pathosymbionts in the inflamed ileal mucosa of Crohn's disease patients. *Gut* 2015; **64**: 1546-1552 [PMID: 25253126 DOI: 10.1136/gutjnl-2014-307289]

35 **Georgiou AN**, Ntritsos G, Papadimitriou N, Dimou N, Evangelou E. Cigarette Smoking, Coffee Consumption, Alcohol Intake, and Risk of Crohn's Disease and Ulcerative Colitis: A Mendelian Randomization Study. *Inflamm Bowel Dis* 2021; **27**: 162-168 [PMID: 32628751 DOI: 10.1093/ibd/izaa152]

36 **Grimm WA**, Messer JS, Murphy SF, Nero T, Lodolce JP, Weber CR, Logsdon MF, Bartulis S, Sylvester BE, Springer A, Dougherty U, Niewold TB, Kupfer SS, Ellis N, Huo D, Bissonnette M, Boone DL. The Thr300Ala variant in ATG16L1 is associated with improved survival in human colorectal cancer and enhanced production of type I interferon. *Gut* 2016; **65**: 456-464 [PMID: 25645662 DOI: 10.1136/gutjnl-2014-308735]

World Journal of Gastroenterology

Submit a Manuscript: https://www.f6publishing.com

World J Gastroenterol 2022 July 14; 28(26): 3071-3080

DOI: 10.3748/wjg.v28.i26.3071

ISSN 1007-9327 (print) ISSN 2219-2840 (online)

MINIREVIEWS

Anabolic androgenic steroid-induced liver injury: An update

Ana Petrovic, Sonja Vukadin, Renata Sikora, Kristina Bojanic, Robert Smolic, Davor Plavec, George Y Wu, Martina Smolic

Specialty type: Gastroenterology and hepatology

Provenance and peer review: Invited article; Externally peer reviewed.

Peer-review model: Single blind

Peer-review report's scientific quality classification

Grade A (Excellent): 0
Grade B (Very good): B, B
Grade C (Good): C
Grade D (Fair): D
Grade E (Poor): 0

P-Reviewer: He F, China; Kreisel W, Germany; Liu P, China

Received: January 11, 2022
Peer-review started: January 11, 2022
First decision: March 8, 2022
Revised: March 22, 2022
Accepted: June 18, 2022
Article in press: June 18, 2022
Published online: July 14, 2022

Ana Petrovic, Sonja Vukadin, Robert Smolic, Martina Smolic, Department of Pharmacology and Biochemistry, Faculty of Dental Medicine and Health Osijek, J. J. Strossmayer University of Osijek, Osijek 31000, Croatia

Ana Petrovic, Sonja Vukadin, Martina Smolic, Department of Pharmacology, Faculty of Medicine Osijek, J. J. Strossmayer University of Osijek, Osijek 31000, Croatia

Renata Sikora, Department of Dental Medicine, Faculty of Dental Medicine and Health Osijek, J. J. Strossmayer University of Osijek, Osijek 31000, Croatia

Renata Sikora, Department of Dental Medicine, Health Center Osijek-Baranja County, Osijek 31000, Croatia

Kristina Bojanic, Department of Otorhinolaryngology, Neurosurgery and Radiology, Faculty of Dental Medicine and Health Osijek, J. J. Strossmayer University of Osijek, Osijek 31000, Croatia

Kristina Bojanic, Department of Biophysics and Radiology, Faculty of Medicine Osijek, J. J. Strossmayer University of Osijek, Osijek 31000, Croatia

Kristina Bojanic, Department of Radiology, Health Center Osijek-Baranja County, Osijek 31000, Croatia

Davor Plavec, Research Department, Srebrnjak Children's Hospital, Zagreb 10000, Croatia

George Y Wu, Department of Medicine, Division of Gastrenterology/Hepatology, University of Connecticut Health Center, Farmington, CT 06030, United States

Corresponding author: Martina Smolic, MD, PhD, Professor, Department of Pharmacology and Biochemistry, Faculty of Dental Medicine and Health Osijek, J. J. Strossmayer University of Osijek, 10E Cara Hadrijana, Osijek 31000, Croatia. martina.smolic@mefos.hr

Abstract

Anabolic androgenic steroids (AASs) are a group of molecules including endogenous testosterone and synthetic derivatives that have both androgenic and anabolic effects. These properties make them therapeutically beneficial in medical conditions such as hypogonadism. However, they are commonly bought illegally and misused for their anabolic, skeletal muscle building, and performance-enhancing effects. Supraphysiologic and long-term use of AASs affects all organs, leading to cardiovascular, neurological, endocrine, gastrointestinal, renal, and hematologic disorders. Hepatotoxicity is one of the major concerns regarding

AASs treatment and abuse. Testosterone and its derivatives have been most often shown to induce a specific form of cholestasis, peliosis hepatis, and hepatic benign and malignant tumors. It is currently believed that mechanisms of pathogenesis of these disorders include disturbance of antioxidative factors, upregulation of bile acid synthesis, and induction of hepatocyte hyperplasia. Most toxicity cases are treated with supportive measures and liver function normalizes with discontinuation of AAS. However, some long-term consequences are irreversible. AAS-induced liver injury should be taken in consideration in patients with liver disorders, especially with the increasing unintentional ingestion of supplements containing AAS. In this paper, we review the most current knowledge about AAS-associated adverse effects on the liver, and their clinical presentations, prevalence, and pathophysiological mechanisms.

Key Words: Androgens; Steroids; Cholestasis; Fibrosis; Liver; Chemical and drug induced liver injury

Core Tip: There is a great deal of literature on the prevalence, pathophysiology, and therapeutic options for anabolic androgenic steroid (AAS)-associated adverse effects. However, AAS-induced liver injury is perhaps still underreported and poorly understood. In this paper, we review the latest knowledge obtained about molecular mechanisms of AAS-associated liver injury from most recent *in vitro* and animal studies, as well as the latest case reports regarding adverse effects of AASs in dietary supplements.

Citation: Petrovic A, Vukadin S, Sikora R, Bojanic K, Smolic R, Plavec D, Wu GY, Smolic M. Anabolic androgenic steroid-induced liver injury: An update. *World J Gastroenterol* 2022; 28(26): 3071-3080
URL: https://www.wjgnet.com/1007-9327/full/v28/i26/3071.htm
DOI: https://dx.doi.org/10.3748/wjg.v28.i26.3071

INTRODUCTION

Anabolic androgenic steroids (AASs) are group of compounds that include endogenous androgens, most importantly testosterone, and their synthetic derivatives[1]. Testosterone and synthetic AASs have been commonly used for their androgenic masculinizing effects resulting in male secondary characteristics, as well as anabolic skeletal muscle building effects due to enhanced protein utilization and synthesis mechanisms[2,3]. AASs are medically indicated in conditions such as male primary and secondary hypogonadism, aplastic anemia, muscle wasting in human immunodeficiency virus-infected patients, osteoporosis, libido dysfunction, chronic kidney disease, and breast cancer[4]. However, they are often misused because of their performance-enhancing and anabolic effects resulting in increased fat-free mass and improved muscle fiber size and strength. Abuse of AASs for aesthetic purposes and athletic performance improvement has surged as a public health problem in the past few decades among both professional and recreational athletes and bodybuilders[5,6]. Unmodified testosterone is rapidly metabolized when administered orally or parenterally and exerts a similar proportion of anabolic and androgenic effects. Chemical modifications of testosterone allow prolonged effective blood concentrations and changes to its pharmacodynamic properties, therefore enhancing desired anabolic or androgenic effects. In its synthetic derivatives used for aestethic and performance-enhancing purposes, testosterone is altered mainly through alkylation and esterification to enhance bioavailability by reducing hepatic metabolism, prolong duration of action, and maximize anabolic properties, though all of the synthetic compounds still exert significant androgenic effects. Supraphysiologic doses and prolonged unsupervised use of AASs have major impacts on users, affecting all organs and causing cardiovascular, neuroendocrine, neuropsychiatric, renal, gastrointestinal, musculoskeletal, dermatologic, immune, and hematologic disorders. Testosterone has a major impact on homeostasis of electrolytes, macromolecules, and micromolecules, including alterations in systemic iron balance and erythropoiesis. It has been established that AAS-induced erythropoiesis is mediated by erythropoietin [7]. Most recent studies also imply suppression of hepcidin (a negative regulator of the iron transporter ferroportin) as a mechanism of androgen-induced enhanced iron absorbtion and incorporation into red blood cells[8]. Some of the most common adverse effects related to AASs are dyslipidemia, hypertension, hypogonadism and infertility, aggression and mood disorders, addiction, and liver and kidney injury[9-11]. This has led to stricter laws regarding availability of AASs, mainly in professional sports organizations which ban anabolic steroid use, and test competitors for the presence of illegal steroids not only because of the unfair advantage in performance, but also because of their potentially dangerous side effects. In legal terms, AASs are classified in the United States as schedule 3 drugs by the

Drug Enforcement Agency, meaning that they can be legally obtained as prescription-only drugs. However, they are illegally sold among teammates, trainers, and fitness centers, through black market or counterfeit prescriptions. Furthermore, many AASs are legally bought and consumed unknowingly in over-the-counter dietary supplements advertised as energy, virility, and muscle strength enhancers [12-14]. Although the precise number of AAS users is difficult to determine, it is estimated that the prevalence across the world is 1%-5%[15]. A study in 2013 found that the prevalence of AAS use among male elite college students in the United States during their lifetime is about 20%[16]. In Norway high school population, a prevalence of 4% was found[17]. While it is difficult to establish a true prevalence of AAS use due to underreporting of this socially undesirable behavior, all the surveys nevertheless found significantly higher AAS use in male compared to female persons and the majority of AAS users are or were professional or near professional athletes[15]. With the liver being the main site of steroid clearance, hepatotoxicity is one of the major adverse effects of chronic AAS use. The aim of this paper is to focus on the most recent studies and knowledge obtained regarding AAS-induced liver injury.

HEPATOTOXICITY

Since the 1950s, a significant number of studies and case reports have raised concerns regarding hepatotoxic effects including cholestasis, hepatic neoplasms, hepatocyte toxicity, and peliosis hepatis related to use of AASs[11,18]. Correlation between steroids and these effects has been attributed to the role of the liver as the primary clearance site for AASs. As mentioned before, synthetic steroids are usually modified to prevent first-pass hepatic metabolism, preventing their clearance by the liver and, therefore, elevating their risk of hepatotoxicity[19]. Most studies of long-term use have not identified exact dosages and concentrations, administration paths, and types of steroid compounds often used simultaneously. Prospective studies with supraphysiologic doses are difficult to gain institutional review board (IRB) approval due to ethical and legal considerations[20], therefore randomized controlled trials are lacking and in this minireview we discuss data from case reports, *in vitro* studies, and studies on animal models.

Proposed mechanisms of liver injury include anabolic steroid-induced infiltration of inflammatory cells in the hepatic tissue, and Kupffer cell activation resulting in production of inflammatory cytokines and collagen deposition, increased oxidative stress and reactive oxygen species with subsequent mitochondrial degeneration in liver cells, and stimulation of intracellular androgenic steroid receptors inducing unregulated growth of hepatocytes. An *in vitro* study in 2021 reported that disruption of mitochondrial respiratory chain reactions occurs early in the pathogenesis of liver injury caused by supraphysiologic doses of nandrolone, a synthetic AAS commonly used for performance enhancement. It specifically inhibits respiratory chain complexes I and III, which causes accumulation of reactive oxygen species and oxidative stress[21]. Indeed, earlier animal studies detected a reduced amount of glutathione and enzymes that serve as free radical scavengers (superoxide dismutase and catalase) as well as increasing thiobarbituric acid-reactive substances indicating impaired redox homeostasis[22,23]. Furthermore, oxidative stress interfered with mitochondrial membrane potential dynamics[24] and altogether resulted in reduced cell energy supply leading to malfunction and necrosis of hepatocytes. Apart from disturbance in cellular function, distortion in mitochondrial morphology and increased number of lysosomes in hepatocytes were observed by electron microscopy[25]. Another process observed after prolonged administration of nandrolone in animal studies was excess collagen deposition in liver parenchyma. It is known that AASs induce infiltration of the liver with inflammatory cells, which together with activated Kupffer cells, favor a pro-inflammatory state by releasing nuclear factor-κB (NF-κB) and inflammatory cytokines transforming growth factor beta1 (TGF-β1), tumor necrosis factor alpha (TNFα), and interleukin-1B (IL-1B). Such conditions also lead to activation of liver stellate cells, resulting in excessive collagen synthesis and deposition[26]. Interestingly, AASs can also promote collagen synthesis by activating their intracellular receptor and activation of transcription factors involved in collagen synthesis[27]. A recent study also gave convincing evidence for a role of testosterone in the pathophysiology of liver diseases with higher occurrences in males than in females. It demonstrated that the susceptibility of the mouse liver to injury was correlated with excessive inflammatory response mediated by androgen receptors (ARs) and testosterone-induced NOD-like receptor family pyrin domain containing 3 (NLRP3) inflammasome activation associated with a variety of chronic diseases[28]. Hepatotoxicity of AASs may also vary due to individual susceptibility, pre-existing liver conditions, and genetic factors. Most frequently reported liver disorders related to AASs are cholestasis, peliosis hepatis, and development of liver tumors[11,29-32]. Figure 1 shows an overview of proposed mechanisms of hepatotoxicity caused by AAS.

AAS drug-induced liver injury (AAS DILI) has also been frequently reported to cause serum liver enzyme elevations in AAS users. Elevated aspartate aminotransferase (AST), alanine aminotransferase (ALT), and lactate dehydrogenase (LDH) activities are, in general, regarded as indicators of hepatocellular damage. Transient elevation of AST and ALT in plasma has been largely reported in AAS users [33], but liver damage may not be the cause of the elevations because of the possible contribution of heavy and intense workouts with consequent muscle damage and rhabdomyolysis. Thus, liver enzymes

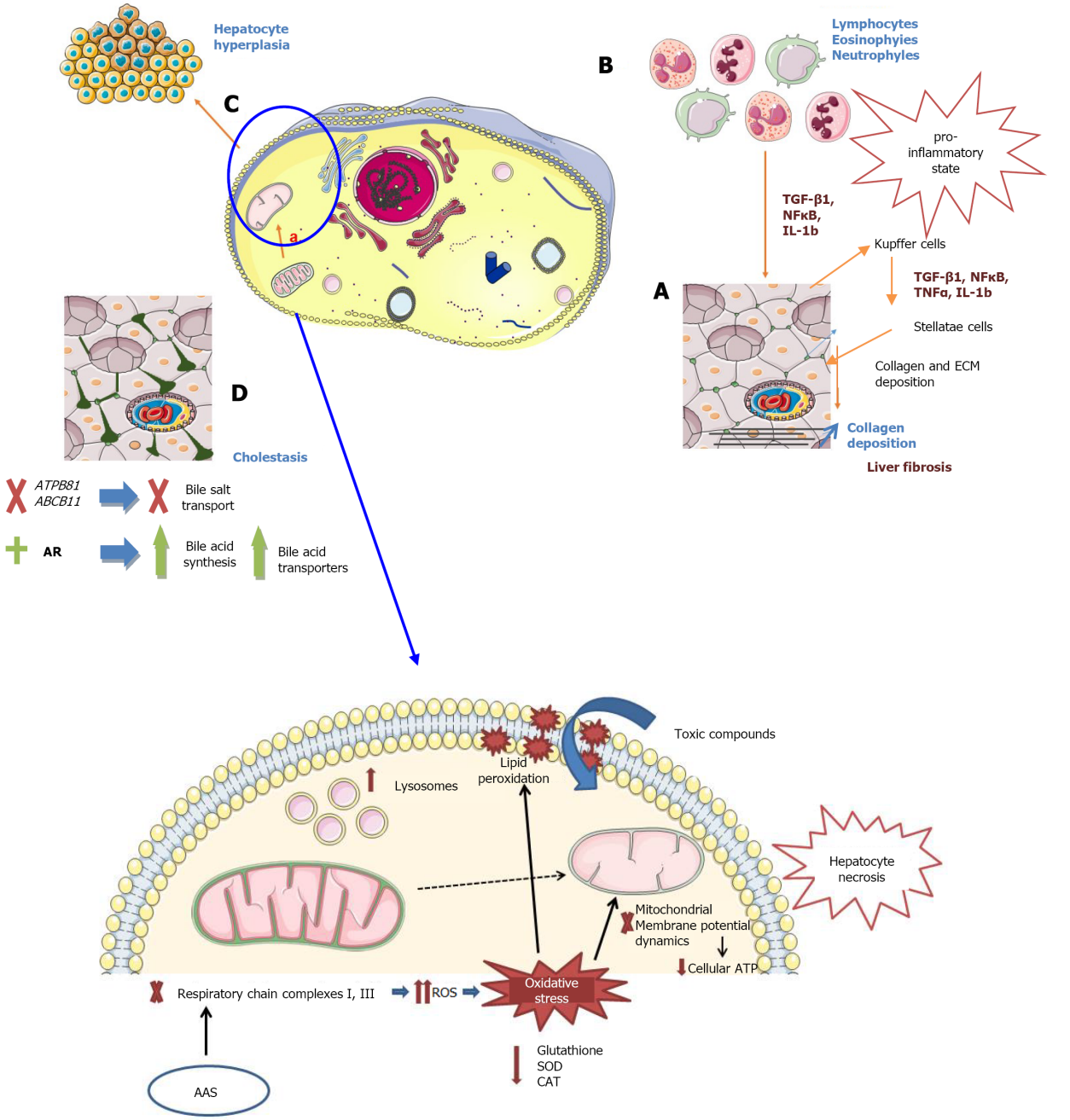

DOI: 10.3748/wjg.v28.i26.3071

Figure 1 Proposed mechanisms of anabolic androgen steroid-induced liver injury. A: Oxidative stress in the mitochondria. Anabolic androgenic steroids (AASs) impair mitochondrial respiratory function, which leads to reactive oxygen species (ROS) accumulation. Cell membrane is damaged due to lipid peroxidation and intracellular ATP depletion occurs due to mitochondrial impairment. This results in cellular dysfunction at many levels (*e.g.*, toxic compounds can enter the cell). Mitochondrial morphology is also changed, with reduced cristae and swelling. In addition, there is an increase in lysosome number. Lack of energy supply eventually leads to hepatocyte necrosis; B: Immune cell infiltration of liver parenchyma. Long-term treatment with AASs like nandrolone is associated with immune cell infiltration which maintains proinflammatory state in liver tissue. Under such conditions, Kupffer cells release transforming growth factor beta1 (TGF-β1), tumor necrosis factor alpha (TNFα), and interleukin-1B (IL-1B) which mediate hepatic stellate cell activation: Extracellular matrix and collagen deposition leading to liver fibrosis; C: Hepatocyte hyperplasia causes formation of hepatic tumors. In rats treated with high-dose nandrolone, it was observed that it supported the viability of hepatic stem cells, which are potential reservoir of cancer stem cells. Nodular hepatocyte hyperplasia causes parenchyma distortion and mechanical blockage of vasculature which forms cystic lesions filled with blood, known as peliosis hepatic; D: "Bland cholestasis". Activation of androgen receptors (ARs) by AASs interferes with bile transporters, mediates intrahepatic microfilament damage, and increases expression of genes for acid bile and bile transporter synthesis, and these changes result in bile acid accumulation, cholestasis, and cholestatic jaundice. SOD: Superoxide dismutase; CAT: Catalase; AR: Androgene receptor; AAS: Anabolic androgenic steroid; AR: Androgen receptor. Figure created with Servier Medical Art, https://smart.servier.com/.

can be elevated independent of androgenic steroid use. Studies showing elevations of creatine kinase (CK) and AST, with no ALT and gamma glutamyl transferase (GGT) elevations, support this concept and suggest that hepatotoxicity related to AASs may be over-estimated if serum ALT, AST, and GGT concentrations are the sole criteria used[34]. Furthermore, a recent multi-center prospective study regarding the incidence of liver injury in transgender patients treated with hormone therapy including AASs showed no significant ALT, AST, alkaline phosphatase (ALP), or GGT elevations[35]. Most of the hepatotoxic effects, cholestasis, peliosis, and liver tumors are associated with orally administered AASs such as testosterone cypionate, enanthate, propionate, methyltestosterone, oxymetholone, danazol, stanozolol, formebolone, and methandienone[36,37], but intramuscular preparations were also linked to hepatotoxic effects[38]. Patil *et al*[38] reported three cases of AAS-induced hepatotoxicity which all manifested differently. The first case was a 31-year-old man who developed cholestatic liver injury after 2 mo of oxymetholone use, the second case was a 24-year-old man who developed well-differentiated hepatocellular carcinomas (HCC) and multiple hepatic adenomas after 3 years of intramuscular testosterone decanoate and daily oral stanozolol use, and the third case was a 36-year-old man with steatohepatitis after 2 mo of intramuscular nandrolone decanoate use[38]. The exact incidence of AAS DILI is difficult to establish due to both underreporting and lack of awareness. On the other hand, even when a history of AAS use is known, it may be difficult to establish the causality, particularly when multiple agents are used concomitantly or if there is an underlying liver condition. However, there has been a trend of increased AAS DILI reporting in recent years which may lead to new insights into pathophysiology and disease course. According to currently available data, AAS DILI has a good prognosis as the majority of cases recover completely and only a very small number of cases develop hepatic failure or die[39].

CHOLESTASIS

Although cholestasis is unlikely in patients treated with parenterally administered unmodified testosterone, 17α-alkyl-substituted steroids, which are designed to decrease hepatic metabolism, directly contribute to a highly characteristic form of acute cholestasis, ranging from very mild to severe. Some characteristic clinical manifestations are nausea, pruritus, fatigue, jaundice, and dark urine with elevated bilirubin and ALP, but without significant elevations of AST, ALT, and GGT. Such characteristics are indicative of cholestasis with minimal inflammation of the liver or bile duct. Resolution usually occurs upon discontinuation of anabolic steroids, although some case reports indicate benefits of hydrocortisone and ursodeoxycholic acid treatment[13,39-42].

Some animal model studies have suggested AAS-induced disruption of intrahepatic microfilaments and interference with bile transporter proteins as a pathophysiological mechanism of this syndrome rather than inflammation and injury to the liver and bile duct[29,43]. El-Sherrif *et al*[13] reported two cases of cholestatic DILI caused by the short-term use of AAS-containing dietary supplement Mass-Drol. The authors found that inhibition of expression of genes *ATPB81* and *ABCB11* by AAS may play a crucial role as the underlying mechanism of cholestatic injury. This leads to impaired bile salt transport and also reduced excretion of different hepatic ectoenzymes. Indeed, both patients presented with cholestasis with marked hyperbilirubinemia, but lack of GGT rise. The authors postulated that individuals who are carriers of c.2093G >A mutation in *ABCB11* may be specifically susceptible to cholestatic hepatic injury caused by AASs due to this mechanism[13]. Additionally, the role of multidrug-related proteins (MRP2, MRP3, and MRP4) is important in bile acid transfer as a complimentary mechanism. It was shown that testosterone metabolites are substrates of MRP2 protein, which has reduced activity in Dubin-Johnson syndrome (DJS). The effect of AAS in DJS has not been investigated to our knowledge, whereas it was found that pregnancy and oral contraceptives increase bilirubin levels in women with DJS[44]. Different underlying mechanism was proposed by Petrov *et al*[45], who used an *in vitro* model to demonstrate that AR activation may upregulate the expression of bile acid synthesis genes as well as bile acid transporters. Most recent studies have reported that the patterns of "bland" cholestasis in AAS users are so specific that this picture can be virtually sufficient to make a diagnosis of AAS-induced cholestasis[46]. Many reports refer to these phenomena as AAS DILI[39,47].

PELIOSIS HEPATIS

Peliosis hepatis is a rare condition characterized by hypervascular liver parenchyma and blood-filled cysts that is known to be associated with use of AASs and several other drugs like estrogens, corticosteroids, and azathioprine. So far, disruption of hepatic extracellular matrix and direct endothelial cell injury have been suggested as generating mechanisms for liver peliosis. It has also been proposed that steroid-induced hepatocyte hyperplasia results in mechanical obstruction of hepatic vascular system, causing dilatation and loss of endothelial barrier function[11,30,48]. Molecular mechanisms in pathophysiology of peliosis remain poorly understood; however, an important role of vascular

endothelial growth factor (VEGF) has been suggested in recent studies. VEGF induces angiogenesis, capillary permeability, and proliferation of endothelial cells in liver and other tissues. Tzirogiannis *et al* [49] found a major protective effect of VEGF which almost totally reversed the extent of peliosis in a model of cadmium-induced toxic liver injury and peliosis, implying that it preserves endothelial cell function. However, a study of peliosis hepatis in a patient with follicular lymphoma found elevated VEGF and suggested that lesions could be caused by elevation of VEGF and its angiogenic effects[50]. An animal model study of peliosis hepatis associated with melanoma supports a concept that a tumor-derived factor such as VEGF could induce development of peliosis due to its endothelial cell proliferation effect[51]. These conclusions indicate a need for further research of pathophysiology in peliosis hepatis as well as AASs and their impact on growth factors. Peliosis hepatis is commonly asymptomatic, but case reports described presentation characterized by sharp abdominal pain and hemoperitoneum in cases of cyst rupture[52]. Peliosis is usually treated with supportive care and the condition has shown to regress with discontinuation of AASs[53,54]. The condition has been reported not only in use of 17-alpha-alkylated steroids, but also in patients treated with unmodified testosterone[19]. Given its benign nature, most cases of peliosis hepatis are incidentally found and the most appropriate diagnostic modalities are magnetic resonance imaging[55] and histological examination. Once diagnosed, the offending drug should be discontinued and the condition closely monitored to reduce the risk of rupture, especially with larger lesions.

NEOPLASMS

Hepatic tumors, ranging from benign adenomas to malignant hepatocellular carcinoma, have been reported in patients with long-term anabolic steroid therapy[56-58]. Studies have suggested a higher hepatic cancer prevalence in males than in females. Higher endogenous concentrations of androgens may be a major factor in the development of liver carcinomas. Having both the estrogen and ARs, the liver is a hormone sensitive organ. The use of AASs is highly associated with hepatocyte proliferation and liver tumors[59]. An i*n vitro* study on HepG2 cells showed that a supraphysiologic dose of nandrolone changed their phenotype to be stem-like, but the mechanism of this transformation remains to be elucidated. In the same study, nandrolone administered *in vivo* in a mouse model promoted "stemness" in healthy organs, primarily ones naturally rich in stem cells such as the liver. Cell "stemness" phenotype is a metabolically latent state in which there is a lower oxygen consumption in the mitochondria. Expression of *Nanog*, *Lin28*, *Myc*, and *Klf4* genes and CD133 membrane protein is also considered to be markers of cell stemness. This led to a hypothesis that long-term supraphysiologic doses of nandrolone in young healthy individuals possibly increase the risk of malignancy in stem-cell rich organs by increasing the reservoir of stem cells which over a period of time under additional toxic stimuli may turn into cancer stem cells[21]. Studies to date indicate that most of AAS-induced tumors occur with use of agents containing a 17-alpha-alkyl group, but it has also been reported in patients treated with unmodified testosterone[56,60,61]. Histologically, these tumors are most commonly hepatic adenomas or HCC, but cholangiocarcinomas and angiosarcomas have also been reported with long-term AAS use[20]. Given the possibility of malignant transformation of hepatic adenoma, which occurs 10 times more commonly in men than in women, it is recommended that surgical resection be the most appropriate approach in men. In women, estrogen-containing oral contraceptives are a common cause, so their cessation, together with periodic surveillance, is an acceptable approach[62,63]. Solimini *et al*[11] reviewed case reports regarding liver tumors as well as cholestatic hepatitis associated with AASs and reported that several different AAS agents were associated with such liver pathology. Notably, chronic AAS use of several years is linked to development of HCC, while benign neoplasms were mostly linked to short-term use of AAS[11].

ADDITIONAL CONCERNS REGARDING AASS AND THE LIVER

Other hepatic disorders associated with AASs include toxicant-associated fatty liver disease (TAFLD), and possible increased risk of hepatitis B and C infections due to unsafe administration of AASs[64]. In addition, a negative effect on lipoproteins with reduced HDL-cholesterol and increased LDL-cholesterol concentrations has been reported mostly in long-term steroid users[65,66], which contribute to increased risk of coronary disease with AAS use.

Another concerning issue is the increasing number of mislabeled over-the-counter dietary supplements sold legally and containing significant amount of AASs. This has also been associated with adverse effects, but remains underreported and poorly understood. However, new case reports have been published on DILI with jaundice, cholestasis, dyslipidemia, and elevated serum liver enzyme panels in patients directly associated with dietary supplement use. After discontinuation of supplements, liver function commonly returned to normal[67,68]. Consumers may unknowingly use AASs which can result in acute, but also chronic, health problems that are difficult to link to these products and lead to re-exposure[69-71].

CONCLUSION

AAS use is closely linked to hepatotoxicity and serious hepatic conditions such as cholestasis, peliosis hepatis, and benign and malignant hepatic tumors, as well as steatohepatitis and dyslipidemia with multiple studies supporting a causal association. Several pathophysiological mechanisms have been proposed including AR receptor-mediated inflammatory response, disturbance of hepatic antioxidant factors, promotion of hepatocyte hyperplasia, and upregulation of bile acid synthesis. Most of these conditions have been reported with 17-alpha-alkylated steroids. Liver function usually returns to normal with discontinuation of use, but a higher HCC prevalence with AASs is concerning. Another important fact is the increasing number of case reports presenting patients with dietary supplements-associated liver conditions that are still underreported. Given all of the above, screening for liver pathology in known AAS users should be considered in order to possibly reverse the condition. Also, if certain liver pathology is diagnosed incidentally, a history of AAS as potential causal agent should be actively sought, and if found, addressed promptly.

FOOTNOTES

Author contributions: Petrovic A, Smolic R, Smolic M, and Wu GY designed the research study; Petrovic A, Vukadin S, Sikora R, Bojanic K, Plavec D, and Smolic M performed the research; Petrovic A and Vukadin S analyzed the data and wrote the manuscript; all authors have read and approved the final manuscript.

Conflict-of-interest statement: There are no conflicts of interest to report.

Country/Territory of origin: Croatia

ORCID number: Ana Petrovic 0000-0001-5585-3121; Sonja Vukadin 0000-0002-1636-2538; Renata Sikora 0000-0001-8594-549X; Kristina Bojanic 0000-0003-4473-5706; Robert Smolic 0000-0003-4614-4344; Davor Plavec 0000-0003-2020-8119; George Y. Wu 0000-0003-0068-1072; Martina Smolic 0000-0002-6867-826X.

S-Editor: Chen YL
L-Editor: Wang TQ
P-Editor: Chen YL

REFERENCES

1 **Roman M**, Roman DL, Ostafe V, Ciorsac A, Isvoran A. Computational Assessment of Pharmacokinetics and Biological Effects of Some Anabolic and Androgen Steroids. *Pharm Res* 2018; **35**: 41 [PMID: 29404794 DOI: 10.1007/s11095-018-2353-1]
2 **Mullen C**, Whalley BJ, Schifano F, Baker JS. Anabolic androgenic steroid abuse in the United Kingdom: An update. *Br J Pharmacol* 2020; **177**: 2180-2198 [PMID: 31989581 DOI: 10.1111/bph.14995]
3 **Barceloux DG**, Palmer RB. Anabolic-androgenic steroids. *Dis Mon* 2013; **59**: 226-248 [PMID: 23719201 DOI: 10.1016/j.disamonth.2013.03.010]
4 **Margo K**, Winn R. Testosterone treatments: why, when, and how? *Am Fam Physician* 2006; **73**: 1591-1598 [PMID: 16719252]
5 **Basaria S**. Androgen abuse in athletes: detection and consequences. *J Clin Endocrinol Metab* 2010; **95**: 1533-1543 [PMID: 20139230 DOI: 10.1210/jc.2009-1579]
6 **Bhasin S**, Storer TW, Berman N, Callegari C, Clevenger B, Phillips J, Bunnell TJ, Tricker R, Shirazi A, Casaburi R. The effects of supraphysiologic doses of testosterone on muscle size and strength in normal men. *N Engl J Med* 1996; **335**: 1-7 [PMID: 8637535 DOI: 10.1056/NEJM199607043350101]
7 **Shahidi NT**. Androgens and erythropoiesis. *N Engl J Med* 1973; **289**: 72-80 [PMID: 4575719 DOI: 10.1056/NEJM197307122890205]
8 **Beggs LA**, Yarrow JF, Conover CF, Meuleman JR, Beck DT, Morrow M, Zou B, Shuster JJ, Borst SE. Testosterone alters iron metabolism and stimulates red blood cell production independently of dihydrotestosterone. *Am J Physiol Endocrinol Metab* 2014; **307**: E456-E461 [PMID: 25074984 DOI: 10.1152/ajpendo.00184.2014]
9 **Hoffman JR**, Ratamess NA. Medical issues associated with anabolic steroid use: are they exaggerated? *J Sports Sci Med* 2006; **5**: 182-193 [PMID: 24259990]
10 **Pope HG Jr**, Wood RI, Rogol A, Nyberg F, Bowers L, Bhasin S. Adverse health consequences of performance-enhancing drugs: an Endocrine Society scientific statement. *Endocr Rev* 2014; **35**: 341-375 [PMID: 24423981 DOI: 10.1210/er.2013-1058]

11 **Solimini R**, Rotolo MC, Mastrobattista L, Mortali C, Minutillo A, Pichini S, Pacifici R, Palmi I. Hepatotoxicity associated with illicit use of anabolic androgenic steroids in doping. *Eur Rev Med Pharmacol Sci* 2017; **21**: 7-16 [PMID: 28379599]

12 **Rahnema CD**, Crosnoe LE, Kim ED. Designer steroids - over-the-counter supplements and their androgenic component: review of an increasing problem. *Andrology* 2015; **3**: 150-155 [PMID: 25684733 DOI: 10.1111/andr.307]

13 **El Sherrif Y**, Potts JR, Howard MR, Barnardo A, Cairns S, Knisely AS, Verma S. Hepatotoxicity from anabolic androgenic steroids marketed as dietary supplements: contribution from ATP8B1/ABCB11 mutations? *Liver Int* 2013; **33**: 1266-1270 [PMID: 23750872 DOI: 10.1111/liv.12216]

14 **DEA**. Drugs of abuse. In: Administration. United States department of justice, 2020

15 **Anawalt BD**. Diagnosis and Management of Anabolic Androgenic Steroid Use. *J Clin Endocrinol Metab* 2019; **104**: 2490-2500 [PMID: 30753550 DOI: 10.1210/jc.2018-01882]

16 **Buckman JF**, Farris SG, Yusko DA. A national study of substance use behaviors among NCAA male athletes who use banned performance enhancing substances. *Drug Alcohol Depend* 2013; **131**: 50-55 [PMID: 23688842 DOI: 10.1016/j.drugalcdep.2013.04.023]

17 **Jenssen IH**, Johannessen KB. Aggression and body image concerns among anabolic androgenic steroid users, contemplators, and controls in Norway. *Body Image* 2015; **12**: 6-13 [PMID: 25261635 DOI: 10.1016/j.bodyim.2014.08.009]

18 **Quaglio G**, Fornasiero A, Mezzelani P, Moreschini S, Lugoboni F, Lechi A. Anabolic steroids: dependence and complications of chronic use. *Intern Emerg Med* 2009; **4**: 289-296 [PMID: 19468827 DOI: 10.1007/s11739-009-0260-5]

19 **Shahidi NT**. A review of the chemistry, biological action, and clinical applications of anabolic-androgenic steroids. *Clin Ther* 2001; **23**: 1355-1390 [PMID: 11589254 DOI: 10.1016/s0149-2918(01)80114-4]

20 **Niedfeldt MW**. Anabolic Steroid Effect on the Liver. *Curr Sports Med Rep* 2018; **17**: 97-102 [PMID: 29521706 DOI: 10.1249/JSR.0000000000000467]

21 **Agriesti F**, Tataranni T, Pacelli C, Scrima R, Laurenzana I, Ruggieri V, Cela O, Mazzoccoli C, Salerno M, Sessa F, Sani G, Pomara C, Capitanio N, Piccoli C. Nandrolone induces a stem cell-like phenotype in human hepatocarcinoma-derived cell line inhibiting mitochondrial respiratory activity. *Sci Rep* 2020; **10**: 2287 [PMID: 32041983 DOI: 10.1038/s41598-020-58871-1]

22 **Sadowska-Krępa E**, Kłapcińska B, Nowara A, Jagsz S, Szołtysek-Bołdys I, Chalimoniuk M, Langfort J, Chrapusta SJ. High-dose testosterone supplementation disturbs liver pro-oxidant/antioxidant balance and function in adolescent male Wistar rats undergoing moderate-intensity endurance training. *PeerJ* 2020; **8**: e10228 [PMID: 33240609 DOI: 10.7717/peerj.10228]

23 **Lima EM**, Cassaro KODS, Silva CLD, Silva MA, Poltronieri MP, Nascimento AMD, Andrade TU, Bissoli NS, Brasil GA. Eight weeks of treatment with nandrolone decanoate in female rats promotes disruption in the redox homeostasis and impaired renal function. *Life Sci* 2020; **242**: 117227 [PMID: 31881226 DOI: 10.1016/j.lfs.2019.117227]

24 **Carteri RB**, Kopczynski A, Rodolphi MS, Strogulski NR, Wannmacher CMD, Franceschi ID, Hammerschmitt ME, Driemeier D, Portela LV. Anabolic-androgenic steroids impair mitochondrial function and redox status in the heart and liver of mice. *Steroids* 2021; **172**: 108861 [PMID: 33984388 DOI: 10.1016/j.steroids.2021.108861]

25 **Gragera R**, Saborido A, Molano F, Jiménez L, Muñiz E, Megías A. Ultrastructural changes induced by anabolic steroids in liver of trained rats. *Histol Histopathol* 1993; **8**: 449-455 [PMID: 8358156]

26 **Shalaby AM**, Bahey NG. Reversal of the hepatic damage induced by the supraphysiological dose of nandrolone decanoate after its withdrawal in the adult male rat. *Tissue Cell* 2018; **53**: 44-52 [PMID: 30060826 DOI: 10.1016/j.tice.2018.05.013]

27 **Markova MS**, Zeskand J, McEntee B, Rothstein J, Jimenez SA, Siracusa LD. A role for the androgen receptor in collagen content of the skin. *J Invest Dermatol* 2004; **123**: 1052-1056 [PMID: 15610513 DOI: 10.1111/j.0022-202X.2004.23494.x]

28 **Ma X**, Zhou Y, Qiao B, Jiang S, Shen Q, Han Y, Liu A, Chen X, Wei L, Zhou L, Zhao J. Androgen aggravates liver fibrosis by activation of NLRP3 inflammasome in CCl_4-induced liver injury mouse model. *Am J Physiol Endocrinol Metab* 2020; **318**: E817-E829 [PMID: 32182125 DOI: 10.1152/ajpendo.00427.2019]

29 **Neri M**, Bello S, Bonsignore A, Cantatore S, Riezzo I, Turillazzi E, Fineschi V. Anabolic androgenic steroids abuse and liver toxicity. *Mini Rev Med Chem* 2011; **11**: 430-437 [PMID: 21443508 DOI: 10.2174/138955711795445916]

30 **Vieira RP**, França RF, Damaceno-Rodrigues NR, Dolhnikoff M, Caldini EG, Carvalho CR, Ribeiro W. Dose-dependent hepatic response to subchronic administration of nandrolone decanoate. *Med Sci Sports Exerc* 2008; **40**: 842-847 [PMID: 18408615 DOI: 10.1249/MSS.0b013e3181666f1c]

31 **Schwingel PA**, Cotrim HP, Salles BR, Almeida CE, dos Santos CR Jr, Nachef B, Andrade AR, Zoppi CC. Anabolic-androgenic steroids: a possible new risk factor of toxicant-associated fatty liver disease. *Liver Int* 2011; **31**: 348-353 [PMID: 21040407 DOI: 10.1111/j.1478-3231.2010.02346.x]

32 **Riezzo I**, Turillazzi E, Bello S, Cantatore S, Cerretani D, Di Paolo M, Fiaschi AI, Frati P, Neri M, Pedretti M, Fineschi V. Chronic nandrolone administration promotes oxidative stress, induction of pro-inflammatory cytokine and TNF-α mediated apoptosis in the kidneys of CD1 treated mice. *Toxicol Appl Pharmacol* 2014; **280**: 97-106 [PMID: 25065671 DOI: 10.1016/j.taap.2014.06.031]

33 **Hartgens F**, Kuipers H. Effects of androgenic-anabolic steroids in athletes. *Sports Med* 2004; **34**: 513-554 [PMID: 15248788 DOI: 10.2165/00007256-200434080-00003]

34 **Dickerman RD**, Pertusi RM, Zachariah NY, Dufour DR, McConathy WJ. Anabolic steroid-induced hepatotoxicity: is it overstated? *Clin J Sport Med* 1999; **9**: 34-39 [PMID: 10336050 DOI: 10.1097/00042752-199901000-00007]

35 **A Stangl T**, M Wiepjes C, Defreyne J, Conemans E, D Fisher A, Schreiner T, T'Sjoen G, den Heijer M. Is there a need for liver enzyme monitoring in people using gender-affirming hormone therapy? *Eur J Endocrinol* 2021; **184**: 513-520 [PMID: 33524005 DOI: 10.1530/EJE-20-1064]

36 **Büttner A**, Thieme D. Side effects of anabolic androgenic steroids: pathological findings and structure-activity relationships. *Handb Exp Pharmacol* 2010; 459-484 [PMID: 20020376 DOI: 10.1007/978-3-540-79088-4_19]

37 **Maravelias C**, Dona A, Stefanidou M, Spiliopoulou C. Adverse effects of anabolic steroids in athletes. A constant threat. *Toxicol Lett* 2005; **158**: 167-175 [PMID: 16005168 DOI: 10.1016/j.toxlet.2005.06.005]

38 **Patil V**, Jothimani D, Harika K, Hakeem AR, Sachan D, Vij M, Rela M. Versatility of Anabolic Androgenic Steroid-

Induced Hepatotoxicity. *J Clin Exp Hepatol* 2022; **12**: 216-221 [PMID: 35068803 DOI: 10.1016/j.jceh.2021.03.003]

39 **Abeles RD**, Foxton M, Khan S, Goldin R, Smith B, Thursz MR, Verma S. Androgenic anabolic steroid-induced liver injury: two case reports assessed for causality by the updated Roussel Uclaf Causality Assessment Method (RUCAM) score and a comprehensive review of the literature. *BMJ Open Gastroenterol* 2020; **7** [PMID: 33214235 DOI: 10.1136/bmjgast-2020-000549]

40 **Robles-Diaz M**, Gonzalez-Jimenez A, Medina-Caliz I, Stephens C, García-Cortes M, García-Muñoz B, Ortega-Alonso A, Blanco-Reina E, Gonzalez-Grande R, Jimenez-Perez M, Rendón P, Navarro JM, Gines P, Prieto M, Garcia-Eliz M, Bessone F, Brahm JR, Paraná R, Lucena MI, Andrade RJ; Spanish DILI Registry; SLatinDILI Network. Distinct phenotype of hepatotoxicity associated with illicit use of anabolic androgenic steroids. *Aliment Pharmacol Ther* 2015; **41**: 116-125 [PMID: 25394890 DOI: 10.1111/apt.13023]

41 **Kafrouni MI**, Anders RA, Verma S. Hepatotoxicity associated with dietary supplements containing anabolic steroids. *Clin Gastroenterol Hepatol* 2007; **5**: 809-812 [PMID: 17509944 DOI: 10.1016/j.cgh.2007.02.036]

42 **Stępień PM**, Reczko K, Wieczorek A, Zarębska-Michaluk D, Pabjan P, Król T, Kryczka W. Severe intrahepatic cholestasis and liver failure after stanozolol usage - case report and review of the literature. *Clin Exp Hepatol* 2015; **1**: 30-33 [PMID: 28856252 DOI: 10.5114/ceh.2015.51376]

43 **Modlinski R**, Fields KB. The effect of anabolic steroids on the gastrointestinal system, kidneys, and adrenal glands. *Curr Sports Med Rep* 2006; **5**: 104-109 [PMID: 16529682 DOI: 10.1097/01.csmr.0000306529.74500.f6]

44 **Erlinger S**, Arias IM, Dhumeaux D. Inherited disorders of bilirubin transport and conjugation: new insights into molecular mechanisms and consequences. *Gastroenterology* 2014; **146**: 1625-1638 [PMID: 24704527 DOI: 10.1053/j.gastro.2014.03.047]

45 **Petrov PD**, Fernández-Murga L, Conde I, Martínez-Sena T, Guzmán C, Castell JV, Jover R. Epistane, an anabolic steroid used for recreational purposes, causes cholestasis with elevated levels of cholic acid conjugates, by upregulating bile acid synthesis (CYP8B1) and cross-talking with nuclear receptors in human hepatocytes. *Arch Toxicol* 2020; **94**: 589-607 [PMID: 31894354 DOI: 10.1007/s00204-019-02643-y]

46 **Chopra S**, Gawrieh S, Vuppalanchi R, Saxena R. Role of the Surgical Pathologist in Diagnosis of Drug-induced Liver Injury: Recognizing Specific Patterns of Drug Injury. *Adv Anat Pathol* 2021; **28**: 383-395 [PMID: 34050060 DOI: 10.1097/PAP.0000000000000307]

47 **Goh HG**, Lee YJ, Kim TH. Severe Persistent Jaundice after the Abuse of an Anabolic Androgenic Steroid Analogue. *Korean J Gastroenterol* 2020; **76**: 167-170 [PMID: 32969366 DOI: 10.4166/kjg.2020.76.3.167]

48 **Tsirigotis P**, Sella T, Shapira MY, Bitan M, Bloom A, Kiselgoff D, Levin M, Libster D, Abdul Hai A, Gesundheit B, Or R, Slavin S, Resnick I. Peliosis hepatis following treatment with androgen-steroids in patients with bone marrow failure syndromes. *Haematologica* 2007; **92**: e106-e110 [PMID: 18024386 DOI: 10.3324/haematol.11343]

49 **Tzirogiannis KN**, Papadimas GK, Kondyli VG, Kourentzi KT, Demonakou MD, Kyriakou LG, Mykoniatis MG, Hereti RI, Panoutsopoulos GI. Peliosis hepatis: microscopic and macroscopic type, time pattern, and correlation with liver cell apoptosis in a model of toxic liver injury. *Dig Dis Sci* 2006; **51**: 1998-2006 [PMID: 17053957 DOI: 10.1007/s10620-006-9242-x]

50 **de la Mano EP**, Martín-Sánchez G, López RL, Galán MAF, Ríos ST, Jiménez MJM, de Morales JMGR, Santos MAC, Núñez GM. Peliosis hepatis associated with follicular lymphoma with a rise in vascular endothelial growth factor and anaemia of inflammation. *Ecancermedicalscience* 2018; **12**: 882 [PMID: 30679949 DOI: 10.3332/ecancer.2018.882]

51 **Edwards R**, Colombo T, Greaves P. "Have you seen this? *Toxicol Pathol* 2002; **30**: 521-523 [PMID: 12187943 DOI: 10.1080/01926230290105686]

52 **Choi SK**, Jin JS, Cho SG, Choi SJ, Kim CS, Choe YM, Lee KY. Spontaneous liver rupture in a patient with peliosis hepatis: a case report. *World J Gastroenterol* 2009; **15**: 5493-5497 [PMID: 19916182 DOI: 10.3748/wjg.15.5493]

53 **Nadell J**, Kosek J. Peliosis hepatis. Twelve cases associated with oral androgen therapy. *Arch Pathol Lab Med* 1977; **101**: 405-410 [PMID: 577673]

54 **Fidelman N**, LaBerge JM, Kerlan RK Jr. SCVIR 2002 Film Panel case 4: massive intraperitoneal hemorrhage caused by peliosis hepatis. *J Vasc Interv Radiol* 2002; **13**: 542-545 [PMID: 11997366 DOI: 10.1016/s1051-0443(07)61539-5]

55 **Hui CL**, Lee ZJ. Hepatic disorders associated with exogenous sex steroids: MR imaging findings. *Abdom Radiol (NY)* 2019; **44**: 2436-2447 [PMID: 30955069 DOI: 10.1007/s00261-019-01941-4]

56 **Nakao A**, Sakagami K, Nakata Y, Komazawa K, Amimoto T, Nakashima K, Isozaki H, Takakura N, Tanaka N. Multiple hepatic adenomas caused by long-term administration of androgenic steroids for aplastic anemia in association with familial adenomatous polyposis. *J Gastroenterol* 2000; **35**: 557-562 [PMID: 10905366 DOI: 10.1007/s005350070081]

57 **Evert M**, Dombrowski F. [Hepatocellular carcinoma in the non-cirrhotic liver]. *Pathologe* 2008; **29**: 47-52 [PMID: 18057936 DOI: 10.1007/s00292-007-0953-3]

58 **Socas L**, Zumbado M, Pérez-Luzardo O, Ramos A, Pérez C, Hernández JR, Boada LD. Hepatocellular adenomas associated with anabolic androgenic steroid abuse in bodybuilders: a report of two cases and a review of the literature. *Br J Sports Med* 2005; **39**: e27 [PMID: 15849280 DOI: 10.1136/bjsm.2004.013599]

59 **Velazquez I**, Alter BP. Androgens and liver tumors: Fanconi's anemia and non-Fanconi's conditions. *Am J Hematol* 2004; **77**: 257-267 [PMID: 15495253 DOI: 10.1002/ajh.20183]

60 **El-Serag HB**. Hepatocellular carcinoma: recent trends in the United States. *Gastroenterology* 2004; **127**: S27-S34 [PMID: 15508094 DOI: 10.1053/j.gastro.2004.09.013]

61 **Tanaka K**, Sakai H, Hashizume M, Hirohata T. Serum testosterone:estradiol ratio and the development of hepatocellular carcinoma among male cirrhotic patients. *Cancer Res* 2000; **60**: 5106-5110 [PMID: 11016636]

62 **Farges O**, Ferreira N, Dokmak S, Belghiti J, Bedossa P, Paradis V. Changing trends in malignant transformation of hepatocellular adenoma. *Gut* 2011; **60**: 85-89 [PMID: 21148580 DOI: 10.1136/gut.2010.222109]

63 **European Association for the Study of the Liver (EASL)**. EASL Clinical Practice Guidelines on the management of benign liver tumours. *J Hepatol* 2016; **65**: 386-398 [PMID: 27085809 DOI: 10.1016/j.jhep.2016.04.001]

64 **Aitken C**, Delalande C, Stanton K. Pumping iron, risking infection? *Drug Alcohol Depend* 2002; **65**: 303-308 [PMID: 11841901 DOI: 10.1016/s0376-8716(01)00174-0]

65 **Hartgens F**, Rietjens G, Keizer HA, Kuipers H, Wolffenbuttel BH. Effects of androgenic-anabolic steroids on apolipoproteins and lipoprotein (a). *Br J Sports Med* 2004; **38**: 253-259 [PMID: 15155420 DOI: 10.1136/bjsm.2003.000199]

66 **Kouri EM**, Pope HG Jr, Oliva PS. Changes in lipoprotein-lipid levels in normal men following administration of increasing doses of testosterone cypionate. *Clin J Sport Med* 1996; **6**: 152-157 [PMID: 8792045 DOI: 10.1097/00042752-199607000-00003]

67 **Magee CD**, Witte S, Kwok RM, Deuster PA. Mission Compromised? *Mil Med* 2016; **181**: e1169-e1171 [PMID: 27612377 DOI: 10.7205/MILMED-D-15-00502]

68 **Cabb E**, Baltar S, Powers DW, Mohan K, Martinez A, Pitts E. The Diagnosis and Manifestations of Liver Injury Secondary to Off-Label Androgenic Anabolic Steroid Use. *Case Rep Gastroenterol* 2016; **10**: 499-505 [PMID: 27721739 DOI: 10.1159/000448883]

69 **García-Cortés M**, Robles-Díaz M, Ortega-Alonso A, Medina-Caliz I, Andrade RJ. Hepatotoxicity by Dietary Supplements: A Tabular Listing and Clinical Characteristics. *Int J Mol Sci* 2016; **17**: 537 [PMID: 27070596 DOI: 10.3390/ijms17040537]

70 **Pascale B**, Steele C, Attipoe S, O'Connor FG, Deuster PA. Dietary Supplements: Knowledge and Adverse Event Reporting Among American Medical Society for Sports Medicine Physicians. *Clin J Sport Med* 2016; **26**: 139-144 [PMID: 26035683 DOI: 10.1097/JSM.0000000000000213]

71 **Medina-Caliz I**, Garcia-Cortes M, Gonzalez-Jimenez A, Cabello MR, Robles-Diaz M, Sanabria-Cabrera J, Sanjuan-Jimenez R, Ortega-Alonso A, García-Muñoz B, Moreno I, Jimenez-Perez M, Fernandez MC, Ginés P, Prieto M, Conde I, Hallal H, Soriano G, Roman E, Castiella A, Blanco-Reina E, Montes MR, Quiros-Cano M, Martin-Reyes F, Lucena MI, Andrade RJ; Spanish DILI Registry. Herbal and Dietary Supplement-Induced Liver Injuries in the Spanish DILI Registry. *Clin Gastroenterol Hepatol* 2018; **16**: 1495-1502 [PMID: 29307848 DOI: 10.1016/j.cgh.2017.12.051]

World Journal of Gastroenterology

Submit a Manuscript: https://www.f6publishing.com

World J Gastroenterol 2022 July 14; 28(26): 3081-3091

DOI: 10.3748/wjg.v28.i26.3081

ISSN 1007-9327 (print) ISSN 2219-2840 (online)

MINIREVIEWS

Epidemiological and clinical aspects of hepatitis B virus infection in Italy over the last 50 years

Caterina Sagnelli, Antonello Sica, Massimiliano Creta, Armando Calogero, Massimo Ciccozzi, Evangelista Sagnelli

Specialty type: Gastroenterology and hepatology

Provenance and peer review: Invited article; Externally peer reviewed.

Peer-review model: Single blind

Peer-review report's scientific quality classification

Grade A (Excellent): 0
Grade B (Very good): B
Grade C (Good): C, C
Grade D (Fair): D
Grade E (Poor): 0

P-Reviewer: Dang SS, China; Gu JY, China; Inoue J, Japan; Biswas S, Ireland
A-Editor: Liu X, China

Received: January 12, 2022
Peer-review started: January 12, 2022
First decision: March 8, 2022
Revised: March 16, 2022
Accepted: June 18, 2022
Article in press: June 18, 2022
Published online: July 14, 2022

Caterina Sagnelli, Evangelista Sagnelli, Department of Mental Health and Public Medicine, Section of Infectious Diseases, University of Campania "Luigi Vanvitelli", Naples 80138, Italy

Antonello Sica, Department of Precision Medicine, University of Campania "Luigi Vanvitelli", Naples 80131, Italy

Massimiliano Creta, Department of Neurosciences, Reproductive Sciences and Odontostomatology, University of Naples Federico II, Naples 80138, Italy

Armando Calogero, Department of Advanced Biomedical Sciences-UO General Surgery, University Federico II of Naples, Naples 80127, Italy

Massimo Ciccozzi, Medical Statistics and Molecular Epidemiology Unit, Campus Bio-Medico University, Rome 80138, Italy

Corresponding author: Caterina Sagnelli, Doctor, MD, PhD, Doctor, Postdoc, Professor, Research Scientist, Department of Mental Health and Public Medicine, Section of Infectious Diseases, University of Campania "Luigi Vanvitelli", 5 Via L. Armanni, Naples 80138, Italy. caterina.sagnelli@unicampania.it

Abstract

A relevant gradual reduction of both the incidence rate of acute hepatitis B (AHB) and prevalence of chronic hepatitis B has occurred in Italy in the last 50 years, due to substantial epidemiological changes: Improvement in socioeconomic and hygienic conditions, reduction of the family unit, accurate screening of blood donations, abolition of re-usable glass syringes, hepatitis B virus (HBV)-universal vaccination started in 1991, use of effective well tolerated nucleo(t)side analogues able to suppress HBV replication available from 1998, and educational mediatic campaigns against human immunodeficiency virus infection focusing on the prevention of sexual and parenteral transmission of infections. As an example, AHB incidence has gradually decreased from 10/100000 inhabitants in 1985 to 0.21 in 2020. Unfortunately, the coronavirus disease 2019 (COVID-19) pandemic has interrupted the trend towards HBV eradication. In fact, several HBV chronic carriers living in the countryside have become unable to access healthcare facilities for screening, diagnosis, clinical management, and nucleo(t)side analogue therapy in the COVID-19 pandemic, mainly for anxiety of becoming infected with severe acute respiratory syndrome coronavirus 2 (SARS-CoV-2), movement restrictions, and reduced gains from job loss. In addition, one-third of

healthcare facilities and personnel for HBV patients have been devolved to the COVID-19 assistance.

Key Words: Hepatitis B virus; Hepatitis B virus epidemiology; Acute hepatitis B; COVID-19

Core Tip: An impressive reduction in the spread of hepatitis B virus (HBV) infection has been observed over the past 5 decades in Italy. This review article analyzes, in Italy, the effects of various events on HBV endemicity: Reduction of the impact of several risk factors, HBV-universal vaccination started in 1991, the nucleo(t)side analogue therapy started in 1996, the increased immigration flows from countries at high HBV endemicity, and the restrictions generated by the coronavirus disease 2019 (COVID-19) pandemic. Particular attention has been directed at the negative effects of the COVID-19 pandemic that threaten to interrupt the favorable trend towards HBV eradication.

Citation: Sagnelli C, Sica A, Creta M, Calogero A, Ciccozzi M, Sagnelli E. Epidemiological and clinical aspects of hepatitis B virus infection in Italy over the last 50 years. *World J Gastroenterol* 2022; 28(26): 3081-3091
URL: https://www.wjgnet.com/1007-9327/full/v28/i26/3081.htm
DOI: https://dx.doi.org/10.3748/wjg.v28.i26.3081

INTRODUCTION

Hepatitis B virus (HBV) infection is a global health problem with 3.61% of the world population chronically infected and 890000 deaths per year for cirrhosis, liver failure, or hepatocellular carcinoma (HCC)[1,2]. Despite the availability of an effective recombinant HBV vaccine from 1991[3] and of effective well-tolerated nucleo(t)side analogues since 1998, the rate of individuals persistently infected with HBV does not decrease worldwide and, unfortunately, it is increasing in some developing countries[4]. Several factors support the level of endemicity of HBV infection: (1) Most patients with chronic infections are asymptomatic and undiagnosed for years[5]; (2) 70% of the individuals with chronic HBV infections live in developing areas where HBV vaccination does not have the character of universality, with 95.3 million in Western Pacific areas and 75.6 million in Africa, where there is a prevalence of hepatitis B surface antigen (HBsAg) chronic carriers of 5.26% and 8.83%, respectively[6]; and (3) Nucleo(t)side analogues suppress but do not eradicate chronic HBV infection. Instead, in the last 30 years, a trend to HBV eradication has been observed in northern America, western Europe, and Japan [7].

As far as Italy, HBV endemicity has progressively decreased over the last 50 years, due to universal HBV vaccination since 1991, the improvement in socioeconomic conditions correlated to better standard of hygiene, substantial reduction of the family unit, and continuous mediatic human immunodeficiency virus (HIV) campaigns organized and financed by the Italian government[8].

Italy is experiencing a continuous migratory flow, more frequently from eastern Europe and sub-Saharan Africa for 20 years and today migrants represent about 9% of the resident population. As an effect of immigration, some HBV genotypes previously rare in Italy are currently responsible for about 40% of acute hepatitis B (AHB) cases[9-12]. There is the fear that the continuous immigrant flows from countries with high or intermediated HBV endemicity will adversely affect the low endemicity level of Italy. As an example, of 882 asymptomatic undocumented migrants or refugees observed in southern Italy in 2015, 78 (9%) were HBsAg positive. This rate was 14% in 444 sub-Saharan Africa subjects, 6% in 198 eastern Europe subjects, and 2%-3% in the 240 migrants from northern Africa, Bangladesh, India, Pakistan, or Sri Lanka, percentages much higher than the 0.8% registered in the people born and living in Italy[13]. The regional office of the World Health Organization (WHO) for Europe reported that a high percentage of immigrants are not vaccinated against HBV upon their arrival in host countries[14] and therefore at risk of becoming infected even in geographic areas with a low HBV endemicity level; accordingly, in Italy one fifth of the new AHB cases are represented by the immigrant population.

Like for numerous other sectors of medicine, the severe acute respiratory syndrome coronavirus 2 (SARS-CoV-2) pandemic reduced care levels also for HBV-related diseases. A recent web-based survey performed in Italy registered that a quarter of healthcare centers and personnel dedicated to liver diseases had been intended for coronavirus disease 2019 (COVID-19) and that 23% of cases with chronic hepatitis B (CHB) undergoing HBV suppression with nuclo(t)side analogues have suffered interruptions of therapeutic plans[15]. There is therefore a suggestion for the healthcare institutions of Italy not to neglect the need of patients with HBV infection throughout this long terrible COVID-19 pandemic, not to lose in short time the advantages obtained with decades of considerable efforts and economic

commitment.

EPIDEMIOLOGICAL AND CLINICAL CHANGES OF AHB IN ITALY OVER LAST FIVE DECADES

HBV is a non-cytopathic virus that induces liver cell necrosis through cytolytic action of human cytotoxic T cells made able to recognize the viral antigens expressed on the surface of infected hepatocytes from a previous pre-sensitization to HBV. The degree of immune response depends on the age of the host at the acquisition of HBV infection, being absent or low in infants and young children who often develop an asymptomatic acute hepatitis frequently progressing to an HBsAg chronic carriage, but high in young adults and adults who usually develop a self-limiting symptomatic acute hepatitis, progressing to chronicity in only 2%-5% of cases. Fulminant hepatitis occurs in only 1%-3% of cases, more frequently in adolescents and young adults, with a mortality rate of 70%, and in most cases requiring liver transplantation[16-19]. In its classic form, AHB begins with generic symptoms such as fever, malaise, headache, nausea, anorexia, vomiting, and diarrhea, followed by jaundice common in adults and rare in children. The aminotransferases serum levels are usually normal or moderately increased in children and high in adults, reflecting the extension of liver damage. High serum titers of IgM to hepatitis B core antigen identify HBV as the etiological factor, simultaneously with serum HBsAg positivity. Hepatitis B e antigen (HBeAg) and serum HBV DNA are signs of high infectivity; they can be found in the early stage of the disease and are no more detectable in the elimination phase of the virus, event accompanied by seroconversion to anti-HBe. A Cochrane's review of seven randomized controlled trials involving a total number of 597 participants found that antiviral treatment has no benefit for AHB[20], since any evolution to chronicity is strongly determined by the reactivity of the patient's immune system. Some more severe cases, however, may require supportive therapy.

All yearly AHB cases occurred in Italy in the sixties were registered by the Italian Institute of Statistic (ISTAT) under one single entry, with an incidence rate of 98 cases per 100000 inhabitants, followed by a subsequent gradual decline to 20 cases per 100000 inhabitants until 1987[8]. Reliable data on AHB incidence in Italy are reported since 1985, when the surveillance of the integrate epidemiological system of acute viral hepatitis (SEIEVA) registered 12 cases per 100000 inhabitants. This incidence gradually decreased in subsequent years, driven by two important events: (1) The beginning in 1985 of mediatic HIV educational campaigns that advised the condoms for sexual intercourses at risk and to avoid syringe sharing[21]; and (2) since 1991, the national universal HBV vaccination continued so far without interruption; currently all Italian people aged 0 to 41 have been vaccinated[22]. The AHB incidence in 1987 decreased to 10.4 cases per 100000 inhabitants, 5.4 in 1990, 0.9 in 2012, 0.6 in 2016, and 0.21 in 2020 (Table 1).

These data testify the strong contribution of the HBV vaccination to reduction of AHB incidence, but it is equally evident that this reduction had already begun before the universal HBV vaccination campaign had started in 1991. The reason for this is that other factors have contributed to the decrease of AHB incidence in Italy, such as the obligation to test blood donations for HBV markers and not to transfuse the samples testing positive, improvement of socioeconomic and hygienic conditions, and some behavioral changes that have led to the reduction of domestic contacts with a chronic HBsAg carrier and not to use non-disposable or improperly sterilized instruments for medical and surgical practice, piercings, tattoos, manicures, pedicures, acupuncture, and barber's shop[23-25]. Vertical transmission of HBV is no longer a route of HBV transmission in Italy from 1991, due to the mandatory screening for HBV infection among women in pregnancy or at delivery, and to the mandatory, in babies born of HBsAg-positive mothers, active and passive immune prophylaxis. Two routes of HBV transmission remain active, the parenteral one because of the exchange of syringes or other objects between intravenous drug users and the sexual one because of the unusual use of condom in sexual intercourses. It should also be underlined that the impact of these two risk factors on HBV endemicity has progressively lowered, due to the positive effect of universal HBV vaccination which currently covers the Italian population aged 0-41.

Analyzed by the age classes, 0-14 years, 15-24 years, and 25 years or more, the data registered by SEIEVA in 1985 showed 6 subjects with AHB per 100000 inhabitants in age class 0-14, 41 in age class 15-24, and 7 in age class 25 or more. The progressive decline was observed in subsequent years in all the three age classes: (1) In 1990: 1, 17, and 4 cases per 100000 inhabitants, respectively; (2) in 1995: 1, 6, and 3 cases, respectively; (3) in 2000: 0.1, 2, and 2 cases, respectively; (4) in 2005: 0, 5, and 1.8 cases, respectively; and (5) in 2011: 0, 0.5, and 1.2 cases per 100000 inhabitants, respectively[26] (Table 1).

Patients with acute viral hepatitis B registered by SEIEVA from 2009 to 2020 were allocated in five age classes (0-14, 15-24, 25-34, 35-54, and 55 or more), with an incidence close to zero in age classes 0-14 and 15-24 and with a continuous downtrend in older age classes up to 2020[26] (Table 1). The cases of AHB in SEIEVA in the period 1991-2019 have been also analyzed by their geographical distribution[26,27], northern + central Italy *vs* southern Italy + main islands (Sicily and Sardinia), a distribution reflecting historical events and the behaviors of the respective inhabitants (Figure 1).

Table 1 Incidence rate of acute hepatitis B in Italy: Cases per 100000 inhabitants per year, according to age classes

Age classes	1985	1990	1995	2000	2005	2009	2010	2011	2012	2013	2014	2015	2016	2017	2018	2019	2020
0-14	6.00	1.00	1.00	0.10	0.00	0.00	0.00	0.00	0.04	0.10	0.03	0.05	0.00	0.00	0.03	0.03	0.00
15-24	41.00	17.00	6.00	2.00	5.00	0.50	0.50	0.45	0.40	0.30	0.28	0.30	0.20	0.15	0.32	0.08	0.08
> 25	7.00	4.00	3.00	2.00	1.80	-	-	-	-	-	-	-	-	-	-	-	-
25-34	-	-	-	-	-	1.20	1.20	1.20	0.80	0.70	0.46	0.33	0.30	0.23	0.34	0.26	0.26
35-54	-	-	-	-	-	1.90	1.80	2.00	1.70	1.90	1.76	1.40	1.10	1.04	0.76	0.69	0.34
> 55	-	-	-	-	-	0.70	0.50	0.50	0.60	0.70	0.51	0.46	0.60	0.48	0.39	0.38	0.20
Total	12.00	5.00	3.00	2.00	1.30	1.00	0.90	1.00	0.85	0.90	0.80	0.70	0.60	0.51	0.44	0.38	0.21

Figure 1 shows a clear trend towards an overtime reduction of the total number of cases in Italy, and moderate changes in cases distribution, increased in northern and central regions and decreased in southern and island areas[26,27].

In Italy, the uninterrupted flux of migrants over the last 20 years brought that about 9% of resident population are composed of immigrants, more frequently from eastern Europe and sub-Saharan Africa. Out of the 4981 AHB cases reported to SEIEVA from 2004 to 2019 by 10 of the 20 Italian regions, 849 (17.0%) occurred in immigrants, of whom 53.4% had come from eastern Europe, 14.6% from Asia, 21.6% from Africa, 8.9% from central/southern America, 0.1% from North America, and 0.1% from Oceania. The comparison between the AHB incidence rates among people born in Italy and foreigners, reported by the "Strong Migratory Pressure Countries", report among foreigners values up to 4 times higher until 2008, a difference progressively decreased from 2009 to 2019, when the standardized rates were 0.4 per 100000 for Italians, and 0.6 for foreigners[26,27].

In Italy, the uninterrupted flux of migrants modified the AHB molecular evolution, where, for decades, genotype D was observed in 95% of patients. Coppola *et al*[28] showed that in 123 AHB-patients, a significant increase in HBV genotypes non-D, from 11% in 1999-2003 to 41.1% in 2004-2008, associated with unsafe sexual habits. In good agreement, Ferraro *et al*[10] showed a high rate of cases with acute hepatitis B due to HBV genotypes non-D in Sicily in 2012 (44% genotype A, 3% genotype E), infected mainly through unsafe sexual intercourses.

In 2015, Zuccaro *et al*[11] reported that HBV genotypes non-D were responsible of nearly half of 103 consecutive cases of acute hepatitis B, mainly HBV genotypes A and F, associated with unsafe sexual exposure. In addition, mutations of antiviral resistance or viral mutants in the antigenic determinant "a" of HBsAg have been reported in AHB-patients[28].

Even clinical presentation and outcome of AHB have changed over time in Italy since, in abolishing the circulation of the virus in subjects aged 0-41, the universal HBV vaccination has confined acute hepatitis B to older ages when the disease is more severe[28,29].

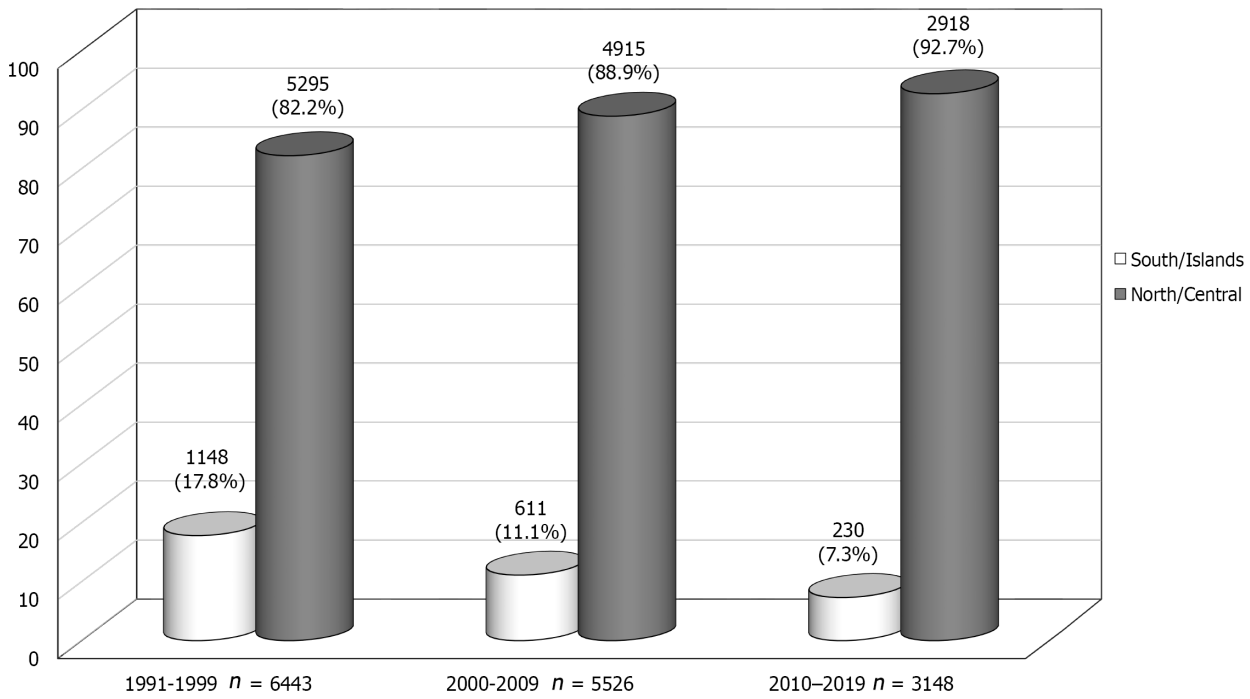

DOI: 10.3748/wjg.v28.i26.3081

Figure 1 Geographic distribution of 15117 new cases of acute hepatitis B registered in the surveillance of the integrate epidemiological system of acute viral hepatitis (SEIEVA) system from 1991 to 2019, according to the time of occurrence.

EPIDEMIOLOGICAL AND CLINICAL CHANGES OF CHB IN ITALY IN THE LAST 50 YEARS

The worldwide prevalence of subjects with chronic HBV infection is estimated at around 5%, with wide differences from a geographic area to another, 0.1%-2.0% in northern America and northwestern Europe, 1.0%-8.0% Japan and African countries overlooking the Mediterranean sea, and 8.0%-20.0% in Southeast Asia/sub-Saharan regions[16,17]. HBV genotype A prevails in northern America and northwestern Europe, HBV genotypes B and C in Asia, genotype D in southern Europe, northern Africa, India, and Middle East, HBV genotype E in western Africa, HBV genotype F in southern/central America, HBV genotype G in the USA and France, and genotype H in Mexico and some countries of South America[30]. CHB, defined as the persistence of HBsAg in serum for more than 6 mo, is a dynamic process which develops through five main phases: (1) "Immune tolerant" phase with mild/absent necroinflammation with normal/low aminotransferase levels, high HBV DNA levels, and HBeAg positivity, with no/slow evolution to fibrosis; (2) "immune reactive phase" characterized by liver necroinflammation, increased or fluctuating aminotransferase serum values, low or intermediate HBV-DNA level, HBeAg positivity, and progression to liver fibrosis or cirrhosis; (3) "inactive HBV carrier state" with low/absent necroinflammation, low/normal aminotransferase serum levels and with very low or undetectable serum HBV DNA, commonly, seroconversion to anti-HBe; (4) "HBeAg-negative CHB" characterized by mild to severe necroinflammation, fluctuating serum levels of aminotransferases and HBV-DNA, linked to e-minus HBV variant unable to express HBeAg[31]; and (5) "occult HBV infection" with HBsAg negativity and low HBV replication with detection of HBV DNA in the liver cells and also in serum (some cases) which clinical impact needs further investigation[32,33].

A complete clinical history should always be the first approach to patients with chronic hepatitis B, including family history, alcohol consumption analysis, metabolic risk assessment, and vaccinations performed. Physical examination should be complete and especially directed at identifying signs indicative of cirrhosis[1]. The laboratory tests useful to define the degree of viral replication and the stage of chronic hepatitis include the search for HBeAg/anti-HBe in serum, HBV DNA load, the blood count, the detection of aminotransferases, total bilirubin, and alkaline phosphatase serum values, and any other tests eventually necessary for the patient under examination[1].

For untreated adult patients, the 5-year cumulative incidence of developing cirrhosis varies between 8% to 20% across studies, and the risk of HCC from 2% to 5%[1]. Among the instrumental investigations, liver biopsy is needed to evaluate the degree of inflammation and fibrosis, a technique, however, sometimes burdened by serious complications, while transient elastography is considered sufficient for the evaluation of fibrosis alone; hepatic ultrasound is of great use for monitoring the clinical course of liver cirrhosis and, in particular, for the early identification of intrahepatic nodules of HCC. Better definition of HCC can be obtained with computed tomography and magnetic resonance imaging.

Drugs recommended and most frequently used to treat CHB are nucleus(t)side analogues tenofovir disoproxil fumarate or tenofovir alafenamide and entecavir, chosen in relation to their high genetic barrier, antiviral potency, and excellent profiles of resistance, tolerability, and safety[1,34]. The duration of treatment remains indefinite because these drugs suppress HBV replication but do not eradicate viral infection and reactivation of both viral replication and chronic disease occurs frequently upon treatment suspension, sometimes with a serious clinical impact[1,34].

At the end of 1970s, the HBV endemicity was considered intermediate, with a prevalence of HBsAg chronic carriers nearly 3%[35,36] and with an increasing gradient from North to South of Italy, where 5% of people were HBsAg positive[37,38]. At that time, the main routes of transmission were vertical transmission at delivery, intravenous drug use (IVDU), and living with an HBsAg chronic carrier, mainly between siblings.

As a result of the reduced HBV circulation, the percentage of HBsAg chronic carriers has decreased overtime in Italy. An impressive decline in HBsAg prevalence in children and teenagers has been observed even before the universal HBV vaccination had been introduced. As an example, the rate of HBsAg positivity decreased from 2.2% in 1980 to 0.8% in 1988 in schoolchildren aged 7-12 years in the city of Naples[39]. This decline has been confirmed in subsequent studies in pregnant women tested at the delivery[40], and in young adults at their enrolment in the army[41].

The rate of HBsAg positivity in patients with chronic hepatitis of all etiologies, either inpatients or outpatients of numerous Italian liver units, was: 61% in 1975[42], 44% in 1980, 34% in 1989[43], and 12.2% in 2001[43-45]. At present, only 0.8% of subjects born in Italy are HBsAg positive, also thanks to the universal HBV vaccination. Additional evidence of efficacy of HBV vaccination in Italy was the increase in the mean age of patients with CHB, from 30.8 years in 1980-1989[42] to 57.3 years in 2019[46].

The positive effects of HBV vaccination to reduce levels of HBV endemicity were also observed in countries with a high level of endemicity. About that, it seems interesting to evaluate the data reported by some authors from China, a nation that like Italy has achieved a remarkable socio-economic improvement in the last decades, where an extensive vaccination campaign against HBV infection has been conducted. A national cross-sectional epidemiological study performed in China in 1992 reported a 9.8% rate of HBsAg chronic carriers[47]. A reduction of this prevalence to 7.2%, due also to a series of measures implemented by the Chinese government, has been reported by Tedder *et al*[48] in 2006. A tendency to a further decline has been shown by a meta-analysis by Wang *et al*[49] who, analyzing the data published in 27 studies from January 2013 to December 2017, estimated a 6.89 HBsAg prevalence in the Chinese population, with more than 90% of HBV infected subjects aging more than 20 years[49]. The data reported by the above-mentioned studies indicate that even starting from very high level of endemicity, the correct application of general and special prophylactic measures, including a wide vaccination campaign against HBV, can yield significant results.

Italy, as mentioned above, has now a country of migration from geographical areas with high or intermediate HBV endemicity in the last two decades. Currently, nearly 9% of the 60 million of inhabitants are immigrants, of whom the major part has not received HBV vaccination and 250000 are estimated to be HBsAg chronic carriers with a 30% rate of HBeAg positivity[50]. The integration of immigrants is proceeding slowly, and it is unlikely that their continuous flow could not impair the favorable results obtained in Italy in the last five decades. El-Hamad *et al*[23] observed 3.728 migrants, mainly undocumented, 12.4% from northern Africa, 21.4% from sub-Saharan Africa, 16.8% from Asia, 44% from eastern Europe, and 5.4% from Central/South America, have come to Italy from 2006 to 2010. The mean rate of HBsAg positivity was 6%, different in the various geographic groups as well as the prevailing HBV genotype, both reflecting those of the country of origin. Coppola *et al*[13] studied 882 undocumented migrants/refugees who lived in the South Italy (period of study January 2012-June 2013), of whom 9% were HBsAg positive. This percentage was 14% in 444 individuals from sub-Saharan Africa, 6% in 198 individuals from Eastern Europe, and 2%-3% in the remaining 240 migrants from other geographic areas[13]. Zermiani *et al*[51] found a 3.5% HBsAg positive rate in migrant female sex workers. A cross-sectional Italy study[50] carried out in 3760 HBV chronic carriers from February to July 2008, reported that 37.1% (932 cases) were migrants from Far East, 35.4% from eastern Europe, 17.5% from sub-Saharan Africa, 5.5% from northern Africa, and 4.5% from other sites. HBV genotype D was detected in 40% of migrants and in 87% of subjects born in Italy. Migrants more frequently than subjects born in Italy were HBV-inactive carriers and less frequently showed CHB, cirrhosis, and HCC.

Sagnelli *et al*[52] evaluated 53 HBsAg chronic carriers with genotype E, immigrated in Southern Italy, of whom 47 (88.7%) were from sub-Saharan Africa, 4 (7.5%) from eastern Europe, and 1 (1.9%) from Asia. The molecular epidemiology study disclosed four statistically supported clusters and traced the genetic evolution and phylogenesis. In addition, phylogenetic analysis on a time scale considering the year of arrival in Italy showed that 52 immigrants had contracted genotype E infection in their country of origin before they arrived in Italy[52].

CONCLUSION

In Italy, the level of HBV endemicity has progressively decreased over the last 50 years. The main

contribution to the downward trend of AHB incidence and of the prevalence of their chronic sequelae is mainly attributable to improvement in socioeconomic and hygienic conditions, the effective educational HIV infection campaigns, and the HBV vaccination since 1991 continued without interruptions until now[43]. There was a consequent strong reduction in the impact of major risk factors for HBV infection acquisition. Vertical transmission from HBsAg positive mother to their newborn babies is just a memory, due to mandatory determination of serum HBsAg in pregnant women, and to passive and active immunization of babies born of HBsAg positive mothers. Besides, the impressive reduction in size of families, particularly in the South Italy regions and islands, has strongly impaired HBV transmission through household contacts with HBsAg-positive chronic carriers. A strong contribution to the significant reduction of HBV endemicity in Italy has been also given by the mandatory screening of blood donations for HBV markers and by the remarkable reduction or abolition of improperly sterilized instruments for medical, surgical, and cosmetic procedures. Also, the role of IVDU has progressively reduced by extension of vaccination to persons aged up to 41. Currently, sexual transmission plays the major role in HBV transmission in Italy, due to infrequent use of condom in unsafe sexual activity[53].

As a consequence of the reduced impact of risk factors for HBV infection acquisition, the prevalence of HBV chronic carriers in the general population has undergone an impressive continuous decrease and to date is 0.8%; similarly, the current AHB incidence B has been reduced to 0.21 per 100000 inhabitants, higher in males than in females, most of cases occurring in Italian citizens with unsafe sexual habits aged over 41 and in unvaccinated migrants[27]. In this regard, most immigrants who come to Italy are not vaccinated against hepatitis B and are three times more likely to acquire HBV infection than Italian citizens[13,26,52,53]. The WHO Regional Office for Europe strongly motivated the national health authorities of the host countries to set up national hepatitis B vaccination protocols for all unvaccinated migrants and instruct local health authorities how to apply them[14]. It should be also emphasized that HBsAg positive migrants should be entrusted to local healthcare facilities for further diagnostic information and clinical therapeutic follow-up.

Like for numerous other sectors of medicine, SARS-CoV2 pandemic has reduced care level also for HBV related diseases. In this period, nearly half people worldwide have not been able to enter clinical center for HBV prevention, diagnosis, and treatment due to breakdowns or other restrictions on the movement imposed by individual governments, absence, or reduction of earnings due to loss of work activities and for the subject' fear to acquire SARS-CoV-2 infection in clinical environments[54]. Furthermore, the activity of clinical structures dedicated to HBsAg positive patients has been greatly reduced, with a sharp contraction in the number of beds for hospitalization, day hospital facilities and healthcare personnel, devolved to assistance for SARS-CoV-2 patients. In Italy, recent web-based survey performed by the Italian Association for the Study of the Liver (AISF) registered that a quarter of hepatology centers have been transformed into divisions for the management of COVID-19 patients and also a quarter of other health services for liver outpatients have been suspended[15]. A continuous clinical/therapeutic follow up has been provided only to 32.5% of patients with decompensated cirrhosis and to 18% of those with HCC; in addition, 23% of CHB patients treated with nuclo(t)side analogues have undergone temporary interruptions of therapy[15]. In this regard international guidelines give clear indications on how to apply therapy with entecavir or tenofovir for an effective long-term suppression of viral replication in CHB patients: Start therapy at first diagnosis, and then continue without interruption to avoid serious and sometimes life-threatening virus reactivations[55,56].

The percentage of subjects vaccinated against COVID-19 in developing countries is decidedly low. In addition, many children have not yet been vaccinated and a minority of adults has refused vaccination in countries with a high socioeconomic level. All this has favored the development of viral variants more and more infectious that is leading the pandemic to its fifth wave. Nevertheless, by reducing SARS-CoV-2 circulation, COVID-19 vaccination is exerting a favorable effect on CHB management, whose consistency, however, is not yet fully assessable because liver units and transplant centers are still suffering severe limitations. Furthermore, most of the damages produced by COVID-19 to patients with liver diseases will come both from the delays in screening, diagnosis and start of treatment and from the interruptions of clinical activities for outpatients, damages not yet calculable. However, the consequences of the first 3 waves of the COVID-19 pandemic have been analysed by Tapper *et al*[57] who reported that all screening procedures were significantly delayed and that this has resulted in a substantial increase in early diagnoses in the advanced stages of liver diseases or at the onset of complications. Analysing the events following the pandemic waves, these Authors identified three phases: The first one taking place in lockdown and other social distances, characterized by high priority for the needs of COVID-19 patients and a strong delay for elective and routine activities regarding other pathologies; the second one following abolition of physical distancing, with a rapid increase in morbidity and decompensation of non-COVID-19 diseases and by a crowding of health facilities forced to solve old and new problems; a long third stage heavily burdened by consequences of delays in diagnosis and start of treatment and by the interruptions of clinical-therapeutic follow-up[57]. More tuned with the problems of HBsAg positive subjects, Mandel *et al*[58] analysed the effect of three waves of COVID-19 pandemic on HBV testing volume in Ontario, a state of Canada with a high socioeconomic level. Test volume for HBV DNA decreased by 37% during the first pandemic wave, by 27% in second one and by 20% in the third one, reflecting reduction in HBsAg testing, 33%, 18% and 15%, respectively. These reductions are most likely due to both an adaptation of citizens to subsequent pandemic waves,

and a favorable effect of an overtime increase in COVID-19 vaccination coverage.

In numerous developing countries, the COVID-19 pandemic is also severely damaging the programs of the HBV-vaccination, as demonstrated by an analysis by the Institute for Health Metrics and Evaluation which showed in 2020 a dropped of vaccination activity to 1990s levels[59].

In clinical practice, telemedicine was increased over the past 20 years[60], with a sharp increase in 2020 and 2021 due to social distancing measures mandatory to curb COVID-19. Consent to the use of telemedicine was expressed by American Association for the Study of Liver Diseases and EASL-ESCMID experts who recommended it in COVID-19 emergency for the care of chronic hepatitis patients, those on waiting for liver transplantation, and those already transplanted[61,62]. On the strength of the experiences gained in waves of COVID-19, telemedicine can usefully be introduced in programs of prevention and screening, diagnosis, clinical, and therapeutic follow-up of HBV patients, with particular advantage for those living in rural areas and for those who have serious trouble getting to a liver unit.

The COVID-19 has caused quickly significant damage to hepatitis B setting that has lost some of the beneficial impact of several scientific research on clinical practice and on technological application, and huge economic investments. Local health authorities should monitor the damages inflicted to HBV patients by COVID-19 pandemic and work to reduce and, when possible, abolish them. Also, a greater spread of telemedicine could reduce the impact of COVID-19 pandemic.

To prevent onset of new SARS-CoV-2 variants highly infectious, nations with high economic levels should contribute to increase the coverage of COVID-19 vaccination in low- or moderate-income nations; the development of new low-cost vaccines suitable for countries with limited health resources will be of help in solving this problem. As far HBV infection, the HBV-universal vaccination must continue worldwide without interruption and health authorities should extend their HBV vaccination protocols to all unvaccinated migrants.

FOOTNOTES

Author contributions: Sagnelli C, Sica A, and Creta M contributed to conceptualization, methodology, validation, formal analysis, investigation, data curation, and original draft preparation; Calogero A and Ciccozzi M contributed to validation and data curation; Sagnelli E contributed to manuscript writing, review, and editing, visualization, and supervision; all authors have read and agreed to the published version of the manuscript.

Conflict-of-interest statement: There are no conflicts of interest to report.

Country/Territory of origin: Italy

ORCID number: Caterina Sagnelli 0000-0002-6413-7810; Antonello Sica 0000-0002-8676-4620; Massimiliano Creta 0000-0003-2082-3330; Armando Calogero 0000-0003-2315-0610; Massimo Ciccozzi 0000-0003-3866-9239; Evangelista Sagnelli 0000-0003-2817-8436.

S-Editor: Chen YL
L-Editor: Wang TQ
P-Editor: Chen YL

REFERENCES

1 **Terrault NA**, Bzowej NH, Chang KM, Hwang JP, Jonas MM, Murad MH; American Association for the Study of Liver Diseases. AASLD guidelines for treatment of chronic hepatitis B. *Hepatology* 2016; **63**: 261-283 [PMID: 26566064 DOI: 10.1002/hep.28156]

2 **Goldstein ST**, Zhou F, Hadler SC, Bell BP, Mast EE, Margolis HS. A mathematical model to estimate global hepatitis B disease burden and vaccination impact. *Int J Epidemiol* 2005; **34**: 1329-1339 [PMID: 16249217 DOI: 10.1093/ije/dyi206]

3 **Huzair F**, Sturdy S. Biotechnology and the transformation of vaccine innovation: The case of the hepatitis B vaccines 1968-2000. *Stud Hist Philos Biol Biomed Sci* 2017; **64**: 11-21 [PMID: 28511068 DOI: 10.1016/j.shpsc.2017.05.004]

4 **Thomas DL**. Global Elimination of Chronic Hepatitis. *N Engl J Med* 2019; **380**: 2041-2050 [PMID: 31116920 DOI: 10.1056/NEJMra1810477]

5 **Global Burden of Disease Study 2013 Collaborators**. Global, regional, and national incidence, prevalence, and years lived with disability for 301 acute and chronic diseases and injuries in 188 countries, 1990-2013: a systematic analysis for the Global Burden of Disease Study 2013. *Lancet* 2015; **386**: 743-800 [PMID: 26063472 DOI:

10.1016/S0140-6736(15)60692-4]
6 **World Health Organization (WHO)**. Hepatitis B; WHO fact sheet. July 27, 2021. [cited 10 January 2022]. Available from: https://www.who.int/news-room/fact-sheets/detail/hepatitis-b
7 **Chen DS**. Toward elimination and eradication of hepatitis B. *J Gastroenterol Hepatol* 2010; **25**: 19-25 [PMID: 20136972 DOI: 10.1111/j.1440-1746.2009.06165.x]
8 **Crovari P**. Epidemiology of viral hepatitis B in Italy. *Vaccine* 1995; **13** Suppl 1: S26-S30 [PMID: 7571823 DOI: 10.1016/0264-410x(95)80043-d]
9 **Sagnelli E**, Sagnelli C, Pisaturo M, Macera M, Coppola N. Epidemiology of acute and chronic hepatitis B and delta over the last 5 decades in Italy. *World J Gastroenterol* 2014; **20**: 7635-7643 [PMID: 24976701 DOI: 10.3748/wjg.v20.i24.7635]
10 **Ferraro D**, Urone N, Pizzillo P, Gussio M, Magliocco S, Cacopardo B, Craxì A, Di Marco V, Di Stefano R. Phylogenetic analysis of isolates from new cases of HBV infection in Southern Italy. *Infect Genet Evol* 2012; **12**: 1591-1596 [PMID: 22824417 DOI: 10.1016/j.meegid.2012.07.006]
11 **Zuccaro O**, Romanò L, Mele A, Mariano A, Clementi M, Tosti ME, Taliani G, Galli C, Zanetti AR, Spada E; Study Group. Clinical, epidemiological and virological features of acute hepatitis B in Italy. *Infection* 2015; **43**: 431-441 [PMID: 25697541 DOI: 10.1007/s15010-015-0747-0]
12 **Romanò L**, Paladini S, Zanetti AR. Twenty years of universal vaccination against hepatitis B in Italy: achievements and challenges. *J Public Health Res* 2012; **1**: 126-129 [PMID: 25170454 DOI: 10.4081/jphr.2012.e18]
13 **Coppola N**, Alessio L, Gualdieri L, Pisaturo M, Sagnelli C, Caprio N, Maffei R, Starace M, Angelillo IF, Pasquale G, Sagnelli E. Hepatitis B virus, hepatitis C virus and human immunodeficiency virus infection in undocumented migrants and refugees in southern Italy, January 2012 to June 2013. *Euro Surveill* 2015; **20**: 30009 [PMID: 26530499 DOI: 10.2807/1560-7917.ES.2015.20.35.30009]
14 **World Health Organization Regional Office for Europe (WHO-EURO)**. Health of Refugees and Migrants Regional Situation Analysis, Practices, Experiences, Lessons Learned and Ways Forward, WHO European Region. 2018. [cited 10 January 2022]. Available from: https://www.euro.who.int/en/publications/abstracts/report-on-the-health-of-refugees-and-migrants-in-the-who european-region-no-public- health-without-refugee-and-migrant
15 **Aghemo A**, Masarone M, Montagnese S, Petta S, Ponziani FR, Russo FP; Associazione Italiana Studio Fegato (AISF). Assessing the impact of COVID-19 on the management of patients with liver diseases: A national survey by the Italian association for the study of the Liver. *Dig Liver Dis* 2020; **52**: 937-941 [PMID: 32703730 DOI: 10.1016/j.dld.2020.07.008]
16 **Lavanchy D**. Worldwide epidemiology of HBV infection, disease burden, and vaccine prevention. *J Clin Virol* 2005; **34** Suppl 1: S1-S3 [PMID: 16461208 DOI: 10.1016/S1386-6532(05)00384-7]
17 **Liaw YF**, Chu CM. Hepatitis B virus infection. *Lancet* 2009; **373**: 582-592 [PMID: 19217993 DOI: 10.1016/S0140-6736(09)60207-5]
18 **McMahon BJ**, Alward WL, Hall DB, Heyward WL, Bender TR, Francis DP, Maynard JE. Acute hepatitis B virus infection: relation of age to the clinical expression of disease and subsequent development of the carrier state. *J Infect Dis* 1985; **151**: 599-603 [PMID: 3973412 DOI: 10.1093/infdis/151.4.599]
19 **Coppola N**, Sagnelli C, Pisaturo M, Minichini C, Messina V, Alessio L, Starace M, Signoriello G, Gentile I, Filippini P, Sagnelli E. Clinical and virological characteristics associated with severe acute hepatitis B. *Clin Microbiol Infect* 2014; **20**: O991-O997 [PMID: 24930916 DOI: 10.1111/1469-0691.12720]
20 **Mantzoukis K**, Rodríguez-Perálvarez M, Buzzetti E, Thorburn D, Davidson BR, Tsochatzis E, Gurusamy KS. Pharmacological interventions for acute hepatitis B infection: an attempted network meta-analysis. *Cochrane Database Syst Rev* 2017; **3**: CD011645 [PMID: 28321877 DOI: 10.1002/14651858.CD011645.pub2]
21 **Stroffolini T**. The changing pattern of hepatitis B virus infection over the past three decades in Italy. *Dig Liver Dis* 2005; **37**: 622-627 [PMID: 15996630 DOI: 10.1016/j.dld.2005.02.010]
22 **Romanò L**, Paladini S, Tagliacarne C, Zappa A, Zanetti AR. The changing face of the epidemiology of type A, B, and D viral hepatitis in Italy, following the implementation of vaccination. *Vaccine* 2009; **27**: 3439-3442 [PMID: 19200848 DOI: 10.1016/j.vaccine.2009.01.056]
23 **El-Hamad I**, Pezzoli MC, Chiari E, Scarcella C, Vassallo F, Puoti M, Ciccaglione A, Ciccozzi M, Scalzini A, Castelli F; ad-hoc Working Group for Hepatitis B in migrants. Point-of-care screening, prevalence, and risk factors for hepatitis B infection among 3,728 mainly undocumented migrants from non-EU countries in northern Italy. *J Travel Med* 2015; **22**: 78-86 [PMID: 25424439 DOI: 10.1111/jtm.12176]
24 **Lai A**, Sagnelli C, Presti AL, Cella E, Angeletti S, Spoto S, Costantino S, Sagnelli E, Ciccozzi M. What is changed in HBV molecular epidemiology in Italy? *J Med Virol* 2018; **90**: 786-795 [PMID: 29315661 DOI: 10.1002/jmv.25027]
25 **Sagnelli C**, Ciccozzi M, Alessio L, Cella E, Gualdieri L, Pisaturo M, Minichini C, Di Caprio G, Starace M, Onorato L, Capoprese M, Occhiello L, Angeletti S, Scotto G, Macera M, Sagnelli E, Coppola N. HBV molecular epidemiology and clinical condition of immigrants living in Italy. *Infection* 2018; **46**: 523-531 [PMID: 29796738 DOI: 10.1007/s15010-018-1153-1]
26 **L'epidemiologia per la sanità pubblica**, Istituto Superiore di Sanità. Sistema epidemiologico integrato dell'epatite virale acuta (SEIEVA). December 22, 2017. Available from: https://www.epicentro.iss.it/epatite/dati-seieva
27 **Stroffolini T**, Morisco F, Ferrigno L, Pontillo G, Iantosca G, Cossiga V, Crateri S, Tosti ME; The Seieva Collaborating Group. Effectiveness of Hepatitis B Vaccination Campaign in Italy: Towards the Control of HBV Infection for the First Time in a European Country. *Viruses* 2022; **14** [PMID: 35215839 DOI: 10.3390/v14020245]
28 **Coppola N**, Tonziello G, Colombatto P, Pisaturo M, Messina V, Moriconi F, Alessio L, Sagnelli C, Cavallone D, Brunetto M, Sagnelli E. Lamivudine-resistant HBV strain rtM204V/I in acute hepatitis B. *J Infect* 2013; **67**: 322-328 [PMID: 23796869 DOI: 10.1016/j.jinf.2013.06.006]
29 **Zanetti AR**, Mariano A, Romanò L, D'Amelio R, Chironna M, Coppola RC, Cuccia M, Mangione R, Marrone F, Negrone FS, Parlato A, Zamparo E, Zotti C, Stroffolini T, Mele A; Study Group. Long-term immunogenicity of hepatitis B vaccination and policy for booster: an Italian multicentre study. *Lancet* 2005; **366**: 1379-1384 [PMID: 16226616 DOI: 10.1016/S0140-6736(05)67568-X]
30 **Kao JH**. Role of viral factors in the natural course and therapy of chronic hepatitis B. *Hepatol Int* 2007; **1**: 415-430 [PMID:

19669337 DOI: 10.1007/s12072-007-9033-2]
31 **Lok AS**, McMahon BJ. Chronic hepatitis B. *Hepatology* 2007; **45**: 507-539 [PMID: 17256718 DOI: 10.1002/hep.21513]
32 **Raimondo G**, Allain JP, Brunetto MR, Buendia MA, Chen DS, Colombo M, Craxì A, Donato F, Ferrari C, Gaeta GB, Gerlich WH, Levrero M, Locarnini S, Michalak T, Mondelli MU, Pawlotsky JM, Pollicino T, Prati D, Puoti M, Samuel D, Shouval D, Smedile A, Squadrito G, Trépo C, Villa E, Will H, Zanetti AR, Zoulim F. Statements from the Taormina expert meeting on occult hepatitis B virus infection. *J Hepatol* 2008; **49**: 652-657 [PMID: 18715666 DOI: 10.1016/j.jhep.2008.07.014]
33 **Coppola N**, Gentile I, Pasquale G, Buonomo AR, Capoluongo N, D'Armiento M, Borgia G, Sagnelli E. Anti-HBc positivity was associated with histological cirrhosis in patients with chronic hepatitis C. *Ann Hepatol* 2013; **13**: 20-26 [PMID: 24378262 DOI: 10.1016/S1665-2681(19)30900-7]
34 **Ghany MG**. Current treatment guidelines of chronic hepatitis B: The role of nucleos(t)ide analogues and peginterferon. *Best Pract Res Clin Gastroenterol* 2017; **31**: 299-309 [PMID: 28774412 DOI: 10.1016/j.bpg.2017.04.012]
35 **Dardanoni L**, Mele A, Polizzi MC. Epidemiology of hepatitis B in Italy. *Ann Ist Super Sanita* 1987; **24**: 235-243 [PMID: 3453605]
36 **Stroffolini T**. Epidemiologia dell'epatite B in Italia. In: La vaccinazione contro l'Epatite da virus B: una scelta prioritaria di politica sanitaria ed economica. Milan: Franco Angelini, 1990: 17-28
37 **Giusti G**, Galanti B, Gaeta GB, Piccinino F, Ruggiero G. HBsAg carriers among blood donors in Italy; a retrospective survey of data from 189 blood banks. *Hepatogastroenterology* 1981; **28**: 96-98 [PMID: 7216155]
38 **Pasquini P**, Kahn HA, Pileggi D, Panà A, Terzi J, Guzzanti E. Prevalence of hepatitis B markers in Italy. *Am J Epidemiol* 1983; **118**: 699-709 [PMID: 6637996 DOI: 10.1093/oxfordjournals.aje.a113680]
39 **D'Argenio P**, Esposito D, Mele A, Ortolani G, Adamo B, Rapicetta M, Forte P, Pisani A, Soldo L, Sarrecchia B. Decline in the exposure to hepatitis A and B infections in children in Naples, Italy. *Public Health* 1989; **103**: 385-389 [PMID: 2798751 DOI: 10.1016/s0033-3506(89)80009-5]
40 **Stroffolini T**, Bianco E, Szklo A, Bernacchia R, Bove C, Colucci M, Cristina Coppola R, D'Argenio P, Lopalco P, Parlato A, Ragni P, Simonetti A, Zotti C, Mele A. Factors affecting the compliance of the antenatal hepatitis B screening programme in Italy. *Vaccine* 2003; **21**: 1246-1249 [PMID: 12559805 DOI: 10.1016/S0264-410X(02)00439-5]
41 **D'Amelio R**, Stroffolini T, Nisini R, Matricardi PM, Rapicetta M, Spada E, Napoli A, Pasquini P. Incidence of hepatitis B virus infection among an Italian military population: evidence of low infection spread. *Eur J Epidemiol* 1994; **10**: 105-107 [PMID: 7957780 DOI: 10.1007/BF01717462]
42 **Giusti G**, Sagnelli E, Gallo C, Piccinino F, Galanti B, Gaeta GB. The etiology of chronic hepatitis in Italy: a multicenter study. *Hepatogastroenterology* 1994; **41**: 397-400 [PMID: 7959581]
43 **Stroffolini T**, Sagnelli E, Mele A, Craxì A, Almasio P; Italian Hospitals Collaborating Group. The aetiology of chronic hepatitis in Italy: results from a multicentre national study. *Dig Liver Dis* 2004; **36**: 829-833 [PMID: 15646431 DOI: 10.1016/j.dld.2004.07.013]
44 **Sagnelli E**, Pasquale G, Coppola N, Marrocco C, Scarano F, Imparato M, Sagnelli C, Scolastico C, Piccinino F. Liver histology in patients with HBsAg negative anti-HBc and anti-HCV positive chronic hepatitis. *J Med Virol* 2005; **75**: 222-226 [PMID: 15602732 DOI: 10.1002/jmv.20260]
45 **Sagnelli E**, Stroffolini T, Mele A, Imparato M, Sagnelli C, Coppola N, Almasio PL. Impact of comorbidities on the severity of chronic hepatitis B at presentation. *World J Gastroenterol* 2012; **18**: 1616-1621 [PMID: 22529690 DOI: 10.3748/wjg.v18.i14.1616]
46 **Stroffolini T**, Ciancio A, Furlan C, Vinci M, Niro GA, Russello M, Colloredo G, Morisco F, Coppola N, Babudieri S, Ferrigno L, Sagnelli C, Sagnelli E; Collaborating group. Chronic hepatitis B virus infection in Italy during the twenty-first century: an updated survey in 2019. *Eur J Clin Microbiol Infect Dis* 2021; **40**: 607-614 [PMID: 33029767 DOI: 10.1007/s10096-020-04065-6]
47 **Xia GL**, Liu CB, Cao HL, Bi SL, Zhan MY, Su CA, Nanc JH, Qic XQ. Prevalence of hepatitis B and C virus infections in the general Chinese population. Results from a nationwide cross-sectional seroepidemiologic study of hepatitis A, B, C, D, and E virus infections in China, 1992. *Int Hepatol Comm* 1996; **5**: 62-73 [DOI: 10.1016/S0928-4346(96)82012-3]
48 **Tedder RS**, Rodger AJ, Fries L, Ijaz S, Thursz M, Rosenberg W, Naoumov N, Banatvala J, Williams R, Dusheiko G, Chokshi S, Wong T, Rosenberg G, Moreea S, Bassendine M, Jacobs M, Mills PR, Mutimer D, Ryder SD, Bathgate A, Hussaini H, Dillon JF, Wright M, Bird G, Collier J, Anderson M, Johnson AM; Collaborative UK Study of Chronic Hepatitis B Infection (CUSHI-B) Study Group. The diversity and management of chronic hepatitis B virus infections in the United Kingdom: a wake-up call. *Clin Infect Dis* 2013; **56**: 951-960 [PMID: 23223601 DOI: 10.1093/cid/cis1013]
49 **Wang H**, Men P, Xiao Y, Gao P, Lv M, Yuan Q, Chen W, Bai S, Wu J. Hepatitis B infection in the general population of China: a systematic review and meta-analysis. *BMC Infect Dis* 2019; **19**: 811 [PMID: 31533643 DOI: 10.1186/s12879-019-4428-y]
50 **Fasano M**, Saracino A, Carosi G, Mazzotta F, Marino N, Sagnelli E, Gaeta GB, Angarano G, Verucchi G, Bellissima P, Angeletti C, Santantonio T. Hepatitis B and immigrants: a SIMIT multicenter cross-sectional study. *Infection* 2013; **41**: 53-59 [PMID: 23264094 DOI: 10.1007/s15010-012-0384-9].]
51 **Zermiani M**, Mengoli C, Rimondo C, Galvan U, Cruciani M, Serpelloni G. Prevalence of sexually transmitted diseases and hepatitis C in a survey of female sex workers in the north-East of Italy. *Open AIDS J* 2012; **6**: 60-64 [PMID: 22833775 DOI: 10.2174/1874613601206010060]
52 **Sagnelli C**, Ciccozzi M, Coppola N, Minichini C, Lo Presti A, Starace M, Alessio L, Macera M, Cella E, Gualdieri L, Caprio N, Pasquale G, Sagnelli E. Molecular diversity in irregular or refugee immigrant patients with HBV-genotype-E infection living in the metropolitan area of Naples. *J Med Virol* 2017; **89**: 1015-1024 [PMID: 27805272 DOI: 10.1002/jmv.24724]
53 **Mele A**, Catapano R, Ferrigno L, Marzolini A, Stazi MA, Martelli A, Pasquini P. Sistema Epidemiologico Integrato dell'epatite Virale Acuta. Rapporto. annuale 1991. Roma: Rapporti Istituto Superiore di sanità, 1993: 16
54 **Wingrove C**, Ferrier L, James C, Wang S. The impact of COVID-19 on hepatitis elimination. *Lancet Gastroenterol Hepatol* 2020; **5**: 792-794 [PMID: 32730783 DOI: 10.1016/S2468-1253(20)30238-7]

55 **Reddy KR**. SARS-CoV-2 and the Liver: Considerations in Hepatitis B and Hepatitis C Infections. *Clin Liver Dis (Hoboken)* 2020; **15**: 191-194 [PMID: 32489654 DOI: 10.1002/cld.970]

56 **Terrault NA**, Lok ASF, McMahon BJ, Chang KM, Hwang JP, Jonas MM, Brown RS Jr, Bzowej NH, Wong JB. Update on prevention, diagnosis, and treatment of chronic hepatitis B: AASLD 2018 hepatitis B guidance. *Hepatology* 2018; **67**: 1560-1599 [PMID: 29405329 DOI: 10.1002/hep.29800]

57 **Tapper EB**, Asrani SK. The COVID-19 pandemic will have a long-lasting impact on the quality of cirrhosis care. *J Hepatol* 2020; **73**: 441-445 [PMID: 32298769 DOI: 10.1016/j.jhep.2020.04.005]

58 **Mandel E**, Peci A, Cronin K, Capraru CI, Shah H, Janssen HLA, Tran V, Biondi MJ, Feld JJ. The impact of the first, second and third waves of covid-19 on hepatitis B and C testing in Ontario, Canada. *J Viral Hepat* 2022; **29**: 205-208 [PMID: 34820967 DOI: 10.1111/jvh.13637]

59 **Gates B**, Gates M. Covid-19 a global perspective 2020 golakeepers report. 2020. [cited 10 January 2022]. Available from: https://www.gatesfoundation.org/goalkeepers/downloads/2020-report/report_a4_en.pdf

60 **Kahn EN**, La Marca F, Mazzola CA. Neurosurgery and Telemedicine in the United States: Assessment of the Risks and Opportunities. *World Neurosurg* 2016; **89**: 133-138 [PMID: 26852710 DOI: 10.1016/j.wneu.2016.01.075]

61 **Fix OK**, Hameed B, Fontana RJ, Kwok RM, McGuire BM, Mulligan DC, Pratt DS, Russo MW, Schilsky ML, Verna EC, Loomba R, Cohen DE, Bezerra JA, Reddy KR, Chung RT. Clinical Best Practice Advice for Hepatology and Liver Transplant Providers During the COVID-19 Pandemic: AASLD Expert Panel Consensus Statement. *Hepatology* 2020; **72**: 287-304 [PMID: 32298473 DOI: 10.1002/hep.31281]

62 **Boettler T**, Newsome PN, Mondelli MU, Maticic M, Cordero E, Cornberg M, Berg T. Care of patients with liver disease during the COVID-19 pandemic: EASL-ESCMID position paper. *JHEP Rep* 2020; **2**: 100113 [PMID: 32289115 DOI: 10.1016/j.jhepr.2020.100113]

World Journal of Gastroenterology

Submit a Manuscript: https://www.f6publishing.com

World J Gastroenterol 2022 July 14; 28(26): 3092-3100

DOI: 10.3748/wjg.v28.i26.3092

ISSN 1007-9327 (print) ISSN 2219-2840 (online)

MINIREVIEWS

Shared decision-making in the management of patients with inflammatory bowel disease

Kai Song, Dong Wu

Specialty type: Gastroenterology and hepatology

Provenance and peer review: Invited article; Externally peer reviewed.

Peer-review model: Single blind

Peer-review report's scientific quality classification

Grade A (Excellent): A
Grade B (Very good): 0
Grade C (Good): C
Grade D (Fair): 0
Grade E (Poor): 0

P-Reviewer: Kaur M, United States; Razzaque MS, United States

Received: January 16, 2022
Peer-review started: January 16, 2022
First decision: April 11, 2022
Revised: April 21, 2022
Accepted: June 19, 2022
Article in press: June 19, 2022
Published online: July 14, 2022

Kai Song, Dong Wu, Department of Gastroenterology, State Key Laboratory of Complex Severe and Rare Diseases, Peking Union Medical College Hospital, Chinese Academy of Medical Sciences, Peking Union Medical College, Beijing 100730, China

Corresponding author: Dong Wu, MD, Professor, Department of Gastroenterology, State Key Laboratory of Complex Severe and Rare Diseases, Peking Union Medical College Hospital, Chinese Academy of Medical Sciences, Peking Union Medical College, No. 1 Shuaifuyuan, Dongcheng District, Beijing 100730, China. wudong@pumch.cn

Abstract

The rapid progress of research into inflammatory bowel disease (IBD) has resulted in increasingly more treatment options. Different options have different advantages and disadvantages, and the preferences of patients may also differ. If patients can be invited to the formulation of medical decision-making, their compliance and satisfaction would be improved, thus possibly achieving better therapeutic results. The present review aims to summarize the current literature on shared decision-making (SDM) in the management of IBD, with the goal of promoting the application of SDM.

Key Words: Inflammatory bowel diseases; Decision making; Shared; Therapeutics

Core Tip: It is often challenging to make therapeutic decisions for patients with inflammatory bowel disease (IBD), given the uncertainty of therapeutic options and diverse patient values. Shared decision-making (SDM) is a process to formulate treatment with patients, trying to clarify and take account of the preferences of patients, increasing their compliance and satisfaction. We summarize current evidence and illustrate the necessity of applying SDM in IBD management.

Citation: Song K, Wu D. Shared decision-making in the management of patients with inflammatory bowel disease. *World J Gastroenterol* 2022; 28(26): 3092-3100
URL: https://www.wjgnet.com/1007-9327/full/v28/i26/3092.htm
DOI: https://dx.doi.org/10.3748/wjg.v28.i26.3092

INTRODUCTION

Inflammatory bowel disease (IBD) refers to a group of chronic inflammatory diseases of the gastrointestinal tract, mainly including Crohn's disease (CD) and ulcerative colitis (UC), which are lifelong diseases that tend to affect individuals aged 20–40 years[1,2]. IBD affects nearly all aspects of living, including patients' private, occupational and social lives. In total, 50%–80% of UC patients and about 67% of CD patients suffer from relapses and remissions, which is a clinical feature of IBD. Around 15%–30% of UC patients fail to achieve sustained remission, while only 13% of CD patients have a relapse-free course[3,4]. Therefore, IBD has a large socioeconomic burden, and direct and indirect costs caused by UC reach 0.81–1.49 billion dollars per year in the United States[5].

Previous research on the mechanism of IBD suggests that genetic susceptibility, intestinal microbiota, environmental factors (such as diet and stress), and the association between proinflammatory and anti-inflammatory cells and factors are involved in the occurrence and development of IBD[6,7]. An increasing number of therapeutic agents have been investigated, including the tumor necrosis factor (TNF)-α antagonist infliximab, and the effectiveness of these agents has been confirmed[8]. Although the large number of treatment options available for IBD is a positive aspect, it complicates the choice of optimal treatment for individual patients.

TRADITIONAL THERAPEUTIC STRATEGIES

The primary therapeutic aim for IBD is to induce and maintain remission[9], of which mucosal healing is the most important target[10]. Besides clinical remission, the most important objective is to achieve mucosal healing under endoscopy[1,2,9,11], which is associated with reduction in recurrence, surgical interventions, intestinal damage and steroid dependence[12,13]. The current treatment regimens for UC and CD are stratified according to severity. A step-up strategy is usually used to treat mild-to-moderate IBD[1,2,14]. For example, mild-to-moderate UC would be first subjected to 5-aminosalicylic acid (5-ASA). When efficacy is unsatisfactory, treatments are escalated to glucocorticoid and/or immunosuppressants, while biologicals are usually used as the final resort. By contrast, for severe IBD or steroid-refractory IBD, immunosuppressants or biologicals may be considered in the earlier stage.

Although the majority of patients with mild-to-moderate UC who receive 5-ASA achieved symptomatic relief within 8 wk, 41% of patients who achieve induced remission eventually experience relapse[15,16]. Thus, daily medication over a longer period of time is necessary to maintain remission. In addition, multiple daily doses of 5-ASA are required in the stage of induced remission, which may impair compliance, particularly for outpatients without regular medication reminders. Additionally, when 5-ASA administration is reduced to once daily during the induction or maintenance of remission stage[16,17], patient compliance may drop to 40%[18]. Poor compliance is a key obstacle for the induction and maintenance of remission[19].

Glucocorticoids constitute an important treatment for the induction of remission in active disease, particularly in CD. However, about 16% of CD patients do not respond to glucocorticoids after treatment for 30 d[20]. In addition, glucocorticoid therapy is often accompanied by a variety of side effects, including diabetes, hypertension, opportunistic infections, and osteoporosis[21,22]. More than 28% of patients with CD develop steroid dependence[20]. Glucocorticoids are not effective in maintaining remission, and the risks associated with long-term use are marked; thus, the dose of glucocorticoids needs to be tapered at the onset of clinical remission[9,16]. When mucosal remission is not achieved, complications such as fistula and stenosis can easily occur[23,24].

Contrary to traditional step-up therapy, the TOP-DOWN trial[25] confirmed that early combination of immunosuppressants led to a higher remission rate than standard step-up therapy in patients without steroids. Evidence has confirmed that the early use of biologicals may benefit certain patients with mild-to-moderate IBD[26]. The CHARM[27], SONIC[24], PRECISE 2[28] and GEMINI 2[29] trials demonstrated the advantages of early biological treatment over step-up therapy in patients with CD, involving anti-TNFα (infliximab and certolizumab) and anti-integrins (vedolizumab). Without sufficient evidence in patients with UC, previous studies showed lower remission rates in patients who had a shorter course of the disease[30], while other studies suggested that early use of vedolizumab increased remission in patients with UC[31].

However, no consensus has formed regarding the early use of biologicals for patients with mild-to-moderate IBD. The Pharmaceutical Benefits Scheme (PBS) of Australia specifies that biologicals should be considered only when the disease remains clinically active after 6 wk of steroids and 3 mo of immunosuppressants[9]. Despite current evidence supporting early use of biologicals, particularly for patients with CD, clinical decision-making needs to involve patients when treatment is economically demanding. It would be improper for clinicians to use biologicals at an early stage solely relying on the personal opinion of the physician, as it could generate conflicts between physicians and patients.

Refractory IBD patients with severe complications (uncontrolled hemorrhage, perforation, abscesses or malignancy) are candidates for surgery[1,2]. However, a previous study showed that gastroenterologists might differ from IBD patients in the willingness to surgery. Patients were more willing than

gastroenterologists to take risks to undergo surgery, and surgeons agreed with patients in the majority of cases[32]. The differences in perceptions among physicians and surgeons have a marked impact on patients, including the timing of referral for surgery.

Due to the convenience of wide access to information, patients may have their own ideas about treatment. Ignoring patients' values or preferences may lead to patient dissatisfaction, poor compliance, and eventually reduced treatment efficacy. Therefore, it is advisable to involve patients in decision-making and to discuss patients' preference after they have been fully informed about the treatment options, which can share the risks and improve patients' compliance. This is called shared decision-making (SDM).

SDM

SDM is an approach where clinicians and patients share the best available evidence when faced with decision-making, and that patients are supported to consider options to achieve informed preferences [33]. Different from traditional diagnosis and treatment procedures, SDM requires that clinicians provide alternative choices of examinations and treatments, and describe the associated risks and benefits, while patients express their preferences and values, and both sides ultimately make decisions that are appropriate and are consistent with patients' best interests[34].

SDM consists of three key steps: (1) Clinicians inform patients of alternative decisions and provide relevant, high-quality, accessible information; (2) Clinicians consider the patients' values and preferences, particularly the most desired therapeutic targets; and (3) Physicians integrate the patients' preferences and values into the decisions to be made[34-36]. The three-talk model is practical to distribute the aforementioned three steps into three conversations, including team talk, option talk and decision talk[37,38]. In the team talk, physicians first actively promote patient participation, inform patients of the current options available for consideration, help patients realize that this is a bidirectional treatment requiring their own participation, and allow patients to think about the primary therapeutic target. In the options talk, physicians introduce each choice to the patients in detail, including the associated advantages and disadvantages, so that patients can compare each option based on their values. For example, for patients with CD, it is necessary to discuss treatment options, such as medical, surgical, and endoscopic therapy, and evidence-based information should be used to explain the remission rate, risks, and costs of each option, so as to objectively demonstrate the advantages and disadvantages of each choice to allow the patients to balance the pros and cons of each approach according to their own preferences and values. In the decision talk, physicians should elicit the patients' preferences and values; thus, the physicians need to understand what is most important to the patients, and make the appropriate decision together with the patients based on the patients' preferences and values. It should be emphasized that it is a course of patients' deliberation, from the stage of being aware of the options to that of understanding those options and having sufficient time to think about what is most important to them with the support of the physicians.

Decision aids can be used for patient education during SDM[39,40]. Decision aids are tools based on evidence-driven medical information. For example, patients can be intuitively told of the clinical remission rate of CD under infliximab monotherapy, and the approximate increased infection rate as well. These tools can be accessed online, on paper, or in video form[34,41,42], and aim to help patients to make deliberate choices among various treatment alternatives[43]. These tools can help patients to obtain relevant clinical evidence, include patients' preferences when medical decision-making dilemmas occur, allow patients to understand the possible long- and short-term results, and promote high-quality decision-making. In terms of decision aids for biological agents, Almario *et al*[44] designed the online decision aid tool IBD and me, which covers the commonly used cetuzumab, viduzumab, adalimumab, infliximab, galimumab and eutecumab; and introduces the timing and frequency of biological use, route of administration, side effects (mainly infectious and oncogenic risks), and common adverse effects of hormones and immunosuppressants. A personalized decision preference report can be obtained after finishing the questionnaire online.

SDM IN IBD

Surveys have shown that the majority of IBD patients agree to be involved in decision-making, and want to be informed about alternative treatments[45-48]. The majority of patients who participate in SDM experience improved clinical satisfaction, higher trust in doctors, and better compliance[49-51]. However, SDM is not suitable for all cases. Medical decisions include effective decisions and preference-sensitive decisions[52]. For effective decisions, it has been demonstrated that the benefits outweigh the risks, so the decisions are undoubtedly the best strategy. For example, coloproctectomy is required in UC patients with complicated colorectal cancer. However, for preference-sensitive decisions, there is no sufficient evidence to demonstrate which treatment is the best, as there may be multiple reasonable treatment options (even including follow-up observation); thus, the judgement of the benefit/risk ratio

falls upon patients, such as whether the treatment target they value has been achieved, or whether the side effects they are concerned about have occurred in the past. Of the two decision types, SDM only fits in the preference-sensitive decisions, which is often present in the management of IBD. IBD is a complex disease with large individual variation, and each treatment has particular advantages and disadvantages. Therefore, SDM is suitable for the management of IBD.

In addition to the aforementioned selection of step up therapy or top-down early intervention treatment strategy, SDM can be used for choosing biologicals. A number of biologicals are currently available for the treatment of IBD, including infliximab, adalimumab, certolizumab, golimumab, natalizumab, vedolizumab and ustekinumab, with differences in the mechanism, route of administration, and side effects[53]. However, it was not until 2019 that the first head-to-head VARSITY trial[54] compared the efficacy and safety of intravenous vedolizumab to subcutaneous adalimumab. Other head-to-head trials of different biologicals are still awaited[55]. Clinicians' selection of biologicals especially for CD patients is varied, because the majority of real-world data on CD show no significant differences in clinical remission rate[56]. Under these circumstances, it is a preference-sensitive decision to choose biologicals. For example, infliximab is administered intravenously, while adalimumab is administered subcutaneously, thus the length of hospital stay varies. While infliximab is administered at intervals of 0, 2 and 6 wk to induce remission, and then administered every 8 wk, adalimumab is administered every 2 wk. In such a case, some patients may be more concerned with the frequency or route of administration due to the distance to the hospital, and therefore may choose infliximab treatment at longer intervals, whereas other patients may give priority to side effects. In a study involving 640 patients with IBD[44], factors that influenced the choice of biologicals for patients with UC were in the following order: long-term remission rate, route/frequency of administration, and risk of lymphoma. For patients with CD, these factors were short-term remission rate, risk of lymphoma, and route/frequency of administration. Of note, a small percentage of patients (3.6%) cited the mechanism of action as the primary factor for their selection of a given biological. At the same time, physicians' assumption of patients' acceptance of biologicals and their preferred route of administration differs from the patients' opinion[57]. If doctors impose on their patients what they think is universally applicable instead of incorporating the patients' preference into the decision-making process, patients may be forced to agree to a treatment plan against their own values. Patients who do not trust their doctors may develop a self-protective mechanism of rejection, thus leading to poor compliance. This awkward situation can be avoided to a large extent by involving patients in the decision-making process.

For the past 20 years, it has been discussed whether biologicals alone or in combination with immunosuppressants should be used for the treatment of IBD. The results of the SONIC study showed the advantages of the combination treatment[58]. Infliximab combined with immunosuppressants achieved higher rates of clinical remission and mucosal healing compared with infliximab or azathioprine alone in corticosteroid-free patients with CD. This may be associated with the fact that immunosuppressants reduce the generation of antidrug antibodies and increase the blood concentration of biological agents[58,59]. Although there is increasing evidence that combination treatment is superior to single-drug treatment[59-61], and the early use of infliximab with azathioprine or methotrexate for ≥ 1 year has been recommended[62], to date, not all the studies support the use of combination treatment, particularly in the case of biologicals other than infliximab[63-67]. In terms of safety, previous studies have shown that biologicals combined with immunosuppressants can increase the incidence of infection and malignancy[68-72]. Therefore, the benefit/risk ratio remains unclear regarding the combination of biological agents with immunosuppressants; thus, clinicians need to explain the benefits and risks to patients. More importantly, the preferences of the patients need to be considered to determine whether the patients would be willing to accept the risk of increased infection and tumor incidence to achieve an increase in remission rate. By involving patients in the decision-making process, the risk of increased side effects can be shared by both doctors and patients.

IBD patients have a risk of relapse after reduction or withdrawal of 5-ASA, glucocorticoids, immunosuppressants, biologicals, or combination therapy. Approximately 30% of patients with CD or UC who stop immunosuppressant monotherapy relapse within 2 years, while 50%–75% relapse within 5 years. By contrast, the risk of relapse after stopping anti-TNF therapy is 30%–40% at 1 year and > 50% at 2 years[73]. The therapeutic cost associated with the long-term use of aforementioned drugs is high, and some side effects may be related to the duration of use, such as the risk of cancer after the use of biologicals. Therefore, whether the treatment should be stopped or the dose tapered needs to be weighed with regard to the possible benefits, costs and risks, and decisions must be made individually. Given the high recurrence rate of IBD and the uncertainty about the optimal timing for clinical, biochemical and endoscopic follow-up, follow-up plans after drug withdrawal or dose reduction should also be made together with patients, taking their preferences into account[73].

As mentioned above, in addition to requiring informed consent, whether patients with IBD should undergo surgery also requires SDM. Controversies exist regarding the choice of surgery[74]. Ileal pouch–anal anastomosis (IPAA) has become the standard surgical option offered to patients with UC, with endoanal mucosal resection being the second choice. IPAA preserves the anal transition zone, which improves fecal continence. However, the elimination of colonic mucosa is the goal of surgical intervention; thus, what IPAA preserves will put the patient at risk of developing dysplasia and

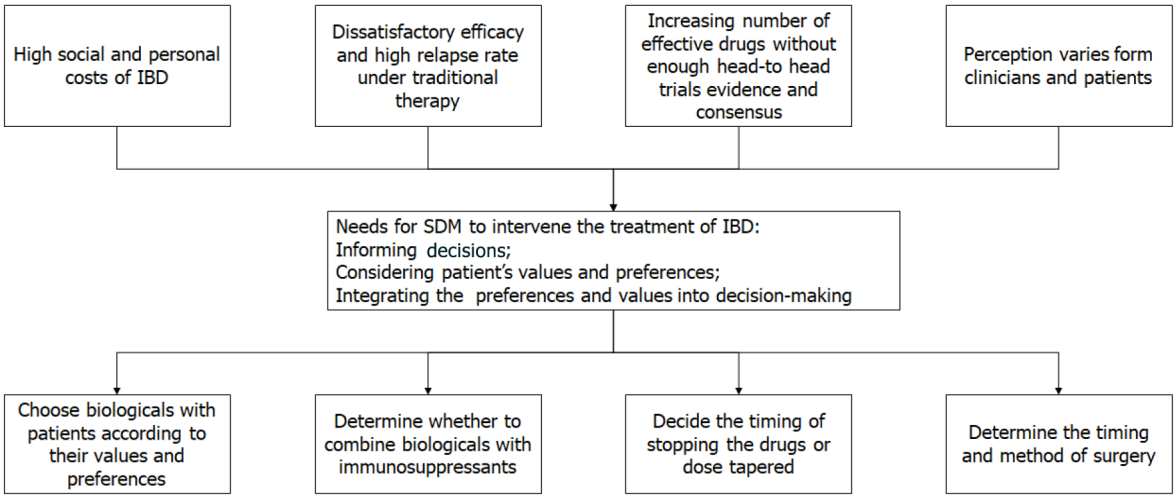

DOI: 10.3748/wjg.v28.i26.3092

Figure 1 The reasons and fields of application for shared decision making in inflammatory bowel disease treatments. IBD: Inflammatory bowel disease; SDM: Shared decision making.

residual disease in the remaining anal canal epithelium, while mucosectomy can decrease dysplasia risk. Therefore, doctors and patients should balance the benefits against potential relapse and malignant change in the retained mucosa.

DISCUSSION

In multiple aspects of IBD management, SDM has shown potential. We believe that SDM can and should be used in IBD therapy (Figure 1). As mentioned, the treatment of IBD is a preference-sensitive choice; the advantages and disadvantages of which need to be weighed by the patients. Clinicians need to invite patients to the decision-making process, even though not all situations are suitable for SDM. For example, when perforation occurs in a UC patient with toxic megacolon, there is no doubt about the choice of treatment, but patients still need to be aware of the need to undergo surgery. Therefore, clinicians must determine whether it is a preference-sensitive decision and whether SDM is required. If patients decline to participate in the SDM even after multiple invitations by doctors, clinicians may not have to continue spending their time on persuading patients.

SDM is a type of informed consent based on evidence-based medicine, putting forward certain requirements for doctors and patients. Challenges inevitably exist in the implementation of SDM. From the aspect of clinicians, as mentioned above, it is important to consider whether doctors are fully aware of the pros and cons of the drugs they choose as new treatments emerge and research advances rapidly. Although it can be resolved with the help of decision aids tools, the tools also should be updated continually. In addition, clinicians should have the awareness and techniques of SDM, and need to receive professional education. With the SDM skills, physicians' willingness to impart relevant knowledge to patients should be emphasized. In addition, different perceptions of IBD between physicians and surgeons may influence patients' perceptions. However, it is worth mentioning that diagnosis and treatment after discussion with a multidisciplinary team is a model that will help bridge the cognitive gap between physicians and surgeons. IBD patients' preferences and disease patterns vary [44], meaning that no SDM plan fits all patients once and for all. Doctors need to be flexible, and patients need to have unlimited access to information and they should be actively invited to the decision-making process. The implementation of SDM undoubtedly needs policy support. For example, biologicals obtained in a first-tier city may not be available in other less-developed cities, which is a restriction for SDM. Unfortunately, SDM is not adequately addressed in current medical education, leading to less awareness of what it is and how to implement it. Therefore, we can't emphasize it too much that the healthcare providers should be trained in their early stage of career to increase the benefits of implementing of SDM. And the early stage training hopefully will cultivate physicians' habit unconsciously to take advantage of SDM in the medical practice.

These challenges need to be carefully considered before SDM can be implemented. Although SDM is theoretically suitable for patients with IBD, studies comparing SDM with traditional decision-making methods remain sparse and are eagerly awaited in the future. We hope that this review will promote the use of SDM in the management of IBD.

CONCLUSION

The investigations delineated in the present article revealed the dilemma of choosing individualized treatments for patients with IBD. We also discussed the advantages of SDM and the aspects in which SDM can be used. Current evidence showed the limitations of conventional step-up therapy for IBD. However, lack of head-to-head clinical trials and diverse treatment preferences of patients lead to difficulty of individualized decision-making. We demonstrate the latest advance of SDM with the support of clinical data, hoping that SDM will be better used by physicians caring for IBD patients.

ACKNOWLEDGEMENTS

We thank Pro. Ji Li for his comment upon this article.

FOOTNOTES

Author contributions: Song K proposed the article framework and performed the majority of the writing; and Wu D settled down the outline and revised the article

Supported by Peking Union Medical College, No. 2019zlgc0503.

Conflict-of-interest statement: All authors report no relevant conflicts of interest for this article.

Country/Territory of origin: China

ORCID number: Kai Song 0000-0003-4459-7059; Dong Wu 0000-0001-9430-9874.

S-Editor: Ma YJ
L-Editor: A
P-Editor: Ma YJ

REFERENCES

1 **Torres J**, Mehandru S, Colombel JF, Peyrin-Biroulet L. Crohn's disease. *Lancet* 2017; **389**: 1741-1755 [PMID: 27914655 DOI: 10.1016/S0140-6736(16)31711-1]
2 **Ungaro R**, Mehandru S, Allen PB, Peyrin-Biroulet L, Colombel JF. Ulcerative colitis. *Lancet* 2017; **389**: 1756-1770 [PMID: 27914657 DOI: 10.1016/S0140-6736(16)32126-2]
3 **Holtmann MH**, Galle PR. Current concept of pathophysiological understanding and natural course of ulcerative colitis. *Langenbecks Arch Surg* 2004; **389**: 341-349 [PMID: 14760536 DOI: 10.1007/s00423-003-0448-5]
4 **Gajendran M**, Loganathan P, Catinella AP, Hashash JG. A comprehensive review and update on Crohn's disease. *Dis Mon* 2018; **64**: 20-57 [PMID: 28826742 DOI: 10.1016/j.disamonth.2017.07.001]
5 **Cohen RD**, Yu AP, Wu EQ, Xie J, Mulani PM, Chao J. Systematic review: the costs of ulcerative colitis in Western countries. *Aliment Pharmacol Ther* 2010; **31**: 693-707 [PMID: 20064142 DOI: 10.1111/j.1365-2036.2010.04234.x]
6 **Guan Q**. A Comprehensive Review and Update on the Pathogenesis of Inflammatory Bowel Disease. *J Immunol Res* 2019; **2019**: 7247238 [PMID: 31886308 DOI: 10.1155/2019/7247238]
7 **Khor B**, Gardet A, Xavier RJ. Genetics and pathogenesis of inflammatory bowel disease. *Nature* 2011; **474**: 307-317 [PMID: 21677747 DOI: 10.1038/nature10209]
8 **Ngo B**, Farrell CP, Barr M, Wolov K, Bailey R, Mullin JM, Thornton JJ. Tumor necrosis factor blockade for treatment of inflammatory bowel disease: efficacy and safety. *Curr Mol Pharmacol* 2010; **3**: 145-152 [PMID: 20799925 DOI: 10.2174/1874467211003030145]
9 **Wright EK**, Ding NS, Niewiadomski O. Management of inflammatory bowel disease. *Med J Aust* 2018; **209**: 318-323 [PMID: 30257634 DOI: 10.5694/mja17.01001]
10 **Jeong DY**, Kim S, Son MJ, Son CY, Kim JY, Kronbichler A, Lee KH, Shin JI. Induction and maintenance treatment of inflammatory bowel disease: A comprehensive review. *Autoimmun Rev* 2019; **18**: 439-454 [PMID: 30844556 DOI: 10.1016/j.autrev.2019.03.002]
11 **Siegel CA**, Whitman CB, Spiegel BMR, Feagan B, Sands B, Loftus EV Jr, Panaccione R, D'Haens G, Bernstein CN, Gearry R, Ng SC, Mantzaris GJ, Sartor B, Silverberg MS, Riddell R, Koutroubakis IE, O'Morain C, Lakatos PL, McGovern DPB, Halfvarson J, Reinisch W, Rogler G, Kruis W, Tysk C, Schreiber S, Danese S, Sandborn W, Griffiths A, Moum B,

Gasche C, Pallone F, Travis S, Panes J, Colombel JF, Hanauer S, Peyrin-Biroulet L. Development of an index to define overall disease severity in IBD. *Gut* 2018; **67**: 244-254 [PMID: 27780886 DOI: 10.1136/gutjnl-2016-312648]

12 **Shah SC**, Colombel JF, Sands BE, Narula N. Systematic review with meta-analysis: mucosal healing is associated with improved long-term outcomes in Crohn's disease. *Aliment Pharmacol Ther* 2016; **43**: 317-333 [PMID: 26607562 DOI: 10.1111/apt.13475]

13 **Shah SC**, Colombel JF, Sands BE, Narula N. Mucosal Healing Is Associated With Improved Long-term Outcomes of Patients With Ulcerative Colitis: A Systematic Review and Meta-analysis. *Clin Gastroenterol Hepatol* 2016; **14**: 1245-1255.e8 [PMID: 26829025 DOI: 10.1016/j.cgh.2016.01.015]

14 **Seyedian SS**, Nokhostin F, Malamir MD. A review of the diagnosis, prevention, and treatment methods of inflammatory bowel disease. *J Med Life* 2019; **12**: 113-122 [PMID: 31406511 DOI: 10.25122/jml-2018-0075]

15 **Feagan BG**, Macdonald JK. Oral 5-aminosalicylic acid for maintenance of remission in ulcerative colitis. *Cochrane Database Syst Rev* 2012; **10**: CD000544 [PMID: 23076890 DOI: 10.1002/14651858.CD000544.pub3]

16 **Bressler B**, Marshall JK, Bernstein CN, Bitton A, Jones J, Leontiadis GI, Panaccione R, Steinhart AH, Tse F, Feagan B; Toronto Ulcerative Colitis Consensus Group. Clinical practice guidelines for the medical management of nonhospitalized ulcerative colitis: the Toronto consensus. *Gastroenterology* 2015; **148**: 1035-1058.e3 [PMID: 25747596 DOI: 10.1053/j.gastro.2015.03.001]

17 **Feagan BG**, Macdonald JK. Oral 5-aminosalicylic acid for induction of remission in ulcerative colitis. *Cochrane Database Syst Rev* 2012; **10**: CD000543 [PMID: 23076889 DOI: 10.1002/14651858.CD000543.pub3]

18 **Kane SV**, Cohen RD, Aikens JE, Hanauer SB. Prevalence of nonadherence with maintenance mesalamine in quiescent ulcerative colitis. *Am J Gastroenterol* 2001; **96**: 2929-2933 [PMID: 11693328 DOI: 10.1111/j.1572-0241.2001.04683.x]

19 **Jackson B**, De Cruz P. Algorithms to facilitate shared decision-making for the management of mild-to-moderate ulcerative colitis. *Expert Rev Gastroenterol Hepatol* 2018; **12**: 1079-1100 [PMID: 30284911 DOI: 10.1080/17474124.2018.1530109]

20 **Faubion WA Jr**, Loftus EV Jr, Harmsen WS, Zinsmeister AR, Sandborn WJ. The natural history of corticosteroid therapy for inflammatory bowel disease: a population-based study. *Gastroenterology* 2001; **121**: 255-260 [PMID: 11487534 DOI: 10.1053/gast.2001.26279]

21 **Rezaie A**, Kuenzig ME, Benchimol EI, Griffiths AM, Otley AR, Steinhart AH, Kaplan GG, Seow CH. Budesonide for induction of remission in Crohn's disease. *Cochrane Database Syst Rev* 2015; CD000296 [PMID: 26039678 DOI: 10.1002/14651858.CD000296.pub4]

22 **Benchimol EI**, Seow CH, Steinhart AH, Griffiths AM. Traditional corticosteroids for induction of remission in Crohn's disease. *Cochrane Database Syst Rev* 2008; CD006792 [PMID: 18425970 DOI: 10.1002/14651858.CD006792.pub2]

23 **Bouguen G**, Peyrin-Biroulet L. Surgery for adult Crohn's disease: what is the actual risk? *Gut* 2011; **60**: 1178-1181 [PMID: 21610273 DOI: 10.1136/gut.2010.234617]

24 **Peyrin-Biroulet L**, Reinisch W, Colombel JF, Mantzaris GJ, Kornbluth A, Diamond R, Rutgeerts P, Tang LK, Cornillie FJ, Sandborn WJ. Clinical disease activity, C-reactive protein normalisation and mucosal healing in Crohn's disease in the SONIC trial. *Gut* 2014; **63**: 88-95 [PMID: 23974954 DOI: 10.1136/gutjnl-2013-304984]

25 **D'Haens G**, Baert F, van Assche G, Caenepeel P, Vergauwe P, Tuynman H, De Vos M, van Deventer S, Stitt L, Donner A, Vermeire S, Van De Mierop FJ, Coche JR, van der Woude J, Ochsenkühn T, van Bodegraven AA, Van Hootegem PP, Lambrecht GL, Mana F, Rutgeerts P, Feagan BG, Hommes D; Belgian Inflammatory Bowel Disease Research Group; North-Holland Gut Club. Early combined immunosuppression or conventional management in patients with newly diagnosed Crohn's disease: an open randomised trial. *Lancet* 2008; **371**: 660-667 [PMID: 18295023 DOI: 10.1016/S0140-6736(08)60304-9]

26 **Berg DR**, Colombel JF, Ungaro R. The Role of Early Biologic Therapy in Inflammatory Bowel Disease. *Inflamm Bowel Dis* 2019; **25**: 1896-1905 [PMID: 30934053 DOI: 10.1093/ibd/izz059]

27 **Schreiber S**, Reinisch W, Colombel JF, Sandborn WJ, Hommes DW, Robinson AM, Huang B, Lomax KG, Pollack PF. Subgroup analysis of the placebo-controlled CHARM trial: increased remission rates through 3 years for adalimumab-treated patients with early Crohn's disease. *J Crohns Colitis* 2013; **7**: 213-221 [PMID: 22704916 DOI: 10.1016/j.crohns.2012.05.015]

28 **Schreiber S**, Colombel JF, Bloomfield R, Nikolaus S, Schölmerich J, Panés J, Sandborn WJ; PRECiSE 2 Study Investigators. Increased response and remission rates in short-duration Crohn's disease with subcutaneous certolizumab pegol: an analysis of PRECiSE 2 randomized maintenance trial data. *Am J Gastroenterol* 2010; **105**: 1574-1582 [PMID: 20234346 DOI: 10.1038/ajg.2010.78]

29 **Sandborn WJ**, Feagan BG, Rutgeerts P, Hanauer S, Colombel JF, Sands BE, Lukas M, Fedorak RN, Lee S, Bressler B, Fox I, Rosario M, Sankoh S, Xu J, Stephens K, Milch C, Parikh A; GEMINI 2 Study Group. Vedolizumab as induction and maintenance therapy for Crohn's disease. *N Engl J Med* 2013; **369**: 711-721 [PMID: 23964933 DOI: 10.1056/NEJMoa1215739]

30 **Murthy SK**, Greenberg GR, Croitoru K, Nguyen GC, Silverberg MS, Steinhart AH. Extent of Early Clinical Response to Infliximab Predicts Long-term Treatment Success in Active Ulcerative Colitis. *Inflamm Bowel Dis* 2015; **21**: 2090-2096 [PMID: 26099066 DOI: 10.1097/MIB.0000000000000474]

31 **Feagan BG**, Rubin DT, Danese S, Vermeire S, Abhyankar B, Sankoh S, James A, Smyth M. Efficacy of Vedolizumab Induction and Maintenance Therapy in Patients With Ulcerative Colitis, Regardless of Prior Exposure to Tumor Necrosis Factor Antagonists. *Clin Gastroenterol Hepatol* 2017; **15**: 229-239.e5 [PMID: 27639327 DOI: 10.1016/j.cgh.2016.08.044]

32 **Byrne CM**, Solomon MJ, Young JM, Selby W, Harrison JD. Patient preferences between surgical and medical treatment in Crohn's disease. *Dis Colon Rectum* 2007; **50**: 586-597 [PMID: 17380368 DOI: 10.1007/s10350-006-0847-0]

33 **Elwyn G**, Laitner S, Coulter A, Walker E, Watson P, Thomson R. Implementing shared decision making in the NHS. *BMJ* 2010; **341**: c5146 [PMID: 20947577 DOI: 10.1136/bmj.c5146]

34 **Barry MJ**, Edgman-Levitan S. Shared decision making--pinnacle of patient-centered care. *N Engl J Med* 2012; **366**: 780-781 [PMID: 22375967 DOI: 10.1056/NEJMp1109283]

35 **Barratt A**. Evidence Based Medicine and Shared Decision Making: the challenge of getting both evidence and preferences into health care. *Patient Educ Couns* 2008; **73**: 407-412 [PMID: 18845414 DOI: 10.1016/j.pec.2008.07.054]

36 **Elwyn G**, Tsulukidze M, Edwards A, Légaré F, Newcombe R. Using a 'talk' model of shared decision making to propose an observation-based measure: Observer OPTION 5 Item. *Patient Educ Couns* 2013; **93**: 265-271 [PMID: 24029581 DOI: 10.1016/j.pec.2013.08.005]

37 **Elwyn G**, Frosch D, Thomson R, Joseph-Williams N, Lloyd A, Kinnersley P, Cording E, Tomson D, Dodd C, Rollnick S, Edwards A, Barry M. Shared decision making: a model for clinical practice. *J Gen Intern Med* 2012; **27**: 1361-1367 [PMID: 22618581 DOI: 10.1007/s11606-012-2077-6]

38 **Elwyn G**, Durand MA, Song J, Aarts J, Barr PJ, Berger Z, Cochran N, Frosch D, Galasiński D, Gulbrandsen P, Han PKJ, Härter M, Kinnersley P, Lloyd A, Mishra M, Perestelo-Perez L, Scholl I, Tomori K, Trevena L, Witteman HO, Van der Weijden T. A three-talk model for shared decision making: multistage consultation process. *BMJ* 2017; **359**: j4891 [PMID: 29109079 DOI: 10.1136/bmj.j4891]

39 **Stacey D**, Légaré F, Lewis K, Barry MJ, Bennett CL, Eden KB, Holmes-Rovner M, Llewellyn-Thomas H, Lyddiatt A, Thomson R, Trevena L. Decision aids for people facing health treatment or screening decisions. *Cochrane Database Syst Rev* 2017; **4**: CD001431 [PMID: 28402085 DOI: 10.1002/14651858.CD001431.pub5]

40 **Trevena LJ**, Zikmund-Fisher BJ, Edwards A, Gaissmaier W, Galesic M, Han PK, King J, Lawson ML, Linder SK, Lipkus I, Ozanne E, Peters E, Timmermans D, Woloshin S. Presenting quantitative information about decision outcomes: a risk communication primer for patient decision aid developers. *BMC Med Inform Decis Mak* 2013; **13** Suppl 2: S7 [PMID: 24625237 DOI: 10.1186/1472-6947-13-S2-S7]

41 **Allen LA**, McIlvennan CK, Thompson JS, Dunlay SM, LaRue SJ, Lewis EF, Patel CB, Blue L, Fairclough DL, Leister EC, Glasgow RE, Cleveland JC Jr, Phillips C, Baldridge V, Walsh MN, Matlock DD. Effectiveness of an Intervention Supporting Shared Decision Making for Destination Therapy Left Ventricular Assist Device: The DECIDE-LVAD Randomized Clinical Trial. *JAMA Intern Med* 2018; **178**: 520-529 [PMID: 29482225 DOI: 10.1001/jamainternmed.2017.8713]

42 **Staszewska A**, Zaki P, Lee J. Computerized Decision Aids for Shared Decision Making in Serious Illness: Systematic Review. *JMIR Med Inform* 2017; **5**: e36 [PMID: 28986341 DOI: 10.2196/medinform.6405]

43 **Chenel V**, Mortenson WB, Guay M, Jutai JW, Auger C. Cultural adaptation and validation of patient decision aids: a scoping review. *Patient Prefer Adherence* 2018; **12**: 321-332 [PMID: 29535507 DOI: 10.2147/PPA.S151833]

44 **Almario CV**, Keller MS, Chen M, Lasch K, Ursos L, Shklovskaya J, Melmed GY, Spiegel BMR. Optimizing Selection of Biologics in Inflammatory Bowel Disease: Development of an Online Patient Decision Aid Using Conjoint Analysis. *Am J Gastroenterol* 2018; **113**: 58-71 [PMID: 29206816 DOI: 10.1038/ajg.2017.470]

45 **Conrad S**, Hüppe A, Raspe H. [Preference of patients with inflammatory bowel disease regarding information and shared decision-making: results from a cross-sectional survey in Germany]. *Z Gastroenterol* 2012; **50**: 364-372 [PMID: 22467539 DOI: 10.1055/s-0031-1281949]

46 **Baars JE**, Markus T, Kuipers EJ, van der Woude CJ. Patients' preferences regarding shared decision-making in the treatment of inflammatory bowel disease: results from a patient-empowerment study. *Digestion* 2010; **81**: 113-119 [PMID: 20093836 DOI: 10.1159/000253862]

47 **Mahlich J**, Matsuoka K, Sruamsiri R. Shared Decision Making and Treatment Satisfaction in Japanese Patients with Inflammatory Bowel Disease. *Dig Dis* 2017; **35**: 454-462 [PMID: 28380481 DOI: 10.1159/000471795]

48 **Morishige R**, Nakajima H, Yoshizawa K, Mahlich J, Sruamsiri R. Preferences Regarding Shared Decision-Making in Japanese Inflammatory Bowel Disease Patients. *Adv Ther* 2017; **33**: 2242-2256 [PMID: 27807816 DOI: 10.1007/s12325-016-0436-0]

49 **Siegel CA**, Lofland JH, Naim A, Gollins J, Walls DM, Rudder LE, Reynolds C. Novel Statistical Approach to Determine Inflammatory Bowel Disease: Patients' Perspectives on Shared Decision Making. *Patient* 2016; **9**: 79-89 [PMID: 25963447 DOI: 10.1007/s40271-015-0126-z]

50 **Lofland JH**, Johnson PT, Ingham MP, Rosemas SC, White JC, Ellis L. Shared decision-making for biologic treatment of autoimmune disease: influence on adherence, persistence, satisfaction, and health care costs. *Patient Prefer Adherence* 2017; **11**: 947-958 [PMID: 28572722 DOI: 10.2147/PPA.S133222]

51 **Veilleux S**, Noiseux I, Lachapelle N, Kohen R, Vachon L, Guay BW, Bitton A, Rioux JD; iGenoMed Consortium. Patients' perception of their involvement in shared treatment decision making: Key factors in the treatment of inflammatory bowel disease. *Patient Educ Couns* 2018; **101**: 331-339 [PMID: 28760459 DOI: 10.1016/j.pec.2017.07.028]

52 **O'Connor AM**, Légaré F, Stacey D. Risk communication in practice: the contribution of decision aids. *BMJ* 2003; **327**: 736-740 [PMID: 14512487 DOI: 10.1136/bmj.327.7417.736]

53 **Patel DB**, van Deen WK, Almario CV, Khalil C, Warui E, Bonthala N, Melmed GY, Spiegel BMR. Assessing Patient Decision-Making on Biologic and Small-Molecule Therapies in Inflammatory Bowel Diseases: Insights From a Conjoint Analysis in the United States, Canada, and the United Kingdom. *Inflamm Bowel Dis* 2021; **27**: 1593-1601 [PMID: 33300555 DOI: 10.1093/ibd/izaa311]

54 **Sands BE**, Peyrin-Biroulet L, Loftus EV Jr, Danese S, Colombel JF, Törüner M, Jonaitis L, Abhyankar B, Chen J, Rogers R, Lirio RA, Bornstein JD, Schreiber S; VARSITY Study Group. Vedolizumab versus Adalimumab for Moderate-to-Severe Ulcerative Colitis. *N Engl J Med* 2019; **381**: 1215-1226 [PMID: 31553834 DOI: 10.1056/NEJMoa1905725]

55 **Pouillon L**, Travis S, Bossuyt P, Danese S, Peyrin-Biroulet L. Head-to-head trials in inflammatory bowel disease: past, present and future. *Nat Rev Gastroenterol Hepatol* 2020; **17**: 365-376 [PMID: 32303700 DOI: 10.1038/s41575-020-0293-9]

56 **Meserve J**, Barsky M, Dulai PS. In the absence of head-to-head trials, what do real world studies tell us about the comparative effectiveness of biologics in Crohn's disease. *Best Pract Res Clin Gastroenterol* 2019; **38-39**: 101619 [PMID: 31327408 DOI: 10.1016/j.bpg.2019.05.006]

57 **Kariburyo MF**, Xie L, Teeple A, Tan H, Ingham M. Predicting Pre-emptive Discussions of Biologic Treatment: Results from an Openness and Preference Survey of Inflammatory Bowel Disease Patients and Their Prescribers. *Adv Ther* 2017; **34**: 1398-1410 [PMID: 28484953 DOI: 10.1007/s12325-017-0545-4]

58 **Colombel JF**, Sandborn WJ, Reinisch W, Mantzaris GJ, Kornbluth A, Rachmilewitz D, Lichtiger S, D'Haens G, Diamond RH, Broussard DL, Tang KL, van der Woude CJ, Rutgeerts P; SONIC Study Group. Infliximab, azathioprine, or

combination therapy for Crohn's disease. *N Engl J Med* 2010; **362**: 1383-1395 [PMID: 20393175 DOI: 10.1056/NEJMoa0904492]

59 **Panaccione R**, Ghosh S, Middleton S, Márquez JR, Scott BB, Flint L, van Hoogstraten HJ, Chen AC, Zheng H, Danese S, Rutgeerts P. Combination therapy with infliximab and azathioprine is superior to monotherapy with either agent in ulcerative colitis. *Gastroenterology* 2014; **146**: 392-400.e3 [PMID: 24512909 DOI: 10.1053/j.gastro.2013.10.052]

60 **Christophorou D**, Funakoshi N, Duny Y, Valats JC, Bismuth M, Pineton De Chambrun G, Daures JP, Blanc P. Systematic review with meta-analysis: infliximab and immunosuppressant therapy vs. infliximab alone for active ulcerative colitis. *Aliment Pharmacol Ther* 2015; **41**: 603-612 [PMID: 25678223 DOI: 10.1111/apt.13102]

61 **Targownik LE**, Benchimol EI, Bernstein CN, Singh H, Tennakoon A, Zubieta AA, Coward S, Jones J, Kaplan GG, Kuenzig ME, Murthy SK, Nguyen GC, Peña-Sánchez JN. Combined Biologic and Immunomodulatory Therapy is Superior to Monotherapy for Decreasing the Risk of Inflammatory Bowel Disease-Related Complications. *J Crohns Colitis* 2020; **14**: 1354-1363 [PMID: 32648579 DOI: 10.1093/ecco-jcc/jjaa050]

62 **Bots S**, Gecse K, Barclay M, D'Haens G. Combination Immunosuppression in IBD. *Inflamm Bowel Dis* 2018; **24**: 539-545 [PMID: 29462391 DOI: 10.1093/ibd/izx065]

63 **Chalhoub JM**, Rimmani HH, Gumaste VV, Sharara AI. Systematic Review and Meta-analysis: Adalimumab Monotherapy Versus Combination Therapy with Immunomodulators for Induction and Maintenance of Remission and Response in Patients with Crohn's Disease. *Inflamm Bowel Dis* 2017; **23**: 1316-1327 [PMID: 28719541 DOI: 10.1097/MIB.0000000000001203]

64 **Reinisch W**, Sandborn WJ, Hommes DW, D'Haens G, Hanauer S, Schreiber S, Panaccione R, Fedorak RN, Tighe MB, Huang B, Kampman W, Lazar A, Thakkar R. Adalimumab for induction of clinical remission in moderately to severely active ulcerative colitis: results of a randomised controlled trial. *Gut* 2011; **60**: 780-787 [PMID: 21209123 DOI: 10.1136/gut.2010.221127]

65 **Colombel JF**, Sandborn WJ, Rutgeerts P, Enns R, Hanauer SB, Panaccione R, Schreiber S, Byczkowski D, Li J, Kent JD, Pollack PF. Adalimumab for maintenance of clinical response and remission in patients with Crohn's disease: the CHARM trial. *Gastroenterology* 2007; **132**: 52-65 [PMID: 17241859 DOI: 10.1053/j.gastro.2006.11.041]

66 **Feagan BG**, McDonald JW, Panaccione R, Enns RA, Bernstein CN, Ponich TP, Bourdages R, Macintosh DG, Dallaire C, Cohen A, Fedorak RN, Paré P, Bitton A, Saibil F, Anderson F, Donner A, Wong CJ, Zou G, Vandervoort MK, Hopkins M, Greenberg GR. Methotrexate in combination with infliximab is no more effective than infliximab alone in patients with Crohn's disease. *Gastroenterology* 2014; **146**: 681-688.e1 [PMID: 24269926 DOI: 10.1053/j.gastro.2013.11.024]

67 **Hu A**, Kotze PG, Burgevin A, Tan W, Jess A, Li PS, Kroeker K, Halloran B, Panaccione R, Peyrin-Biroulet L, Ma C, Ananthakrishnan AN. Combination Therapy Does Not Improve Rate of Clinical or Endoscopic Remission in Patients with Inflammatory Bowel Diseases Treated With Vedolizumab or Ustekinumab. *Clin Gastroenterol Hepatol* 2021; **19**: 1366-1376.e2 [PMID: 32668338 DOI: 10.1016/j.cgh.2020.07.012]

68 **Toruner M**, Loftus EV Jr, Harmsen WS, Zinsmeister AR, Orenstein R, Sandborn WJ, Colombel JF, Egan LJ. Risk factors for opportunistic infections in patients with inflammatory bowel disease. *Gastroenterology* 2008; **134**: 929-936 [PMID: 18294633 DOI: 10.1053/j.gastro.2008.01.012]

69 **D'haens G**, Reinisch W, Satsangi J, Loftus E, Panaccione R, Alperovich G, Kalabic J, Bereswill M, Arikan D, Petersson J, Robinson A. P353 Long-term safety of adalimumab in patients with Crohn's disease: final data from PYRAMID registry. *J Crohns Colitis* 2017; **11**: S256-257 [DOI: 10.1093/ecco-jcc/jjx002.478]

70 **Osterman MT**, Sandborn WJ, Colombel JF, Robinson AM, Lau W, Huang B, Pollack PF, Thakkar RB, Lewis JD. Increased risk of malignancy with adalimumab combination therapy, compared with monotherapy, for Crohn's disease. *Gastroenterology* 2014; **146**: 941-949 [PMID: 24361468 DOI: 10.1053/j.gastro.2013.12.025]

71 **Lichtenstein GR**, Rutgeerts P, Sandborn WJ, Sands BE, Diamond RH, Blank M, Montello J, Tang L, Cornillie F, Colombel JF. A pooled analysis of infections, malignancy, and mortality in infliximab- and immunomodulator-treated adult patients with inflammatory bowel disease. *Am J Gastroenterol* 2012; **107**: 1051-1063 [PMID: 22613901 DOI: 10.1038/ajg.2012.89]

72 **Lemaitre M**, Kirchgesner J, Rudnichi A, Carrat F, Zureik M, Carbonnel F, Dray-Spira R. Association Between Use of Thiopurines or Tumor Necrosis Factor Antagonists Alone or in Combination and Risk of Lymphoma in Patients With Inflammatory Bowel Disease. *JAMA* 2017; **318**: 1679-1686 [PMID: 29114832 DOI: 10.1001/jama.2017.16071]

73 **Doherty G**, Katsanos KH, Burisch J, Allez M, Papamichael K, Stallmach A, Mao R, Berset IP, Gisbert JP, Sebastian S, Kierkus J, Lopetuso L, Szymanska E, Louis E. European Crohn's and Colitis Organisation Topical Review on Treatment Withdrawal ['Exit Strategies'] in Inflammatory Bowel Disease. *J Crohns Colitis* 2018; **12**: 17-31 [PMID: 28981623 DOI: 10.1093/ecco-jcc/jjx101]

74 **Larson DW**, Pemberton JH. Current concepts and controversies in surgery for IBD. *Gastroenterology* 2004; **126**: 1611-1619 [PMID: 15168371 DOI: 10.1053/j.gastro.2004.03.063]

World Journal of Gastroenterology

Submit a Manuscript: https://www.f6publishing.com

World J Gastroenterol 2022 July 14; 28(26): 3101-3115

DOI: 10.3748/wjg.v28.i26.3101

ISSN 1007-9327 (print) ISSN 2219-2840 (online)

MINIREVIEWS

Clinical implications and mechanism of histopathological growth pattern in colorectal cancer liver metastases

Bing-Tan Kong, Qing-Sheng Fan, Xiao-Min Wang, Qing Zhang, Gan-Lin Zhang

Specialty type: Oncology

Provenance and peer review: Invited article; Externally peer reviewed.

Peer-review model: Single blind

Peer-review report's scientific quality classification
Grade A (Excellent): 0
Grade B (Very good): 0
Grade C (Good): C, C, C
Grade D (Fair): 0
Grade E (Poor): 0

P-Reviewer: Arigami T, Japan; Cassese G, Italy; Morera-Ocon FJ, Spain

Received: January 17, 2022
Peer-review started: January 17, 2022
First decision: April 11, 2022
Revised: April 21, 2022
Accepted: June 16, 2022
Article in press: June 16, 2022
Published online: July 14, 2022

Bing-Tan Kong, Qing-Sheng Fan, Xiao-Min Wang, Qing Zhang, Gan-Lin Zhang, Department of Oncology, Beijing Hospital of Traditional Chinese Medicine, Capital Medical University, Beijing 100010, China

Bing-Tan Kong, School of Graduates, Beijing University of Chinese Medicine, Beijing 100029, China

Corresponding author: Gan-Lin Zhang, PhD, Associate Research Scientist, Department of Oncology, Beijing Hospital of Traditional Chinese Medicine, Capital Medical University, No. 23 Back Road of Art Gallery, Dongcheng District, Beijing 100010, China.
kalinezhang@163.com

Abstract

Liver is the most common site of metastases of colorectal cancer, and liver metastases present with distinct histopathological growth patterns (HGPs), including desmoplastic, pushing and replacement HGPs and two rare HGPs. HGP is a miniature of tumor-host reaction and reflects tumor biology and pathological features as well as host immune dynamics. Many studies have revealed the association of HGPs with carcinogenesis, angiogenesis, and clinical outcomes and indicates HGP functions as bond between microscopic characteristics and clinical implications. These findings make HGP a candidate marker in risk stratification and guiding treatment decision-making, and a target of imaging observation for patient screening. Of note, it is crucial to determine the underlying mechanism shaping HGP, for instance, immune infiltration and extracellular matrix remodeling in desmoplastic HGP, and aggressive characteristics and special vascularization in replacement HGP (rHGP). We highlight the importance of aggressive features, vascularization, host immune and organ structure in formation of HGP, hence propose a novel "advance under camouflage" hypothesis to explain the formation of rHGP.

Key Words: Colorectal cancer liver metastases; Histopathological growth pattern; Desmoplastic histopathological growth pattern; Replacement histopathological growth pattern; Prognostic value; Vessel co-option

Core Tip: Histopathological growth pattern (HGP) reflects tumor–host interaction, vascularization, aggressiveness and immune infiltration. Remarkable performance on predicting survival and recurrence and distinct response to therapies makes HGP a promising prognostic biomarker and stratification parameter in pretreatment decision-making. Exploiting on mechanism of HGP would provide potential therapeutic targets. In this context, we propose one novel "advance under camouflage" hypothesis to interpret formation of replacement HGP.

Citation: Kong BT, Fan QS, Wang XM, Zhang Q, Zhang GL. Clinical implications and mechanism of histopathological growth pattern in colorectal cancer liver metastases. *World J Gastroenterol* 2022; 28(26): 3101-3115
URL: https://www.wjgnet.com/1007-9327/full/v28/i26/3101.htm
DOI: https://dx.doi.org/10.3748/wjg.v28.i26.3101

INTRODUCTION

Colorectal cancer (CRC) is the third most frequent tumor worldwide and the second most common in Europe. In diagnosed CRC, 20%–25% of patients are classified as stage IV and 15%–25% of those develop liver metastases[1]. For these whose metastases are confined to the liver, the only opportunity to cure is radical surgical resection. However, not all patients are fit for surgery and there is still a high rate of intrahepatic recurrence after curative resection. Therefore, the attempt on seeking for more comprehensive prognostic and stratification markers is of utmost importance. Deriving from this aim, the invasive margin as one pathological variable was selected to construct a prognostic system for rectal cancer patients[2]. There, tumor margin was classified into expanding type (pushing or well circumscribed) and infiltrating type. Based on these studies, the histopathological growth pattern (HGP) initially came into shape.

In 2016, international consensus guidelines[3] for scoring HGPs of liver metastasis were produced. Three common HGPs, *i.e.*, desmoplastic HGP (dHGP), pushing HGP (pHGP) and replacement HGP (rHGP), and two rare HGPs, *i.e.*, sinusoidal HGP and portal HGP are described in these consensus guidelines. In principle, HGPs could be distinguished according to the character of the invasive margin and morphology of the tumor, which is usually observed in light microscopy on standard hematoxylin and eosin (H&E)-stained tissue sections. Distinct biological and invasive patterns are presented in different HGPs. The key histopathological characteristic of dHGP is that there is a broad desmoplastic rim at the tumor periphery, which separates tumor cells from normal liver tissue. rHGP tumor cells mimic the liver architecture and replace the hepatocytes within liver plates, and the tumor displays an infiltrative border and irregular contours. pHGP tumor expands in a pushing way and the adjacent liver is compressed. Its interface is as sharp as that of dHGP but without a desmoplastic rim[3]. Figurative knowledge of dHGP and rHGP is presented in Figure 1.

PROGNOSTIC VALUE OF HGPS

Frequently, HGP predicts overall survival and recurrence in patients resected for CRC liver metastasis (CRCLM). HGPs have been extensively characterized not only in liver metastases but also in the primary cancer and metastases in lung, brain and skin; therefore, there are different categorization about HGPs in different tissues. They are ordinarily classified into dHGP and non-dHGP or expanding and infiltrative HGP[2] when used as prognostic biomarkers. In this fashion, dHGP refers to pure dHGP with a 100% desmoplastic interface on every section, while non-dHGP actually includes pushing, replacement and a mixed (pushing-replacement) pattern. As the major form in most cases, rHGP represents non-dHGPs and infiltrative HGP. One of the most important findings from studies on predictive value of HGP is that CRCLM patients with dHGP, especially pure dHGP, are prone to longer overall survival. dHGP is verified as an independent factor for superior overall survival (OS) and progression-free survival (PFS)[4-8], while non-dHGPs are strong prognostic indicators of worse survival[8-14]. More than in CRCLM, a similar trend has been observed in liver metastases from cutaneous melanoma[15], which implies that the prognostic value of HGP is generally applied in various liver metastases.

For CRCLM patients who have undergone hepatectomy, high recurrence rate may cause repeat resection and impair their survival. Non-dHGP might be responsible for this damage from intrahepatic as well as overall recurrences[12]. Compared with dHGP, rHGP and pHGP more frequently experience multiorgan recurrence, while dHGP has more liver-limited disease recurrence[16-18]. Evidence supports that dHGP predicts good outcomes, but the infiltrative pattern or rHGP indicates poorer outcomes and higher recurrence. In this context, we provide an overview of studies focusing on prognostic and strati-

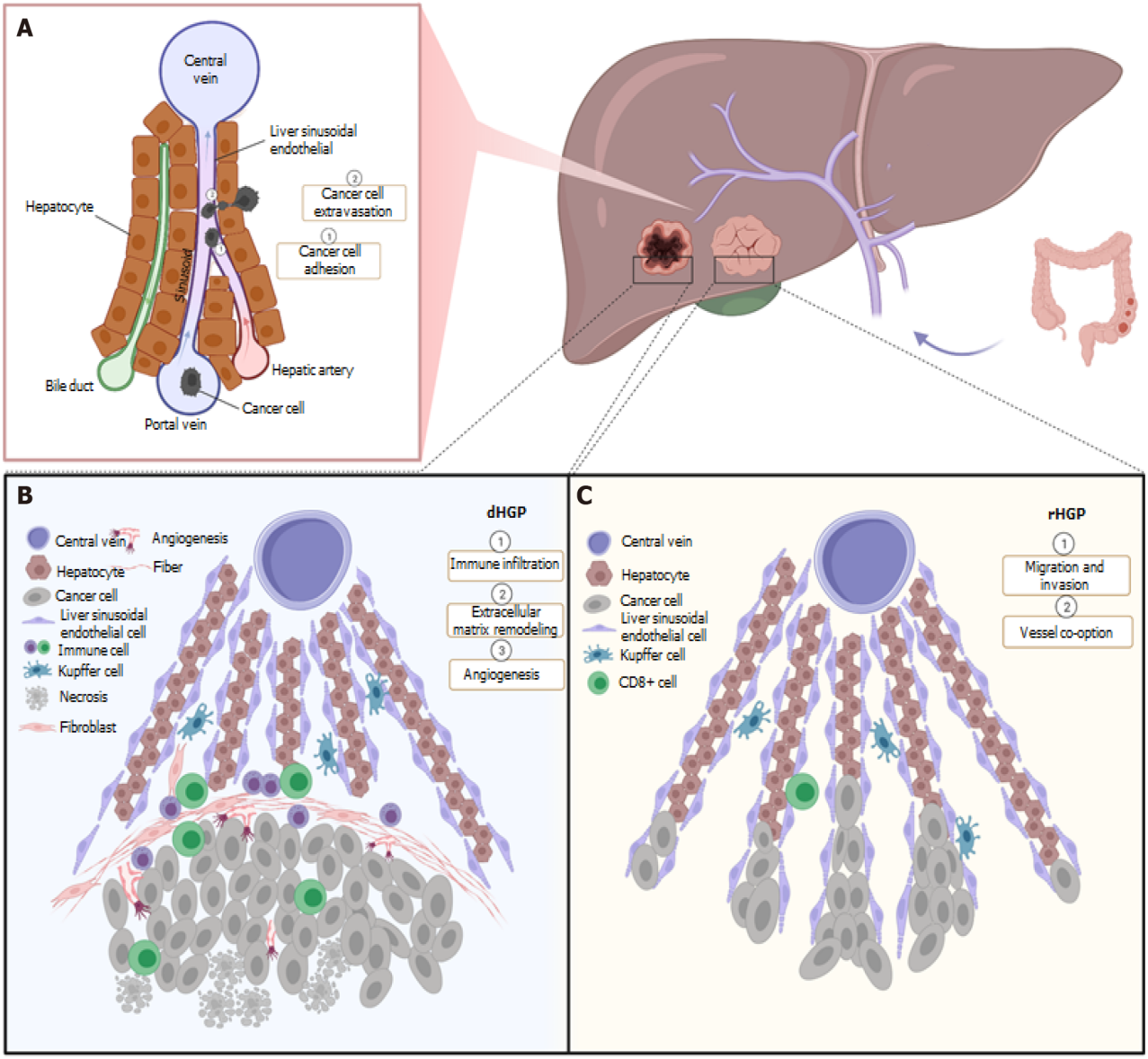

DOI: 10.3748/wjg.v28.i26.3101

Figure 1 Formation and mechanism of desmoplastic histopathological growth pattern and replacement histopathological growth pattern. A: Cancer cells originating from colorectal cancer arrive in the liver *via* portal vein, adhere to lumen of liver sinusoid and migrate with extravasation through fenestrae on liver sinusoidal endothelial cells (LSECs); B: There is a desmoplastic rim in interface of tumor with desmoplastic histopathological growth pattern, with tumor cells destroying liver plate, causing immune infiltration and extracellular matrix remodeling induced by activated fibroblasts and deposited fiber. Both angiogenesis and necrosis are presented in the tumor; C: In replacement histopathological growth pattern, tumor cells with highly migration and invasion replace hepatocytes and co-opt LSECs but without disturbing the liver structure and extensive immune infiltration. dHGP: Desmoplastic histopathological growth pattern; rHGP: Replacement histopathological growth pattern.

fication value of HGPs in Table 1.

Apart from predicting survival, the growth pattern of primary CRC was also found to predict the HGP of liver metastases. The primary CRCs with expanding growth pattern significantly tend to form dHGP liver metastasis, while CRC patients presenting with infiltrating growth pattern are more likely to have rHGP liver metastasis[19]. It seems that some invasive characteristics are inherited from primary tumor to secondary metastases. However, there are few reports about this. Wu *et al*[19] found several specific gene mutations, among which representative gene mutation *PIK3CA* appearing in 40% of primary CRC patients with dHGP liver metastasis was speculated to mediate vascular development and angiogenesis through the vascular endothelial growth factor (VEGF) signaling pathway, further supporting dHGP. Nevertheless, these findings have not revealed the genomic correlation between growth pattern in primary CRC and HGP in liver metastases.

Some relevant factors such as surgical margin, immunoscore[20] and glucose uptake[21,22] were also widely investigated as predictor in outcomes of CRC. The combination of HGP with resection margin, parameters of immune status, genes and metabolism also paves the way for creating comprehensive and accurate predictive models. Surgical margin in tumorectomy is a critical but controversial issue as

Table 1 Studies on stratification value of histopathological growth pattern in colorectal cancer liver metastasis

Year	Factors	Prediction	Distribution of HGPs	Ref.
Survival stratification				
2018-2019	dHGP and rHGP (based on radiomics)	dHGP *vs* rHGP and mixed HGP: longer PFS (no detail)	119 patients: dHGP (206 lesions), rHGP (140 lesions)	Wei *et al* [43]
2004-2019	Pushing GP and infiltrative GP	Infiltrative GP *vs* pushing GP: Worse OS (50.2 mo *vs* 92 mo) and DFS (10.5 mo *vs* 21.5 mo), higher intrahepatic recurrence (75% *vs* 20%)	266 patients: Infiltrative (n = 182, 68.4%) and pushing (n = 84, 31.6%)	Jayme *et al* [16]
2005-2017	dHGP and non-dHGP group; metabolic-clinical risk score	dHGP *vs* non-dHGP: Longer 5 yr OS (83.3% *vs* 34.3%) and 10 yr OS (62.5% *vs* 22.8%) and DFS (14.4 mo *vs* 8.3 mo)	108 patients: dHGP (26, 20%), non-dHGP (38, 35%)	Bohlok *et al* [23]
2000-2015	dHGP and non-dHGP; positive resection margins (R1) and negative resection margins(R0)	Non-dHGP *vs* dHGP: worse OS (50 mo *vs* 80 mo), higher risk of positive resection margins (76.6% *vs* 23.4%)	1302 patients: dHGP (305, 23%) and non-dHGP (997, 77%); R1 (170, 13%) and R0 (1132, 87%)	Nierop *et al* [9]
2004-2017	dHGP and non-dHGP, clinical risk score, the immunoscore	dHGP *vs* non-dHGP: Higher immunoscore (51.9% *vs* 33%), longer relapse free survival (32 mo *vs* 12 mo) and OS (not reached *vs* 40 mo)	166 patients: dHGP (54, 32.5%), non-dHGP (112, 67.5%)	Liang *et al* [4]
2012-2017	Expanding GP, infiltrating GP; low tumor budding score, and Crohn's disease-like response	Expanding GP in primary CRC: dHGP liver metastasis and better OS (no detail); infiltrating GP in primary carcinoma: rHGP liver metastasis and worse OS (no detail)	29 patients; primary CRC: expanding GP (11, 37.9%) and infiltrating GP (18, 62.1%); liver metastasis: dHGP (15, 51.7%) and rHGP (14, 48.2%)	Wu *et al*[19]
2000-2015	dHGP and non-dHGP	dHGP *vs* non-dHGP: More liver-limited disease recurrence (43% *vs* 31%); less frequently experience multi-organ recurrence (19% *vs* 34%)	690 patients: dHGP (173, 25%) and non-dHGP (517, 75%)	Nierop *et al* [17]
2000-2009	Infiltrative and pushing tumor margin	Infiltrative margin *vs* pushing margin: poorer 5 yr DFS (20.2% *vs* 40.5%)	91 patients: infiltrative margin (54, 59.3%) and pushing margin (37, 40.7%)	Pinheiro *et al*[12]
2007-2011	dHGP, rHGP, pHGP, mixed HGP	rHGP *vs* dHGP, pHGP and mixed HGP: Poorer OS (22.8 mo *vs* > 60 mo, 44.2 mo and 40.3 mo)	217 patients: pHGP(33%), dHGP(32%), rHGP(11%) and mixed HGP(24%)	Nielsen *et al* [8]
1997-2005	dHGP, rHGP, pHGP, mixed HGP	pHGP *vs* dHGP, rHGP and mixed HGP: Poorer 2 yr OS (43.8% *vs* 72.5%, 70.2%, and 54.3%)	205 patients: pHGP (15.6%), dHGP (34.6%), rHGP (27.8%) and mixed HGP (17.6 %)	Van den Eynden *et al* [13]
Therapy response stratification				
2000-2016	dHGP and non-dHGP	Non-dHGP: Superior response to adjuvant systemic chemotherapy on improving OS and DFS but only in patients that were not treated with chemotherapy	1236 patients; 580 not pretreated patients (46.9%): dHGP (91, 15.6%) and non-dHGP (489, 84.4%); 656 pretreated patients (53.1%), dHGP (189, 28.8%) and non-dHGP (467, 71.2%).	Buisman *et al*[27]
2000-2015	dHGP and non-dHGP	dHGP *vs* non-dHGP: Better 5-year PFS (50% *vs* 19%) and 5 yr OS (70% *vs* 37%) but only in chemo-naive patients with resecting CRCLM	732 patients; in the chemo-naive patient cohort (n = 367), dHGP (68, 19%) and non-dHGP (299, 81%); in the neoadjuvantly treated patient cohort (n = 365), dHGP (109, 30%) and non-dHGP (256, 70%)	Galjart *et al* [6]
2010-2013	dHGP, rHGP, pHGP, mixed HGP	pHGP: Worse OS and DFS; significantly associated with Oxaliplatin-based chemotherapy	110 patients: pHGP (33, 30%), dHGP (23, 21%), rHGP (19, 18%) and mixed HGP (34, 31%)	Falcao *et al* [11]

HGP: Histopathological growth pattern; GP: Growth pattern; dHGP: Desmoplastic histopathological growth pattern; rHGP: Replacement histopathological growth pattern; pHGP: Pushing histopathological growth pattern; OS: Overall survival; DFS: Disease-free survival; PFS: Progression-free survival.

biologic factors driving margin-based differences may lead to the need for larger surgical margins, which indicate less chance of residual tumor cells and recurrence. Nierop *et al*[9] found that patients with non-dHGP are at higher risk of positive resection margins. It seems to be necessary to enlarge resection margin size when tumors present more aggressive borders or worse HGPs. Partly answering this question, Jayme *et al*[16] found that those with infiltrative-type borders indeed presented with worse overall and disease-free survival, and had a 2.32 higher risk of hepatic recurrence than patients with pushing borders. However, a larger resection margin (> 10 mm) in patients with infiltrative borders did not affect the prognosis. It could be pointed out that what really counts is tumor biology rather than tumor size. In parallel with HGPs, high preoperative glucose uptake representing high metabolism rate is associated with poor prognosis in CRCLM[21,22]. When integrating preoperative metabolic parameters with HGPs, the postoperative prognostic value could be improved[23]. As

expected, similar results appeared in studies on correlation between HGPs and immunophenotype and genomic mutation[19,24].

HGPS AND THERAPIES

HGP is also a useful tool to stratify patients for their response to therapy. For both resectable and unresectable patients, additional chemotherapy and angiogenesis inhibitors (AIs) are regarded as essential adjuvant therapy, however, their timing of administration and effect remains a matter of debate. Previous studies showed perioperative chemotherapy was not that beneficial as expected[25,26]. Retrospective analysis on long-term outcomes of 236 resectable CRCLMs suggested that there were no measurable differences between groups receiving adjuvant and perioperative chemotherapy[26]. Whereas an interesting phenomenon is that the effectiveness of adjuvant therapies varies with different HGP subgroups. For patients who were not pretreated with chemotherapy, non-dHGP subgroup have longer OS and disease-free survival (DFS) after adjuvant chemotherapy[27]. dHGP and pHGP are more sensitive to triplets + cetuximab and triplets + bevacizumab, respectively, while rHGP has poor response to the both therapies[28]. In other words, HGPs may determine the sensitivity to chemotherapy and AIs. Besides, chemotherapy somehow changes the component of HGPs. One study found more than half (55%) of chemonaive resected CRCLMs showed rHGP, while patients with neoadjuvant therapy presented the opposite phenomenon, in which dHGP comprised the major proportion (66%)[6]. Chemotherapy as an independent relevant factor induced an HGP phenotypic change with an increase of dHGP. A similar trend was shown in another study in which Nierop *et al*[29] evaluated the effect of preoperative systemic chemotherapy on the HGPs of CRCLM, and obtained multiple verification in three independent cohorts. Conclusively, HGP could be a stratification factor when considering the effectiveness of adjuvant chemotherapy after resection.

The remarkable results with AIs in preclinical studies brought hope to patients; however, with passing decades, AIs have failed to demonstrate a survival advantage. Increasing findings strongly imply that rHGP is insensitive to AIs and increasing proportion of rHGP furtherly drives reactive resistance after AIs therapy, all of which is mainly due to vessel co-option being as predominant vascularization. Serial clinical studies in patients with liver metastases verified that rHGP is prevalent in post-treatment patients and rHGP subgroup poorly responds to AI therapy[30]. Whereas, supplementary inhibition of rHGP through suppressing cancer cell motility and migration facilitated effectiveness of AIs *in vivo*. Other direct evidence supporting vessel co-option (rHGP) as a mechanism of acquiring resistance to AI therapy was obtained from an orthotopic human hepatocellular carcinoma (HCC) model[31]. The researchers paid more attention to vascularization within the tumor instead of the interface between the tumor and liver, and found the number of co-option vessels was elevated from 23.3% in untreated controls to 75% in resistant tumors, along with a shift from angiogenesis (dHGP) to vessel co-option (rHGP)[31]. These observations make it clear that rHGP induces resistance to AI therapy in *in vivo* and *in vitro*.

Collectively, HGPs determine the sensitivity to therapy, and both chemotherapy and AIs somehow change the components of HGPs. Chemotherapy tends to the change with increase of dHGP, while AIs make a shift from angiogenesis (dHGP) to vessel co-option (rHGP). Considering prognostic significance and drug response of HGP in liver metastases, HGP could be used to guide treatment for CRCLM patients, select out ideal subgroup, design precision therapy for individual patient, even develop approaches to transform HGP of drug-resistant group to one sensitive type so that they can benefit from current therapy.

HGPS AND VASCULARIZATION

Tumors adopt various forms of vascularization, among which, angiogenesis occupies a dominant position. Yet, increasing evidence shows that vessel co-option is a crucially alternative nonangiogenic strategy by which tumor cells hijack the pre-existing vessels instead of creating new vessels and gain access to nutrients to support tumor survival, growth and metastasis. Different HGPs correspond with distinct vascularization patterns, which also vary with metastatic organs. In CRCLM, rHGP and dHGP obtain blood supply *via* different routes, *i.e.*, the former is vessel co-option while the latter is sprouting angiogenesis. This difference of vascularization contributes to distinct therapy response.

For a long time, dHGP has been known to represent an angiogenic growth pattern. Different from rHGP, tumors with dHGP completely destroy liver architecture and form neovascularization. Chemotherapy and antiangiogenic agents caused 100% necrosis and few surviving carcinoma cells left under the desmoplastic rim[32]. It is believed that leakiness of immature vascular allows cytotoxic agents sufficient interaction with malignant cells contributing to more efficient of chemotherapy on dHGP. In the process of sprouting angiogenesis, with extracellular matrix (ECM) and basement membrane degrading, endothelial cells and pericytes proliferate, migrate and eventually form immature vasculature[33,34]. Like a double-edged sword, abnormal basement and loose pericytes of new vessels

lead to leakiness and heavily impair blood supply to the whole tumor which causes hypoxia and acidosis[35]. This leakiness may affect drug delivery and only after normalizing the abnormal tumor vasculature can chemotherapy as well as oxygen efficiently penetrate throughout tumor[35]. AIs has been verified with the ability to prune proliferating vessels, render tumor vasculature normalized and enhance the delivery and efficacy of cytotoxic agents[36,37]. Collectively, sprouting angiogenic vascularization contributes to favorable effect of chemotherapy on dHGP.

In contrast, rHGP tumors expand in a "conventional way" by replacing liver cells, attaching liver sinusoidal endothelial cells (LSECs) and co-opting liver vessels with liver structure preserved. The data from Frentzas and colleagues[30] provide direct evidence supporting cancer cells utilizing pre-existing sinusoidal blood vessels in rHGP liver tumors. They found invading tumor cells followed the "RR" rule that tumor cells replaced hepatocytes in the liver parenchyma but respected the sinusoidal blood vessels, leaving the sinusoidal space complete. Sinusoidal vessels with one end embedded in the tumors were frequently observed, with the other end originating from normal liver. Different from dHGP, there were more mature vessels in continuity with the sinusoidal network in rHGP. rHGP lesions preserve more viable carcinoma cells, more microvascular density (MVD) and showed no necrosis after chemotherapy and antiangiogenic agents[32].

These vascularization characteristics could partly explain why rHGP tumors initiate less response to chemotherapy and antiangiogenic therapy than dHGP tumors do, and even resistance to antiangiogenic therapy. Tumor with rHGP lacks proliferating vasculature, while the co-opted liver sinusoidal capillary network as a mature and endogenous vascular network does not respond to AIs. Current studies on vascularization of HGPs extensively pay attention to tumor periphery other than central region, and particularly co-option vessels were only observed in interface. In this case, what the vascularization in central region of rHGP tumor requires further investigation.

IDENTIFYING HGPS IN NONINVASIVE METHODS

In spite of strong prognostic and stratification value, HGP has not been put into clinical decision-making, which is mainly because of its limitation of requiring histopathological assessment of surgical resection specimens. Thus, a noninvasive method identifying HGP is urgently needed, especially when selecting optimal therapies for patients with untreated and unresectable liver metastasis and predicting their survival for long-term healthcare. Rim enhancement as a hotspot topic has attracted much attention. Radiomics stands out with a remarkable performance in identifying HGPs and predicting outcomes and several novel predictive models combining morphological score or not have superior ability to conventional response evaluation criteria.

Over the years, several noninvasive approaches, such as computed tomography (CT), magnetic resonance imaging (MRI) and ultrasound, were used to identify HGP and explore their correlation with response to therapy and even survival forecasting. There are some common imaging features of HGPs, *e.g.*, a significantly enhanced rim and clear tumor–liver interface in dHGP, compared with an indefinite margin and no rim enhancement in rHGP. Earlier studies on the correlation between radiology images and morphological features concentrated on rim enhancement since knowledge on HGP was insufficient. In the 1990s, scientists studied the enhancing rim through comparing radiology images with histopathological slides, attributed this phenomenon to blood flow and perfusion and believed that the morphological substrate of rim enhancement of colorectal metastases seen by CT was compressed liver parenchyma[38]. The compressed liver parenchyma lacked a portal blood supply but was compensated by an increase in the arterial blood supply, and the rim enhancement of metastases could only be seen during hepatic arteriography. Similarly, Terayama *et al*[39] found two-way blood flow between the tumor and the adjacent liver tissues contributed to peritumoral enhancement. This abnormal blood circulation and occlusion in the tumoral–peritumoral area caused sinusoidal congestion, the thickness of which reflected thickness the perilesional hyperintense rim[40]. The findings from Semelka *et al*[41] implied that the level of compression of hepatic parenchyma was not positively correlated with the degree of perilesional enhancement. The concomitant reactions such as peritumoral desmoplastic reaction, vascular proliferation and peritumoral inflammation contributed a lot to the increase in rim enhancement. Above all, these findings on the mechanism of rim enhancement focusing on inflammatory infiltration and reactive vascularization step forward to comprehensive knowledge on HGP.

Nevertheless, in some cases, it is difficult to recognize some minor differences in rim enhancement because distinct vascularization for HGPs cannot be exactly and quantitatively identified visually. Current studies have focused on the correlation between HGPs and radiomics. Radiomics is a promising tool to predict HGPs but still faces great challenges. Radiomics containing pre- and post-contrast (arterial and portal venous phase) multidetector CT images were demonstrated to improve distinguishing accuracy on HGPs in the training cohort[42]. Importantly, the performance predicting HGPs of radiomics models alone did not differ from combining clinical and qualitative imaging factors[42]. Given the diagnostic performance of this model with area under the curve > 0.9, another study verified its potential for predicting survival[43]. In unresected patients additionally treated with bevacizumab-

containing chemotherapy, the dHGP subgroup had > 1-year PFS, which was in line with HGP prediction on resected specimens[43].

CT criteria based on morphological forecast outcomes superior to Response Evaluation Criteria In Solid Tumors (RECIST) based on tumor size and number[44,45]. A radiomics model based on tumor-liver interface exhibited better predictive value compared with a model based on tumor zone; nevertheless, combination of the two models was superior to any single one, even clinical model[46]. Some evaluative and predictive models, *e.g.*, SPECTRA-score[47] based on a radiomic nomogram, displayed superior sensitivity and accuracy to standard evaluation with RECIST 1.1. Even though CT, MRI and positron emission tomography/CT have comparative diagnostic value in detecting CRCLM, gadoxetate-disodium-enhanced MRI was found to have greater accuracy in a systemic review[48]. These imply that the combined prediction model of morphological characteristics and imaging studies perform better than the mono-model.

UNDERLYING MECHANISM OF HGPS

dHGP: Immune infiltration and ECM remodeling

Immune infiltration: The tumor microenvironment not only carries out major tumor-relevant activities including antitumor response and stromal remodeling but also involves in formation of distinct pathological phenotypes. The immunoscore of patients with dHGP remains high, which implies that dHGP is an abundant immune status. As unique marker of dHGP tumor, the desmoplastic rim usually indicates active antitumor response meanwhile rim itself is a product of matrix deposition and immune infiltration. Here, adaptive lymphocytes participate in both cytotoxic and immunosuppressive effects. In dHGP, there was an increase of $CD3^+$ T cells, $CD8^+$ T cells, $CD20^+$ B cells and CD8/CD4 ratio; all of which enhance antitumor immunity, while decrease of $CD4^+$ T cells[4,5]. That this phenomenon appeared in peritumoral and intratumoral regions and even distant tumor-free liver but not peripheral blood suggested local immune situation instead of systemic immunity drove and determined the HGP phenotype. In dHGP, Eefsen *et al*[49] observed macrophages accumulating at the tumor border in patients given neoadjuvant chemotherapy and higher level of urokinase-type plasminogen activation receptor in chemonaive patients. As part of the plasminogen activation system, urokinase-type plasminogen activation receptor is mainly expressed in macrophages and myofibroblasts and some cancer cells[50], and induces changes in the macrophages during tumor invasion. Therefore, higher urokinase-type plasminogen activation receptor expression in desmoplastic metastases may be a secondary reaction of the tumor cells to the desmoplasia.

ECM remodeling: Desmoplasia is also a host-specific reaction to protect against malignant cells invasion of adjacent parenchyma and plays a protective role in tumor progression. On formation of desmoplasia, cancer-associated fibroblasts (CAFs) play a pivotal role through producing collagen and fiber, coupled with the role of self-produced cytokines and growth factors, thereby remodeling the ECM [51]. When stromal content automatically decreases within tumor microenvironment or inducing stromal depletion with medication, *e.g.*, type I collagen, the tumor will become more aggressive, with lower tissue stiffness and rapid growth, leading to poorer overall survival of the host[52]. This desmoplastic capsule mainly consists of collagen fibers originating from activated myofibroblasts. Capsule formation typically occurs when there is a high level of infiltration by $CD4^+$, $CD45RO^+$ and $CD8^+$ T cells in the near stromal region[53]. However, the distant stromal area with low density of immune cells hardly ever forms a capsule. The desmoplastic rim may be a complicated collection of several components, *e.g.*, fibers, blood vessels, fibroblasts and immune cells. This rim originates from the antitumor response, and functions as a barrier separating malignant cells from normal tissues.

rHGP: Aggressive characteristics and special vascularization

Metastatic capability: Cell motility, invasion and migration: To our knowledge, rHGP was initially described as infiltrating growth pattern[2] other than replacement growth pattern, implying that this type of tumor has aggressive biology and is prone to adopt an infiltrative growth patten. Tumor cells with rHGP present a highly motile, invasive and adhesive phenotype, which accelerates infiltration of the adjacent liver and utilizes the pre-existing vasculature.

For molecules involved in cancer cell motility supporting rHGP, the actin-related protein 2/3 (ARP2/3) complex is indispensable. It has been demonstrated ARP2/3 mediates the nucleation of actin filaments at the frontier cells to drive cell movement and facilitate the motility and invasion of breast and colorectal cancer cells[54]. ARP2/3 subunit ARPC3 is highly expressed in rHGP human CRCLM specimens, and its knockdown results in a significant decrease of rHGP in animal models[30]. *In vitro* data have shown that ARPC3 silencing suppresses migration other than proliferation of CRC cells. Apart from ARP2/3, Runt-related transcription factor (RUNX)1 also regulates motility and epithelial–mesenchymal transition (EMT) in cancer cells. As a key upstream transcriptional regulator of ARP2/3, RUNX1 is overexpressed in rHGP CRCLM lesions[55], and its inhibition could suppress tumor cell motility and EMT. Downstream proteins ARP2/3 and thrombospondin 1 are also reported to

facilitate cancer cell motility; however, whether RUNX1 support of rHGP is ARP2/3 dependent needs more investigation.

Tumor with strong adhesion to hepatocytes has potential to develop rHGP. Claudins as critical components of tight-junctional complexes that modulate carcinogenesis and metastasis[56]. Claudin-2 acts as an essential determinant in the formation of rHGP liver metastases from either CRC or breast cancer[57]. During tumor metastasis to the liver, there is functional shift in claudin-2 from tight-junctional complex to adhesion molecule between cancer cells and hepatocytes[58,59]. Claudin-2 promotes tumor cell adhesion to hepatocytes and is specifically expressed at high levels in rHGP; at the same time, claudin-8 is specifically expressed at high levels in dHGP[57].

Co-opting vessels: Different HGPs are associated with different types of tumor vascularization. In rHGP, tumor cells replace hepatocytes to spread and co-opt liver vessels to obtain blood. Since rHGP corresponds with vessel co-option, those regulating vascular factors should be paid attention. Angiopoietin (Ang)1 and Ang2 are vascular growth factors that act as agonists to active their ligand Tie2, which then together induce endothelial cell (EC) formation, survival, proliferation and migration. Ang1 has a distinct vascular-relevant effect, protects against EC apoptosis, and mediates vessel maturation by enhancing pericyte recruitment. Ang2 has a proangiogenic function through mediating pericyte detachment and blood vessel destabilization[60]. In human resected CRCLM specimens with rHGP, Ang1 supporting vessel co-option displays higher expression in the liver adjacent to tumor[61]. To demonstrate the critical role of Ang1, an animal model of Ang1 knockout was established and showed a change from rHGP to dHGP along with a decrease of liver metastases[61]. This verified that high expression of Ang1 in the host liver supported rHGP. Additionally, some inflammatory molecules partly participated in rHGP. RNA sequencing showed that two genes, *CXCL6* and *LOXL4*, were significantly upregulated in rHGP tumors *vs* dHGP tumors, and were involved in cell migration and wound healing[62]. Neutrophils expressing *LOXL4* concentrated at the tumor–liver interface and in areas of inflammation in rHGP lesions, and circulating neutrophil expression of LOXL4 protein is increased in CRCLM patients. It indicates that the chemoattraction and subsequent activation of neutrophils may be vital in promoting rHGP in CRCLM[62].

Hypothesis for HGPs

Liver injury hypothesis: When coping with exogenous or endogenous injuries, the liver has both the potential for healthy regeneration following acute injury and the potential for repair toward fibrosis under persistent damage[63]. Given malignant cells proliferate within the liver, causing injury and activating host reactions, van Dam *et al*[64] proposed the hypothesis that HGPs represent the response patterns of the liver to injury.

Development of liver metastases has similar pathological changes to those in liver injury. In liver fibrosis, portal fibroblasts and hepatic stellate cells transform to activated myofibroblasts, binding with components of ECM (crosslinking collagen), and together induce fibrogenic activation and support fibrogenic units based on activation and reorganization of cholangiocytes, accounting for fibrotic progression[65]. For dHGP, the peripheral desmoplastic rim shares one common ECM remodeling and ductular reaction with liver fibrosis, among which the activated cholangiocytes proliferate and form small nonfunctional bile ducts. Differently, rHGP adopts an analogous pattern with liver regeneration where the process of new cells replacing older hepatocytes takes place. In the context of vascularization, in liver regeneration, regenerating liver cells co-opt pre-existing sinusoidal capillaries instead of sprouting angiogenesis which is akin to rHGP. Even though it is far from reaching a certain conclusion that dHGP and rHGP exemplify liver fibrosis and regeneration, but there is still similarity between formation of liver metastasis and liver development and regeneration; knowledge of which would enable us to determine the underlying mechanism of HGPs.

Advance under camouflage hypothesis: Researchers have detailed knowledge of the mechanism of dHGP, but there is little ideal explanation for the formation of rHGP. Except for some tumoral phenotypic and molecular drivers observed in rHGP, there is still no systematic model to support the explanation. We put forward a hypothesis that malignant cells benumb and educate the immune system, and advance by an unknown path under camouflage (Figure 2).

The tumor cells with an infiltrative pattern paralyze or tame the local immune system *via* interaction with LSECs and induce immune tolerance. LSECs are a major group of hepatic cells that specialize in detection and capture of pathogens from the blood. However, in some cases, this group also downregulates T-cell response through crosstalk with immune cell subsets, leading to immune escape[64,66]. Through programmed death (PD) ligand 1 on T cells binding to PD-1 on LSECs, $CD8^+$ T cells are activated to a dynamic but nonlicensed type, which fails to produce effector cytokines (*e.g.*, interferon-γ) and have decreased cellular cytotoxicity[67]. Similar suppressive immune activity takes place with mediation of another specific surface protein LSECtin, through which LSECs directly identify activated T cells and inhibit immune-response-mediated T cells[68]. These strongly imply that LSECs are important players in immune tolerance, which enhances invasive and metastatic potential of tumor cells. Taking advantage of this point, tumor cells obtain sufficient interaction with LSECs and hepatocytes, so that tumor cells educate these normal liver cells and remodel the immune microenvir-

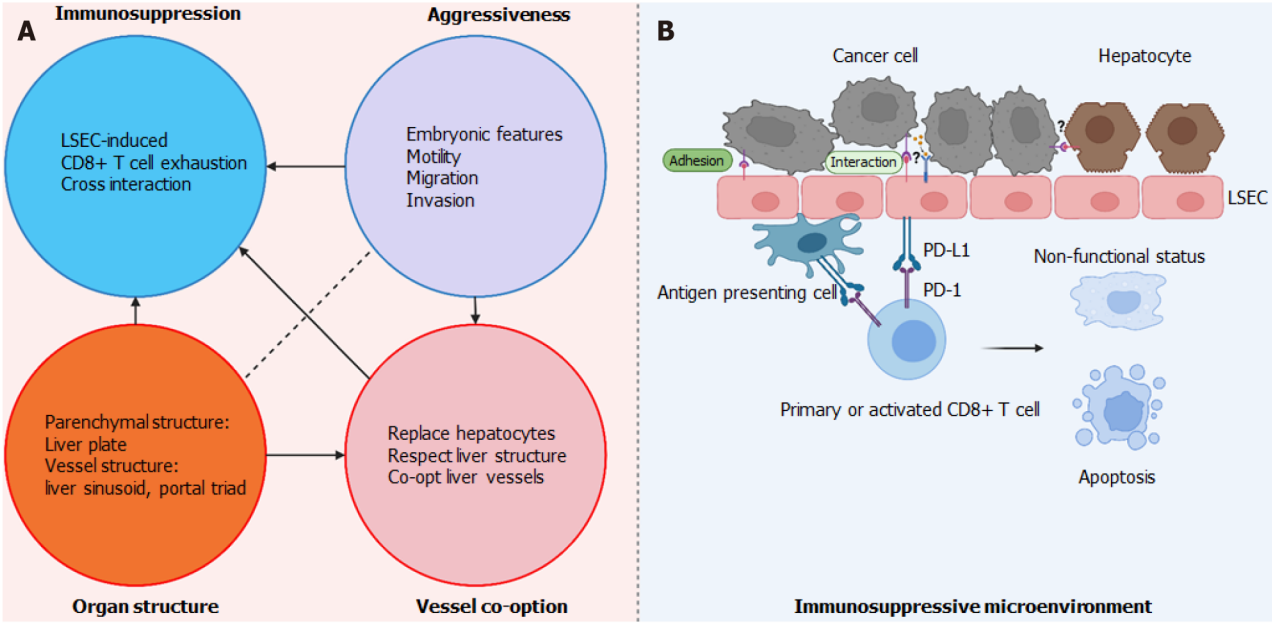

DOI: 10.3748/wjg.v28.i26.3101

Figure 2 "Advance under camouflage" hypothesis for replacement histopathological growth pattern. A: "Advance under camouflage" hypothesis of replacement histopathological growth pattern (rHGP) includes four elements. Embryonic features, motility, migration and adhesion contributes to aggressiveness of tumor, which drives tumor progression as an intrinsic factor. Tumor cells interact with liver sinusoidal endothelial cells (LSECs) and hepatocytes, so that tumor cells educate these normal liver cells and remodel the immune microenvironment into a tolerance state *via* CD8+ T cells. In this manner, under camouflage of LSECs, tumor cells are able to survive and slowly progress. Co-opting LSECs enable the tumor to obtain sufficient blood supply and less chance of exposure to immune system. With its unique parenchymal and vessel structure, organ architecture of liver supports the whole advance process; B: Immunosuppressive microenvironment in tumor with rHGP. Under cross interaction of cancer cells and LSECs and other immune cells (unknown mechanism), programmed death (PD) ligand 1 on LSECs and antigen presenting cells binds to PD-1 on T cells making CD8+ T cells activated to a dynamic but nonfunctional type which fails to produce effector cytokines and has decreased cellular cytotoxicity, or is apoptostic. LSEC: Liver sinusoidal endothelial cell; PD: Programmed death.

onment into a state of tolerance. In this manner, under camouflage of LSECs, tumor cells are able to survive and slowly advance. To expand further, the leading cells at the tumor border also initiate adaptive changes, *e.g.*, enhanced metastatic capacity including cell motility, adhesion and migration. Many of them are driven by some embryonic features that are relevant to co-option-type metastases[69,70]. As a whole, embryonic characteristics, interaction between tumor and normal liver cells, and immunological inertia allows efficient and safe advance of tumor cells. Two other factors must be paid attention: (1) Co-opting normal hepatic vasculature reduces the chance of direct exposure of the tumor to the immune system and achieves normalization of the blood supply. In this case, the intratumoral microvessel keep their normal structure and evenly perfuse the whole nodule, which reduces hypoxia and necrosis and is conducive to overall development of the tumor; and (2) Organ structure is another essential aspect. In an organ with a clear and distinct architecture such as the lungs and liver, the metastatic foci can often expand and develop along with its structure[71,72], which implies that organ architecture sometimes directs how tumor cells expand. We propose a complex axis that 'embryonic characteristics playing a primitive driving role - tumor hepatic sinusoidal endothelial cell interaction as the mediator - organ structure as the support' and advance under camouflage hypothesis to explain the underlying mechanism of rHGP.

CONCLUSION

We proposed a novel hypothesis to explain the mechanism of rHGP formation. We denoted four elements, *i.e.*, intrinsic features of cancer cells, tumor vascularization, immunosuppressive microenvironment and host organ structure in the HGP formation. Vascularization and tumor microenvironment have been emphasized in previous studies while the pivotal role of organ structure is addressed for the first time in this review. Common features in angiogenic HGP, for instance, desmoplastic reaction, immune infiltration and sprouting angiogenesis, have been shown. Organ specific morphology was only observed in non-angiogenic HGP, exhibiting angio-tropism and structure-dependent properties. It was observed that non-angiogenic HGP metastases in brain[73] and skin[74] adopted pericytic mimicry and extravascular migratory behavior to get access to the blood. Similarly, metastatic cells remained the mesenchymal structure (pulmonary alveoli and hepatic plate) and presented with alveolar HGP, interstitial HGP and perivascular cuffing HGP in the lung[75], as well as rHGP in the liver. Thus, it

Table 2 Characteristics of desmoplastic histopathological growth pattern and replacement histopathological growth pattern in colorectal cancer liver metastasis

Aspects	dHGP	rHGP
Morphology	Sharp desmoplastic rim separating tumor cells from adjacent liver	Ill-defined border; Tumor cells replace normal hepatocytes along with the architecture of liver plate
Invasion pattern	Expanding and mild	Infiltrative and aggressive
Immune phenotype	Abundant	Desert
Vascularization	Angiogenesis	Non-angiogenesis (vessel co-option)
Organ-specific	No, widely appears in brain, lung and liver	Yes, only appears in liver
Therapy response	Superior response	Inferior response and drug resistance
Clinical outcome	Longer OS, DFS and PFS	Poorer survival and high recurrence

dHGP: Desmoplastic histopathological growth pattern; rHGP: Replacement histopathological growth pattern; OS: Overall survival; DFS: Disease-free survival; PFS: Progression-free survival.

could be hypothesized that the organ architecture provides metastatic tumor cells with attachment and support for their growth. We also highlight the specific interaction of tumor cells with LSECs in rHGP which might indirectly contribute to tumor progress. However, it is still a pure conceptual idea and it remains to be verified.

Clinical implications of HGP are as follows: (1) The association of HGP with clinical outcomes suggests that HGP can be used to stratify patients by survival risk. Early risk stratification helps provide individualized care and guide long-term follow-up; (2) Patients with dHGP are more likely to benefit from systematic therapy, those with rHGP are prone to acquire resistance to AIs and those with non-dHGP are at high risk of positive surgical margin, indicating that HGP can serve as a biomarker for therapy. Based on pre-treatment prediction of HGP, stratification of patients may help clinicians in treatment decision-making and surgical planning for CRCLM patients. The patients with non-dHGP tumor are at higher risk of hepatic recurrence, therefore radical surgery may be of utmost importance. Furthermore, combination therapy would be an inevitable choice for the subgroup with rHGP. Nevertheless, the above benefit from HGP is on the premise of identifying HGP by a non-interventional method. In this regard, radiomics aiming to distinguish HGP in combination with other markers may be a powerful tool in classification of patients; and (3) Studies of mechanism of HGP favor development of therapeutic approaches, and it is encouraging that there have been relevant preliminary trails. For instance, vessel co-option was found to be inhibited through suppressing cancer cell motility and migration in rHGP tumor, and inhibitors targeting both angiogenesis and vessel co-option were more effective *in vivo*[30]. Considering the enrichment of fibrotic and angiogenic reaction of dHGP tumors, anti-angiogenic and anti-fibrotic therapies may be effective for these tumors. However, even though both anti-fibrotic[76,77] and anti-VEGF[78] treatment could restore the immune response, these treatments should be used with caution due to the unsatisfying results shown in trials[79].

In addition, we put forward our perspectives on some hot topics. HGP is a miniature of tumor-host reaction and reflects tumor biology and pathological features as well as host immune dynamics. In this sense, HGP builds a bridge between microscopic characteristics and clinical implications. Is HGP plastic? With existence of spatial and temporal heterogeneity, tumors utilize different vascularization at different stages, and their HGP also changes with development of tumor, but knowledge about this is still lacking. What is the key motivation shaping HGP? In addition to motility, invasion and migration giving rise to formation of HGP, the association between HGP and other biological characteristics such as embryonic features, stemness, and spontaneous mutation should be explored. In summary, HGP is a paradox involving several dimensions: malignant and normal cells, central and peripheral sites, angiogenesis and non-angiogenesis, and aggressive and mild characteristics (the summary on characteristics of dHGP and rHGP is listed out in Table 2). Combination of AIs with immune checkpoint inhibitors and AIs with vessel co-option inhibitors showed better effects, suggesting that complex targeted treatment would be a direction for the precision therapy in the future.

FOOTNOTES

Author contributions: Kong BT performed the majority of the writing, and prepared the figures and tables; Fan QS, Wang XM and Zhang Q conceptualized the manuscript; Zhang GL revised the manuscript, provided guidance on the overall concept and execution of the manuscript; and All authors have read and approved the final manuscript.

Supported by National Nature Science Foundation, No. 81873111, No. 82174454, and No. 82074182; Natural Science Foundation of Beijing, No. 7202066.

Conflict-of-interest statement: All authors report no relevant conflicts of interest for this article.

Country/Territory of origin: China

ORCID number: Bing-Tan Kong 0000-0001-5352-1406; Qing-Sheng Fan 0000-0002-5648-2833; Xiao-Min Wang 0000-0003-1274-224X; Qing Zhang 0000-0003-3713-4785; Gan-Lin Zhang 0000-0003-3674-3060.

S-Editor: Ma YJ
L-Editor: A
P-Editor: Ma YJ

REFERENCES

1 **Adam R**, de Gramont A, Figueras J, Kokudo N, Kunstlinger F, Loyer E, Poston G, Rougier P, Rubbia-Brandt L, Sobrero A, Teh C, Tejpar S, Van Cutsem E, Vauthey JN, Påhlman L; of the EGOSLIM (Expert Group on OncoSurgery management of LIver Metastases) group. Managing synchronous liver metastases from colorectal cancer: a multidisciplinary international consensus. *Cancer Treat Rev* 2015; **41**: 729-741 [PMID: 26417845 DOI: 10.1016/j.ctrv.2015.06.006]

2 **Jass JR**, Love SB, Northover JM. A new prognostic classification of rectal cancer. *Lancet* 1987; **1**: 1303-1306 [PMID: 2884421 DOI: 10.1016/s0140-6736(87)90552-6]

3 **van Dam PJ**, van der Stok EP, Teuwen LA, Van den Eynden GG, Illemann M, Frentzas S, Majeed AW, Eefsen RL, Coebergh van den Braak RRJ, Lazaris A, Fernandez MC, Galjart B, Laerum OD, Rayes R, Grünhagen DJ, Van de Paer M, Sucaet Y, Mudhar HS, Schvimer M, Nyström H, Kockx M, Bird NC, Vidal-Vanaclocha F, Metrakos P, Simoneau E, Verhoef C, Dirix LY, Van Laere S, Gao ZH, Brodt P, Reynolds AR, Vermeulen PB. International consensus guidelines for scoring the histopathological growth patterns of liver metastasis. *Br J Cancer* 2017; **117**: 1427-1441 [PMID: 28982110 DOI: 10.1038/bjc.2017.334]

4 **Liang JY**, Xi SY, Shao Q, Yuan YF, Li BK, Zheng Y, Wang DS, Wu XJ, Ding PR, Chen G, Li LR, Wang FH, Wang ZQ, Pan ZZ, Xu RH, Li YH. Histopathological growth patterns correlate with the immunoscore in colorectal cancer liver metastasis patients after hepatectomy. *Cancer Immunol Immunother* 2020; **69**: 2623-2634 [PMID: 32601799 DOI: 10.1007/s00262-020-02632-6]

5 **Höppener DJ**, Nierop PMH, Hof J, Sideras K, Zhou G, Visser L, Gouw ASH, de Jong KP, Sprengers D, Kwekkeboom J, Vermeulen PB, Grünhagen DJ, Verhoef C. Enrichment of the tumour immune microenvironment in patients with desmoplastic colorectal liver metastasis. *Br J Cancer* 2020; **123**: 196-206 [PMID: 32418992 DOI: 10.1038/s41416-020-0881-z]

6 **Galjart B**, Nierop PMH, van der Stok EP, van den Braak RRJC, Höppener DJ, Daelemans S, Dirix LY, Verhoef C, Vermeulen PB, Grünhagen DJ. Angiogenic desmoplastic histopathological growth pattern as a prognostic marker of good outcome in patients with colorectal liver metastases. *Angiogenesis* 2019; **22**: 355-368 [PMID: 30637550 DOI: 10.1007/s10456-019-09661-5]

7 **Siriwardana PN**, Luong TV, Watkins J, Turley H, Ghazaley M, Gatter K, Harris AL, Hochhauser D, Davidson BR. Biological and Prognostic Significance of the Morphological Types and Vascular Patterns in Colorectal Liver Metastases (CRLM): Looking Beyond the Tumor Margin. *Medicine (Baltimore)* 2016; **95**: e2924 [PMID: 26937938 DOI: 10.1097/MD.0000000000002924]

8 **Nielsen K**, Rolff HC, Eefsen RL, Vainer B. The morphological growth patterns of colorectal liver metastases are prognostic for overall survival. *Mod Pathol* 2014; **27**: 1641-1648 [PMID: 24851832 DOI: 10.1038/modpathol.2014.4]

9 **Nierop PMH**, Höppener DJ, van der Stok EP, Galjart B, Buisman FE, Balachandran VP, Jarnagin WR, Kingham TP, Allen PJ, Shia J, Vermeulen PB, Groot Koerkamp B, Grünhagen DJ, Verhoef C, D'Angelica MI. Histopathological growth patterns and positive margins after resection of colorectal liver metastases. *HPB (Oxford)* 2020; **22**: 911-919 [PMID: 31735649 DOI: 10.1016/j.hpb.2019.10.015]

10 **Li X**, Zhao Q, An B, Qi J, Wang W, Zhang D, Li Z, Qin C. Prognostic and predictive value of the macroscopic growth pattern in patients undergoing curative resection of colorectal cancer: a single-institution retrospective cohort study of 4,080 Chinese patients. *Cancer Manag Res* 2018; **10**: 1875-1887 [PMID: 30013394 DOI: 10.2147/CMAR.S165279]

11 **Falcão D**, Alexandrino H, Caetano Oliveira R, Martins J, Ferreira L, Martins R, Serôdio M, Martins M, Tralhão JG, Cipriano MA, Castro E Sousa F. Histopathologic patterns as markers of prognosis in patients undergoing hepatectomy for colorectal cancer liver metastases - Pushing growth as an independent risk factor for decreased survival. *Eur J Surg Oncol* 2018; **44**: 1212-1219 [PMID: 29691114 DOI: 10.1016/j.ejso.2018.03.023]

12 **Pinheiro RS**, Herman P, Lupinacci RM, Lai Q, Mello ES, Coelho FF, Perini MV, Pugliese V, Andraus W, Cecconello I, D'Albuquerque LC. Tumor growth pattern as predictor of colorectal liver metastasis recurrence. *Am J Surg* 2014; **207**: 493-

498 [PMID: 24112674 DOI: 10.1016/j.amjsurg.2013.05.015]

13 **Van den Eynden GG**, Bird NC, Majeed AW, Van Laere S, Dirix LY, Vermeulen PB. The histological growth pattern of colorectal cancer liver metastases has prognostic value. *Clin Exp Metastasis* 2012; **29**: 541-549 [PMID: 22476470 DOI: 10.1007/s10585-012-9469-1]

14 **Rajaganeshan R**, Prasad R, Guillou PJ, Scott N, Poston G, Jayne DG. Expression patterns of hypoxic markers at the invasive margin of colorectal cancers and liver metastases. *Eur J Surg Oncol* 2009; **35**: 1286-1294 [PMID: 19540709 DOI: 10.1016/j.ejso.2009.05.008]

15 **Barnhill R**, van Dam PJ, Vermeulen P, Champenois G, Nicolas A, Rawson RV, Wilmott JS, Thompson JF, Long GV, Cassoux N, Roman-Roman S, Busam KJ, Scolyer RA, Lazar AJ, Lugassy C. Replacement and desmoplastic histopathological growth patterns in cutaneous melanoma liver metastases: frequency, characteristics, and robust prognostic value. *J Pathol Clin Res* 2020; **6**: 195-206 [PMID: 32304183 DOI: 10.1002/cjp2.161]

16 **Jayme VR**, Fonseca GM, Amaral IMA, Coelho FF, Kruger JAP, Jeismann VB, Pinheiro RSN, de Mello ES, Herman P. Infiltrative Tumor Borders in Colorectal Liver Metastasis: Should We Enlarge Margin Size? *Ann Surg Oncol* 2021; **28**: 7636-7646 [PMID: 33834322 DOI: 10.1245/s10434-021-09916-w]

17 **Nierop PMH**, Galjart B, Höppener DJ, van der Stok EP, Coebergh van den Braak RRJ, Vermeulen PB, Grünhagen DJ, Verhoef C. Salvage treatment for recurrences after first resection of colorectal liver metastases: the impact of histopathological growth patterns. *Clin Exp Metastasis* 2019; **36**: 109-118 [PMID: 30843120 DOI: 10.1007/s10585-019-09960-7]

18 **Nyström H**, Naredi P, Berglund A, Palmqvist R, Tavelin B, Sund M. Liver-metastatic potential of colorectal cancer is related to the stromal composition of the tumour. *Anticancer Res* 2012; **32**: 5183-5191 [PMID: 23225415 DOI: 10.1016/j.ejso.2012.06.187]

19 **Wu JB**, Sarmiento AL, Fiset PO, Lazaris A, Metrakos P, Petrillo S, Gao ZH. Histologic features and genomic alterations of primary colorectal adenocarcinoma predict growth patterns of liver metastasis. *World J Gastroenterol* 2019; **25**: 3408-3425 [PMID: 31341365 DOI: 10.3748/wjg.v25.i26.3408]

20 **Mlecnik B**, Van den Eynde M, Bindea G, Church SE, Vasaturo A, Fredriksen T, Lafontaine L, Haicheur N, Marliot F, Debetancourt D, Pairet G, Jouret-Mourin A, Gigot JF, Hubert C, Danse E, Dragean C, Carrasco J, Humblet Y, Valge-Archer V, Berger A, Pagès F, Machiels JP, Galon J. Comprehensive Intrametastatic Immune Quantification and Major Impact of Immunoscore on Survival. *J Natl Cancer Inst* 2018; **110** [PMID: 28922789 DOI: 10.1093/jnci/djx123]

21 **Shim JR**, Lee SD, Han SS, Lee SJ, Lee DE, Kim SK, Kim SH, Park SJ, Oh JH. Prognostic significance of ^{18}F-FDG PET/CT in patients with colorectal cancer liver metastases after hepatectomy. *Eur J Surg Oncol* 2018; **44**: 670-676 [PMID: 29459018 DOI: 10.1016/j.ejso.2018.01.243]

22 **Nemeth Z**, Wijker W, Lengyel Z, Hitre E, Borbely K. Metabolic Parameters as Predictors for Progression Free and Overall Survival of Patients with Metastatic Colorectal Cancer. *Pathol Oncol Res* 2020; **26**: 2683-2691 [PMID: 32661836 DOI: 10.1007/s12253-020-00865-5]

23 **Bohlok A**, Duran Derijckere I, Azema H, Lucidi V, Vankerckhove S, Hendlisz A, Van Laethem JL, Vierasu I, Goldman S, Flamen P, Larsimont D, Demetter P, Dirix L, Vermeulen P, Donckier V. Clinico-metabolic characterization improves the prognostic value of histological growth patterns in patients undergoing surgery for colorectal liver metastases. *J Surg Oncol* 2021; **123**: 1773-1783 [PMID: 33751583 DOI: 10.1002/jso.26466]

24 **Baldin P**, Van den Eynde M, Mlecnik B, Bindea G, Beniuga G, Carrasco J, Haicheur N, Marliot F, Lafontaine L, Fredriksen T, Lanthier N, Hubert C, Navez B, Huyghe N, Pagès F, Jouret-Mourin A, Galon J, Komuta M. Prognostic assessment of resected colorectal liver metastases integrating pathological features, RAS mutation and Immunoscore. *J Pathol Clin Res* 2021; **7**: 27-41 [PMID: 32902189 DOI: 10.1002/cjp2.178]

25 **Allard MA**, Nishioka Y, Beghdadi N, Imai K, Gelli M, Yamashita S, Kitano Y, Kokudo T, Yamashita YI, Sa Cunha A, Vibert E, Elias D, Cherqui D, Goere D, Adam R, Baba H, Hasegawa K. Multicentre study of perioperative *versus* adjuvant chemotherapy for resectable colorectal liver metastases. *BJS Open* 2019; **3**: 678-686 [PMID: 31592094 DOI: 10.1002/bjs5.50174]

26 **Araujo R**, Gonen M, Allen P, Blumgart L, DeMatteo R, Fong Y, Kemeny N, Jarnagin W, D'Angelica M. Comparison between perioperative and postoperative chemotherapy after potentially curative hepatic resection for metastatic colorectal cancer. *Ann Surg Oncol* 2013; **20**: 4312-4321 [PMID: 23897009 DOI: 10.1245/s10434-013-3162-8]

27 **Buisman FE**, van der Stok EP, Galjart B, Vermeulen PB, Balachandran VP, Coebergh van den Braak RRJ, Creasy JM, Höppener DJ, Jarnagin WR, Kingham TP, Nierop PMH, Sadot E, Shia J, Groot Koerkamp B, Grünhagen DJ, D'Angelica M, Verhoef C. Histopathological growth patterns as biomarker for adjuvant systemic chemotherapy in patients with resected colorectal liver metastases. *Clin Exp Metastasis* 2020; **37**: 593-605 [PMID: 32691187 DOI: 10.1007/s10585-020-10048-w]

28 **Cremolini C**, Milione M, Marmorino F, Morano F, Zucchelli G, Mennitto A, Prisciandaro M, Lonardi S, Pellegrinelli A, Rossini D, Bergamo F, Aprile G, Urbani L, Morelli L, Schirripa M, Cardellino GG, Fassan M, Fontanini G, de Braud F, Mazzaferro V, Falcone A, Pietrantonio F. Differential histopathologic parameters in colorectal cancer liver metastases resected after triplets plus bevacizumab or cetuximab: a pooled analysis of five prospective trials. *Br J Cancer* 2018; **118**: 955-965 [PMID: 29531324 DOI: 10.1038/s41416-018-0015-z]

29 **Nierop PM**, Höppener DJ, Buisman FE, van der Stok EP, Galjart B, Balachandran VP, Jarnagin WR, Kingham TP, Shia J, Mauer M, Nordlinger B, Julié C, Groot Koerkamp B, Doukas M, Vermeulen PB, Grünhagen DJ, D'Angelica MI, Verhoef C. Preoperative systemic chemotherapy alters the histopathological growth patterns of colorectal liver metastases. *J Pathol Clin Res* 2022; **8**: 48-64 [PMID: 34480530 DOI: 10.1002/cjp2.235]

30 **Frentzas S**, Simoneau E, Bridgeman VL, Vermeulen PB, Foo S, Kostaras E, Nathan M, Wotherspoon A, Gao ZH, Shi Y, Van den Eynden G, Daley F, Peckitt C, Tan X, Salman A, Lazaris A, Gazinska P, Berg TJ, Eltahir Z, Ritsma L, Van Rheenen J, Khashper A, Brown G, Nystrom H, Sund M, Van Laere S, Loyer E, Dirix L, Cunningham D, Metrakos P, Reynolds AR. Vessel co-option mediates resistance to anti-angiogenic therapy in liver metastases. *Nat Med* 2016; **22**: 1294-1302 [PMID: 27748747 DOI: 10.1038/nm.4197]

31 **Kuczynski EA**, Yin M, Bar-Zion A, Lee CR, Butz H, Man S, Daley F, Vermeulen PB, Yousef GM, Foster FS, Reynolds

AR, Kerbel RS. Co-option of Liver Vessels and Not Sprouting Angiogenesis Drives Acquired Sorafenib Resistance in Hepatocellular Carcinoma. *J Natl Cancer Inst* 2016; **108** [PMID: 27059374 DOI: 10.1093/jnci/djw030]

32 **Lazaris A**, Amri A, Petrillo SK, Zoroquiain P, Ibrahim N, Salman A, Gao ZH, Vermeulen PB, Metrakos P. Vascularization of colorectal carcinoma liver metastasis: insight into stratification of patients for anti-angiogenic therapies. *J Pathol Clin Res* 2018; **4**: 184-192 [PMID: 29654716 DOI: 10.1002/cjp2.100]

33 **Hillen F**, Griffioen AW. Tumour vascularization: sprouting angiogenesis and beyond. *Cancer Metastasis Rev* 2007; **26**: 489-502 [PMID: 17717633 DOI: 10.1007/s10555-007-9094-7]

34 **Paku S**, Paweletz N. First steps of tumor-related angiogenesis. *Lab Invest* 1991; **65**: 334-346 [PMID: 1716330]

35 **Jain RK**. Normalization of tumor vasculature: an emerging concept in antiangiogenic therapy. *Science* 2005; **307**: 58-62 [PMID: 15637262 DOI: 10.1126/science.1104819]

36 **Batchelor TT**, Sorensen AG, di Tomaso E, Zhang WT, Duda DG, Cohen KS, Kozak KR, Cahill DP, Chen PJ, Zhu M, Ancukiewicz M, Mrugala MM, Plotkin S, Drappatz J, Louis DN, Ivy P, Scadden DT, Benner T, Loeffler JS, Wen PY, Jain RK. AZD2171, a pan-VEGF receptor tyrosine kinase inhibitor, normalizes tumor vasculature and alleviates edema in glioblastoma patients. *Cancer Cell* 2007; **11**: 83-95 [PMID: 17222792 DOI: 10.1016/j.ccr.2006.11.021]

37 **Tolaney SM**, Boucher Y, Duda DG, Martin JD, Seano G, Ancukiewicz M, Barry WT, Goel S, Lahdenrata J, Isakoff SJ, Yeh ED, Jain SR, Golshan M, Brock J, Snuderl M, Winer EP, Krop IE, Jain RK. Role of vascular density and normalization in response to neoadjuvant bevacizumab and chemotherapy in breast cancer patients. *Proc Natl Acad Sci U S A* 2015; **112**: 14325-14330 [PMID: 26578779 DOI: 10.1073/pnas.1518808112]

38 **Irie T**, Tsushima Y, Terahata S, Hatsuse K, Kusano S. Rim enhancement in colorectal metastases at CT during infusion hepatic arteriography. Does it represent liver parenchyma or live tumor cell zone? *Acta Radiol* 1997; **38**: 416-421 [PMID: 9191433 DOI: 10.1080/02841859709172093]

39 **Terayama N**, Matsui O, Ueda K, Kobayashi S, Sanada J, Gabata T, Kawamori Y, Kadoya M. Peritumoral rim enhancement of liver metastasis: hemodynamics observed on single-level dynamic CT during hepatic arteriography and histopathologic correlation. *J Comput Assist Tomogr* 2002; **26**: 975-980 [PMID: 12488746 DOI: 10.1097/00004728-200211000-00021]

40 **Kanematsu M**, Matsuo M, Yamada Y, Semelka RC, Kondo H, Goshima S, Hoshi H, Moriyama N. Perilesional hyperintense rim of malignant hepatic tumors on ferumoxide-enhanced T1-weighted gradient-echo MR images: correlation between MR imaging and histopathologic findings. *J Magn Reson Imaging* 2003; **18**: 40-48 [PMID: 12815638 DOI: 10.1002/jmri.10328]

41 **Semelka RC**, Hussain SM, Marcos HB, Woosley JT. Perilesional enhancement of hepatic metastases: correlation between MR imaging and histopathologic findings-initial observations. *Radiology* 2000; **215**: 89-94 [PMID: 10751472 DOI: 10.1148/radiology.215.1.r00mr2989]

42 **Cheng J**, Wei J, Tong T, Sheng W, Zhang Y, Han Y, Gu D, Hong N, Ye Y, Tian J, Wang Y. Prediction of Histopathologic Growth Patterns of Colorectal Liver Metastases with a Noninvasive Imaging Method. *Ann Surg Oncol* 2019; **26**: 4587-4598 [PMID: 31605342 DOI: 10.1245/s10434-019-07910-x]

43 **Wei S**, Han Y, Zeng H, Ye S, Cheng J, Chai F, Wei J, Zhang J, Hong N, Bao Y, Zhou J, Ye Y, Meng X, Zhou Y, Deng Y, Qiu M, Tian J, Wang Y. Radiomics diagnosed histopathological growth pattern in prediction of response and 1-year progression free survival for colorectal liver metastases patients treated with bevacizumab containing chemotherapy. *Eur J Radiol* 2021; **142**: 109863 [PMID: 34343846 DOI: 10.1016/j.ejrad.2021.109863]

44 **Chun YS**, Vauthey JN, Boonsirikamchai P, Maru DM, Kopetz S, Palavecino M, Curley SA, Abdalla EK, Kaur H, Charnsangavej C, Loyer EM. Association of computed tomography morphologic criteria with pathologic response and survival in patients treated with bevacizumab for colorectal liver metastases. *JAMA* 2009; **302**: 2338-2344 [PMID: 19952320 DOI: 10.1001/jama.2009.1755]

45 **Shindoh J**, Loyer EM, Kopetz S, Boonsirikamchai P, Maru DM, Chun YS, Zimmitti G, Curley SA, Charnsangavej C, Aloia TA, Vauthey JN. Optimal morphologic response to preoperative chemotherapy: an alternate outcome end point before resection of hepatic colorectal metastases. *J Clin Oncol* 2012; **30**: 4566-4572 [PMID: 23150701 DOI: 10.1200/JCO.2012.45.2854]

46 **Han Y**, Chai F, Wei J, Yue Y, Cheng J, Gu D, Zhang Y, Tong T, Sheng W, Hong N, Ye Y, Wang Y, Tian J. Identification of Predominant Histopathological Growth Patterns of Colorectal Liver Metastasis by Multi-Habitat and Multi-Sequence Based Radiomics Analysis. *Front Oncol* 2020; **10**: 1363 [PMID: 32923388 DOI: 10.3389/fonc.2020.01363]

47 **Dohan A**, Gallix B, Guiu B, Le Malicot K, Reinhold C, Soyer P, Bennouna J, Ghiringhelli F, Barbier E, Boige V, Taieb J, Bouché O, François E, Phelip JM, Borel C, Faroux R, Seitz JF, Jacquot S, Ben Abdelghani M, Khemissa-Akouz F, Genet D, Jouve JL, Rinaldi Y, Desseigne F, Texereau P, Suc E, Lepage C, Aparicio T, Hoeffel C; PRODIGE 9 Investigators and PRODIGE 20 Investigators. Early evaluation using a radiomic signature of unresectable hepatic metastases to predict outcome in patients with colorectal cancer treated with FOLFIRI and bevacizumab. *Gut* 2020; **69**: 531-539 [PMID: 31101691 DOI: 10.1136/gutjnl-2018-316407]

48 **Choi SH**, Kim SY, Park SH, Kim KW, Lee JY, Lee SS, Lee MG. Diagnostic performance of CT, gadoxetate disodium-enhanced MRI, and PET/CT for the diagnosis of colorectal liver metastasis: Systematic review and meta-analysis. *J Magn Reson Imaging* 2018; **47**: 1237-1250 [PMID: 28901685 DOI: 10.1002/jmri.25852]

49 **Eefsen RL**, Engelholm L, Alpizar-Alpizar W, Van den Eynden GG, Vermeulen PB, Christensen IJ, Laerum OD, Rolff HC, Høyer-Hansen G, Vainer B, Osterlind K, Illemann M. Inflammation and uPAR-Expression in Colorectal Liver Metastases in Relation to Growth Pattern and Neo-adjuvant Therapy. *Cancer Microenviron* 2015; **8**: 93-100 [PMID: 26268716 DOI: 10.1007/s12307-015-0172-z]

50 **Illemann M**, Bird N, Majeed A, Laerum OD, Lund LR, Danø K, Nielsen BS. Two distinct expression patterns of urokinase, urokinase receptor and plasminogen activator inhibitor-1 in colon cancer liver metastases. *Int J Cancer* 2009; **124**: 1860-1870 [PMID: 19123477 DOI: 10.1002/ijc.24166]

51 **Garcia-Vicién G**, Mezheyeuski A, Bañuls M, Ruiz-Roig N, Molleví DG. The Tumor Microenvironment in Liver Metastases from Colorectal Carcinoma in the Context of the Histologic Growth Patterns. *Int J Mol Sci* 2021; **22** [PMID: 33546502 DOI: 10.3390/ijms22041544]

52 **Jiang H**, Torphy RJ, Steiger K, Hongo H, Ritchie AJ, Kriegsmann M, Horst D, Umetsu SE, Joseph NM, McGregor K, Pishvaian MJ, Blais EM, Lu B, Li M, Hollingsworth M, Stashko C, Volmar K, Yeh JJ, Weaver VM, Wang ZJ, Tempero MA, Weichert W, Collisson EA. Pancreatic ductal adenocarcinoma progression is restrained by stromal matrix. *J Clin Invest* 2020; **130**: 4704-4709 [PMID: 32749238 DOI: 10.1172/JCI136760]

53 **Brunner SM**, Kesselring R, Rubner C, Martin M, Jeiter T, Boerner T, Ruemmele P, Schlitt HJ, Fichtner-Feigl S. Prognosis according to histochemical analysis of liver metastases removed at liver resection. *Br J Surg* 2014; **101**: 1681-1691 [PMID: 25331841 DOI: 10.1002/bjs.9627]

54 **Iwaya K**, Oikawa K, Semba S, Tsuchiya B, Mukai Y, Otsubo T, Nagao T, Izumi M, Kuroda M, Domoto H, Mukai K. Correlation between liver metastasis of the colocalization of actin-related protein 2 and 3 complex and WAVE2 in colorectal carcinoma. *Cancer Sci* 2007; **98**: 992-999 [PMID: 17459058 DOI: 10.1111/j.1349-7006.2007.00488.x]

55 **Rada M**, Kapelanski-Lamoureux A, Petrillo S, Tabariès S, Siegel P, Reynolds AR, Lazaris A, Metrakos P. Runt related transcription factor-1 plays a central role in vessel co-option of colorectal cancer liver metastases. *Commun Biol* 2021; **4**: 950 [PMID: 34376784 DOI: 10.1038/s42003-021-02481-8]

56 **Tabariès S**, Siegel PM. The role of claudins in cancer metastasis. *Oncogene* 2017; **36**: 1176-1190 [PMID: 27524421 DOI: 10.1038/onc.2016.289]

57 **Tabariès S**, Annis MG, Lazaris A, Petrillo SK, Huxham J, Abdellatif A, Palmieri V, Chabot J, Johnson RM, Van Laere S, Verhoef C, Hachem Y, Yumeen S, Meti N, Omeroglu A, Altinel G, Gao ZH, Yu ASL, Grünhagen DJ, Vermeulen P, Metrakos P, Siegel PM. Claudin-2 promotes colorectal cancer liver metastasis and is a biomarker of the replacement type growth pattern. *Commun Biol* 2021; **4**: 657 [PMID: 34079064 DOI: 10.1038/s42003-021-02189-9]

58 **Tabariès S**, Dupuy F, Dong Z, Monast A, Annis MG, Spicer J, Ferri LE, Omeroglu A, Basik M, Amir E, Clemons M, Siegel PM. Claudin-2 promotes breast cancer liver metastasis by facilitating tumor cell interactions with hepatocytes. *Mol Cell Biol* 2012; **32**: 2979-2991 [PMID: 22645303 DOI: 10.1128/MCB.00299-12]

59 **Tabariès S**, McNulty A, Ouellet V, Annis MG, Dessureault M, Vinette M, Hachem Y, Lavoie B, Omeroglu A, Simon HG, Walsh LA, Kimbung S, Hedenfalk I, Siegel PM. Afadin cooperates with Claudin-2 to promote breast cancer metastasis. *Genes Dev* 2019; **33**: 180-193 [PMID: 30692208 DOI: 10.1101/gad.319194.118]

60 **Ahmad SA**, Liu W, Jung YD, Fan F, Wilson M, Reinmuth N, Shaheen RM, Bucana CD, Ellis LM. The effects of angiopoietin-1 and -2 on tumor growth and angiogenesis in human colon cancer. *Cancer Res* 2001; **61**: 1255-1259 [PMID: 11245414 DOI: 10.1002/1097-0142(20010215)91:4<874::AID-CNCR1076>3.0.CO;2-O]

61 **Ibrahim NS**, Lazaris A, Rada M, Petrillo SK, Huck L, Hussain S, Ouladan S, Gao ZH, Gregorieff A, Essalmani R, Seidah NG, Metrakos P. Angiopoietin1 Deficiency in Hepatocytes Affects the Growth of Colorectal Cancer Liver Metastases (CRCLM). *Cancers (Basel)* 2019; **12** [PMID: 31877668 DOI: 10.3390/cancers12010035]

62 **Palmieri V**, Lazaris A, Mayer TZ, Petrillo SK, Alamri H, Rada M, Jarrouj G, Park WY, Gao ZH, McDonald PP, Metrakos P. Neutrophils expressing lysyl oxidase-like 4 protein are present in colorectal cancer liver metastases resistant to anti-angiogenic therapy. *J Pathol* 2020; **251**: 213-223 [PMID: 32297656 DOI: 10.1002/path.5449]

63 **Cordero-Espinoza L**, Huch M. The balancing act of the liver: tissue regeneration versus fibrosis. *J Clin Invest* 2018; **128**: 85-96 [PMID: 29293095 DOI: 10.1172/JCI93562]

64 **van Dam PJ**, Daelemans S, Ross E, Waumans Y, Van Laere S, Latacz E, Van Steen R, De Pooter C, Kockx M, Dirix L, Vermeulen PB. Histopathological growth patterns as a candidate biomarker for immunomodulatory therapy. *Semin Cancer Biol* 2018; **52**: 86-93 [PMID: 29355613 DOI: 10.1016/j.semcancer.2018.01.009]

65 **Schuppan D**, Kim YO. Evolving therapies for liver fibrosis. *J Clin Invest* 2013; **123**: 1887-1901 [PMID: 23635787 DOI: 10.1172/JCI66028]

66 **Arteta B**, Lasuen N, Lopategi A, Sveinbjörnsson B, Smedsrød B, Vidal-Vanaclocha F. Colon carcinoma cell interaction with liver sinusoidal endothelium inhibits organ-specific antitumor immunity through interleukin-1-induced mannose receptor in mice. *Hepatology* 2010; **51**: 2172-2182 [PMID: 20513002 DOI: 10.1002/hep.23590]

67 **Kubes P**, Jenne C. Immune Responses in the Liver. *Annu Rev Immunol* 2018; **36**: 247-277 [PMID: 29328785 DOI: 10.1146/annurev-immunol-051116-052415]

68 **Tang L**, Yang J, Liu W, Tang X, Chen J, Zhao D, Wang M, Xu F, Lu Y, Liu B, Sun Q, Zhang L, He F. Liver sinusoidal endothelial cell lectin, LSECtin, negatively regulates hepatic T-cell immune response. *Gastroenterology* 2009; **137**: 1498-508.e1 [PMID: 19632227 DOI: 10.1053/j.gastro.2009.07.051]

69 **Lugassy C**, Kleinman HK, Vermeulen PB, Barnhill RL. Angiotropism, pericytic mimicry and extravascular migratory metastasis: an embryogenesis-derived program of tumor spread. *Angiogenesis* 2020; **23**: 27-41 [PMID: 31720876 DOI: 10.1007/s10456-019-09695-9]

70 **Sakariassen PØ**, Prestegarden L, Wang J, Skaftnesmo KO, Mahesparan R, Molthoff C, Sminia P, Sundlisaeter E, Misra A, Tysnes BB, Chekenya M, Peters H, Lende G, Kalland KH, Øyan AM, Petersen K, Jonassen I, van der Kogel A, Feuerstein BG, Terzis AJ, Bjerkvig R, Enger PØ. Angiogenesis-independent tumor growth mediated by stem-like cancer cells. *Proc Natl Acad Sci U S A* 2006; **103**: 16466-16471 [PMID: 17056721 DOI: 10.1073/pnas.0607668103]

71 **Donnem T**, Reynolds AR, Kuczynski EA, Gatter K, Vermeulen PB, Kerbel RS, Harris AL, Pezzella F. Non-angiogenic tumours and their influence on cancer biology. *Nat Rev Cancer* 2018; **18**: 323-336 [PMID: 29520090 DOI: 10.1038/nrc.2018.14]

72 **Kuczynski EA**, Vermeulen PB, Pezzella F, Kerbel RS, Reynolds AR. Vessel co-option in cancer. *Nat Rev Clin Oncol* 2019; **16**: 469-493 [PMID: 30816337 DOI: 10.1038/s41571-019-0181-9]

73 **Berghoff AS**, Rajky O, Winkler F, Bartsch R, Furtner J, Hainfellner JA, Goodman SL, Weller M, Schittenhelm J, Preusser M. Invasion patterns in brain metastases of solid cancers. *Neuro Oncol* 2013; **15**: 1664-1672 [PMID: 24084410 DOI: 10.1093/neuonc/not112]

74 **Lugassy C**, Zadran S, Bentolila LA, Wadehra M, Prakash R, Carmichael ST, Kleinman HK, Péault B, Larue L, Barnhill RL. Angiotropism, pericytic mimicry and extravascular migratory metastasis in melanoma: an alternative to intravascular cancer dissemination. *Cancer Microenviron* 2014; **7**: 139-152 [PMID: 25304454 DOI: 10.1007/s12307-014-0156-4]

75 **Bridgeman VL**, Vermeulen PB, Foo S, Bilecz A, Daley F, Kostaras E, Nathan MR, Wan E, Frentzas S, Schweiger T, Hegedus B, Hoetzenecker K, Renyi-Vamos F, Kuczynski EA, Vasudev NS, Larkin J, Gore M, Dvorak HF, Paku S, Kerbel

RS, Dome B, Reynolds AR. Vessel co-option is common in human lung metastases and mediates resistance to anti-angiogenic therapy in preclinical lung metastasis models. *J Pathol* 2017; **241**: 362-374 [PMID: 27859259 DOI: 10.1002/path.4845]

76 **Feig C**, Jones JO, Kraman M, Wells RJ, Deonarine A, Chan DS, Connell CM, Roberts EW, Zhao Q, Caballero OL, Teichmann SA, Janowitz T, Jodrell DI, Tuveson DA, Fearon DT. Targeting CXCL12 from FAP-expressing carcinoma-associated fibroblasts synergizes with anti-PD-L1 immunotherapy in pancreatic cancer. *Proc Natl Acad Sci U S A* 2013; **110**: 20212-20217 [PMID: 24277834 DOI: 10.1073/pnas.1320318110]

77 **Kraman M**, Bambrough PJ, Arnold JN, Roberts EW, Magiera L, Jones JO, Gopinathan A, Tuveson DA, Fearon DT. Suppression of antitumor immunity by stromal cells expressing fibroblast activation protein-alpha. *Science* 2010; **330**: 827-830 [PMID: 21051638 DOI: 10.1126/science.1195300]

78 **Wallin JJ**, Bendell JC, Funke R, Sznol M, Korski K, Jones S, Hernandez G, Mier J, He X, Hodi FS, Denker M, Leveque V, Cañamero M, Babitski G, Koeppen H, Ziai J, Sharma N, Gaire F, Chen DS, Waterkamp D, Hegde PS, McDermott DF. Atezolizumab in combination with bevacizumab enhances antigen-specific T-cell migration in metastatic renal cell carcinoma. *Nat Commun* 2016; **7**: 12624 [PMID: 27571927 DOI: 10.1038/ncomms12624]

79 **Özdemir BC**, Pentcheva-Hoang T, Carstens JL, Zheng X, Wu CC, Simpson TR, Laklai H, Sugimoto H, Kahlert C, Novitskiy SV, De Jesus-Acosta A, Sharma P, Heidari P, Mahmood U, Chin L, Moses HL, Weaver VM, Maitra A, Allison JP, LeBleu VS, Kalluri R. Depletion of carcinoma-associated fibroblasts and fibrosis induces immunosuppression and accelerates pancreas cancer with reduced survival. *Cancer Cell* 2014; **25**: 719-734 [PMID: 24856586 DOI: 10.1016/j.ccr.2014.04.005]

World Journal of Gastroenterology

Submit a Manuscript: https://www.f6publishing.com

World J Gastroenterol 2022 July 14; 28(26): 3116-3131

DOI: 10.3748/wjg.v28.i26.3116

ISSN 1007-9327 (print) ISSN 2219-2840 (online)

MINIREVIEWS

Role of gadoxetic acid-enhanced liver magnetic resonance imaging in the evaluation of hepatocellular carcinoma after locoregional treatment

Marco Gatti, Cesare Maino, Fatemeh Darvizeh, Alessandro Serafini, Eleonora Tricarico, Alessia Guarneri, Riccardo Inchingolo, Davide Ippolito, Umberto Ricardi, Paolo Fonio, Riccardo Faletti

Specialty type: Gastroenterology and hepatology

Provenance and peer review: Invited article; Externally peer reviewed.

Peer-review model: Single blind

Peer-review report's scientific quality classification

Grade A (Excellent): 0
Grade B (Very good): B
Grade C (Good): C
Grade D (Fair): 0
Grade E (Poor): 0

P-Reviewer: Chai RM, China; Hu Q, China
A-Editor: Dong QJ, China

Received: February 25, 2022
Peer-review started: February 25, 2022
First decision: April 5, 2022
Revised: April 25, 2022
Accepted: June 16, 2022
Article in press: June 16, 2022
Published online: July 14, 2022

Marco Gatti, Alessandro Serafini, Paolo Fonio, Riccardo Faletti, Department of Surgical Sciences, University of Turin, Turin 10126, Italy

Cesare Maino, Davide Ippolito, Department of Diagnostic Radiology, University of Milano-Bicocca, Monza 20900, Italy

Cesare Maino, Davide Ippolito, Department of Diagnostic Radiology, Ospedale San Gerardo, Monza 20900, Italy

Fatemeh Darvizeh, School of Medicine, Vita-Salute San Raffaele University, Milan 20121, Italy

Eleonora Tricarico, Department of Radiology, "F. Perinei" Hospital, Altamura (BA) 70022, Italy

Alessia Guarneri, Umberto Ricardi, Department of Oncology, University of Turin, Turin 10126, Italy

Riccardo Inchingolo, Interventional Radiology Unit, "F. Miulli" Regional General Hospital, Acquaviva delle Fonti (BA) 70021, Italy

Corresponding author: Marco Gatti, MD, Research Fellow, Department of Surgical Sciences, University of Turin, Via Genova 3, Turin 10126, Italy. marcogatti17@gmail.com

Abstract

Locoregional treatments, as alternatives to surgery, play a key role in the management of hepatocellular carcinoma (HCC). Liver magnetic resonance imaging (MRI) enables a multiparametric assessment, going beyond the traditional dynamic computed tomography approach. Moreover, the use of hepatobiliary agents can improve diagnostic accuracy and are becoming important in the diagnosis and follow-up of HCC. However, the main challenge is to quickly identify classical responses to loco-regional treatments in order to determine the most suitable management strategy for each patient. The aim of this review is to provide a summary of the most common and uncommon liver MRI findings in patients who underwent loco-regional treatments for HCC, with a special focus on ablative therapies (radiofrequency, microwaves and cryoablation), trans-arterial chemoembolization, trans-arterial radio-embolization and stereotactic ablative radiotherapy techniques, considering the usefulness of gadoxetate

disodium (Gd-EOB-DTPA) contrast agent.

Key Words: Carcinoma; Hepatocellular; Magnetic resonance imaging; Gd-EOB-DTPA; Radiofrequency ablation; Catheter ablation; Ablation techniques

Core Tip: Ablation techniques are useful tools in the treatment of patients with hepatocellular carcinoma, both in case with a small lesion and as a bridging option prior to surgical resection or liver transplantation and in addition to palliative treatment in advanced disease. In clinical practice it is of utmost importance to acquire a specific skill to identify classical magnetic resonance imaging appearance of the treated lesion and for early detection of tumor recurrence, to guarantee the best possible management for each patient.

Citation: Gatti M, Maino C, Darvizeh F, Serafini A, Tricarico E, Guarneri A, Inchingolo R, Ippolito D, Ricardi U, Fonio P, Faletti R. Role of gadoxetic acid-enhanced liver magnetic resonance imaging in the evaluation of hepatocellular carcinoma after locoregional treatment. *World J Gastroenterol* 2022; 28(26): 3116-3131
URL: https://www.wjgnet.com/1007-9327/full/v28/i26/3116.htm
DOI: https://dx.doi.org/10.3748/wjg.v28.i26.3116

INTRODUCTION

Hepatocellular carcinoma (HCC) is the most common primary liver cancer and represents a major public health issue worldwide[1]. Treatment of patients with HCC is closely related to Barcelona Clinic Liver Cancer (BCLC) stage. Locoregional treatments, as alternatives to surgery, play a key role in the management of HCC. Percutaneous thermoablation strategies are considered as an alternative to surgery in patients with BCLC 0-A, transcatheter embolization therapies are essential in patients with more advanced disease (*i.e.*, BCLC B) and both together with Stereotactic Body Radiation Therapy (SBRT) are useful in patients who are not a surgical candidate[2].

The evaluation of both short- and long-term treatment outcomes is crucial for patient management. According to the guidelines, this evaluation should be performed using either dynamic computed tomography (CT) or magnetic resonance imaging (MRI)[2].

Liver MRI enables a multiparametric assessment, going beyond the vascularity assessment provided by traditional dynamic CT[3,4]. In recent years, liver MRI has made significant advances in the evaluation of HCC thanks to the introduction of new sequences for non-contrast evaluation (*e.g.*, diffusion-weighted sequences), the high temporal resolution sequences for optimal contrast enhancement assessment[5,6] and finally, the use of hepatobiliary contrast agents (gadoxetate disodium: Gd-EOB-DTPA, Eovist/Primovist; gadobenate disodium: Gd-BOPTA, Multihance). Gd-EOB–DTPA combines the properties of an extracellular agent, allowing for conventional contrast-enhanced multiphasic imaging, and a hepatocyte agent, allowing for hepatocyte uptake and biliary excretion evaluation, with the added benefit of tumor assessment in the transitional phase (TP) and delayed hepatobiliary phase (HBP) (20-min)[4,7,8]. This contrast agent improves the diagnostic accuracy and is becoming increasingly important in the detection of HCC[9].

The use of liver MRI with hepatobiliary contrast agents has become critical in patients with HCC. Therefore, understanding the typical and atypical features of treatment outcomes and recurrences is of paramount importance for proper treatment strategy.

The purpose of this review is to provide a comprehensive overview of locoregional therapies and to describe how to assess treatment outcomes using contrast-enhanced hepatobiliary MRI.

ABLATIVE THERAPIES

There are several ablation techniques available for the treatment of HCC as reported in a recent literature review by Makary *et al*[10], such as radiofrequency ablation (RFA), microwaves (MWA), cryoablation (CA), irreversible electroporation (IRE), laser-induced interstitial thermotherapy (LITT), and high-intensity focused ultrasound (HIFU). The process of choosing among alternative techniques is principally based on institutional expertise and should be fitted to each patient. The main target for the abovementioned treatment methods is an early-stage HCC with a maximum axial diameter of 3 cm with BCLC class 0 or A. Moreover, this approach may lead to better clinical outcomes in patients with larger HCC lesions (axial diameter of 3 cm to 5 cm), when combined with trans-arterial chemoembolization

(TACE)[10].

Even though the ablation techniques are widely performed, they are not risk-free: it is important to underline that the treated patients can present post-ablation syndrome, loco-regional bleeding, and adjacent organs injuries. The ablative therapy shows similar outcomes to surgical resection in the treatment of HCC with a maximum diameter of 3 cm, with a remarkable advantage of no pre-and post-surgical complications[10].

Most published studies on electronic medical databases including PubMed and Web of Science are strictly linked to RFA and MWA, while CA, IRE, LITT, and HIFU are not deeply evaluated and consequently data regarding response to therapy are lacking. On this basis, we'll present the most common MR imaging findings regarding RFA, MWA and CA therapies.

RFA

RFA technique relies on the destruction of tumoral tissue by producing frictional heat using rapidly alternating electrical current thanks to the application of at least one electrode inside the region of treatment. The ablation zone includes a wider region than the tumor itself, of at least 5 mm to 10 mm[8]. The use of RFA results in hyperthermia-induced coagulation necrosis and represents a heterogeneous low or mixed signal intensity on T1-weighted (T1w) and homogeneously low signal intensity on T2-weighted (T2w) images.

After contrast media administration (extracellular or hepatobiliary agents), the RFA zone manifests as a well-demarcated hypointense area with the absence of contrast enhancement[8]. The presence of slight rim signal intensity on T2w images and contrast enhancement especially in the equilibrium phase should be considered as a physiological response to thermal injury, mainly during early follow-up[11]. The typical appearance of HCC recurrence is the hypervascularity on arterial phase [arterial phase hyperenhancement (APHE)], hypointensity on portal-venous and HBPs. However, in clinical practice, the discrimination between hyperemia and residual HCC might be difficult. This aspect was demonstrated by Mikami *et al*[12], who reported a typical enhancement pattern in only 17.5% of recurrent HCCs, while 40.6% with APHE without washout in the portal venous phase and 11.9% with portal venous phase washout without APHE.

In this setting, the use of Gd-EOB-DTPA can help to distinguish vascular pseudolesions from hypervascular tumors including recurrent HCC[13]. Since 2013, it has been reported[14] the efficacy of EOB-MRI in the decision-making of curative treatment for HCC: it was demonstrated that the HBP improves the diagnostic accuracy and treatment decision making in the early-stage HCC and these results can perfectly fit candidates to RFA. Imai *et al*[15], by enrolling 97 patients who underwent RFA, revealed that EOB-MRI had higher diagnostic accuracy and sensitivity for detection of recurrent hypervascular HCC (44 *vs* 24, $P < 0.001$) in comparison to CT. They also reported a good inter-observer agreement between the 2 readers, underlying the effectiveness of EOB-MRI.

As known, the main advantage of EOB-MRI is the HBP, where the radiologist can face a hypointense nodule without significant hypervascular appearance. On this basis, it is important to determine the risk of non-hypervascular HCC recurrence after loco-regional treatment. The systematic review and meta-analysis by Kim *et al*[16] demonstrated the post-ablation recurrence of HCC: they showed that hypointense nodules in the HBP represent a high-risk factor for recurrence (hazard ratio = 1.74-3.07), underlying the importance of EOB-MRI in the detection of HCC recurrence post-RFA.

More recently, a retrospective study by Bae *et al*[17] on 183 patients who underwent different treatments including RFA, showed that satellite nodules and peritumoral hypointensity on HBP images were associated with poor disease-free survival and overall survival ($P = 0.018$ and $P = 0.016$, respectively).

On the other hand, the study by Rimola *et al*[18], on 49 patients who underwent locoregional treatment, determined that MRI with extracellular agents has a similar specificity in detecting viable HCC in comparison to EOB-MRI (84% *vs* 85%, respectively), with a higher AUROC (0.80 *vs* 0.72, respectively). These findings are not in line with most studies, however, should be carefully considered due to the small sample size and the remarkable risk of bias, since different ablation techniques were evaluated.

Finally, EOB-MRI was found efficient not only in the evaluation of treatment response but also in the feasibility of ablative margin grading before RFA. Koda *et al*[19] by enrolling 124 HCCs, showed that EOB-MRI enables an early assessment of RFA effectiveness in the majority of HCC nodules with the tumor size as an independent predictor factor for local tumor progression.

To conclude, EOB-MRI can be considered as a useful tool in the detection of HCC recurrence after RFA treatment, however, large prospective studies are needed to determine a more accurate evaluation of diagnostic performance.

Figure 1 depicts a liver MRI after RF treatment with no evidence of disease persistence or relapse, and Figure 2 depicts its evolution. Figure 3 depicts a case of HCC recurrence after RF treatment.

Microwave ablation

MWA technique is based on analogous physical principles of RFA, however, it employs an antenna that produces electromagnetic waves which can interact with water molecules and, consequently, raises the temperature[20].

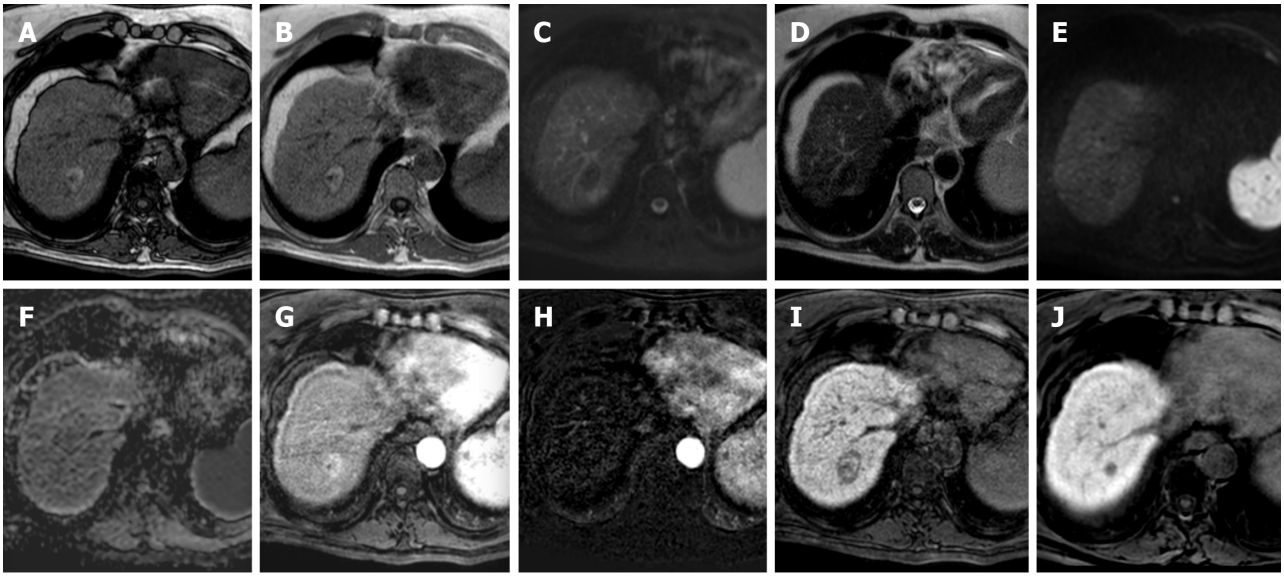

DOI: 10.3748/wjg.v28.i26.3116

Figure 1 hree-month follow-up liver magnetic resonance imaging of a 69-yr-old male post radiofrequency ablation of right hepatic lobe hepatocellular carcinoma (segment VII). A: Out-phase T1-weighted image; B: In-phase T1-weighted image; C: T2-spectral attenuated inversion recovery; D: T2-weighted image; E: High b-value diffusion weighted imaging; F: Apparent diffusion coefficient map; G: Arterial phase magnetic resonance imaging (MRI); H: Arterial phase MRI with image subtraction technique; I and J: Hepatobiliary phase MRI. Follow-up MRI (A-I) after 3 mo post treatment revealed a good outcome characterized by inhomogeneous high signal hyperintensity in T1 sequences due to the presence of coagulative necrosis with associated signal hypointensity in T2 weighted sequences and the absence signal hyperintensity in diffusion weighted imaging. Dynamic study showed no enhancement in arterial phase with inhomogeneous hypointensity during hepatobiliary excretion. Findings are suggestive of complete tumor ablation also when compared to the similar pre-treatment sequences (J).

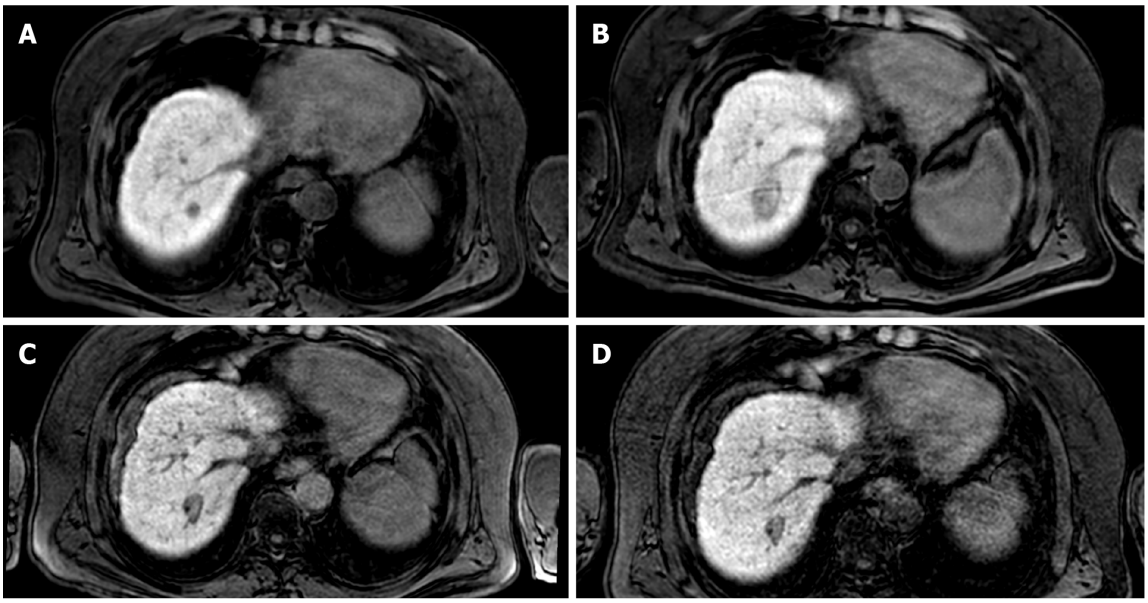

DOI: 10.3748/wjg.v28.i26.3116

Figure 2 The evolution of the ablation zone shown in Figure 1. A: Hepatobiliary phase (HBP) phase magnetic resonance imaging (MRI) prior to radiofrequency ablation (RFA); B: HBP MRI 3 mo after RFA; C: HBP MRI 9 mo after RFA; D: HBP MRI 19 mo after RFA. Liver MRIs demonstrate a progressive reduction of ablation zone together with fibrotic changes.

MR findings after MWA are like those reported for RFA. On unenhanced T1w images, the ablated lesion shows a target-like appearance: linear hypointensity in the center of the ablation zone surrounded by hyperintense region due to coagulative necrosis, and outer hypointense areas of signal intensity corresponding to a slight to high signal intensity on T2w images due to inflammation[21]. After injection of contrast media, no APHE should be seen to consider a complete response. However, only a few studies evaluated the usefulness of EOB-MRI in the detection of HCC recurrence after MWA. Imai *et al*[15] reported that the diagnostic value of EOB-MRI is better than CT to evaluate HCC after

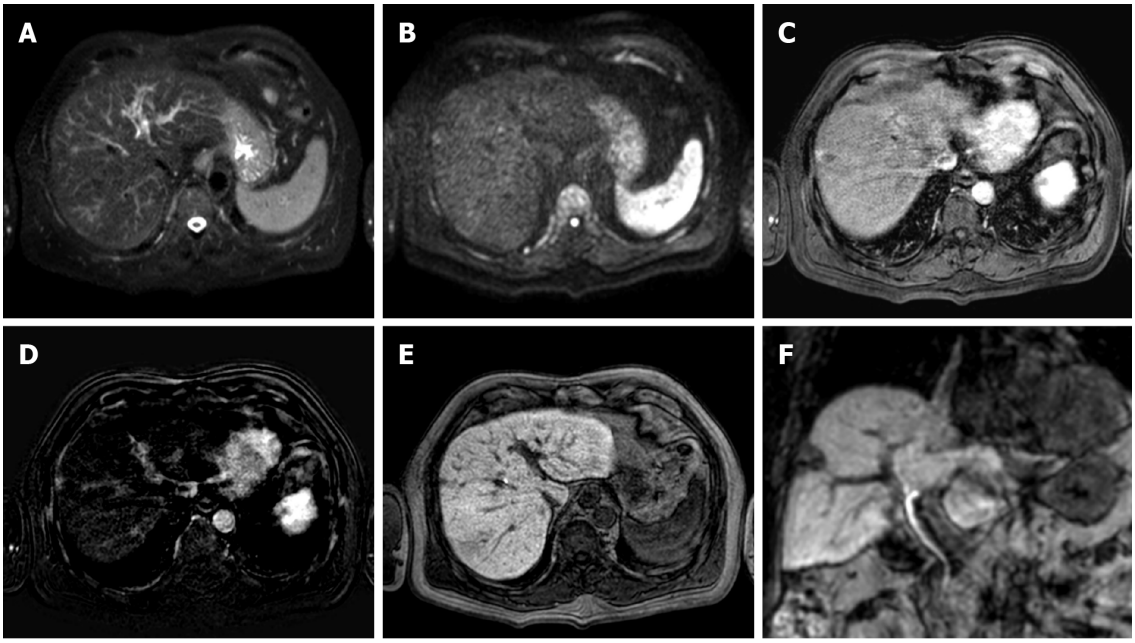

DOI: 10.3748/wjg.v28.i26.3116

Figure 3 Two-years liver magnetic resonance imaging follow-up of a 71-yr-old male with liver cirrhosis and previous subcapsular hepatocellular carcinoma in segment VIII underwent radiofrequency ablation. A: T2-spectral attenuated inversion recovery; B: High b-value diffusion weighted imaging; C: Arterial phase magnetic resonance imaging (MRI); D: Arterial phase MRI with image subtraction technique; E and F: Hepatobiliary phase MRI. Liver MRI showed recurrent hepatocellular carcinoma (8 mm) located infero-lateral to the radiofrequency scar, characterized by moderate to high signal hyperintensity in T2, hyperintensity in high b-value diffusion sequences, with arterial "wash in" and hypointensity in hepatobiliary excretion phase.

treatment by image-guided tumor procedures, including patients who underwent both ablation and chemoembolization.

CA

As reported by Song[22], CA should be included in the family of thermal ablation in HCC patients. The physical bases are like RFA and MWA, however, the employed temperature is not hot but cold, thanks to chemical agents such as liquid nitrogen. According to a recent meta-analysis[23], the effects of MWA and CA appeared to be similar to those of RFA, but there were lower rates of local tumor progression and higher rates of complete thermal ablation in large tumors compared to RFA ($P < 0.05$). MR imaging findings after the CA procedure are similar to RFA and MWA, as reported above: the ablation zone at 24h appears hypointense and heterogeneously hyperintense on T1w and T2w images, respectively[24]. Foci of inhomogeneous signal intensities on T1w and T2w images should be principally due to blood products and can be present in further follow-up examinations[24]. The peripheral zone shows a slight to hyper- signal intensity on T2w images, due to inflammation and granulation tissue formation. The residual tumor presents analogous imaging features to the treated lesion, while the recurrence can be seen as an area of APHE with consequent hypointensity on portal-venous and HBP. Even if not fully reported in the literature, a focal hypointense area of HBP images without APHE might be referred to a suspected recurrence.

TACE AND TRANS-ARTERIAL RADIOEMBOLIZATION

Treatment options for HCC depend on tumor burden and extent, patient's performance status, liver function, extra-hepatic disease, and co-morbidities, according to the BCLC system[10]. Intra-arterial therapies, including TACE and trans-arterial radio-embolization (TARE), come into play to improve survival and quality of life where curative treatments like ablation, liver resection, or liver transplantation are not applicable[10,25]. TACE and TARE are regarded as a standard of care for a patient with intermediate-stage HCC (BCLC class B, Child-Pugh A-B) not eligible for surgical resection or transplantation and without portal vein thrombosis or extrahepatic spread. Moreover, the application of these techniques range from curative-intent for small tumors, to downstaging or bridging to resection and transplantation for early and intermediate disease, and locoregional control and palliation for advanced disease[26].

The main contraindications to TACE and TARE are decompensated liver cirrhosis, bilobar liver involvement, and technical infeasibility; absolute contraindication specific to TARE is the presence of

hepato-pulmonary shunt or hepato-enteric shunts[10].

In the case of portal vein thrombosis, in clinical practice, TACE is contraindicated, even if Patidar *et al* [27] described a good outcome of patients with segmental-branch or first-border branch portal vein thrombosis treated with TACE. On the contrary, TARE may have applications even if there is portal vein thrombosis because of the reduced embolic effect of the technique[10].

TACE

TACE is performed by cannulation of the arteries that feed the HCC through a catheter or a microcatheter and releasing both the chemotherapeutic agent and embolic particles. The treatment may be performed in two ways, conventional TACE that uses lipiodol, an oily radiopaque material mixed with one or more chemotherapeutics agents, followed by administration of an embolic agent and drug-eluting beads TACE (DEB-TACE) with slowing releasing of chemotherapy by particles[26].

Multiphasic MRI is performed to evaluate the response to treatment and to detect new HCCs from 1 mo to 3 mo after treatment for the first imaging study, followed by every 3 mo for 2 years[28]. As previously mentioned, MRI may use gadolinium-based extracellular contrast agents, or gadolinium-based hepatobiliary agents[28,29].

MRI imaging after TACE is related to tumor necrosis caused by ischemic injury from arterial embolization and chemotoxic injury from the administered chemotherapy[28]. Gd-EOB-DTPA allows similar dynamic acquisition of extracellular agents in arterial and portal phases, essential in detection of a viable tumor. If the treatment is successful the expected findings are: absence of APHE, associated with surrounding perfusion changes related to edema and arterial embolization, a thin APHE phase due to inflammatory, that may persist up to a year, and a volumetric reduction of the treated lesion over time[28]. The HBP contributes to the diagnosis of complete response to treatment, showing a corresponding hypointensity of the lesion if complete necrosis occurs. A thin, continuous, and smooth APHE rim associated with a corresponding isointense area in the HBP defines a benign finding[30].

After treatment, the damage of the liver parenchyma around the treated lesion may cause geographic perfusion changes and corresponding hypointensity on the HBP, a feature that needs careful evaluation and examination of additional sequences to avoid diagnostic mistakes of infiltrative disease[31]. If pseudolesions related to treatment occur (arterial-venous shunt and portal vein obstruction), they usually don't show hypointensity on the HBP, an element that helps in the diagnosis of benignity, although hypointense pseudolesions on the HBP mimicking malignancy have been described by Motosugi *et al*[32].

The sign of residual and/or recurrent disease is represented by the presence of thick, peripheral, irregular, eccentric, nodular APHE with or without washout within the treated lesion, or enhancement similar to pre-treatment tumor. Aslam *et al*[30] showed findings suggestive of the presence of viable tumor after thermoablation, applicable for TACE too: the presence of thick, nodular and eccentric hypointense signal on HBP or a discontinuous hypointense rim. Considering these findings on the HBP-like viable tumor is much more important when there is equivocal APHE, consisting of viable isoenhance or hypoenhance tumor in arterial phase[33].

Figure 4 depicts a pre-treatment CT images and subsequent TACE treatment of an HCC nodule, the results of which are illustrated in Figure 5.

TARE

TARE is a trans-arterial catheter treatment based on delivering microspheres (glass or resin) coated with ^{90}Y. ^{90}Y is an unstable isotope that releases a beta particle during its decay into a stable element, zirconium 90, inducing destruction of the target tumor with a limited depth of penetration to minimize radiation exposure of surrounding parenchyma[33].

^{90}Y microspheres have a main radiant effect and a small microembolic effect due to the little diameter of microspheres; therefore, tumor necrosis related to TARE is mostly radiation-induced and the arterial flow to adjacent parenchyma is largely conserved, which is an important advantage in the case of portal venous thrombosis (*i.e.*, contraindication for TACE)[33].

Multiphasic MRI after TARE is performed at 3-mo intervals even for the first examination, because imaging performed earlier may show exuberant arterial phase involving the treated lesion and the surrounding parenchyma with consequently difficult interpretation[29]. MRI imaging findings in TACE and TARE are not similar because of the different mechanisms of action: TARE induces modifications that evolve because of the impact of radiation on the liver parenchyma surrounding the lesion[28,30].

The expected Gd-EOB-DTPA imaging findings of TARE-treated HCC are persistent APHE or portal washout that can persist for at least one year, geographic peri-tumoral APHE, complete loss of APHE, thin rim of peripheral APHE, transitory growth in the size of the tumor due to edema, and cytostatic effect of radiation, a delay in tumor decreasing size. In TARE, in the immediate post-treatment setting, the penetration of beta particles in the surrounding liver parenchyma causing inflammation, edema, hemorrhage, leads to a heterogeneous enhancement, more accentuated than TACE. Even in this case, Gd-EOB-DTPA may show a related hypointensity on the HBP, an important element to be assessed since it can be misdiagnosed with an infiltrative disease. This finding may usually resolve after 6 mo, so in the early phase is very important to consider other sequences to make the differential diagnosis, especially T2w and DWI images. The changes in the lesion diameter should be characterized with

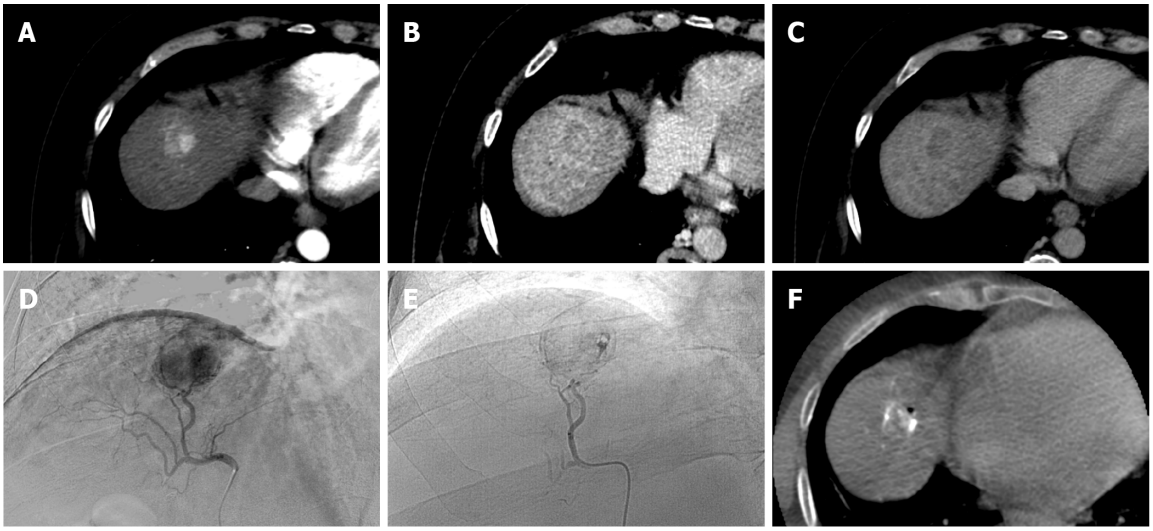

DOI: 10.3748/wjg.v28.i26.3116

Figure 4 A 62-yr-old male with typical hepatocellular carcinoma in segment IVa who underwent trans-arterial chemoembolization with microparticles (Lifepearl 100 +/- 25 microns) preloaded with 50 mg of Farmorubicin and later with non-loadable Hydropearl 400 +/- 75 microns microparticles. A: Pre-treatment computed tomography (CT) images: arterial phase; B: Pre-treatment CT images: portal phase; C: Pre-treatment CT images: delayed phase; D: Pre-trans-arterial chemoembolization (TACE) angiographic image; E: Post-TACE angiographic image; F: Post-TACE cone beam CT.

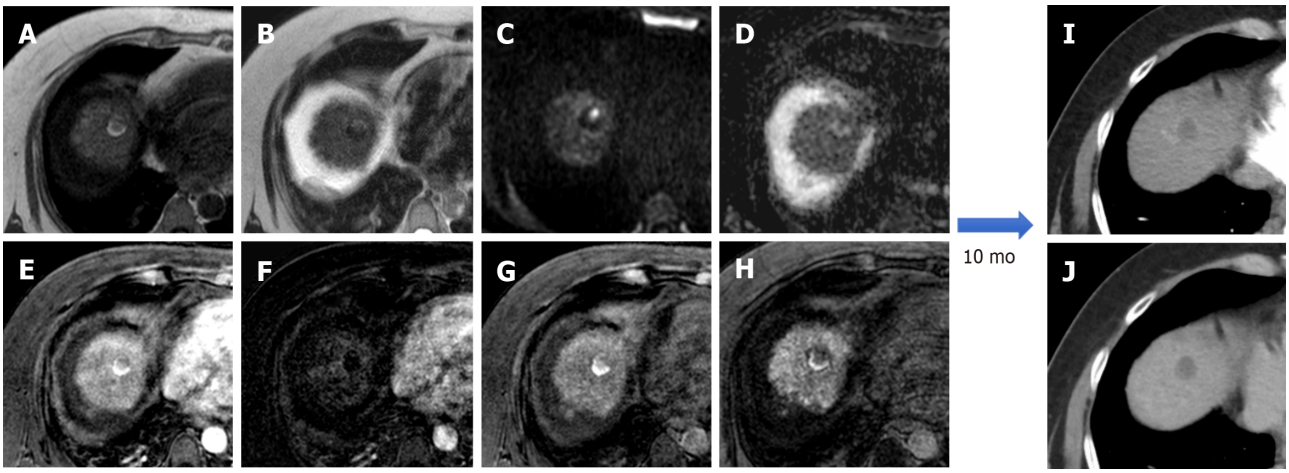

DOI: 10.3748/wjg.v28.i26.3116

Figure 5 Post-trans-arterial chemoembolization follow-up magnetic resonance imaging with hepatospecific contrast agent in the same patient described in Figure 4. A: In-phase T1-weighted image; B: T2-weighted image C: High b-value diffusion weighted imaging (DWI); D: Apparent diffusion coefficient map; E: Arterial phase magnetic resonance imaging (MRI); F: Arterial phase MRI with image subtraction technique; G: Portal venous phase MRI; H: Hepatobiliary phase MRI; I: Ten-month computed tomography (CT) follow-up: arterial phase; J: Ten-month CT follow-up: delayed phase. Liver MRI shows an inhomogeneously hyperintense nodule in T1WI in its right posterior portion, coexisting with a more hyperintense area in T2WI with high signal intensity in high b-value DWI in the left anterior portion. Dynamic study showed no arterial enhancement confirmed with the subtraction technique image, absence of vascularization in the portal phase and inhomogeneous hypointensity in the hepatobiliary phase. The findings are suggestive of good treatment outcome with presence of both coagulative and colliquative necrosis and no residual disease and CT scans control after 10 mo confirmed the outcome.

caution based on the persistent APHE and typical washout of the lesion after TARE. Viable tumor manifests itself with an increase in the size of the treated nodule with new or growing nodular enhancement within or beyond the margin of the post-radiation zone with hypointense signal on the HBP[28,30].

For both TARE and TACE techniques the use of Gd-EOB-DTPA implies knowledge of some technical concerns. An optimal arterial phase may be more difficult to obtain compared to extracellular-contrast agents because of acute transient severe motion artifacts affecting EOB-MRI. Several approaches have been applied to reduce motion artifacts: (1) Lowering thecontrast injection rate; (2) Using multiple arterial phasetechnique; (3) Shortening the scanning time; and (4) Using a modified breathing command, and dilutingcontrast medium[5,34]. Moreover, "washout" evaluation of the nodule has to be assessed in the portal phase because hypointensity during the TP could be related to true washout or

pseudo-washout resulting from the hyperintensity of the surrounding parenchyma[34]. Another element to be considered is the adequacy of the HBP, strictly linked to the assessment of the degree of contrast uptake in the liver parenchyma relative to the hepatic vessels and of the presence of contrast excretion into the biliary system. A signal intensity ratio of 1.8 between liver and vein, with the maximal enhancement of liver parenchyma and hypointensity of the veins, is the best predictor of the ideal phase. In a functional liver, this ideal condition is achieved at 15-20 min after contrast injection[35]. In this setting, the main limitation of Gd-EOB-DTPA is the necessity of a functional liver for an optimal HBP; the cirrhotic liver may have diminished or delayed parenchymal enhancement leading to failure of the mechanism of contrast uptake and excretion. Therefore, in a situation with deeply compromised liver function (Child-Pugh B-C) acquisition of delayed HBP beyond the 20 min is necessary.

At present, the treatment response algorithms used in the clinical practice, such as Modified Response Evaluation Criteria in Solid Tumors (mRECIST), European Association for the Study of the Liver Disease Criteria, and Liver Imaging and Reporting Data System Treatment Response Algorithm are enhancement-based classification systems that don't include transitional or HBP obtained by Gd-EOB-DTPA[28-30]. However, many authors have analyzed the contribution of EOB-MRI in follow-up after TACE and TARE with promising results. To the best of our knowledge the actual studies published in the literature, have analyzed the impact of Gd-EOB-DTPA in the follow-up of loco-regional therapy group (for example both ablation and TACE) without examination of the single procedure, therefore next considerations are almost effective for both TACE and TARE.

In a recent study, Kim *et al*[33] showed an increased sensitivity in the detection of viable tumor considering all ancillary features (HBP hypointensity, restricted diffusion, and intermediate signal on T2w) with growing sensitivity into the LI-RADS-TR viable category of 57%-87% *vs* 39%-65% without changing in specificity. Park *et al*[36] obtained similar results for TACE and ablation, with increased sensitivity of 84% *vs* 76%.

Kim *et al*[37] first, in a recent retrospective study, analyzed the impact of the incorporation of the individual ancillary feature instead of multiple ancillary features on the diagnostic performance of the LI-RADS-TR for viable tumor. They found that hypointense signal during the transition and/or HBP can improve the sensitivity than contrast dynamic assessment alone.

Conversely, Rimola *et al*[18] show a small contribution of HBP in the evaluation of tumor response after loco-regional therapy, with greater accuracy, sensitivity, and inter-reader agreement using extracellular agents in comparison with Gd-EOB-DTPA[37]. These results may depend on better conspicuity of the APHE with extracellular agents and to the misdiagnosis of viable tumor for hypointense areas on the HBP related to damaged liver parenchyma, an avoidable mistake considering additional sequences[18,30].

Another important fact is that EOB-MRI in follow-up after TACE and TARE significantly contributes not only to determination of viable tumors on the treated cavity but also for detection of new HCC lesions, that may be disguised by the post-treatment changes of the surrounding hepatic parenchyma [30].

The use of EOB-MRI after TACE and TARE is widespread in the clinical practice and its contribution with transitional and HBP to identify the viable tumor, necrotic cavity, damaged liver tissue, and new HCC has been shown in the literature, although it still has not been included in treatment response algorithms.

Figure 6 depicts the pre-treatment liver MRI and preoperative planning for TARE of a patient with voluminous infiltrating HCC. Figure 7 illustrates the outcome of treatment.

STEREOTACTIC ABLATIVE RADIOTHERAPY

Recent improvements in image guidance and conformal radiation techniques have made it possible to administer high doses of radiation to liver tumors with minimal damage to adjacent parenchymal tissue [38]. Although SBRT is not part of the current BCLC system, it is included as a treatment option in the most recent version of the National Comprehensive Cancer Network (NCCN) for primary liver cancer for unresectable disease or medically inoperable patients[38,39].

Indications for SBRT are applicable in the following cases: (1) Early-stage HCC, not eligible for surgical resection, liver transplantation, or local ablation; (2) Intermediate or advance stage HCC not eligible or not responsive to TACE; (3) Palliative purpose for symptomatic end-stage HCC; and (4) Bridging or downstaging therapy for liver transplantation in patients not eligible for other locoregional therapies[40].

Factors that generally hinder percutaneous ablative therapies, such as proximity of the tumor to vascular structures, bile ducts or the diaphragmatic surface are not contraindication to treatment[41]. SBRT is most appropriate in patients with cirrhotic disease in Child-Pugh class A. Treatment is available for patients up to Child-Pugh B7, for whom close clinical monitoring and dose reduction are recommended due to the increased risk of radiation-induced liver disease (RILD). From a technical point of view, the number of target lesions, together with their intraparenchymal location, are potential limitations during treatment planning and dose delivery.

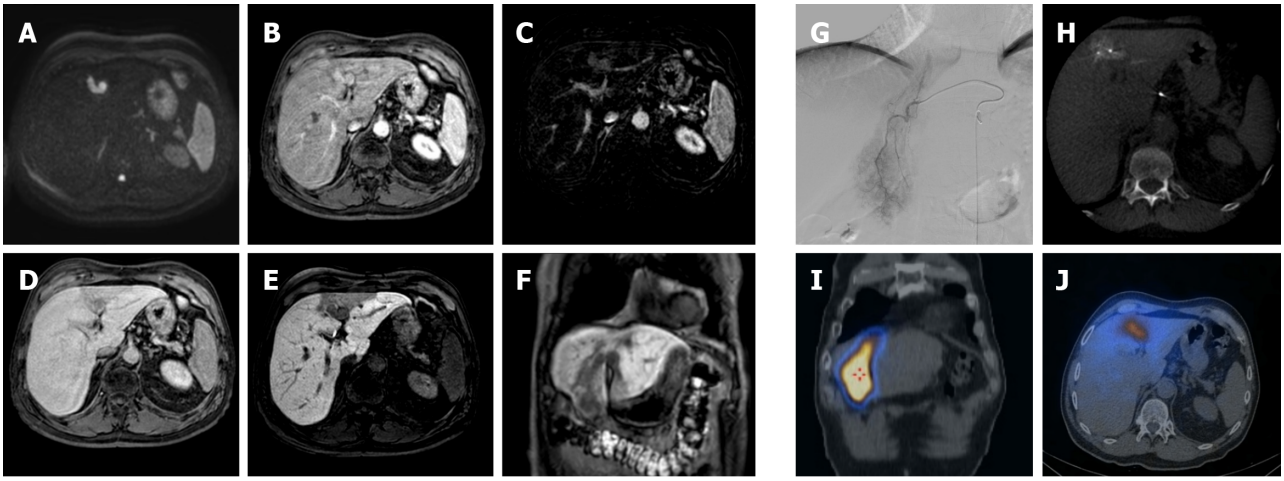

DOI: 10.3748/wjg.v28.i26.3116

Figure 6 A 62-yr-old patient with infiltrative hepatocellular carcinoma with associated neoplastic portal vein thrombosis. A: High-b-value diffusion-weighted image; B: Arterial phase magnetic resonance imaging (MRI); C: Arterial phase MRI with image subtraction technique; D: Portal venous phase MRI; E and F: Hepatobiliary phase MRI; G: Pre-treatment arteriography; H: Pre-treatment cone beam computed tomography (CT); I and J: Post trans-arterial radio-embolization single photon emission computed tomography (SPECT) images. Left panel shows pre-treatment liver MRI, illustrating the cranial portion of the lesion with portal branch infiltration; whereas the right panel shows pre-treatment arteriography, the cone beam CT of the cranial portion of the lesion with the portal vein infiltration, and preoperative planning with SPECT images post administration of Tc-99m-labeled albumin macroaggregates with hyperfixation at both lesion site and portal thrombosis.

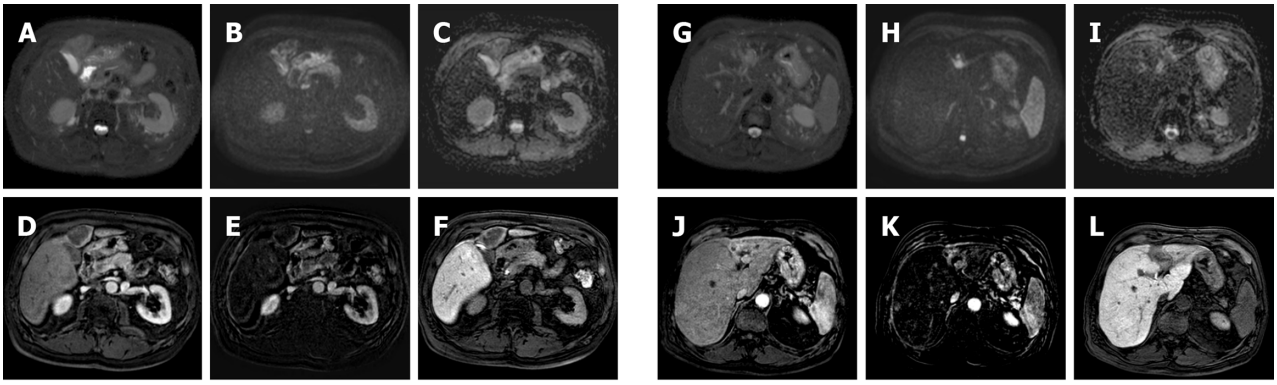

DOI: 10.3748/wjg.v28.i26.3116

Figure 7 Post-trans-arterial radio-embolization images in the patient mentioned in Figure 6. A: T2-spectral attenuated inversion recovery; B: High b-value diffusion weighted imaging; C: Apparent diffusion coefficient (ADC) map; D: Arterial phase magnetic resonance imaging (MRI); E: Arterial phase MRI with image subtraction technique; F: Hepatobiliary phase (HBP) MRI; G: T2-spectral attenuated inversion recovery; H: High b-value diffusion weighted imaging; I: ADC map; J: Arterial phase MRI; K: Arterial phase MRI with image subtraction technique; L: HBP MRI. The liver MRIs reveal almost no signal restriction in DWI and no enhancement in dynamic study in the caudal portion of the lesion (left panel) which are suggestive of a good outcome. Whereas in the cranial infiltrating part of the lesion (right panel) at portal branch level, the high signal in DWI with arterial enhancement is suspected for residual disease.

Ionizing radiations directly impairs the DNA replication process by causing breaks and thus preventing cancer cells from replicating, most powerfully on tissues with a high cell turnover. After radiotherapy, centrilobular hepatocytes die by a hypoxic process secondary to vascular congestion, which does not recover until several months later[42]. Furthermore, proinflammatory mechanisms will be set on the treated region. These histological changes initially lead to an acute reduction in cellular vascular supply, with peripheral hypervascularization induced by the proinflammatory mechanisms, while over time, fibrosis leads to a reduction of tumor size and vascular supply[43]. Damage also occurs in the surrounding liver parenchyma with the evolution of the chronic inflammatory context, characterized initially by edema and subsequently by fibrosis, leading to capsular retraction[42].

Acute, subacute and chronic stages can be distinguished by assessing the evolution of histological changes. In the acute stage (1-3 mo) typical peripheral hyperarterialization, defined as a ring-like enhancement during the arterial and portal venous phases, can be observed. In the subacute stage (3-6 mo), the involved parenchyma shows relative hypointensity before and after contrast media injection especially on the portal-venous phase, with progressive enhancement in the late phases, concerning the occlusion of the centrilobular veins and to the reduced clearance of intravenous contrast. In the chronic

stage (> 6 mo), imaging will reveal changes caused by radio-induced fibrosis. The subcapsular location of the target lesions also correlates with the progressive occurrence of capsular retraction. This reaction typically appears as a band-like finding, a typical appearance that can help the differential diagnosis with residual or recurrent tumor[44]. Finally, the classic RILD generally occurs within 4 mo of total or subtotal hepatic irradiation, and manifests with hepatomegaly, ascites, and increased alkaline phosphatase levels, without a radiological intrahepatic progression disease. Nowadays, this complication is effectively prevented by sparing a sufficient portion of the parenchyma during therapy.

Patients with pre-existing chronic liver disease undergoing this type of treatment tend to experience a different spectrum of toxicity than with classic RILD, including a general decline in liver function, a marked increase in transaminases or jaundice within 3 mo of the end of therapy, collectively referred as "non-classic" RILD[44].

The radiological findings of SBRT treated lesions differ from the imaging of other locoregional therapies. Indeed, while the latter results in immediate tumor devascularization, SBRT leads to gradual histological changes in the lesion and surrounding parenchyma over time, which may lead to the incorrect assumption of a lack of efficacy.

As previously mentioned, different algorithms are employed to determine the response evaluation, such as mRECIST, applied to CT and MRI[45]. The intensity of arterial enhancement may appear quite early (15-45 d after SBRT) and may persist over time. Therefore, lesions dimensionally stable over time with a reduced arterial hypervascularization should be considered as a responder. The decrease in size occurs more slowly, over 22-24 mo, due to progressive necrosis up to 12 mo after treatment, which results in a slower evolution of structural changes.

In post-SBRT MRI examinations it is common to find a hyperintense perilesional halo on T2w due to the inflammatory reaction and venous congestion induced by veno-occlusive disease or, in subsequent follow-ups, a slight signal hyperintensity on T2w in the whole irradiated field, a direct sign of parenchymal fibrosis. Moreover, the application of DWI sequences can provide information on tissue cellularity and the integrity of cell membranes. In fact, during the early phase after treatment, hepatic edema occurs due to decreased venous outflow secondary to centrilobular obstruction, and there may be mild restricted diffusion and a slight increase in apparent diffusion coefficient (ADC).

Finally, tumor response after SBRT can be challenging, as described above: tumor shrinkage may not happen in the immediate months after SBRT. Even in the absence of volumetric reduction, progressive reduction in tumor enhancement is consistent with treatment response. This is typically accompanied by a corresponding increase in ADC. An increment in ADC of 20%-25% was found to be an indicator of SBRT response in a few small retrospective studies[46,47]. Thus, in stereotactic radiotherapy, a statistically significant increase in ADC values measured in HCC undergoing radiofrequency was found to be the most important independent factor in recurrence and survival rates.

The use of hepatobiliary contrast agents allows the assessment of both lesion and the adjacent hepatocytes: The presence of a hypointense nodular lesion during HBP nearby an SBRT-treated HCC may signify either the presence of neoplastic cells or a scar. The picture is further complicated by the manifestation in such sequences of the focal hepatic reaction induced by radiotherapy. This alteration can be demarcated as a band-like area of signal hypointensity, such as hyperintensity on T2w, related to altered hepatocyte function in the irradiated field[48].

Figure 8 depicts the radiotherapy treatment plan; Figure 9 shows the SBRT treatment outcomes; Figure 10 depicts the treated zone's evolution; and Figure 11 illustrates the outcome 20 mo after treatment.

LIVER MRI ACCURACY AND LIMITATIONS

Although MRI is notably known as a highly sensitive and accurate imaging technique in detection and characterization of focal liver lesions, there is still no consensus regarding the best imaging follow-up modality for patients affected with HCC after locoregional treatments. Moreover, to date, only few studies have conducted a comparison among imaging techniques after locoregional treatments, and this raises the scientific interest in further investigations.

Kubota *et al*[49], by evaluating 84 HCCs underwent TACE treatment, showed the superiority of MRI to CT for early detection of lesion. Authors reported 76.0% sensitivity, 67.6% specificity and 72.6% accuracy for lipiodol-CT in comparison to 100% sensitivity, specificity and accuracy for dynamic MRI. Moreover, DWI and ADC values can help identify the early HCC recurrence: the presence of pathological tissues results in a higher signal intensity on DWI relative to normal liver parenchyma and a low signal on ADC maps, differentiating it from treated lesion (necrotic/edematous area) which manifests as high ADC values[50]. In these settings, the use of Gd-EOB-DTPA can maintain the highest diagnostic values, as mentioned above.

MRI was demonstrated to be useful also prior to treatment, especially by evaluating the HBP. Kim *et al*[16] found that HBP hypointense nodules without APHE are risk factors for intrahepatic distant recurrence in HCC patients treated with RFA or hepatectomy in a meta-analysis of 842 patients. In patients with HCC who have these nodules on pretreatment gadoxetic acid-enhanced MRI, stratification

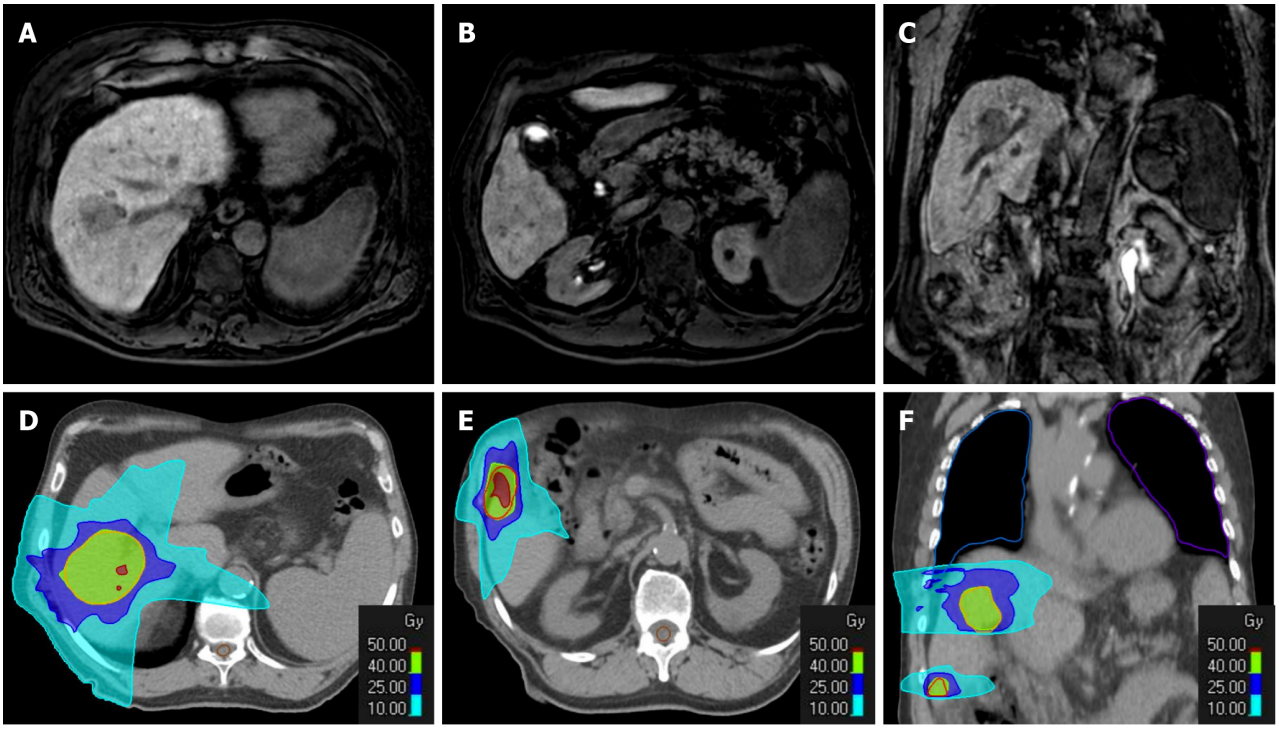

DOI: 10.3748/wjg.v28.i26.3116

Figure 8 Radiotherapy treatment planning of a 70-yr-old male patient with two hypovascular hepatocellular carcinomas in segment VIII (4.3 cm) and segment VI (1.3 cm). A-C: Hepatobiliary phase magnetic resonance imaging (MRI); D-F: Computed tomography (CT) simulation for radiation therapy planning. In the upper panel from A to C are reported hepatobiliary phase MRI images prior to stereotactic ablative radiotherapy treatment. In the bottom panel from D to F are reported CT images from radiotherapy treatment plan with isodose curve distributions.

of patient management in terms of performing additional tests or treatment for these nodules, as well as modification of proper follow-up strategies, may be required.

Considering the therapeutic response to RFA, literature may not be much of a help since the two most important studies in this field were published in the early 2000s[51]. Both studies reported that MRI may have an edge over CT in the early detection of local regrowth in particular after 4 mo of treatment [51]. This aspect should be carefully considered according to readers' experience, MR image quality, and the scattered use of hepatobiliary contrast agents, which was not widely used 20 years ago.

Regarding therapeutic response to TACE, it is important to underline that beam hardening artifacts can lead to the underestimation of hyperenhancement during the CT arterial phase and thus reducing the sensitivity and accuracy dramatically[49,52]. On the other hand, the wider use of DEB-TACE can partially solve this issue due to the lack of beam hardening artifacts[53]. The abovementioned issues can be partially left out when using MR to detect recurrence. On the other hand, the use of dual-energy CT can help increase diagnostic accuracy, even if not widely available[54]. CT and MR diagnostic accuracy can be considered completely superimposable after TARE[26], although the added value of HBP imaging was not deeply evaluated.

In the recent years, perfusion techniques, both with CT and MR, were used to diagnose HCC and determine different treatment responses, especially after medical therapy: in this setting CT perfusion can be considered a reliable tool in the early detection of recurrence, as reported by Choi *et al*[55]. More recently the effectiveness of CT perfusion was evaluated by Ruff *et al*[56], demonstrating that residual tumor perfusion parameters are linked to HCC recurrence. However, both CT and MR perfusion imaging need an extra time, added costs and are not widely available to be considered convenient tool in daily clinical practice[57].

In the recent years, radiomics models based especially on texture analysis are showing promising results[58]. Zhang *et al*[59], by enrolling 132 patients who underwent locoregional therapies, demonstrated that radiomic features extracted from Gd-EOB-DTPA MR imaging associated with clinical data can predict the early tumor recurrence. Even if pioneering, radiomics analyses should be carefully evaluated, especially due to different types of software and MR techniques used which vary between centers. However, further studies should focus on these aspects to validate its potential values[60].

Overall, it is important to underline the presence of artifacts during MR acquisition, especially in the arterial phase when using Gd-EOB-DTPA studies. As previously reported and demonstrated[61], flow rate and acquisition protocol[5] can lead to the degradation of the arterial phase and should be carefully managed to avoid the leak of important data, linked to the risk of early recurrence.

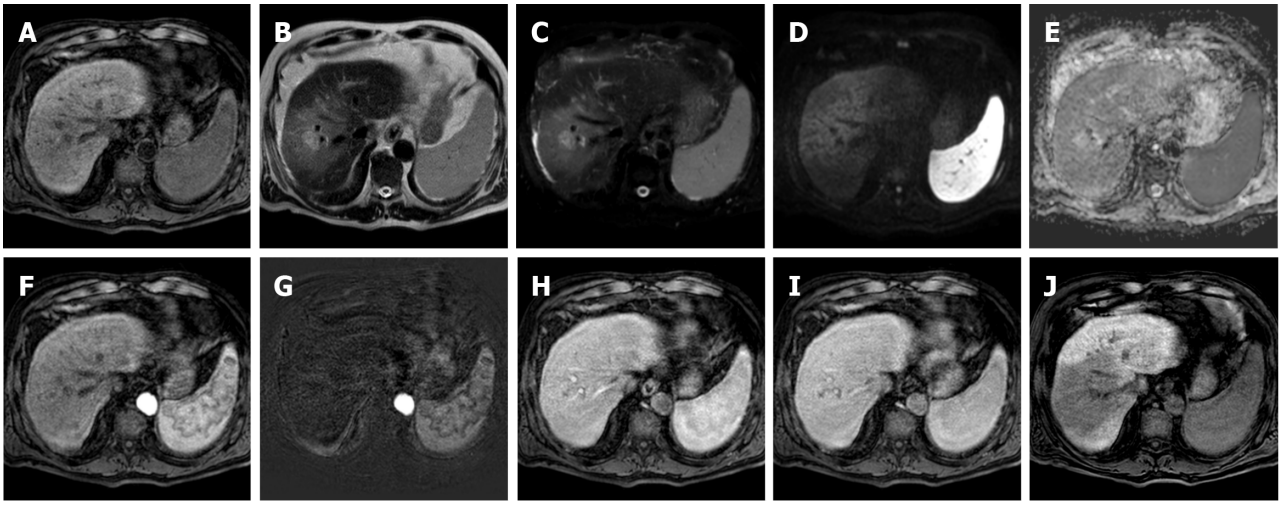

DOI: 10.3748/wjg.v28.i26.3116

Figure 9 Four-months follow-up post stereotactic body radiation therapy liver magnetic resonance imaging of the hepatocellular carcinoma in segment VIII shown in the Figure 8. A: Non contrast T1-weighted high resolution isotropic volume examination; B: T2-weighted image; C: T2-spectral attenuated inversion recovery; D: High b-value diffusion weighted imaging (DWI); E: Apparent diffusion coefficient (ADC) map; F: Arterial phase magnetic resonance imaging (MRI); G: Arterial phase MRI with image subtraction technique; H: Portal venous phase MRI; I: Delayed phase MRI; J: Hepatobiliary phase MRI. The liver MRI shows an ill-defined area of signal hypointensity in T1 in the treatment zone with a blurred and inhomogeneous signal hyperintensity with evidence of increased signal hyperintensity in the residual nodule. A shaded signal hyperintensity on DWI without signal hyperintensity of the previous lesion, with higher ADC values relative to the surrounding liver parenchyma. No areas of enhancement are shown, and a coarse hypointense signal in the hepatobiliary phase due to the initial fibrotic evolution of the treated zone is evident.

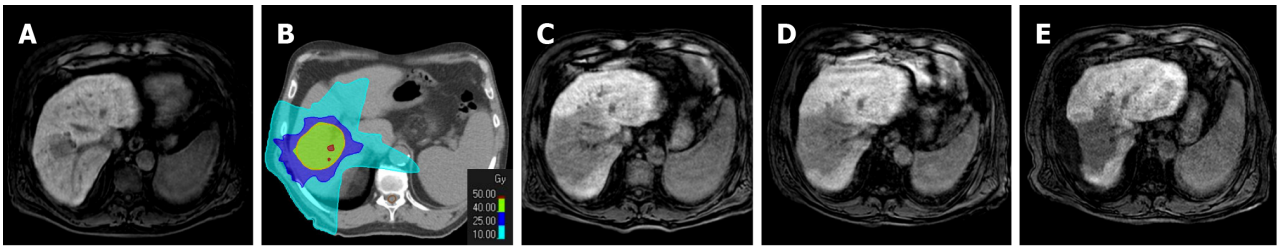

DOI: 10.3748/wjg.v28.i26.3116

Figure 10 The evolution of the hepatocellular carcinoma stereotactic body radiation therapy treatment zone in patient shown in Figures 8 and 9. A: Hepatobiliary phase (HBP) magnetic resonance imaging (MRI) prior to stereotactic body radiation therapy (SBRT); B: SBRT plan with isodose curve distributions; C: HBP MRI 4 mo after treatment; D: HBP MRI 8 mo after treatment; E: HBP MRI 20 mo after treatment. The MRIs demonstrated the progressive fibrotic evolution of the treatment area.

Finally, the use of CT or MRI is strictly linked to each institution's flow charts: it is important to underline the low CT associated costs, the need for less patient cooperation, and its usefulness when ascites is present[62]. Also in these settings, a direct comparison with MR with HBP imaging is lacking and further studies are needed to validate the abovementioned data.

CONCLUSION

Locoregional therapy is critical in the treatment of patients with HCC. The accurate evaluation of tumor response using imaging modalities is essential for optimal management. Gadoxetic acid-enhanced liver MRI is an important radiological tool in these patients because it allows for optimal non-invasive tissue characterization using a multiparametric approach. For HCC patients to get proper therapeutic management, radiologists must know the usual post-treatment imaging findings associated with locoregional therapy, as well as a thorough comparison of imaging before and after therapy. Overall, gadoxetic acid-enhanced liver MRI is a critical modality in the assessment of results following locoregional HCC therapy, having a significant impact on patient management.

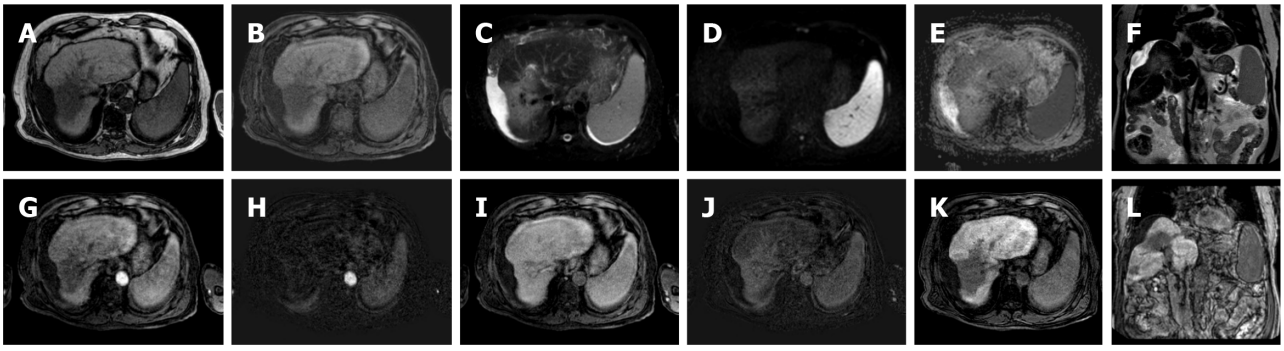

DOI: 10.3748/wjg.v28.i26.3116

Figure 11 Follow-up liver magnetic resonance imaging of abovementioned patient (Figures 8-10), 20 mo after stereotactic body radiation therapy. A: Out-phase T1-weighted image; B: Non contrast T1-weighted high resolution isotropic volume examination; C: T2-spectral attenuated inversion recovery; D: High b-value diffusion weighted imaging; E: Apparent diffusion coefficient map; F: T2-weighted image; G: Arterial phase magnetic resonance imaging (MRI); H: Arterial phase MRI with image subtraction technique; I: Portal venous phase MRI; J: Portal venous phase MRI with image subtraction technique; K and L: Hepatobiliary phase MRI. MRI revealed parenchymal retraction with signal hypointensity on T1-weighted images corresponding to inhomogeneous hyperintensity in axial and coronal T2 sequences, with no significant increase in diffusion signal. Dynamic perfusion study after contrast medium administration: no enhancement in arterial phase and a progressive enhancement in delayed phase with corresponding hypointense signal in the hepatobiliary excretion phase testifying the fibrotic evolution of the treated liver and the absence of locoregional recurrence.

FOOTNOTES

Author contributions: Gatti M was involved in conception and design of the study; Gatti M, Maino C, Serafini A and Tricarico E were involved in literature review, analysis and writing of the original draft; Darvizeh F was involved in writing of the original draft; Guarneri A, Inchingolo R, Ippolito D, Ricardi U and Fonio P took part in supervision of the study; Faletti R took part in supervision of the study and is the guarantor of the study; all the authors worked together to editing, reviewing and final approval of article.

Conflict-of-interest statement: All the authors report no relevant conflicts of interest for this article.

Country/Territory of origin: Italy

ORCID number: Marco Gatti 0000-0001-8168-5280; Cesare Maino 0000-0002-5742-802X; Fatemeh Darvizeh 0000-0002-3735-0472; Alessandro Serafini 0000-0002-4992-4824; Eleonora Tricarico 0000-0001-9805-2551; Alessia Guarneri 0000-0003-1711-3645; Riccardo Inchingolo 0000-0002-0253-5936; Davide Ippolito 0000-0002-2696-7047; Umberto Ricardi 0000-0003-4406-7621; Paolo Fonio 0000-0002-1106-2990; Riccardo Faletti 0000-0002-8865-8637.

S-Editor: Gao CC
L-Editor: A
P-Editor: Chen YX

REFERENCES

1 **Yang J**, Pan G, Guan L, Liu Z, Wu Y, Lu W, Li S, Xu H, Ouyang G. The burden of primary liver cancer caused by specific etiologies from 1990 to 2019 at the global, regional, and national levels. *Cancer Med* 2022; **11**: 1357-1370 [PMID: 34989144 DOI: 10.1002/cam4.4530]

2 **Vogel A**, Cervantes A, Chau I, Daniele B, Llovet JM, Meyer T, Nault JC, Neumann U, Ricke J, Sangro B, Schirmacher P, Verslype C, Zech CJ, Arnold D, Martinelli E; ESMO Guidelines Committee. Hepatocellular carcinoma: ESMO Clinical Practice Guidelines for diagnosis, treatment and follow-up. *Ann Oncol* 2018; **29**: iv238-iv255 [PMID: 30285213 DOI: 10.1093/annonc/mdy308]

3 **Ippolito D**, Inchingolo R, Grazioli L, Drago SG, Nardella M, Gatti M, Faletti R. Recent advances in non-invasive magnetic resonance imaging assessment of hepatocellular carcinoma. *World J Gastroenterol* 2018; **24**: 2413-2426 [PMID: 29930464 DOI: 10.3748/wjg.v24.i23.2413]

4 **Inchingolo R**, Faletti R, Grazioli L, Tricarico E, Gatti M, Pecorelli A, Ippolito D. MR with Gd-EOB-DTPA in assessment of liver nodules in cirrhotic patients. *World J Hepatol* 2018; **10**: 462-473 [PMID: 30079132 DOI: 10.4254/wjh.v10.i7.462]

5 **Grazioli L**, Faletti R, Frittoli B, Battisti G, Ambrosini R, Romanini L, Gatti M, Fonio P. Evaluation of incidence of acute

transient dyspnea and related artifacts after administration of gadoxetate disodium: a prospective observational study. *Radiol Med* 2018; **123**: 910-917 [PMID: 30084108 DOI: 10.1007/s11547-018-0927-y]

6 **Gatti M**, Calandri M, Bergamasco L, Darvizeh F, Grazioli L, Inchingolo R, Ippolito D, Rousset S, Veltri A, Fonio P, Faletti R. Characterization of the arterial enhancement pattern of focal liver lesions by multiple arterial phase magnetic resonance imaging: comparison between hepatocellular carcinoma and focal nodular hyperplasia. *Radiol Med* 2020; **125**: 348-355 [PMID: 31916102 DOI: 10.1007/s11547-019-01127-4]

7 **Inchingolo R**, Maino C, Gatti M, Tricarico E, Nardella M, Grazioli L, Sironi S, Ippolito D, Faletti R. Gadoxetic acid magnetic-enhanced resonance imaging in the diagnosis of cholangiocarcinoma. *World J Gastroenterol* 2020; **26**: 4261-4271 [PMID: 32848332 DOI: 10.3748/wjg.v26.i29.4261]

8 **Granata V**, Grassi R, Fusco R, Belli A, Cutolo C, Pradella S, Grazzini G, La Porta M, Brunese MC, De Muzio F, Ottaiano A, Avallone A, Izzo F, Petrillo A. Diagnostic evaluation and ablation treatments assessment in hepatocellular carcinoma. *Infect Agent Cancer* 2021; **16**: 53 [PMID: 34281580 DOI: 10.1186/s13027-021-00393-0]

9 **Yinzhong W**, Xiaoxue T, Jinhui T, Pengcheng Y, Xiaoying L, Junqiang L. Is Gadoxetic Acid Disodium (Gd-EOB-DTPA)-Enhanced Magnetic Resonance Imaging an Accurate Diagnostic Method for Hepatocellular Carcinoma? *Curr Med Imaging* 2022; **18**: 633-647 [PMID: 34533447 DOI: 10.2174/1573405617666210917124404]

10 **Makary MS**, Khandpur U, Cloyd JM, Mumtaz K, Dowell JD. Locoregional Therapy Approaches for Hepatocellular Carcinoma: Recent Advances and Management Strategies. *Cancers (Basel)* 2020; **12** [PMID: 32679897 DOI: 10.3390/cancers12071914]

11 **Minami Y**, Nishida N, Kudo M. Therapeutic response assessment of RFA for HCC: contrast-enhanced US, CT and MRI. *World J Gastroenterol* 2014; **20**: 4160-4166 [PMID: 24764654 DOI: 10.3748/wjg.v20.i15.4160]

12 **Mikami S**, Tateishi R, Akahane M, Asaoka Y, Kondo Y, Goto T, Shiina S, Yoshida H, Koike K. Computed tomography follow-up for the detection of hepatocellular carcinoma recurrence after initial radiofrequency ablation: a single-center experience. *J Vasc Interv Radiol* 2012; **23**: 1269-1275 [PMID: 22999746 DOI: 10.1016/j.jvir.2012.06.032]

13 **Yoon JH**, Lee EJ, Cha SS, Han SS, Choi SJ, Juhn JR, Kim MH, Lee YJ, Park SJ. Comparison of gadoxetic acid-enhanced MR imaging *vs* four-phase multi-detector row computed tomography in assessing tumor regression after radiofrequency ablation in subjects with hepatocellular carcinomas. *J Vasc Interv Radiol* 2010; **21**: 348-356 [PMID: 20116285 DOI: 10.1016/j.jvir.2009.11.014]

14 **Yoo SH**, Choi JY, Jang JW, Bae SH, Yoon SK, Kim DG, Yoo YK, Rha SE, Lee YJ, Jung ES. Gd-EOB-DTPA-enhanced MRI is better than MDCT in decision making of curative treatment for hepatocellular carcinoma. *Ann Surg Oncol* 2013; **20**: 2893-2900 [PMID: 23649931 DOI: 10.1245/s10434-013-3001-y]

15 **Imai Y**, Katayama K, Hori M, Yakushijin T, Fujimoto K, Itoh T, Igura T, Sakakibara M, Takamura M, Tsurusaki M, Takahashi H, Nakanishi K, Usuki N, Tsuji K, Ohashi H, Kim T, Takehara T, Murakami T. Prospective Comparison of Gd-EOB-DTPA-Enhanced MRI with Dynamic CT for Detecting Recurrence of HCC after Radiofrequency Ablation. *Liver Cancer* 2017; **6**: 349-359 [PMID: 29234638 DOI: 10.1159/000481416]

16 **Kim TH**, Woo S, Han S, Suh CH, Lee DH, Lee JM. Hepatobiliary phase hypointense nodule without arterial phase hyperenhancement: are they at risk of HCC recurrence after ablation or surgery? *Eur Radiol* 2020; **30**: 1624-1633 [PMID: 31776747 DOI: 10.1007/s00330-019-06499-9]

17 **Bae JS**, Kim JH, Lee DH, Han JK. Hepatobiliary phase of gadoxetic acid-enhanced MRI in patients with HCC: prognostic features before resection, ablation, or TACE. *Eur Radiol* 2021; **31**: 3627-3637 [PMID: 33211146 DOI: 10.1007/s00330-020-07499-w]

18 **Rimola J**, Davenport MS, Liu PS, Brown T, Marrero JA, McKenna BJ, Hussain HK. Diagnostic accuracy of MRI with extracellular vs. hepatobiliary contrast material for detection of residual hepatocellular carcinoma after locoregional treatment. *Abdom Radiol (NY)* 2019; **44**: 549-558 [PMID: 30218239 DOI: 10.1007/s00261-018-1775-x]

19 **Koda M**, Tokunaga S, Okamoto T, Hodozuka M, Miyoshi K, Kishina M, Fujise Y, Kato J, Matono T, Sugihara T, Oyama K, Hosho K, Okano J, Murawaki Y, Kakite S, Yamashita E. Clinical usefulness of the ablative margin assessed by magnetic resonance imaging with Gd-EOB-DTPA for radiofrequency ablation of hepatocellular carcinoma. *J Hepatol* 2015; **63**: 1360-1367 [PMID: 26232269 DOI: 10.1016/j.jhep.2015.07.023]

20 **Vogl TJ**, Nour-Eldin NA, Hammerstingl RM, Panahi B, Naguib NNN. Microwave Ablation (MWA): Basics, Technique and Results in Primary and Metastatic Liver Neoplasms - Review Article. *Rofo* 2017; **189**: 1055-1066 [PMID: 28834968 DOI: 10.1055/s-0043-117410]

21 **Bouda D**, Lagadec M, Alba CG, Barrau V, Dioguardi Burgio M, Moussa N, Vilgrain V, Ronot M. Imaging review of hepatocellular carcinoma after thermal ablation: The good, the bad, and the ugly. *J Magn Reson Imaging* 2016; **44**: 1070-1090 [PMID: 27505619 DOI: 10.1002/jmri.25369]

22 **Song KD**. Percutaneous cryoablation for hepatocellular carcinoma. *Clin Mol Hepatol* 2016; **22**: 509-515 [PMID: 28081593 DOI: 10.3350/cmh.2016.0079]

23 **Luo W**, Zhang Y, He G, Yu M, Zheng M, Liu L, Zhou X. Effects of radiofrequency ablation *vs* other ablating techniques on hepatocellular carcinomas: a systematic review and meta-analysis. *World J Surg Oncol* 2017; **15**: 126 [PMID: 28693505 DOI: 10.1186/s12957-017-1196-2]

24 **Ratanaprasatporn L**, Sainani N, Duda JB, Aghayev A, Tatli S, Silverman SG, Shyn PB. Imaging findings during and after percutaneous cryoablation of hepatic tumors. *Abdom Radiol (NY)* 2019; **44**: 2602-2626 [PMID: 31004203 DOI: 10.1007/s00261-019-01999-0]

25 **Couri T**, Pillai A. Goals and targets for personalized therapy for HCC. *Hepatol Int* 2019; **13**: 125-137 [PMID: 30600478 DOI: 10.1007/s12072-018-9919-1]

26 **Young S**, Taylor AJ, Sanghvi T. Post Locoregional Therapy Treatment Imaging in Hepatocellular Carcinoma Patients: A Literature-based Review. *J Clin Transl Hepatol* 2018; **6**: 189-197 [PMID: 29951364 DOI: 10.14218/JCTH.2017.00059]

27 **Patidar Y**, Basavaraj 1, Mukund A, Sarin SK. Transarterial Chemoembolization in Unresectable Hepatocellular Carcinoma with Portal Vein Tumor Thrombosis: A Tertiary Care Center Experience. *Indian J Radiol Imaging* 2021; **31**: 270-276 [PMID: 34556907 DOI: 10.1055/s-0041-1734367]

28 **Mendiratta-Lala M**, Masch WR, Shampain K, Zhang A, Jo AS, Moorman S, Aslam A, Maturen KE, Davenport MS. MRI

Assessment of Hepatocellular Carcinoma after Local-Regional Therapy: A Comprehensive Review. *Radiol Imaging Cancer* 2020; **2**: e190024 [PMID: 33778692 DOI: 10.1148/rycan.2020190024]

29 **American College of Radiology**. CT/MRI LI-RADS v2018. [cited 15 February 2022]. In: American College of Radiology [Internet]. Available from: https://www.acr.org/Clinical-Resources/Reporting-and-Data-Systems/LI-RADS/CT-MRI-LI-RADS-v2018

30 **Aslam A**, Kamath A, Spieler B, Maschiocchi M, Sabottke CF, Chernyak V, Lewis SC. Assessing locoregional treatment response to Hepatocellular Carcinoma: comparison of hepatobiliary contrast agents to extracellular contrast agents. *Abdom Radiol (NY)* 2021; **46**: 3565-3578 [PMID: 33856509 DOI: 10.1007/s00261-021-03076-x]

31 **Yaghmai V**, Besa C, Kim E, Gatlin JL, Siddiqui NA, Taouli B. Imaging assessment of hepatocellular carcinoma response to locoregional and systemic therapy. *AJR Am J Roentgenol* 2013; **201**: 80-96 [PMID: 23789661 DOI: 10.2214/AJR.13.10706]

32 **Motosugi U**, Ichikawa T, Sou H, Sano K, Tominaga L, Muhi A, Araki T. Distinguishing hypervascular pseudolesions of the liver from hypervascular hepatocellular carcinomas with gadoxetic acid-enhanced MR imaging. *Radiology* 2010; **256**: 151-158 [PMID: 20574092 DOI: 10.1148/radiol.10091885]

33 **Kim SW**, Joo I, Kim HC, Ahn SJ, Kang HJ, Jeon SK, Lee JM. LI-RADS treatment response categorization on gadoxetic acid-enhanced MRI: diagnostic performance compared to mRECIST and added value of ancillary features. *Eur Radiol* 2020; **30**: 2861-2870 [PMID: 32006170 DOI: 10.1007/s00330-019-06623-9]

34 **Chernyak V**, Fowler KJ, Heiken JP, Sirlin CB. Use of gadoxetate disodium in patients with chronic liver disease and its implications for liver imaging reporting and data system (LI-RADS). *J Magn Reson Imaging* 2019; **49**: 1236-1252 [PMID: 30609194 DOI: 10.1002/jmri.26540]

35 **Bashir MR**, Breault SR, Braun R, Do RK, Nelson RC, Reeder SB. Optimal timing and diagnostic adequacy of hepatocyte phase imaging with gadoxetate-enhanced liver MRI. *Acad Radiol* 2014; **21**: 726-732 [PMID: 24717550 DOI: 10.1016/j.acra.2014.02.005]

36 **Park S**, Joo I, Lee DH, Bae JS, Yoo J, Kim SW, Lee JM. Diagnostic Performance of LI-RADS Treatment Response Algorithm for Hepatocellular Carcinoma: Adding Ancillary Features to MRI Compared with Enhancement Patterns at CT and MRI. *Radiology* 2020; **296**: 554-561 [PMID: 32692297 DOI: 10.1148/radiol.2020192797]

37 **Kim YY**, Kim MJ, Yoon JK, Shin J, Roh YH. Incorporation of Ancillary MRI Features Into the LI-RADS Treatment Response Algorithm: Impact on Diagnostic Performance After Locoregional Treatment of Hepatocellular Carcinoma. *AJR Am J Roentgenol* 2022; **218**: 484-493 [PMID: 34585608 DOI: 10.2214/AJR.21.26677]

38 **Schaub SK**, Hartvigson PE, Lock MI, Høyer M, Brunner TB, Cardenes HR, Dawson LA, Kim EY, Mayr NA, Lo SS, Apisarnthanarax S. Stereotactic Body Radiation Therapy for Hepatocellular Carcinoma: Current Trends and Controversies. *Technol Cancer Res Treat* 2018; **17**: 1533033818790217 [PMID: 30068240 DOI: 10.1177/1533033818790217]

39 **Benson AB 3rd**, D'Angelica MI, Abbott DE, Abrams TA, Alberts SR, Saenz DA, Are C, Brown DB, Chang DT, Covey AM, Hawkins W, Iyer R, Jacob R, Karachristos A, Kelley RK, Kim R, Palta M, Park JO, Sahai V, Schefter T, Schmidt C, Sicklick JK, Singh G, Sohal D, Stein S, Tian GG, Vauthey JN, Venook AP, Zhu AX, Hoffmann KG, Darlow S. NCCN Guidelines Insights: Hepatobiliary Cancers, Version 1.2017. *J Natl Compr Canc Netw* 2017; **15**: 563-573 [PMID: 28476736 DOI: 10.6004/jnccn.2017.0059]

40 **European Association for Study of Liver**. European Organisation for Research and Treatment of Cancer. EASL-EORTC clinical practice guidelines: management of hepatocellular carcinoma. *Eur J Cancer* 2012; **48**: 599-641 [PMID: 22424278 DOI: 10.1016/j.ejca.2011.12.021]

41 **Sapisochin G**, Barry A, Doherty M, Fischer S, Goldaracena N, Rosales R, Russo M, Beecroft R, Ghanekar A, Bhat M, Brierley J, Greig PD, Knox JJ, Dawson LA, Grant DR. Stereotactic body radiotherapy vs. TACE or RFA as a bridge to transplant in patients with hepatocellular carcinoma. An intention-to-treat analysis. *J Hepatol* 2017; **67**: 92-99 [PMID: 28257902 DOI: 10.1016/j.jhep.2017.02.022]

42 **Olsen CC**, Welsh J, Kavanagh BD, Franklin W, McCarter M, Cardenes HR, Gaspar LE, Schefter TE. Microscopic and macroscopic tumor and parenchymal effects of liver stereotactic body radiotherapy. *Int J Radiat Oncol Biol Phys* 2009; **73**: 1414-1424 [PMID: 18990508 DOI: 10.1016/j.ijrobp.2008.07.032]

43 **Macià I Garau M**. Radiobiology of stereotactic body radiation therapy (SBRT). *Rep Pract Oncol Radiother* 2017; **22**: 86-95 [PMID: 28490978 DOI: 10.1016/j.rpor.2017.02.010]

44 **Velec M**, Haddad CR, Craig T, Wang L, Lindsay P, Brierley J, Brade A, Ringash J, Wong R, Kim J, Dawson LA. Predictors of Liver Toxicity Following Stereotactic Body Radiation Therapy for Hepatocellular Carcinoma. *Int J Radiat Oncol Biol Phys* 2017; **97**: 939-946 [PMID: 28333016 DOI: 10.1016/j.ijrobp.2017.01.221]

45 **Kudo M**, Ikeda M, Ueshima K, Sakamoto M, Shiina S, Tateishi R, Nouso K, Hasegawa K, Furuse J, Miyayama S, Murakami T, Yamashita T, Kokudo N. Response Evaluation Criteria in Cancer of the liver version 6 (Response Evaluation Criteria in Cancer of the Liver 2021 revised version). *Hepatol Res* 2022; **52**: 329-336 [PMID: 35077590 DOI: 10.1111/hepr.13746]

46 **Lall C**, Bhargava P, Sandrasegaran K, Shanbhogue AK, Ramsinghani N, Koh YW, Choi JY, Choi JI. Three-dimensional conformal radiation therapy in the liver: MRI findings along a time continuum. *J Comput Assist Tomogr* 2015; **39**: 356-364 [PMID: 25700224 DOI: 10.1097/RCT.0000000000000219]

47 **Yip C**, Cook GJR, Owczarczyk K, Goh V. Challenges in imaging assessment following liver stereotactic body radiotherapy: pitfalls to avoid in clinical practice. *Chin Clin Oncol* 2017; **6**: S11 [PMID: 28917249 DOI: 10.21037/cco.2017.06.06]

48 **Mendiratta-Lala M**, Gu E, Owen D, Cuneo KC, Bazzi L, Lawrence TS, Hussain HK, Davenport MS. Imaging Findings Within the First 12 Months of Hepatocellular Carcinoma Treated With Stereotactic Body Radiation Therapy. *Int J Radiat Oncol Biol Phys* 2018; **102**: 1063-1069 [PMID: 29029891 DOI: 10.1016/j.ijrobp.2017.08.022]

49 **Kubota K**, Hisa N, Nishikawa T, Fujiwara Y, Murata Y, Itoh S, Yoshida D, Yoshida S. Evaluation of hepatocellular carcinoma after treatment with transcatheter arterial chemoembolization: comparison of Lipiodol-CT, power Doppler sonography, and dynamic MRI. *Abdom Imaging* 2001; **26**: 184-190 [PMID: 11178697 DOI: 10.1007/s002610000139]

50 **Gluskin JS**, Chegai F, Monti S, Squillaci E, Mannelli L. Hepatocellular Carcinoma and Diffusion-Weighted MRI:

Detection and Evaluation of Treatment Response. *J Cancer* 2016; **7**: 1565-1570 [PMID: 27471573 DOI: 10.7150/jca.14582]

51 **Dromain C**, de Baere T, Elias D, Kuoch V, Ducreux M, Boige V, Petrow P, Roche A, Sigal R. Hepatic tumors treated with percutaneous radio-frequency ablation: CT and MR imaging follow-up. *Radiology* 2002; **223**: 255-262 [PMID: 11930075 DOI: 10.1148/radiol.2231010780]

52 **Takayasu K**, Arii S, Matsuo N, Yoshikawa M, Ryu M, Takasaki K, Sato M, Yamanaka N, Shimamura Y, Ohto M. Comparison of CT findings with resected specimens after chemoembolization with iodized oil for hepatocellular carcinoma. *AJR Am J Roentgenol* 2000; **175**: 699-704 [PMID: 10954453 DOI: 10.2214/ajr.175.3.1750699]

53 **Lee JM**, Yoon JH, Joo I, Woo HS. Recent Advances in CT and MR Imaging for Evaluation of Hepatocellular Carcinoma. *Liver Cancer* 2012; **1**: 22-40 [PMID: 24159569 DOI: 10.1159/000339018]

54 **Yue X**, Jiang Q, Hu X, Cen C, Song S, Qian K, Lu Y, Yang M, Li Q, Han P. Quantitative dual-energy CT for evaluating hepatocellular carcinoma after transarterial chemoembolization. *Sci Rep* 2021; **11**: 11127 [PMID: 34045528 DOI: 10.1038/s41598-021-90508-9]

55 **Choi SH**, Chung JW, Kim HC, Baek JH, Park CM, Jun S, Kim MU, Lee ES, Cho HR, Jae HJ, Lee W, Park JH. The role of perfusion CT as a follow-up modality after transcatheter arterial chemoembolization: an experimental study in a rabbit model. *Invest Radiol* 2010; **45**: 427-436 [PMID: 20440211 DOI: 10.1097/RLI.0b013e3181e07516]

56 **Ruff C**, Artzner C, Syha R, Grosse U, Hoffmann R, Bitzer M, Partovi S, Horger M, Nikolaou K, Grözinger G. Transarterial Chemoembolization of Hepatocellular Carcinoma Using Radiopaque Drug-Eluting Embolics: Impact of Embolic Density and Residual Tumor Perfusion on Tumor Recurrence and Survival. *Cardiovasc Intervent Radiol* 2021; **44**: 1403-1413 [PMID: 34021375 DOI: 10.1007/s00270-021-02858-6]

57 **Chen X**, Xiao E, Shu D, Yang C, Liang B, He Z, Bian D. Evaluating the therapeutic effect of hepatocellular carcinoma treated with transcatheter arterial chemoembolization by magnetic resonance perfusion imaging. *Eur J Gastroenterol Hepatol* 2014; **26**: 109-113 [PMID: 24284371 DOI: 10.1097/MEG.0b013e328363716e]

58 **Castaldo A**, De Lucia DR, Pontillo G, Gatti M, Cocozza S, Ugga L, Cuocolo R. State of the Art in Artificial Intelligence and Radiomics in Hepatocellular Carcinoma. *Diagnostics (Basel)* 2021; **11** [PMID: 34209197 DOI: 10.3390/diagnostics11071194]

59 **Zhang L**, Cai P, Hou J, Luo M, Li Y, Jiang X. Radiomics Model Based on Gadoxetic Acid Disodium-Enhanced MR Imaging to Predict Hepatocellular Carcinoma Recurrence After Curative Ablation. *Cancer Manag Res* 2021; **13**: 2785-2796 [PMID: 33790652 DOI: 10.2147/CMAR.S300627]

60 **van Timmeren JE**, Cester D, Tanadini-Lang S, Alkadhi H, Baessler B. Radiomics in medical imaging-"how-to" guide and critical reflection. *Insights Imaging* 2020; **11**: 91 [PMID: 32785796 DOI: 10.1186/s13244-020-00887-2]

61 **Ichikawa S**, Motosugi U, Sato K, Shimizu T, Wakayama T, Onishi H. Transient Respiratory-motion Artifact and Scan Timing during the Arterial Phase of Gadoxetate Disodium-enhanced MR Imaging: The Benefit of Shortened Acquisition and Multiple Arterial Phase Acquisition. *Magn Reson Med Sci* 2021; **20**: 280-289 [PMID: 32863326 DOI: 10.2463/mrms.mp.2020-0064]

62 **Westwood M**, Joore M, Grutters J, Redekop K, Armstrong N, Lee K, Gloy V, Raatz H, Misso K, Severens J, Kleijnen J. Contrast-enhanced ultrasound using SonoVue® (sulphur hexafluoride microbubbles) compared with contrast-enhanced computed tomography and contrast-enhanced magnetic resonance imaging for the characterisation of focal liver lesions and detection of liver metastases: a systematic review and cost-effectiveness analysis. *Health Technol Assess* 2013; **17**: 1-243 [PMID: 23611316 DOI: 10.3310/hta17160]

World Journal of Gastroenterology

Submit a Manuscript: https://www.f6publishing.com

World J Gastroenterol 2022 July 14; 28(26): 3132-3149

DOI: 10.3748/wjg.v28.i26.3132

ISSN 1007-9327 (print) ISSN 2219-2840 (online)

ORIGINAL ARTICLE

Basic Study

Neutrophil extracellular traps participate in the development of cancer-associated thrombosis in patients with gastric cancer

Jia-Cheng Li, Xiao-Ming Zou, Shi-Feng Yang, Jia-Qi Jin, Lei Zhu, Chang-Jian Li, Hao Yang, An-Ge Zhang, Tian-Qi Zhao, Chong-Yan Chen

Specialty type: Gastroenterology and hepatology

Provenance and peer review: Unsolicited article; Externally peer reviewed.

Peer-review model: Single blind

Peer-review report's scientific quality classification

Grade A (Excellent): 0
Grade B (Very good): B, B, B
Grade C (Good): C
Grade D (Fair): 0
Grade E (Poor): 0

P-Reviewer: Ferreira GSA, Brazil; Mohamed SY, Egypt; Morozov S, Russia; Singh I, United States

Received: October 19, 2021
Peer-review started: October 19, 2021
First decision: January 11, 2022
Revised: January 20, 2022
Accepted: March 16, 2022
Article in press: March 16, 2022
Published online: July 14, 2022

Jia-Cheng Li, Xiao-Ming Zou, Shi-Feng Yang, Lei Zhu, Chang-Jian Li, Hao Yang, An-Ge Zhang, Tian-Qi Zhao, Chong-Yan Chen, Department of Gastrointestinal Surgery, The Second Affiliated Hospital of Harbin Medical University, Harbin 150001, Heilongjiang Province, China

Jia-Cheng Li, Shi-Feng Yang, Jia-Qi Jin, Lei Zhu, Hao Yang, An-Ge Zhang, The Key Laboratory of Myocardial Ischemia, Harbin Medical University, Harbin 150001, Heilongjiang Province, China

Jia-Qi Jin, Department of Neurosurgery, The Second Affiliated Hospital of Harbin Medical University, Harbin 150001, Heilongjiang Province, China

Corresponding author: Xiao-Ming Zou, MD, PhD, Chief Doctor, Professor, Surgeon, Department of Gastrointestinal Surgery, The Second Affiliated Hospital of Harbin Medical University, No. 246 Xuefu Road, Nangang District, Harbin 150001, Heilongjiang Province, China. zou4930@163.com

Abstract

BACKGROUND

The development of venous thromboembolism (VTE) is associated with high mortality among gastric cancer (GC) patients. Neutrophil extracellular traps (NETs) have been reported to correlate with the prothrombotic state in some diseases, but are rarely reported in GC patients.

AIM

To investigate the effect of NETs on the development of cancer-associated thrombosis in GC patients.

METHODS

The levels of NETs in blood and tissue samples of patients were analyzed by ELISA, flow cytometry, and immunofluorescence staining. NET generation and hypercoagulation of platelets and endothelial cells (ECs) *in vitro* were observed by immunofluorescence staining. NET procoagulant activity (PCA) was determined by fibrin formation and thrombin–antithrombin complex (TAT) assays. Thrombosis *in vivo* was measured in a murine model induced by flow stenosis in the inferior vena cava (IVC).

RESULTS

NETs were likely to form in blood and tissue samples of GC patients compared with healthy individuals. *In vitro* studies showed that GC cells and their conditioned medium, but not gastric mucosal epithelial cells, stimulated NET release from neutrophils. In addition, NETs induced a hypercoagulable state of platelets by upregulating the expression of phosphatidylserine and P-selectin on the cells. Furthermore, NETs stimulated the adhesion of normal platelets on glass surfaces. Similarly, NETs triggered the conversion of ECs to hypercoagulable phenotypes by downregulating the expression of their intercellular tight junctions but upregulating that of tissue factor. Treatment of normal platelets or ECs with NETs augmented the level of plasma fibrin formation and the TAT complex. In the models of IVC stenosis, tumor-bearing mice showed a stronger ability to form thrombi, and NETs abundantly accumulated in the thrombi of tumor-bearing mice compared with control mice. Notably, the combination of deoxyribonuclease I, activated protein C, and sivelestat markedly abolished the PCA of NETs.

CONCLUSION

GC-induced NETs strongly increased the risk of VTE development both *in vitro* and *in vivo*. NETs are potential therapeutic targets in the prevention and treatment of VTE in GC patients.

Key Words: Neutrophil extracellular traps; Gastric cancer; Platelet; Endothelial cells; Venous thromboembolism

Core tip: We found that gastric cancer (GC)-induced neutrophil extracellular traps (NETs) strongly increase the risk of venous thromboembolism (VTE) development in GC patients. NETs are potential therapeutic targets in the prevention and treatment of VTE in GC patients.

Citation: Li JC, Zou XM, Yang SF, Jin JQ, Zhu L, Li CJ, Yang H, Zhang AG, Zhao TQ, Chen CY. Neutrophil extracellular traps participate in the development of cancer-associated thrombosis in patients with gastric cancer. *World J Gastroenterol* 2022; 28(26): 3132-3149

URL: https://www.wjgnet.com/1007-9327/full/v28/i26/3132.htm

DOI: https://dx.doi.org/10.3748/wjg.v28.i26.3132

INTRODUCTION

Gastric cancer (GC) is one of the most prevalent gastrointestinal tumors and the third most fatal cancer in the world[1,2]. Additionally, venous thromboembolism (VTE) is a more common complication among GC patients when compared to healthy individuals[3-5]. Notably, VTE is associated with a high mortality in GC patients[6,7]. Several factors, such as tumor stage, neoadjuvant chemotherapy, and surgery, contribute to the development of VTE in GC patients[8,9]. Cancer cells exert a procoagulant activity (PCA) in their microenvironment, which is related to activation of the coagulation system[10]. However, the molecular mechanism underlying PCA in GC patients is poorly understood. Uncovering molecular targets associated with VTE in GC patients can help in the development of appropriate therapy, which can improve the clinical outcomes of these patients.

Neutrophil extracellular traps (NETs) are web-like structures composed of filamentous DNA and histones, decorated with antimicrobial protein granules and enzymes, including neutrophil elastase (NE), myeloperoxidase (MPO), matrix metalloproteinase-9 (MMP-9), and cathepsin G (CatG)[11,12]. They result from interactions between neutrophils and bacterial or other stimulating factors[13,14]. Overall, they protect the host from pathogen-related damage. NETs were initially described as an antimicrobial reaction, but some undesirable effects of NETs have been reported in autoimmune diseases[15-17]. Citrullinated histone H3 (citH3) is proposed as a biomarker reflecting NETs formation. Recent studies have linked NETs to the development of metastasis and cancer-associated thrombosis[18,19]. In particular, NETs result in arterial and venous thrombosis, both of which are mediated by neutrophils[20]. Furthermore, using mouse models, it has been shown that thrombosis in breast cancer tissues is closely linked to the formation of NETs[21]. This finding suggests the potential relationship between NETs and cancer-associated thrombosis.

A recent study revealed that priming metastatic pancreatic cancer cells with platelets stimulates neutrophils to release NETs, which promotes thrombosis in both static and dynamic states[22]. We first reported that platelets derived from GC can stimulate neutrophils to release NETs. NETs enhance PCA in GC patients, which is positively correlated with the expression of the thrombin–antithrombin (TAT)

complex and the level of serum D-dimers[23]. Moreover, both human and animal studies suggest that enhanced thrombosis may result from increased activated platelets[24,25]. Nevertheless, little is known about the interaction between NETs and platelet activation in GC patients. Venous endothelial cell (EC) injury in cancer patients is also closely related to venous thrombosis[26,27]. Interestingly, the cytotoxicity of NETs against ECs enhances PCA in oral squamous cancer, even in patients with obstructive jaundice and inflammatory bowel disease[28-30]. Even so, the potential mechanism underlying EC injury in GC patients is poorly understood.

Our central hypothesis is that GC-induced NETs participate in VTE responses by platelet activation and endothelial injury. Therefore, we first explored the complex relationship between NET formation and platelet activation as well as EC injury. Furthermore, we showed the effect of NETs on thrombosis in an inferior vena cava (IVC) stenosis mouse model. In general, our results may indicate that NETs are potential therapeutic targets in the prevention and treatment of VTE in GC patients.

MATERIALS AND METHODS

Patients and tissue samples

Sixty-three patients newly diagnosed with primary GC and 13 healthy donors (HDs) attending the Second Affiliated Hospital of Harbin Medical University between October 2019 and April 2021 were enrolled in this study. GC diagnoses were performed based on pathological examinations. Pathological tumor-node-metastasis (TNM) staging and histological classification of GC were performed according to the 7th American Joint Committee on Cancer (AJCC) guidelines[31]. Patients who were < 18 years old or pregnant, those on antitumor or anticoagulant treatment before surgical treatment, or those with underlying complications such as endocrine, cardiovascular, hematological and other cancers or infectious disease were all excluded. The main clinical characteristics of the patients with GC and HDs are shown in Table 1. We extracted tumor and adjacent normal tissues from GC patients who consented to this study in writing. Blood samples of preoperative patients were obtained at first diagnosis before any clinical treatment, and blood samples of postoperative patients were obtained from 1 mo after surgery before adjuvant therapy to avoid errors caused by postoperative stress. The protocol for this study was approved by the Ethics Committee of the Second Affiliated Hospital of Harbin Medical University (No. KY2016-032).

Isolation of human plasma, platelets, and neutrophils

Fresh whole venous blood was collected into tubes containing 3.2% sodium citrate using 21-gauge needles. The patients underwent overnight fasting before blood collection. The blood was centrifuged at 150 *g* for 20 min at room temperature (RT) to obtain platelet-rich plasma (PRP), within 1 h of collection. Clean top PRP layer was collected in a new tube, diluted with platelet wash buffer (TBD, Tianjin, China), and centrifuged at 460 *g* for 20 min at RT to obtain clean platelets and platelet-free plasma (PFP) [32]. The platelets were resuspended in prewarmed modified Tyrode's buffer (137 mmoL/L NaCl, 2.8 mmoL/L KCl, 1.0 mmoL/L $MgCl_2$, 12 mmoL/L $NaHCO_3$, 0.4 mmoL/L Na_2HPO_4, 5.5 mmoL/L glucose, pH 7.4; Solarbio, Beijing, China). Neutrophils were isolated based on the density gradient centrifugation, using the whole blood neutrophil isolation kit (TBD). After lysing erythrocytes based on the red blood cell lysis buffer (150 mmoL/L NH_4CL, 10 mmoL/L $KHCO_3$, 0.2 mmoL/L Na_2EDTA, pH 7.4; TBD), the purity (> 96%) and viability (> 96%) of neutrophils were assessed using Wright–Giemsa staining and Trypan blue staining, respectively.

Cell lines and conditioned medium

The human metastatic GC KATO-III and MKN-45 cell lines, human primary GC AGS cell line, human gastric mucosal epithelial cell (GES-1) line, human umbilical cord endothelial cell (HUVEC) line, and mouse forestomach squamous carcinoma (MFC) cell line were purchased from PROCELL (Wuhan, China). All cell lines were characterized using short tandem repeat (STR) profiling. The GES-1, AGS, MKN-45 and MFC cells were cultured in RPMI 1640 (Gibco, USA), KATO-III cells were cultured in IMDM (Gibco), and HUVECs were cultured in DME/F12 (HyClone, Logan, UT, USA). All media were supplemented with 10% fetal bovine serum (FBS; Gibco) and 1% penicillin–streptomycin solution (Beyotime, Beijing, China). Incubation was performed at 37°C under 5% CO_2in a humidified environment. To prepare conditioned medium (CM), the cells were cultured to 90% confluence in medium supplemented with 10% FBS, washed three times using 1 × PBS, and recultured for 48 h in medium without FBS. The supernatant was centrifuged at 1500 *g* for 10 min at 4°C to remove cell debris. The CM was collected and stored at -80°C until use.

Animal models

The animal protocol was designed to minimize pain or discomfort to the animals. Wild-type male C57BL/6 mice (7–9 wk old, weighing 20–26 g) were purchased from the Animal Experimental Center of Harbin Medical University, and all procedures were approved by the Animal Care and Use Committee

Table 1 Main clinical and laboratory features of 13 healthy subjects and 63 patients diagnosed with gastric cancer

Characteristics (n = 76, DF = 4)	Control (n = 13)	Stage I (n = 14)	Stage II (n = 15)	Stage III (n = 22)	Stage IV (n = 12)
Male (%)	61.5	50	53.3	72.7	66.6
Age(yr)	58.46 ± 5.43	57.0 ± 10.07	63.07 ± 9.12	60.32 ± 11.54	63.64 ± 9.68
Erythrocytes (× 10^{12}/L)	4.70 ± 0.57	4.46 ± 0.32	4.12 ± 0.83	4.13 ± 0.69	4.03 ± 0.81
Leukocytes (× 10^9/L)	6.87 ± 2.86	6.57 ± 2.04	8.60 ± 2.54[a]	8.58 ± 4.66[a]	10.60 ± 5.25[b]
Neutrophils (× 10^9/L)	4.36 ± 3.0	4.62 ± 2.54	6.36 ± 2.82[a]	6.75 ± 4.92[a]	8.53 ± 5.46[c]
Hb (g/L)	140.84 ± 20.31	137.23 ± 10.76	121.29 ± 26.65	121.23 ± 29.72	111 ± 33.23[a]
PLT (× 10^9)	259.15 ± 59.0	242.69 ± 52.19	293.29 ± 83.74	250.64 ± 104.63	302.0 ± 156.9
ALB (g/L)	44.84 ± 3.27	43.33 ± 4.84	38.06 ± 6.29	37.39 ± 9.23	35.59 ± 4.08[a]
PT (s)	11.24 ± 1.03	12.66 ± 4.16	12.42 ± 2.03	12.05 ± 0.86	12.24 ± 1.57
APTT (s)	35.06 ± 2.71	36.03 ± 7.54	34.52 ± 3.46	33.49±3.81	35.08±4.68
D-dimer (mg/L)	53.30 ± 48.16	238.46 ± 265.28[c]	280.21 ± 269.55[c]	291.23 ± 262.88[c]	950.0 ± 743.72[d]
Fibrinogen (g/L)	2.46 ± 0.43	2.69 ± 0.58	3.67 ± 0.98[a]	3.19 ± 0.61[a]	4.68 ± 2.61[b]

[a]$P < 0.05$ *vs* healthy control.
[b]$P < 0.01$ *vs* healthy control.
[c]$P < 0.001$ *vs* healthy control.
[d]$P < 0.0001$ *vs* healthy control.
Data are presented as numbers (percentages) or the mean ± SD. DF: Degree of freedom; Hb: Hemoglobin; PLT: Platelets; ALB: Albumin; PT: Prothrombin time; APTT: Activated partial thromboplastin time.

of the Second Affiliated Hospital of Harbin Medical University (No. KY2016-032). The animals were individually housed and maintained under standard conditions (12 h/12 h light/dark cycle, 22 ± 1 °C, 50% humidity) and provided with a conventional laboratory diet and an unrestricted supply of drinking water. In the subcutaneous tumor models, mice were injected with MFC cells (2 × 10^7 cells/mL) subcutaneously into the right axilla, and the tumor volumes were measured every 3 d from 7 d after injection with MFC cells and allowed to reach 1000 mm^3 (usually 28–35 d). The volume was calculated by measuring the length (L) and width (W) of the tumor: Tumor volume = $\pi/6 \times L \times W^2$. Thereafter, a murine model of deep vein thrombosis (DVT) was developed as previously described[33]. The mice were anesthetized by intraperitoneal injection of 2,2,2-tribromoethanol (Sigma, St . Louis, MO, USA), and the intestines were removed to expose the IVC after entering the abdominal cavity through a median abdominal incision. The IVC was carefully separated below the left renal vein plane. After 5-0 (1 mm) sutures passed through the IVC, 3-0 (2 mm) sutures were placed at the parallel part of the IVC as the blocking line. The IVC was ligated and 3-0 sutures were carefully extracted. This procedure has been shown to decrease the vascular lumen by approximately 90%. The other branches of the IVC were ligated to the level of the iliac vein. Thereafter, the abdominal incision was closed, mice were sacrificed after 6 or 48 h, and thrombi that had formed in the IVC were harvested. The IVC stenosis mice in the treatment groups were injected with DNase I (50 μg/mouse; Roche, Switzerland) intraperitoneally every 12 h until the time of death. All animals were killed for tissue collection. Blood (300 μL/mouse) was drawn from the periorbital eye plexus and stabilized with 0.5 mmoL/L EDTA. Plasma was obtained as described above. Thrombi of control and tumor-bearing mice were fixed in 4% paraformaldehyde for 24 h, embedded in Optimal Cutting Temperature (OCT) compound (SAKURA, Torrance, CA, USA), and cryosectioned at a thickness of 4 μm for immunofluorescence staining.

Quantification of plasma NETs marker

Plasma cell-free DNA (cf-DNA), MPO-DNA and citH3-DNA complexes were quantified using capture ELISA as previously described[34]. The quantification of cf-DNA was performed using the Quant-iT PicoGreen dsDNA assay kit (Invitrogen, Carlsbad, CA, USA). For detection of NET-DNA complexes, 5 μg/mL anti-MPO (ab90810; Abcam, Cambridge, UK) or anti-citH3 antibody (ab5103; Abcam) was coated onto 96-well plates overnight at 4°C. After blocking in 1% bovine serum albumin (BSA), the plasma from GC patients or healthy individuals was added per well and incubated at RT for 2 h. After washing five times with PBST, Quant-iT PicoGreen dsDNA Reagent was added. The values were then read with a fluorometer with a filter setting of 480 nm/520 nm excitation/emission wavelengths.

Fibrin formation and TAT complex assay

Fibrin formation of platelets and ECs was detected by turbidity as previously described[35]. To assess

the fibrin formation in the setting of platelet or EC monolayers, cell monolayers in 96-well plates were stimulated by NETs with or without DNase I, activated protein C (APC), and sivelestat treatment alone or together for 4 h, followed by two washes with Hank's balanced salt solution (137 mmoL/L NaCl, 5.3 mmoL/L KCl, 4.17 mmoL/L $NaHCO_3$, 0.33 mmoL/L Na_2HPO_4, 5.5 mmoL/L glucose, pH 7.4) and then 150 μL PFP from HDs was cocultured with cells at 37°C for 2 min, followed by the addition of 50 μL prewarmed 25 mmoL/L $CaCl_2$. The fibrin formation was tested using turbidity measurements and quantified as the maximum value by measuring the OD at 405 nm every 10 s for 30 min on a SpectraMax 340 PC plate reader. To assess the fibrin formation in the plasma of mice, 150 μL PFP from control, tumor-bearing mice, or DNase I infused tumor-bearing mice was cultured at 37°C for 2 min, followed by addition of 50 μL prewarmed 25 mmoL/L $CaCl_2$. To detect the level of TAT complex, a human and mouse TAT complex ELISA kit (Jingkbio, Shanghai, China) was used as previously described[36].

Flow cytometry

Circulating NETs were measured using flow cytometry. Here, whole blood from HDs and GC patients was diluted with 1 × PBS and incubated in the dark at RT for 30 min with FITC-conjugated-citH3 (eBioscience, San Diego, CA, USA) and PE-conjugated MPO (eBioscience) antibodies. For the assessment of phosphatidylserine (PS) and P-selectin expression on platelets, platelets (2×10^6 cells) isolated from the blood of HDs and GC patients were incubated with FITC-conjugated lactadherin (Haematologic, Essex Junction, VT, USA), APC-conjugated CD62P (Biolegend, San Diego, CA, USA), and PerCP-conjugated CD41 (Biolegend) antibodies.

Immunofluorescence staining of NETs

Tumor and paratumor tissues of GC patients were fixed in 4% paraformaldehyde for 24 h, embedded in OCT compound (SAKURA), and cryosectioned into slices of 4-μm thickness. The samples were cultured overnight at 4°C with primary rabbit anti-histone H3 (1:500, ab5103; Abcam) and mouse anti-MPO (1:500, ab90810; Abcam) antibodies, and washed three times with PBS before incubation for 1 h at RT with Alexa Fluor 594-conjugated goat anti-rabbit (1:200; Proteintech, China) and Alexa Fluor 488-conjugated goat anti-mouse (1:200; Proteintech) secondary antibodies. The tissues were stained for 5 min at RT in the dark with 4′,6-diamidino-2-phenylindole (DAPI) and anti-fade mounting medium (Solarbio, Beijing, China). Thrombi in the IVC of tumor models or control mice were stained with primary rabbit anti-histone H3 (1:500, ab5103; Abcam) and rat anti-Ly6G (1:500, Novus, St. Charles, MO, USA), and the specimens were incubated with the Alexa Fluor 488-conjugated goat anti-rabbit (1:200; Proteintech) and Alexa Fluor 594-conjugated goat anti-rat (1:200; Proteintech) secondary antibodies as previously described[37]. The tissue images were captured using a confocal microscope (LSM 800; Zeiss, Germany).

Neutrophils (5×10^5 cells) isolated from HDs were seeded and incubated in glass-based poly-L-lysine-coated 24-well plates for 1 h at 37°C under 5% CO_2. Thereafter, cell suspensions of KATO-III, MKN-45, AGS, and GES-1 (2×10^5 cells) or CM from GC cells were cocultured with neutrophils for 4 h at 37°C under 5% CO_2. To detect and quantify NETs, the samples of the CM group were incubated with primary rabbit anti-histone H3 and mouse anti-MPO antibodies and then fluorescent secondary antibodies. For the samples of cell-cell contact groups, NETs were stained with Sytox Green (Solarbio) for 10 min in the dark at RT. All images were captured using a confocal microscope (LSM 800; Zeiss) and analyzed with ImageJ software (National Institutes of Health, Bethesda, MD, USA).

Preparation of cell-free NETs

Cell-free NETs were isolated from neutrophils of GC patients as previously described, with modifications[38]. Neutrophils (10^7 cells/mL) were cultured for 4 h at 37°C under 5% CO_2 in medium supplemented with 500 nM PMA (HY-18739; MedChemExpress, Monmouth Junction, NJ, USA). The supernatant was discarded, and ice-cold 1 × PBS was added to wash down the cell layer of neutrophils to obtain the NET medium and centrifuged at 1500 *g* for 10 min at 4°C to remove cell debris. Thereafter, 1.5 mL supernatant (sterile DNA–protein complex) was centrifuged at 15 000 *g* for 15 min at 4°C. The resultant pellets were suspended in ice-cold 1 × PBS, followed by DNA concentration measurement in the medium obtained using spectrophotometry (Biospec-nano, Japan). An adequate DNA concentration in the medium should range between 50 and 100 μg/mL. The medium containing the NETs was stored at -80°C for subsequent experiments.

Platelet activation and adhesion assays

Platelet activation and adhesion assays were performed as previously described[22]. Glass-based wells of 24-well plates were coated with cell-free NETs after overnight incubation in the corresponding medium at 4°C in a humidified chamber. For controls, 1% denatured BSA was used. Denatured BSA was prepared by heating the solution in PBS without calcium or magnesium to 80°C for 3 min and immediately placing it on ice until cool; it was then stored at 20°C until use. Platelet suspensions (10^7 cells/mL) were then seeded in the wells, cultured for 1 h at 37°C under 5% CO_2, fixed for 15 min at RT with 4% paraformaldehyde, and washed three times using 1 × PBS before 20 min permeabilization

using 0.1% Triton-X 100. The platelets were then incubated for 30 min with Alexa Fluor 594-conjugated phalloidin primary antibody (1:300; Thermo Fisher, Waltham, MA, USA). To assess PS and P-selectin expression, the platelet suspension was incubated for 1 h at 37°C under 5% CO_2, and the cells were stimulated with NETs for 1 h, followed by FITC-conjugated lactadherin (Hematologic) staining for 30 min. Platelets were washed twice with PBS before fixation for 15 min at RT with 4% paraformaldehyde, permeabilized using 0.1% Triton-X 100 for 20 min, and then stained with primary rabbit anti-P-selectin (1:200; Proteintech) and mouse anti-CD41 (1:500; Novus) antibodies. Images were captured using a confocal microscope (LSM 800; Zeiss) and analyzed with ImageJ software (National Institutes of Health).

HUVECs stimulation assay

HUVECs were incubated with cell-free NETs or PBS in 24-well plates for 4 h when the cells grew to a confluent monolayer. The cells were fixed in 4% paraformaldehyde for 15 min at RT, washed three times using 1 × PBS, and blocked for 1 h using 10% goat serum with 1% BSA solution in PBS. For detection of tissue factor (TF) expression, ECs were incubated overnight at 4 °C with rabbit anti-TF (1:500, ab228968; Abcam) and mouse anti-CD31 (1:500, ab9498; Abcam) primary antibodies. The cells were washed with PBS and reincubated for 1 h at RT with Alexa Fluor 594-conjugated (Proteintech) goat anti-rabbit and Alexa Fluor 488-conjugated (Proteintech) goat anti-mouse secondary antibodies. For detection of intercellular junctions of cells, cells were incubated overnight at 4°C with rabbit anti-VE-cadherin (1:500, ab33168; Abcam) primary antibody, followed by Alexa Fluor 488-conjugated (Proteintech) goat anti-rabbit secondary antibody, and were further incubated with Alexa Fluor 594-conjugated phalloidin primary antibody (1:300; Thermo Fisher, Waltham, MA, USA). They were stained with DAPI and fixed with mounting medium (Solarbio) for 5 min at RT in the dark. The cells were observed and photographed using a confocal microscope. The photos were analyzed with ImageJ software.

Platelet and HUVEC inhibition assays

For inhibition assays, platelets and HUVECs were cocultured with cell-free NETs for 1 h at 37°C in a humidifier chamber in the presence of DNase I (100 U/mL, Roche), APC (100 nM, HY-P1918; MedChemExpress), and sivelestat (100 nM, HY-17443; MedChemExpress) alone or together. DNase I cleaves NET DNA, whereas APC and sivelestat disrupt histones and NE functions, respectively.

Statistical analysis

Data are expressed as the mean ± SD. Data were analyzed to assess distribution normality. For normally distributed data, statistical significance was analyzed using Student's *t*-tests and one-way analysis of variance. For non-normally distributed data, statistical significance was analyzed using the Mann–Whitney test and Kruskal–Wallis test. All analyses were performed using GraphPad Prism version 8.0 and SPSS 16.0 statistical software. Spearman's correlation was used to evaluate the association between two variables. $P < 0.05$ was considered statistically significant.

RESULTS

GC patients display greater NET formation

The levels of plasma cf-DNA, citH3-DNA,and MPO-DNA complexes in GC patients ($n = 63$) and HDs ($n = 13$), which reflect the concentration of NETs, were measured using capture ELISA. The levels of NET markers were significantly higher in patients with stage II/III/IV GC than in HDs (Figure 1A–C). There was also a significant difference in preoperative and postoperative plasma NET marker levels in GC patients (Figure 1D–F). The levels of NET markers positively correlated with those of serum D-dimer (cf-DNA: $r = 0.5595$, $P < 0.0001$; citH3-DNA: $r = 0.5469$, $P < 0.0001$; MPO-DNA: $r = 0.5479$, $P < 0.0001$), suggesting that NETs were associated with hypercoagulation and VTE development in GC patients. The levels of NETs (MPO^+/$citH3^+$ neutrophils) in the circulation in GC patients and HDs were measured using flow cytometry. Circulating NETs were higher in the blood of patients with either GC stage (II–IV) than in their HD counterparts (Figure 1G and H). Furthermore, based on MPO and citH3 levels, immunofluorescence staining revealed that NETs were significantly higher in the tumor microenvironment than in the paratumor tissue of the same patients (Figure 1I–M).

GC cells stimulate formation of NETs by neutrophils

To assess whether GC cells directly stimulated NET formation, we analyzed the expression of NETs in a coculture of GC cell lines and neutrophils. Immunofluorescence analysis revealed that compared with GES-1 cells, the rate of NET formation was significantly higher in GC cells (Figure 2A). However, the formation of NETs was greater in the metastatic GC cell line than in the nonmetastatic GC cell line (Figure 2B). We measured NET formation when normal neutrophils were cocultured with CM from KATO-III, MKN-45, AGS and GES-1 cells. Immunofluorescence analysis further revealed that the CM of KATO-III and MKN-45 cells exerted greater neutrophil activation for NET formation than the CM of

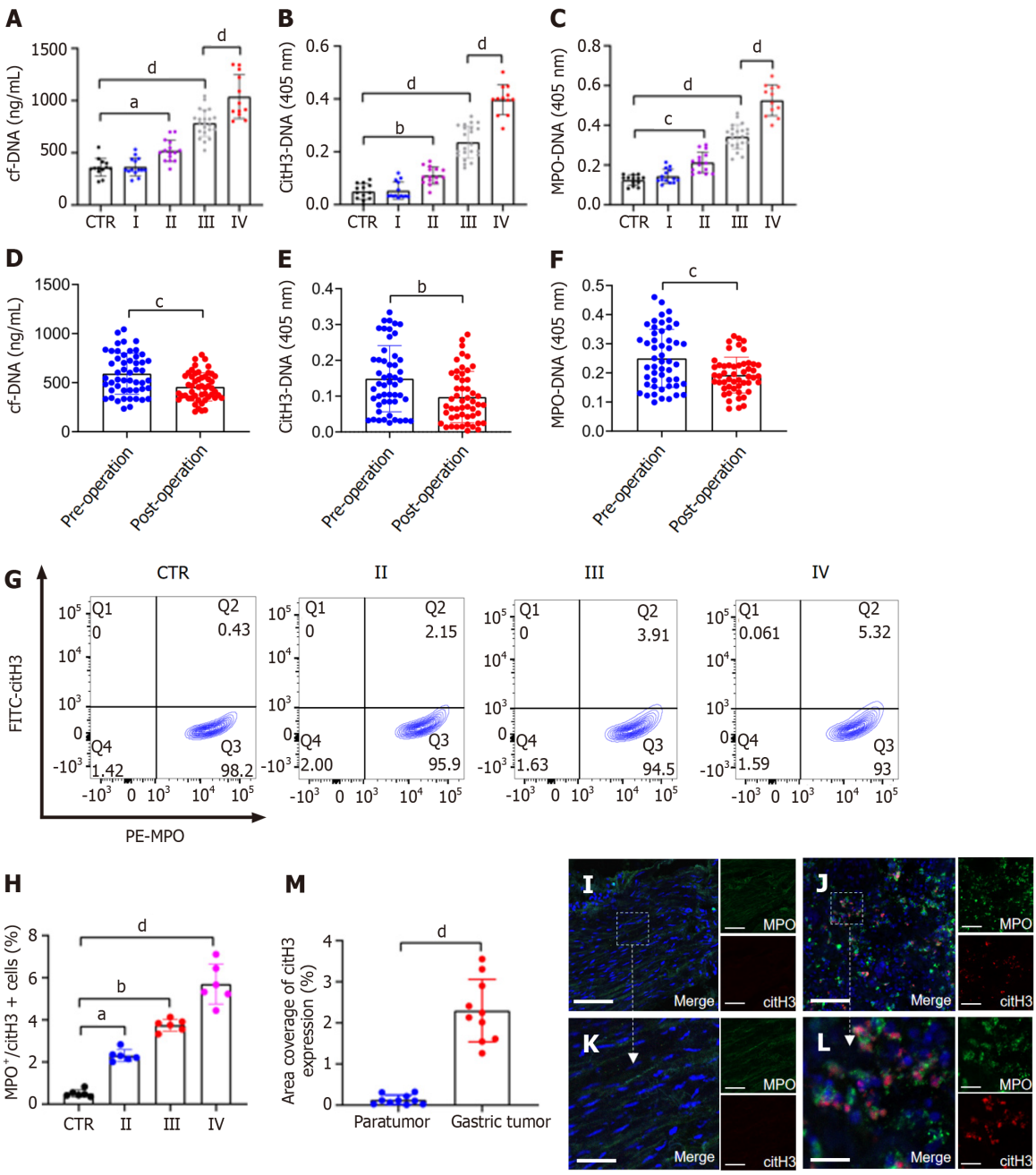

DOI: 10.3748/wjg.v28.i26.3132

Figure 1 NETs are accumulated in samples of GC patients. A–C: Plasma levels of NET markers cf-DNA, citH3-DNA, and MPO-DNA in GC patients and healthy individuals were measured by ELISA. Healthy individuals, n = 13; stage I, n = 14; II, n = 15; III, n = 22; IV, n = 12; D-F: Comparison of cf-DNA, citH3-DNA and MPO-DNA in the plasma of patients with GC preoperatively and postoperatively by ELISA. n = 51; G and H: The rate of activated neutrophils in the circulating environment of GC patients and healthy individuals was measured by flow cytometry with APC-MPO and FITC-citH3 staining. Each group: n = 6; I and J: NET accumulation was detected by confocal microscopy with MPO and citH3 staining in paratumor and tumor samples from the same GC patient. Magnification 20×; scale bars: 50 μm. Red-citH3, Green-MPO and Blue-DAPI; K and L: Magnified (40×) part of MPO and citH3 colocation in paratumor and tumor samples from the same patient. Scale bars: 10 μm. Red-citH3, Green-MPO and Blue-DAPI; M: The percentage of area coverage of citH3 expression was defined as the rate of red area in total area and analyzed with ImageJ software; all values are the mean ± SD. $^{a}P < 0.05$; $^{b}P < 0.01$; $^{c}P < 0.001$; $^{d}P < 0.0001$. NET: Neutrophil extracellular trap; GC: Gastric cancer; cf-DNA: Cell-free DNA; MPO: Myeloperoxidase; citH3: Citrullinated histone H3.

AGS cells. However, the CM of GES-1 cells had no effect on NET formation (Figure 2C and D). Overall, these findings demonstrate that GC cells stimulate NET formation through both intercellular contact and noncontact mechanisms.

NETs contribute to hypercoagulation of platelets

To examine the effect of NETs on platelet activation, we measured the levels of PS and P-selectin expression in these cells. Flow cytometry revealed that compared to HDs, the expression of PS and P-selectin was significantly higher on platelets of patients with GC (Figure 3). In addition, platelets

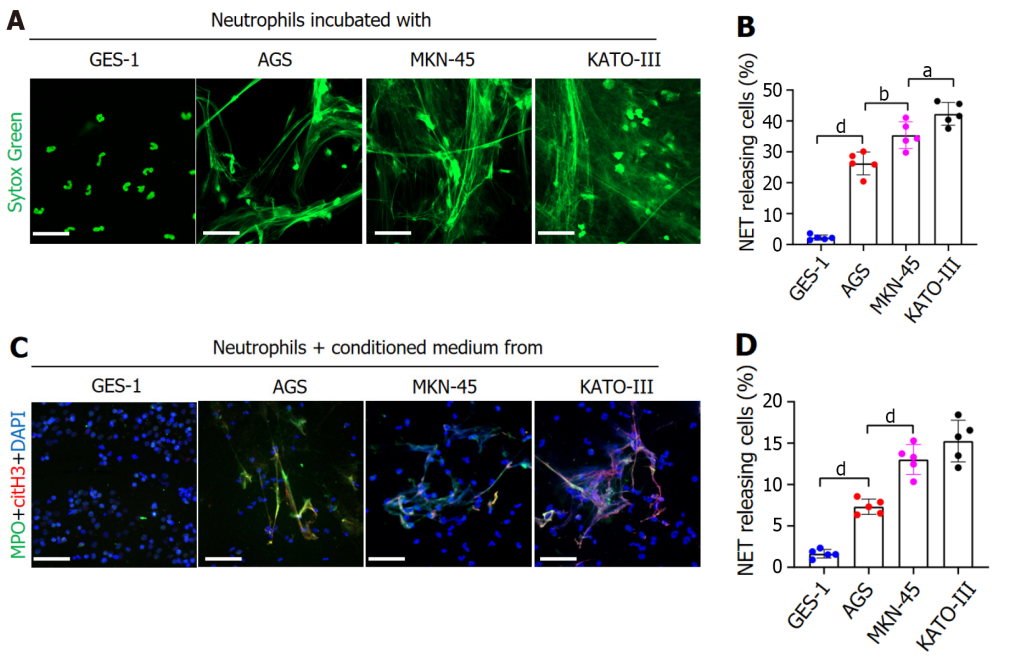

DOI: 10.3748/wjg.v28.26.3132

Figure 2 GC cells can stimulate neutrophils to form NETs. A and B: Control neutrophils were cocultured with normal gastric mucosal epithelial cells (GES-1) or GC cells (AGS, MKN-45 and KATO-III) and NET formation was measured by confocal microscopy with cell-impermeable Sytox-Green staining. Magnification 20×; scale bars: 50 μm. Green: Neutrophils; C and D: Control neutrophils were cocultured with CM from GES-1 or GC cells, and stained with MPO and citH3. The percentage of NET-releasing cells was defined as the ratio of the calculated NET releasing neutrophils to the total number of neutrophils. Magnification 20×; scale bars: 50 μm. Red-citH3, Green-MPO, and Blue-DAPI. All values are the mean ± SD. $^{a}P < 0.05$; $^{b}P < 0.01$; $^{c}P < 0.001$; $^{d}P < 0.0001$. GC: Gastric cancer; GES-1: Gastric mucosal epithelial cells; NET: Neutrophil extracellular trap; CM: Conditioned medium; MPO: Myeloperoxidase; citH3: Citrullinated histone H3.

isolated from HDs were cocultured with NET medium or PBS before analyzing PS and P-selectin expression. We found that NETs stimulated PS and P-selectin expression on platelets by confocal microscopy (Figure 4A–C). Flow cytometry also demonstrated this hypercoagulable phenotype of platelets which was stimulated by NETs (Figure 4D and E). In the inhibition assay, we added DNase I, APC and sivelestat alone or together to cleave DNA, histones and NE, which were the most functional factors of NETs. At the highest concentration of NETs (0.5 μg DNA/mL), flow cytometry revealed that DNase I, APC, sivelestat, or a combination of the three inhibited 60.2%, 47.1%, 41.9% and 83.2% of PS expression, respectively (Figure 4D), and 55.2%, 47.0%, 41.0%, and 91.76% of P-selectin expression on platelets, respectively (Figure 4E).

NETs promote platelet adhesion and prothrombotic state

Previous studies have shown that NETs promote thrombosis in murine late-stage breast cancer models and DVT models[19,39]. However, whether NETs derived from GC neutrophils have the ability to stimulate platelet adhesion under static conditions is unknown. To determine the effect of NETs on platelet adhesion, platelets isolated from HDs were seeded in NET-coated wells to measure the effects of NETs on the adherence of platelets to blood vessels. Confocal microscopy revealed that NETs enhanced adherence of platelets to glass slides (Figure 5A and B), indicating that NETs induce the development of thrombosis. Moreover, the results revealed that fibrin formation and TAT complex levels were increased when control plasma was cocultured with platelets activated by NETs (Figure 5C and D).

Inhibition assays revealed that digestion of NET DNA using DNase I modulated the adhesion of platelets on glass surfaces. Even so, a few platelets still adhered to the NET-coated well pretreated with DNase I (Figure 5A). This suggested that other protein components other than NET-DNA participated in the adhesion of platelets. NETs treated with DNase I, APC, sivelestat, or a combination of the three inhibited 67.1%, 56.6%, 38.9%, and 91.8% of platelet adhesion, respectively (Figure 5B). The degree of platelet adhesion in the combination group was comparable to that of the controls. We found that DNase I, APC, sivelestat, or a combination of the three reduced fibrin formation by 81.1%, 73.9%, 64.3%, and 90.7%, respectively (Figure 5C), and inhibited 78.9%, 57.4%, 51.2%, and 91.9% of TAT complex level, respectively (Figure 5D), at the highest concentration of NETs. Taken together, these findings demonstrate that NETs play a role in the development of thrombosis.

NETs drive hypercoagulation of ECs

To detect the effect of NETs on EC thrombogenicity, HUVECs were cocultured with NET medium. Confocal microscopy revealed that NETs destroyed the normal intercellular junctions between ECs

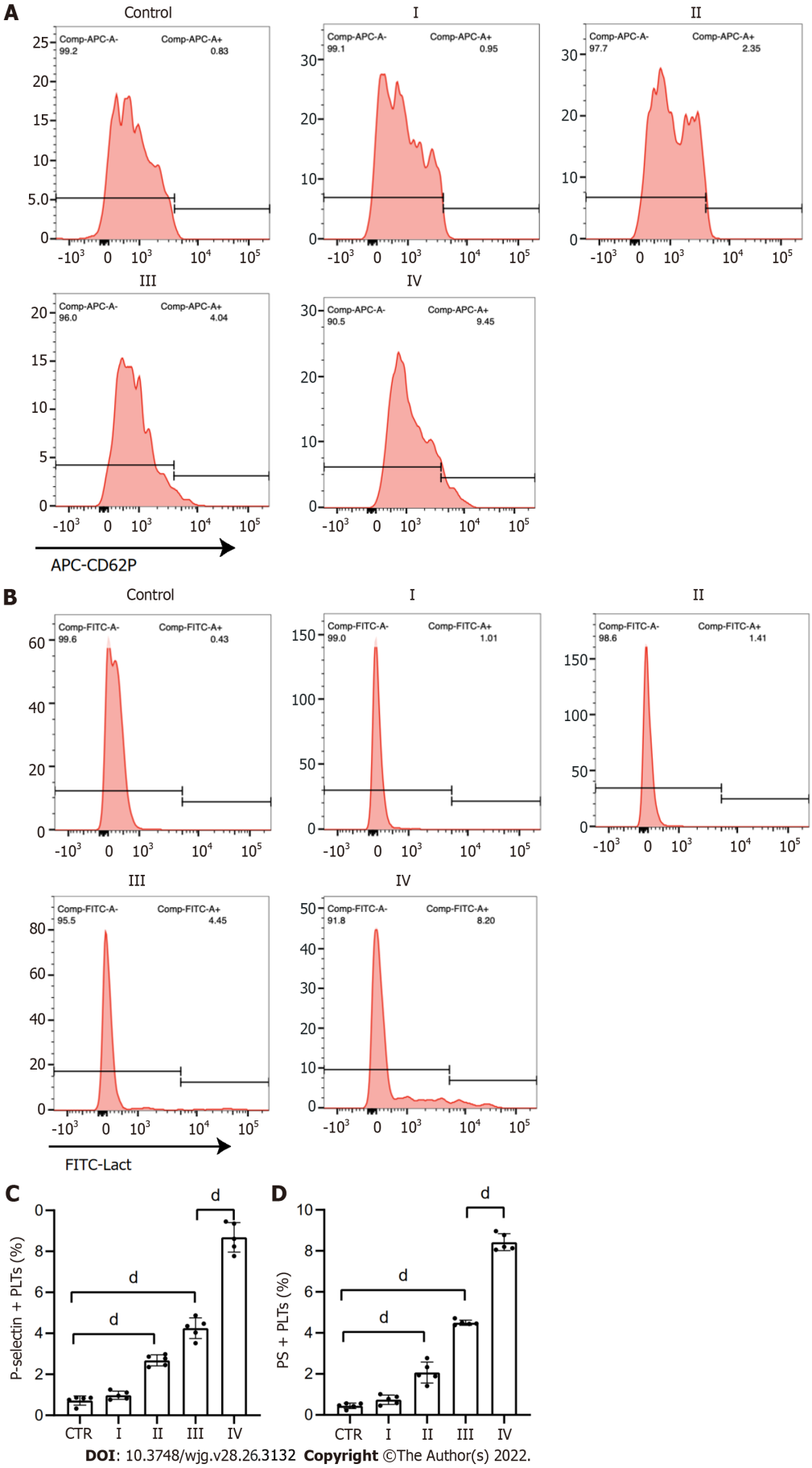

DOI: 10.3748/wjg.v28.26.3132

Figure 3 Platelets are activated in patients with GC. A and C: Flow cytometry showed the rate of P-selectin-positive platelets from each stage GC patients

and healthy individuals; B and D: Rate of phosphatidylserine-positive platelets from each stage GC patients and healthy individuals. All values are the mean ± SD. $^{d}P < 0.0001$. PS: Phosphatidylserine; GC: Gastric cancer. CD62P: P-selectin; Lact: Lactadherin.

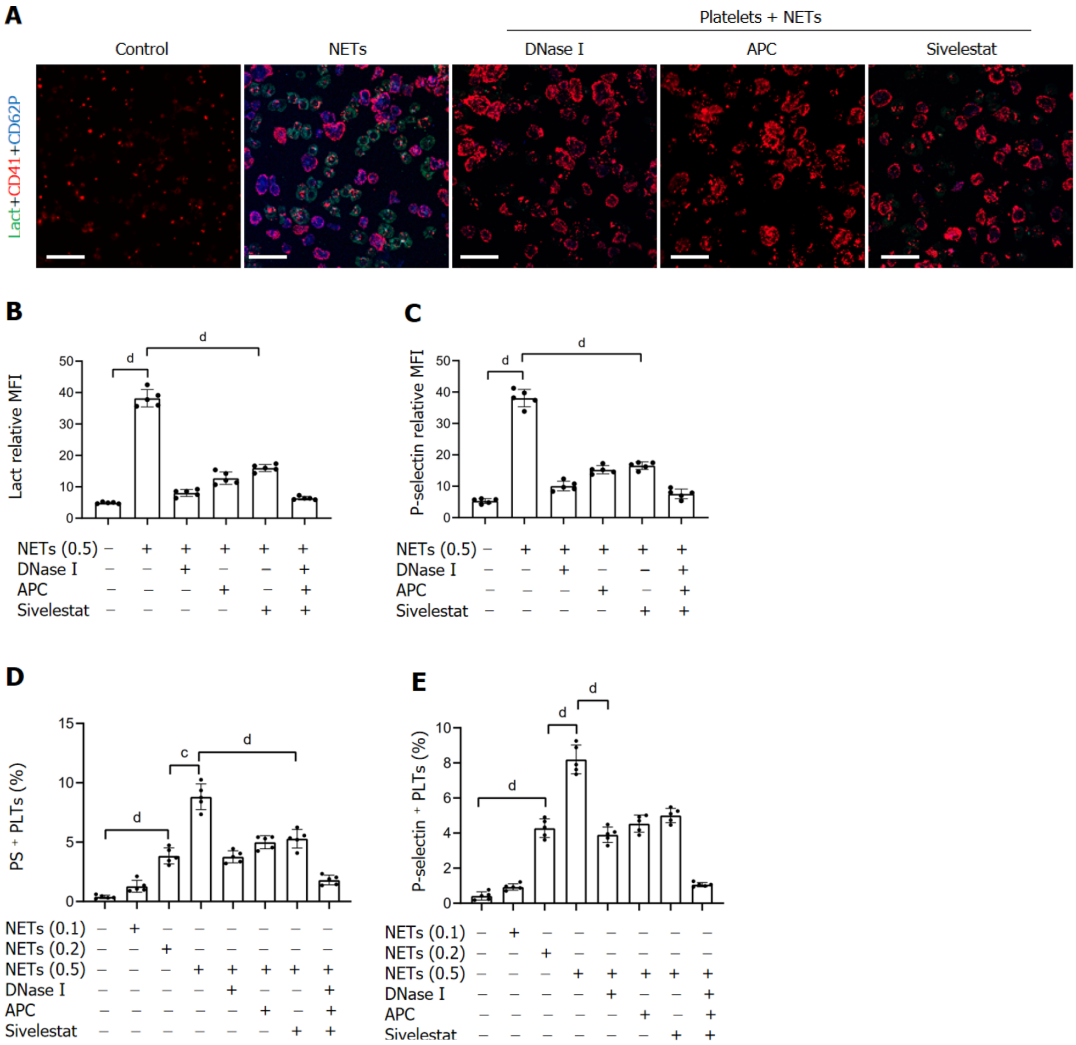

DOI: 10.3748/wjg.v28.26.3132

Figure 4 NETs contribute to hypercoagulation of platelets. A: PS exposure and P-selectin expression were measured when isolated platelets were cocultured with BETs (μg, DNA/mL) or in the presence of DNase I, activated protein C, and sivelestat alone or together by confocal microscopy. Magnification 63×; scale bars: 10 μm. Red-platelets, Green-Lactadherin, and Blue-P-selectin; B and C: PS exposure and P-selectin expression are indicated as MFI. MFI was defined as the ratio of total fluorescence intensity to the area; D and E: The rates of PS-positive platelets and P-selectin-positive platelets were detected by flow cytometry. All values are the mean ± SD. $^{c}P < 0.001$; $^{d}P < 0.0001$. PS: Phosphatidylserine; GC: Gastric cancer; DNase I: Deoxyribonuclease I; APC: Activated protein C; MFI: Mean fluorescence intensity; Lact: Lactadherin; CD41: Platelet; NET: Neutrophil extracellular trap.

(Figure 6A and C). NET treatment upregulated expression of TF on the surface membrane of ECs (Figure 6B and D). In addition, plasma fibrin formation and TAT complex levels were significantly increased when control plasma was incubated with EC monolayers activated by NETs (Figure 6E and F). Further inhibition assays were performed to assess the effect of NETs on ECs after pretreatment with DNase I, APC, sivelestat, or a combination of the three. We found that NET treatment after incubation with DNase I, APC, sivelestat, or all three drugs returned 47.5%, 36.3%, 33.4%, and 86.5%, respectively, of VE expression on ECs (Figure 6C), whereas similar treatment inhibited 60.4%, 44.8%, 38.6%, and 95.5%, respectively, of TF expression (Figure 6D). Additionally, we found that NET treat-ment after incubation with the above inhibitors inhibited 59.7%, 54.4%, 54.0%, and 91.5% of fibrin formation level, respectively (Figure 6E), and inhibited 51.2%, 35.6%, 25.9%, and 84.3% of TAT complex level, respectively (Figure 6F). Taken together, these findings suggest that NETs promote hypercoagulation of ECs; thus, inhibiting NET function can protect against venous injury.

NETs promote formation of thrombi in tumor-bearing IVC flow restriction mice

Based on these findings *in vitro* and the pivotal role of NETs in thrombosis, we hypothesized that GC-

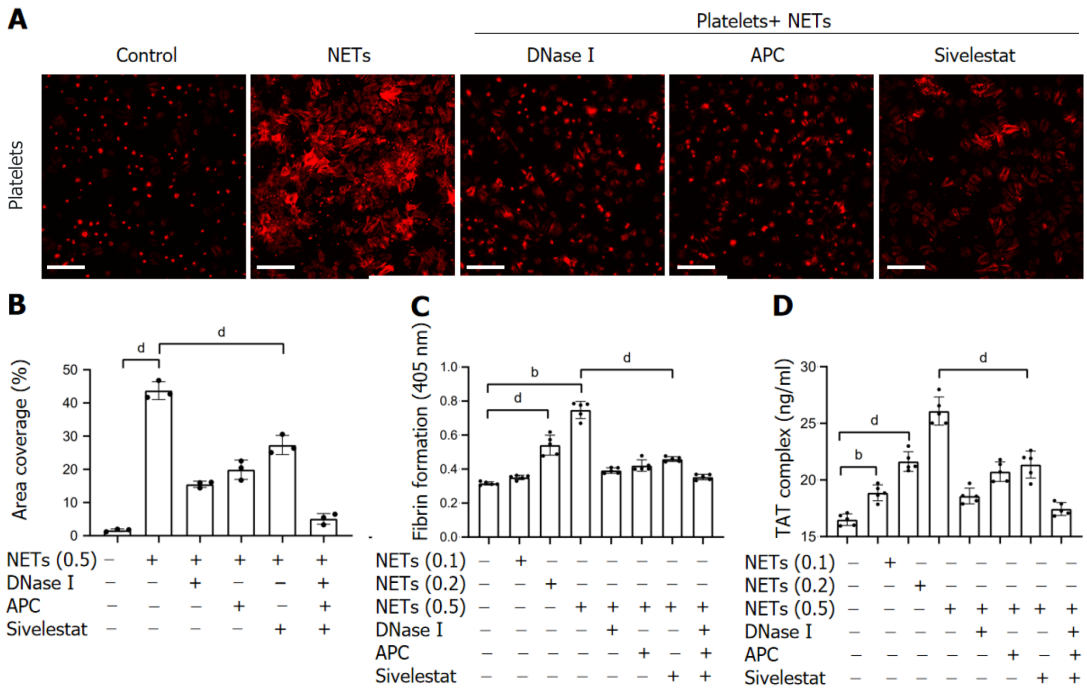

DOI: 10.3748/wjg.v28.26.3132

Figure 5 NETs promote platelet adhesion and prothrombotic state. A: Isolated platelets were incubated on glass slides which were coated with 1% dBSA, NETs (μg DNA/mL), or NETs pretreated with DNase I, APC, and sivelestat alone or together, followed by the F-actin components of platelets with 594-phalloidin staining. Magnification 63×; scale bars: 10 μm. Red-platelets; B: The percentage of area coverage of platelet adhesion was defined as the rate of red area in the total area and analyzed with ImageJ software; C: Isolated platelets were cocultured with different concentrations of NETs for 30 min with or without DNase I, APC and sivelestat treatment alone or together, and plasma fibrin formation was tested using turbidity measurements and monitored OD at 405 nm; D: TAT complex level of activated platelets was analyzed by ELISA. All values are the mean ± SD. $^{a}P < 0.05$; $^{b}P < 0.01$; $^{c}P < 0.001$; $^{d}P < 0.0001$. dBSA: Denatured bovine serum albumin; NETs: Neutrophil extracellular traps; DNase I: Deoxyribonuclease I; APC: Activated protein C; TAT: Thrombin–antithrombin.

induced NETs can also promote thrombosis *in vivo*. Here, in a mouse IVC flow stenosis model, tumor-bearing mice demonstrated more capacity to form thrombi and showed heavier weight and longer length of thrombi compared to control mice (Figure 7A–D). In the 6 h models, three of nine of control mice showed thrombi, whereas seven of nine of tumor-bearing mice formed thrombi. In the 48 h models, all mice demonstrated thrombi in the IVC. In addition, confocal images of thrombi formed in the tumor-bearing mice after 48 h of IVC stenosis showed that NETs were significantly accumulated compared to control mice (Figure 7E–H). The thrombi of control mice included some neutrophils (Ly6G+) but were not activated to form NETs (Figure 7E and G). Furthermore, tumor-bearing mice showed higher fibrin formation and TAT complex levels than control mice (Figure 7I and J).

In the inhibition assay, we infused DNase I into mice immediately after IVC stenosis and examined thrombosis after 6 or 48 h of surgery. We found that treatment with DNase I significantly inhibited thrombi formation in tumor-bearing IVC stenosis mice (Figure 7A–D). Furthermore, fibrin formation and TAT complex levels in tumor-bearing mice were significantly decreased by DNase I treatment (Figure 7I and J). These data suggest that NETs play a role in thrombosis *in vivo*, which was induced by GC, and inhibiting NETs by DNase I had a protective effect on thrombosis in this mouse model.

DISCUSSION

Inflammation is one of the hallmarks of cancer. Additionally, neutrophils are among the most important immune cells implicated in promoting tumor progression[40,41]. NETs participate in cancer progression by promoting the proliferation, invasion, metastasis and angiogenesis of cancer cells as well as thrombosis in numerous tumor types[42-44]. A recent study using mouse models with Jak^{2V617F} knock-in revealed that most myeloproliferative neoplasms display NET formation and DVT[45]. Our previous studies revealed that NETs promote the migration and metastasis of GC cells both *in vitro* and *in vivo* through epithelial mesenchymal transition[46]. Intriguingly, inhibition of NETs promotes apoptosis and inhibits the invasion of GC cells by regulating the expression of Bcl-2, Bax and nuclear factor-κB proteins[47]. Our initial studies revealed that NETs released by neutrophils in GC patients promoted the conversion of thrombin and fibrin[23]. Accordingly, we hypothesized that NETs promote thrombosis in GC patients. We investigated the interactions between GC cells, neutrophils, platelets and ECs, with a keen focus on their role in cancer-associated thrombosis.

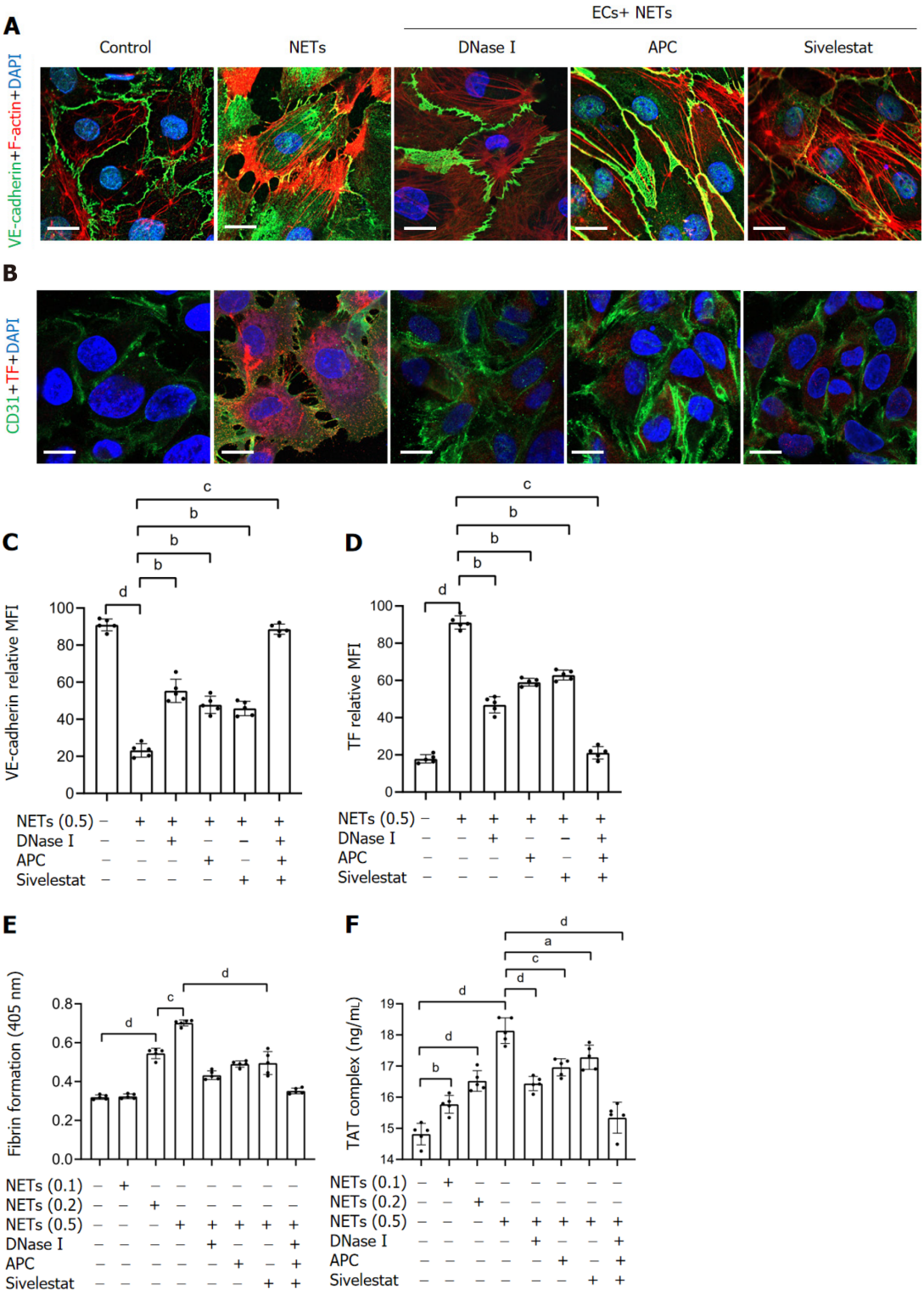

DOI: 10.3748/wjg.v28.26.3132

Figure 6 NETs drive hypercoagulation of ECs. A: ECs were cocultured with NETs (μg DNA/mL) or PBS in the presence of DNase I, APC, or sivelestat alone or together for 4 h and analyzed by confocal microscopy. The intercellular junctions of ECs were stained with VE–cadherin and phalloidin. Magnification 63×; scale bars: 10 μm. Red-phalloidin, Green-VE, and Blue-DAPI; B: EC activation was stained with CD31 and TF. Magnification 63×; scale bars: 10 μm. Red-TF, Green-CD31, and Blue-DAPI; C and D: VE–cadherin expression and TF expression on ECs were detected by confocal microscopy and analyzed with ImageJ software (expression indicated as MFI). MFI was defined as the ratio of total fluorescence intensity to the area; E and F: EC monolayers were stimulated with various concentrations of NETs for 4 h, followed by determination of fibrin formation by turbidity measurement at 405 nm, and the TAT complex level was detected by ELISA. All values are the mean ± SD. $^{a}P < 0.05$; $^{b}P < 0.01$; $^{c}P < 0.001$; $^{d}P < 0.0001$. NETs: Neutrophil extracellular traps; ECs: Endothelial cells; DNase I: Deoxyribonuclease I; APC: Activated protein C; TF: Tissue factor; TAT: Thrombin–antithrombin; MFI: Mean fluorescence intensity.

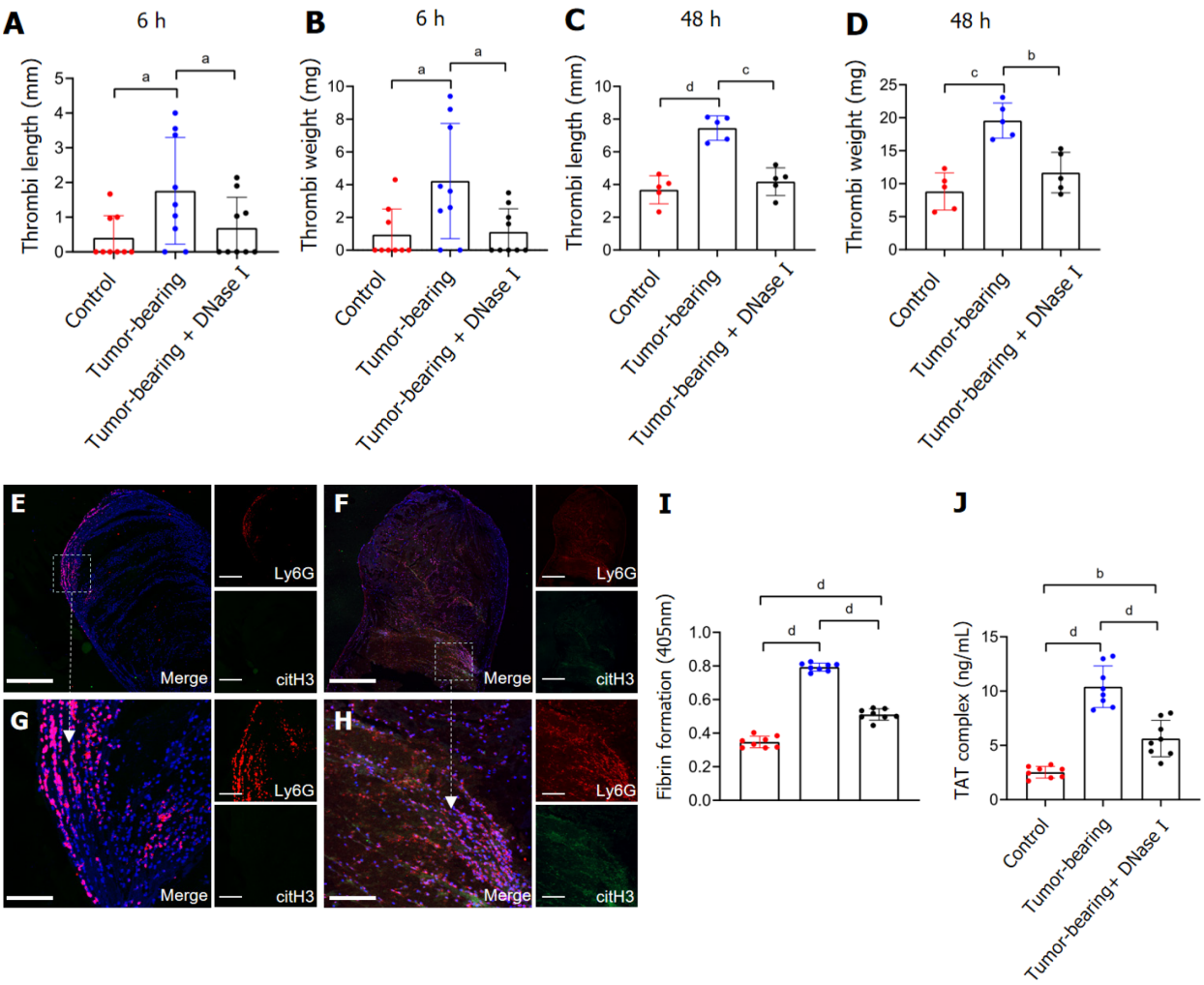

DOI: 10.3748/wjg.v28.i26.3132

Figure 7 Tumor-bearing mice show a greater ability to form thrombi by inferior vena cava flow restriction. A and B: The values for weight and length of thrombi present in control, tumor-bearing mice, DNase I infused tumor-bearing mice at 6 h after surgery. Each group, n = 9; C and D: Values for weight and length of thrombi present in mice at 48 h after surgery. Each group, n = 5; E and F: Confocal imaging of thrombi derived from control mice and tumor-bearing mice with Ly6G and citH3 staining. Magnification 10×; scale bars: 200 μm. Red-Ly6G, Green-citH3, and Blue-DAPI; G and H: Magnified (40×) part of thrombi derived from control mice and tumor-bearing mice. Scale bars: 50 μm. Red-Ly6G, Green-citH3, and Blue-DAPI; I and J: Fibrin formation levels in the plasma of control, tumor-bearing mice, or DNase-I-infused tumor-bearing mice were detected by turbidity measurement at 405 nm, and TAT complex levels were detected by ELISA. Each group, n = 8. All values are the mean ± SD. $^{a}P < 0.05$; $^{b}P < 0.01$; $^{c}P < 0.001$; $^{d}P < 0.0001$. DNase I: Deoxyribonuclease I; TAT: Thrombin–antithrombin.

In this study, we found that the levels of plasma NET markers and citH3-positive neutrophils were significantly higher in GC patients than in HDs. Expression of NETs decreased significantly after resection of GC tissues. Neutrophil infiltration and NET formation were upregulated in tumor tissues, relative to adjacent paratumor tissues of the same GC patient. The levels of serum D-dimer were positively correlated with tumor TNM stage, consistent with previous findings[48]. These findings suggest that the expression of NETs promotes GC development and thrombosis in the same group of patients.

It has been reported that hepatocellular cancer and hypoxic CM stimulate the production of NETs by neutrophils[44]. However, the relationship between GC cells and neutrophils is poorly understood. Our experiments demonstrated that both metastatic and nonmetastatic GC cancer cells directly stimulated production of NETs from neutrophils, contrary to GES-1 cells. CM of GC cells, but not that of GES-1, also induced the formation of neutrophil-related NETs. This suggests that NET formation is also mediated by factors secreted by GC cells. Inflammatory cytokines, such as interleukin (IL)-1β, IL-6, IL-8, and tumor necrosis factor-, as well as damage-associated molecular patterns, all overexpressed in tumor microenvironments, stimulate neutrophils to release NETs[49,50]. Although IL-8 is the cytokine with the highest overexpression in GC patients, whether it is the main mediator of NET formation and the subsequent underlying mechanism in GC remain to be validated.

A recent study showed that NETs promote thrombosis by activating and promoting the adhesion of platelets in the venous walls of pancreatic cancer patients[22]. Activated platelets express PS on their surface membranes[51]. Additionally, P-selectin expression on the surface membrane of platelets is also

associated with thrombosis[52]. In this study, we found that compared to HDs, PS and P-selectin expression on platelets was significantly higher in GC patients, particularly those with stage III/IV GC. NET treatment upregulated PS and P-selectin expression on platelets. Additionally, NETs stimulated the adhesion of normal platelets on glass slides. However, even though DNase I treatment modulated this phenomenon, some platelets still adhered to the glass slides, suggesting that other secretory factors participated in the adhesion property.

Previous studies have shown that histones in NETs promote thrombosis in colorectal cancer patients [53]. NE is another most abundant protein that binds NETs. Although this potent protein stimulates tumor progression both *in vitro* and *in vivo*, the mechanisms underlying NE-mediated cancer-associated thrombosis remain to be clarified. A recent study on DVT using mouse models showed that NE deficiency or NE inhibition alone does not completely inhibit DVT[54]. In this study, we found that hypercoagulation of platelets was not completely mediated by NET DNA, but also by other secretory proteins in the NETs, such as histones and NE. Consequently, DNase I treatment of NETs had no complete effect on hypercoagulation of platelets. However, a combination of DNase I, APC and sivelestat treatment almost completely inhibited hypercoagulation of platelets. Although sivelestat did not show a strong antihypercoagulation effect similar to DNase I, it nonetheless modulated the activation and adhesion of platelets. This demonstrated that histones and NE also participate in the activation and adhesion of platelets.

DVT can be triggered by injury to vascular ECs. Previous studies have shown that under certain malignancies, NETs can induce dysfunction and apoptosis of ECs[35]. In patients with chronic pancreatic disease and pancreatic cancer, NETs exert their cytotoxicity against ECs *via* intercellular cell adhesion molecule-1 and vascular cell adhesion molecule-1 expression[26]. Recent studies have shown that treatment of ECs with NETs derived from patients with colorectal cancer promotes and enhances the production of fibrin and the corresponding coagulation[53]. In this study, we found that NET treatment inhibited the secretion of intercellular junctions in ECs and promoted hypercoagulation of platelets by upregulating TF expression. Moreover, NET treatment upregulated the expression of PS on ECs. ECs activated by NETs significantly increased the level of TAT complexes and fibrin generation in the plasma of HDs. Given that a combination of DNase I, APC and sivelestat treatment completely inhibited hypercoagulation, the process was regulated through numerous mechanisms. These findings strongly suggest that NETs contribute to GC-associated thrombosis.

In the late stage of murine mammary tumor models, thrombi were found in lung vessels, and NETs accumulated, indicating that cancer-induced NETs contribute to the cancer-associated thrombosis[19]. Here, we demonstrated that GC-bearing mice have a greater ability to form thrombi than control mice have and that NETs were abundantly present in the thrombi of tumor-bearing mouse IVC stenosis models. Most of this response can be blocked by DNase I treatment, which was similar to previous studies. In DVT models, flow restriction of the IVC may result in a hypoxic microenvironment to recruit neutrophils and stimulate NET release. In addition, cancer cells often secrete more inflammatory factors, which aggravate the recruitment of neutrophils to form NETs under a hypoxic conditions[50]. Therefore, neutrophils are exposed to two major triggers of NET release: A tumor hypoxic environment and IVC flow restriction, which then participate in the development of thrombi in GC.

CONCLUSION

Our findings demonstrate that GC cells can directly induce NET formation, which in turn strongly increases the risks of VTE development both *in vitro* and *in vivo*. In addition, we found that not only NET DNA but also histones and NE participate in the development of cancer-associated thrombosis. Accordingly, NETs are potential therapeutic targets against VTE in GC patients.

ARTICLE HIGHLIGHTS

Research background

The development of venous thromboembolism (VTE) is associated with high mortality among gastric cancer (GC) patients. Neutrophil extracellular traps (NETs) have been reported to correlate with the prothrombotic state in some diseases, but it was rarely reported in GC patients.

Research motivation

Cancer cells exert a procoagulant activity (PCA) in their microenvironment, which is related to activation of the coagulation system. However, the molecular mechanism underlying PCA in GC patients is poorly understood.

Research objectives
The present study aimed to investigate the effect of NETs on the development of cancer-associated thrombosis in GC patients.

Research methods
The levels of NETs in blood and tissue samples of patients were analyzed by ELISA, flow cytometry, and immunofluorescence staining. NET generation and hypercoagulation of platelets and endothelial cells (ECs) *in vitro* were observed by immunofluorescence staining. NET PCA was determined by fibrin formation and thrombin–antithrombin complex assays. Thrombosis *in vivo* was measured in a murine model induced by flow stenosis in the inferior vena cava (IVC).

Research results
NETs were likely to form in blood and tissue samples of GC patients compared with healthy individuals. *In vitro* studies showed that GC cells and their conditioned medium, but not gastric mucosal epithelial cells, can stimulate NET release from neutrophils. Furthermore, NETs induced hypercoagulable state of platelets and ECs. In a model of IVC stenosis, tumor-bearing mice showed a stronger ability to form thrombi, and NETs abundantly accumulated in the thrombi of tumor-bearing mice compared with control mice. Notably, the combination of deoxyribonuclease, activated protein C, and sivelestat markedly abolished the PCA of NETs.

Research conclusions
Our findings demonstrate that GC-induced NETs strongly increase the risk of VTE development both *in vitro* and *in vivo*. NETs are potential therapeutic targets in the prevention and treatment of VTE in GC patients.

Research perspectives
The treatment strategies can consider the combination of traditional anticoagulant drugs and NETs inhibiting drugs, so as to reduce the risk of cancer associated thrombosis in patients with GC and improve the clinical treatment effect.

FOOTNOTES

Author contributions: Zou XM and Li JC designed the study, completed the experiments, and drafted the manuscript; Yang SF, Zhao TQ, and Jin JQ collected the patient clinical data and performed part of the experiments; Zhu L, Li CJ, and Chen CY participated in the animal experiments; Yang H and Zhang AG performed the statistical analysis; all authors have read and approved the final manuscript.

Supported by National Natural Science Foundation of China, No. 81672355.

Institutional review board statement: The study was reviewed and approved by the ethics committee of the Second Affiliated Hospital of Harbin Medical University (No. KY2016-032).

Institutional animal care and use committee statement: All animal experiments in this study were approved by the ethics committee of the Second Affiliated Hospital of Harbin Medical University (No. KY2016-032).

Conflict-of-interest statement: The authors declare no conflict of interest for this manuscript.

Data sharing statement: No additional data are available.

ARRIVE guidelines statement: The authors have read the ARRIVE guidelines, and the manuscript was prepared and revised according to the ARRIVE guidelines.

Country/Territory of origin: China

ORCID number: Jia-Cheng Li 0000-0002-0467-7225; Xiao-Ming Zou 0000-0002-9689-5026; Shi-Feng Yang 0000-0002-4395-6753; Jia-Qi Jin 0000-0002-7635-5452; Lei Zhu 0000-0002-7495-606X; Chang-Jian Li 0000-0003-0441-0368; Hao Yang 0000-0003-0952-3345; An-Ge Zhang 0000-0003-4772-1254; Tian-Qi Zhao 0000-0002-1938-1419; Chong-Yan Chen 0000-0003-2749-4891.

S-Editor: Fan JR
L-Editor: Kerr C Wang TQ
P-Editor: Fan JR

REFERENCES

1 **Sung H**, Ferlay J, Siegel RL, Laversanne M, Soerjomataram I, Jemal A, Bray F. Global Cancer Statistics 2020: GLOBOCAN Estimates of Incidence and Mortality Worldwide for 36 Cancers in 185 Countries. *CA Cancer J Clin* 2021; **71**: 209-249 [PMID: 33538338 DOI: 10.3322/caac.21660]

2 **Banks M**, Graham D, Jansen M, Gotoda T, Coda S, di Pietro M, Uedo N, Bhandari P, Pritchard DM, Kuipers EJ, Rodriguez-Justo M, Novelli MR, Ragunath K, Shepherd N, Dinis-Ribeiro M. British Society of Gastroenterology guidelines on the diagnosis and management of patients at risk of gastric adenocarcinoma. *Gut* 2019; **68**: 1545-1575 [PMID: 31278206 DOI: 10.1136/gutjnl-2018-318126]

3 **Farge D**, Bounameaux H, Brenner B, Cajfinger F, Debourdeau P, Khorana AA, Pabinger I, Solymoss S, Douketis J, Kakkar A. International clinical practice guidelines including guidance for direct oral anticoagulants in the treatment and prophylaxis of venous thromboembolism in patients with cancer. *Lancet Oncol* 2016; **17**: e452-e466 [PMID: 27733271 DOI: 10.1016/S1470-2045(16)30369-2]

4 **Kang MJ**, Ryoo BY, Ryu MH, Koo DH, Chang HM, Lee JL, Kim TW, Kang YK. Venous thromboembolism (VTE) in patients with advanced gastric cancer: an Asian experience. *Eur J Cancer* 2012; **48**: 492-500 [PMID: 22169121 DOI: 10.1016/j.ejca.2011.11.016]

5 **Khan F**, Tritschler T, Kahn SR, Rodger MA. Venous thromboembolism. *Lancet* 2021; **398**: 64-77 [PMID: 33984268 DOI: 10.1016/S0140-6736(20)32658-1]

6 **Tanizawa Y**, Bando E, Kawamura T, Tokunaga M, Makuuchi R, Iida K, Nanri K, Yoneyama M, Terashima M. Prevalence of deep venous thrombosis detected by ultrasonography before surgery in patients with gastric cancer: a retrospective study of 1140 consecutive patients. *Gastric Cancer* 2017; **20**: 878-886 [PMID: 27987041 DOI: 10.1007/s10120-016-0677-2]

7 **Jung YJ**, Seo HS, Park CH, Jeon HM, Kim JI, Yim HW, Song KY. Venous Thromboembolism Incidence and Prophylaxis Use After Gastrectomy Among Korean Patients With Gastric Adenocarcinoma: The PROTECTOR Randomized Clinical Trial. *JAMA Surg* 2018; **153**: 939-946 [PMID: 30027281 DOI: 10.1001/jamasurg.2018.2081]

8 **Wada T**, Fujiwara H, Morita S, Fukagawa T, Katai H. Incidence of and risk factors for preoperative deep venous thrombosis in patients undergoing gastric cancer surgery. *Gastric Cancer* 2017; **20**: 872-877 [PMID: 28120128 DOI: 10.1007/s10120-017-0690-0]

9 **Osaki T**, Saito H, Fukumoto Y, Kono Y, Murakami Y, Shishido Y, Kuroda H, Matsunaga T, Sato K, Hirooka Y, Fujiwara Y. Risk and incidence of perioperative deep vein thrombosis in patients undergoing gastric cancer surgery. *Surg Today* 2018; **48**: 525-533 [PMID: 29234961 DOI: 10.1007/s00595-017-1617-4]

10 **Varki A**. Trousseau's syndrome: multiple definitions and multiple mechanisms. *Blood* 2007; **110**: 1723-1729 [PMID: 17496204 DOI: 10.1182/blood-2006-10-053736]

11 **Brinkmann V**, Reichard U, Goosmann C, Fauler B, Uhlemann Y, Weiss DS, Weinrauch Y, Zychlinsky A. Neutrophil extracellular traps kill bacteria. *Science* 2004; **303**: 1532-1535 [PMID: 15001782 DOI: 10.1126/science.1092385]

12 **Brinkmann V**, Zychlinsky A. Beneficial suicide: why neutrophils die to make NETs. *Nat Rev Microbiol* 2007; **5**: 577-582 [PMID: 17632569 DOI: 10.1038/nrmicro1710]

13 **McDonald B**, Urrutia R, Yipp BG, Jenne CN, Kubes P. Intravascular neutrophil extracellular traps capture bacteria from the bloodstream during sepsis. *Cell Host Microbe* 2012; **12**: 324-333 [PMID: 22980329 DOI: 10.1016/j.chom.2012.06.011]

14 **Zeng H**, Fu X, Cai J, Sun C, Yu M, Peng Y, Zhuang J, Chen J, Chen H, Yu Q, Xu C, Zhou H, Cao Y, Hu L, Li J, Cao S, Gu C, Yan F, Chen G. Neutrophil Extracellular Traps may be a Potential Target for Treating Early Brain Injury in Subarachnoid Hemorrhage. *Transl Stroke Res* 2022; **13**: 112-131 [PMID: 33852132 DOI: 10.1007/s12975-021-00909-1]

15 **Zuo Y**, Yalavarthi S, Gockman K, Madison JA, Gudjonsson JE, Kahlenberg JM, Joseph McCune W, Bockenstedt PL, Karp DR, Knight JS. Anti-Neutrophil Extracellular Trap Antibodies and Impaired Neutrophil Extracellular Trap Degradation in Antiphospholipid Syndrome. *Arthritis Rheumatol* 2020; **72**: 2130-2135 [PMID: 32729667 DOI: 10.1002/art.41460]

16 **Cichon I**, Ortmann W, Bednarz A, Lenartowicz M, Kolaczkowska E. Reduced Neutrophil Extracellular Trap (NET) Formation During Systemic Inflammation in Mice With Menkes Disease and Wilson Disease: Copper Requirement for NET Release. *Front Immunol* 2019; **10**: 3021 [PMID: 32010131 DOI: 10.3389/fimmu.2019.03021]

17 **Marcos V**, Zhou Z, Yildirim AO, Bohla A, Hector A, Vitkov L, Wiedenbauer EM, Krautgartner WD, Stoiber W, Belohradsky BH, Rieber N, Kormann M, Koller B, Roscher A, Roos D, Griese M, Eickelberg O, Döring G, Mall MA, Hartl D. CXCR2 mediates NADPH oxidase-independent neutrophil extracellular trap formation in cystic fibrosis airway inflammation. *Nat Med* 2010; **16**: 1018-1023 [PMID: 20818377 DOI: 10.1038/nm.2209]

18 **Martins-Cardoso K**, Almeida VH, Bagri KM, Rossi MID, Mermelstein CS, König S, Monteiro RQ. Neutrophil Extracellular Traps (NETs) Promote Pro-Metastatic Phenotype in Human Breast Cancer Cells through Epithelial-Mesenchymal Transition. *Cancers (Basel)* 2020; **12** [PMID: 32545405 DOI: 10.3390/cancers12061542]

19 **Demers M**, Krause DS, Schatzberg D, Martinod K, Voorhees JR, Fuchs TA, Scadden DT, Wagner DD. Cancers predispose neutrophils to release extracellular DNA traps that contribute to cancer-associated thrombosis. *Proc Natl Acad Sci U S A* 2012; **109**: 13076-13081 [PMID: 22826226 DOI: 10.1073/pnas.1200419109]

20 **Thålin C**, Hisada Y, Lundström S, Mackman N, Wallén H. Neutrophil Extracellular Traps: Villains and Targets in Arterial, Venous, and Cancer-Associated Thrombosis. *Arterioscler Thromb Vasc Biol* 2019; **39**: 1724-1738 [PMID: 31315434 DOI: 10.1161/ATVBAHA.119.312463]

21 **Gomes T**, Várady CBS, Lourenço AL, Mizurini DM, Rondon AMR, Leal AC, Gonçalves BS, Bou-Habib DC, Medei E, Monteiro RQ. IL-1β Blockade Attenuates Thrombosis in a Neutrophil Extracellular Trap-Dependent Breast Cancer Model.

Front Immunol 2019; **10**: 2088 [PMID: 31552036 DOI: 10.3389/fimmu.2019.02088]

22 **Abdol Razak N**, Elaskalani O, Metharom P. Pancreatic Cancer-Induced Neutrophil Extracellular Traps: A Potential Contributor to Cancer-Associated Thrombosis. *Int J Mol Sci* 2017; **18** [PMID: 28245569 DOI: 10.3390/ijms18030487]

23 **Yang C**, Sun W, Cui W, Li X, Yao J, Jia X, Li C, Wu H, Hu Z, Zou X. Procoagulant role of neutrophil extracellular traps in patients with gastric cancer. *Int J Clin Exp Pathol* 2015; **8**: 14075-14086 [PMID: 26823721]

24 **Zhao L**, Bi Y, Kou J, Shi J, Piao D. Phosphatidylserine exposing-platelets and microparticles promote procoagulant activity in colon cancer patients. *J Exp Clin Cancer Res* 2016; **35**: 54 [PMID: 27015840 DOI: 10.1186/s13046-016-0328-9]

25 **Suzuki-Inoue K**. Platelets and cancer-associated thrombosis: focusing on the platelet activation receptor CLEC-2 and podoplanin. *Blood* 2019; **134**: 1912-1918 [PMID: 31778548 DOI: 10.1182/blood.2019001388]

26 **Gasiorowska A**, Talar-Wojnarowska R, Kaczka A, Borkowska A, Czupryniak L, Małecka-Panas E. Subclinical Inflammation and Endothelial Dysfunction in Patients with Chronic Pancreatitis and Newly Diagnosed Pancreatic Cancer. *Dig Dis Sci* 2016; **61**: 1121-1129 [PMID: 26597191 DOI: 10.1007/s10620-015-3972-6]

27 **Chang Z**, Zhang Y, Liu J, Zheng Y, Li H, Kong Y, Li P, Peng H, Shi Y, Cao B, Ran F, Chen Y, Song Y, Ye Q, Ding L. Snail promotes the generation of vascular endothelium by breast cancer cells. *Cell Death Dis* 2020; **11**: 457 [PMID: 32541667 DOI: 10.1038/s41419-020-2651-5]

28 **Li B**, Liu Y, Hu T, Zhang Y, Zhang C, Li T, Wang C, Dong Z, Novakovic VA, Shi J. Neutrophil extracellular traps enhance procoagulant activity in patients with oral squamous cell carcinoma. *J Cancer Res Clin Oncol* 2019; **145**: 1695-1707 [PMID: 31020419 DOI: 10.1007/s00432-019-02922-2]

29 **Zhang J**, Yu M, Liu B, Zhou P, Zuo N, Wang Y, Feng Y, Zhang Y, Wang J, He Y, Wu Y, Dong Z, Hong L, Shi J. Neutrophil extracellular traps enhance procoagulant activity and thrombotic tendency in patients with obstructive jaundice. *Liver Int* 2021; **41**: 333-347 [PMID: 33159371 DOI: 10.1111/liv.14725]

30 **Li T**, Wang C, Liu Y, Li B, Zhang W, Wang L, Yu M, Zhao X, Du J, Zhang J, Dong Z, Jiang T, Xie R, Ma R, Fang S, Zhou J, Shi J. Neutrophil Extracellular Traps Induce Intestinal Damage and Thrombotic Tendency in Inflammatory Bowel Disease. *J Crohns Colitis* 2020; **14**: 240-253 [PMID: 31325355 DOI: 10.1093/ecco-jcc/jjz132]

31 **Edge SB**, Compton CC. The American Joint Committee on Cancer: the 7th edition of the AJCC cancer staging manual and the future of TNM. *Ann Surg Oncol* 2010; **17**: 1471-1474 [PMID: 20180029 DOI: 10.1245/s10434-010-0985-4]

32 **Koupenova M**, Corkrey HA, Vitseva O, Manni G, Pang CJ, Clancy L, Yao C, Rade J, Levy D, Wang JP, Finberg RW, Kurt-Jones EA, Freedman JE. The role of platelets in mediating a response to human influenza infection. *Nat Commun* 2019; **10**: 1780 [PMID: 30992428 DOI: 10.1038/s41467-019-09607-x]

33 **Brill A**, Fuchs TA, Chauhan AK, Yang JJ, De Meyer SF, Köllnberger M, Wakefield TW, Lämmle B, Massberg S, Wagner DD. von Willebrand factor-mediated platelet adhesion is critical for deep vein thrombosis in mouse models. *Blood* 2011; **117**: 1400-1407 [PMID: 20959603 DOI: 10.1182/blood-2010-05-287623]

34 **Yang LY**, Luo Q, Lu L, Zhu WW, Sun HT, Wei R, Lin ZF, Wang XY, Wang CQ, Lu M, Jia HL, Chen JH, Zhang JB, Qin LX. Increased neutrophil extracellular traps promote metastasis potential of hepatocellular carcinoma *via* provoking tumorous inflammatory response. *J Hematol Oncol* 2020; **13**: 3 [PMID: 31907001 DOI: 10.1186/s13045-019-0836-0]

35 **Folco EJ**, Mawson TL, Vromman A, Bernardes-Souza B, Franck G, Persson O, Nakamura M, Newton G, Luscinskas FW, Libby P. Neutrophil Extracellular Traps Induce Endothelial Cell Activation and Tissue Factor Production Through Interleukin-1α and Cathepsin G. *Arterioscler Thromb Vasc Biol* 2018; **38**: 1901-1912 [PMID: 29976772 DOI: 10.1161/ATVBAHA.118.311150]

36 **Zhou P**, Li T, Jin J, Liu Y, Li B, Sun Q, Tian J, Zhao H, Liu Z, Ma S, Zhang S, Novakovic VA, Shi J, Hu S. Interactions between neutrophil extracellular traps and activated platelets enhance procoagulant activity in acute stroke patients with ICA occlusion. *EBioMedicine* 2020; **53**: 102671 [PMID: 32114386 DOI: 10.1016/j.ebiom.2020.102671]

37 **Brill A**, Fuchs TA, Savchenko AS, Thomas GM, Martinod K, De Meyer SF, Bhandari AA, Wagner DD. Neutrophil extracellular traps promote deep vein thrombosis in mice. *J Thromb Haemost* 2012; **10**: 136-144 [PMID: 22044575 DOI: 10.1111/j.1538-7836.2011.04544.x]

38 **Najmeh S**, Cools-Lartigue J, Giannias B, Spicer J, Ferri LE. Simplified Human Neutrophil Extracellular Traps (NETs) Isolation and Handling. *J Vis Exp* 2015 [PMID: 25938591 DOI: 10.3791/52687]

39 **Fuchs TA**, Brill A, Duerschmied D, Schatzberg D, Monestier M, Myers DD Jr, Wrobleski SK, Wakefield TW, Hartwig JH, Wagner DD. Extracellular DNA traps promote thrombosis. *Proc Natl Acad Sci U S A* 2010; **107**: 15880-15885 [PMID: 20798043 DOI: 10.1073/pnas.1005743107]

40 **Bodac A**, Meylan E. Neutrophil metabolism in the cancer context. *Semin Immunol* 2021; 101583 [PMID: 34963565 DOI: 10.1016/j.smim.2021.101583]

41 **Ustyanovska Avtenyuk N**, Visser N, Bremer E, Wiersma VR. The Neutrophil: The Underdog That Packs a Punch in the Fight against Cancer. *Int J Mol Sci* 2020; **21** [PMID: 33105656 DOI: 10.3390/ijms21217820]

42 **Zha C**, Meng X, Li L, Mi S, Qian D, Li Z, Wu P, Hu S, Zhao S, Cai J, Liu Y. Neutrophil extracellular traps mediate the crosstalk between glioma progression and the tumor microenvironment **via** the HMGB1/RAGE/IL-8 axis. *Cancer Biol Med* 2020; **17**: 154-168 [PMID: 32296583 DOI: 10.20892/j.issn.2095-3941.2019.0353]

43 **Itatani Y**, Yamamoto T, Zhong C, Molinolo AA, Ruppel J, Hegde P, Taketo MM, Ferrara N. Suppressing neutrophil-dependent angiogenesis abrogates resistance to anti-VEGF antibody in a genetic model of colorectal cancer. *Proc Natl Acad Sci U S A* 2020; **117**: 21598-21608 [PMID: 32817421 DOI: 10.1073/pnas.2008112117]

44 **Tohme S**, Yazdani HO, Al-Khafaji AB, Chidi AP, Loughran P, Mowen K, Wang Y, Simmons RL, Huang H, Tsung A. Neutrophil Extracellular Traps Promote the Development and Progression of Liver Metastases after Surgical Stress. *Cancer Res* 2016; **76**: 1367-1380 [PMID: 26759232 DOI: 10.1158/0008-5472.CAN-15-1591]

45 **Wolach O**, Sellar RS, Martinod K, Cherpokova D, McConkey M, Chappell RJ, Silver AJ, Adams D, Castellano CA, Schneider RK, Padera RF, DeAngelo DJ, Wadleigh M, Steensma DP, Galinsky I, Stone RM, Genovese G, McCarroll SA, Iliadou B, Hultman C, Neuberg D, Mullally A, Wagner DD, Ebert BL. Increased neutrophil extracellular trap formation promotes thrombosis in myeloproliferative neoplasms. *Sci Transl Med* 2018; **10** [PMID: 29643232 DOI: 10.1126/scitranslmed.aan8292]

46 **Zhu T**, Zou X, Yang C, Li L, Wang B, Li R, Li H, Xu Z, Huang D, Wu Q. Neutrophil extracellular traps promote gastric

cancer metastasis by inducing epithelialmesenchymal transition. *Int J Mol Med* 2021; **48** [PMID: 34013374 DOI: 10.3892/ijmm.2021.4960]

47 **Li R**, Zou X, Zhu T, Xu H, Li X, Zhu L. Destruction of Neutrophil Extracellular Traps Promotes the Apoptosis and Inhibits the Invasion of Gastric Cancer Cells by Regulating the Expression of Bcl-2, Bax and NF-κB. *Onco Targets Ther* 2020; **13**: 5271-5281 [PMID: 32606746 DOI: 10.2147/OTT.S227331]

48 **Zhang Y**, Hu Y, Ma C, Sun H, Wei X, Li M, Wei W, Zhang F, Yang F, Wang H, Gu K. Diagnostic, Therapeutic Predictive, and Prognostic Value of Neutrophil Extracellular Traps in Patients With Gastric Adenocarcinoma. *Front Oncol* 2020; **10**: 1036 [PMID: 32714865 DOI: 10.3389/fonc.2020.01036]

49 **Keshari RS**, Jyoti A, Dubey M, Kothari N, Kohli M, Bogra J, Barthwal MK, Dikshit M. Cytokines induced neutrophil extracellular traps formation: implication for the inflammatory disease condition. *PLoS One* 2012; **7**: e48111 [PMID: 23110185 DOI: 10.1371/journal.pone.0048111]

50 **Liu Y**, Yan W, Tohme S, Chen M, Fu Y, Tian D, Lotze M, Tang D, Tsung A. Hypoxia induced HMGB1 and mitochondrial DNA interactions mediate tumor growth in hepatocellular carcinoma through Toll-like receptor 9. *J Hepatol* 2015; **63**: 114-121 [PMID: 25681553 DOI: 10.1016/j.jhep.2015.02.009]

51 **Harper MT**, Poole AW. Chloride channels are necessary for full platelet phosphatidylserine exposure and procoagulant activity. *Cell Death Dis* 2013; **4**: e969 [PMID: 24357800 DOI: 10.1038/cddis.2013.495]

52 **Cleary SJ**, Hobbs C, Amison RT, Arnold S, O'Shaughnessy BG, Lefrançais E, Mallavia B, Looney MR, Page CP, Pitchford SC. LPS-induced Lung Platelet Recruitment Occurs Independently from Neutrophils, PSGL-1, and P-Selectin. *Am J Respir Cell Mol Biol* 2019; **61**: 232-243 [PMID: 30768917 DOI: 10.1165/rcmb.2018-0182OC]

53 **Zhang Y**, Wang C, Yu M, Zhao X, Du J, Li Y, Jing H, Dong Z, Kou J, Bi Y, Novakovic VA, Zhou J, Shi J. Neutrophil extracellular traps induced by activated platelets contribute to procoagulant activity in patients with colorectal cancer. *Thromb Res* 2019; **180**: 87-97 [PMID: 31271975 DOI: 10.1016/j.thromres.2019.06.005]

54 **Martinod K**, Witsch T, Farley K, Gallant M, Remold-O'Donnell E, Wagner DD. Neutrophil elastase-deficient mice form neutrophil extracellular traps in an experimental model of deep vein thrombosis. *J Thromb Haemost* 2016; **14**: 551-558 [PMID: 26712312 DOI: 10.1111/jth.13239]

World Journal of Gastroenterology

Submit a Manuscript: https://www.f6publishing.com

World J Gastroenterol 2022 July 14; 28(26): 3150-3163

DOI: 10.3748/wjg.v28.i26.3150

ISSN 1007-9327 (print) ISSN 2219-2840 (online)

ORIGINAL ARTICLE

Basic Study

Activation of natural killer T cells contributes to Th1 bias in the murine liver after 14 d of ethinylestradiol exposure

Meng-Zhi Zou, Wei-Chao Kong, Heng Cai, Meng-Tao Xing, Zi-Xun Yu, Xin Chen, Lu-Yong Zhang, Xin-Zhi Wang

Specialty type: Toxicology

Provenance and peer review: Invited article; Externally peer reviewed.

Peer-review model: Single blind

Peer-review report's scientific quality classification

Grade A (Excellent): 0
Grade B (Very good): B
Grade C (Good): 0
Grade D (Fair): 0
Grade E (Poor): 0

P-Reviewer: Imai Y, Japan
A-Editor: Lin FY, China

Received: October 26, 2021
Peer-review started: October 26, 2021
First decision: April 16, 2022
Revised: April 25, 2022
Accepted: May 22, 2022
Article in press: May 22, 2022
Published online: July 14, 2022

Meng-Zhi Zou, Wei-Chao Kong, Heng Cai, Zi-Xun Yu, Xin Chen, Lu-Yong Zhang, Xin-Zhi Wang, New Drug Screening Center, China Pharmaceutical University, Nanjing 210009, Jiangsu Province, China

Meng-Tao Xing, Department of Pharmacology, China Pharmaceutical University, Nanjing 210009, Jiangsu Province, China

Lu-Yong Zhang, Center for Drug Research and Development, Guangdong Pharmaceutical University, Guangzhou 510006, Guangdong Province, China

Corresponding author: Xin-Zhi Wang, PhD, Associate Research Scientist, New Drug Screening Center, China Pharmaceutical University, No. 24 Tongjiaxiang, Nanjing 210009, Jiangsu Province, China. wangxz@cpu.edu.cn

Abstract

BACKGROUND

As the main component of oral contraceptives (OCs), ethinylestradiol (EE) has been widely applied as a model drug to induce murine intrahepatic cholestasis. The clinical counterpart of EE-induced cholestasis includes women who are taking OCs, sex hormone replacement therapy, and susceptible pregnant women. Taking intrahepatic cholestasis of pregnancy (ICP) as an example, ICP consumes the medical system due to its high-risk fetal burden and the impotency of ursodeoxycholic acid in reducing adverse perinatal outcomes.

AIM

To explore the mechanisms and therapeutic strategies of EE-induced cholestasis based on the liver immune microenvironment.

METHODS

Male C57BL/6J mice or invariant natural killer T (iNKT) cell deficiency (Jα18$^{-/-}$ mice) were administered with EE (10 mg/kg, subcutaneous) for 14 d.

RESULTS

Both Th1 and Th2 cytokines produced by NKT cells increased in the liver skewing toward a Th1 bias. The expression of the chemokine/chemokine receptor Cxcr6/Cxcl16, toll-like receptors, Ras/Rad, and PI3K/Bad signaling was upregulated after EE administration. EE also influenced bile acid synthase

Cyp7a1, Cyp8b1, and tight junctions ZO-1 and Occludin, which might be associated with EE-induced cholestasis. iNKT cell deficiency (Jα18$^{-/-}$ mice) robustly alleviated cholestatic liver damage and lowered the expression of the abovementioned signaling pathways.

CONCLUSION

Hepatic NKT cells play a pathogenic role in EE-induced intrahepatic cholestasis. Our research improves the understanding of intrahepatic cholestasis by revealing the hepatic immune microenvironment and also provides a potential clinical treatment by regulating iNKT cells.

Key Words: Natural killer T cell; Th1/Th2; IFN-γ; Estrogen; Cholestasis

Core Tip: In this study, we observed the production of both Th1 and Th2 cytokines by natural killer T (NKT) cells in the liver after 14 d of exposure to ethinylestradiol-induced cholestasis. The liver immune microenvironment was also skewed toward a Th1 bias mainly contributed by NKT cells. Invariant NKT cell deficiency robustly alleviated cholestatic liver damage and downregulated the associated signaling pathways, highlighting the pathogenic role and therapeutic potential of hepatic NKT cells in cholestatic liver diseases.

Citation: Zou MZ, Kong WC, Cai H, Xing MT, Yu ZX, Chen X, Zhang LY, Wang XZ. Activation of natural killer T cells contributes to Th1 bias in the murine liver after 14 d of ethinylestradiol exposure. *World J Gastroenterol* 2022; 28(26): 3150-3163

URL: https://www.wjgnet.com/1007-9327/full/v28/i26/3150.htm

DOI: https://dx.doi.org/10.3748/wjg.v28.i26.3150

INTRODUCTION

Cholestasis is a mild and common phenomenon during liver diseases but also a crucial triggering element of severe hepatopathy, such as fibrosis, cirrhosis, and hepatic venous thrombosis[1]. Both estrogen and oral contraceptives (OCs) can elicit intrahepatic cholestasis (IHC), whose effects manifest as retention of toxic bile acids in the liver and circulation[2]. 17α-ethinylestradiol (EE) is used as a model drug to induce murine IHC. As the predominant component of OCs and hormone replacement therapy, the clinical counterpart of EE-induced IHC includes women who are taking OCs, postmenopausal replacement therapy and susceptible pregnant women. Sex steroids may lead to alterations in bile components and the elevation of total bile acids (TBAs), which may induce apoptosis and oxidative stress and thus have harmful effects on hepatocytes and other organs[3]. In clinical studies, administration of EE to both males and females leads to increased serum TBA levels and decreased clearance of sulfobromophthalein[4]. In murine studies, the mechanisms involve the activation of AMP-activated protein kinase[5] and estrogen receptor α[6], the inhibition of farnesoid X receptor (FXR), bile acid transporters, bile acid synthase and metabolism enzymes, and inflammatory reactions[7-9]. The first-line therapy ursodeoxycholic acid (UDCA) for cholestatic diseases is a naturally hydrophilic bile acid, although its potency is limited, as approximately 40% of patients are not responsive to UDCA treatment [10].

Among these predisposing factors, the significance of the local immune microenvironment in the liver has been emphasized because sex hormones are immunomodulators that are metabolized in the liver. In a murine model of EE-induced cholestasis, hepatic expression of TNF-α and IL-6 was greatly upregulated[8]. Proinflammatory mediators can affect nuclear receptors and transporters and then cause bile acid equilibrium disorder, increased cytokine secretion, and further exacerbated cholestasis, forming a positive regulation loop[8]. In patients with intrahepatic cholestasis of pregnancy (ICP), an increase in Th1-type cytokines and a decrease in Th2-type cytokines suggest the involvement of proinflammatory and cytotoxic Th1 biases in ICP[11]. However, the impotency of corticosteroids in the treatment of cholestasis indicates that promising therapies or active agents are in heavy demand[12].

Natural killer T (NKT) cells are one of the most abundant lymphocytes in the liver, and their role in cholestasis is noteworthy[13]. NKT cells behave similarly to conventional T cells and function as both effector and regulatory immune cells. Jα18$^{-/-}$ mice are not prone to developing cholestatic liver injury after alpha-naphthylisothiocyanate (ANIT) administration due to the invariant NKT-cell (iNKT cell) knockout-related reduction in cytokines and the restored expression of transporters and bile acid metabolism enzymes[14]. Recent work also demonstrated that IL-4 secreted by type 1 NKT cells (iNKT cells) may inhibit type 2 NKT cells and upregulate immunoregulators, affecting the expression of bile

acid nuclear receptors, transporters, and CYP450 enzymes, thus exacerbating triptolide-induced cholestatic liver damage[15]. However, Jα18$^{-/-}$ mice showed aggravation of liver damage after bile duct ligation (BDL) surgery compared with wild-type mice due to the increase in neutrophils, chemokines and cytokines[16]. Moreover, knockout of the bile acid sensor FXR gene increases liver NKT cells and aggravates liver damage, indicating that FXR can regulate the activation of liver NKT cells[17]. Certain antigens that can activate NKT cells exist in the bile of patients with chronic liver diseases[18]. Thus, the aim of the present study was to investigate the effects and mechanisms of NKT cells in a murine model of EE-induced cholestatic hepatotoxicity.

MATERIALS AND METHODS

Reagents

17α-EE (CAS:57-63-6, batch number: E0037, contents > 98.0% (T) high performance liquid chromatography) was purchased from tcichemicals (Shanghai, China). EE was dissolved in an 80% 1,2-propylene glycol solution and diluted with physiological saline to a dosing concentration of 10 mg/kg before the experiment. Anti-CD16/32 antibody (clone: 2.4G2), which was used for blocking before staining, anti-CD3e-FITC antibody (clone: 145-2C11), anti-CD49b-APC antibody (clone: DX5), leukocyte activation cocktail with BD GolgiPlug™, anti-IFN-γ-PE antibody (clone: XMG1.2), and anti-IL-4-PE antibody (clone: 11B11) were purchased from BD Pharmingen (San Diego, CA, United States).

Animals and treatment

Male C57BL/6J mice (6-8 wk of age and 18-20 g of weight) were obtained from SLAC Laboratory Animal Co., Ltd. (Shanghai, China). iNKT cell-deficient Jα18$^{-/-}$ mice on a C57BL/6 background (6 to 8 wk old) were kindly provided by Dr. Li Bai (University of Science and Technology of China). All mice were administered physiological saline or EE (10 mg/kg) subcutaneously (s.c.) for 14 continuous d. Each group contained 6 mice. All mice were maintained and bred under controlled conditions (pathogen-free, 22 ± 2 °C, 12:12-h light-dark regular photoperiod) with ad libitum mouse chow and water access. The animals were housed in the laboratory for 1 wk prior to experiments to acclimate. All procedures involved in this study were performed under the Ethical Committee of China Pharmaceutical University and the Laboratory Animal Management Committee of Jiangsu Province guidelines (Approval No.: 2021-10-003).

Nonparenchymal cell isolation and labeling

After perfusing saline solution into the heart to eliminate blood, the mouse liver was minced through a 200-gauge nylon mesh and washed with cold PBS. After centrifugation at 50 × g for 2 min in the crude solution, the separated supernatant was centrifuged for another 10 min at 800 × g. The cell pellets were resuspended in 40% Percoll for centrifugation at 1250 × g for 15 min. After nonparenchymal cell (NPC) isolation from the cell pellets by red blood cell lysis solution (0.15 M NH4Cl and 0.1 mmol/L Na2EDTA) treatment and 2 washes, NPCs were stimulated with leukocyte activation cocktail for 4-5 h (BD Pharmingen).

After stimulation, NPCs were blocked with anti-CD16/32 and then surface-labeled with FITC-conjugated anti-mouse CD3e and APC-CD49b antibodies. NPCs were permeabilized with Cytofix/Cytoperm (Becton Dickinson) following the manufacturer's instructions, and intracellular staining was performed by incubation with IFN-γ or IL-4 antibodies. After each step, unbound antibodies were excluded from the system by centrifugation. Then, the cells were analyzed using a FACSCalibur flow cytometer (Becton Dickinson, Palo Alto, CA, United States), with 50000 events recorded per tube. The results were processed using FlowJo version 10 software (FlowJo, Ashland, OR, United States). The gating strategy was as follows: first, NPCs were gated by FSC and SSC, followed by the gating of CD3e$^+$ or CD3e$^-$ cells. CD49b$^+$ IFN-γ$^+$, CD49b$^+$ IL-4$^+$ or CD49b$^-$ IFN-γ$^+$, and CD49b$^-$ IL-4$^+$ cells were then gated and analyzed.

Blood biochemical analysis

Anticoagulant-free serum was collected and then analyzed for the levels of alkaline phosphatase (ALP), total bile acid (TBA), alanine transaminase (ALT), and aspartate transaminase (AST) using the ALP, ALT, and AST quantification kit (Whitman Biotech, Nanjing, China) and TBA quantification kit (Jiancheng Bioengineering Institute, Nanjing, China).

Histopathology and immunohistochemistry

The liver lobules were fixed, paraffin embedded, sectioned, and stained with hematoxylin and eosin for histopathological examination. Slides were coded, randomized, and assessed by pathologists who, during the evaluation of the slides, were blinded to the treatment groups. Scoring for liver injury was conducted according to the following criteria: no hepatocellular necrosis, proliferation of pseudocholangiolar duct, or inflammatory cell infiltration, 0; mild, 1; moderate, 2; severe, 3. The other sections were

Table 1 The primer sequence used for real-time polymerase chain reaction in mice

Name	Forward (5' to 3')	Reserve (5' to 3')
Gapdh	CATCACTGCCACCCAGAAGACTG	ATGCCAGTGAGCTTCCCGTTCAG
Tlr2	TGCTCCTGCGAACTCCTATC	CAGACTCCAGACACCAGTGC
Tlr4	AGCTTCTCCAATTTTTCAGAACTTC	TGAGAGGTGGTGTAAGCCATGC
Tlr6	AGCCAAGACAGAAAACCCATC	GGGGTCATGCTTCCGACTAT
Tlr7	CACCACCAATCTTACCCTTACC	CAGATGGTTCAGCCTACGGAA
Tlr9	GCTGTCAATGGCTCTCAGTTCC	CCTGCAACTGTGGTAGCTCACT
Cxcr6	GGTTCTTCCTGCCATTGCTCAC	GCAGGAACACAGCCACTACAAG
Cxcl16	GCAGGGTACTTTGGATCACATCC	AGTTCACGGACCCACTGGTCTT
Ras	TCGCACTGTTGAGTCTCGGCAG	TATGCTGCCGAATCTCACGGAC
Raf	CGCCAAGTCAATCATCCACAGAG	CACCGAGATTTCACTGTGGCTAG
Pi3k	CACCTGAACAGACAAGTAGAGGC	GCAAAGCATCCATGAAGTCTGGC
Bad	GGGAGCAACATTCATCAGCAGG	CGTCCTCGAAAAGGGCTAAGCT

subjected to IHC for semiquantification of the expression of toll-like receptor (TLR) 9 (Novus, 26C593.2, dilution percentage: 1:200).

RNA extraction and real-time polymerase chain reaction

RNA was extracted from liver sections by TRIzol reagent (Vazyme Biotech, Nanjing, China). Isolated RNA was processed by the HiScript™ Q RT SuperMix for quantitative polymerase chain reaction (qPCR) (+ gDNA wiper) kit (Vazyme Biotech) for cDNA synthesis. A 20 μL real-time PCR system was prepared according to the manufacturer's instructions. The mRNA levels were normalized to the housekeeping gene *Gapdh*. The primer sequences used are shown in Table 1.

Statistical analysis

Values are expressed as the means ± SE. The groups were evaluated using Student's *t* test. A P value < 0.05 was considered statistically significant.

RESULTS

EE promotes hepatic NKT-cell proliferation along with biased Th1 cytokine production

Increased activation of NKT cells, T cells, or NK cells has been reported to contribute to the pathophysiology of cholestasis[15,19,20]. Here, we measured and analyzed their percentages and Th1/Th2 cytokine production to evaluate their activation. Hepatic NKT cells, $CD3^+$ T cells (excluding NKT cells) and NK cells were defined as $CD3e^+CD49b^+$ (Figure 1A upper right), $CD3e^+CD49b^-$ (Figure 1A lower right), and $CD3e^-CD49b^+$ (Figure 1A upper left), respectively. After EE administration, the percentage of hepatic NKT cells expanded more than 3-fold compared with the control group, while the frequencies of $CD3^+$ T cells and NK cells showed no significant changes (Figure 1A-D). Both IFN-γ and IL-4 secreted from NKT cells increased, which further indicated NKT-cell activation. Moreover, the upregulated Th1/Th2 ratios indicated that a skewed hepatic Th1 immune response was due to NKT cells (Figure 1E–I). Compared with the control group, IL-4 secreted by $CD3^+$ T cells and NK cells increased, and their IFN-γ secretion and Th1/Th2 ratios remained unaltered (Figure 1J–Q).

iNKT cells exacerbate EE-induced cholestatic liver damage

For further investigation of the NKT-cell effect, cholestatic liver injury was compared between iNKT cell knockout mice (Jα18$^{-/-}$ mice) and C57BL/6J mice after EE administration. Compared with the control group, EE induced increased levels of ALP, TBA, ALT, and AST in C57BL/6J mice. Compared with C57BL/6J mice, Jα18$^{-/-}$ mice demonstrated significantly lower levels of ALP, TBA, ALT, and AST (Figure 2A-D). Based on the scoring criteria[21], the histopathological and hepatic injury score results showed proliferation of pseudocholangiolar duct (yellow arrows), inflammatory cell infiltration (red arrows) and hepatocyte necrosis (black arrows) after EE treatment, whereas Jα18$^{-/-}$ mice exhibited reduced proliferation of the pseudocholangiolar duct, inflammatory cell infiltration, and necrosis (Figure 2E-G). These results showed that iNKT cell-deficient mice can inhibit the development of cholestatic hepatotoxicity induced by EE, indicating a pathogenic effect exerted by iNKT cells on EE-

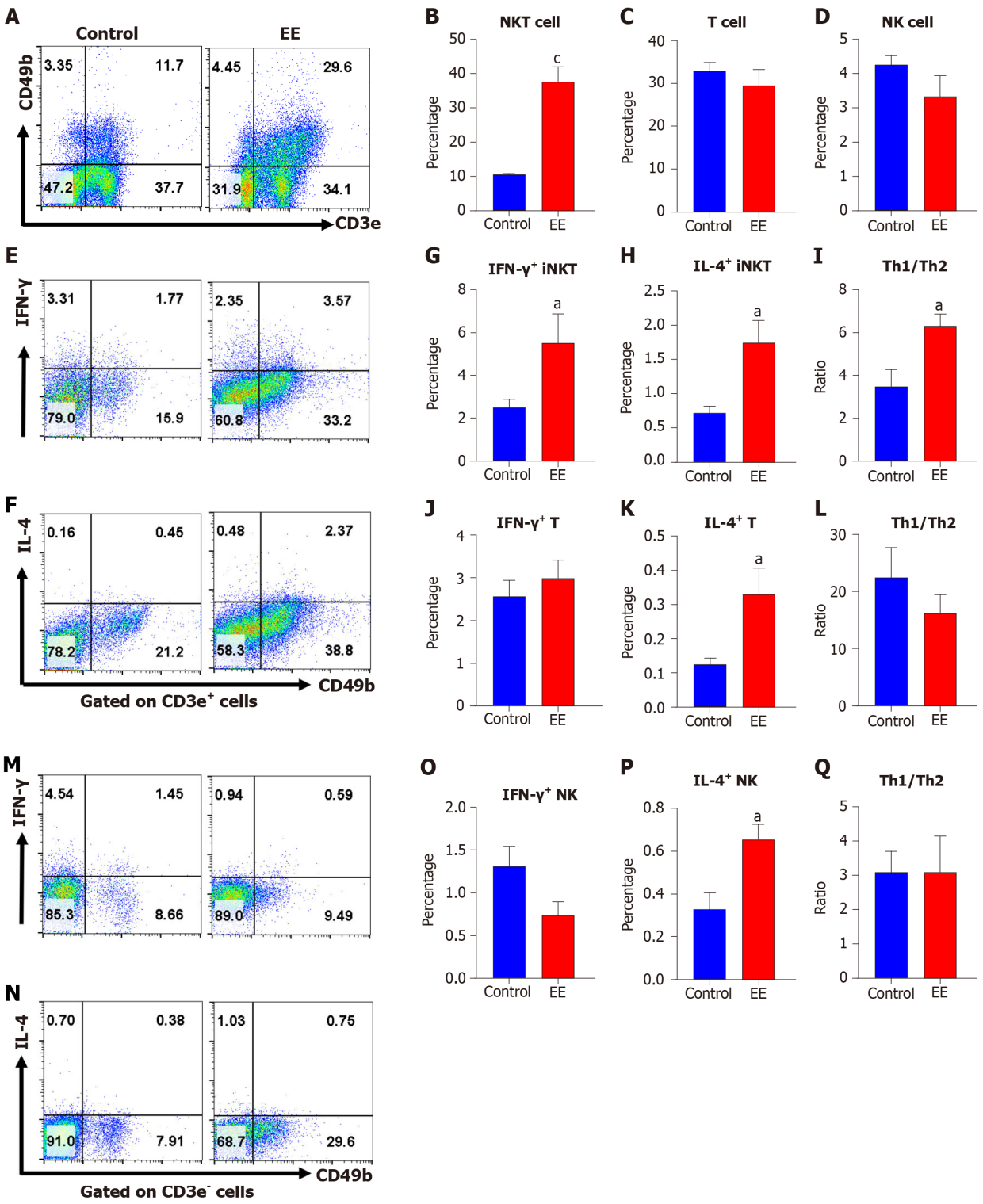

DOI: 10.3748/wjg.v28.i26.3150

Figure 1 Ethinylestradiol promotes hepatic natural killer T cell proliferation along with biased Th1 cytokine production. A: The percentage of hepatic natural killer T (NKT) cells, T cells and NK cells were detected and defined as $CD3e^+CD49b^+$ (upper right), $CD3e^+CD49b^-$ (lower right), $CD3e^-CD49b^+$ (upper left), respectively; B: Proportion analysis and comparison of NKT cells; C: Proportion analysis and comparison of T cells; D: Proportion analysis and comparison of NK cells; E and F: Th1 cytokine (IFN-γ) (E) and Th2 cytokine (IL-4) (F) produced by NKT cells and T cells were detected, respectively; G: IFN-γ produced by NKT cells; H: IL-4 produced by NKT cells; I: The ratio of Th1/Th2 by NKT cells; J: IFN-γ produced by T cells; K: IL-4 produced by T cells; L: The ratio of Th1/Th2 by T cells; M and N: Th1 cytokine (IFN-γ) (M) and Th2 cytokine (IL-4) (N) produced by NK cells were detected; O: IFN-γ produced by NK cells; P: IL-4 produced by NK cells; Q: The ratio of Th1/Th2 by NK cells. All values are the means ± SE (n = 4-6). $^aP < 0.05$, $^cP < 0.001$ *vs* control.

induced cholestatic liver damage.

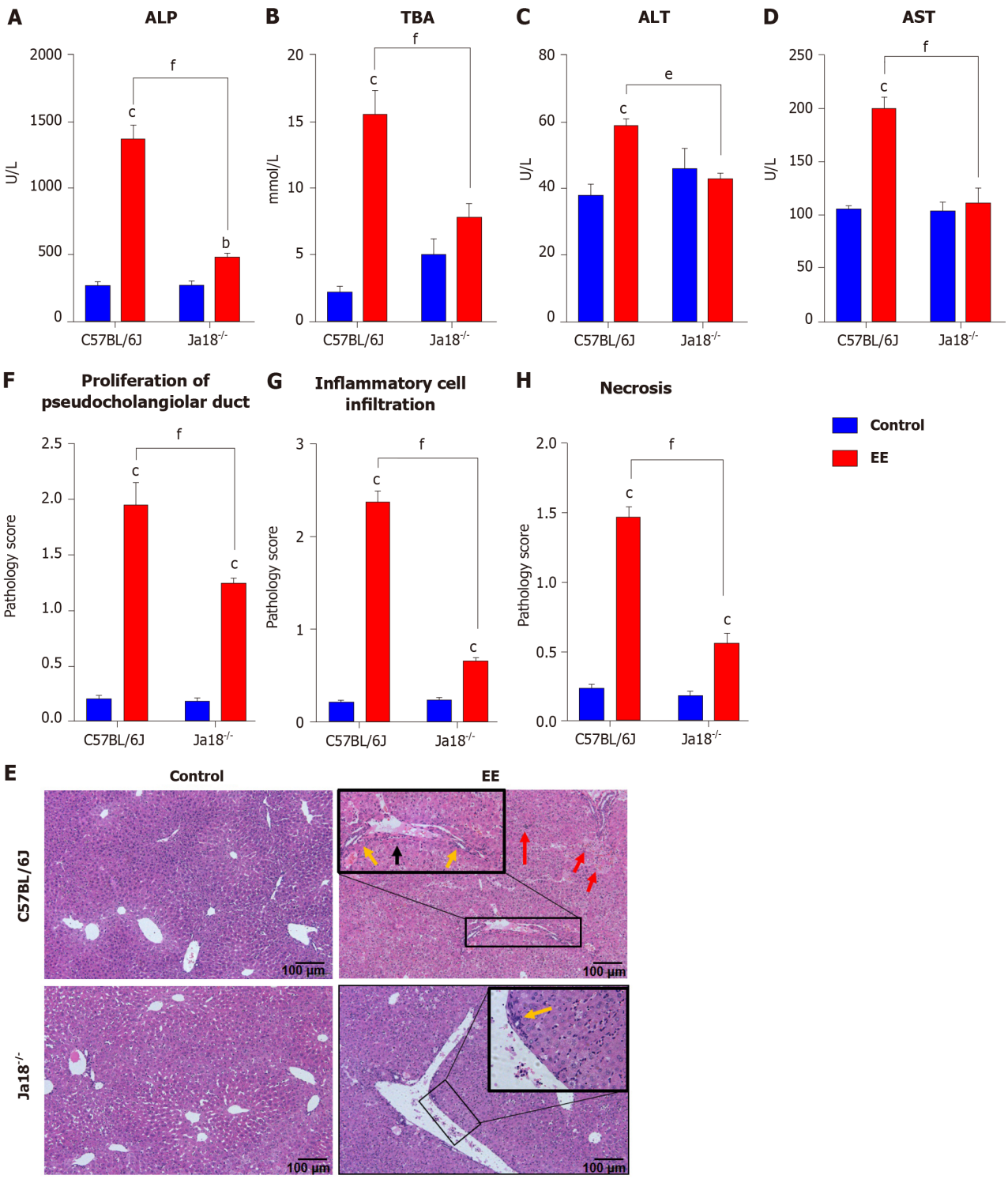

DOI: 10.3748/wjg.v28.i26.3150

Figure 2 Invariant natural killer T cells exacerbate ethinylestradiol-induced cholestatic liver damage. A-D: The serum levels of ALP (A), TBA (B), ALT (C) and AST (D); E: Liver sections stained with hematoxylin and eosin (10×); F: Proliferation of pseudocholangiolar duct (yellow arrows); G and H: Inflammatory cell infiltration (G, red arrows) and hepatocyte necrosis (H, black arrows) were compared as pathology scores. All values are the means ± SE (n = 4-6). $^{b}P < 0.01$, $^{c}P < 0.001$ *vs* control; $^{e}P < 0.01$, $^{f}P < 0.001$ *vs* C57BL/6J group.

iNKT cell deficiency lowers the hepatic expression of chemokine/chemokine receptors

CXCR6, the receptor for chemokine CXCL16, is expressed on the surface of several hepatic lymphocytes, including NKT cells. The CXCR6-dependent infiltration of NKT cells into the liver induces enhanced inflammation in a murine model of chronic hepatic damage[22]. The qPCR results showed that EE promoted the hepatic mRNA expression of Cxcr6/Cxcl16 in C57BL/6J mice. Compared with C57BL/6J mice, iNKT cell deficiency significantly suppressed the mRNA expression of Cxcr6/Cxcl16, which may be related to the absence of the need for hepatic recruitment of NKT cells (Figure 3).

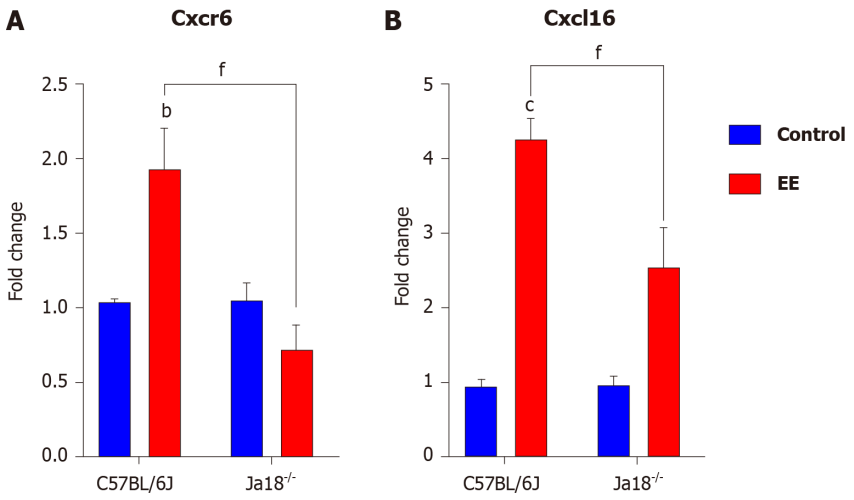

DOI: 10.3748/wjg.v28.i26.3150

Figure 3 Invariant natural killer T cell deficiency lowers the hepatic expression of chemokine/chemokine receptors. A and B: Hepatic mRNA expressions of Cxcr6 (A) and Cxcl16 (B) were determined and compared. All values are the means ± SE (n = 4-6). $^{b}P < 0.01$, $^{c}P < 0.001$ *vs* control; $^{f}P < 0.001$ *vs* C57BL/6J group.

Absence of iNKT cells alters the expression of TLRs and associated signaling pathways

Accumulating evidence suggests that TLRs contribute to the development of hepatobiliary damage[23]. TLRs have also been reported to contribute to the activation and subsequent cytokine production of NKT cells[24]. Intriguingly, iNKT cells have been reported to express certain TLRs, some of which are functional[25]. In the present study, TLRs associated with NKT-cell activation or liver disease were measured and analyzed. The results showed that the mRNA expression levels of Tlr2, Tlr4, Tlr6, Tlr7, and Tlr9 were significantly upregulated after EE administration. Deficiency of iNKT cells significantly downregulated the expression of the above TLRs compared with that in C57BL/6J mice (Figure 4), which suggested that the absence of iNKT cells may influence the expression of TLRs. The hepatic immunohistochemistry results of TLR9 showed a trend similar to that of mRNA (Figure 4F).

TLRs or T cell receptors (TCRs) can stimulate T cells, leading to MAPK signaling pathway activation, which is required for the effects of T cells[26]. iNKT cell activation by TCR stimulation has also been reported to be mediated by ERK and p38 MAPK[27]. In the present study, the expression of both MAPK and PI3K signaling was investigated after EE administration in C57BL/6J and Jα18$^{-/-}$ mice. The hepatic mRNA expression levels of MAPK upstream Ras and Raf as well as Pi3k and its downstream Bad, which might be associated with TLR activation, were increased in C57BL/6J mice after EE administration. The above mRNA levels were remarkably inhibited in Jα18$^{-/-}$ mice compared with C57BL/6J mice, which suggested that the absence of iNKT cells changes the expression of MAPK and PI3K signaling pathways (Figure 5).

Knockout of iNKT cells may inhibit the synthesis of bile acid and weaken the inhibition of hepatocyte polarity

Dysregulated bile acid homeostasis may be attributed to the disorder of bile acid synthesis/metabolism and/or the dysfunction of tight junctions (TJs)[28]. To investigate the possible mechanism of the alleviation of cholestatic liver injury in NKT-cell knockout mice, the levels of CYP450 synthase and TJs were detected. The mRNA levels of Cyp7a1 and Cyp8b1 were upregulated after EE administration in C57BL/6J mice, whereas a nonsignificant difference was shown in Jα18$^{-/-}$ mice. In comparison to C57BL/6J mice, the mRNA expression of Cyp7a1 and Cyp8b1 was inhibited in Jα18$^{-/-}$ mice after EE administration, indicating the relatively reduced synthesis of bile acid (Figure 6A and B). The IHC results showed that, in comparison to the control group, fewer cells positively stained for ZO-1 or Occludin after EE treatment in C57BL/6J mice, and positive cells remained unaltered between the control and EE groups in Jα18$^{-/-}$ mice (Figure 6C and D). These data suggested that knockout of iNKT cells can inhibit bile acid synthase and weaken the inhibition of hepatocyte polarity, thereby reducing cholestatic liver injury.

DISCUSSION

As the most common hepatic disorder, the principal pathogenic factors of EE-induced IHC include estrogen and toxic bile acid, both of which are correlated with immune imbalance. Increased activation

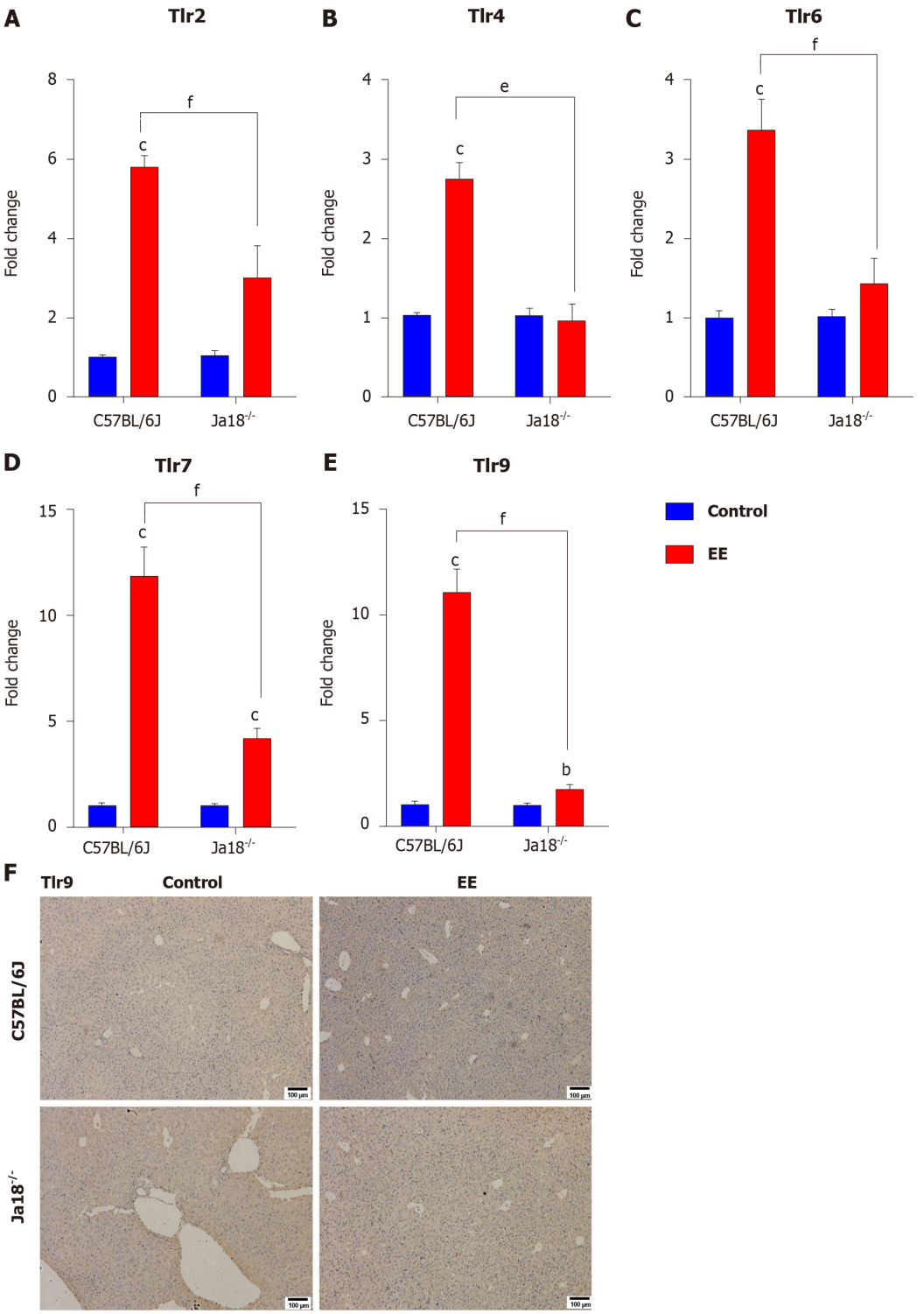

DOI: 10.3748/wjg.v28.i26.3150

Figure 4 Absence of invariant natural killer T cells alters the expression of toll-like receptors. A-E: Hepatic mRNA levels of Tlr2 (A), Tlr4 (B), Tlr6 (C), Tlr7 (D) and Tlr9 (E) were determined and compared; F: Changes in the protein level of TLR9 were determined by immunohistochemistry. All values are the means ± SE (n = 4-6). $^{b}P < 0.01$, $^{c}P < 0.001$ *vs* control; $^{e}P < 0.01$, $^{f}P < 0.001$ *vs* C57BL/6J group.

status of NKT cells, T cells, or NK cells has been reported to contribute to the pathophysiology of cholestatic diseases[15,19,20]. Therefore, the percentages of hepatic NKT cells, CD3^{+}T cells, and NK cells along with their Th1/Th2 cytokine secretion and bias were compared in the present study. Surprisingly, in EE-induced cholestasis, only the NKT-cell percentage and its Th1/Th2 cytokine secretion and ratio significantly increased, indicating their activation and Th1-biased immune response. The percentage of CD3^{+}T cells and NK cells, along with their secretion of Th1 cytokines, remained unaltered. Th2 cytokines from CD3^{+}T cells and NK cells showed a rising trend, which did not seem to affect the Th1/Th2 balance (Figure 1). Our results revealed that both Th1 and Th2 cytokines existed in the liver,

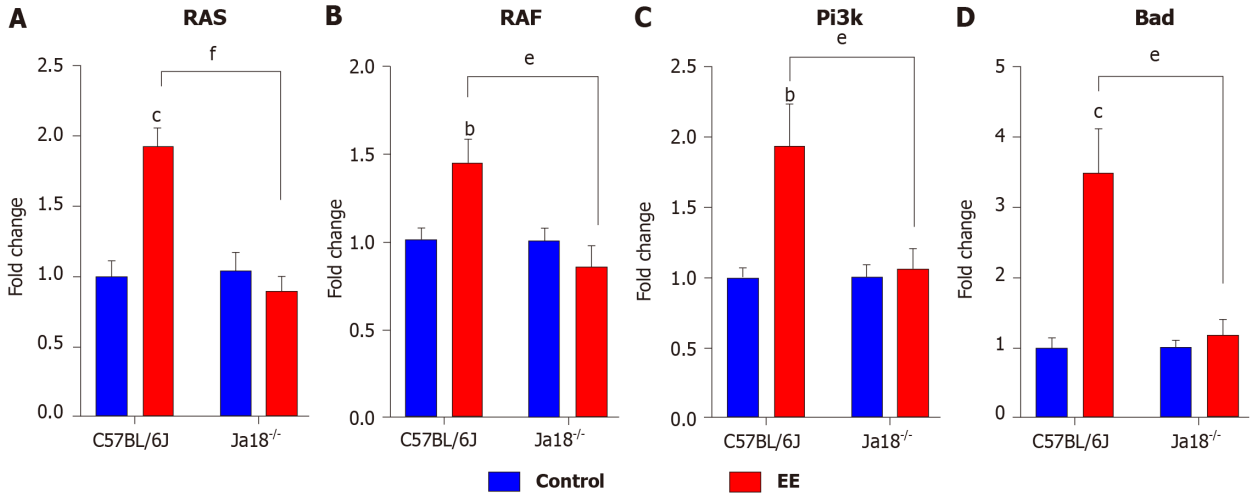

DOI: 10.3748/wjg.v28.i26.3150

Figure 5 Absence of invariant natural killer T cells alters the expression of Ras/Raf and PI3K/Bad signaling pathways. A-D: Hepatic gene expressions of Ras (A), Raf (B), Pi3k (C) and Bad (D) were determined and compared. All values are the means ± SE (n = 4-6), $^{b}P < 0.01$, $^{c}P < 0.001$ *vs* control; $^{e}P < 0.01$, $^{f}P < 0.001$ *vs* C57BL/6J group.

consistent with previous studies[14,29], and the Th1 bias was mainly contributed by NKT cells. To further confirm the effect of NKT cells in EE-induced cholestasis, cholestatic liver damage was compared between iNKT cell-deficient mice and C57BL/6J mice after EE administration. Jα18$^{-/-}$ mice showed significantly reduced blood biochemistry parameters, including levels of ALP, TBA, ALT, and AST, and alleviated liver histopathological changes, suggesting that NKT cells have a harmful effect on EE-induced cholestasis. NKT cells have been accepted as a key connection between innate and adaptive immunity. Upon activation, NKT cells can activate and influence most innate and adaptive immune cells by rapid and abundant cytokine production[30,31]. NKT cells, whose role is noteworthy in cholestasis, are mostly abundant in the liver rather than other organs. In the PBC mouse model, NKT cells are highly activated and secrete enormous amounts of IFN-γ. In comparison to mice with PBC, cholangitis and liver inflammation are significantly alleviated in mice with NKT-cell deficiency[32]. Our previous investigations also found that iNKT cells and their cytokines aggravate ANIT- and triptolide-induced cholestasis by disrupting bile acid homeostasis[14,15]. Although NKT cells can be protective by suppressing neutrophils in an extrahepatic cholestasis model[16], our research data suggest the harmful effects of NKT cells in EE-induced cholestasis. The above studies indicate that the role of NKT cells may vary in different diseases and models.

Under physiological conditions, CXCR6/CXCL16 regulate the migration of NKT cells in hepatic sinusoids[33]. Under the early pathologic states of chronic liver damage, they specifically mediate the hepatic accumulation of NKT cells, exacerbating hepatic inflammation and promoting fibrogenesis[22]. CXCL16 can be expressed in hepatobiliary tissues of patients with hepatopathy[34] but also in mouse liver sinusoidal endothelial cells triggered by intestinal microorganism-induced bile acids, indicating that its expression is related to hepatobiliary damage[33,35]. Our results showed that the hepatic gene levels of Cxcr6 and Cxcl16 were upregulated (Figure 3). Inflammatory cytokines, such as IFN-γ, which was increased in the present model, are capable of further inducing CXCL16 expression, forming a positive regulation loop[36]. In the present study, iNKT cell deficiency inhibited the mRNA levels of Cxcr6 and Cxcl16, which may be linked to the absence of hepatic infiltration of NKT cells (Figure 3).

Activation of iNKT cells can be caused by direct interaction with TCR or indirect effects of TLR agonists and/or IL-12[37]. TLRs, which are widely expressed in the liver, can stimulate hepatic inflammation and actively participate in the initiation and development of liver damage under pathological conditions[38,39]. Lipopolysaccharide (LPS), a specific TLR4 Ligand, activates hepatic iNKT cells and leads to their secretion of IL-4 within 2 h *in vivo* or in vitro, demonstrating that TLR4 is expressed and functional in iNKT cells[40]. In alcoholic liver disease, TLR4 inhibition results in drastically reduced levels of hepatic proinflammatory mediators[41]. TLR4 deletion nearly eliminates inflammatory cell infiltration in the liver and hepatocyte injury in a murine model of ischemia reperfusion[42]. In EE-induced cholestatic liver injury, hepatic mRNA levels of Tlr2, 4, 6, 7, and 9 were markedly increased (Figure 4). CD1d knockout mice (lacking NKT cells) exhibit enhanced (> 4-fold) proinflammatory cytokine secretion and higher mRNA levels of TLR4 in the kidney of a nonalcoholic fatty liver disease model[43]. In the present study, iNKT cell deficiency significantly downregulated the expression of the above TLRs compared with C57BL/6J mice (Figure 4), suggesting the effect of iNKT cells on the expression of TLRs. NKT cells have been found to express certain functional TLRs[24]. The IHC results of TLR9 showed a similar trend as the mRNA levels (Figure 4F). In a murine autoimmune hepatitis model induced by concanavalin A, NKT cells infiltrate and are activated, promoted by TLR9

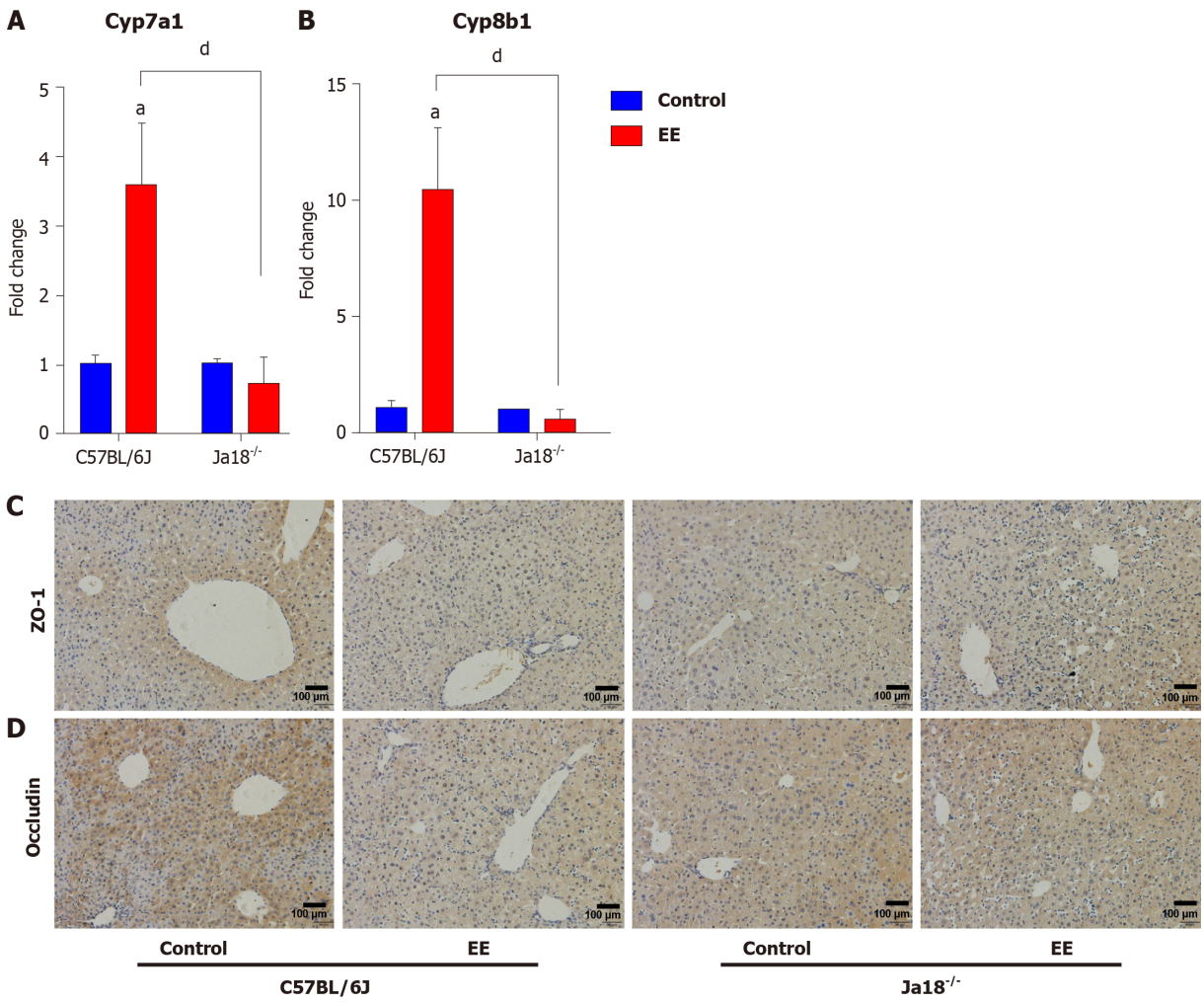

DOI: 10.3748/wjg.v28.i26.3150

Figure 6 Knockout of invariant natural killer T cells may inhibit the synthesis of bile acid and weaken the inhibition of hepatocyte polarity. A and B: Hepatic gene levels of bile acid synthase Cyp7a1 (A) and Cyp8b1 (B) were determined and compared; C and D: Changes in the protein expressions of tight junction Zo-1 (C) and Occludin (D) were determined by immunohistochemistry. All values are the means ± SE (n = 6), $^{a}P < 0.05$ *vs* control; $^{d}P < 0.05$ *vs* C57BL/6J group.

stimulation, thereby leading to aggravated hepatotoxicity[44]. The PI3K/Akt and Ras/Raf/MEK/ERK signaling pathways are considered to be activated and function following inflammation[45], which further upregulates proinflammatory mediators in cholestasis[46]. Our data demonstrated that the mRNA levels of the downstream pathways Ras/Raf and Pi3k/Bad were also upregulated, while iNKT cell deficiency suppressed their upregulation (Figure 5). These results indicated that iNKT cell deletion affected TLRs and their downstream Ras/Raf and PI3K/Bad signaling.

Growing numbers of studies have reported that hepatocyte TJs, constituting hepatocyte polarization, play a pivotal role in the maintenance of the epithelial barrier and permeability; therefore, their structural disruption can lead to the leakage of bile components into blood circulation, bile acid homeostasis disorder, and cholestatic liver injury[47]. TJ damage can be found in obstructive jaundice patients[48] and murine cholestatic models of ANIT[28], carbon tetrachloride[49], BDL[50], and EE[51]. Inflammation has been associated with structural and functional alterations of hepatic TJs[52]. In the present study, the results showed that iNKT cell-deficient mice ameliorated disorders of bile acid synthesis and TJs (Figure 6) and restored previously deteriorated bile acid homeostasis and hepatocyte barrier function, contributing to the mitigation of EE-induced cholestatic hepatotoxicity.

CONCLUSION

In EE-induced cholestatic hepatotoxicity, EE promoted hepatic NKT-cell proliferation and activation, which contributed to Th1 cytokine bias and influenced the liver immune microenvironment. EE also upregulated the expression of Cxcr6/Cxcl16, TLRs, and downstream Ras/Rad and PI3K/Bad signaling. Moreover, EE influenced the levels of the bile acid synthase Cyp7a1 and Cyp8b1 and the TJs ZO-1 and

Occludin. iNKT cell deficiency significantly alleviated cholestatic liver damage and downregulated the abovementioned signaling pathways, indicating the pathogenic effects of hepatic iNKT cells in EE-induced cholestatic liver damage. It is noteworthy that mouse and human NKT cells share similar functions, including the killing of tumor/infected cells by cytotoxicity and their crucial role in autoimmunity[53]. Therefore, regulation of NKT-cell activation may serve as a potential therapeutic strategy with clinical implications for cholestatic diseases.

ARTICLE HIGHLIGHTS

Research background

Cholestasis is mild and common during liver diseases but is also a crucial triggering element of severe hepatopathy. As the predominant component of oral contraceptives (OCs) and hormone replacement therapy, 17α-ethinylestradiol (EE) is used as a model drug to induce murine intrahepatic cholestasis (IHC). The clinical counterpart of EE-induced IHC includes women who are taking OCs, postmenopausal replacement therapy, and susceptible pregnant women.

Research motivation

The significance of the local immune microenvironment in the liver has been emphasized because estrogens are immunomodulators that are metabolized in the liver.

Research objectives

The aim of the present study was to investigate the effects and mechanisms of natural killer T (NKT) cells in a murine model of EE-induced cholestatic hepatotoxicity.

Research methods

Male C57BL/6J mice or invariant NKT (iNKT) cell deficiency (Jα18$^{-/-}$ mice) were administered with EE (10 mg/kg, subcutaneous) for 14 d.

Research results

Both Th1 and Th2 cytokines produced by NKT cells increased in the liver skewing toward a Th1 bias. The expression of the chemokine/chemokine receptor Cxcr6/Cxcl16, toll-like receptors, Ras/Rad, and PI3K/Bad signaling was upregulated after EE administration. EE also influenced bile acid synthase Cyp7a1, Cyp8b1, and tight junctions ZO-1 and Occludin, which might be associated with EE-induced cholestasis. iNKT cell deficiency (Jα18$^{-/-}$ mice) robustly alleviated cholestatic liver damage and lowered the expression of the abovementioned signaling pathways.

Research conclusions

The present study demonstrated that hepatic NKT cells play a pathogenic role in EE-induced intrahepatic cholestasis, contributing to the development of the IHC mechanisms and the potential treatment targeting NKT cells.

Research perspectives

Hepatic NKT cells and their Th1 cytokine production play a pathogenic role in a 14-d murine model of EE-induced intrahepatic cholestasis.

ACKNOWLEDGEMENTS

The authors would like to acknowledge Li Bai (University of Science and Technology of China) for kindly providing iNKT cell-deficient (Jα18$^{-/-}$ mice).

FOOTNOTES

Author contributions: Zou MZ and Kong WC contributed equally to the work; Zou MZ, Kong WC, Yu ZX, and Chen X performed the experiments, collected data, and analyzed the data; Xing MT, Zhang LY, and Wang XZ contributed to the guidance of experiments and the final manuscript; Wang XZ and Xing MT designed the study; Wang XZ, Xing MT, Zou MZ and Cai H wrote the manuscript; All the authors have reviewed and approved the final version of the manuscript.

Supported by the National Natural Science Foundation of China, No. 82073948 and 81703626; and National Innovation and Entrepreneurship Training Program for Undergraduate, No. 202210316040Z.

Institutional animal care and use committee statement: All animal experiments involved in this study were performed under the Ethical Committee of China Pharmaceutical University and the Laboratory Animal Management Committee of Jiangsu Province guidelines (Approval No.: 2021-10-003).

Conflict-of-interest statement: All authors have nothing to disclose.

Data sharing statement: No additional data are available.

ARRIVE guidelines statement: The authors have read the ARRIVE guidelines, and the manuscript was prepared and revised according to the ARRIVE guidelines.

Country/Territory of origin: China

ORCID number: Meng-Zhi Zou 0000-0001-5303-7550; Wei-Chao Kong 0000-0001-9083-2609; Heng Cai 0000-0001-6544-2414; Meng-Tao Xing 0000-0003-3816-4214; Zi-Xun Yu 0000-0002-7272-7394; Xin Chen 0000-0002-5330-6543; Lu-Yong Zhang 0000-0003-1164-7371; Xin-Zhi Wang 0000-0001-9624-0102.

S-Editor: Zhang H
L-Editor: A
P-Editor: Guo X

REFERENCES

1 **Xiang D**, Xu Y, He W, Yang J, Zhang C, Liu D. Bioinformatics-based identification of key pathways and candidate genes for estrogeninduced intrahepatic cholestasis using DNA microarray analysis. *Mol Med Rep* 2019; **20**: 303-311 [PMID: 31115536 DOI: 10.3892/mmr.2019.10256]

2 LiverTox: Clinical and Research Information on Drug-Induced Liver Injury [Internet]. Bethesda (MD): National Institute of Diabetes and Digestive and Kidney Diseases; 2012–. Estrogens and Oral Contraceptives. [PMID: 31643857]

3 **McIlvride S**, Dixon PH, Williamson C. Bile acids and gestation. *Mol Aspects Med* 2017; **56**: 90-100 [PMID: 28506676 DOI: 10.1016/j.mam.2017.05.003]

4 **Reyes H**, Ribalta J, González MC, Segovia N, Oberhauser E. Sulfobromophthalein clearance tests before and after ethinyl estradiol administration, in women and men with familial history of intrahepatic cholestasis of pregnancy. *Gastroenterology* 1981; **81**: 226-231 [PMID: 7195358]

5 **Li X**, Liu R, Luo L, Yu L, Chen X, Sun L, Wang T, Hylemon PB, Zhou H, Jiang Z, Zhang L. Role of AMP-activated protein kinase α1 in 17α-ethinylestradiol-induced cholestasis in rats. *Arch Toxicol* 2017; **91**: 481-494 [PMID: 27090119 DOI: 10.1007/s00204-016-1697-8]

6 **Yamamoto Y**, Moore R, Hess HA, Guo GL, Gonzalez FJ, Korach KS, Maronpot RR, Negishi M. Estrogen receptor alpha mediates 17alpha-ethynylestradiol causing hepatotoxicity. *J Biol Chem* 2006; **281**: 16625-16631 [PMID: 16606610 DOI: 10.1074/jbc.M602723200]

7 **Wang J**, Fu T, Dong R, Wang C, Liu K, Sun H, Huo X, Ma X, Yang X, Meng Q. Hepatoprotection of auraptene from the peels of citrus fruits against 17α-ethinylestradiol-induced cholestasis in mice by activating farnesoid X receptor. *Food Funct* 2019; **10**: 3839-3850 [PMID: 31210195 DOI: 10.1039/c9fo00318e]

8 **Yu L**, Liu X, Li X, Yuan Z, Yang H, Zhang L, Jiang Z. Protective effects of SRT1720 *via* the HNF1α/FXR signalling pathway and anti-inflammatory mechanisms in mice with estrogen-induced cholestatic liver injury. *Toxicol Lett* 2016; **264**: 1-11 [PMID: 27818225 DOI: 10.1016/j.toxlet.2016.10.016]

9 **Milona A**, Owen BM, Cobbold JF, Willemsen EC, Cox IJ, Boudjelal M, Cairns W, Schoonjans K, Taylor-Robinson SD, Klomp LW, Parker MG, White R, van Mil SW, Williamson C. Raised hepatic bile acid concentrations during pregnancy in mice are associated with reduced farnesoid X receptor function. *Hepatology* 2010; **52**: 1341-1349 [PMID: 20842631 DOI: 10.1002/hep.23849]

10 **Jansen PL**, Ghallab A, Vartak N, Reif R, Schaap FG, Hampe J, Hengstler JG. The ascending pathophysiology of cholestatic liver disease. *Hepatology* 2017; **65**: 722-738 [PMID: 27981592 DOI: 10.1002/hep.28965]

11 **Peng B**, Liu S. [Study of relationship between T helper cell type-1 and type-2 cytokines and intrahepatic cholestasis of pregnancy]. *Zhonghua Fu Chan Ke Za Zhi* 2002; **37**: 516-518 [PMID: 12411008]

12 **Jin F**, Cheng D, Tao JY, Zhang SL, Pang R, Guo YJ, Ye P, Dong JH, Zhao L. Anti-inflammatory and anti-oxidative effects of corilagin in a rat model of acute cholestasis. *BMC Gastroenterol* 2013; **13**: 79 [PMID: 23641818 DOI: 10.1186/1471-230X-13-79]

13 **Zou M**, Wang A, Wei J, Cai H, Yu Z, Zhang L, Wang X. An insight into the mechanism and molecular basis of dysfunctional immune response involved in cholestasis. *Int Immunopharmacol* 2021; **92**: 107328 [PMID: 33412394 DOI: 10.1016/j.intimp.2020.107328]

14 **Nong C**, Zou M, Xue R, Bai L, Liu L, Jiang Z, Sun L, Huang X, Zhang L, Wang X. The role of invariant natural killer T cells in experimental xenobiotic-induced cholestatic hepatotoxicity. *Biomed Pharmacother* 2020; **122**: 109579 [PMID: 31794947 DOI: 10.1016/j.biopha.2019.109579]

15 **Zou M**, Nong C, Yu Z, Cai H, Jiang Z, Xue R, Huang X, Sun L, Zhang L, Wang X. The role of invariant natural killer T cells and associated immunoregulatory factors in triptolide-induced cholestatic liver injury. *Food Chem Toxicol* 2020; **146**: 111777 [PMID: 32987112 DOI: 10.1016/j.fct.2020.111777]

16 **Duwaerts CC**, Sun EP, Cheng CW, van Rooijen N, Gregory SH. Cross-activating invariant NKT cells and kupffer cells suppress cholestatic liver injury in a mouse model of biliary obstruction. *PLoS One* 2013; **8**: e79702 [PMID: 24260285 DOI: 10.1371/journal.pone.0079702]

17 **Mencarelli A**, Renga B, Migliorati M, Cipriani S, Distrutti E, Santucci L, Fiorucci S. The bile acid sensor farnesoid X receptor is a modulator of liver immunity in a rodent model of acute hepatitis. *J Immunol* 2009; **183**: 6657-6666 [PMID: 19880446 DOI: 10.4049/jimmunol.0901347]

18 **Valestrand L**, Berntsen NL, Zheng F, Schrumpf E, Hansen SH, Karlsen TH, Blumberg RS, Hov JR, Jiang X, Melum E. Lipid antigens in bile from patients with chronic liver diseases activate natural killer T cells. *Clin Exp Immunol* 2021; **203**: 304-314 [PMID: 33089489 DOI: 10.1111/cei.13541]

19 **Sun K**, Ma S, Tian S, Zhang M, Liu Y, Li B, Zhou X, Zheng X, Wang L, Han Y. An enhanced level of LAMP-2A participates in $CD4^+$T cell hyperactivity in patients with primary biliary cholangitis. *Ann Transl Med* 2021; **9**: 101 [PMID: 33569403 DOI: 10.21037/atm-20-2427]

20 **Hydes TJ**, Blunt MD, Naftel J, Vallejo AF, Seumois G, Wang A, Vijayanand P, Polak ME, Khakoo SI. Constitutive Activation of Natural Killer Cells in Primary Biliary Cholangitis. *Front Immunol* 2019; **10**: 2633 [PMID: 31803181 DOI: 10.3389/fimmu.2019.02633]

21 **Zhang YY**, Zhang CX, Li Y, Jiang X, Wang YF, Sun Y, Wang J, Ji WY, Liu Y. Development of a novel rat model of heterogeneous hepatic injury by injection with colchicine *via* the splenic vein. *World J Gastroenterol* 2018; **24**: 5005-5012 [PMID: 30510375 DOI: 10.3748/wjg.v24.i44.5005]

22 **Wehr A**, Baeck C, Heymann F, Niemietz PM, Hammerich L, Martin C, Zimmermann HW, Pack O, Gassler N, Hittatiya K, Ludwig A, Luedde T, Trautwein C, Tacke F. Chemokine receptor CXCR6-dependent hepatic NK T Cell accumulation promotes inflammation and liver fibrosis. *J Immunol* 2013; **190**: 5226-5236 [PMID: 23596313 DOI: 10.4049/jimmunol.1202909]

23 **Liu W**, Jing ZT, Xue CR, Wu SX, Chen WN, Lin XJ, Lin X. PI3K/AKT inhibitors aggravate death receptor-mediated hepatocyte apoptosis and liver injury. *Toxicol Appl Pharmacol* 2019; **381**: 114729 [PMID: 31445927 DOI: 10.1016/j.taap.2019.114729]

24 **Kulkarni RR**, Villanueva AI, Read LR, Brisbin JT, Bhaumik SK, LaMarre J, Murali-Krishna K, Sharif S. CpG oligonucleotide-mediated co-stimulation of mouse invariant natural killer T cells negatively regulates their activation status. *Cell Tissue Res* 2017; **369**: 541-554 [PMID: 28550425 DOI: 10.1007/s00441-017-2631-y]

25 **Kulkarni R**, Behboudi S, Sharif S. Insights into the role of Toll-like receptors in modulation of T cell responses. *Cell Tissue Res* 2011; **343**: 141-152 [PMID: 20680345 DOI: 10.1007/s00441-010-1017-1]

26 **Dong C**, Davis RJ, Flavell RA. MAP kinases in the immune response. *Annu Rev Immunol* 2002; **20**: 55-72 [PMID: 11861597 DOI: 10.1146/annurev.immunol.20.091301.131133]

27 **Stuart JK**, Bisch SP, Leon-Ponte M, Hayatsu J, Mazzuca DM, Maleki Vareki S, Haeryfar SM. Negative modulation of invariant natural killer T cell responses to glycolipid antigens by p38 MAP kinase. *Int Immunopharmacol* 2010; **10**: 1068-1076 [PMID: 20584631 DOI: 10.1016/j.intimp.2010.06.007]

28 **Yang T**, Wang X, Zhou Y, Yu Q, Heng C, Yang H, Yuan Z, Miao Y, Chai Y, Wu Z, Sun L, Huang X, Liu B, Jiang Z, Zhang L. SEW2871 attenuates ANIT-induced hepatotoxicity by protecting liver barrier function *via* sphingosine 1-phosphate receptor-1-mediated AMPK signaling pathway. *Cell Biol Toxicol* 2021; **37**: 595-609 [PMID: 33400020 DOI: 10.1007/s10565-020-09567-9]

29 **Caielli S**, Conforti-Andreoni C, Di Pietro C, Usuelli V, Badami E, Malosio ML, Falcone M. On/off TLR signaling decides proinflammatory or tolerogenic dendritic cell maturation upon CD1d-mediated interaction with invariant NKT cells. *J Immunol* 2010; **185**: 7317-7329 [PMID: 21078913 DOI: 10.4049/jimmunol.1000400]

30 **Zeissig S**, Blumberg RS. Analyzing Antigen Recognition by Natural Killer T Cells. *Methods Mol Biol* 2019; **1988**: 439-453 [PMID: 31147957 DOI: 10.1007/978-1-4939-9450-2_30]

31 **Terabe M**, Berzofsky JA. The immunoregulatory role of type I and type II NKT cells in cancer and other diseases. *Cancer Immunol Immunother* 2014; **63**: 199-213 [PMID: 24384834 DOI: 10.1007/s00262-013-1509-4]

32 **Chuang YH**, Lian ZX, Yang GX, Shu SA, Moritoki Y, Ridgway WM, Ansari AA, Kronenberg M, Flavell RA, Gao B, Gershwin ME. Natural killer T cells exacerbate liver injury in a transforming growth factor beta receptor II dominant-negative mouse model of primary biliary cirrhosis. *Hepatology* 2008; **47**: 571-580 [PMID: 18098320 DOI: 10.1002/hep.22052]

33 **Geissmann F**, Cameron TO, Sidobre S, Manlongat N, Kronenberg M, Briskin MJ, Dustin ML, Littman DR. Intravascular immune surveillance by CXCR6+ NKT cells patrolling liver sinusoids. *PLoS Biol* 2005; **3**: e113 [PMID: 15799695 DOI: 10.1371/journal.pbio.0030113]

34 **Heydtmann M**, Lalor PF, Eksteen JA, Hübscher SG, Briskin M, Adams DH. CXC chemokine ligand 16 promotes integrin-mediated adhesion of liver-infiltrating lymphocytes to cholangiocytes and hepatocytes within the inflamed human liver. *J Immunol* 2005; **174**: 1055-1062 [PMID: 15634930 DOI: 10.4049/jimmunol.174.2.1055]

35 **Ma C**, Han M, Heinrich B, Fu Q, Zhang Q, Sandhu M, Agdashian D, Terabe M, Berzofsky JA, Fako V, Ritz T, Longerich T, Theriot CM, McCulloch JA, Roy S, Yuan W, Thovarai V, Sen SK, Ruchirawat M, Korangy F, Wang XW, Trinchieri G, Greten TF. Gut microbiome-mediated bile acid metabolism regulates liver cancer *via* NKT cells. *Science* 2018; **360** [PMID: 29798856 DOI: 10.1126/science.aan5931]

36 **Abel S**, Hundhausen C, Mentlein R, Schulte A, Berkhout TA, Broadway N, Hartmann D, Sedlacek R, Dietrich S, Muetze B, Schuster B, Kallen KJ, Saftig P, Rose-John S, Ludwig A. The transmembrane CXC-chemokine ligand 16 is induced by IFN-gamma and TNF-alpha and shed by the activity of the disintegrin-like metalloproteinase ADAM10. *J Immunol* 2004;

172: 6362-6372 [PMID: 15128827 DOI: 10.4049/jimmunol.172.10.6362]

37 **Anderson CK**, Reilly SP, Brossay L. The Invariant NKT Cell Response Has Differential Signaling Requirements during Antigen-Dependent and Antigen-Independent Activation. *J Immunol* 2021; **206**: 132-140 [PMID: 33229442 DOI: 10.4049/jimmunol.2000870]

38 **Kiziltas S**. Toll-like receptors in pathophysiology of liver diseases. *World J Hepatol* 2016; **8**: 1354-1369 [PMID: 27917262 DOI: 10.4254/wjh.v8.i32.1354]

39 **Chu AJ**. Antagonism by bioactive polyphenols against inflammation: a systematic view. *Inflamm Allergy Drug Targets* 2014; **13**: 34-64 [PMID: 24251781 DOI: 10.2174/1871528112666131119211002]

40 **Askenase PW**, Itakura A, Leite-de-Moraes MC, Lisbonne M, Roongapinun S, Goldstein DR, Szczepanik M. TLR-dependent IL-4 production by invariant Valpha14+Jalpha18+ NKT cells to initiate contact sensitivity in vivo. *J Immunol* 2005; **175**: 6390-6401 [PMID: 16272291 DOI: 10.4049/jimmunol.175.10.6390]

41 **Ishida K**, Kaji K, Sato S, Ogawa H, Takagi H, Takaya H, Kawaratani H, Moriya K, Namisaki T, Akahane T, Yoshiji H. Sulforaphane ameliorates ethanol plus carbon tetrachloride-induced liver fibrosis in mice through the Nrf2-mediated antioxidant response and acetaldehyde metabolization with inhibition of the LPS/TLR4 signaling pathway. *J Nutr Biochem* 2021; **89**: 108573 [PMID: 33388347 DOI: 10.1016/j.jnutbio.2020.108573]

42 **Uchida Y**, Ke B, Freitas MC, Yagita H, Akiba H, Busuttil RW, Najafian N, Kupiec-Weglinski JW. T-cell immunoglobulin mucin-3 determines severity of liver ischemia/reperfusion injury in mice in a TLR4-dependent manner. *Gastroenterology* 2010; **139**: 2195-2206 [PMID: 20637206 DOI: 10.1053/j.gastro.2010.07.003]

43 **Alhasson F**, Dattaroy D, Das S, Chandrashekaran V, Seth RK, Schnellmann RG, Chatterjee S. NKT cell modulates NAFLD potentiation of metabolic oxidative stress-induced mesangial cell activation and proximal tubular toxicity. *Am J Physiol Renal Physiol* 2016; **310**: F85-F101 [PMID: 26447219 DOI: 10.1152/ajprenal.00243.2015]

44 **Jiang W**, Sun R, Zhou R, Wei H, Tian Z. TLR-9 activation aggravates concanavalin A-induced hepatitis *via* promoting accumulation and activation of liver CD4+ NKT cells. *J Immunol* 2009; **182**: 3768-3774 [PMID: 19265155 DOI: 10.4049/jimmunol.0800973]

45 **Choi SH**, Harkewicz R, Lee JH, Boullier A, Almazan F, Li AC, Witztum JL, Bae YS, Miller YI. Lipoprotein accumulation in macrophages *via* toll-like receptor-4-dependent fluid phase uptake. *Circ Res* 2009; **104**: 1355-1363 [PMID: 19461045 DOI: 10.1161/CIRCRESAHA.108.192880]

46 **Xiang D**, Yang J, Xu Y, Lan L, Li G, Zhang C, Liu D. Estrogen cholestasis induces gut and liver injury in rats involving in activating PI3K/Akt and MAPK signaling pathways. *Life Sci* 2021; **276**: 119367 [PMID: 33775691 DOI: 10.1016/j.lfs.2021.119367]

47 **Gissen P**, Arias IM. Structural and functional hepatocyte polarity and liver disease. *J Hepatol* 2015; **63**: 1023-1037 [PMID: 26116792 DOI: 10.1016/j.jhep.2015.06.015]

48 **Assimakopoulos SF**, Tsamandas AC, Louvros E, Vagianos CE, Nikolopoulou VN, Thomopoulos KC, Charonis A, Scopa CD. Intestinal epithelial cell proliferation, apoptosis and expression of tight junction proteins in patients with obstructive jaundice. *Eur J Clin Invest* 2011; **41**: 117-125 [PMID: 20840373 DOI: 10.1111/j.1365-2362.2010.02379.x]

49 **Horikoshi Y**, Kitatani K, Toriumi K, Fukunishi N, Itoh Y, Nakamura N, Ohno S, Matsura T, Takekoshi S. Aberrant activation of atypical protein kinase C in carbon tetrachloride-induced oxidative stress provokes a disturbance of cell polarity and sealing of bile canalicular lumen. *Am J Pathol* 2015; **185**: 958-968 [PMID: 25688837 DOI: 10.1016/j.ajpath.2014.12.015]

50 **Fallon MB**, Mennone A, Anderson JM. Altered expression and localization of the tight junction protein ZO-1 after common bile duct ligation. *Am J Physiol* 1993; **264**: C1439-C1447 [PMID: 8333499 DOI: 10.1152/ajpcell.1993.264.6.C1439]

51 **Landmann L**. Cholestasis-induced alterations of the trans- and paracellular pathways in rat hepatocytes. *Histochem Cell Biol* 1995; **103**: 3-9 [PMID: 7736278 DOI: 10.1007/BF01464469]

52 **Han X**, Fink MP, Uchiyama T, Yang R, Delude RL. Increased iNOS activity is essential for hepatic epithelial tight junction dysfunction in endotoxemic mice. *Am J Physiol Gastrointest Liver Physiol* 2004; **286**: G126-G136 [PMID: 12946943 DOI: 10.1152/ajpgi.00231.2003]

53 **Takahashi T**, Chiba S, Nieda M, Azuma T, Ishihara S, Shibata Y, Juji T, Hirai H. Cutting edge: analysis of human V alpha 24+CD8+ NK T cells activated by alpha-galactosylceramide-pulsed monocyte-derived dendritic cells. *J Immunol* 2002; **168**: 3140-3144 [PMID: 11907064 DOI: 10.4049/jimmunol.168.7.3140]

World Journal of Gastroenterology

Submit a Manuscript: https://www.f6publishing.com

World J Gastroenterol 2022 July 14; 28(26): 3164-3176

DOI: 10.3748/wjg.v28.i26.3164

ISSN 1007-9327 (print) ISSN 2219-2840 (online)

ORIGINAL ARTICLE

Basic Study

Bifidobacterium infantis regulates the programmed cell death 1 pathway and immune response in mice with inflammatory bowel disease

Lin-Yan Zhou, Ying Xie, Yan Li

Specialty type: Gastroenterology and hepatology

Provenance and peer review: Unsolicited article; Externally peer reviewed.

Peer-review model: Single blind

Peer-review report's scientific quality classification

Grade A (Excellent): A
Grade B (Very good): B, B
Grade C (Good): 0
Grade D (Fair): 0
Grade E (Poor): 0

P-Reviewer: Bozkurt HS, Turkey; Rodrigues AT, Brazil; Serban ED, Romania

Received: December 6, 2021
Peer-review started: December 6, 2021
First decision: January 8, 2022
Revised: January 12, 2022
Accepted: June 16, 2022
Article in press: June 16, 2022
Published online: July 14, 2022

Lin-Yan Zhou, Ying Xie, Yan Li, Department of Gastroenterology, Shengjing Hospital of China Medical University, Shenyang 110004, Liaoning Province, China

Corresponding author: Yan Li, PhD, Chief Doctor, Professor, Department of Gastroenterology, Shengjing Hospital of China Medical University, No. 36 Sanhao Road, Heping District, Shenyang 110004, Liaoning Province, China. liy@sj-hospital.org

Abstract

BACKGROUND

Inflammatory bowel disease (IBD) is caused by an abnormal immune response. Programmed cell death 1 (PD-1) is an immunostimulatory molecule, which interacts with PD ligand (PD-L1) playing a prime important role among autoimmune diseases. *Bifidobacterium infantis* (*B. infantis*) can promote the differentiation of CD (cluster of differentiation) 4^+ T cells into regulatory T cells (Tregs). Tregs participate in the development of IBD and may be related to disease activity. *B. infantis* amplify the expression level of PD-1, PD-L1 and Tregs' nuclear transcription factor forkhead box protein 3 (Foxp3). But the mechanism of *B. infantis* on PD-1/PD-L1 signaling remains unclear.

AIM

To explore the mechanism of *B. infantis* regulating the immune response in IBD.

METHODS

Forty-eight-week-old BALB/c mice were randomly divided into five groups: The control group, dextran sulphate sodium (DSS) model group, DSS + *B. infantis* group, DSS + *B. infantis* + anti-PD-L1 group, and DSS + anti-PD-L1 group. The control group mice were given drinking water freely, the other four groups were given drinking water containing 5% DSS freely. The control group, DSS model group, and DSS + anti-PD-L1 group were given normal saline (NS) 400 μL daily by gastric lavage, and the DSS + *B. infantis* group and DSS + *B. infantis* + anti-PD-L1 group were given NS and 1×10^9 colony-forming unit of *B. infantis* daily by gastric lavage. The DSS + *B. infantis* + anti-PD-L1 group and DSS + anti-PD-L1 group were given 200 μg of PD-L1 blocker intraperitoneally at days 0, 3, 5, and 7; the control group, DSS + anti-PD-L1 group, and DSS + *B. infantis* group were given an intraperitoneal injection of an equal volume of phosphate buffered saline

(PBS). Changes in PD-L1, PD-1, Foxp3, interleukin (IL)-10, and transforming growth factor β (TGF-β) 1 protein and gene expression were observed. Flow cytometry was used to observe changes in $CD4^+$, $CD25^+$, $Foxp3^+$ cell numbers in the blood and spleen.

RESULTS

Compared to the control group, the expression of PD-1, Foxp3, IL-10, and TGF-β1 was significantly decreased in the intestinal tract of the DSS mice ($P < 0.05$). Compared to the control group, the proportion of $CD4^+$, $CD25^+$, $Foxp3^+$ cells in spleen and blood of DSS group was visibly katabatic ($P < 0.05$). *B. infantis* upgraded the express of PD-L1, PD-1, Foxp3, IL-10, and TGF-β1 ($P < 0.05$) and increased the proportion of $CD4^+$, $CD25^+$, $Foxp3^+$ cells both in spleen and blood ($P < 0.05$). After blocking PD-L1, the increase in Foxp3, IL-10, and TGF-β1 protein and gene by *B. infantis* was inhibited ($P < 0.05$), and the proliferation of $CD4^+$, $CD25^+$, $Foxp3^+$ cells in the spleen and blood was also inhibited ($P < 0.05$). After blocking PD-L1, the messenger ribonucleic acid and protein expression of PD-1 were invariant.

CONCLUSION

It is potential that *B. infantis* boost the proliferation of $CD4^+$, $CD25^+$, $Foxp3^+$ T cells in both spleen and blood, as well as the expression of Foxp3 in the intestinal tract by activating the PD-1/PD-L1 pathway.

Key Words: *Bifidobacterium infantis*; Enteritis; Programmed cell death ligand; T-Lymphocytes

Core Tip: *Bifidobacterium infantis* (*B. infantis*) can be used as a therapeutic agent to treat inflammatory bowel disease. It regulates the intestinal microbiota, alleviates inflammation, and regulates the immune response. We found that *B. infantis* increases the expression of forkhead box protein 3 (Foxp3) and the proliferation of $Foxp3^+$ T cells, and activates the programmed cell death 1 (PD-1)/ PD ligand 1 pathway.

Citation: Zhou LY, Xie Y, Li Y. *Bifidobacterium infantis* regulates the programmed cell death 1 pathway and immune response in mice with inflammatory bowel disease. *World J Gastroenterol* 2022; 28(26): 3164-3176
URL: https://www.wjgnet.com/1007-9327/full/v28/i26/3164.htm
DOI: https://dx.doi.org/10.3748/wjg.v28.i26.3164

INTRODUCTION

Inflammatory bowel disease (IBD) results from the aberrant immune responses or the disruption of immune tolerance to intestinal antigens. Several factors, including the immune system, infections, and genetic and environmental factors, may remarkably contribute to the development of IBD[1-4]. To maintain immune tolerance to the intestinal environment, the intestinal immune system monitors changes in the bacterial microbiota and the expression of antigens on the surface of the intestinal mucosa[5,6]. Antigen-presenting cells, including dendritic cells and intestinal epithelial cells, present intestinal antigens to $CD4^+$ T cells and induce their differentiation into regulatory T cells (Tregs), which maintain tolerance to the intestinal microbiota. Hyperactive T cell responses to the intestinal microbiota contribute to the inflammatory response observed in IBD[7].

Programmed cell death protein 1 (PD-1) and PD-ligand 1 (PD-L1), belong to the CD28/B7 superfamily, which primarily functions in T cell-mediated immune responses and is closely related to several diseases and disease states, including autoimmune diseases, tumors, chronic viral infections, and chronic inflammation[8-10]. The role of the PD-1/PD-L1 signaling pathway in glomerulonephritis, systemic lupus erythematosus, rheumatoid arthritis, dilated cardiomyopathy, autoimmune diabetes, and other autoimmune diseases has been widely studied[11,12]; however, few studies have examined the role of the PD-1/PD-L1 signaling pathway in IBD[13].

Tregs are a subpopulation of T lymphocytes with immunoregulatory functions[14]. They can inhibit the activation and proliferation of autoreactive T cells by secreting cytokines such as interleukin (IL)-10 and transforming growth factor β (TGF-β), downregulating the function of auxiliary T cells, and maintaining intestinal homeostasis and immune tolerance[15,16]. Tregs are divided into two categories: Natural Tregs (nTregs) and induced Tregs (iTregs). The nTregs mature in the thymus and are positive for CD4, CD25, and Foxp3. The iTregs are induced by specific antigen stimulation of $CD4^+$ T cells in the presence of IL-2 and TGF-β1, in the intestine, spleen, and other peripheral sites[17]. Animal studies have shown that injecting T cells with no CD4 and Tregs expressing CD25 into T cell-deficient mice can

induce the development of autoimmune colitis, whereas the injection of T cells expressing CD4 with that of $CD25^+$ Tregs can inhibit colitis development. These results suggest that $CD4^+$ and $CD25^+$ Tregs are vital for the inhibition of the intestinal immune response[18]. Maul *et al*[19] found that the percentage of Tregs in the peripheral blood of patients with IBD decreased in the active phase and increased in the remission phase of the disease; however, the number of Tregs in the intestinal epithelium increased in the active phase of the disease but was still significantly lower than that observed in patients with diverticulitis. This suggests a role of Tregs in IBD development.

The adoptive transfer of immature $CD4^+$ T cells into wild-type $rag^{-/-}$ mice and PD-$L1^{-/-}rag^{-/-}$ mice significantly decreases the number of Tregs in PD-$L1^{-/-}rag^{-/-}$ mice, suggesting a dominant role of PD-L1 in Treg differentiation[20]. PD-L1 can enhance Treg function and promote the production of IL-10 by Tregs[21]. Treg differentiation depends on the PD-L1 signaling pathway. Higher levels of PD-L1 expression in hepatodendritic cells result in greater induction of Tregs which maintain the tolerance toward transplanted organs.

We have previously found that *Bifidobacterium infantis* (*B. infantis*) can alleviate intestinal epithelial injury and maintain intestinal immune tolerance in a mouse model of IBD and may have therapeutic implications for the immunological injuries observed in IBD**.** *Bifidobacterium infantis* notably increased the expression levels of PD-L1 and PD-1 in the intestine and promoted the expression of nuclear transcription factors and of anti-inflammatory factors (IL-10 and TGF-β1) in Tregs[22,23]. Therefore, this study aimed to explore the mechanism of action of *B. infantis* in the PD-1/PD-L1 signaling pathway and the differentiation and function of Tregs.

MATERIALS AND METHODS

Reagents and antibodies

Dextran sulfate sodium (DSS; molecular weight 36000-50000) was purchased from MP Biomedicals (Irvine, CA, United States). *B. infantis* freeze-dried powder, containing 1.6×10^{11} colony-forming units (CFU)/g, was provided by Shandong Kexing Biological Products Co., Ltd. (Batch No. 2017012, Shandong Province, China). Invivomab anti-mouse PD-L1 was purchased from BIOX Cell (Lebanon, NH, United States). BALB/c mice were purchased from Huafukang Biotechnology (Beijing, China). Allophycocyanin (APC) rat anti-mouse Cd4, Bb515 rat anti-mouse, P-phycoerythrin (PE) rat anti-mouse Foxp3, and a transcription factor buffer set were purchased from BD Biosciences (Franklin Lakes, NJ, United States). Antibodies against PD-L1, PD-1, and Foxp3 were purchased from Proteintech Group (Rosemont, IL, United States). Antibodies against IL-10 and TGF-β1 were purchased from Abcam (Cambridge, United Kingdom). Real-time quantitative PCR was performed using the following reagents: TRIzol (Invitrogen, Thermo Fisher, Waltham, MA, United States), Primescript™ RT Regent kit with gDNA eraser, quick response training (qRT) PCR kit SYBR® premier ex taq™ II (Tli RNaseH Plus, Takara, Japan), and the specific primers (Biotechnology Co., Ltd., China).

Animals

Forty-eight-week-old BALB/c mice, male and female, weighing 20 g ± 2 g, were raised under pathogen-free conditions in the standalone animal experimental center affiliated with the Shengjing Hospital of China Medical University. The mice were kept at 20 °C-26 °C and in an atmosphere with a relative humidity of 40%-70%, with a 12 h light/dark cycle. Sterilized water and standard feed were provided for free consumption by the animals. The experimental protocol was approved by the ethics committee of the hospital (No. 2017PS353K). The operators ensured that suitable measures were taken to reduce malaise and injury to the animals during experiments.

Experimental grouping and modeling

Forty mice were randomly divided into five groups: Control, DSS, DSS + *B. infantis*, DSS + *B. infantis* + anti-PD-L1, and DSS + anti-PD-L1. Mice in the control group were given free access drinking water for 7 d. The other four groups were administered sterilized water containing 5% DSS for 7 d. The drinking. Drinking water was changed daily. The control, DSS, and DSS + anti-PD-L1 groups were administered 400 μL normal saline (NS) *via* gavage daily, and the DSS + *B. infantis* and DSS + *B. infantis* + anti-PD-L1 groups were administered 400 μL NS *via* gavage and *B. infantis* (1×10^9 CFU) daily. The DSS + *B. infantis* + anti-PD-L1 and DSS + anti-PD-L1 groups were administered an intraperitoneal injection of PD-L1 blocker (200 μg), and the control, DSS model, and DSS + *B. infantis* groups were intraperitoneally injected with phosphate-buffered phosphate buffered saline (PBS) on days 0, 3, 5, and 7.

Specimen collection

General characteristics of the mice: During the experimental period, temperament, reactivity, activity, hair color, weight, eating, and defecation of each mouse were observed seriatim and recorded in detail daily.

Peripheral blood collection: On day 8, all animals were anesthetized *via* isoflurane inhalation, and the beards were removed. Blood was collected through retro-orbital bleeding and placed in blood collection vessels containing EDTA. The blood and EDTA were mixed and stored on ice.

Extraction of single cells from mouse spleen: After blood collection, the sacrificed mice were dissected along the midline, and the spleen was fully exposed. After blunt dissection, the spleen was removed, placed in PBS, and transported on ice. The spleen was then transferred to a glass dish containing RPMI 1640 medium and mashed with ground glass. The cells were then transferred to a centrifuge tube and centrifuged at 1200 rpm for 5 min, and the supernatant was discarded. Next, 2 mL of RBC lysate was added to each sample. PBS (3 mL) was added to dilute and stop the lysis, and the samples were centrifuged again at 400 × *g* for 5 min at 4 °C. The supernatant was discarded and 3 mL of PBS was added. The cells were filtered and centrifuged for 10 min. The supernatant was discarded, and PBS was added to obtain a single-cell suspension. All the procedures were performed at 4 °C to ensure cell viability.

Acquisition of mouse colon: After splenectomy, the colon was exposed and the colon from the blind part to the anus was removed, washed with pre-cooled NS, and divided into four parts. The samples were then transferred to a -80 °C ultra-low-temperature refrigerator in liquid nitrogen for long-term preservation.

Detection of $CD4^+$, $CD25^+$, $Foxp3^+$ T cells by flow cytometry

Spleen: Splenic $CD4^+$, $CD25^+$, and $Foxp3^+$ T cells were detected using flow cytometry. The prepared single-cell spleen suspension (100 μL) was aliquoted into labeled flow tubes. Anti-$CD4^+$ and anti-$CD25^+$ antibodies were then added to the tubes and the tubes were incubated at 4 °C in the dark for 30 min. Next, 1 mL of 1X fix/perm working solution was added to each sample and the samples were incubated at 4 °C in the dark for 40 min to permeabilize the nucleus. Anti-Foxp3 antibody was then added and the resulting solution was incubated at 4 °C in the dark for 40 min. Excess antibodies were removed, and the samples were run on a flow cytometer (FACSCalibur, BD Bioscience).

Peripheral blood: After RBC lysis, flow cytometry was performed on the peripheral blood samples using the protocol described above.

Western blotting

Total protein was extracted from the colon, and the protein concentration was determined. The samples were subjected to electrophoresis at 60 V. After marker separation, the voltage was adjusted to 80 V. After 30 min, the voltage was adjusted to 100 V. Electrophoresis was terminated when the target protein with the lowest molecular weight reached the end of the gel. A voltage of 100 V was used to transfer proteins to the membrane. Proteins with a molecular weight < 25 kDa were transferred for 25 min, and proteins weighing 26-70 kDa were transferred for 70 min. The membrane was blocked with 2.5% bovine serum albumin (BSA) at room temperature for 1.5 h. Primary antibodies against PD-L1 (1:750), PD-1 (1:500), Foxp3 (1:1000), IL-10 (1:800), TGF-β1 (1:500), and GAPDH (1:10000) were added and the membrane was incubated at 4 °C overnight. Then, goat anti-rabbit IgG secondary antibody labeled with horseradish peroxidase was added to the membrane, followed by incubation at room temperature for 1.5 h. In a dark room, a chemiluminescence imaging analysis system was used to visualize the membranes. GelPro software was used to analyze the images and to perform quantitative analysis using the following formula: Protein content = grey value of the target protein of the sample/grey value of the same sample.

Real time qPCR

The experiment consists of 5 steps: (1) Ribonucleic acid (RNA) purification: DSS can reduce the purity of RNA, so extra purification of the colon RNA was necessary. RNA purification was performed as follows: 30 μL lithium chloride (8 mol/L) + 270 μL ddH_2O was added to 10 μL RNA and placed on ice for 2 h. The samples were then centrifuged at 14000 × g for 30 min. The supernatant was then discarded, and the RNA was dissolved in 90 μL ddH_2O. Next, 10 μL sodium acetate (3 mol/L) + 200 μL anhydrous ethanol was added to the RNA and incubated at -20 °C for 30 min to precipitate the RNA. The samples were then centrifuged at 14000 × g for 30 min at 4 °C. The supernatant was then discarded, 500 μL 75% ethanol was added, and the samples were gently blown with a pipette to clean the RNA. Next, the samples were centrifuged at 800 × g for 10 min at 4 °C. The supernatant was discarded, and the RNA was dissolved with 10 μL ddH_2O. Finally, the samples were transferred to -80 °C on ice for preservation; (2) detection of RNA concentration: The ratio of A260/A280 was eligible for all of the samples, which indicates that the purity of the RNA was high and suitable for further experiments; (3) preparation of cDNA by RNA reverse transcription: The gDNA was removed, and the specimens were heated to 42 °C for 2 min. For reverse transcription, the reaction solution was prepared according to Table 1. The samples were heated at 37 °C for 15 min and 85 °C for 5 s. The reaction was then stopped and cooled down to 4 °C; (4) concentration and purity of cDNA: After zero adjustment, 1 μL of the cDNA sample to

Table 1 Preparation of reverse transcription system

Reagent	Dose (μL)
5 × prime script buffer	4
Prime sript RT enzyme mix	1
RT primer xix	1
ddH_2O	4

RT: Real time; dd: Double distilled.

be tested was dropped onto the detection probe to determine the concentration and purity. The probe was washed with ddH2O between the evaluation of the two samples; and (5) qRT-PCR: qRT-PCR was carried out as follows: PCR amplification reaction, denaturation at 95 °C for 5 min, PCR reaction at 95 °C for 10 s, and 60 °C for 30 s for 45 cycles.

Statistical analysis

Data are presented as mean ± SD. Differences among the groups were analyzed using the analysis of variance. SPSS (version 23.0; IBM, Armonk, NY, United States) and GraphPad 7.0 (Software, CA, United States) statistical software were used to perform statistical analyses. Two-tailed *P* values were calculated, and statistical significance was set as $P < 0.05$.

RESULTS

The effect of B. infantis on the expression of PD-1 after PD-L1 blockade

Western blot results: Compared to the DSS + *B. infantis* group, PD-1 protein in the DSS + *B. infantis* + anti-PD-L1 group decreased, but the difference was not statistically significant ($P = 0.07$). Compared to DSS model group, the expression of PD-1 was no significant distinction in DSS + anti-PD-L1 group ($P = 0.62$) (Figure 1A-C).

qRT-PCR results: In contrast to control group, PD-1 messenger ribonucleic acid (mRNA) in DSS group decreased significantly ($P < 0.05$). In constrast to DSS group, the expression of DSS + *B. infantis* group increased, but the difference was not statistically significant ($P = 0.36$). Compared to the *B. infantis* group, PD-1 RNA decreased significantly in the DSS + *B. infantis* + anti-PD-L1 group ($P < 0.05$) (Figure 1A-C).

Effect of B. infantis on Tregs and Foxp3 expression after PD-L1 blockade

Western blot results: Compared to the DSS + *B. infantis* group, Foxp3 protein decreased in DSS + *B. infantis* + anti-PD-L1 group, and the difference was statistically significant ($P < 0.05$). There was no significant difference in Foxp3 protein expression between the DSS model group and DSS + anti-PD-L1 group ($P = 0.99$) (Figure 1D-F).

RT-qPCR results: In contrast to control group, Foxp3 mRNA in DSS model group decreased significantly ($P < 0.05$); Foxp3 mRNA in DSS + *B. infantis* group was significantly higher than that in DSS model group ($P < 0.05$). Compared to the *B. infantis* group, the expression of Foxp3 mRNA decreased significantly in the DSS + *B. infantis* + anti-PD-L1 group ($P < 0.05$). In comparison with DSS model group, Foxp3 mRNA in DSS + anti-PD-L1 group was also visible distinction ($P < 0.05$) (Figure 1D-F).

Flow cytometry results

Flow cytometry of peripheral blood: Compared to control group, the proportion of peripheral $CD4^+$, $CD25^+$, $Foxp3^+$ cells decreased visibly ($P < 0.05$) of DSS group and increased visibly in the blood of the DSS + *B. infantis* group ($P < 0.05$). Compared to the DSS + *B. infantis* group, the proportion of $CD4^+$, $CD25^+$, $Foxp3^+$ cells in the peripheral blood of DSS + *B. infantis* + anti-PD-L1 group was significantly lower ($P < 0.05$). The proportion of $CD4^+$, $CD25^+$, $Foxp3^+$ cells in the blood of the DSS + anti-PD-L1 group was also distinctly lower compared to the DSS group ($P < 0.05$) (Figure 2).

Flow cytometry of splenocytes: The ratio of splenic $CD4^+$, $CD25^+$, $Foxp3^+$ cells in DSS model group was significantly lower ($P < 0.05$), comparing to control group. The ratio of $CD4^+$, $CD25^+$, $Foxp3^+$ cells in the DSS + *B. infantis* group was significantly higher than that in the DSS model group ($P < 0.05$). Compared to the DSS + *B. infantis* group, the proportion of $CD4^+$, $CD25^+$, $Foxp3^+$ cells in the DSS + *B. infantis* + anti-

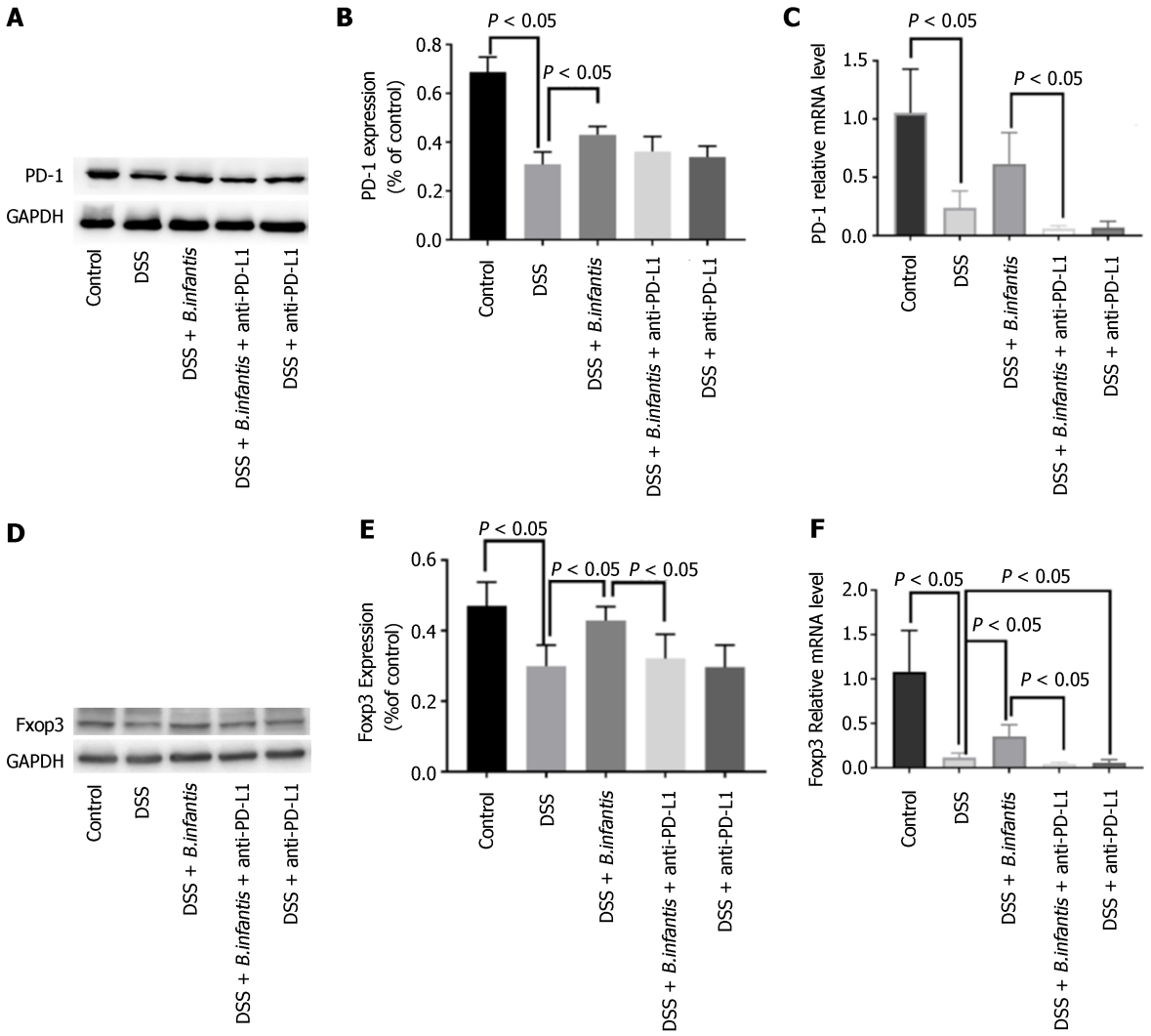

DOI: 10.3748/wjg.v28.i26.3164

Figure 1 The effects of blocking programmed cell death ligand. A: Expression of programmed cell death 1 (PD-1) protein; B: Statistical chart showing the differences in PD-1 protein expression; C: Statistical map showing the differences in PD-1 mRNA expression; D: Western blot showing forkhead box protein 3 protein (Foxp3) expression; E: Statistical chart showing the differences in Foxp3 expression; F: Statistical map showing the differences in Foxp3 mRNA levels. Data are presented as mean ± SD, and comparisons between groups were analyzed by one-way analysis of variance. Statistical significance was set as $P < 0.05$. PD-1: Programmed cell death 1; PD-L1: Programmed cell death ligand; GAPDH: Glyceraldehyde-3-phosphate dehydrogenase; DSS: Dextran sulfate sodium; *B. infantis*: *Bifidobacterium infantis*; Foxp3: Forkhead box protein 3.

PD-L1 group decreased significantly ($P < 0.05$). The proportion of $CD4^+$, $CD25^+$, $Foxp3^+$ cells in the DSS + anti-PD-L1 group also decreased significantly compared to the DSS group ($P < 0.05$) (Figure 3).

The effect of B. infantis on the expression of IL-10 and TGF-β1 after PD-L1 blockade

Western blot results: The expression of IL-10 and TGF-β1 protein in the DSS + *B. infantis* group was lower than that in DSS + *B. infantis* + anti-PD-L1 group ($P < 0.05$). Compared to the DSS model group, there was no apparent distinction in the express of IL-10 ($P = 0.99$) or TGF-β1 in the DSS + anti-PD-L1 group ($P < 0.05$) (Figure 4).

Real time PCR results: In comparison with control group, mRNA of IL-10 and TGF-β1 in the DSS model group decreased ($P < 0.05$), and mRNA of IL-10 and TGF-β1 in the DSS + *B. infantis* group increased clearly ($P < 0.05$). IL-10 and TGF-β1 mRNA expression in DSS + *B. infantis* + anti-PD-L1 group decreased clearly ($P < 0.05$) contrsating to DSS + *B. infantis* group. Compared to the DSS model group, IL-10 and TGF-β1 mRNA in DSS + anti-PD-L1 group were also statistically distinction ($P < 0.05$) (Figure 4).

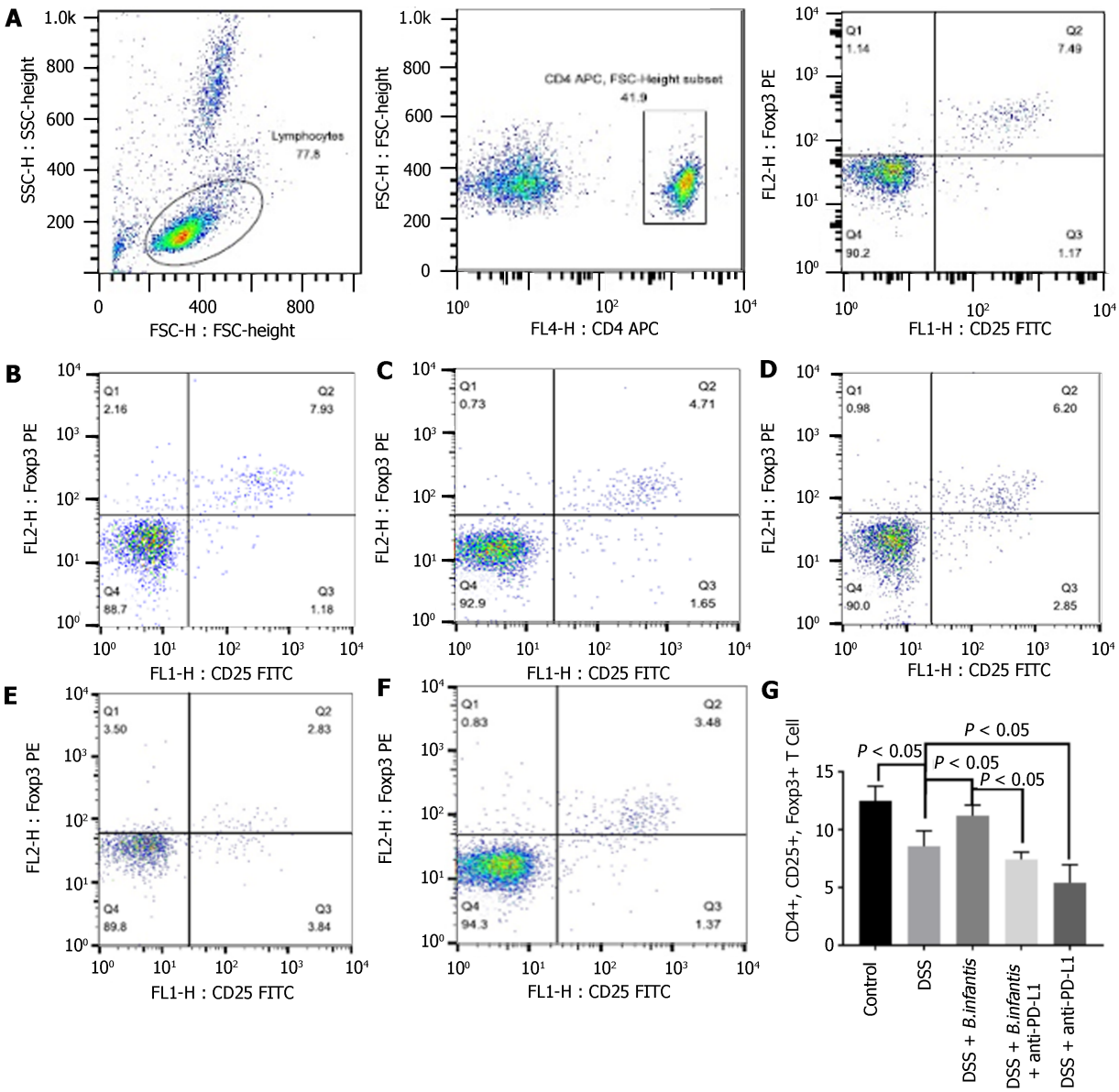

DOI: 10.3748/wjg.v28.i26.3164

Figure 2 Effects of *Bifidobacterium infantis* and programmed cell death ligand inhibition on the proportion of CD4⁺, CD25⁺, and forkhead box protein 3⁺ cells in the blood. A: The strategy of CD4⁺, CD25⁺, and forkhead box protein (Foxp) 3⁺ cells; B-F: Flow cytometry results for the control group (B), the DSS model group (C), the DSS + *B. infantis* group (D), the DSS + *B. infantis* + anti-PD-L1 group (E), the DSS + anti-PD-L1 group (F); G: Statistical chart of the numbers of CD4⁺, CD25⁺, and Foxp3⁺ cells. Data are presented as mean ± SD, and the comparisons among each group were analyzed by one-way analysis of variance. Statistical significance was set as $P < 0.05$. PD-1: Programmed cell death 1; PD-L1: Programmed cell death ligand; DSS: Dextran sulfate sodium; *B. infantis: Bifidobacterium infantis*; Foxp3⁺: Forkhead box protein 3⁺; CD: Cluster of differentiation; SSC: Side scatter; FSC: Forward scatter; FL: Fluorescence; APC: Allophycocyanin; FITC: Fluorescein isothiocyanate; H: Height.

DISCUSSION

The specific pathogenesis of IBD remains unclear; however, abnormal inflammatory responses and continuous inflammatory damage to the intestine are recognized as the basic mechanisms of IBD pathogenesis[24,25]. Intestinal immunity is a complex and interactive process, involving several immune factors such as intestinal mucosal immunity, T cells, cytokines, and intestinal microecology [26]. The intestinal mucosal immune system is responsible for monitoring the intestinal microbiota and surface antigens[27], presenting antigens to CD4⁺ T cells, promoting the interaction between PD-1 and PD-L1, establishing immune tolerance, and preventing the occurrence of autoimmunity. Several inflammatory mediators including interferon γ, tumor necrosis factor α, IL-10, and other cytokines, are involved in the pathogenesis of DSS colitis, suggesting that inflammatory immune responses play a critical role in the pathogenesis of IBD[28-30].

A recently discovered immunostimulatory molecule, PD-1 interacts with its ligand PD-L1 to regulate T cell-mediated immunity and induce immune tolerance, thereby playing a critical role in autoimmune

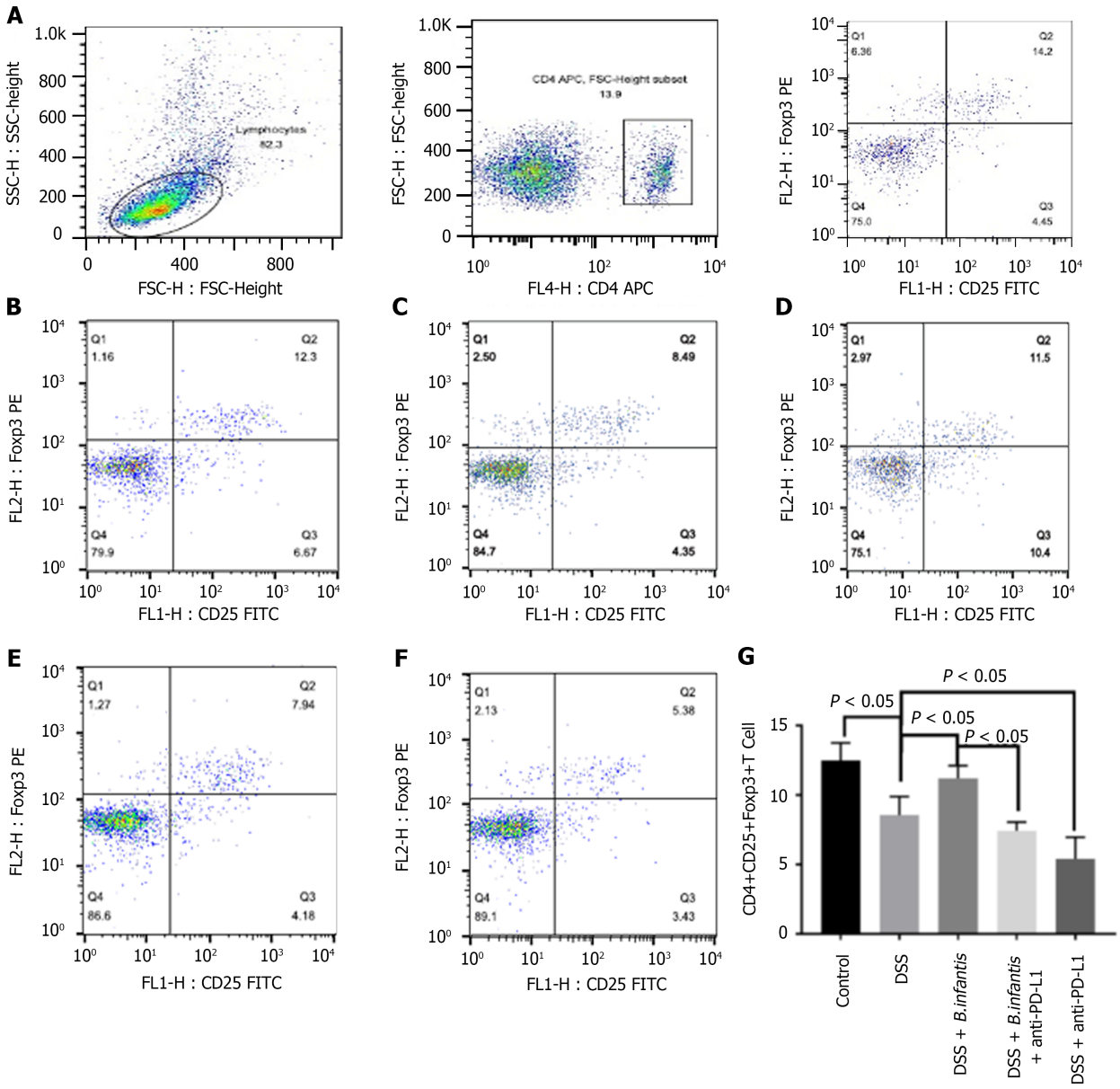

DOI: 10.3748/wjg.v28.i26.3164

Figure 3 Effects of *Bifidobacterium infantis* and programmed cell death ligand inhibition on the proportion of splenic CD4⁺, CD25⁺, and forkhead box protein 3⁺ cells. A: The strategy of CD4⁺, CD25⁺, and forkhead box protein (Foxp) 3⁺ cells; B-F: Flow cytometry results for the the control group (B), the DSS model group (C), the DSS + *B. infantis* group (D), the DSS + *B. infantis* + anti-PD-L1 group (E); and the DSS + anti-PD-L1 group (F); G: Statistical chart of the numbers of CD4⁺, CD25⁺, and Foxp3⁺ cells. Data are presented as mean ± SD, and the comparisons among each group were analyzed by one-way analysis of variance. Statistical significance was set as $P < 0.05$. PD-1: Programmed cell death 1; PD-L1: Programmed cell death ligand; DSS: Dextran sulfate sodium; *B. infantis* : *Bifidobacterium infantis*; Foxp3⁺: Forkhead box protein 3⁺; CD: Cluster of differentiation; SSC: Side scatter; FSC: Forward scatter; FL: Fluorescence; APC: Allophycocyanin; FITC: Fluorescein isothiocyanate; H: Height.

diseases (such as IBD), tumor immunity, and the acceptance of transplanted organs. Studies have shown that PD-1 knockout results in autoimmune diseases in animal models[31-33]. Activation of the PD-1/PD-L1 signaling pathway can induce the differentiation of Tregs[34] and the release of cytokines, such as IL-10 and TGF-β1, to inhibit the activation and proliferation of reactive T cells, thus maintaining intestinal immune tolerance. Additionally, the inhibition of the PD-1/PD-L1 pathway may reduce the proportion of Tregs[35]. These findings indicate that PD-1/PD-L1 signaling plays a critical role in immune tolerance[36]. In this study, we found that PD-L1 inhibition did not alter the PD-1 protein and mRNA levels in the intestine of DSS-induced mice, suggesting that PD-L1 did not affect the transcription or translation of PD-1 in the intestine of the IBD mouse model. However, although the expression of PD-1 mRNA in the intestinal tracts of DSS mice significantly decreased, the expression of PD-1 protein did not change after *B. infantis* administration. We, therefore, speculate that PD-L1 inhibition may indirectly inhibit the *B. infantis*-induced PD-1 gene transcription, but not the post-transcriptional modification and translation of PD-1 protein. This transcriptional inhibition of PD-1 may be due to a negative feedback mechanism caused by the high PD-1 protein levels. Further studies are

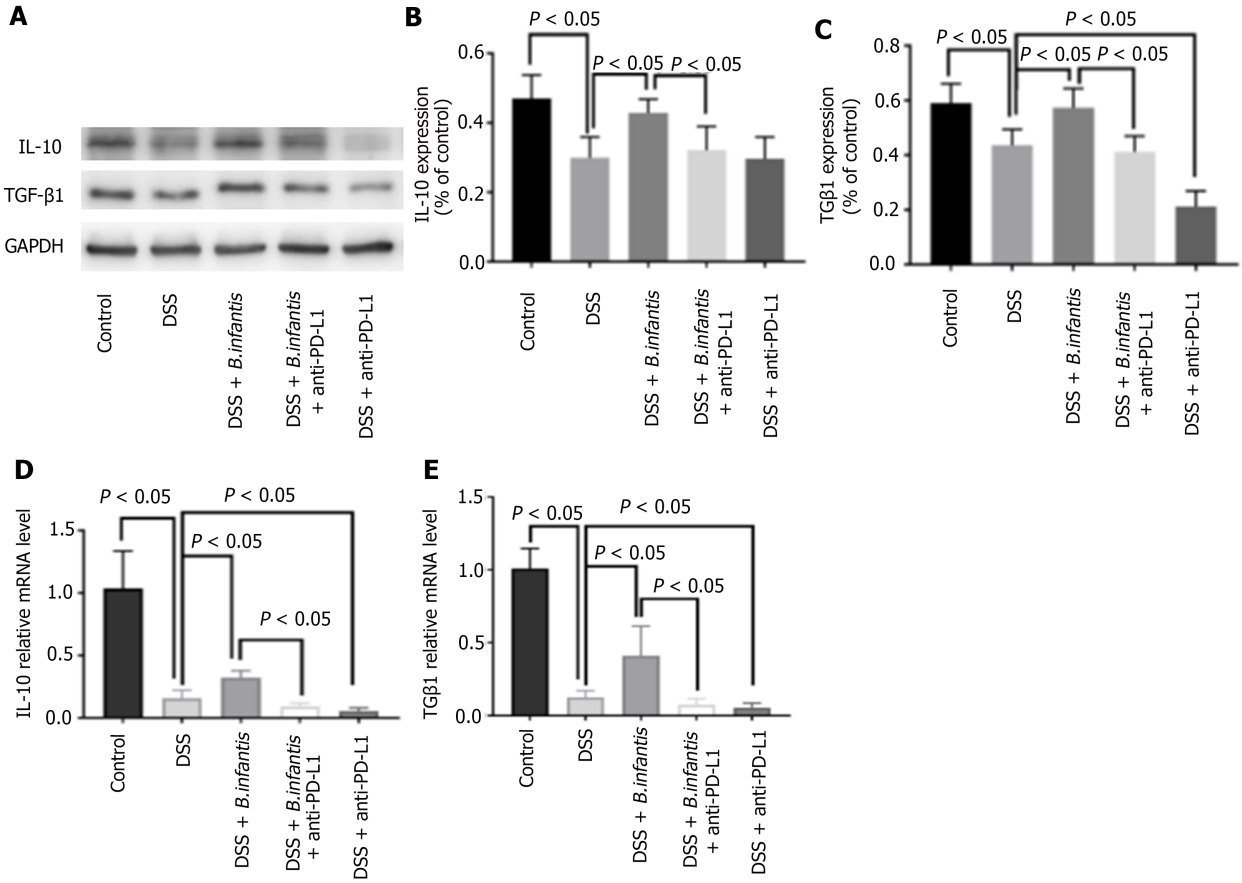

DOI: 10.3748/wjg.v28.i26.3164

Figure 4 Effects of programmed cell death ligand inhibition on the expression of interleukin-10 and transforming growth factor β 1. A: Western blot showing interleukin (IL)-10 and transforming growth factor β (TGF-β) 1 protein expression; B-E: Statistical maps of the differences in IL-10 protein expression (B), TGF-β1 protein expression (C), IL-10 mRNA expression (D), and TGF-β1 expression (E). Data are presented as mean ± SD, and the comparisons among each group were analyzed by one-way analysis of variance. Statistical significance was set as $P < 0.05$. PD-1: Programmed cell death 1; PD-L1: Programmed cell death ligand; DSS: Dextran sulfate sodium; *B. infantis: Bifidobacterium infantis*; IL: Interleukin; TGF-β: Transforming growth factor β; GAPDH: Glyceraldehyde-3-phosphate dehydrogenase; mRNA: Messenger ribonucleic acid.

needed to determine how PD-L1 inhibition suppresses the transcription and translation of PD-1 and the underlying mechanism of action of the effect of *B. infantis* on PD-1 after PD-L1 inhibition.

B. infantis can be used to treat IBD by regulating the intestinal microbiota, alleviating inflammation, and regulating the immune response. *B. infantis* can reduce the intestinal wall permeability, edema, and neutrophil infiltration in IBD mice, and alleviate intestinal inflammatory responses[37]. We have previously shown that a combined administration of *B. infantis* with *Clostridium butyricum* increases the abundance of probiotic bacteria (such as members of the genera *Bifidobacterium* and *Lactobacillus)* in the intestinal microbiota of patients with IBD, reduces the prevalence of enterococci, improves clinical symptoms, and promotes the healing of colonic mucosa[38]. *B. infantis* also plays an important role in immune regulation by promoting the proliferation of Tregs[39] and increasing the expression of IL-10 and TGF-β1. *In vivo* and *in vitro* experiments have revealed that *B. infantis* can significantly accelerate the differentiation of $CD4^+$ T cells into Tregs by inducing the maturation of resistant dendritic cells and further inhibiting the inflammatory response induced by reactive T cell activation. Furthermore, we have previously revealed that, compared to the observations in normal mice, the number of $CD4^+$, $CD25^+$, and $Foxp3^+$ T cells in the blood and spleen of DSS mice and the expression of Foxp3 mRNA in their intestines showed a decrease, suggesting that the differentiation and proliferation of Tregs may be correlated to the pathogenesis of IBD[40]. The number of Tregs in the colon was reported to be related to the intestinal microbiota. Treg populations in the colons of sterile mice are significantly low; however, feeding sterile mice with feces collected from specific pathogen-free mice significantly increases the number of Tregs in the colon[41], indicating that Treg population is dependent on the intestinal microbiota. In patients with IBD, the proportion of normal intestinal bacteria decreases, resulting in intestinal microbiota-associated disorders[42]. Therefore, improving the composition of the intestinal microbiota can help increase the number of Tregs; however, further studies are needed for the elucidation of the underlying mechanism. In the present study, we found that *B. infantis* promotes the proliferation of $CD4^+$, $CD25^+$, and $Foxp3^+$ T cells in the blood and spleen, as well as the expression of Foxp3 mRNA in the intestine. PD-L1 inhibition significantly reduced the numbers of $CD4^+$, $CD25^+$, and

Foxp3$^+$ T cells in the blood and spleen, and decreased the expression of Foxp3 protein and mRNA in the intestine. Therefore, *B. infantis* promotes Treg proliferation by activating the PD-L1/PD-1 pathway.

In addition, our results indicate that *B. infantis* promoted the mRNA expression of IL-10 and TGF-β1 in the mouse intestine. PD-L1 inhibition significantly reduced the protein and mRNA expression levels of IL-10 and TGF-β1 in the intestine. These results further indicate that *B. infantis* affected IL-10 and TGF-β1 expression through the PD-1/PD-L1 pathway. Notably, Tregs mainly secrete TGF-β1 and IL-10 to inhibit inflammatory responses. Further studies are needed to confirm the immunosuppressive effects of *B. infantis* in patients with IBD. Additionally, Francisco *et al*[20] found that PD-L1 can downregulate Protein kinase B (Akt), mammalian target of rapamycin (mTOR), and extracellular regulated protein kinases (ERK2), while upregulating phosphatase and tensin homolog deleted on chromosome ten (PTEN) expression in Tregs; however, whether *B. infantis* can accelerate the differentiation and proliferation of Tregs by activating the PD-1/PD-L1 pathway and regulating Akt, mTOR, or PTEN expression requires further investigation.

CONCLUSION

In conclusion, *B. infantis* may accelerate the proliferation of CD4$^+$, CD25$^+$, and Foxp3$^+$ T cells in the spleen and peripheral blood, and the expression of Foxp3 in the intestine by activating the PD-1/PD-L1 signaling pathway. It can also promote the expression of IL-10 and TGF-β1 to reduce the intestinal inflammatory response, which has a therapeutic effect on IBD mice. We aim to further investigate the role of the PD-1/PD-L1 pathway in IBD and the possible therapeutic effect of *B. infantis* on patients with IBD in future studies.

ARTICLE HIGHLIGHTS

Research background

The immune-inflammatory response plays an important role in the pathogenesis and development of inflammatory bowel disease (IBD). *Bifidobacterium infantis* (*B. infantis*) can repair the acute intestinal mucosal injury and maintain autoimmune tolerance in mice with IBD.

Research motivation

The specific mechanism of action of *B. infantis* in the treatment of IBD is unclear. Understanding this underlying mechanism will help in the treatment of IBD.

Research objectives

To explore if *B. infantis* can promote regulatory T cell Treg differentiation through the programmed cell death 1 (PD-1)/PD ligand (PD-L1) pathway to promote the expression of forkhead box protein 3 (Foxp3), interleukin (IL)-10 and transforming growth factor β (TGF-β) 1, and reduce the inflammatory response.

Research methods

We blocked the expression of PD-L1 in the intestine and performed western blotting and real-time qPCR to observe the effects of *B. infantis* on PD-1, Foxp3, IL-10, and TGF-β1. Flow cytometry was used to examine the changes in the differentiation of CD4$^+$, CD25$^+$, and Foxp3$^+$ cells in the blood and spleen after blocking PD-L1.

Research results

PD-L1 inhibition reduced the promoting effects of *B. infantis* on intestinal PD-1, Foxp3, IL-10, and TGF-β 1. The promoting effect of *B. infantis* on the differentiation of CD4$^+$, CD25$^+$, and Foxp3$^+$ cells was also reduced.

Research conclusions

B. infantis mediates Foxp3 expression through the PD-1/PD-L1 pathway, thereby promoting Treg differentiation and improving IL-10 and TGF-β1 expression to reduce the immune and inflammatory response in IBD. *B. infantis* may act as a therapeutic agent for IBD.

Research perspectives

To explore the mechanism of action of *B. infantis* in the treatment of IBD at the cellular level. Further experiments are essential to determine whether *B. infantis* inhibits the immune response through the PD-1/PD-L1 pathway in the patients with IBD.

ACKNOWLEDGEMENTS

The authors thank Professor Liu DY for her guidance during the experiments.

FOOTNOTES

Author contributions: Zhou LY obtained funding, processed the samples, analyzed the raw data, and wrote manuscript; Xie Y processed the samples, obtained and managed data; Li Y conceived the study protocol, critically revised the manuscript, and approved the final version.

Supported by the Doctoral Start-up Foundation of Liaoning Province, No. 2021-BS-114.

Institutional review board statement: The study was reviewed and approved by the Institutional Review Board at Shengjing Hospital of China Medical University.

Institutional animal care and use committee statement: All animal experiments conformed to the internationally accepted principles for the care and use of laboratory animals, No. 2017PS353K.

Conflict-of-interest statement: The authors declare that they have no conflict of interest.

Data sharing statement: No additional data are available.

ARRIVE guidelines statement: The authors have read the ARRIVE guidelines, and the manuscript was prepared and revised according to the ARRIVE guidelines.

Country/Territory of origin: China

ORCID number: Lin-Yan Zhou 0000-0002-9403-2809; Ying Xie 0000-0001-8226-4242; Yan Li 0000000276903324.

S-Editor: Chen YL
L-Editor: A
P-Editor: Cai YX

REFERENCES

1 **Burisch J**, Zammit SC, Ellul P, Turcan S, Duricova D, Bortlik M, Andersen KW, Andersen V, Kaimakliotis IP, Fumery M, Gower-Rousseau C, Girardin G, Valpiani D, Goldis A, Brinar M, Čuković-Čavka S, Oksanen P, Collin P, Barros L, Magro F, Misra R, Arebi N, Eriksson C, Halfvarson J, Kievit HAL, Pedersen N, Kjeldsen J, Myers S, Sebastian S, Katsanos KH, Christodoulou DK, Midjord J, Nielsen KR, Kiudelis G, Kupcinskas L, Nikulina I, Belousova E, Schwartz D, Odes S, Salupere R, Carmona A, Pineda JR, Vegh Z, Lakatos PL, Langholz E, Munkholm P; Epi-IBD group. Disease course of inflammatory bowel disease unclassified in a European population-based inception cohort: An Epi-IBD study. *J Gastroenterol Hepatol* 2019; **34**: 996-1003 [PMID: 30562421 DOI: 10.1111/jgh.14563]

2 **Olendzki B**, Bucci V, Cawley C, Maserati R, McManus M, Olednzki E, Madziar C, Chiang D, Ward DV, Pellish R, Foley C, Bhattarai S, McCormick BA, Maldonado-Contreras A. Dietary manipulation of the gut microbiome in inflammatory bowel disease patients: Pilot study. *Gut Microbes* 2022; **14**: 2046244 [PMID: 35311458 DOI: 10.1080/19490976.2022.2046244]

3 **Lo Sasso G**, Phillips BW, Sewer A, Battey JND, Kondylis A, Talikka M, Titz B, Guedj E, Peric D, Bornand D, Dulize R, Merg C, Corciulo M, Ouadi S, Yanuar R, Tung CK, Ivanov NV, Peitsch MC, Hoeng J. The reduction of DSS-induced colitis severity in mice exposed to cigarette smoke is linked to immune modulation and microbial shifts. *Sci Rep* 2020; **10**: 3829 [PMID: 32123204 DOI: 10.1038/s41598-020-60175-3]

4 **Algethmi W**, Baumann C, Alnajjar W, Sroji A, Alsahafi M, Jawa H, Qari Y, Peyrin-Biroulet L, Saadah OI, Mosli M. Environmental exposures and the risk of inflammatory bowel disease: a case-control study from Saudi Arabia. *Eur J Gastroenterol Hepatol* 2020; **32**: 358-364 [PMID: 31851095 DOI: 10.1097/MEG.0000000000001619]

5 **Illiano P**, Brambilla R, Parolini C. The mutual interplay of gut microbiota, diet and human disease. *FEBS J* 2020; **287**: 833-855 [PMID: 31955527 DOI: 10.1111/febs.15217]

6 **Lavelle A**, Sokol H. Gut microbiota-derived metabolites as key actors in inflammatory bowel disease. *Nat Rev Gastroenterol Hepatol* 2020; **17**: 223-237 [PMID: 32076145 DOI: 10.1038/s41575-019-0258-z]

7 **Sartor RB**. Mechanisms of disease: pathogenesis of Crohn's disease and ulcerative colitis. *Nat Clin Pract Gastroenterol Hepatol* 2006; **3**: 390-407 [PMID: 16819502 DOI: 10.1038/ncpgasthep0528]

8 **Li J**, Jie HB, Lei Y, Gildener-Leapman N, Trivedi S, Green T, Kane LP, Ferris RL. PD-1/SHP-2 inhibits Tc1/Th1 phenotypic responses and the activation of T cells in the tumor microenvironment. *Cancer Res* 2015; **75**: 508-518 [PMID: 25480946 DOI: 10.1158/0008-5472.CAN-14-1215]

9 **Pauken KE**, Sammons MA, Odorizzi PM, Manne S, Godec J, Khan O, Drake AM, Chen Z, Sen DR, Kurachi M, Barnitz RA, Bartman C, Bengsch B, Huang AC, Schenkel JM, Vahedi G, Haining WN, Berger SL, Wherry EJ. Epigenetic stability of exhausted T cells limits durability of reinvigoration by PD-1 blockade. *Science* 2016; **354**: 1160-1165 [PMID: 27789795 DOI: 10.1126/science.aaf2807]

10 **Garcia-Bates TM**, Palma ML, Shen C, Gambotto A, Macatangay BJC, Ferris RL, Rinaldo CR, Mailliard RB. Contrasting Roles of the PD-1 Signaling Pathway in Dendritic Cell-Mediated Induction and Regulation of HIV-1-Specific Effector T Cell Functions. *J Virol* 2019; **93** [PMID: 30541848 DOI: 10.1128/JVI.02035-18]

11 **Zamani MR**, Aslani S, Salmaninejad A, Javan MR, Rezaei N. PD-1/PD-L and autoimmunity: A growing relationship. *Cell Immunol* 2016; **310**: 27-41 [PMID: 27660198 DOI: 10.1016/j.cellimm.2016.09.009]

12 **Kuol N**, Stojanovska L, Nurgali K, Apostolopoulos V. PD-1/PD-L1 in disease. *Immunotherapy* 2018; **10**: 149-160 [PMID: 29260623 DOI: 10.2217/imt-2017-0120]

13 **Long Y**, Xia C, Sun Y, Ma Y, Xu L, Song Y, Liu C. Increased circulating PD-1^{hi}CXCR5- peripheral helper T cells are associated with disease severity of active ulcerative colitis patients. *Immunol Lett* 2021; **233**: 2-10 [PMID: 33675861 DOI: 10.1016/j.imlet.2021.03.001]

14 **Li JY**, Yu M, Pal S, Tyagi AM, Dar H, Adams J, Weitzmann MN, Jones RM, Pacifici R. Parathyroid hormone-dependent bone formation requires butyrate production by intestinal microbiota. *J Clin Invest* 2020; **130**: 1767-1781 [PMID: 31917685 DOI: 10.1172/JCI133473]

15 **Hartwig T**, Zwicky P, Schreiner B, Yawalkar N, Cheng P, Navarini A, Dummer R, Flatz L, Conrad C, Schlapbach C, Becher B. Regulatory T Cells Restrain Pathogenic T Helper Cells during Skin Inflammation. *Cell Rep* 2018; **25**: 3564-3572.e4 [PMID: 30590032 DOI: 10.1016/j.celrep.2018.12.012]

16 **Barbi J**, Pardoll D, Pan F. Treg functional stability and its responsiveness to the microenvironment. *Immunol Rev* 2014; **259**: 115-139 [PMID: 24712463 DOI: 10.1111/imr.12172]

17 **Vitale A**, Strisciuglio C, Vitale S, Santopaolo M, Bruzzese D, Micillo T, Scarpato E, Miele E, Staiano A, Troncone R, Matarese G, Gianfrani C. Increased frequency of regulatory T cells in pediatric inflammatory bowel disease at diagnosis: a compensative role? *Pediatr Res* 2020; **87**: 853-861 [PMID: 31715619 DOI: 10.1038/s41390-019-0662-7]

18 **O'Garra A**, Vieira P. Regulatory T cells and mechanisms of immune system control. *Nat Med* 2004; **10**: 801-805 [PMID: 15286781 DOI: 10.1038/nm0804-801]

19 **Maul J**, Loddenkemper C, Mundt P, Berg E, Giese T, Stallmach A, Zeitz M, Duchmann R. Peripheral and intestinal regulatory CD4+ CD25(high) T cells in inflammatory bowel disease. *Gastroenterology* 2005; **128**: 1868-1878 [PMID: 15940622 DOI: 10.1053/j.gastro.2005.03.043]

20 **Francisco LM**, Salinas VH, Brown KE, Vanguri VK, Freeman GJ, Kuchroo VK, Sharpe AH. PD-L1 regulates the development, maintenance, and function of induced regulatory T cells. *J Exp Med* 2009; **206**: 3015-3029 [PMID: 20008522 DOI: 10.1084/jem.20090847]

21 **Ding Q**, Lu L, Zhou X, Zhou Y, Chou KY. Human PD-L1-overexpressing porcine vascular endothelial cells induce functionally suppressive human CD4+CD25hiFoxp3+ Treg cells. *J Leukoc Biol* 2011; **90**: 77-86 [PMID: 21498584 DOI: 10.1189/jlb.1210691]

22 **Zhou L**, Liu D, Xie Y, Yao X, Li Y. *Bifidobacterium infantis* Induces Protective Colonic PD-L1 and Foxp3 Regulatory T Cells in an Acute Murine Experimental Model of Inflammatory Bowel Disease. *Gut Liver* 2019; **13**: 430-439 [PMID: 30600673 DOI: 10.5009/gnl18316]

23 **Chaudhary CL**, Gurung P, Jang S, Banskota S, Nam TG, Kim JA, Jeong BS. Synthesis, activity and mechanism of alkoxy-, carbamato-, sulfonamido-, thioureido-, and ureido-derivatives of 2,4,5-trimethylpyridin-3-ol against inflammatory bowel disease. *J Enzyme Inhib Med Chem* 2020; **35**: 1-20 [PMID: 31619080 DOI: 10.1080/14756366.2019.1677637]

24 **Lee KH**, Ahn BS, Cha D, Jang WW, Choi E, Park S, Park JH, Oh J, Jung DE, Park H, Suh Y, Jin D, Lee S, Jang YH, Yoon T, Park MK, Seong Y, Pyo J, Yang S, Kwon Y, Jung H, Lim CK, Hong JB, Park Y, Shin JI, Kronbichler A. Understanding the immunopathogenesis of autoimmune diseases by animal studies using gene modulation: A comprehensive review. *Autoimmun Rev* 2020; **19**: 102469 [PMID: 31918027 DOI: 10.1016/j.autrev.2020.102469]

25 **Eichele DD**, Kharbanda KK. Dextran sodium sulfate colitis murine model: An indispensable tool for advancing our understanding of inflammatory bowel diseases pathogenesis. *World J Gastroenterol* 2017; **23**: 6016-6029 [PMID: 28970718 DOI: 10.3748/wjg.v23.i33.6016]

26 **Yan PG**, Li JN. Advances in the understanding of the intestinal micro-environment and inflammatory bowel disease. *Chin Med J (Engl)* 2020; **133**: 834-841 [PMID: 32106123 DOI: 10.1097/CM9.0000000000000718]

27 **Aden K**, Rehman A, Waschina S, Pan WH, Walker A, Lucio M, Nunez AM, Bharti R, Zimmerman J, Bethge J, Schulte B, Schulte D, Franke A, Nikolaus S, Schroeder JO, Vandeputte D, Raes J, Szymczak S, Waetzig GH, Zeuner R, Schmitt-Kopplin P, Kaleta C, Schreiber S, Rosenstiel P. Metabolic Functions of Gut Microbes Associate With Efficacy of Tumor Necrosis Factor Antagonists in Patients With Inflammatory Bowel Diseases. *Gastroenterology* 2019; **157**: 1279-1292.e11 [PMID: 31326413 DOI: 10.1053/j.gastro.2019.07.025]

28 **Yan Y**, Kolachala V, Dalmasso G, Nguyen H, Laroui H, Sitaraman SV, Merlin D. Temporal and spatial analysis of clinical and molecular parameters in dextran sodium sulfate induced colitis. *PLoS One* 2009; **4**: e6073 [PMID: 19562033 DOI: 10.1371/journal.pone.0006073]

29 **Hall LJ**, Faivre E, Quinlan A, Shanahan F, Nally K, Melgar S. Induction and activation of adaptive immune populations during acute and chronic phases of a murine model of experimental colitis. *Dig Dis Sci* 2011; **56**: 79-89 [PMID: 20467900 DOI: 10.1007/s10620-010-1240-3]

30 **Fukata M**, Michelsen KS, Eri R, Thomas LS, Hu B, Lukasek K, Nast CC, Lechago J, Xu R, Naiki Y, Soliman A, Arditi M, Abreu MT. Toll-like receptor-4 is required for intestinal response to epithelial injury and limiting bacterial translocation in a murine model of acute colitis. *Am J Physiol Gastrointest Liver Physiol* 2005; **288**: G1055-G1065 [PMID: 15826931 DOI: 10.1152/ajpgi.00328.2004]

31 **Chen L**, Pai V, Levinson R, Sharpe AH, Freeman GJ, Braun J, Gordon LK. Constitutive neuronal expression of the immune regulator, programmed death 1 (PD-1), identified during experimental autoimmune uveitis. *Ocul Immunol Inflamm* 2009; **17**: 47-55 [PMID: 19294574 DOI: 10.1080/09273940802491884]

32 **Roosenboom B**, Horjus Talabur Horje CS, Smids C, Leeuwis JW, van Koolwijk E, Groenen MJM, Wahab PJ, van Lochem EG. Distribution of mucosal PD-1 expressing T cells in patients with colitis of different etiologies. *Scand J Gastroenterol* 2021; **56**: 671-679 [PMID: 33779456 DOI: 10.1080/00365521.2021.1906316]

33 **Bodhankar S**, Galipeau D, Vandenbark AA, Offner H. PD-1 Interaction with PD-L1 but not PD-L2 on B-cells Mediates Protective Effects of Estrogen against EAE. *J Clin Cell Immunol* 2013; **4**: 143 [PMID: 24009988 DOI: 10.4172/2155-9899.1000143]

34 **Gianchecchi E**, Fierabracci A. Inhibitory Receptors and Pathways of Lymphocytes: The Role of PD-1 in Treg Development and Their Involvement in Autoimmunity Onset and Cancer Progression. *Front Immunol* 2018; **9**: 2374 [PMID: 30386337 DOI: 10.3389/fimmu.2018.02374]

35 **O'Shaughnessy MJ**, Murray KS, La Rosa SP, Budhu S, Merghoub T, Somma A, Monette S, Kim K, Corradi RB, Scherz A, Coleman JA. Systemic Antitumor Immunity by PD-1/PD-L1 Inhibition Is Potentiated by Vascular-Targeted Photodynamic Therapy of Primary Tumors. *Clin Cancer Res* 2018; **24**: 592-599 [PMID: 28954788 DOI: 10.1158/1078-0432.CCR-17-0186]

36 **Lo YC**, Price C, Blenman K, Patil P, Zhang X, Robert ME. Checkpoint Inhibitor Colitis Shows Drug-Specific Differences in Immune Cell Reaction That Overlap With Inflammatory Bowel Disease and Predict Response to Colitis Therapy. *Am J Clin Pathol* 2021; **156**: 214-228 [PMID: 33555016 DOI: 10.1093/ajcp/aqaa217]

37 **Elian SD**, Souza EL, Vieira AT, Teixeira MM, Arantes RM, Nicoli JR, Martins FS. Bifidobacterium longum subsp. infantis BB-02 attenuates acute murine experimental model of inflammatory bowel disease. *Benef Microbes* 2015; **6**: 277-286 [PMID: 25391346 DOI: 10.3920/BM2014.0070]

38 **Li Hui**, Gong Yi, Li Yan. Clinical efficacy of mesalazine combined with Clostridium butyricum in the treatment of active mild to moderate ulcerative colitis. *Shiyong Yaowu Yu Linchuang* 2016; **19**: 1389-1393 [DOI: 10.14053/j.cnki.ppcr.201611017]

39 **Mi H**, Dong Y, Zhang B, Wang H, Peter CCK, Gao P, Fu H, Gao Y. Bifidobacterium Infantis Ameliorates Chemotherapy-Induced Intestinal Mucositis Via Regulating T Cell Immunity in Colorectal Cancer Rats. *Cell Physiol Biochem* 2017; **42**: 2330-2341 [PMID: 28848081 DOI: 10.1159/000480005]

40 **Fu L**, Song J, Wang C, Fu S, Wang Y. *Bifidobacterium infantis* Potentially Alleviates Shrimp Tropomyosin-Induced Allergy by Tolerogenic Dendritic Cell-Dependent Induction of Regulatory T Cells and Alterations in Gut Microbiota. *Front Immunol* 2017; **8**: 1536 [PMID: 29176981 DOI: 10.3389/fimmu.2017.01536]

41 **Bozkurt HS**, Kara B. A new treatment for ulcerative colitis: Intracolonic Bifidobacterium and xyloglucan application. *Eur J Inflamm* 2020; **18**: 1-7 [DOI: 10.1177/2058739220942626]

42 **Zuo T**, Ng SC. The Gut Microbiota in the Pathogenesis and Therapeutics of Inflammatory Bowel Disease. *Front Microbiol* 2018; **9**: 2247 [PMID: 30319571 DOI: 10.3389/fmicb.2018.02247]

World Journal of Gastroenterology

Submit a Manuscript: https://www.f6publishing.com

World J Gastroenterol 2022 July 14; 28(26): 3177-3200

DOI: 10.3748/wjg.v28.i26.3177

ISSN 1007-9327 (print) ISSN 2219-2840 (online)

ORIGINAL ARTICLE

Basic Study

Involvement of Met receptor pathway in aggressive behavior of colorectal cancer cells induced by parathyroid hormone-related peptide

María Belén Novoa Díaz, Pedro Carriere, Graciela Gigola, Ariel Osvaldo Zwenger, Natalia Calvo, Claudia Gentili

Specialty type: Biochemistry and molecular biology

Provenance and peer review: Invited article; Externally peer reviewed.

Peer-review model: Single blind

Peer-review report's scientific quality classification

Grade A (Excellent): 0
Grade B (Very good): B, B
Grade C (Good): C
Grade D (Fair): D
Grade E (Poor): 0

P-Reviewer: Ding L, China; Gao W, China; Xu HC, China; Wan XH, China
A-Editor: Soldera J, Brazil

Received: January 13, 2022
Peer-review started: January 13, 2022
First decision: March 8, 2022
Revised: March 21, 2022
Accepted: May 27, 2022
Article in press: May 27, 2022
Published online: July 14, 2022

María Belén Novoa Díaz, Pedro Carriere, Graciela Gigola, Natalia Calvo, Claudia Gentili, Departamento de Biología, Bioquímica y Farmacia, Universidad Nacional del Sur (UNS)-INBIOSUR (CONICET-UNS), Bahía Blanca 8000, Buenos Aires, Argentina

Ariel Osvaldo Zwenger, Centro de Estudios Clínicos SAGA, CEC SAGA, Santiago de Chile 8320000, Chile

Corresponding author: Claudia Gentili, PhD, Professor, Research Scientist, Departamento de Biología, Bioquímica y Farmacia, Universidad Nacional del Sur (UNS)- INBIOSUR (CONICET-UNS), 670 San Juan, Bahía Blanca 8000, Buenos Aires, Argentina.
cgentili@criba.edu.ar

Abstract

BACKGROUND

Parathyroid hormone-related peptide (PTHrP) plays a key role in the development and progression of many tumors. We found that in colorectal cancer (CRC) HCT116 cells, the binding of PTHrP to its receptor PTHR type 1 (PTHR1) activates events associated with an aggressive phenotype. In HCT116 cell xenografts, PTHrP modulates the expression of molecular markers linked to tumor progression. Empirical evidence suggests that the Met receptor is involved in the development and evolution of CRC. Based on these data, we hypothesized that the signaling pathway trigged by PTHrP could be involved in the transactivation of Met and consequently in the aggressive behavior of CRC cells.

AIM

To elucidate the relationship among PTHR1, PTHrP, and Met in CRC models.

METHODS

For *in vitro* assays, HCT116 and Caco-2 cells derived from human CRC were incubated in the absence or presence of PTHrP (1-34) (10^{-8} M). Where indicated, cells were pre-incubated with specific kinase inhibitors or dimethylsulfoxide, the vehicle of the inhibitors. The protein levels were evaluated by Western blot technique. Real-time polymerase chain reaction (RT-qPCR) was carried out to determine the changes in gene expression. Wound healing assay and morpho-

logical monitoring were performed to evaluate cell migration and changes related to the epithelial-mesenchymal transition (EMT), respectively. The number of viable HCT116 cells was counted by trypan blue dye exclusion test to evaluate the effects of irinotecan (CPT-11), oxaliplatin (OXA), or doxorubicin (DOXO) with or without PTHrP. For *in vivo* tests, HCT116 cell xenografts on 6-wk-old male N:NIH (S)_nu mice received daily intratumoral injections of PTHrP (40 μg/kg) in 100 μL phosphate-buffered saline (PBS) or the vehicle (PBS) as a control during 20 d. Humanitarian slaughter was carried out and the tumors were removed, weighed, and fixed in a 4% formaldehyde solution for subsequent treatment by immunoassays. To evaluate the expression of molecular markers in human tumor samples, we studied 23 specimens obtained from CRC patients which were treated at the Hospital Interzonal de Graves y Agudos Dr. José Penna (Bahía Blanca, Buenos Aires, Argentina) and the Hospital Provincial de Neuquén (Neuquén, Neuquén, Argentina) from January 1990 to December 2007. Seven cases with normal colorectal tissues were assigned to the control group. Tumor tissue samples and clinical histories of patients were analyzed. Paraffin-embedded blocks from primary tumors were reviewed by hematoxylin-eosin staining technique; subsequently, representative histological samples were selected from each patient. From each paraffin block, tumor sections were stained for immunohistochemical detection. The statistical significance of differences was analyzed using proper statistical analysis. The results were considered statistically significant at $P < 0.05$.

RESULTS

By Western blot analysis and using total Met antibody, we found that PTHrP regulated Met expression in HCT116 cells but not in Caco-2 cells. In HCT116 cells, Met protein levels increased at 30 min ($P < 0.01$) and at 20 h ($P < 0.01$) whereas the levels diminished at 3 min ($P < 0.05$), 10 min ($P < 0.01$), and 1 h to 5 h ($P < 0.01$) of PTHrP treatment. Using an active Met antibody, we found that where the protein levels of total Met decreased (3 min, 10 min, and 60 min of PTHrP exposure), the status of phosphorylated/activated Met increased ($P < 0.01$) at the same time, suggesting that Met undergoes proteasomal degradation after its phosphorylation/activation by PTHrP. The increment of its protein level after these decreases (at 30 min and 20 h) suggests a modulation of Met expression by PTHrP in order to improve Met levels and this idea is supported by our observation that the cytokine increased *Met* mRNA levels at least at 15 min in HCT116 cells as revealed by RT-qPCR analysis ($P < 0.05$). We then proceeded to evaluate the signaling pathways that mediate the phosphorylation/ activation of Met induced by PTHrP in HCT116 cells. By Western blot technique, we observed that PP1, a specific inhibitor of the activation of the proto-oncogene protein tyrosine kinase Src, blocked the effect of PTHrP on Met phosphorylation ($P < 0.05$). Furthermore, the selective inhibition of the ERK 1/2 mitogen-activated protein kinase (ERK 1/2 MAPK) using PD98059 and the p38 MAPK using SB203580 diminished the effect of PTHrP on Met phosphorylation/activation ($P < 0.05$). Using SU11274, the specific inhibitor of Met activation, and trypan blue dye exclusion test, Western blot, wound healing assay, and morphological analysis with a microscope, we observed the reversal of cell events induced by PTHrP such as cell proliferation ($P < 0.05$), migration ($P < 0.05$), and the EMT program ($P < 0.01$) in HCT116 cells. Also, PTHrP favored the chemoresistance to CPT-11 ($P < 0.001$), OXA ($P < 0.01$), and DOXO ($P < 0.01$) through the Met pathway. Taken together, these findings suggest that Met activated by PTHrP participates in events associated with the aggressive phenotype of CRC cells. By immunohistochemical analysis, we found that PTHrP in HCT116 cell xenografts enhanced the protein expression of Met (0.190 ± 0.014) compared to tumors from control mice (0.110 ± 0.012; $P < 0.05$) and of its own receptor (2.27 ± 0.20) compared to tumors from control mice (1.98 ± 0.14; $P < 0.01$). Finally, assuming that the changes in the expression of PTHrP and its receptor are directly correlated, we investigated the expression of both Met and PTHR1 in biopsies of CRC patients by immunohistochemical analysis. Comparing histologically differentiated tumors with respect to those less differentiated, we found that the labeling intensity for Met and PTHR1 increased and diminished in a gradual manner, respectively ($P < 0.05$).

CONCLUSION

PTHrP acts through the Met pathway in CRC cells and regulates Met expression in a CRC animal model. More basic and clinical studies are needed to further evaluate the PTHrP/Met relationship.

Key Words: PTHrP; MET receptor tyrosine kinase; Parathyroid hormone receptor type 1; Colorectal cancer; Drug resistance

Core Tip: Colorectal cancer (CRC) is one of the leading causes of cancer death, and chemoresistance is common in the treatment of CRC patients. Parathyroid hormone-related peptide (PTHrP) and the receptor tyrosine kinase Met are involved in the aggressive behavior of CRC cells. However, to date it is unknown whether PTHrP and Met are related to promoting events associated with the progression and chemoresistance of CRC. Herein we showed, for the first time, a PTHrP/Met axis that could have a positive impact on the knowledge of CRC biology and on the development of new targeted therapies.

Citation: Novoa Díaz MB, Carriere P, Gigola G, Zwenger AO, Calvo N, Gentili C. Involvement of Met receptor pathway in aggressive behavior of colorectal cancer cells induced by parathyroid hormone-related peptide. *World J Gastroenterol* 2022; 28(26): 3177-3200
URL: https://www.wjgnet.com/1007-9327/full/v28/i26/3177.htm
DOI: https://dx.doi.org/10.3748/wjg.v28.i26.3177

INTRODUCTION

Colorectal cancer (CRC) is one of the most frequent tumors of the digestive system and represents the third type of cancer with the highest incidence worldwide[1]. According to statistics, the development of metastasis and resistance to chemotherapeutic drugs causes 90% of deaths in patients with CRC[2]. Although treatment strategies have been improved in the past years, the mortality associated with this oncological disease is still around 50%[1,3]. In this line, the World Cancer Research Fund International indicates that CRC incidence is still increasing and that its prevalence is expected to augment by 60% in the next few years[4]. This is mainly due to the emergence of CRC patients under 50 years old and the appearance of new tumors subtypes that have a refractory response to the usual therapy[5]. Currently, two of the chemotherapeutic agents approved as first and second-line palliative drugs in CRC are oxaliplatin (OXA) and irinotecan (CPT-11)[6,7]. However, more than half of patients with stage II/III disease who underwent surgery and were treated with these drugs relapsed and died[8]. Thus, all these facts evidence an urgent need to elucidate the molecular mechanisms associated with two key aspects of therapy: Effectiveness and resistance.

Parathyroid hormone-related peptide (PTHrP) is a cytokine-like protein that is normally produced in many adult and fetal tissues[9,10]. The N-terminal 13 amino acid residues of PTHrP exhibit high structural homology with the PTH[11]. This allows the binding of both ligands to the same G-protein-coupled receptor, PTH/PTHrP type 1 (PTHR1)[12,13]. It is known that PTHrP and its receptor are expressed in the same cells or neighboring cells. This juxtaposition is directly related to its activity as an autocrine and paracrine factor[14,15].

Regarding the expression of this protein in neoplastic disease, studies in patients show its overexpression in tissues of breast, prostate, lung, and colon cancers[16,17]. Moreover, 95% of colorectal adenocarcinomas have elevated expression of this protein[18-20]. Although PTHrP was initially identified as a major contributor to hypercalcemia in paraneoplastic syndromes, it is known that this peptide also plays a key role in the development and progression of many tumors [10,16,21-23]. In this concern, in CRC-derived cells we found that PTHrP stimulated cell proliferation, survival, and migration, the epithelial-mesenchymal transition (EMT), the release of pro-angiogenic factors, and the resistance to CPT-11[13,24-26]. In xenografts of CRC cells, we have observed that PTHrP also modulates the expression of molecular markers linked to tumor progression[24-27]. Despite these contributions, relevant aspects from the action of this peptide are still unknown, specifically, whether PTHrP could promote resistance to other forms of chemotherapy and the validation of our previous observations using human samples.

Met is a receptor with tyrosine kinase (RTK) activity, and it is expressed in normal tissues and participates in various physiological processes such as embryonic development and wound repair[28]. Only hepatocyte growth factor (HGF) is known as a necessary ligand for its activation. However, cross-communications between this RTK and G-protein-coupled receptors were reported to promote its aberrant activation[29-31]. Met overexpression or its dysregulation can lead to malignant cell transformation and contributes to the development and progression of different types of cancer including colorectal tumors[28,32-35]. Moreover, Met dysregulation is also associated with drug resistance in colon cancer cells[32,35,36]. Several studies demonstrated the overexpression of this RTK in tumor tissue of CRC patients; in this regard, its inhibition is being widely investigated as a complementary treatment to usual therapies[37,38]. Despite this, the value of Met as a prognostic marker or in treatment strategies has not been established yet.

Although empirical evidence suggests that Met and PTHrP play a key role in the development and evolution of CRC, it is still unknown whether PTHrP and Met act cooperatively to promote events associated with the progression and chemoresistance in CRC. Based on our previous studies, we hypothesized that the signaling pathway trigged by PTHR1 after binding to PTHrP could be involved in

the transactivation of the RTK Met and consequently in the aggressive behavior of CRC cells. For this reason, the present work aimed to elucidate the relationship among PTHR1, PTHrP, and Met.

MATERIALS AND METHODS

Reagents and antibodies

Human PTHrP (1-34) and trypan blue dye were obtained from Sigma-Aldrich Chemical Co (St. Louis, MO, United States). Antibodies were purchased from the following sources: Anti-Met and anti-phospho Met (Tyr 1234/1235) and anti-E-cadherin were provided by Cell Signaling Technology (Beverly, MA, United States); anti-PTH/PTHrP receptor type 1, anti-GAPDH, goat anti-rabbit peroxidase conjugated secondary antibody, and goat anti-mouse peroxidase conjugated secondary antibody were from Santa Cruz Biotechnology (Santa Cruz, CA, United States). PD98059, SB203580, and PP1 were obtained from Calbiochem (San Diego, CA, United States) and SU11274 from Sigma-Aldrich Chemical Co. RNase CocktailTM Enzime Mix was from Applied Biosystems (Carlsbad, CA, United States). Protein size markers were from Amersham Biosciences (Piscataway, NJ, United States). Immobilonpolyvinylidene difluoride (PVDF) membranes and electrochemiluminescence (ECL) detection kit were from Amersham (Little Chalfont, Buckinghamshire, England). The chemotherapeutic drugs CPT-11, OXA, and doxorubicin (DOXO) were generously provided by Dr. Ariel Zwenger.

Cell culture and treatment

Human colon cancer cells Caco-2 and HCT116 (American Type Culture Collection, Manassas, VA, United States) were grown at 37 °C in an atmosphere containing 5.5% CO_2 in Dulbecco's Modified Eagle Culture Medium (DMEM) containing 10% heat-inactivated and irradiated fetal bovine serum (FBS), 1% non-essential amino acids, penicillin (100 IU/mL), streptomycin (100 mg/mL), and gentamicin (50 mg/mL). The cells were cultured until reaching 80% confluence and then they were deprived of FBS for 2 h. Treatments were performed by incubating cells with 2.5% FBS-DMEM in the absence or presence of PTHrP (1-34) (10^{-8} M) at different times. This dose was selected based on previous studies[39,40]. Where indicated, cells were pre-incubated for 30 min with PD-98059 (20 μM), an inhibitor of the mitogen-activated protein kinase (MAPK) kinases (MEKs), the upstream kinases of ERK1/2; SB203580 (20 μM), an inhibitor of p38 MAPK; PP1 (10 μM), an inhibitor of Src; or SU11274 (0.5 μM), a Met inhibitor. In previous works, we confirmed the effectiveness of the inhibitors PD98059, SB203580, and PP1[26,27], whereas SU11274 dose was chosen in accordance with the literature[41]. Controls were run by the addition of an equivalent volume of dimethylsulfoxide (DMSO), the vehicle of the inhibitors.

Western blot analysis

Cells were washed with phosphate buffered saline (PBS) with 25 mmol/L NaF and 1 mmol/L Na_3VO_4 and lysed in buffer containing 50 mmol/L Tris-HCl (pH 7.4), 150 mmol/L NaCl, 3 mmol/L KCl, 1 mmol/L ethylenediaminetetraacetic acid (EDTA), 1% Tween 20, 1% Nonidet P-40, 20 μg/mL aprotinin, 20 μg/mL leupeptin, 1 mmol/L phenylmethylsulfonyl fluoride (PMSF), 25 mmol/L NaF, and 1 mmol/L Na_3VO_4. Lysates were vortexed for 45 s, incubated on ice for 10 min, and then centrifuged at 14000 *g* and 4 °C for 15 min. The supernatant was collected and protein quantification was performed by the Bradford method[42]. The proteins present in the samples were separated (30 μg/lane) using sodium dodecyl sulfate (SDS)-polyacrylamide gels (8%-10% acrylamide) and electrotransferred to hydrophilic polyvinylidene fluoride (PVDF) membranes. The membranes were blocked with 5% skim milk in Tris buffered saline-Tween (TBS-T) buffer (50 mmol/L Tris, pH 7.2-7.4, 200 mmol/L NaCl, 0.1% Tween-20), and then incubated overnight with the appropriate dilution of primary antibody (Met #8198 1:3000, p-Met #3077 1:500, E-cadherin #3195 1:1000; GAPDH sc-32233 1:5000) in TBS-T with 2.5% bovine serum albumin. After washing, the membranes were incubated with the appropriate dilution of horseradish peroxidase conjugated secondary antibody in TBS-T with 2.5% skim milk. Finally, proteins were revealed using a commercial electrochemiluminescence kit, and the bands obtained were digitized densitometrically and quantified with Image J program.

Stripping and reprobing membranes

To remove primary and secondary antibodies, membranes were incubated in stripping buffer (62.5 mmol/LTris-HCl pH 6.8, 2% SDS, and 50 mmol/L β-mercaptoethanol) at 55 °C for 30 min in agitation, washed for 10 min in TBS-T (1% Tween-20), and then blocked, as indicated above. After this procedure, it is possible to re-test antibodies in the membranes.

RNA isolation and cDNA synthesis

HCT116 cells were incubated in serum-free DMEM for 2 h and then treated with or without PTHrP (10^{-8} mol/L, in DMEM 2.5% FBS) for 15 min. Total RNA from all samples was isolated using the High Pure RNA Isolation Kit (Roche Diagnostics, Mannheim, Germany) according to the manufacturer's instructions. Total RNA (1 g) from each sample was used for first-strand cDNA synthesis using High

Capacity cDNA Reverse Transcription Kits following the manufacturer's instructions (Applied Biosystems, United States). The cDNA product was quantified and then stored at -20 °C for real-time polymerase chain reaction (RT-qPCR).

RT-qPCR

PCR reactions were carried out on a real-time PCR system (Applied Biosystems, model 7500). The primers used are the following: 5′-GGAAACACCCATCCAGAATGTCATT-3′ (forward) and 5′-TGATATCGAATGCAATGGATGATCT-3′ (reverse) for *Met*; 5′-ACCACAGTCCATGCCATCA-3′ (forward) and 5′-TCCACCACCCTGTTGCTGTA-3′ (reverse) for *GAPDH*. The PCR reactions were prepared using SYBR green master mix (No. 4309159, Applied Biosystems). On ice, the following was added: 5 µL of 2 × SYBR green, 0.8 µL of forward primer (400 nmol/L), 0.8 µL of reverse primer (400 nmol/L), 2 µL of template cDNA (12 ng), and 1.4 µL of Milli Q sterile water. *GAPDH* cDNA was amplified in parallel for all genes to provide an appropriate internal PCR control. For each experiment, water was added as a sample without a template (negative control). Mean Ct of the gene of interest (Met) was calculated from triplicate measurements using the following equation: Ct =Ct of the gene of interest -Ct of *GAPDH*. mRNA levels were calculated by the $2^{-\Delta CT}$ method.

Wound healing assay and morphological monitoring

Once confluence was reached, a cross-shaped wound was made manually in the cell monolayer with a tip and two washes were performed with sterile 1 × PBS to remove debris from the procedure. Then, the treatments were performed in DMEM without FBS as detailed above. Finally, the wounds were visualized under an inverted microscope and each of them was photographed at 0 h, 5 h, and 24 h, where the same fields were photographed. For each condition, the closure of the wound concerning the control was analyzed using ImageJ-NIH program, which allows for quantifying the area that remains cell-free.

To evaluate morphological changes potentially associated with the EMT, cells were treated with PTHrP as detailed above and the same fields were observed with a microscope and photographed during the times when significant molecular changes were observed.

Measurements of drug effects of chemotherapeutics

CPT-11, OXA, and DOXO cytotoxicities were assessed by trypan blue dye exclusion test. HCT116 cells were seeded in a 24-well plate until 80% confluence and then treated with or without PTHrP 10^{-8} M and/or CPT-11(10 µM)/OXA (10 µM)/DOXO (5 µM) in triplicate for 24 h. The doses of these drugs were chosen according to previous works[26,43-45]. Where indicated, HCT116 cells were pre-incubated with SU11274 (0.5 µM)[41] or DMSO, the vehicle of the inhibitor. After the treatment, cells were washed with PBS and then incubated with trypsin-EDTA to separate them from the culture substrate. The cell suspension was diluted in equal volume with trypan blue stain (1:1). The number of cells per field was counted in a Neubauer chamber; cells that exclude the dye were considered viable cells. The number of viable cells was calculated according to the following formula: Total number of viable cells = average number of viable cells × dilution factor × 10^4[46].

Xenograft in nude mice

Xenografts on 6-wk old male N:NIH (S)_nu mice (body weight 20-25 g) were generated through a subcutaneous injection of 1 × 10^6 HCT116 cells in their left dorsal flanks[47]. Four days after this procedure, the animals were randomly separated into treated and control groups (n = 6/group). Mice received a daily intratumoral injection of PTHrP (40 µg/kg) in 100 µL PBS, or PBS as a control. This manner of administration was in order to keep the compound level constant in the tumor area. The dose of PTHrP was selected according to previous studies performed by us and by other investigators with PTH and/or PTHrP in rodents[27,48-50]. Throughout the experiment, animals were kept under strict sanitary barriers in insulated cabins and had access to sterilized food and water *ad libitum*. Besides, they were exposed to 12 h cycles of light and darkness (200 Lux/1 m from the floor), atmospheric pressure, 25 °C, and humidity of 40%-60%. Humanitarian slaughter was carried out after 20 d of treatment by inhalation of the chemical agent CO_2. The tumors were removed, weighed, and fixed in a 4% formaldehyde solution and included in a paraffin block for subsequent treatment in immunoassays. At the end of the trial, the average weights were 0.30 g ± 0.11 g (standard deviation) and 0.40 g ± 0.10 g for control tumors and treated tumors, respectively. Whereas the average volumes were 0.21 mm^3 ± 0.08 mm^3 (standard deviation) and 0.26 mm^3 ± 0.08 mm^3 for control tumors and treated tumors, respectively. The present animal protocol was approved by the Institutional Committee for the Care and Use of Experimental Animals from the Universidad Nacional del Sur (CICUAE-UNS, institutional endorsement updated to 2021) and it was executed in accordance with the National Institutes of Health guide for the care and use of laboratory animals (NIH 1996) in order to minimize pain or discomfort for the animals.

Patients and clinical specimens

The following research protocol (File number 8610-017183/2018, Registry of Investigations in Health (RIS) number N° 11.00.18) has the endorsement of the Advisory Commission on Biomedical Research in

Beings Human Rights (CAIBSH) and the approval of the Health Ministry of the Province of Neuquén, Argentina (provision 0088-18-1-19) and was authorized by the Ethical Committee of the Hospital Interzonal de Graves y Agudos Dr. José Penna, Buenos Aires, Argentina in accordance with article 23 of Law 11044 of the Ministry of Health and the Central Research Ethics Committee (CECI) on research with biological samples from Argentina.

We performed an analysis of specimens obtained from patients with colorectal adenocarcinoma which were admitted to the Hospital Interzonal de Graves y Agudos Dr. José Penna (Bahía Blanca, Buenos Aires, Argentina) and the Hospital Provincial de Neuquén (Neuquén, Neuquén, Argentina) from January 1990 to December 2007. Normal colorectal tissue samples were assigned to a control group. The medical record of each patient was analyzed for the information as follows: Sex; age; primary tumor location; histological grade; and initial stage (according to the TNM staging system issued by the American Joint Committee on Cancer-AJCC and International Union for Cancer Control-UICC). The exclusion criteria were: Patients under 18 years of age due to the low prevalence of this cancer in the child and youth population[51]; pregnant patients due to the fact that high levels of PTHrP have been observed in the placenta and fetal tissues[52]; lactating patients because high levels of PTHrP have been detected in breast tissue and in breast milk and correlate with serum PTHrP levels in these women[53]; patients who have previously developed other types of tumors (liver, lung, and bone) since CRC commonly metastasizes to these sites. These considerations are necessary to exclude cases where the cytokine derived from other tissues may interfere with the analysis of the results from this study. All are exclusion criteria at the time of diagnosis. The confidentiality criteria were based on the regulatory provisions referring to confidentiality in clinical investigations, including Law 11044 and Law 25326 on data protection, from Argentina, the Guide for Health Research of the National Ministry of Health, the UNESCO Declaration on the Protection of Genetic Data and the Declaration of Helsinki of the World Medical Association (version 2008), and the Council for International Organizations of Medical Sciences (CIOMS) Guidelines. This study respected the dignity and rights of the patients. All data derived from the clinical history was treated under strict confidentiality to protect and preserve the patient's identities.

Paraffin-embedded archival blocks from primary tumors were reviewed by hematoxylin-eosin staining technique; subsequently, representative histological samples of each patient were selected for immunoassays.

Immunohistochemistry

From each paraffin block, tumor sections were sliced and prepared for immunohistochemical detection using the primary monoclonal antibody anti-Met (#8198, 1:2000) or anti-PTHR1 antibody (sc-12722-3D1.1, 1:50) according to the manufacturer's protocol. The sections were deparaffinized with xylol for 15 min and subsequently rehydrated in decreasing concentrations of alcohol. Antigenic retrieval was carried out using a pressure cooker with sodium citrate buffer (10 mmol/L, pH 6) for 15 min at 1 atm. The sections were washed twice with PBS and we proceeded to block endogenous peroxidase with 30% $H_2O_2$for 10 min. After two washes with PBS, the corresponding antibody was added to each sample and incubated overnight at 4 °C. Immunohistochemical staining was carried out manually using ABCAM Detection IHC Kit (Abcam, Cambridge, MA, United States) according to the manufacturer's instructions. The images obtained under an optical microscope were analyzed using an open-source image processing package based on ImageJ-NIH program[54,55].

Statistical analysis

To obtain statistical data, three experiments were carried out independently and the results are expressed as the mean ± SD. To determine significant differences between two groups of data, Student's *t*-test (two-tailed, equal variance) was carried out. A P value < 0.05 was considered statistically significant.

For the statistical analysis of human tumor samples, the correlation coefficient between the expression of Met and PTHR1 was evaluated by the Spearman test. Then, the patients were grouped according to clinicopathological characteristics such as age, sex, TNM stage (II, III, and IV), location of the primary tumor (right colon, left colon, and rectum), and histological grade (G1, G2, and G3). The Fisher's exact test was used to evaluate the association of Met or PTHR1 expression with each variable. These statistical analyses were performed using the R programming language version 4.1.1[56]. A P value < 0.05 was considered statistically significant.

RESULTS

PTHrP modulates the expression of the RTK Met in human HCT116 cells

Met is a heterodimeric receptor that is composed of two chains, alpha and beta. Initially, this RTK is synthesized as a single-chain precursor (pro-Met), and it then undergoes posttranslational modifications to produce the mature form[57]. The binding of the HGF to the beta subunit of Met induces its dimerization and the phosphorylation of tyrosine domains in the intracellular portion of the receptor

(Y1234 and Y1235). These events promote the kinase activity of Met and its autophosphorylation (Y1349 and Y1356). Then, various proteins are recruited to these phosphorylated sites, triggering different signaling pathways[33,58].

In CRC cells, Met signaling is activated by various mechanisms to promote tumor development and progression[28,59]. Gene amplification or mutations (that lead to receptor overexpression) and increased activity due to ligand-mediated stimulation induce the aberrant activation of Met[28]. As mentioned earlier, another mechanism that favors its abnormal activation involves the phosphorylation in Met activator domains and is indirectly due to the previous activation of cell-surface receptors like G-protein-coupled receptors[29,31].

In the past years, several authors have reported a correlation between the overexpression of PTHrP and tumor progression in lung, breast, and prostate cancers[16,21,60]. Our research group has shown that this cytokine also promotes the aggressive phenotype of intestinal tumor cells[13,24-26]. This pro-tumor factor exerts its action on CRC cells through several mitogenic signaling pathways[13]. In view of this background, in this work we decided to investigate whether the molecular mechanisms trigged by PTHR1 after binding of PTHrP are capable of modulating the expression of the mature form of the RTK Met and/or its activation in CRC-derived cells. To that end, we initially treated Caco-2 cells and HCT116 cells with PTHrP for different times and then the cell lysates were immunoblotted with an anti-Met antibody. We selected these cell lines from CRC with different aggressive phenotypes because both express the receptor PTHR1 and we had previously verified that their cell responses are mediated exclusively by this receptor[26,40,61]. Met did not change its protein expression when Caco-2 cells were treated with PTHrP over a wide interval of exposure times (data not shown). However, the response of the HCT116 cell line, which is more aggressive than Caco-2 cell line, was different. As seen in Figure 1 (top and middle panels), PTHrP treatment for 30 min increased Met protein levels. However, the protein expression diminished at 3 min and 10 min, and at 1 h to 3 h of exposure to the peptide. Figure 1 (lower panel) shows that at 5 h of treatment, Met protein levels continued to decrease. However, PTHrP increased Met protein expression at 20 h of treatment.

As it happens with other RTKs on the cell surface, after its phosphorylation/activation, Met is internalized with the subsequent decrease in its protein levels due to the proteasomal degradation[62,63]. In this regard, the reduction of Met protein levels observed in HCT116 cells suggested a previous activation of this receptor by PTHrP, and the increment of its protein level after these decreases (at 30 min and 20 h) suggested a modulation of Met expression by PTHrP in order to improve Met levels.

PTHrP promotes Met phosphorylation and activation through Src kinase in human HCT116 cells

Our next goal was to elucidate if the decrease in Met protein levels observed in HCT116 cell line and mediated by exogenous PTHrP could be due to its previous phosphorylation/activation. Thus, we proceeded to evaluate the status of phosphorylated Met under PTHrP action. As shown in Figure 2A, Western blot analysis using a specific antibody that recognizes active Met, revealed that PTHrP treatment for 3 min and 10 min increased the phosphorylation of Met at the residues Tyr 1234 and Tyr 1235. These phosphorylation sites constitute activating domains of the receptor. The decrease in total Met protein levels (showed in Figure 1 and pointed in Figure 2A with arrows) ruled out the possibility that an increase in phosphorylated Met levels at the same time was due to the up-regulation of Met protein expression.

Src is a cytosolic tyrosine kinase deregulated in 80% of CRC patients[64-66]. Previously, we reported the activation of Src in the HCT116 cell line induced by PTHrP at 3 min of treatment[26]. As we mentioned above and taking into account that we observed phosphorylation of Met by PTHrP on specific tyrosine residues that are needed for its activation, we decided to evaluate whether Src is involved in this process induced by the cytokine PTHrP in intestinal tumor cells. For this purpose, the cells were pre-treated with PP1, a specific inhibitor of Src activation, and then with PTHrP for 3 min. As shown in Figure 2B, we observed that PP1 decreased PTHrP-induced phosphorylation of Met at Tyr1234/1235. These findings suggested that in the HCT116 cell line, PTHrP rapidly activate the Src signaling pathway, leading to the phosphorylation and activation of Met.

PTHrP promotes the phosphorylation/activation of Met through the MAPK signaling pathway in human HCT116 cells

It has been described that MAPK signaling pathway activation is very common in CRC and is related to an aggressive phenotype of intestinal tumor cells[67]. Due to its relevance in cancer, in recent decades the possibility of employing MAPK pathway inhibitors has been studied for the treatment of this disease[68,69]. In our laboratory, we found that PTHrP induces the activation of the ERK 1/2 MAPK and p38 MAPK and that the activity of Src converges in the phosphorylation/activation of MAPK in CRC-derived cells [26,27].

Based on our previous results, we next decided to investigate in our model if ERK 1/2 MAPK and p38 MAPK are also involved in the effects of PTHrP on the Met signaling pathway. To that end, the cells were pre-incubated with PD-98059 (a selective inhibitor of MEK, the upstream kinases of ERK 1/2) or with SB-203580 (a specific p38 MAPK inhibitor) and then exposed to PTHrP for 1 h. This time point was selected because the phosphorylation/activation of ERK 1/2 MAPK and p38 MAPK significantly

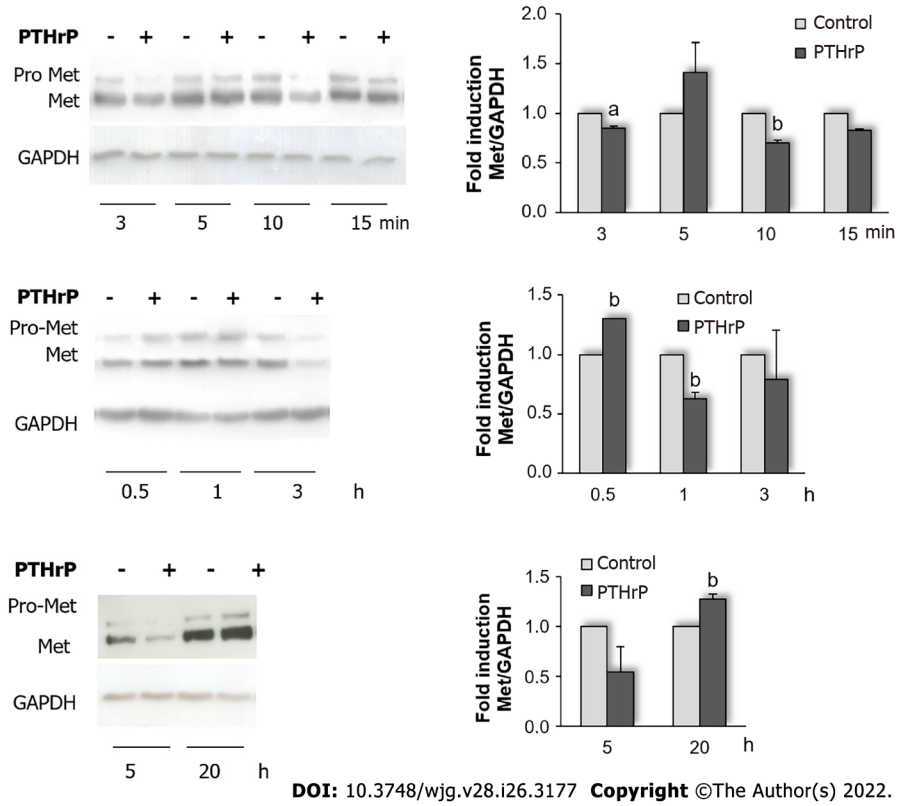

DOI: 10.3748/wjg.v28.i26.3177

Figure 1 Parathyroid hormone-related peptide modulates the protein expression of Met receptor in HCT116 cells. Cells were treated with or without 10^{-8} mol/L parathyroid hormone-related peptide (PTHrP) for different times. The protein levels of pro-Met (Met precursor) and Met [tyrosine kinase receptor (RTK) mature form] were analyzed by Western blot to investigate whether the molecular mechanisms trigged by PTHR type 1 (PTHR1) after binding of PTHrP are capable of modulating the expression of the mature form of the RTK Met in HCT116 cells. GAPDH protein levels were determined as a control of the amount of proteins present in the membrane, since this protein is not substantially modified with the treatment by the cytokine. Graph bars represent the average of the results obtained from three independent experiments. GAPDH: Glyceraldehyde 3-phosphate dehydrogenase; Met: Receptor tyrosine kinase Met; PTHrP: Parathyroid hormone-related peptide. $^{a}P < 0.05$; $^{b}P < 0.01$.

increased at 60 min after PTHrP treatment in HCT116 cells[26,27]. Regarding the cell response when tumor cells were exposed to PTHrP for 1 h (Figure 1), Figure 3 shows an increase in the phosphorylated Met levels, suggesting that the treatment with the cytokine for 1 h also induces the phosphorylation/activation of Met with the subsequent reduction in its protein levels due to its proteasomal degradation. Moreover, Figure 3 reveals that the selective inhibition of MEK MAPK and p38 MAPK averted the effect on Met phosphorylation, suggesting that Met activation is regulated by the ERK 1/2 MAPK and p38 MAPK signaling pathways in HCT116 cells under PTHrP action.

PTHrP increases Met gene expression in human HCT116 cells

As it was commented earlier, the fact that Met, like other RTKs, undergoes proteasomal degradation after its phosphorylation/activation[62,63] explains that at the same time points of PTHrP exposure (3 min, 10 min, and 60 min), the levels of phosphorylated Met increased while the protein levels of total Met decreased. Furthermore, in this work we elucidated that Met is phosphorylated by PTHrP through the Src and MAPK signaling pathways. In view of the results shown in Figure 1, we selected a time before 30 min with the purpose to evaluate whether the increase in Met protein levels initially observed by PTHrP treatment is related to the modulation of gene expression. By real-time PCR, we analyzed the *Met* mRNA levels and found that PTHrP increased *Met* gene expression at 15 min (Figure 4). This result suggested that in HCT116 cells, PTHrP at least at this time promotes the transcription of the *Met* gene and its translation, correlating with the increase of the protein levels observed at 30 min of PTHrP exposure.

Met signaling pathway induced by PTHrP participates in cell events related to the aggressive behavior of human HCT116 cells

Our studies in CRC cell models have demonstrated that PTHrP favors several events associated with the progression of the disease, such as cell proliferation, migration, and the EMT program[13,24,26,27,39]. Based on these previous findings and since Met is modulated by PTHrP in HCT116 cells, we decided to evaluate whether the Met signaling pathway participates in events induced by the cytokine and associated with an aggressive phenotype of CRC-derived cells. For this purpose, cells were incubated

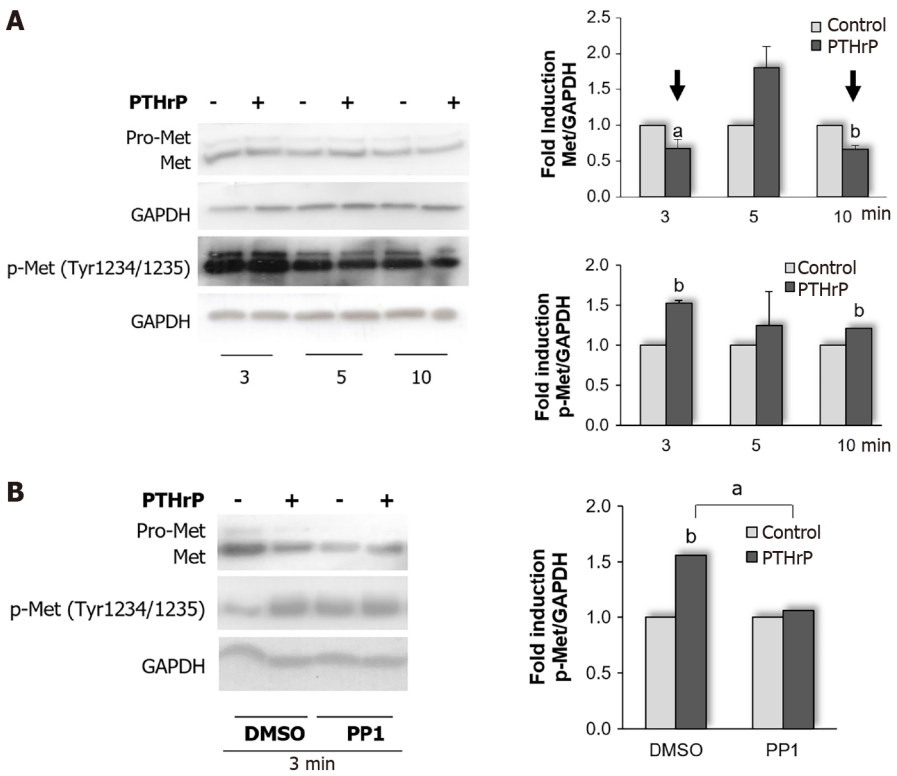

DOI: 10.3748/wjg.v28.i26.3177

Figure 2 Parathyroid hormone-related peptide increases Met phosphorylation and activation through Src kinase in HCT116 cells. A: Cells were exposed to 10^{-8} mol/L parathyroid hormone-related peptide (PTHrP) 10^{-8} mol/L for 3 min, 5 min, and 10 min. The protein levels of Met and p-Met (phosphorylated in the residues Tyr1234 and Tyr1235) were assessed by Western blot to investigate whether PTHrP is capable of modulating Met phosphorylation and activation in HCT116 cells. Graph bars represent the average of the results obtained from three independent experiments; B: Cells were pre-treated with PP1, a selective Src inhibitor, for 30 min and then exposed to 10^{-8} mol/L PTHrP for 3 min to evaluate whether Src kinase mediates the effect of PTHrP on Met activation in HCT116 cells. Controls were run by adding an equivalent volume of DMSO, the vehicle of the inhibitor. The protein levels of p-Met and Met were evaluated by Western blot. Graph bars represent the average of the results obtained from three independent experiments. In all experiments, GAPDH protein levels were determined as a control of the amount of proteins present in the membrane, since this protein is not substantially modified with the treatment by the cytokine. DMSO: Dimethylsulfoxide; GAPDH: Glyceraldehyde 3-phosphate dehydrogenase; Met: Receptor tyrosine kinase Met; p-Me: Phospho-Met (Tyr1234/1235); PTHrP: Parathyroid hormone-related peptide. $^{a}P < 0.05$; $^{b}P < 0.01$.

with SU11274, an ATP competitive inhibitor of the catalytic activity of the Met kinase[70], followed by the treatment with or without PTHrP for different times, and then we performed different procedures as described below. The times of PTHrP exposure were selected based on our previous findings[24,26,27]. As shown in Figure 5A, PTHrP or PTHrP plus DMSO (the vehicle of the inhibitor) at 24 h increased the number of HCT116 cells. However, the treatment with the Met inhibitor significantly decreased the number of viable cells concerning the control. As the Met signaling pathway is involved in the proliferation and survival of intestinal tumor cells[41,71-73], this descent in the cell viability suggests that both cell responses are affected.

By the wound healing assay, we evaluated whether Met signaling is also involved in the migration of HCT116 cells induced by PTHrP. We observed the wound healing in the culture of confluent HCT116 cells to compare the migration between untreated cells and cells treated with PTHrP in the presence or absence of SU11274. Representative photographs, taken at time points 0 h, 5 h, and 24 h of the identical location and the quantification of the results of two separate experiments are shown in Figure 5B. A significant enhancement in wound closure was detected in cells exposed to PTHrP or PTHrP plus DMSO compared to the control at 5 h and 24 h. However, this effect was not observed in cells that had been pre-treated with the Met inhibitor.

We recently published results revealing that PTHrP is able to induce the EMT in HCT116 cells[24]. The EMT is a key program of CRC that participates in the invasion, angiogenesis, and chemoresistance associated with metastasis[74,75]. Based on this previous work, herein we analyzed if PTHrP also induces this program through the Met pathway. To that end, HCT116 cells were incubated with SU11274 and then treated with or without PTHrP. The cells were observed under an inverted microscope after treatment with PTHrP for 5 h and 24 h to analyze the morphological changes associated with the EMT. The arrows in Figure 5C point to morphological changes corresponding to the transition from a polygonal structure to spindle-like structure in cells treated for 24 h with PTHrP or PTHrP plus DMSO. These findings revealed an effective transition to the mesenchymal phenotype and are consistent with our previous work in HCT116 cells[24]. There were no changes between SU 11274

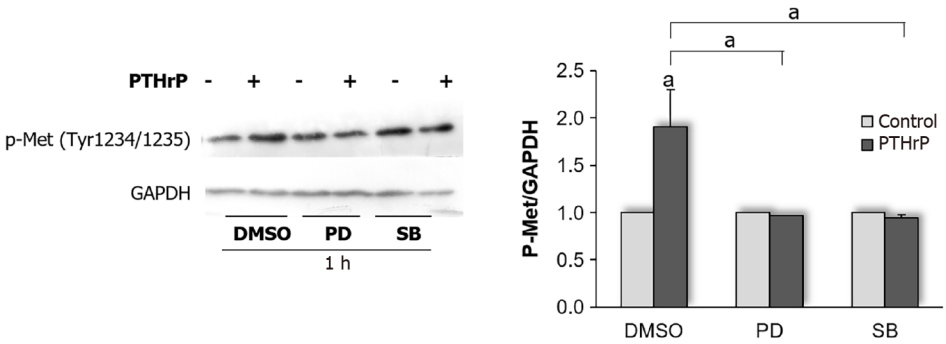

DOI: 10.3748/wjg.v28.i26.3177 **Copyright** ©The Author(s) 2022.

Figure 3 Parathyroid hormone-related peptide modulates Met activation through the mitogen-activated protein kinase signaling pathway in HCT116 cells. Cells were treated with PD-98059 or SB-203580, a selective mitogen-activated protein kinase (MAPK) kinase (MEK) or P38 MAPK inhibitor, respectively, for 30 min and then exposed to 10^{-8} mol/L PTHrP for 1 h to evaluate whether ERK1/2 MAPK and/or p38 MAPK mediate the effect of PTHrP on Met activation in HCT116 cells. Controls were run by adding an equivalent volume of dimethylsulfoxide, the vehicle of the inhibitors. The protein levels of Met phosphorylated in the residues Tyr1234 and Tyr1235 were assessed by Western blot. These phosphorylation sites constitute activating domains of the receptor. GAPDH protein levels were determined as a control of the amount of proteins present in the membrane, since this protein is not substantially modified with the treatment by the cytokine. Graph bars represent the average of the results obtained from three independent experiments. DMSO: Dimethylsulfoxide; GAPDH: Glyceraldehyde 3-phosphate dehydrogenase; Met: Receptor tyrosine kinase Met; p-Met: Phospho-Met (Tyr1234/1235); PTHrP: Parathyroid hormone-related peptide. $^{a}P < 0.05$.

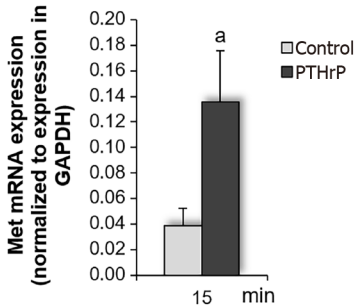

DOI: 10.3748/wjg.v28.i26.3177 **Copyright** ©The Author(s) 2022.

Figure 4 Parathyroid hormone-related peptide increases mRNA levels of *Met* in HCT116 cells. Colon cancer cells were exposed to parathyroid hormone-related peptide (PTHrP) for 15 min, followed by real-time polymerase chain reaction analysis to detect *Met* mRNA levels as described in Materials and Methods to evaluate whether PTHrP modulates *Met* mRNA levels in HCT116 cells. Graph bars represent the average of the results obtained from three independent experiments. GAPDH: Glyceraldehyde 3-phosphate dehydrogenase; Met: Receptor tyrosine kinase Met; PTHrP: Parathyroid hormone-related peptide. $^{a}P < 0.05$.

control cells and those treated with the inhibitor of Met plus PTHrP. To further evaluate the phenotype related to a mesenchymal shape, we measured the minor and major axes in the photomicrographs using the Image J-NIH program. Figure 6 reveal that under PTHrP action, the cells lost their epithelial characteristics. The increase of the relation between the major and minor axes indicated that the exposure to PTHrP for 24 h significantly increased the degree of HCT116 cell elongation, a typical feature of the mesenchymal shape. However, when the cells were pre-incubated with SU11274, the effects of the cytokine were reverted.

It has been shown that the loss of the expression of the epithelial marker E-cadherin is associated with EMT progress in CRC[76,77]. In our recent work[24], we showed that in HCT116 cells, PTHrP at 5 h modulated the expression of E-cadherin and other epithelial markers as well as certain mesenchymal markers. Based on these morphological changes related to the EMT and mediated through Met, we then explored by Western blot analysis whether Met is involved in the modulation of E-cadherin protein expression by the cytokine. As seen in Figure 5C, the effects of the cytokine on E-cadherin protein levels were reverted when the cells were pre-incubated with SU11274. Taken together, these findings suggest that PTHrP induces the EMT program in HCT116 cells through the Met signaling pathway.

In agreement with other works published[78], our findings suggest that the Met signaling pathway induced by PTHrP is involved in cell events related to tumor aggressive behavior in the HCT116 cells.

PTHrP attenuates the cytotoxic effect of CPT-11, OXA, and DOXO in human HCT116 cells through the Met signaling pathway

In CRC-derived cells, our group has previously described a role of PTHrP in the resistance to CPT-11, the most widely used chemotherapeutic drug today[26]. In the treatment of CRC, many pharmaco-

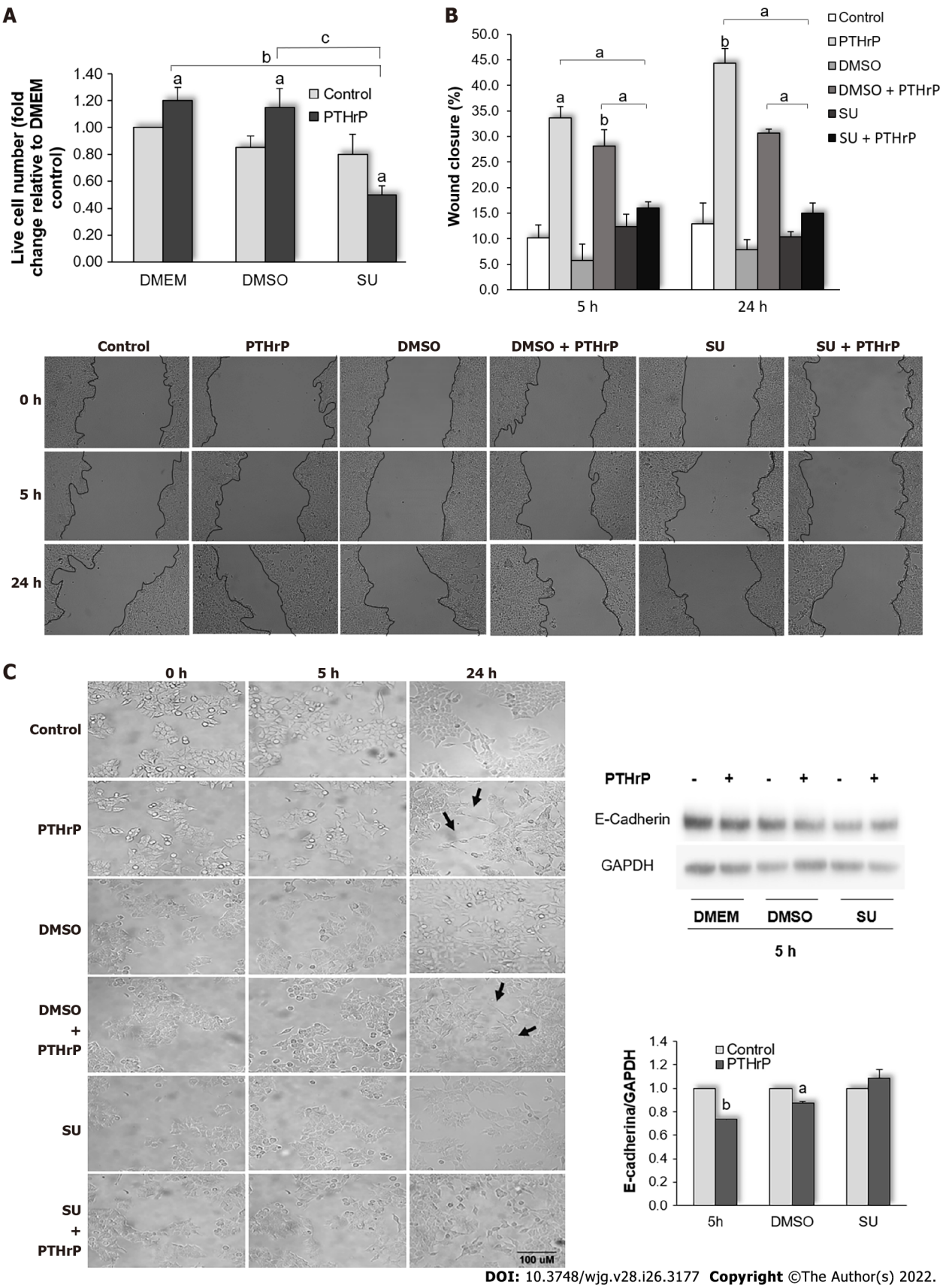

DOI: 10.3748/wjg.v28.i26.3177

Figure 5 Parathyroid hormone-related peptide promotes events related to the aggressive behavior of HCT116 cells through the Met signaling pathway. HCT116 cells were pre-incubated with SU11274, a specific Met inhibitor, for 30 min and then treated with or without parathyroid hormone-related peptide (PTHrP; 10^{-8}M). A: Trypan blue technique showed that Met inhibition decreased the cell proliferation induced by PTHrP at 24 h; B: Images from wound healing assay show that Met inhibition reverted the wound closure promoted by PTHrP at 5 h and 24 h; C: E-cadherin protein levels analyzed by Western blot to investigate whether Met is involved in the decrease of this epithelial-mesenchymal transition (EMT) program marker induced by PTHrP in HCT116 cells. Using the

Image J-NIH program, we performed the analysis of the parameters related to cell morphology. The arrows indicate the morphological changes corresponding to the transition from a polygonal structure to spindle-like structure related to EMT program progress observed when the cells were treated for 24 h with PTHrP or PTHrP plus dimethylsulfoxide (DMSO). In all experiments, a control with DMSO, the vehicle of the inhibitor, was performed. Graph bars represent the average of the results obtained from two independent experiments. DMEM: Dulbecco's Modified Eagle Culture Medium; DMSO: Dimethylsulfoxide; EMT: Epithelial to mesenchymal transition; PTHrP: Parathyroid hormone-related peptide. [a]$P < 0.05$; [b]$P < 0.01$; [c]$P < 0.001$.

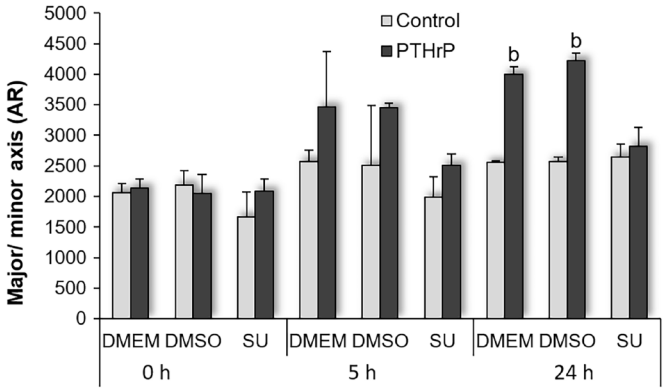

Time	Image J analysis of cells aspect radio (AR)	Area	Perimeter	Major	Minor	AR	Round
0 h	Control	371608.35	83700.44	29714.67	15072.84	2.06	0.51
	PTHrP	445243.58	95072.71	32963.65	16999.08	2.12	0.55
	DMSO	401221.98	90350.81	31896.07	16001.69	2.19	0.53
	DMSO + PTHrP	507695.83	102479.62	35812.26	18038.25	2.02	0.53
	SU	540780.15	104863.69	33247.98	17729.93	1.87	0.53
	SU+ PTHrP	502373.55	104550.15	35027.30	18751.45	2.10	0.57
5 h	Control	549152.49	114728.86	40994.62	20538.01	2.00	0.50
	PTHrP	572497.91	134398.89	48988.78	15197.87	3.47	0.34
	DMSO	459528.84	104492.96	36189.49	16991.24	2.51	0.53
	DMSO + PTHrP	540958.38	132183.13	47145.72	15112.32	3.45	0.36
	SU	433503.43	91961.62	32499.24	17279.31	2.00	0.56
	SU+ PTHrP	474989.59	107135.04	37739.83	16617.10	2.51	0.48
24 h	Control	487973.50	108293.98	37998.97	16948.69	2.55	0.48
	PTHrP	440312.67	134882.49	44247.08	13044.18	3.70	0.32
	DMSO	453802.96	117009.26	37199.63	16191.98	2.57	0.47
	DMSO + PTHrP	492995.40	132117.10	44167.20	13864.80	3.20	0.31
	SU	453382.04	118630.81	37624.58	15650.04	2.50	0.45
	SU+ PTHrP	508934.37	124074.22	41166.22	16517.61	2.80	0.44

DOI: 10.3748/wjg.v28.i26.3177

Figure 6 Analysis of the aspect ratio (major/minor axis) of HCT116 cells, obtained using the Image J-NIH program. The table shows values of parameters associated to cell morphology: Area; perimeter; round; major axis; minor axis; and aspect radio, relation between major axis and minor axis (AR). Graph bars show the AR for each condition. The increase of the degree of cell elongation at 24 h of exposure to parathyroid hormone-related peptide was significantly reversed in the presence of the Met inhibitor. DMSO: Dimethylsulfoxide; PTHrP: Parathyroid hormone-related peptide; SU: SU11274. [b]$P < 0.01$.

logical strategies have been implemented. OXA is another drug commonly employed for this purpose and it exerts its cytotoxic action through different mechanisms with respect to CPT-11. Thereby, the combination of CPT-11 and OXA is generally used to improve the effectiveness of the adjuvant therapy [79,80]. DOXO is another chemotherapeutic agent that has been effective in the treatment of advanced CRC; however, the side effects associated with its use at high doses and the development of chemores-

istance constitute a great challenge to the effective treatment[43,81,82]. Since the greatest problem in CRC treatment is the development of chemoresistance, we proceeded to evaluate if PTHrP affects the cytotoxicity promoted by these other drugs. Trypan blue dye exclusion test revealed that PTHrP not only decreased the sensitivity of intestinal tumor cells to CPT-11 but also to OXA and DOXO (Figure 7).

Studies carried out by colleagues demonstrated the correlation between overexpression and/or hyper-activation of Met in tumor tissues with a poor prognosis of cancer patients and with a chemoresistant phenotype[32,83,84]. These findings support the interest in Met inhibitors as new therapeutic strategies. Since herein we found that Met inhibition substantially reverts the effects of PTHrP on events associated with the malignant behavior such as cell proliferation, migration, and the EMT program, we set out to assess if the signaling pathway trigged by this RTK also promotes chemoresistance in our experimental system. Counting live cells by means of trypan blue dye exclusion test revealed that Met inhibition restored the sensitivity of HCT116 cells to CPT-11 (Figure 7A), OXA (Figure 7B), and DOXO (Figure 7C) even in the presence of PTHrP, suggesting that this cytokine attenuates the cytotoxic effect of these drugs in CRC cells through the Met signaling pathway.

PTHrP enhances the protein expression of Met and its receptor in HCT116 cells tumor xenografts

In a murine model, we have previously observed that the administration of PTHrP in HCT116 cell xenografts changed the protein expression of markers linked to CRC progression, such as Ki67, cyclin D1, ERK1/2 MAPK, CREB/ATF-1[26], RSK[27], VEGF[25], SPARC, and E-cadherin[24]. As Met overexpression promotes events related to tumor progression like proliferation, invasion, and migration[63,70] and taking into account our previous finding in the animal model, in this work we evaluated whether the administration of PTHrP in the same murine model (HCT116 cell xenografts in nude mice N: NIH(S)_nu) also changes the protein levels of Met in tumor tissues. To that end, 12 male mice, between 4 and 6 wk of age and with a body weight between 20 g and 25 g, were randomly divided into two groups (n = 6 each), after an acclimatization period of 4 d. Group 1 received the cytokine vehicle (100 μL PBS), while group 2 received PTHrP at a concentration of 40 μg/kg body weight in 100 μL PBS[49]. The treatment was intra-tumoral daily and until the end of the experiment to maintain the level of the compound constant in the tumor area. The mice were kept throughout the protocol in sterile conditions (see Materials and Methods). The immunohistochemical analysis with the quantification of Met immunoreactivity revealed that Met levels were elevated in tumors from mice treated with PTHrP (0.190 ± 0.014) compared to tumors from control mice (0.110 ± 0.012; $P < 0.05$) (Figure 8, top images). As the present work was aimed to elucidate the relationship between PTHR1, PTHrP, and Met, we also analyzed the immunoreactivity of PTHR1 using an anti-PTHR1 antibody in HCT116 cell xenografts from untreated nude mice (control) and mice treated with PTHrP. Interestingly, as seen in Figure 8 (lower images), PTHrP increased the protein expression of its receptor in the tumor of these animals (2.27 ± 0.20) compared to tumors from control mice (1.98 ± 0.14; $P < 0.01$). The data shown in this section together with those in the first and fourth sections of results indicate that PTHrP modulates the expression of Met both *in vitro* and *in vivo*. Perhaps the cytokine modulates the expression of its own receptor in this animal model in order to amplify its signaling within the cell and thus makes its effects more effective in CRC. More studies are necessary to confirm this hypothesis.

Evaluation of Met and PTHR1 expressions in CRC human samples

As we mentioned before, the Met receptor has the HGF as its only known ligand. However, it could be aberrantly activated by G-protein-coupled receptors[29,31]. The results reported herein in the previous sections suggest that PTHR1 activation (after its binding with PTHrP) is able to trigger the activation of the Met signaling pathway through a cross-talk between both receptors that is mediated by cytosolic kinases like Src. In this context, and taking into account the findings obtained by *in vitro* and *in vivo* assays, we decided to validate our observations and therefore our ultimate objective was to assess the expression of both receptors in CRC human tumor samples with the aim to elucidate if there is a relation between them and with the tumor characteristics. So, we analyzed 23 specimens obtained from patients with colorectal adenocarcinoma. Seven cases with normal colorectal tissues were assigned to the control group. Table 1 shows the patients' characteristics. The average age was 62 years; 48% (n = 11) were male, and 52% (n = 12) were female. Regarding the primary tumor location, 39% (n = 9) presented right-colon cancer, 30.5% (n = 7) presented left-colon cancer, while in 30.5% (n = 7) of patients the location was in the rectum; 61% (n = 14) of the tumors presented a high grade of histological differentiation, while 39% (n = 9) were moderately or poorly differentiated; 48% (n = 11) of the patients with CRC presented stage II, 39% (n = 9) stage III, and 13% (n = 3) stage IV.

The expression of Met and PTHR1 was evaluated in biopsies of patients with well (G1), moderately (G2), and poorly differentiated (G3) colon adenocarcinomas, as well as in normal colon tissue using the immunohistochemical technique. Figure 9A shows the comparison between both quantifications, Met and PTHR1, for each histological grade of differentiation. As shown in Figure 9B, in normal tissue Met receptor labeling is homogeneous throughout the cytoplasm of the epithelial cell. However, in tumor cells, we observed that the intensity of the immunostaining in the membrane increased as tumor differentiation declined. Concerning PTHR1, the intensity of the staining gradually decreased in histologically less differentiated tumors and the receptor seemed to relocate from the plasma membrane of the epithelial cell in G1 to the cytoplasm and the perinuclear zone in G3. Based on these observations, we

Table 1 Clinicopathological characteristics of the patients

Variable	Value
Sex, *n* (%)	
Male	11 (48)
Female	12 (52)
Age, median (range)	62 (58-74)
Primary tumor site, *n* (%)	
Right-side	9 (39)
Left-side	7 (30.5)
Rectum	7 (30.5)
Tumor differentiation, *n* (%)	
Well differentiated	14 (61)
Moderately or poorly differentiated	9 (39)
Initial stage, *n* (%)	
II	11 (48)
III	9 (39)
IV	3 (13)

Data are presented as *n* (%) except where otherwise stated.

decided to investigate whether there is a correlation between the expression of Met and PTHR1. No statistical significance was found between the expression of both receptors in the tumor samples. Additionally, we studied if there is a statistically significant association between the clinicopathological characteristics and the immunohistochemical staining for Met or PTHR1. For this purpose, we dichotomized the specimens into low, medium, and high expression levels of Met or PTHR1. We found that in less differentiated tumors, Met expression increased (P = 0.035), while PTHR1 expression was statistically lower (P = 0.0496). However, we did not find a statistically significant association of Met or PTHR1 with age, sex, primary tumor location, and TNM stage. These results indicate that the expression of PTHR1 is more marked in well-differentiated tumors, while Met showed a higher expression level in poorly differentiated tumors.

DISCUSSION

Resistance to chemotherapeutic drugs constitutes an obstacle in the therapy of CRC[2]. In this context, it is crucial to identify the molecular mechanisms related to the aggressive phenotype of CRC to develop more effective therapeutic strategies and find new prognostic and predictive markers.

PTHrP is expressed in various types of cancer, including CRC[16]. In fact, 95% of colorectal tumors present elevated levels of this protein[18-20,85]. Our research group found that this cytokine modulates different signaling pathways and events associated with the aggressive phenotype in CRC-derived cells [13,24-26].

Several studies have demonstrated the participation of the Met signaling pathway in the evolution of different types of cancer[28,33-35,83]. Moreover, this receptor is overexpressed and/or can be aberrantly activated by several mechanisms in CRC cells, triggering tumor development and progression[28,36,38,59]. A recent study addresses the relationship between the HGF/Met axis and cytokines such as PTHrP in bone metastasis and renal cell cancer progression[86]. In agreement with these observations, the results from this work suggest that the expression and activity of Met are regulated by signaling pathways trigged by the binding of PTHrP to PTHR1. We observed that exogenous PTHrP treatment modulates Met protein and gene expression in HCT116 cells. Despite that the cytokine regulates Met expression in HCT116 cells, our initial observations in Caco-2 cells reveal that PTHrP is not able to modulate its protein levels. In line with these findings, we previously reported that PTHrP modulates the protein levels of SPARC (an invasion marker) and E-cadherin (a marker related with EMT program) in HCT116 cells but not in Caco-2 cells[24]. The fact that the cytokine can modulate the expression of markers associated with the malignant behavior in a more aggressive cell line (HCT116) but not in a less aggressive cell line (Caco-2) may be because these CRC cells have different mutations[87,88] and

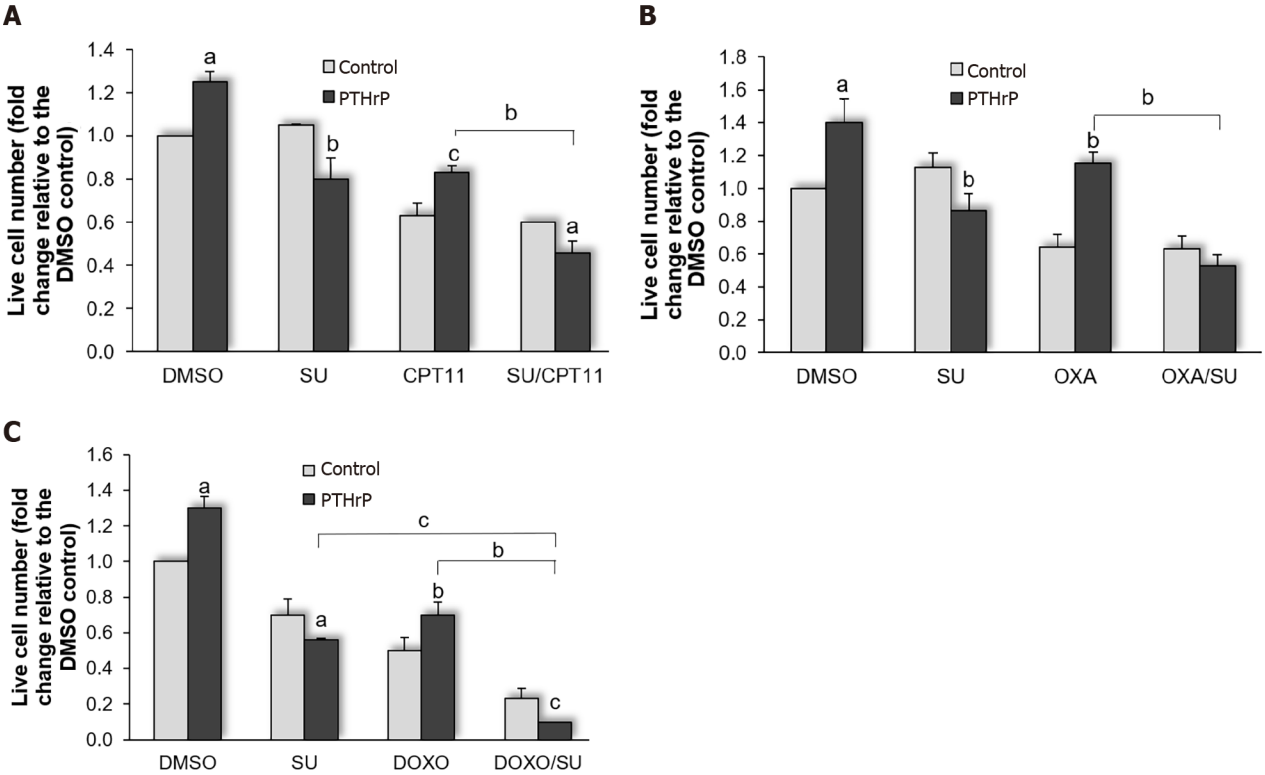

DOI: 10.3748/wjg.v28.i26.3177

Figure 7 Parathyroid hormone-related peptide attenuates the cytotoxicity of CPT11, oxaliplatin, and doxorubicin through the Met signaling pathway. A-C: HCT116 cells were pre-incubated with SU11274, a specific Met inhibitor, and then treated with PTHrP (10^{-8} M) and/or irinotecan (CPT-11, 10 μM) (A), oxaliplatin (OXA, 10 μM) (B), or doxorubicin (DOXO, 5 μM) (C) for 24 h. The number of viable cells was quantified by Trypan blue technique. In each experiment, a control with DOXO, the vehicle of the inhibitor, was performed. Graph bars represent the average of the results obtained from two independent experiments. CPT-11: Irinotecan; DMSO: Dimethylsulfoxide; DOXO: Doxorubicin; OXA: Oxaliplatin; PTHrP: Parathyroid hormone-related peptide; SU: SU11274. $^{a}P < 0.05$; $^{b}P < 0.01$; $^{c}P < 0.001$.

perhaps several events triggered by PTHrP in these two cell lines may be dependent on these mutations explaining the different response between Caco-2 and HCT116 cells.

We found in HCT116 cells that the peptide promotes the activation of Met by phosphorylation on Tyr residues. Bradley and colleagues and later Critchley and his research group, demonstrated that, like other RTKs, Met after its activation is degraded by the proteasomal pathway[62,63]. Consistent with these data, our results suggest that Met protein levels decline after PTHrP-induced phosphorylation.

Previous studies by our research group established that PTHrP in the HCT116 cell line promotes phosphorylation and activation of Src; then this kinase acts upstream of ERK 1/2 MAPK to induce their phosphorylation/activation, though the mechanisms that lead to the phosphorylation/activation of p38 MAPK by the cytokine is still unknown[13,26]. Herein, we demonstrated that PTHrP induces the phosphorylation and activation of Met through Src. Furthermore, PTHrP modulates the phosphorylation/activation of Met through ERK 1/2 and p38 MAPK. The fact that the cytokine diminishes Met protein levels in a range of time between 1 h to 5 h suggests that Met is activated by PTHrP (with its subsequent degradation) not only by the MAPKs but also by some pathway/s that is/are effector/s of the action of these MAPKs. This idea is supported by our finding that the effects of PTHrP is mediated by these MAPKs in HCT116 cells at longer exposure times[26]. More studies are needed to confirm this hypothesis.

Given these observations, the results obtained in this work suggest that at least the Src-ERK 1/2 MAPK and p38 MAPK axis is required for the phosphorylation/activation of Met induced by PTHrP in our model. Since MAPKs are serine-threonine kinases and Met requires phosphorylation on tyrosine residues for its activation, further studies are necessary to determine the link between these molecules.

As we previously mentioned, in CRC, the Met signaling pathway is associated with tumor evolution and also with resistance to chemotherapeutic drugs[32]. Currently, the inhibition of this RTK is being widely studied as a complementary therapy to conventional CRC treatments[37,38]. SU11274 prevents Met activation because it is an ATP competitive inhibitor of Met catalytic activity[70]. We previously showed that PTHrP has several effects on CRC derived cells such as proliferation, survival, migration, and induction of EMT program, among others[13,26,39]; the fact that we found a significant reduction in the viability and migration of HCT116 cells in the presence of an Met inhibitor as well as the reversal of the mesenchymal phenotype induction, even in the presence of PTHrP, indicates that Met mainly

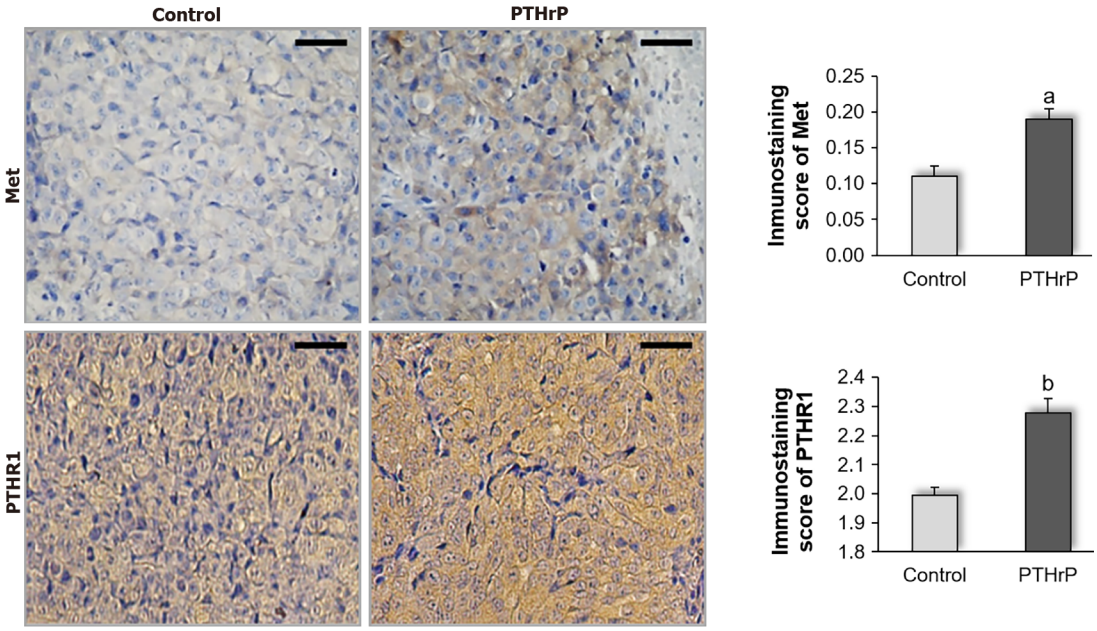

DOI: 10.3748/wjg.v28.i26.3177

Figure 8 Parathyroid hormone-related peptide increases the protein expression of Met and parathyroid hormone receptor type 1 in tumor xenografts. Met and parathyroid hormone-related peptide receptor type 1 (PTHR1) protein levels were evaluated by the immunohistochemistry technique in the HCT116 cell tumor-bearing nude mouse model. Tumor sections were stained with an anti-Met antibody or anti-PTHR1 antibody. Images (400 ×) are from the tumor treated with saline solution (left) or with PTHrP (right). The immunostaining was quantified with the Fiji image processing package of the Image J-NIH program. Scale bar: 50 μM. Met: Receptor tyrosine kinase Met; PTHR1: Parathyroid hormone receptor type 1; PTHrP: Parathyroid hormone-related peptide. $^{a}P < 0.05$; $^{b}P < 0.01$.

participates in the molecular mechanisms that are involved in these cell responses to PTHrP action.

PTHrP favors the aggressive behavior of CRC cells, inducing other events related to the malignant phenotype such as chemoresistance to CPT-11. The tumor cell response to this drug under PTHrP action involves the ERK signaling pathway[26]. Other investigations carried out by Paillas and colleagues demonstrated that the p38 MAPK pathway also modulates the sensitivity of CRC cells to CPT-11[89]. Given the data obtained previously by us and by other researchers and taking into account the link in CRC between Met signaling and the MAPKs pathway showed in this work and by other authors[41], our next motivation was to further investigate the chemoresistance of CRC-derived cells induced by PTHrP by analyzing two key aspects: Whether the cytokine affects the sensitivity of CRC cells to other chemotherapeutic drugs and whether the Met signaling pathway participates in PTHrP-trigged chemoresistance.

Our work shows that the treatment with this cytokine also attenuates the cytotoxicity induced by OXA and DOXO. This is an interesting result as it indicates that PTHrP promotes resistance to different types of cytotoxic agents. Perhaps the mechanisms trigged by this cytokine alter specific targets or the signaling of these drugs. Tumor cells develop different strategies to avoid chemotherapeutic drug effects. To improve the efficacy of the treatment, combinations of multiple agents are usually used[90]. Given that these drugs present different modes of action, pharmacological doses, and side effects[91-93], in the future it will be necessary to continue this research by testing new drugs and combinations thereof as well as elucidating the specific targets of PTHrP for each one.

Besides, the use of SU11274 together with CPT-11, OXA, or DOXO increases the sensitivity of CRC cells to these drugs, suggesting that Met participates in the chemoresistance induced by PTHrP. The inhibitors of markers/pathways related to cancer progression are still under investigation and like all anti-cancer approaches, their applications have challenges in the therapy of the disease[78,94]. With respect to the inhibition of the Met signaling pathway, a recent publication by Du and colleagues proposes to target the HGF/Met axis as a possible strategy for patients with metastatic CRC[94].

So far, our *in vitro* observations have allowed us to suppose the existence of a mechanism based on the action of PTHrP on the regulation of *Met* gene expression and also on its activation through Src kinase and the MAPKs pathway. Once activated, Met signaling leads to molecular changes in the tumor cell to promote chemoresistance to CPT-11, OXA, and DOXO. Probably, the up-regulation of Met expression also collaborates in the induction of events associated with the aggressive behavior of CRC cells (Figure 10). Besides, our results support those studies that suggest the incorporation of Met inhibitors combined with adjuvant drugs as new therapeutic strategies in CRC treatment and establish the need to further investigate whether PTHrP is a predictive and/or prognostic marker of CRC.

In this work, we also performed *in vivo* assays with the aim to evaluate the effects of PTHrP in a different context for tumor cells. As we expected, in agreement with our *in vitro* observations, HCT116

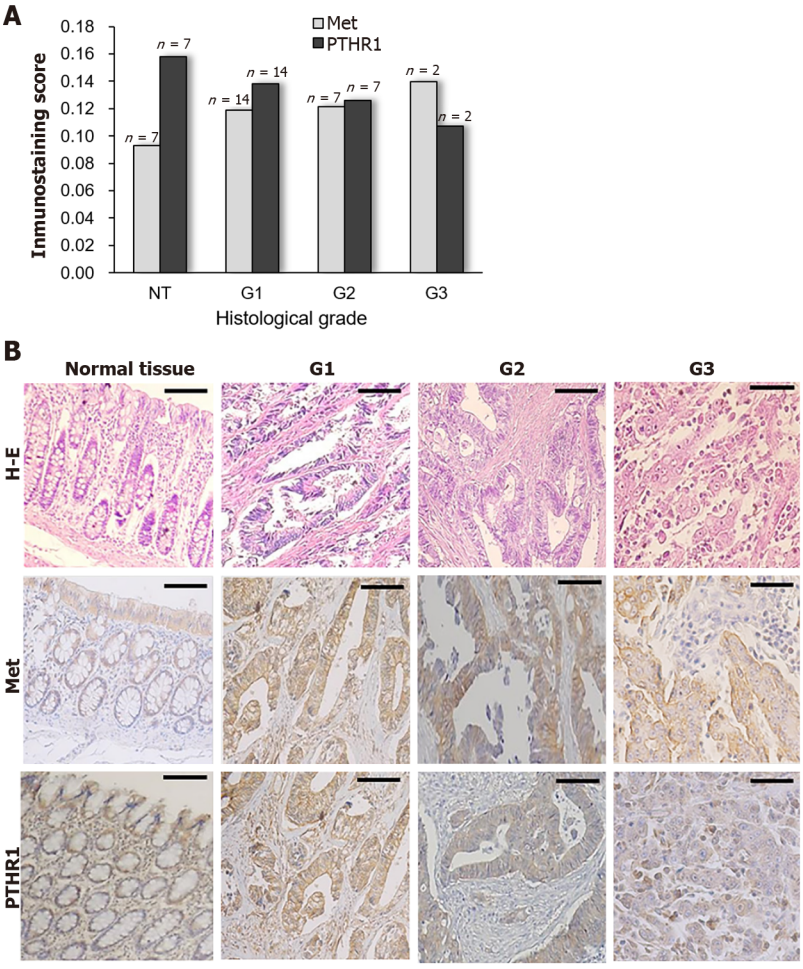

DOI: 10.3748/wjg.v28.i26.3177

Figure 9 Relation of Met and parathyroid hormone receptor type 1 staining intensity with tumor histological differentiation. A: Quantification of the immunostaining by optical density analysis using the FIJI plug-in from the Image J program; B: Representative images (200 ×) obtained by hematoxylin-eosin staining and by the immunohistochemistry technique performed for Met and PTHR1 for normal colorectal tissue and colorectal cancer tissue, with histological grades G1, G2, and G3. Scale bar: 10 μM. H-E: Hematoxylin-eosin staining; Met: Receptor tyrosine kinase Met; NT: Normal tissue; PTHR1: Parathyroid hormone receptor type 1.

cell tumor xenografts treated with the peptide exhibited an increase in Met protein expression concerning the control. PTHrP increases the levels of its own receptor, perhaps to amplify its signaling within the cell, and thus makes its effects more effective in CRC. Despite the limitations of the N:NIH (S)_nu model regarding the interaction of tumor cells with the stroma[13,24], these results allow us to presume a relationship between the aberrant expression of Met already observed in the tumor tissue of CRC patients[38] and PTHrP/PTHR1.

As we previously stated, although HGF is the only known ligand capable of inducing Met phosphorylation and activation, studies have shown that the cross-communication with G-coupled protein receptors transactivates this RTK. Concerning this, it was demonstrated that the prostaglandin E2 receptor EP1 can induce an aberrant activation of RTKs like Met in hepatocellular carcinoma cells [30]. Similar results had previously been obtained by Fischer and colleagues in pancreatic and hepatocellular carcinoma cells[29]. As we previously mentioned, PTHrP has intracrine, autocrine, endocrine, and mainly paracrine actions through the binding to a G-coupled protein receptor, PTHR1[9,10]. For this reason, the peptide and its receptor are expressed in the same cells or adjacent cells and changes in their expression are directly correlated[14,15]. Considering the previously described background, we evaluated Met and PTHR1 expression in normal colorectal tissues and in biopsies from patients with colon adenocarcinoma. Although Lee and colleagues did not find a statistical relevance between Met overexpression and the clinicopathological characteristics of patients with CRC, they demonstrated that it is associated with a lower overall survival and progression-free survival[38]. In contrast, Kim and his research group concluded that Met expression in patients with CRC is not a prognostic indicator for overall survival[95]. Despite these data, there was no information about the association between Met and PTHR1 expression and its impact on the evolution of CRC. As we expected, given that both receptors have a physiological role, Met and the PTHrP receptor are expressed in normal colon tissue. We found a statistically significant result when we compared the staining of tumors with high

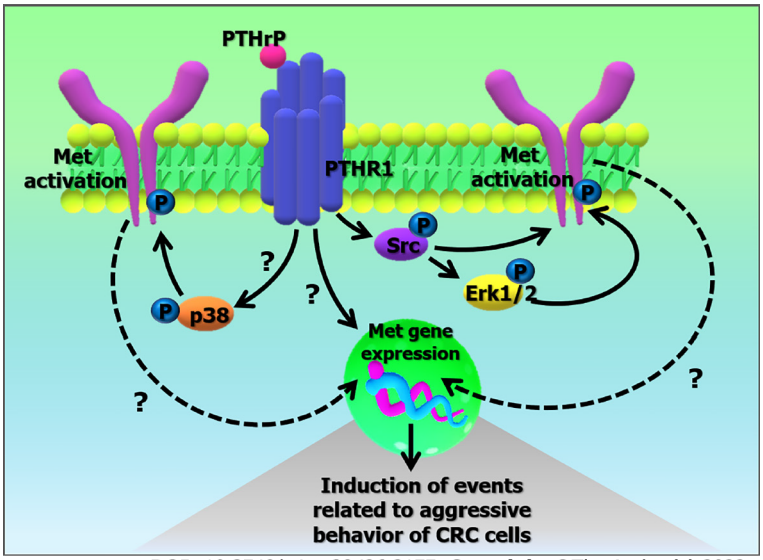

DOI: 10.3748/wjg.v28.i26.3177

Figure 10 Possible mechanism based on the action of parathyroid hormone-related peptide in the regulation of Met gene expression and its activation. The binding of parathyroid hormone-related peptide (PTHrP) to PTHR type 1 (PTHR1) in HCT116 cells promotes the up-regulation of *Met* gene expression. PTHrP also induces the activation of Met through Src kinase and the mitogen-activated protein kinases (MAPKs) pathway (Erk 1/2 MAPK and p38 MAPK). Once activated, Met signaling leads to molecular changes in the tumor cell that promote events related to the aggressive behavior of colorectal cancer cells. CRC: Colorectal cancer; Erk 1/2: Extracellular signal-regulated kinases 1/2; Met: Receptor tyrosine kinase Met; P: Activators domains phosphorylated; PTHR1: Parathyroid hormone receptor type 1; PTHrP: Parathyroid hormone-related peptide.

histological differentiation compared to those more undifferentiated with regard to the immunoreactivity for Met and PTHR1 that gradually increase and diminish, respectively.

Interestingly, García and colleagues showed that in neuroblastoma, PTHrP acts as a growth factor promoting tumor progression and high levels of its receptor are associated with less aggressive tumor characteristics; also, the intracrine and paracrine actions of the cytokine promote phenotypes with different levels of aggressiveness in their experimental models. These researchers found that PTHR1 is poorly expressed in neuroblastoma cell lines that are not well differentiated; however, in those cells with a high degree of differentiation, PTHR1 has greater expression. Furthermore, they observed that the receptor knockdown promotes a much more aggressive phenotype in more differentiated cells[96]. These data support our observations and could be related with the role of PTHrP and PTHR1 in the promotion of an aggressive phenotype of CRC.

We observed that the intensity of Met immunostaining in tumor cell plasma membrane increases as tumor differentiation declines. Concerning the location of PTHR1 in the plasma membrane, the intensity of the staining gradually decreases in histologically less differentiated tumors; also, it is located in the cytoplasm and the perinuclear region of the tumor cell, with immunoreactivity more predominant in samples with histological degree G3. This could be related to an intracrine role of the cytokine most preponderant in less differentiated CRC cells. More studies are necessary to confirm this.

Based on the above, it is presumed that in the early stages of tumor development, PTHrP would act by binding to its receptor in the tumor cell, possibly inducing Met receptor expression. The secretion of this cytokine from tumor stromal cells has also been reported[97] and we have previously demonstrated its influence on the synthesis and release of tumor microenvironment factors that favor an aggressive CRC phenotype[24,25]. Considering that in less differentiated tumors, we observed lower expression of PTHR1, we hypothesize that in this instance the tumor stromal cells adopt a leading role by secreting (perhaps in response to PTHrP) other cytokines that promote the expression and activation of molecular markers related to a worse prognosis of the disease. The high levels of Met in more advanced stages could be mediated not only by the action of PTHrP but also by other cytokines as other researchers have previously demonstrated[63,98]. It is known that the loss of cellular identity, characteristic of an advanced undifferentiated state, is evidenced by changes in the expression of surface molecules including receptors on tumor cells[99]. The high levels of PTHR1 observed in normal samples and primary neoplasms, and its decrease in undifferentiated histological grades could respond to this effect. On the other hand, high expression of Met in tumor samples is observed in association with a low degree of cellular differentiation. In this context, perhaps PTHR1 and Met could act as markers of cellular dedifferentiation. However, more studies are needed to verify this hypothesis.

CONCLUSION

Here we have demonstrated using an *in vitro* model that the PTHrP pathway promotes events that are associated with a worse evolution of CRC through Met activation. We also provide evidence for the association between PTHrP action and Met expression *in vivo*. Given all this information, it will be of great interest to ascertain the participation of Met in other molecular events related to CRC progression trigged by PTHrP and its translational relevance. More studies are needed in the areas of basic and clinical oncology to confirm this.

ARTICLE HIGHLIGHTS

Research background

Colorectal cancer (CRC) patients usually relapse and die due to the development of metastasis and resistance to chemotherapeutic drugs employed in the treatment. Parathyroid hormone-related peptide (PTHrP) is a cytokine that has a key role in the carcinogenesis and the progression of several tumors. Our research group found that the binding of PTHrP to its receptor, the parathyroid hormone receptor type 1 (PTHR1), promotes events associated with the aggressive phenotype of colorectal cancer cells. The receptor tyrosine kinase Met is associated with metastasis and chemoresistance in CRC.

Research motivation

The mechanisms that lead to an aggressive tumor behavior and a worse response to CRC treatment are still unknown. To date, it has not been studied whether there is a cross-talk between the PTHrP and Met signaling pathways to trigger molecular mechanisms associated with CRC progression.

Research objectives

To investigate the relationship between PTHR1, PTHrP, and Met in the aggressive behavior of CRC cells. These findings could have implications for the future diagnosis, prognosis, and treatment of patients with CRC.

Research methods

By RT-PCR and Western blot analysis, we studied whether PTHrP modulates the expression of Met and its activation in CRC cells. By Western blot and using specific inhibitors, we also evaluated the signaling pathways involved in Met activation induced by PTHrP. By Trypan blue technique, Wound healing assay, Western blot, and morphological analysis, we evaluated whether the Met signaling pathway mediates the effects induced by PTHrP in HCT116 cells. By the immunohistochemistry technique, we evaluated the expression of Met and the PTHrP receptor, PTHR1, in HCT116 cell xenografts of nude mice in response to the treatment with or without PTHrP. An observational analysis of human samples was performed to validate the findings obtained by *in vitro* and *in vivo* assays.

Research results

PTHrP modulated the expression of Met and promoted its activation through Src kinase and the mitogen-activated protein kinase (MAPK) signaling pathway in human HCT116 cells. The Met signaling pathway triggered by PTHrP participated in cellular events related to the aggressive behavior of human HCT116 cells such as proliferation, morphological changes associated with epithelial to mesenchymal transition, and migration and in the decrease of the sensitivity to chemotherapy drugs. PTHrP increased the protein expression of its receptor, PTHR1, and of Met in HCT116 cell tumor xenografts. PTHR1 was highly expressed in well-differentiated human CRC samples. In contrast, Met showed an expression pattern that was increased in poorly differentiated CRC tumors.

Research conclusions

PTHrP promotes events associated with a worse behavior of CRC cells through Met activation. To date, our *in vitro* observations suggest that the binding of PTHrP to its receptor, PTHR1, promotes the regulation of *Met* gene expression and also its activation through the Src kinase and the MAPKs pathway. Once activated, Met signaling leads to molecular changes in the tumor cell to promote events associated with the aggressive behavior of CRC cells. Our previous data together with the findings shown herein reveal that PTHrP *in vivo* modulates the expression of markers linked to tumor progression (including Met) and also of its own receptor. These events could favor the tumor phenotype in the CRC animal model studied in this work.

Research perspectives

In the future, it will be of great interest to evaluate whether Met mediates other molecular mechanisms and events triggered by PTHrP that are involved in CRC progression. Concerning translational

relevance, more studies are needed in the areas of basic and clinical oncology.

FOOTNOTES

Author contributions: Novoa Díaz MB and Carriere P contributed to conceptualization, methodology, investigation, formal analysis, visualization, and manuscript drafting, review, and editing; Gigola G and Zwenger AO contributed to conceptualization, methodology, and investigation; Calvo N contributed to conceptualization, methodology, investigation, formal analysis, visualization, supervision, and manuscript drafting, review, and editing; Gentili C contributed to conceptualization, methodology, resources, investigation, formal analysis, visualization, supervision, manuscript drafting, review, and editing, project administration, and funding acquisition.

Supported by the Agencia Nacional de Promoción Científica y Tecnológica, No. PICT-2013-1441; Consejo Nacional de Investigaciones Científicas y Técnicas, No. PIP11220150100350; Instituto Nacional del Cáncer Asistencia Financiera II, RESOL 493/14, No. 2002-4395-14-1; Instituto Nacional del Cáncer Asistencia Financiera III-2016-2017, RESOL-2016-1006-E-APN-MS, No. 2002-3862-16-1 CANCER; Universidad Nacional del Sur, No. PGI: 24/B230 and No. PGI: 24/B303; and Fundación Alberto J. Roemmers of Argentina.

Institutional review board statement: The study was reviewed and approved by the committee of experts on the subject conformed by members of the Department of Biology, Biochemistry and Pharmacy of the National University of the South.

Institutional animal care and use committee statement: All applicable international, national, and/or institutional guidelines for the care and use of animals were followed. All experiments with animals were approved by a local animal committee for ethics (CICUAE-UNS, institutional endorsement updated to 2021), and were carried out in accordance with the National Institutes of Health guide for the care and use of Laboratory animals (NIH 1996).

Conflict-of-interest statement: There are no conflicts of interest to report.

Data sharing statement: No additional data are available.

ARRIVE guidelines statement: The authors have read the ARRIVE Guidelines, and the manuscript was prepared and revised according to the ARRIVE Guidelines.

Country/Territory of origin: Argentina

ORCID number: María Belén Novoa Díaz 0000-0002-6684-4076; Pedro Carriere 0000-0002-5751-8850; Graciela Gigola 0000-0001-7362-3178; Ariel Osvaldo Zwenger 0000-0002-4407-5413; Natalia Calvo 0000-0003-3627-6749; Claudia Gentili 0000-0002-9957-7824.

S-Editor: Chen YL
L-Editor: Wang TQ
P-Editor: Yu HG

REFERENCES

1 **Wang J**, Dong X, Zhu X, Zhao H, Mao D, Zhao X. [Expression of interleukin-9 in colon cancer tissues and its clinical significance]. *Nan Fang Yi Ke Da Xue Xue Bao* 2018; **38**: 943-948 [PMID: 30187869 DOI: 10.3969/j.issn.1673-4254.2018.08.07]
2 **Arnold M**, Sierra MS, Laversanne M, Soerjomataram I, Jemal A, Bray F. Global patterns and trends in colorectal cancer incidence and mortality. *Gut* 2017; **66**: 683-691 [PMID: 26818619 DOI: 10.1136/gutjnl-2015-310912]
3 **Hatano Y**, Fukuda S, Hisamatsu K, Hirata A, Hara A, Tomita H. Multifaceted Interpretation of Colon Cancer Stem Cells. *Int J Mol Sci* 2017; **18** [PMID: 28678194 DOI: 10.3390/ijms18071446]
4 Erratum: Global cancer statistics 2018: GLOBOCAN estimates of incidence and mortality worldwide for 36 cancers in 185 countries. *CA Cancer J Clin* 2020; **70**: 313 [PMID: 32767693 DOI: 10.3322/caac.21609]
5 **Li J**, Huang L, Zhao H, Yan Y, Lu J. The Role of Interleukins in Colorectal Cancer. *Int J Biol Sci* 2020; **16**: 2323-2339 [PMID: 32760201 DOI: 10.7150/ijbs.46651]
6 **Parsons S**, Maldonado EB, Prasad V. Comparison of Drugs Used for Adjuvant and Metastatic Therapy of Colon, Breast, and Non-Small Cell Lung Cancers. *JAMA Netw Open* 2020; **3**: e202488 [PMID: 32275321 DOI:

10.1001/jamanetworkopen.2020.2488]
7 **Chang CL**, Yuan KS, Wu ATH, Wu SY. Adjuvant Therapy for High-Risk Stage II or III Colon Adenocarcinoma: A Propensity Score-Matched, Nationwide, Population-Based Cohort Study. *Cancers (Basel)* 2019; **11** [PMID: 31842371 DOI: 10.3390/cancers11122003]
8 **Meyers BM**, Cosby R, Quereshy F, Jonker D. Adjuvant Chemotherapy for Stage II and III Colon Cancer Following Complete Resection: A Cancer Care Ontario Systematic Review. *Clin Oncol (R Coll Radiol)* 2017; **29**: 459-465 [PMID: 28341242 DOI: 10.1016/j.clon.2017.03.001]
9 **Maioli E**, Fortino V. PTHrP on MCF-7 breast cancer cells: a growth factor or an antimitogenic peptide? *Br J Cancer* 2004; **90**: 1293-4; author reply 1295 [PMID: 15026815 DOI: 10.1038/sj.bjc.6601689]
10 **McCauley LK**, Martin TJ. Twenty-five years of PTHrP progress: from cancer hormone to multifunctional cytokine. *J Bone Miner Res* 2012; **27**: 1231-1239 [PMID: 22549910 DOI: 10.1002/jbmr.1617]
11 **Goltzman D**. Nonparathyroid Hypercalcemia. *Front Horm Res* 2019; **51**: 77-90 [PMID: 30641526 DOI: 10.1159/000491040]
12 **He S**, Tang J, Diao N, Liao Y, Shi J, Xu X, Xie F, Bai L. Parathyroid hormone-related protein activates HSCs *via* hedgehog signalling during liver fibrosis development. *Artif Cells Nanomed Biotechnol* 2019; **47**: 1984-1994 [PMID: 31311343 DOI: 10.1080/21691401.2019.1615931]
13 **Novoa Díaz MB**, Carriere PM, Martín MJ, Calvo N, Gentili C. Involvement of parathyroid hormone-related peptide in the aggressive phenotype of colorectal cancer cells. *World J Gastroenterol* 2021; **27**: 7025-7040 [PMID: 34887626 DOI: 10.3748/wjg.v27.i41.7025]
14 **Martin TJ**. Parathyroid Hormone-Related Protein, Its Regulation of Cartilage and Bone Development, and Role in Treating Bone Diseases. *Physiol Rev* 2016; **96**: 831-871 [PMID: 27142453 DOI: 10.1152/physrev.00031.2015]
15 **Kim MR**, Choi SH, Lee BN, Min KS, Hwang YC. Effect of parathyroid hormone-related protein on odontogenic differentiation in human dental pulp cells. *BMC Oral Health* 2020; **20**: 101 [PMID: 32276610 DOI: 10.1186/s12903-020-01085-8]
16 **Zhang R**, Li J, Assaker G, Camirand A, Sabri S, Karaplis AC, Kremer R. Parathyroid Hormone-Related Protein (PTHrP): An Emerging Target in Cancer Progression and Metastasis. *Adv Exp Med Biol* 2019; **1164**: 161-178 [PMID: 31576548 DOI: 10.1007/978-3-030-22254-3_13]
17 **Kremer R**, Li J, Camirand A, Karaplis AC. Parathyroid hormone related protein (PTHrP) in tumor progression. *Adv Exp Med Biol* 2011; **720**: 145-160 [PMID: 21901625 DOI: 10.1007/978-1-4614-0254-1_12]
18 **Nishihara M**, Kanematsu T, Taguchi T, Razzaque MS. PTHrP and tumorigenesis: is there a role in prognosis? *Ann N Y Acad Sci* 2007; **1117**: 385-392 [PMID: 18056053 DOI: 10.1196/annals.1402.046]
19 **Nishihara M**, Ito M, Tomioka T, Ohtsuru A, Taguchi T, Kanematsu T. Clinicopathological implications of parathyroid hormone-related protein in human colorectal tumours. *J Pathol* 1999; **187**: 217-222 [PMID: 10365097 DOI: 10.1002/(SICI)1096-9896(199901)187:2<217:AID-PATH210>3.0.CO;2-0]
20 **Malakouti S**, Asadi FK, Kukreja SC, Abcarian HA, Cintron JR. Parathyroid hormone-related protein expression in the human colon: immunohistochemical evaluation. *Am Surg* 1996; **62**: 540-4; discussion 544 [PMID: 8651548]
21 **Ongkeko WM**, Burton D, Kiang A, Abhold E, Kuo SZ, Rahimy E, Yang M, Hoffman RM, Wang-Rodriguez J, Deftos LJ. Parathyroid hormone related-protein promotes epithelial-to-mesenchymal transition in prostate cancer. *PLoS One* 2014; **9**: e85803 [PMID: 24465715 DOI: 10.1371/journal.pone.0085803]
22 **Sen S**, Dasgupta P, Kamath G, Srikanth HS. Paratharmone related protein (peptide): A novel prognostic, diagnostic and therapeutic marker in Head & Neck cancer. *J Stomatol Oral Maxillofac Surg* 2018; **119**: 33-36 [PMID: 29081380 DOI: 10.1016/j.jormas.2017.10.016]
23 **Hong N**, Yoon HJ, Lee YH, Kim HR, Lee BW, Rhee Y, Kang ES, Cha BS, Lee HC. Serum PTHrP Predicts Weight Loss in Cancer Patients Independent of Hypercalcemia, Inflammation, and Tumor Burden. *J Clin Endocrinol Metab* 2016; **101**: 1207-1214 [PMID: 26765580 DOI: 10.1210/jc.2015-3785]
24 **Carriere P**, Calvo N, Novoa Díaz MB, Lopez-Moncada F, Herrera A, Torres MJ, Alonso E, Gandini NA, Gigola G, Contreras HR, Gentili C. Role of SPARC in the epithelial-mesenchymal transition induced by PTHrP in human colon cancer cells. *Mol Cell Endocrinol* 2021; **530**: 111253 [PMID: 33781836 DOI: 10.1016/j.mce.2021.111253]
25 **Calvo N**, Carriere P, Martín MJ, Gigola G, Gentili C. PTHrP treatment of colon cancer cells promotes tumor associated-angiogenesis by the effect of VEGF. *Mol Cell Endocrinol* 2019; **483**: 50-63 [PMID: 30639585 DOI: 10.1016/j.mce.2019.01.005]
26 **Martín MJ**, Gigola G, Zwenger A, Carriquiriborde M, Gentil F, Gentili C. Potential therapeutic targets for growth arrest of colorectal cancer cells exposed to PTHrP. *Mol Cell Endocrinol* 2018; **478**: 32-44 [PMID: 30009852 DOI: 10.1016/j.mce.2018.07.005]
27 **Calvo N**, Carriere P, Martin MJ, Gentili C. RSK activation *via* ERK modulates human colon cancer cells response to PTHrP. *J Mol Endocrinol* 2017; **59**: 13-27 [PMID: 28385776 DOI: 10.1530/JME-16-0216]
28 **Choi YJ**, Kim JH, Rho JK, Kim JS, Choi CM, Kim WS, Son J, Lee JC. AXL and MET receptor tyrosine kinases are essential for lung cancer metastasis. *Oncol Rep* 2017; **37**: 2201-2208 [PMID: 28260071 DOI: 10.3892/or.2017.5482]
29 **Fischer OM**, Giordano S, Comoglio PM, Ullrich A. Reactive oxygen species mediate Met receptor transactivation by G protein-coupled receptors and the epidermal growth factor receptor in human carcinoma cells. *J Biol Chem* 2004; **279**: 28970-28978 [PMID: 15123705 DOI: 10.1074/jbc.M402508200]
30 **Han C**, Michalopoulos GK, Wu T. Prostaglandin E2 receptor EP1 transactivates EGFR/MET receptor tyrosine kinases and enhances invasiveness in human hepatocellular carcinoma cells. *J Cell Physiol* 2006; **207**: 261-270 [PMID: 16331686 DOI: 10.1002/jcp.20560]
31 **Cattaneo F**, Guerra G, Parisi M, De Marinis M, Tafuri D, Cinelli M, Ammendola R. Cell-surface receptors transactivation mediated by g protein-coupled receptors. *Int J Mol Sci* 2014; **15**: 19700-19728 [PMID: 25356505 DOI: 10.3390/ijms151119700]
32 **Mezquita B**, Pineda E, Mezquita J, Mezquita P, Pau M, Codony-Servat J, Martínez-Balibrea E, Mora C, Maurel J, Mezquita C. LoVo colon cancer cells resistant to oxaliplatin overexpress c-MET and VEGFR-1 and respond to VEGF with

dephosphorylation of c-MET. *Mol Carcinog* 2016; **55**: 411-419 [PMID: 25647613 DOI: 10.1002/mc.22289]
33 **Mulcahy EQX**, Colón RR, Abounader R. HGF/MET Signaling in Malignant Brain Tumors. *Int J Mol Sci* 2020; **21** [PMID: 33066121 DOI: 10.3390/ijms21207546]
34 **Huang L**, Xie K, Li H, Wang R, Xu X, Chen K, Gu H, Fang J. Suppression of c-Met-Overexpressing Tumors by a Novel c-Met/CD3 Bispecific Antibody. *Drug Des Devel Ther* 2020; **14**: 3201-3214 [PMID: 32982167 DOI: 10.2147/DDDT.S254117]
35 **Wang S**, Qiu J, Liu L, Su C, Qi L, Huang C, Chen X, Zhang Y, Ye Y, Ding Y, Liang L, Liao W. CREB5 promotes invasiveness and metastasis in colorectal cancer by directly activating MET. *J Exp Clin Cancer Res* 2020; **39**: 168 [PMID: 32843066 DOI: 10.1186/s13046-020-01673-0]
36 **Cai P**, Xie Y, Dong M, Zhu Q. Inhibition of *MEIS3* Generates Cetuximab Resistance through c-Met and Akt. *Biomed Res Int* 2020; **2020**: 2046248 [PMID: 33376716 DOI: 10.1155/2020/2046248]
37 **Shali H**, Ahmadi M, Kafil HS, Dorosti A, Yousefi M. IGF1R and c-met as therapeutic targets for colorectal cancer. *Biomed Pharmacother* 2016; **82**: 528-536 [PMID: 27470393 DOI: 10.1016/j.biopha.2016.05.034]
38 **Lee SJ**, Lee J, Park SH, Park JO, Lim HY, Kang WK, Park YS, Kim ST. c-MET Overexpression in Colorectal Cancer: A Poor Prognostic Factor for Survival. *Clin Colorectal Cancer* 2018; **17**: 165-169 [PMID: 29576428 DOI: 10.1016/j.clcc.2018.02.013]
39 **Martín MJ**, Calvo N, de Boland AR, Gentili C. Molecular mechanisms associated with PTHrP-induced proliferation of colon cancer cells. *J Cell Biochem* 2014; **115**: 2133-2145 [PMID: 25053227 DOI: 10.1002/jcb.24890]
40 **Calvo N**, Martín MJ, de Boland AR, Gentili C. Involvement of ERK1/2, p38 MAPK, and PI3K/Akt signaling pathways in the regulation of cell cycle progression by PTHrP in colon adenocarcinoma cells. *Biochem Cell Biol* 2014; **92**: 305-315 [PMID: 25051885 DOI: 10.1139/bcb-2013-0106]
41 **Larsen CA**, Dashwood RH. (-)-Epigallocatechin-3-gallate inhibits Met signaling, proliferation, and invasiveness in human colon cancer cells. *Arch Biochem Biophys* 2010; **501**: 52-57 [PMID: 20361925 DOI: 10.1016/j.abb.2010.03.017]
42 **Bradford MM**. A rapid and sensitive method for the quantitation of microgram quantities of protein utilizing the principle of protein-dye binding. *Anal Biochem* 1976; **72**: 248-254 [PMID: 942051 DOI: 10.1006/abio.1976.9999]
43 **Naba NM**, Tolay N, Erman B, Sayi Yazgan A. Doxorubicin inhibits miR-140 expression and upregulates PD-L1 expression in HCT116 cells, opposite to its effects on MDA-MB-231 cells. *Turk J Biol* 2020; **44**: 15-23 [PMID: 32123492 DOI: 10.3906/biy-1909-12]
44 **Attoub S**, Arafat K, Khalaf T, Sulaiman S, Iratni R. Frondoside A Enhances the Anti-Cancer Effects of Oxaliplatin and 5-Fluorouracil on Colon Cancer Cells. *Nutrients* 2018; **10** [PMID: 29724012 DOI: 10.3390/nu10050560]
45 **Lu X**, Wei H, Zhang X, Zheng W, Chang C, Gu J. Rapamycin synergizes with low-dose oxaliplatin in the HCT116 colon cancer cell line by inducing enhanced apoptosis. *Oncol Lett* 2011; **2**: 643-647 [PMID: 22848242 DOI: 10.3892/ol.2011.299]
46 **Sabit H**, Samy MB, Said OA, El-Zawahri MM. Procaine Induces Epigenetic Changes in HCT116 Colon Cancer Cells. *Genet Res Int* 2016; **2016**: 8348450 [PMID: 27843649 DOI: 10.1155/2016/8348450]
47 **Dunn EF**, Iida M, Myers RA, Campbell DA, Hintz KA, Armstrong EA, Li C, Wheeler DL. Dasatinib sensitizes KRAS mutant colorectal tumors to cetuximab. *Oncogene* 2011; **30**: 561-574 [PMID: 20956938 DOI: 10.1038/onc.2010.430]
48 **Zhou H**, Iida-Klein A, Lu SS, Ducayen-Knowles M, Levine LR, Dempster DW, Lindsay R. Anabolic action of parathyroid hormone on cortical and cancellous bone differs between axial and appendicular skeletal sites in mice. *Bone* 2003; **32**: 513-520 [PMID: 12753867 DOI: 10.1016/s8756-3282(03)00057-7]
49 **Stewart AF**, Cain RL, Burr DB, Jacob D, Turner CH, Hock JM. Six-month daily administration of parathyroid hormone and parathyroid hormone-related protein peptides to adult ovariectomized rats markedly enhances bone mass and biomechanical properties: a comparison of human parathyroid hormone 1-34, parathyroid hormone-related protein 1-36, and SDZ-parathyroid hormone 893. *J Bone Miner Res* 2000; **15**: 1517-1525 [PMID: 10934650 DOI: 10.1359/jbmr.2000.15.8.1517]
50 **Frolik CA**, Cain RL, Sato M, Harvey AK, Chandrasekhar S, Black EC, Tashjian AH Jr, Hock JM. Comparison of recombinant human PTH(1-34) (LY333334) with a C-terminally substituted analog of human PTH-related protein(1-34) (RS-66271): In vitro activity and in vivo pharmacological effects in rats. *J Bone Miner Res* 1999; **14**: 163-172 [PMID: 9933468 DOI: 10.1359/jbmr.1999.14.2.163]
51 **Sierrasesµmaga L**. Tumores sólidos más frecuentes en la infancia. *AnPediatriContin* 2004; 153
52 **Farrugia W**, de Gooyer T, Rice GE, Moseley JM, Wlodek ME. Parathyroid hormone(1-34) and parathyroid hormone-related protein(1-34) stimulate calcium release from human syncytiotrophoblast basal membranes *via* a common receptor. *J Endocrinol* 2000; **166**: 689-695 [PMID: 10974662 DOI: 10.1677/joe.0.1660689]
53 **Lassoued S**, Caulier M, Poey C, Fournié B, Fournié A. [Lumbago-sciatica disclosing a spinal lipoma. A case report]. *Rev Rhum Mal Osteoartic* 1990; **57**: 563-565 [PMID: 2149201 DOI: 10.1089/bfm.2010.0101]
54 **Crowe AR**, Yue W. Semi-quantitative Determination of Protein Expression using Immunohistochemistry Staining and Analysis: An Integrated Protocol. *Bio Protoc* 2019; **9** [PMID: 31867411 DOI: 10.21769/BioProtoc.3465]
55 **Schindelin J**, Arganda-Carreras I, Frise E, Kaynig V, Longair M, Pietzsch T, Preibisch S, Rueden C, Saalfeld S, Schmid B, Tinevez JY, White DJ, Hartenstein V, Eliceiri K, Tomancak P, Cardona A. Fiji: an open-source platform for biological-image analysis. *Nat Methods* 2012; **9**: 676-682 [PMID: 22743772 DOI: 10.1038/nmeth.2019]
56 **R Core Team**. A language and environment for statistical computing. 2020. [cited 20 March 2022]. Available from: https://www.R-project.org/
57 **Chen R**, Li J, Feng CH, Chen SK, Liu YP, Duan CY, Li H, Xia XM, He T, Wei M, Dai RY. c-Met function requires N-linked glycosylation modification of pro-Met. *J Cell Biochem* 2013; **114**: 816-822 [PMID: 23060267 DOI: 10.1002/jcb.24420]
58 **Zhang J**, Wang Z, Zhang S, Chen Y, Xiong X, Li X, Tonks NK, Fan G. Spatial regulation of signaling by the coordinated action of the protein tyrosine kinases MET and FER. *Cell Signal* 2018; **50**: 100-110 [PMID: 29920310 DOI: 10.1016/j.cellsig.2018.06.006]
59 **Ma DJ**, Cao Z, Wang BS, Sun YL. [Effect of silencing hepatocyte growth factor receptor c-Met expression on biological

characteristics of colon cancer cells]. *Zhonghua Zhong Liu Za Zhi* 2020; **42**: 362-368 [PMID: 32482024 DOI: 10.3760/cma.j.cn112152-112152-20191106-00714]

60 **Hastings RH**, Montgrain PR, Quintana RA, Chobrutskiy B, Davani A, Miyanohara A, Mahooti S. Lung carcinoma progression and survival versus amino- and carboxyl-parathyroid hormone-related protein expression. *J Cancer Res Clin Oncol* 2017; **143**: 1395-1407 [PMID: 28342003 DOI: 10.1007/s00432-017-2396-4]

61 **Calvo N**, German O, Russo de Boland A, Gentili C. Pro-apoptotic effects of parathyroid hormone in intestinal cells. *Biochem Cell Biol* 2009; **87**: 389-400 [PMID: 19370057 DOI: 10.1139/O08-143]

62 **Critchley WR**, Pellet-Many C, Ringham-Terry B, Harrison MA, Zachary IC, Ponnambalam S. Receptor Tyrosine Kinase Ubiquitination and De-Ubiquitination in Signal Transduction and Receptor Trafficking. *Cells* 2018; **7** [PMID: 29543760 DOI: 10.3390/cells7030022]

63 **Bradley CA**, Dunne PD, Bingham V, McQuaid S, Khawaja H, Craig S, James J, Moore WL, McArt DG, Lawler M, Dasgupta S, Johnston PG, Van Schaeybroeck S. Transcriptional upregulation of c-MET is associated with invasion and tumor budding in colorectal cancer. *Oncotarget* 2016; **7**: 78932-78945 [PMID: 27793046 DOI: 10.18632/oncotarget.12933]

64 **Martínez-Pérez J**, Lopez-Calderero I, Saez C, Benavent M, Limon ML, Gonzalez-Exposito R, Soldevilla B, Riesco-Martínez MC, Salamanca J, Carnero A, Garcia-Carbonero R. Prognostic relevance of Src activation in stage II-III colon cancer. *Hum Pathol* 2017; **67**: 119-125 [PMID: 28601656 DOI: 10.1016/j.humpath.2017.05.025]

65 **Steeg PS**. Targeting metastasis. *Nat Rev Cancer* 2016; **16**: 201-218 [PMID: 27009393 DOI: 10.1038/nrc.2016.25]

66 **Chen J**, Elfiky A, Han M, Chen C, Saif MW. The role of Src in colon cancer and its therapeutic implications. *Clin Colorectal Cancer* 2014; **13**: 5-13 [PMID: 24361441 DOI: 10.1016/j.clcc.2013.10.003]

67 **Braicu C**, Buse M, Busuioc C, Drula R, Gulei D, Raduly L, Rusu A, Irimie A, Atanasov AG, Slaby O, Ionescu C, Berindan-Neagoe I. A Comprehensive Review on MAPK: A Promising Therapeutic Target in Cancer. *Cancers (Basel)* 2019; **11** [PMID: 31652660 DOI: 10.3390/cancers11101618]

68 **Yuan J**, Dong X, Yap J, Hu J. The MAPK and AMPK signalings: interplay and implication in targeted cancer therapy. *J Hematol Oncol* 2020; **13**: 113 [PMID: 32807225 DOI: 10.1186/s13045-020-00949-4]

69 **Degirmenci U**, Wang M, Hu J. Targeting Aberrant RAS/RAF/MEK/ERK Signaling for Cancer Therapy. *Cells* 2020; **9** [PMID: 31941155 DOI: 10.3390/cells9010198]

70 **Gao W**, Bing X, Li M, Yang Z, Li Y, Chen H. Study of critical role of c-Met and its inhibitor SU11274 in colorectal carcinoma. *Med Oncol* 2013; **30**: 546 [PMID: 23536000 DOI: 10.1007/s12032-013-0546-3]

71 **Matsumoto K**, Umitsu M, De Silva DM, Roy A, Bottaro DP. Hepatocyte growth factor/MET in cancer progression and biomarker discovery. *Cancer Sci* 2017; **108**: 296-307 [PMID: 28064454 DOI: 10.1111/cas.13156]

72 **Gao SH**, Liu C, Wei J, Feng Y. Effect of c-Met inhibitor SU11274 on human colon cancer cell growth. *Chin Med J (Engl)* 2013; **126**: 2705-2709 [PMID: 23876900]

73 **Troiani T**, Martinelli E, Napolitano S, Vitagliano D, Ciuffreda LP, Costantino S, Morgillo F, Capasso A, Sforza V, Nappi A, De Palma R, D'Aiuto E, Berrino L, Bianco R, Ciardiello F. Increased TGF-α as a mechanism of acquired resistance to the anti-EGFR inhibitor cetuximab through EGFR-MET interaction and activation of MET signaling in colon cancer cells. *Clin Cancer Res* 2013; **19**: 6751-6765 [PMID: 24122793 DOI: 10.1158/1078-0432.CCR-13-0423]

74 **Loboda A**, Nebozhyn MV, Watters JW, Buser CA, Shaw PM, Huang PS, Van't Veer L, Tollenaar RA, Jackson DB, Agrawal D, Dai H, Yeatman TJ. EMT is the dominant program in human colon cancer. *BMC Med Genomics* 2011; **4**: 9 [PMID: 21251323 DOI: 10.1186/1755-8794-4-9]

75 **Tsoumas D**, Nikou S, Giannopoulou E, Champeris Tsaniras S, Sirinian C, Maroulis I, Taraviras S, Zolota V, Kalofonos HP, Bravou V. ILK Expression in Colorectal Cancer Is Associated with EMT, Cancer Stem Cell Markers and Chemoresistance. *Cancer Genomics Proteomics* 2018; **15**: 127-141 [PMID: 29496692 DOI: 10.21873/cgp.20071]

76 **Gurzu S**, Silveanu C, Fetyko A, Butiurca V, Kovacs Z, Jung I. Systematic review of the old and new concepts in the epithelial-mesenchymal transition of colorectal cancer. *World J Gastroenterol* 2016; **22**: 6764-6775 [PMID: 27570416 DOI: 10.3748/wjg.v22.i30.6764]

77 **Druzhkova I**, Ignatova N, Prodanets N, Kiselev N, Zhukov I, Shirmanova M, Zagainov V, Zagaynova E. E-Cadherin in Colorectal Cancer: Relation to Chemosensitivity. *Clin Colorectal Cancer* 2019; **18**: e74-e86 [PMID: 30415989 DOI: 10.1016/j.clcc.2018.10.003]

78 **Jeon HM**, Lee J. MET: roles in epithelial-mesenchymal transition and cancer stemness. *Ann Transl Med* 2017; **5**: 5 [PMID: 28164090 DOI: 10.21037/atm.2016.12.67]

79 **Mocellin S**, Baretta Z, Roqué I Figuls M, Solà I, Martin-Richard M, Hallum S, Bonfill Cosp X. Second-line systemic therapy for metastatic colorectal cancer. *Cochrane Database Syst Rev* 2017; **1**: CD006875 [PMID: 28128439 DOI: 10.1002/14651858.CD006875.pub3]

80 **Goldberg RM**, Sargent DJ, Morton RF, Fuchs CS, Ramanathan RK, Williamson SK, Findlay BP, Pitot HC, Alberts SR. A randomized controlled trial of fluorouracil plus leucovorin, irinotecan, and oxaliplatin combinations in patients with previously untreated metastatic colorectal cancer. *J Clin Oncol* 2004; **22**: 23-30 [PMID: 14665611 DOI: 10.1200/JCO.2004.09.046]

81 **Zhou X**, Xiao D. Long non-coding RNA GAS5 is critical for maintaining stemness and induces chemoresistance in cancer stem-like cells derived from HCT116. *Oncol Lett* 2020; **19**: 3431-3438 [PMID: 32269616 DOI: 10.3892/ol.2020.11471]

82 **Yang C**, Ran Q, Zhou Y, Liu S, Zhao C, Yu X, Zhu F, Ji Y, Du Q, Yang T, Zhang W, He S. Doxorubicin sensitizes cancer cells to Smac mimetic *via* synergistic activation of the CYLD/RIPK1/FADD/caspase-8-dependent apoptosis. *Apoptosis* 2020; **25**: 441-455 [PMID: 32418059 DOI: 10.1007/s10495-020-01604-6]

83 **Delitto D**, Vertes-George E, Hughes SJ, Behrns KE, Trevino JG. c-Met signaling in the development of tumorigenesis and chemoresistance: potential applications in pancreatic cancer. *World J Gastroenterol* 2014; **20**: 8458-8470 [PMID: 25024602 DOI: 10.3748/wjg.v20.i26.8458]

84 **Cañadas I**, Rojo F, Taus Á, Arpí O, Arumí-Uría M, Pijuan L, Menéndez S, Zazo S, Dómine M, Salido M, Mojal S, García de Herreros A, Rovira A, Albanell J, Arriola E. Targeting epithelial-to-mesenchymal transition with Met inhibitors reverts chemoresistance in small cell lung cancer. *Clin Cancer Res* 2014; **20**: 938-950 [PMID: 24284055 DOI: 10.1158/1078-0432.CCR-13-1330]

85 **Soki FN**, Park SI, McCauley LK. The multifaceted actions of PTHrP in skeletal metastasis. *Future Oncol* 2012; **8**: 803-817 [PMID: 22830401 DOI: 10.2217/fon.12.76]

86 **Silva Paiva R**, Gomes I, Casimiro S, Fernandes I, Costa L. c-Met expression in renal cell carcinoma with bone metastases. *J Bone Oncol* 2020; **25**: 100315 [PMID: 33024658 DOI: 10.1016/j.jbo.2020.100315]

87 **Ahmed D**, Eide PW, Eilertsen IA, Danielsen SA, Eknæs M, Hektoen M, Lind GE, Lothe RA. Epigenetic and genetic features of 24 colon cancer cell lines. *Oncogenesis* 2013; **2**: e71 [PMID: 24042735 DOI: 10.1038/oncsis.2013.35]

88 **Ilyas M**, Tomlinson IP, Rowan A, Pignatelli M, Bodmer WF. Beta-catenin mutations in cell lines established from human colorectal cancers. *Proc Natl Acad Sci U S A* 1997; **94**: 10330-10334 [PMID: 9294210 DOI: 10.1073/pnas.94.19.10330]

89 **Paillas S**, Boissière F, Bibeau F, Denouel A, Mollevi C, Causse A, Denis V, Vezzio-Vié N, Marzi L, Cortijo C, Ait-Arsa I, Askari N, Pourquier P, Martineau P, Del Rio M, Gongora C. Targeting the p38 MAPK pathway inhibits irinotecan resistance in colon adenocarcinoma. *Cancer Res* 2011; **71**: 1041-1049 [PMID: 21159664 DOI: 10.1158/0008-5472.CAN-10-2726]

90 **Gelibter AJ**, Caponnetto S, Urbano F, Emiliani A, Scagnoli S, Sirgiovanni G, Napoli VM, Cortesi E. Adjuvant chemotherapy in resected colon cancer: When, how and how long? *Surg Oncol* 2019; **30**: 100-107 [PMID: 31500770 DOI: 10.1016/j.suronc.2019.06.003]

91 **Murai J**, Thomas A, Miettinen M, Pommier Y. Schlafen 11 (SLFN11), a restriction factor for replicative stress induced by DNA-targeting anti-cancer therapies. *Pharmacol Ther* 2019; **201**: 94-102 [PMID: 31128155 DOI: 10.1016/j.pharmthera.2019.05.009]

92 **Riddell IA**. Cisplatin and Oxaliplatin: Our Current Understanding of Their Actions. *Met Ions Life Sci* 2018; **18** [PMID: 29394020 DOI: 10.1515/9783110470734-007]

93 **Dasari S**, Tchounwou PB. Cisplatin in cancer therapy: molecular mechanisms of action. *Eur J Pharmacol* 2014; **740**: 364-378 [PMID: 25058905 DOI: 10.1016/j.ejphar.2014.07.025]

94 **Du F**, Li X, Feng W, Qiao C, Chen J, Jiang M, Qiu Z, Qian M, Tian D, Nie Y, Fan D, Wu K, Xia L. SOX13 promotes colorectal cancer metastasis by transactivating SNAI2 and c-MET. *Oncogene* 2020; **39**: 3522-3540 [PMID: 32111984 DOI: 10.1038/s41388-020-1233-4]

95 **Kim HJ**, Baek MJ, Kang DH, Lee SC, Bae SB, Lee KT, Lee N, Kim H, Jeong D, Ahn TS, Lee MS, Hong DS, Won JH. Association Between c-Met and Lymphangiogenic Factors in Patients With Colorectal Cancer. *Ann Coloproctol* 2018; **34**: 88-93 [PMID: 29742856 DOI: 10.3393/ac.2017.10.10]

96 **García M**, Rodríguez-Hernández CJ, Mateo-Lozano S, Pérez-Jaume S, Gonçalves-Alves E, Lavarino C, Mora J, de Torres C. Parathyroid hormone-like hormone plays a dual role in neuroblastoma depending on PTH1R expression. *Mol Oncol* 2019; **13**: 1959-1975 [PMID: 31293052 DOI: 10.1002/1878-0261.12542]

97 **Cowan RW**, Singh G, Ghert M. PTHrP increases RANKL expression by stromal cells from giant cell tumor of bone. *J Orthop Res* 2012; **30**: 877-884 [PMID: 22102368 DOI: 10.1002/jor.22020]

98 **Takeuchi H**, Bilchik A, Saha S, Turner R, Wiese D, Tanaka M, Kuo C, Wang HJ, Hoon DS. c-MET expression level in primary colon cancer: a predictor of tumor invasion and lymph node metastases. *Clin Cancer Res* 2003; **9**: 1480-1488 [PMID: 12684423]

99 **Kim WT**, Ryu CJ. Cancer stem cell surface markers on normal stem cells. *BMB Rep* 2017; **50**: 285-298 [PMID: 28270302 DOI: 10.5483/BMBRep.2017.50.6.039]

World Journal of Gastroenterology

Submit a Manuscript: https://www.f6publishing.com

World J Gastroenterol 2022 July 14; 28(26): 3201-3217

DOI: 10.3748/wjg.v28.i26.3201

ISSN 1007-9327 (print) ISSN 2219-2840 (online)

ORIGINAL ARTICLE

Basic Study

Intracellular alpha-fetoprotein mitigates hepatocyte apoptosis and necroptosis by inhibiting endoplasmic reticulum stress

Yun-Fen Chen, Si-Ying Liu, Qi-Jiao Cheng, Yu-Jiao Wang, Shuang Chen, Yi-Yang Zhou, Xia Liu, Zhi-Gang Jiang, Wei-Wei Zhong, Yi-Huai He

Specialty type: Gastroenterology and hepatology

Provenance and peer review: Unsolicited article; Externally peer reviewed.

Peer-review model: Single blind

Peer-review report's scientific quality classification
Grade A (Excellent): A
Grade B (Very good): 0
Grade C (Good): C
Grade D (Fair): 0
Grade E (Poor): 0

P-Reviewer: Kai K, Japan; Salgado LP, United States

Received: January 13, 2022
Peer-review started: January 13, 2022
First decision: March 8, 2022
Revised: March 22, 2022
Accepted: May 13, 2022
Article in press: May 13, 2022
Published online: July 14, 2022

Yun-Fen Chen, Si-Ying Liu, Qi-Jiao Cheng, Shuang Chen, Yi-Yang Zhou, Xia Liu, Yi-Huai He, Department of Infectious Diseases, The Affiliated Hospital of Zunyi Medical University, Zunyi 563000, Guizhou Province, China

Yu-Jiao Wang, Department of General Medicine, The Affiliated Hospital of Zunyi Medical University, Zunyi 563000, Guizhou Province, China

Zhi-Gang Jiang, School of Public Health, Zunyi Medical University, Zunyi 563099, Guizhou Province, China

Wei-Wei Zhong, Department of Endoscopy, Jingmen No.1 People's Hospital, Jingmen 448000, Hubei Province, China

Corresponding author: Yi-Huai He, MM, Director, Department of Infectious Diseases, The Affiliated Hospital of Zunyi Medical University, No. 201 Dalian Street, Zunyi 563000, Guizhou Province, China. 993565989@qq.com

Abstract

BACKGROUND
Endoplasmic reticulum (ER) stress contributes to the pathogenesis of chronic liver diseases, but how hepatocytes respond to ER stress has not been clarified. Alpha-fetoprotein (AFP) is secreted by hepatoma cells and elevated levels of serum AFP are associated with development of liver malignancies.

AIM
To investigate whether and how AFP could regulate ER stress and hepatocyte injury.

METHODS
The distribution of AFP and the degrees of ER stress in liver tissues and liver injury were characterized by histology, immunohistochemistry, and Western blot in biopsied human liver specimens, two mouse models of liver injury and a cellular model. The levels of AFP in sera and the supernatants of cultured cells were quantified by chemiluminescence.

RESULTS
High levels of intracellular AFP were detected in liver tissues, particularly in the

necrotic areas, from patients with chronic liver diseases and mice after carbon tetrachloride (CCl_4) administration or induction of ER stress, but not from the controls. The induced intracellular AFP was accompanied by elevated activating transcription factor-6 (ATF6) expression and protein kinase R-like ER kinase (PERK) phosphorylation in mouse livers. ER stress induced AFP expression in LO2 cells and decreased their viability. ATF6, but not PERK, silencing mitigated the ER-stress-induced AFP expression in LO2 cells. Conversely, AFP silencing deteriorated the ER stress-mediated LO2 cell injury and CCl_4 administration-induced liver damages by increasing levels of cleaved caspase-3, the C/enhancer binding protein homologous protein expression, mixed lineage kinase domain-like pseudokinase and PERK phosphorylation, but decreasing ATF6 expression.

CONCLUSION

ER stress upregulated intra-hepatocyte AFP expression by activating ATF6 during the process of liver injury and intracellular AFP attenuated hepatocyte apoptosis and necroptosis by alleviating ER stress.

Key Words: Alpha-fetoprotein; Endoplasmic reticulum stress; Necroptosis; Apoptosis; Liver injury

Core Tip: During the process of liver injury, alpha-fetoprotein (AFP) expression was up-regulated in hepatocytes, especially in the necrotic areas, but it did not increase the serum AFP level. Endoplasmic reticulum (ER) stress induced intracellular AFP expression through activating activating transcription factor-6 and the up-regulated intracellular AFP expression attenuated hepatocyte apoptosis and necroptosis by feedback-down-regulating ER stress.

Citation: Chen YF, Liu SY, Cheng QJ, Wang YJ, Chen S, Zhou YY, Liu X, Jiang ZG, Zhong WW, He YH. Intracellular alpha-fetoprotein mitigates hepatocyte apoptosis and necroptosis by inhibiting endoplasmic reticulum stress. *World J Gastroenterol* 2022; 28(26): 3201-3217
URL: https://www.wjgnet.com/1007-9327/full/v28/i26/3201.htm
DOI: https://dx.doi.org/10.3748/wjg.v28.i26.3201

INTRODUCTION

Chronic liver diseases, such as chronic hepatitis B (CHB), affect many patients, especially in East Asia, such as China. However, the pathogenesis of chronic liver diseases remains unclear. Although human liver has powerful capacity to compensate the disease-related liver injury, how hepatocytes respond and defense against these diseases has not been clarified. Hence, it is of great significance to clarify it for the management of patients with chronic liver diseases.

Alpha-fetoprotein (AFP) is a protein with similar biological function to albumin and secreted mainly by embryonic tissue cells physiologically and malignant hepatocytes pathologically after birth. Elevated levels of serum AFP have been considered as a reliable biomarker for prediction of birth defect and diagnosis of liver cancer, teratoma, renal cell carcinoma, and pancreatic cancer[1] although moderate serum AFP levels can be temporarily detected in individuals with aberrant liver regeneration, hepatitis, and chronic liver disease. Furthermore, low levels of serum AFP have been continually observed in patients with liver cirrhosis and positively correlated with the degrees of liver inflammation and fibrosis [2,3]. The low and moderate levels of serum AFP are likely from the activation and proliferation of liver precursor cells, including oval cells, hepatic progenitor cells, in response to severe liver damages, particularly in liver failure[4-6]. While hepatocyte proliferation usually compensates for mild and moderate liver injury, liver precursor cells can differentiate into hepatocytes and bile duct cells, promoting liver regeneration. The activated liver precursor cells can secrete AFP and high levels of serum AFP have been suggested to be a biomarker of better prognosis of liver failure[7,8]. However, it is unclear whether chronic liver injury can induce AFP expression and secretion in differentiated mature hepatocytes, and how the induced AFP modulates the pathogenic process of chronic liver diseases.

It is notable that endoplasmic reticulum (ER) stress contributes to the pathogenesis of chronic liver diseases[9,10] and is regulated by inositol requiring enzyme-1 and activating transcription factor-6 (ATF6) and protein kinase R-like ER kinase (PERK)/eukaryotic translational initiation factor 2 alpha (eIF2α) signaling[11,12]. Aberrant ER stress can activate cell injury reactions, such as apoptosis and necroptosis by activating the C/enhancer binding protein (EBP)-homologous protein (CHOP) pathway,

caspase-3 cleavage and mixed lineage kinase domain-like pseudokinase (MLKL) phosphorylation[13, 14]. Our previous study has shown that ER stress inhibits the AFP secretion in hepatoma cells and the increase in the levels of intracellular AFP feedback attenuates the ER stress-related apoptosis and necroptosis in hepatoma cells[15]. However, it is unknown how ER stress can regulate AFP expression and secretion, and how intracellular AFP can modulate the ER stress-induced liver injury during the pathogenic process of chronic liver diseases.

In this research, we focus on whether intracellular AFP exists in hepatocytes during the liver injury, its regulatory relationship with ER stress, and its role in hepatocyte injury through clinical research, *in vivo* and *in vitro* experiments.

MATERIALS AND METHODS

Clinical samples

A total of 34 biopsied liver specimens were collected from CHB patients, eight surgical liver specimens were obtained from patients with hepatic trauma, and another eight surgical liver specimens were obtained from patients with hepatocellular carcinoma (HCC) in the Department of Infectious Diseases, or Hepatobiliary Surgery, the Affiliated Hospital of Zunyi Medical University since 2012. The patients with CHB were diagnosed, according to the Guidelines for Prevention and Treatment of Chronic Hepatitis B revised in 2019[16]. Individual patients were excluded if she/he had current infectious disease, autoimmune liver disease, liver malignant tumor, alcoholic liver disease, drug-induced liver disease, multiple organ dysfunction syndrome, obvious bleeding tendency, deep jaundice, obvious ascites, or another situation not suitable for liver biopsy. Their demographic and clinical data are shown in Table 1. The experimental protocol was approved by the Ethics Committee of Affiliated Hospital of Zunyi Medical University (ZYFYLS[2018] 28).

Establishment of liver injury in mice

Male BALB/c mice (25.0 g ± 3.0 g) were purchased from the Animal Center of Zunyi Medical University (Guizhou Province, China; SYXK[Qin] 2021-0004). The mice were maintained in a specific pathogen-free facility with a controlled temperature (20 °C-24 °C), a 12-h light/dark cycle and allowed free access to food and water *ad libitum*. The experimental protocol was established, according to the Animal Care and Research guidelines[17] and approved by the Animal Experiment Ethics Committee of Zunyi Medical University (LS[2020] 2-231).

To induce liver injury by carbon tetrachloride (CCl_4) administration, the mice were randomized using a random number table into the healthy control group (NC; untreated), solvent control group (olive oil, 5 mL/kg, intraperitoneally, *i.p.*) and CCl_4 group (1 mL/kg mixed with 4 mL of olive oil, *i.p.*) (n = 12 per group). The mice in the solvent and CCl_4 group were administrated with solvent or CCl_4 once or twice per week for 8 wk. Their peripheral blood samples were collected 24 h after the last dose, euthanized and their liver tissues were dissected.

To induce ER stress-related liver injury, the mice were randomized into the healthy NC (untreated), solvent control (phosphate buffer saline, PBS, 10 mL/kg) and tunicamycin (TM; an inhibitor of protein glycosylation) groups (2 mg/kg in the same volume of PBS, *i.p.*; Sigma) once (n = 12 per time point group). One or two days later, their peripheral blood samples were collected, euthanized and their liver tissues were dissected.

To test the role of AFP in the CCl_4-induced liver injury, the mice were randomized and treated intravenously with 1×10^{10} recombinant serotype 8 adeno-associated virus (rAAV8) for expression of control short hairpin RNA (shRNA) or *Afp*-specific shRNA (Table 2, Genechem, Beijing, China). Six weeks after infection, the levels of AFP expression in the livers of mice were analyzed by Western blot to confirm *Afp* silencing. The mice with control shRNA or *Afp*-specific shRNA were administrated with olive oil or CCl_4 as the control shRNA + olive oil, CCl_4 (control shRNA + CCl_4), *Afp* shRNA + olive oil, or *Afp* shRNA + CCl_4 (*Afp* shRNA + CCl_4). Their peripheral blood samples were collected, euthanized and their livers were dissected at 36 h (n = 12 per group) post CCl_4 administration, based on our preliminary studies.

Cell lines and culture

Human hepatocyte LO2 and hepatoma HepG2 cell lines were obtained from the Type Culture Collection of the Chinese Academy of Sciences (Shanghai, China) and identified by STR. The cells were cultured in RPMI-1640 containing 10% fetal bovine serum, 100 Units/mL of penicillin and 100 μg/mL of streptomycin at 37 °C in a 5% CO_2 incubator. To induce ER stress, LO2 cells were treated with, or without (NC group), solvent control group (dimethyl sulfoxide, DMSO) and 0.5 μmol/L thapsigargin (TG; an inhibitor of intracellular calcium balance) in DMSO (Sigma, TG group) for 12 h, 24 h and 48 h, respectively.

In addition, LO2 cells (1.2×10^6 cell/well) were cultured in 6-well plates overnight and transfected with plasmids for control shRNA, *PERK*-specific shRNA and *ATF6*-specific shRNA (Beijing Genechem) using lipofectamine 3000 (Fisher). Two days later, the cells were treated with vehicle DMSO or TG for 24

Table 1 The demographic and clinical data of subjects

Group	CHB	Control	HCC
n	34	8	8
Age (years; 25%, 75%)	41.00 (35.00, 48.75)	32.50 (28.25, 41.85)	47.00 (40.25, 53.42)
ALT (U/L; 25%, 75%)	137.50 (59.00, 221.50)	31.5000 (14.5000, 63.1725)	48.50 (39.00, 65.25)
TBil (μmol/L; 25%, 75%)	16.300 (11.500, 24.225)	10.80 (9.42, 20.58)	20.6 (14.5, 32.5)
AFP (ng/mL; 25%, 75%)	4.5400 (2.9850, 13.1725)	2.02 (1.05, 4.75)	179.80 (14.65, 207.53)

CHB: Chronic hepatitis B; HCC: Hepatocellular carcinoma; AFP: Alpha-fetoprotein; ALT: Serum alanine aminotransferase; TBil: Total bilirubin.

Table 2 The sequences of short hairpin RNAs

Insert content			5'-3'
Mouse	*Afp* shRNA	Target sequence	GCATCCATTGCAAAGGAATTA
		shRNA sequence	GCATCCATTGCAAAGGAATTACGAA*TAATTCCTTTGCAATGGATGC*
	Control shRNA	shRNA sequence	AAACGTGACACGTTCGGAGAACGAATTCTCCGAACGTGTCACGTTT
Human	*PERK* shRNA	Target sequence	GCACTTTAGATGGGAGAATTG
		shRNA sequence	GCACTTTAGATGGGAGAATTGCGAA*CAATTCTCCCATCTAAAGTGC*
	Control shRNA	shRNA sequence	AAACGTGACACGTTCGGAGAACGAATTCTCCGAACGTGTCACGTTT
	ATF6 shRNA	Target sequence	GCAGGTCCTCCTGTTATTAGA
		shRNA sequence	GCAGGTCCTCCTGTTATTAGACGAA*TCTAATAACAGGAGGACCTGC*
	Control shRNA	shRNA sequence	AAACGTGACACGTTCGGAGAA CGAATTCTCCGAACGTGTCACGTTT
	AFP shRNA	Target sequence	GCTTCCATATTGGATTCTTAC
		shRNA sequence	GCTTCCATATTGGATTCTTAC CGAA*GTAAGAATCCAATATGGAAGC*
	Control shRNA	shRNA sequence	AAACGTGACACGTTCGGAGAA CGAATTCTCCGAACGTGTCACGTTT

AFP: Alpha-fetoprotein; ATF6: Activating transcription factor-6; PERK: Protein kinase R-like ER kinase; shRNA: Short hairpin RNA.

h. Additionally, LO2 cells were transfected with plasmid for the expression of control shRNA or *AFP*-specific shRNA (Beijing Genechem) for 48 h and treated with DMSO or TG for 36 h, respectively.

Western blot analysis

LO2, HepG2 cells, or individual liver samples were homogenized in immunoprecipitation assay lysis buffer (R0010, Solarbio, Beijing, China). After centrifugation, individual liver lysates (40 μg) were separated in sodium dodecyl sulfate polyacrylamide gel on 10% gels and transferred to polyvinylidene fluoride membranes (Millipore, Billerica, MA, United States). The membranes were blocked with 5% skim dry milk in TBST (Tris-HCl buffer salt solution + Tween 20) and probed with mouse monoclonal antibodies (mAb) against AFP (sc-130302; Santa Cruz Biotechnology, Santa Cruz, CA, United States), ATF6 (sc-166659, 1:1000, Santa Cruz Biotechnology), GAPDH (sc-166545, 1:10000, Santa Cruz Biotechnology), CHOP (GADD153, sc-71136, 1:10000, Santa Cruz Biotechnology), eIF2α (sc-133132, 1:10000, Santa Cruz Biotechnology), phosphorylated PERK (p-PERK, MA5-15033, 1:1000, Thermofisher Scientific, United States), and PERK (sc-377400, 1:10000, Santa Cruz Biotechnology), or rabbit monoclonal antibodies against cleaved caspase-3 (9664, 1:10000, Cell Signaling Technology), and phosphorylated eIF2α (p-eIF2α, 3398, 1:10000, Cell Signaling Technology), or rabbit polyclonal antibodies against phosphorylated MLKL (p-MLKL, PA5-105677, 1:2000, Thermofisher Scientific), and MLKL (PA5-34733, 1:3000, Thermofisher Scientific). After reaction with horseradish peroxidase (HRP)-conjugated anti-mouse or anti-rabbit IgG, the immunocomplexes were visualized with enhanced chemiluminescent reagents. Quantity One software (Bio-Rad, Hercules, CA, United States) was used to determine the relative levels of each targeted protein to the control (standardized as 1)[18].

Pathological analysis of liver tissue

Fresh liver tissues (5 mm × 5 mm in size from each mouse or 1 mm × 30 mm in size from one patient)

were fixed in 4% paraformaldehyde for ≥ 24 h, paraffin-embedded and cut. The liver tissue sections (5 μm) were dewaxed, rehydrated and routine-stained with hematoxylin and eosin (H&E). The sections were examined under a light microscope (OLYMPUS CX31) using CaseViewer 2.4 software (3DHISTECH, Hungary). The necrotic areas in the liver were analyzed by Image-Pro Plus 6.0 (Media Cybernetics, United States)[19]. The Histology Activity Index-Knodell scores were determined by two pathologists blindly[20].

Immunohistochemistry

The liver tissue sections were dewaxed, rehydrated and blocked with 3% of bovine serum albumin for 20 min. The sections were incubated with mAb against AFP (sc-130302, 1:250) at 4 °C overnight and the bound antibodies were detected with HRP-conjugated anti-mouse IgG, followed by visualizing with diaminobenzidine. The intensity of anti-AFP staining was evaluated by Image Pro Plus 6.0[19].

TUNEL assay

The effect of *Afp* silencing on the frequency of apoptotic hepatocytes in liver sections was determined by terminal deoxynucleotidyl transferase (TdT)-mediated deoxyribonucleotide derivative digoxigenin (dUTP) nick end labeling (TUNEL) using a specific kit (Roche, 11684817910), according to the manufacturer's instruction. Briefly, the paraffin-embedded liver sections were dehydrated, permeabilized, and incubated with a mixture of TdT and dUTP at 1:14 in a humidified chamber for 2 h at 37 °C. The labeled cells were detected with detection solution and after being washed, the sections were counterstained with 4′, 6-diamidino-2-phenylindole. The TUNEL signals were examined under a fluorescent microscope. The apoptotic cells were defined by nuclear green staining while non-apoptotic cells with blue nuclear staining. Five visual fields in each section were randomly selected and the percentages of apoptotic cells in each section were calculated using the formula of positive cells/total cells × 100%.

Analysis of AFP levels

AFP levels in the supernatant of cultured cells and mouse serum samples were measured by chemiluminescence immunoassay on the Beckman Coulter Auto Analyzer (Model DX1800; 04481798190, Roche Diagnostics GmbH) as previously described[21]. Samples were centrifuged to remove the remaining cells and possible cell debris before testing the AFP concentration.

Alanine aminotransferase and total bilirubin levels

The levels of serum alanine aminotransferase (ALT), total bilirubin (TBil) were two commonly used measures of liver injury, and analyzed by an auto-analyzer (AU5800, Beckman Coulter, United States) [22].

Cell viability assay

The impact of specific gene silencing or ER stress on LO2 cell viability was determined using the cell counting kit-8 (CCK-8; Cat. No. 40203ES60; Yeasen Biotechnology, Shanghai, China), per the product instruction. Briefly, LO2 cells (5000 cells/100 μL medium/well in 96-well plates) were treated with, or without, TG for 48 h (5 replicates per sample). During the last one-hour culture, the cells were exposed to CCK-8 and the absorbance of individual wells was detected at a wavelength of 450 nm (Bio-Rad, CA, United States). The relative cell viability (%) = (OD value of the treatment group-OD value of the blank group)/(OD value of the control group-OD value of the blank group) × 100.

Statistical analysis

Data are representative images or expressed as the mean ± SD of each group from 3 separate experiments. The difference of normally distributed values among groups was analyzed by one-way ANOVA and post hoc Tukey's method. The difference between groups was analyzed by Student's *t*-test. Survival rates were estimated using the Kaplan-Meier method and analyzed by the log-rank test. A *P*-value less than 0.05 was considered statistically significant.

RESULTS

AFP expression is induced in the liver of patients with chronic liver injury

To explore the potential role of AFP in the progression of chronic hepatocyte injury, we analyzed AFP expression in liver tissues of patients with CHB (n = 34), controls (liver trauma; n = 8), and those with HCC (positive controls, n = 8). While there were healthy hepatocytes without degeneration and necrosis in the control liver tissues there were many hepatocytes undergoing degeneration and necrosis (Figure 1A). Immunohistochemistry indicated positive anti-AFP staining in the liver tissues from patients with HCC or CHB, but little in the controls. Interestingly, the positively stained anti-AFP was particularly in the regions with hepatocyte degeneration and necrosis of the liver tissues from CHB

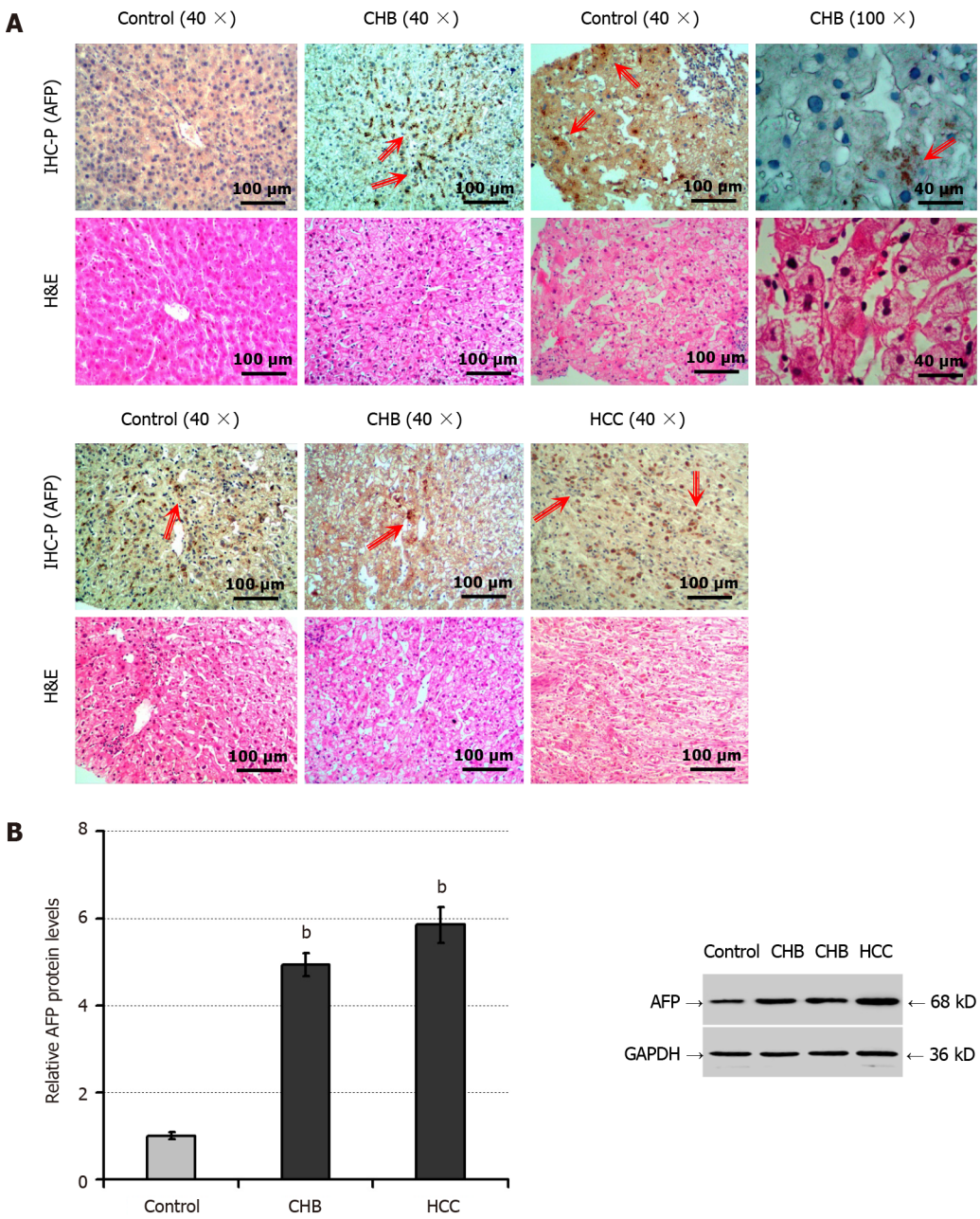

DOI: 10.3748/wjg.v28.i26.3201

Figure 1 The intrahepatic levels of alpha-fetoprotein protein are elevated in injured livers. A: Immunohistochemistry and hematoxylin and eosin (H&E) staining analyzed alpha-fetoprotein (AFP) expression and pathological changes, respectively, in liver tissues of patients with chronic hepatitis B (CHB, n = 34), trauma (n = 8) or hepatocellular carcinoma (HCC, the positive control group, n = 8). The upper panels display immunohistochemical staining, and the lower panels exhibit H&E staining in sequential tissue sections. The positive expression of AFP was stained with brownish yellow by immunohistochemistry and indicated by the arrows; B: The relative levels of AFP protein expression were analyzed by Western blot in the liver specimens indicated. H&E: Hematoxylin and eosin; IHC-P: Immunohistochemistry-paraffin; AFP: Alpha-fetoprotein; HCC: Hepatocellular carcinoma; CHB: Chronic hepatitis B. $^{b}P < 0.01$, compared with the control group.

patients. Further Western blot displayed significantly increased levels of AFP expression in the livers from HCC or CHB patients, relative to that in the controls ($P < 0.01$, Figure 1B). Such data indicated that AFP expression was induced in hepatocytes, associated with hepatocyte degeneration and necrosis in humans during the process of hepatocyte injury.

Induction of liver injury enhances AFP expression and ER stress in the liver of mice following CCl_4 administration

Next, we tested whether AFP expression could be induced in the liver of mouse model of CCl_4-induced hepatocyte injury. As expected, CCl_4 administration significantly elevated serum ALT ($P < 0.05$; Figure 2A), TBil ($P < 0.05$; Figure 2B) levels, accompanied by increased areas of liver tissue necrosis in mice, relative to the NC and the control groups (olive oil) of mice ($P < 0.05$; Figure 2C), particularly in the livers of mice following administration with CCl_4 for 8 wk. There were similarly low levels of serum

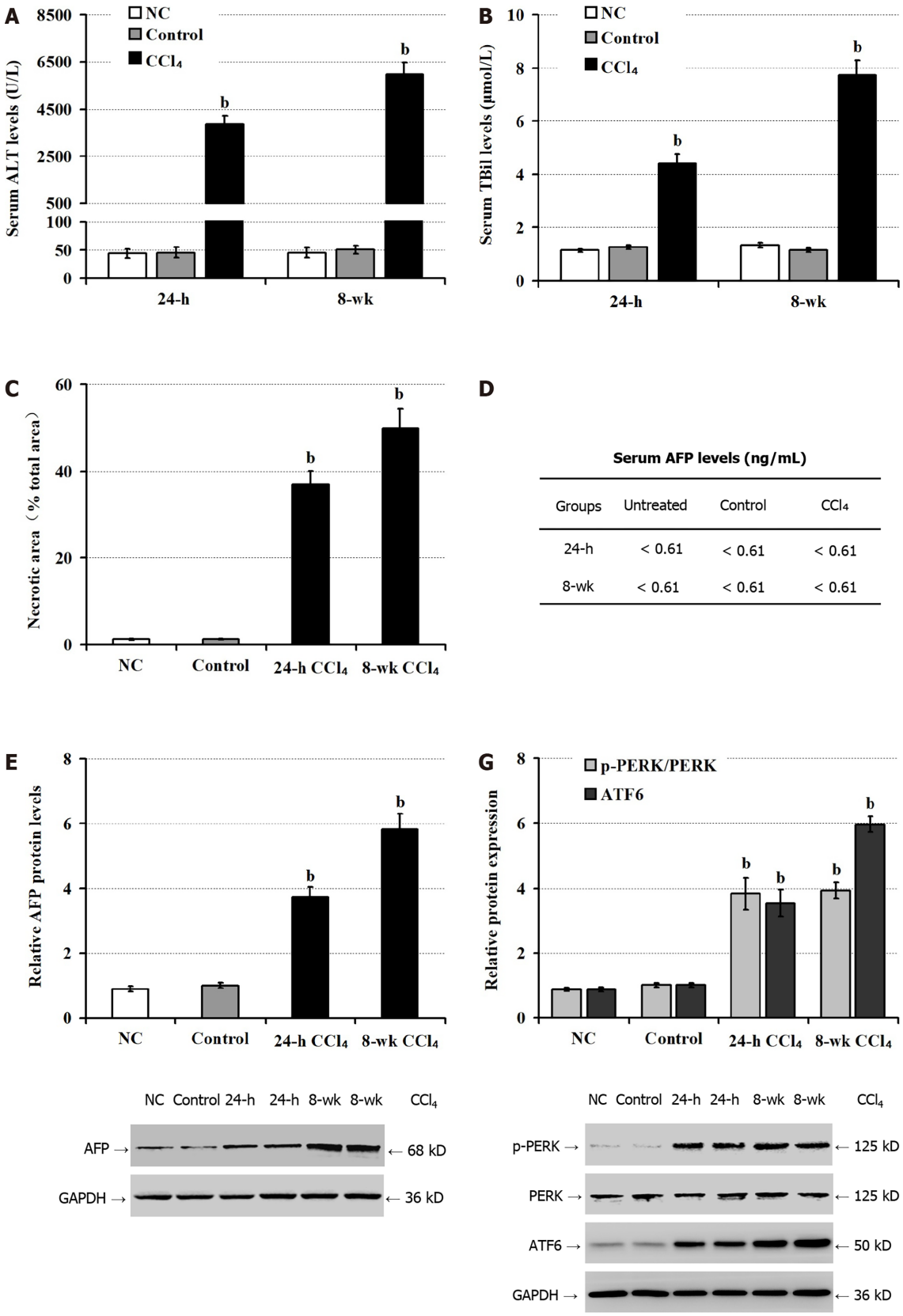
A
Serum ALT levels (U/L)
NC
Control
CCl4
24-h
8-wk
B
Serum TBil levels (μmol/L)
C
Necrotic area（% total area）
NC
Control
24-h CCl4
8-wk CCl4
D
Serum AFP levels (ng/mL)
Groups | Untreated | Control | CCl4
24-h | < 0.61 | < 0.61 | < 0.61
8-wk | < 0.61 | < 0.61 | < 0.61
E
Relative AFP protein levels
NC Control 24-h 24-h 8-wk 8-wk CCl4
AFP
68 kD
GAPDH
36 kD
G
Relative protein expression
p-PERK/PERK
ATF6
NC Control 24-h 24-h 8-wk 8-wk CCl4
p-PERK
125 kD
PERK
125 kD
ATF6
50 kD
GAPDH
36 kD

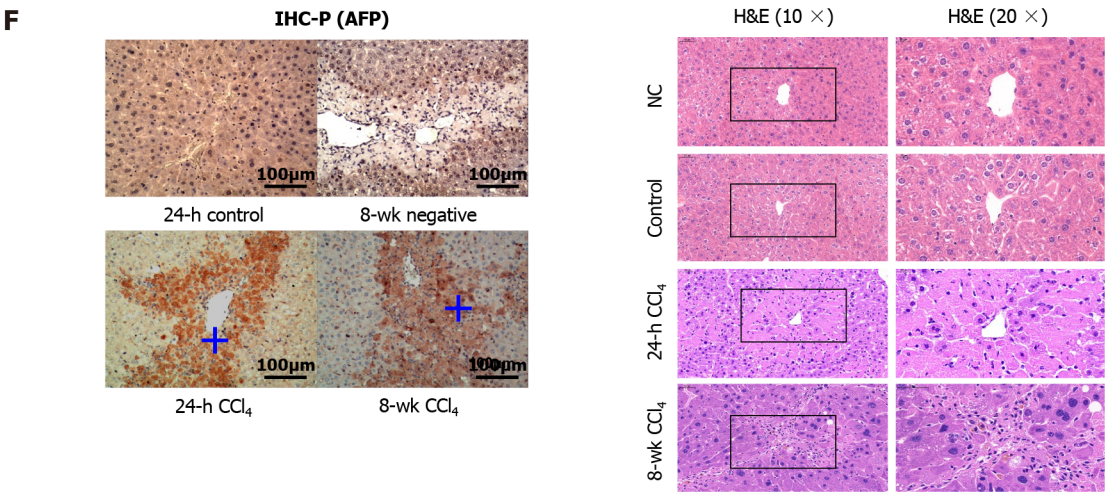

DOI: 10.3748/wjg.v28.i26.3201

Figure 2 Administration with carbon tetrachloride induces alpha-fetoprotein expression, endoplasmic reticulum stress and liver injury in mice. Male BALB/c mice were untreated (NC), or administrated with olive oil (control) or carbon tetrachloride (CCl_4) for 24 h, or 8 wk. A: Serum alanine aminotransferase levels; B: Serum total bilirubin levels; C: Hematoxylin and eosin staining analysis of pathological changes in mouse liver tissues at 24-h and 8-wk post CCl_4; D: Chemiluminescence immunoassay of serum alpha-fetoprotein (AFP) levels; E: Western blot analysis of the relative levels of AFP expression in liver tissues of mice; F: Immunohistochemical staining of AFP expression in liver tissue of mice at 24-h post CCl_4, the positive expression of AFP was stained with brownish yellow and indicated by a plus sign; G: Western blot analysis of the relative levels of protein kinase R-like endoplasmic reticulum kinase phosphorylation and activating transcription factor-6 expression in liver tissues of mice. AFP: Alpha-fetoprotein; ALT: Alanine aminotransferase; ATF6: Activating transcription factor-6; CCl_4: Carbon tetrachloride; H&E: Hematoxylin and eosin; PERK: Protein kinase R-like endoplasmic reticulum kinase; TBil: Total bilirubin. $^bP < 0.01$ compared with the control group.

AFP detected in the different groups of mice (about 0.61 ng/mL, Figure 2D). In contrast, Western blot revealed that CCl_4 administration obviously up-regulated AFP expression in the livers of mice in a trend of time-dependence ($P < 0.05$; Figure 2E). Further immunohistochemistry exhibited that the up-regulated AFP expression was mainly accumulated in the injured liver areas (Figure 2F). Finally, CCl_4 administration significantly enhanced the relative levels of PERK phosphorylation and ATF6 expression ($P < 0.05$; Figure 2G), the hallmarks of enhancing ER stress in the livers of mice. Collectively, CCl_4 administration induced hepatocyte injury and ER stress, and up-regulated AFP expression, but not its secretion in mice.

ER stress up-regulates AFP expression in hepatocytes

Given that up-regulated AFP expression was associated with enhanced ER stress, we tested whether induction of ER stress could up-regulate AFP expression in TM-injected mice. Compared with the NC and vehicle controls, significantly elevated levels of serum ALT ($P < 0.05$; Figure 3A) and TBil ($P < 0.05$; Figure 3B) were detected in mice at 24 h and 48 h post TM injection, implicating that induction of ER stress induced liver damages in mice. Consistently, Western blot revealed that TM injection obviously up-regulated ATF6, and AFP expression and PERK phosphorylation in the livers of mice, relative to that of the controls ($P < 0.05$; Figure 3C). Interestingly, there were damaged liver areas with strong anti-AFP staining in the mice with TM injection (Figure 3D). However, there were similar levels of serum AFP in the different groups of mice (< 0.61 ng/mL, Figure 3E). Furthermore, while there was no detectable AFP in the supernatants of cultured human non-tumor hepatocyte LO2 cells, even after treatment with TG, the levels of AFP in the supernatants of cultured HepG2 cells increased in a time-dependent manner (Figure 3F). Moreover, TG treatment significantly decreased the viability of LO2 cells at 24 h and 48 h post treatment ($P < 0.05$, Figure 3G), but TG treatment significantly enhanced the relative levels of AFP and ATF6 expression and PERK phosphorylation in LO2 cells ($P < 0.05$, Figure 3H). Thus, induction of ER stress induced hepatocyte injury and AFP expression.

ATF6 silencing mitigates the TG-induced AFP expression in LO2 cells

To understand how ER stress promoted AFP expression, we transfected LO2 cells with *PERK* or *ATF6*-specific shRNA. We found that *PERK* silencing significantly reduced the viability of LO2 cells ($P < 0.05$), and deteriorated the TG-induced damages in LO2 cells ($P < 0.01$; Figure 4A). While *PERK* silencing significantly reduced the levels of PERK protein expression in both regular cultures and TG-treated LO2 cells, and mitigated the relative levels of TG-enhanced eIF2α phosphorylation in LO2 cells, *PERK* silencing failed to significantly alter AFP protein expression in LO2 cells regardless of TG treatment (Figure 4B). In contrast, *ATF6* silencing significantly reduced the viability of LO2 cells, but enhanced the TG-induced damages in LO2 cells ($P < 0.01$; Figure 4C). Moreover, transfection with *ATF6* shRNA not

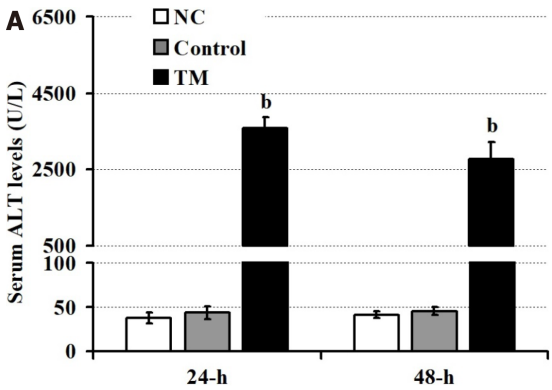

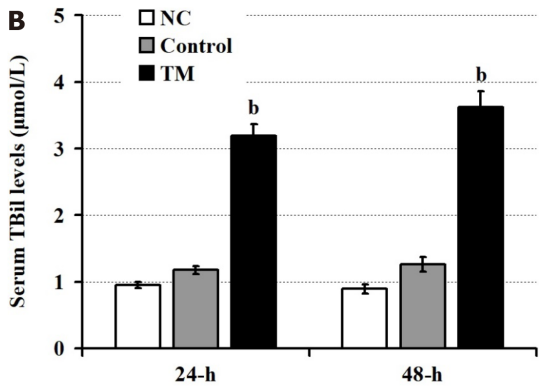

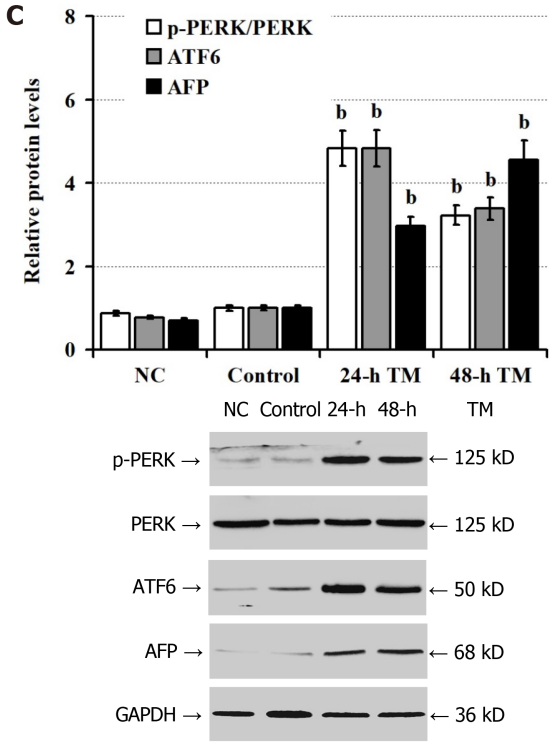

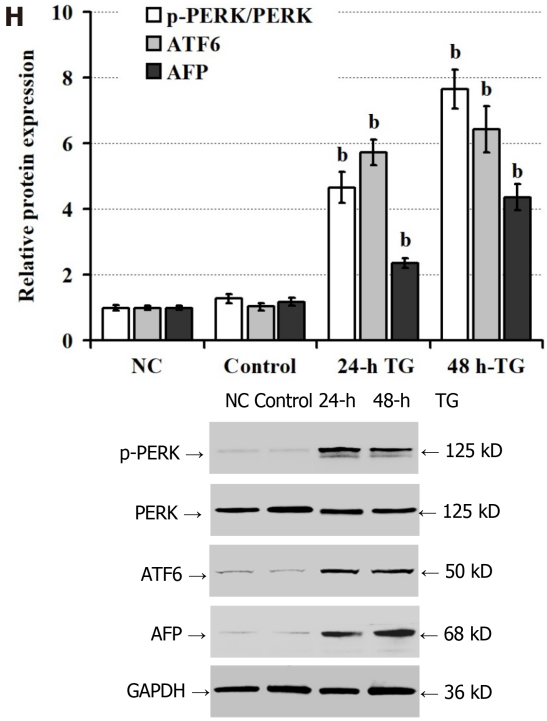

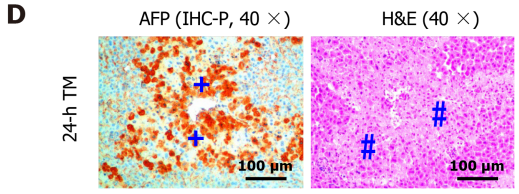

E

Serum AFP levels (ng/mL)

Time	NC	Control	TM
24-h	< 0.61	< 0.61	< 0.61
48-h	< 0.61	< 0.61	< 0.61

F

Supernanat AFP levels (ng/mL)

Time (h)	LO2 cells		HepG2 cells
	Control	TG	
0	< 0.61	< 0.61	4.75 ± 0.37
12	< 0.61	< 0.61	9.54 ± 1.57[d]
24	< 0.61	< 0.61	23.80 ± 1.85[d]
48	< 0.61	< 0.61	40.05 ±3.06[d]

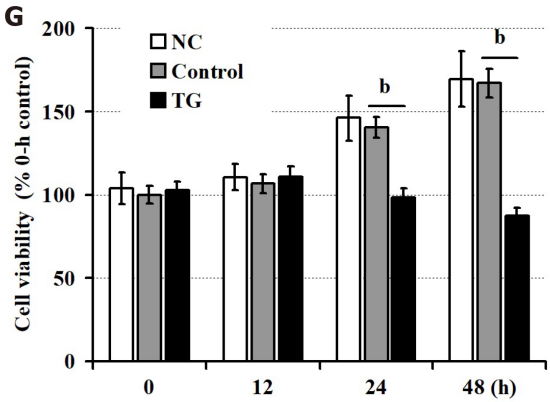

DOI: 10.3748/wjg.v28.i26.3201

Figure 3 Endoplasmic reticulum stress up-regulates alpha-fetoprotein expression in hepatocytes. Male BALB/c mice were untreated (NC), or

treated with phosphate buffer saline (control) or TM for 24 h or 48 h. LO2 cells were untreated (NC), or treated with dimethyl sulfoxide (control) or thapsigargin (TG) for 24 h, and 48 h. A: Serum alanine aminotransferase levels; B: Serum total bilirubin levels; C: Western blot analysis of the relative levels of proteins; D: Immunohistochemical analysis of alpha-fetoprotein (AFP) expression and hematoxylin and eosin staining analysis of liver injury in mice at 24 h post endoplasmic reticulum stress. The positive expression of AFP was stained with brownish yellow and indicated by a plus sign. Hash sign indicates the area of necrosis; E: Chemiluminescence immunoassay of serum AFP levels in mice; F: The levels of AFP in the supernatants of cultured cells; G: Cell counting kit-8 analysis of the cell viability; H: Western blot analysis of the relative levels of p-protein kinase R-like endoplasmic reticulum kinase, ATF6 and AFP expression in LO2 cells. AFP: Alpha-fetoprotein; ALT: Alanine aminotransferase; ATF6: Activating transcription factor-6; CCl_4: Carbon tetrachloride; CCK-8: Cell counting kit-8; DMSO: Dimethyl sulfoxide; H&E: Hematoxylin and eosin; IHC-P: Immunohistochemistry-paraffin; PBS: Phosphate buffer saline; p-PERK: Phosphorylated protein kinase R-like endoplasmic reticulum kinase; TBil: Total Bilirubin; TM: Tunicamycin; TG: Thapsigargin. $^{b}P < 0.01$, compared with the control group; $^{d}P < 0.01$, compared with the 0 h group in HepG2 cells.

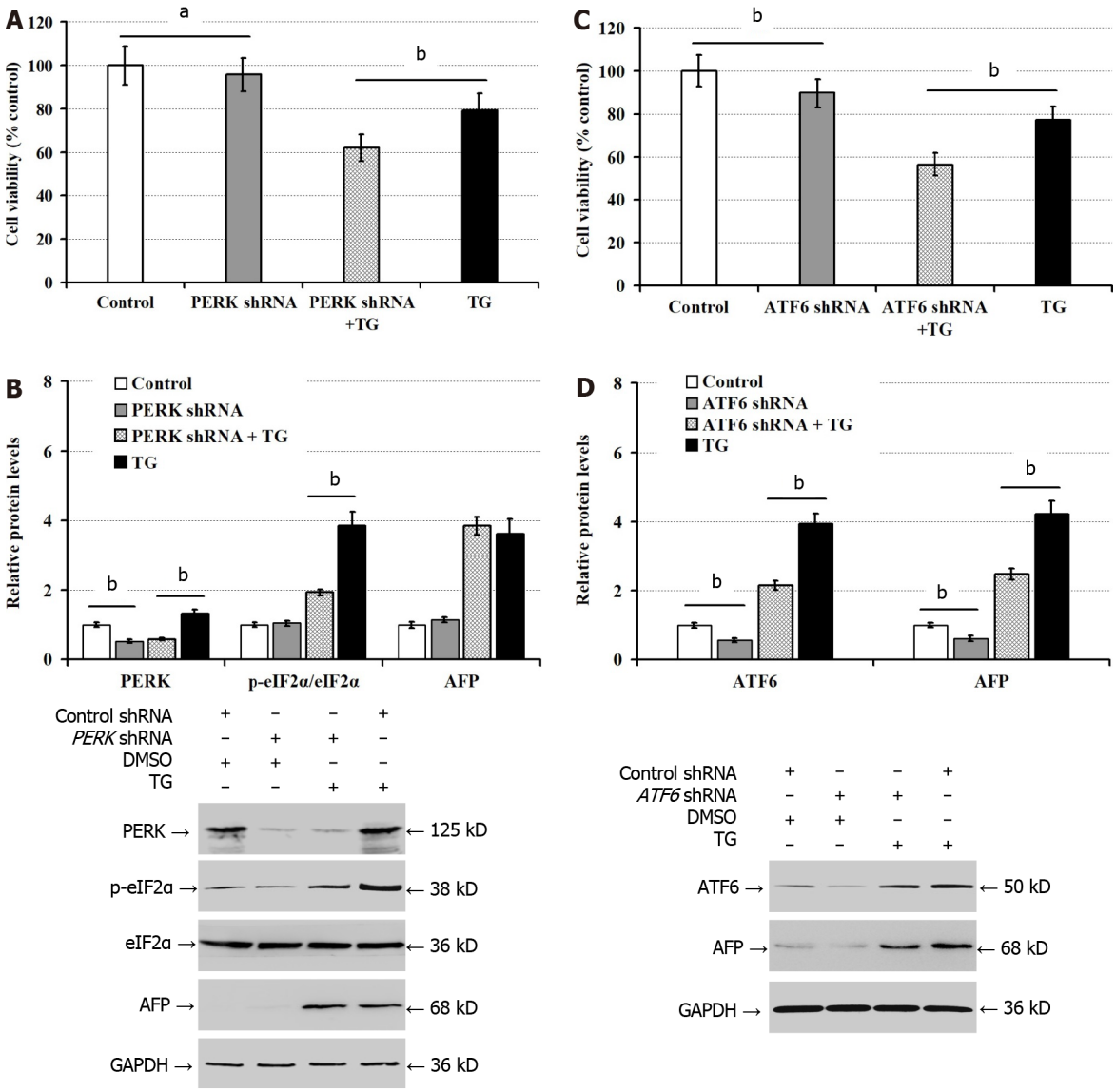

DOI: 10.3748/wjg.v28.i26.3201

Figure 4 Activating transcription factor-6 silencing inhibits the expression of alpha-fetoprotein induced by thapsigargin *in vitro*. LO2 cells were transfected with control shRNA, *protein kinase R-like endoplasmic reticulum kinase* (*PERK*)-shRNA, or *activating transcription factor-6* (*ATF6*)-shRNA for 48 h, and treated with dimethyl sulfoxide (control) or thapsigargin for 24 h. A: Cell counting kit-8 (CCK-8) analysis of cell viability; B: Western blot analysis of p-PERK, phosphorylated eukaryotic translational initiation factor 2 alpha, and alpha-fetoprotein expression; C: CCK-8 analysis of cell viability; D: Western blot analysis of the relative levels of ATF6 and AFP protein expression. AFP: Alpha-fetoprotein; ATF6: Activating transcription factor-6; CCK-8: Cell counting kit-8; DMSO: Dimethyl sulfoxide; p-eIF2α: Phosphorylated eukaryotic translational initiation factor 2 alpha; p-PERK: Phosphorylated protein kinase R-like endoplasmic reticulum kinase; TG: Thapsigargin. $^{a}P < 0.05$, $^{b}P < 0.01$, compared with these two groups.

only significantly inhibited ATF6 expression, but also attenuated the relative levels of AFP expression in both regular cultures and TG-treated LO2 cells ($P < 0.01$; Figure 4D). Hence, *ATF6* silencing mitigated the TG-induced AFP expression in LO2 cells.

AFP silencing increases the TG-induced hepatocyte apoptosis and necroptosis in LO2 cells

To understand the importance of AFP in ER stress-induced hepatocyte injury, we further explored the impact of *AFP* silencing on the ER stress-induced hepatocyte injury *in vitro*. Compared with the control LO2 cells, transfection with *AFP*-specific shRNA, but not the control shRNA, dramatically reduced AFP expression in LO2 cells ($P < 0.01$; Figure 5A), and deteriorated the TG-induced damages ($P < 0.01$), but it did not significantly alter the viability of LO2 cells ($P > 0.05$, Figure 5B). Furthermore, the *AFP* silencing significantly increased the levels of cleaved caspase-3 and MLKL phosphorylation regardless of TG treatment ($P < 0.05$, Figure 5C). Consistently, *AFP* silencing also significantly increased CHOP expression and PERK phosphorylation, but decreased ATF6 expression in LO2 cells ($P < 0.01$, Figure 5D). These results clearly indicated that *AFP* silencing enhanced spontaneous and TG-induced ER stress, apoptosis and necroptosis in LO2 cells.

AFP silencing deteriorates the CCl_4-induced liver injury in mice

Finally, we tested whether induction of *Afp* silencing could modulate the CCl_4-induced liver injury in mice. After intravenous administration with rAAV8 virus for the expression of control or *Afp*-specific shRNA for 6 wk, the levels of AFP expression in the liver tissues were reduced dramatically, confirming the *Afp* silencing ($P < 0.01$, Figure 6A). Both groups of mice were administrated with vehicle olive oil or CCl_4 and 36 h later, we found that *Afp* silencing increased serum ALT ($P < 0.01$, Figure 6B), and TBil levels ($P < 0.01$, Figure 6C), regardless of CCl_4 administration. Compared with the control mice, *Afp* silencing increased the percentages of necrotic areas in the livers of mice ($P < 0.01$, Figure 6D). Furthermore, *Afp* silencing decreased AFP expression, but remarkably increased the relative levels of cleaved caspase-3 expression, MLKL phosphorylation ($P < 0.01$, Figure 6E) and the percentages of apoptotic hepatocytes in the livers of both vehicle and CCl_4-treated mice ($P < 0.01$, Figure 6F). Finally, *Afp* silencing significantly increased CHOP expression and PERK phosphorylation, but decreased ATF6 expression in the livers of CCl_4-treated mice ($P < 0.01$; Figure 6G). Therefore, *Afp* silencing enhanced ER stress and liver injury induced by CCl4 in mice.

DISCUSSION

In this study, we investigated AFP expression, its regulatory mechanism, and its effect on hepatocyte injury during the process of liver injury. We detected high levels of AFP expression in the livers, particularly in the areas of hepatocyte necrosis, of patients with CHB, but not in those with hepatic trauma. Similarly, high levels of AFP expression were observed in the livers of mice following CCl_4 administration and ER stress induction. The induced AFP expression was accompanied by liver injury in those patients and mice. Interestingly, there was no significant difference in the levels of serum AFP in those experimental patients and mice, compared to the controls. Moreover, induction of ER stress in human non-tumor hepatocyte LO2 cells also induced AFP expression, hepatocyte apoptosis and necroptosis, but failed to detect AFP in the supernatants of cultured cells. These indicated that during chronic liver diseases, ER stress and other inducers triggered hepatocyte apoptosis and necroptosis and stimulated AFP expression, but limited its secretion, leading to increased levels of intracellular AFP in hepatocytes. These novel data extended our previous study on hepatoma cells[15], and support the notion that AFP can be induced during the process of chronic liver diseases[7,23]. Our findings may shed light on the liver responses to ER stress in the pathogenic process of chronic liver diseases.

Low levels of serum AFP are detected in patients with chronic liver disease, and are positively correlated with the degrees of liver damages[8,24]. Although high levels of AFP expression were detected in mouse livers, we did not detect abnormally high levels of serum AFP in liver-injured mice, consistent with our observation in hepatoma cells[15]. These indicated that ER stress induced intracellular AFP expression by limiting its secretion. Given that healthy hepatocytes do not express AFP in adults it is possible that ER stress-induced hepatocyte injury may also induce compensative hepatocyte proliferation to repair liver damages in these models. However, the induced intracellular AFP is unlikely from the proliferation and differentiation of liver precursor cells. We are interested in further investigating how ER stress limits the secretion of AFP in hepatocytes during the process of chronic liver diseases.

AFP expression is regulated in a manner of tissue-specific and time-restriction[25]. Previous studies have shown that AFP expression is regulated by transcription factors, such as hepatocyte nuclear factor-1 (HNF1), ACCAAT-enhancer binding protein (C/EBP) and NF-1 and their enhancers[26-28]. Furthermore, the mutation in the AFP promoter region can increase the binding affinity of HNF1, leading to sustained increase in the levels of AFP expression[29]. Moreover, the AFP promoter activity is also regulated by the competitive modulation of these transcription factors, activators and inhibitors [30]. In this study, we explored how ER stress induced AFP expression in hepatocytes. ER stress mainly enhances eIF2α activation and regulates the expression of target molecules through ATF4, ATF6, and XBP1 to enhance cell ability to eliminate and degrade misfolded proteins[11]. We found that *ATF6*, but not *PERK*, silencing significantly mitigated the ER stress-induced AFP expression in LO2 cells. These data suggest that ATF6 may promote AFP expression in hepatocytes under an ER stress condition.

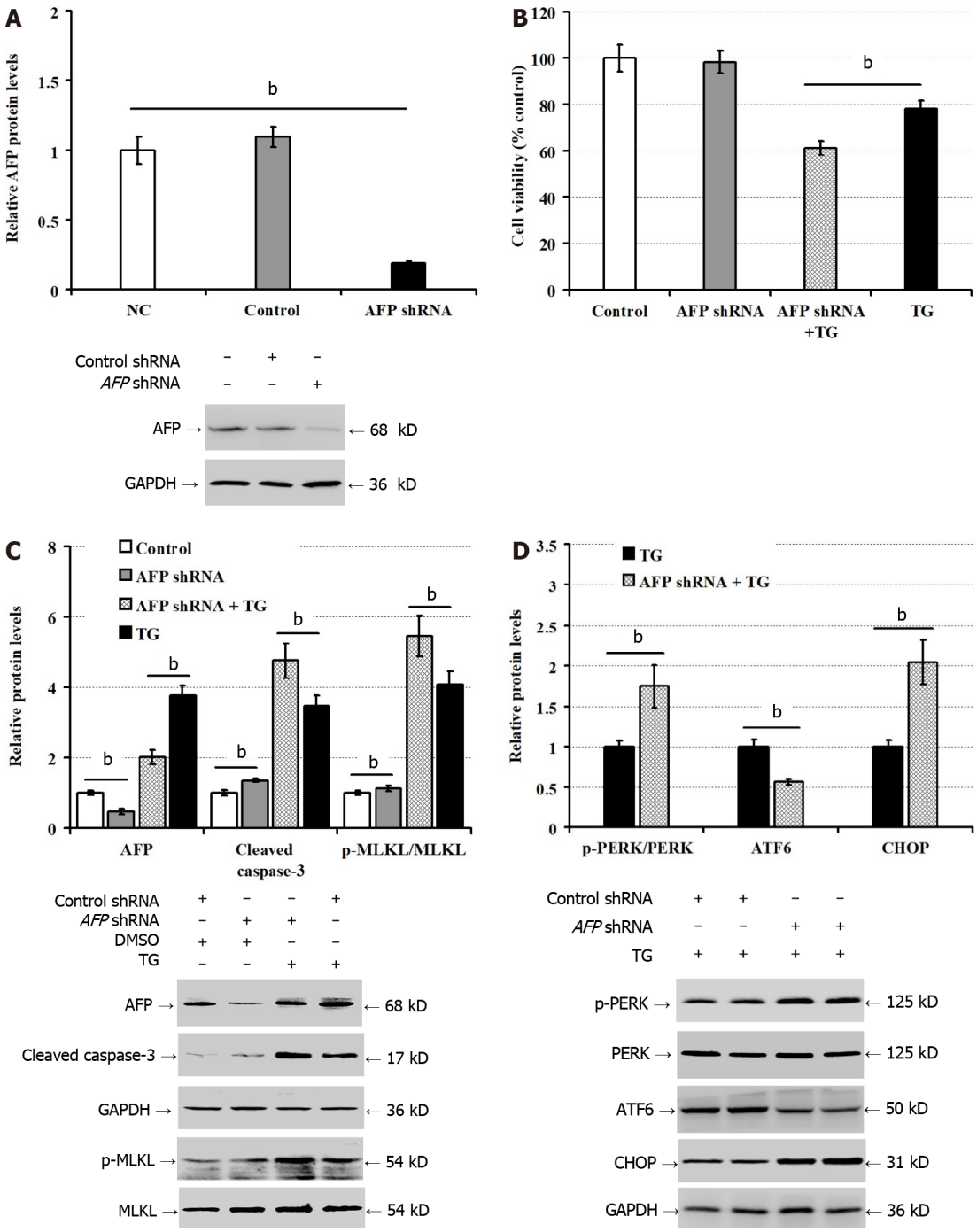

DOI: 10.3748/wjg.v28.i26.3201

Figure 5 Silencing of *alpha-fetoprotein* exacerbates the thapsigargin-induced LO2 cell injury. A: Western blot determined alpha-fetoprotein silencing in LO2 cells; B: Cell counting kit-8 analysis of LO2 cell viability; C: Western blot for the relative levels of indicated protein expression in LO2 cells; D: Western blot for the relative levels of endoplasmic reticulum stress-related protein. AFP: Alpha-fetoprotein; CCK-8: Cell counting kit-8; ER: Endoplasmic reticulum; TG: Thapsigargin; p-MLKL: Phosphorylated mixed lineage kinase domain-like pseudokinase; p-PERK: Phosphorylated protein kinase R-like endoplasmic reticulum kinase. Data are typical images or expressed as the mean ± SD of each group from 3 separate experiments. $^{b}P < 0.01$ compared with these two groups.

Functionally, AFP can act as a carrier to maintain plasma colloidal osmotic pressure and transport bilirubin, estrogen, fatty acids, retinoids, steroids and progesterone to regulate hormone homeostasis [31]. Second, AFP can induce immune cell apoptosis and down-regulates the gene expression of a variety of inflammatory factors, inhibiting autoimmunity and aberrant inflammation by protecting the fetus from maternal immune attack and attenuating the immune clearance of tumors[32,33]. Furthermore, AFP can enhance the malignant behavior of hepatoma cells by inhibiting their apoptosis and autophagy[34,35]. Accordingly, AFP can promote the survival and growth of a variety of tumor and non-tumor cells[36,37]. AFP can reduce the tumor necrosis factor alpha (TNF-α)-mediated damages of liver cancer cells or hepatocytes, and promotes their proliferation[38,39]. Studies have found that AFP can enhance the expression of p53, c-fos, c-jun, N-ras and hepatocyte growth factor receptor by binding

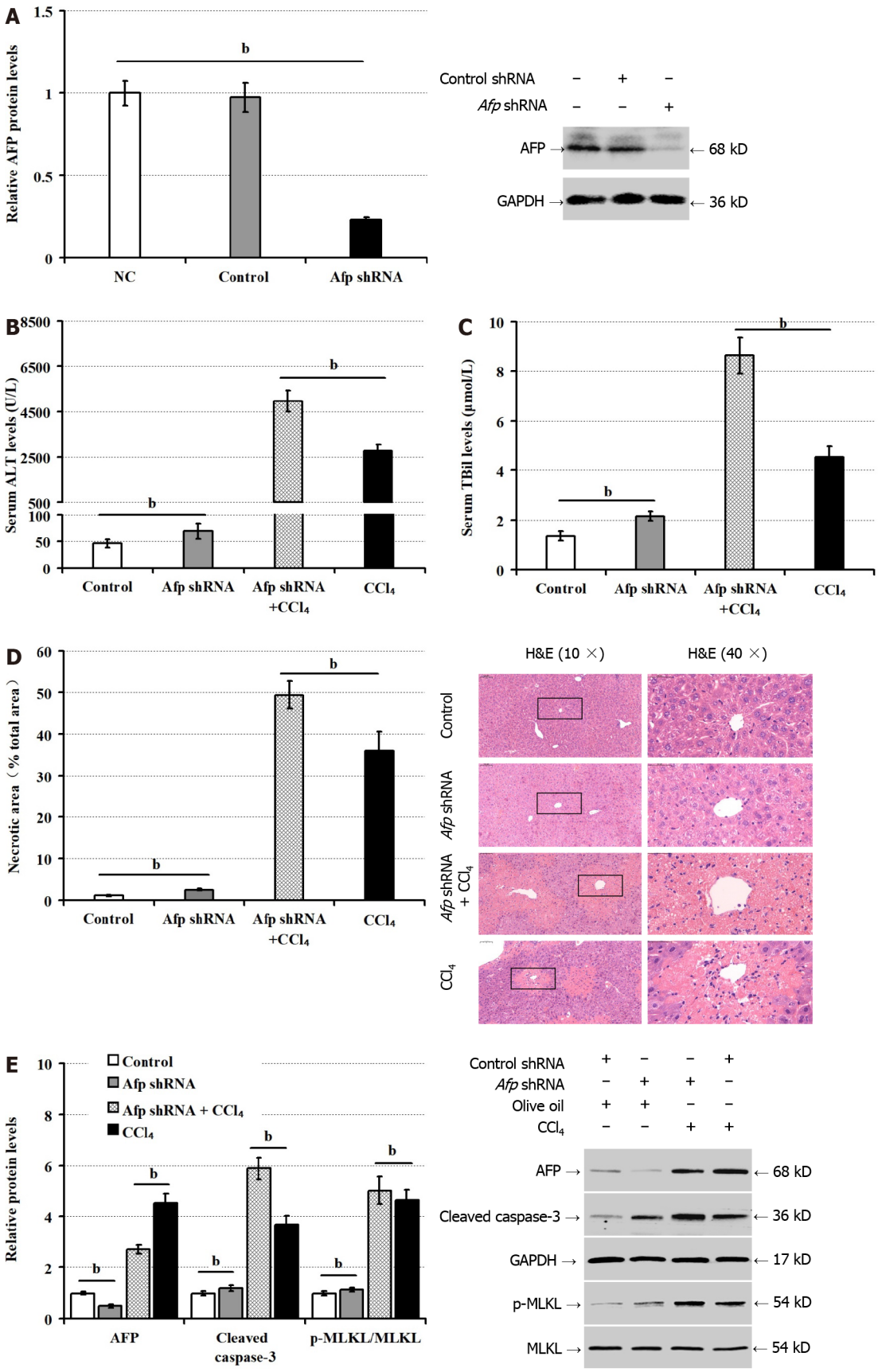
A
Relative AFP protein levels
1.5
1
0.5
0
b
NC
Control
Afp shRNA
Control shRNA
Afp shRNA
AFP
GAPDH
68 kD
36 kD
B
Serum ALT levels (U/L)
8500
6500
4500
2500
500
100
50
0
b
Control
Afp shRNA
Afp shRNA +CCl4
CCl4
C
Serum TBil levels (μmol/L)
10
8
6
4
2
0
b
Control
Afp shRNA
Afp shRNA +CCl4
CCl4
D
Necrotic area（% total area）
60
50
40
30
20
10
0
b
Control
Afp shRNA
Afp shRNA +CCl4
CCl4
H&E (10 ×)
H&E (40 ×)
Control
Afp shRNA
Afp shRNA + CCl4
CCl4
E
Relative protein levels
10
8
6
4
2
0
Control
Afp shRNA
Afp shRNA + CCl4
CCl4
b
AFP
Cleaved caspase-3
p-MLKL/MLKL
Control shRNA
Afp shRNA
Olive oil
CCl4
AFP
Cleaved caspase-3
GAPDH
p-MLKL
MLKL
68 kD
36 kD
17 kD
54 kD
54 kD

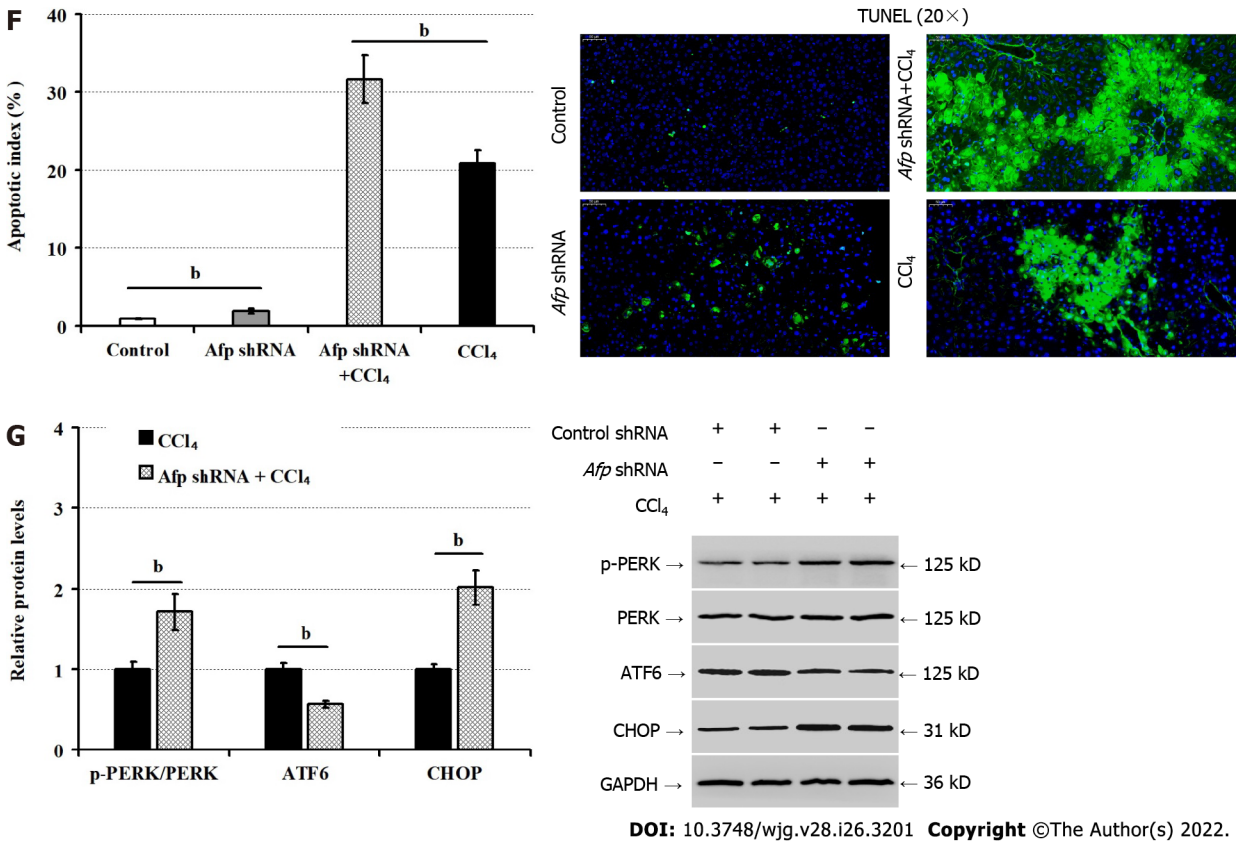

DOI: 10.3748/wjg.v28.i26.3201

Figure 6 Silencing of *alpha-fetoprotein* increases liver injury in mice following CCl_4 administration. A: Western blot for the protein levels of alpha-fetoprotein (AFP) in the liver tissues of mice; B: Serum alanine aminotransferase levels; C: Serum levels of total bilirubin; D: Liver sections stained by hematoxylin and eosin and measurements of necrotic areas in mice; E: Western blot for the relative levels of AFP, cleaved caspase-3, and phosphorylated mixed lineage kinase domain-like pseudokinase expression in the liver tissues; F: TUNEL analysis of hepatocyte apoptosis; G: The relative levels of phosphorylated protein kinase R-like ER kinase, activating transcription factor-6 and C/enhancer binding protein homologous protein protein in liver tissues. AFP: Alpha-fetoprotein; ALT: Alanine aminotransferase; ATF6: Activating transcription factor-6; CCl_4: Carbon tetrachloride; CHOP: C/enhancer binding protein homologous protein; H&E: Hematoxylin and eosin; p-MLKL: Phosphorylated mixed lineage kinase domain-like pseudokinase; p-PERK: Phosphorylated protein kinase R-like ER kinase; TBil: Total bilirubin; TUNEL: Terminal deoxynucleotidyl transferase-mediated dUTP nick end labeling. $^{b}P < 0.01$ compared with these two groups.

to its receptors to activate the cyclic adenosine 3′, 5′-monophosphate (cAMP)-protein kinase A (PKA) pathway and induce Ca^{2+} influx. This process increases intracellular cAMP and PKA, and promotes the proliferation, differentiation and regeneration of hepatocytes. In this study, *Afp* silencing deteriorated the ER stress-mediated apoptosis and necroptosis of LO2 cells *in vitro*. Preferable liver *Afp* silencing also aggravated the CCl_4-induced liver damages, hepatocyte apoptosis, and necroptosis in mice. The results suggest that the induced AFP expression in the liver by ER stress may enhance the resistance of hepatocytes to apoptosis and necroptosis stimulators, alleviating liver injury. Interestingly, we found that AFP silencing also exacerbated the ER stress, but lowed ATF6 expression in LO2 cells and in hepatocytes of liver tissues in mice, consistent with our previous observation[15]. These findings suggest that intracellular AFP induced by the ATF6 signaling may feedback-attenuate the ER stress-induced hepatocyte apoptosis and necroptosis, partially by up-regulating ATF6 expression. Given that AFP is not a transcription factor for the ATF6 expression the ER stress-induced AFP expression may through signal-crosstalk induce the ATF6-specific transcription factor and activator expression, indirectly inducing ATF6 expression in hepatocytes in a condition of ER stress.

We have reported that ATF6 is important for hepatocyte apoptosis and programmed necrosis[40]. It is possible that intracellular AFP may interact with intracellular proteins, transcription factors, kinases, co-activators and cell cycle regulators, such as PTEN to activate the PI3K/AKT/mTOR signaling to support the hepatocyte survival[41]. In addition, intracellular AFP may also interact with the apoptosis-related signaling to enhance apoptosis resistance by up-regulating Bcl-2 expression[35]. However, how intracellular AFP mitigates the ER stress-induced hepatocyte injury remains to be further examined.

CONCLUSION

ER stress induced intracellular AFP expression through activating ATF6 and the induced intracellular AFP feedback-attenuated the ER stress-induced hepatocyte injury. Thus, our findings may shed lights

on the molecular regulation by which hepatocytes respond to ER stress, promoting compensative liver repair following ER stress-induced liver injury.

ARTICLE HIGHLIGHTS

Research background

Endoplasmic reticulum (ER) stress plays an important role in the pathogenesis of chronic liver diseases, but how hepatocytes respond to ER stress has not been clarified. Alpha-fetoprotein (AFP) is secreted by hepatoma cells and elevated levels of serum AFP are associated with development of liver malignancies.

Research motivation

Anti-injury response is an important force for hepatocytes to resist liver injury mediated by various reasons, which has a close relationship to the progress and prognosis of liver injury. Studying the anti-injury mechanism of hepatocytes is important for the diagnosis and treatment of liver injury in the clinic.

Research objectives

To investigate whether and how AFP could regulate ER stress and hepatocyte injury.

Research methods

The distribution of AFP and the degrees of ER stress in liver tissues were characterized by histology, immunohistochemistry, and Western blot in biopsied human liver specimens, two mouse models of liver injury and a cellular model. The levels of AFP in sera and the supernatants of cultured cells were quantified by chemiluminescence.

Research results

ER stress induces liver injury and increases intracellular AFP expression in hepatocytes. ER stress up-regulates intracellular AFP expression by up-regulating activating transcription factor-6 (ATF6). Upregulated AFP feedback attenuates ER stress, forming a regulatory loop. Upregulated AFP mitigates the ER stress-induced hepatocyte apoptosis and necroptosis.

Research conclusions

ER stress upregulated intracellular AFP expression in hepatocytes by up-regulating ATF6 during the process of liver injury and intracellular AFP feedback-attenuated hepatocyte apoptosis and necroptosis by alleviating ER stress.

Research perspectives

Intracellular AFP induced by ER stress alleviates hepatocyte apoptosis and necroptosis by activating ATF6.

FOOTNOTES

Author contributions: Chen YF, Liu SY, and Cheng QJ contributed equally to this work; Chen YF, Liu SY, Cheng QJ, and He YH conceived and designed research; Chen YF, Liu SY, Wang YJ, Chen S, Zhou YY, and Liu X collected data and conducted research; Jiang ZG, Chen YF, and Zhong WW analyzed and interpreted data; Chen YF, Liu SY, and Cheng QJ wrote the initial paper; He YH and Zhong WW revised the paper; He YH had primary responsibility for final content; all authors read and approved the final manuscript.

Supported by the National Natural Science Foundation of China, No. 81560110; Tian Qing Liver Disease Research Fund Project of the Chinese Foundation for Hepatitis Prevention and Control, No. TQGB20200001; and the Science and Technology Planning Projects of Guizhou Province and Zunyi City, No. QKH·ZC[2019] 2803, No. QKHJC-ZK[2022]YB642, No. QKH·PTRC[2017]5733-013, No. gzwjkj2020-1-041, No. ZSKHSZ[2020]230, and No. ZMC·YZ[2018]38.

Institutional review board statement: The study was reviewed and approved by the Ethics Committee of Affiliated Hospital of Zunyi Medical University (ZYFYLS[2018] 28).

Institutional animal care and use committee statement: All procedures involving animals were reviewed and approved by the Animal Experiment Ethics Committee of Zunyi Medical University (LS[2020] 2-231).

Conflict-of-interest statement: There are no conflicts of interest to report.

Data sharing statement: The datasets generated and analyzed during the current study are available from the corresponding author on reasonable request.

ARRIVE guidelines statement: The authors have read the ARRIVE guidelines, and the manuscript was prepared and revised according to the ARRIVE guidelines.

Country/Territory of origin: China

ORCID number: Yun-Fen Chen 0000-0002-7940-7481; Si-Ying Liu 0000-0001-9938-4232; Qi-Jiao Cheng 0000-0002-3746-5923; Yu-Jiao Wang 0000-0002-9077-4979; Shuang Chen 0000-0001-9879-7529; Yi-Yang Zhou 0000-0002-1549-1821; Xia Liu 0000-0003-4140-184X; Zhi-Gang Jiang 0000-0003-4539-6988; Wei-Wei Zhong 0000-0002-9736-8148; Yi-Huai He 0000-0002-8639-3436.

S-Editor: Chen YL
L-Editor: A
P-Editor: Yuan YY

REFERENCES

1 **Galle PR**, Foerster F, Kudo M, Chan SL, Llovet JM, Qin S, Schelman WR, Chintharlapalli S, Abada PB, Sherman M, Zhu AX. Biology and significance of alpha-fetoprotein in hepatocellular carcinoma. *Liver Int* 2019; **39**: 2214-2229 [PMID: 31436873 DOI: 10.1111/liv.14223]

2 **Fouad R**, Elsharkawy A, Abdel Alem S, El Kassas M, Alboraie M, Sweedy A, Afify S, Abdellatif Z, Khairy M, Esmat G. Clinical impact of serum α-fetoprotein and its relation on changes in liver fibrosis in hepatitis C virus patients receiving direct-acting antivirals. *Eur J Gastroenterol Hepatol* 2019; **31**: 1129-1134 [PMID: 30896550 DOI: 10.1097/MEG.0000000000001400]

3 **Tai WC**, Hu TH, Wang JH, Hung CH, Lu SN, Changchien CS, Lee CM. Clinical implications of alpha-fetoprotein in chronic hepatitis C. *J Formos Med Assoc* 2009; **108**: 210-218 [PMID: 19293036 DOI: 10.1016/S0929-6646(09)60054-1]

4 **Fausto N**, Campbell JS. The role of hepatocytes and oval cells in liver regeneration and repopulation. *Mech Dev* 2003; **120**: 117-130 [PMID: 12490302 DOI: 10.1016/s0925-4773(02)00338-6]

5 **Vessey CJ**, de la Hall PM. Hepatic stem cells: a review. *Pathology* 2001; **33**: 130-141 [PMID: 11358043]

6 **Kuhlmann WD**, Peschke P. Hepatic progenitor cells, stem cells, and AFP expression in models of liver injury. *Int J Exp Pathol* 2006; **87**: 343-359 [PMID: 16965562 DOI: 10.1111/j.1365-2613.2006.00485.x]

7 **Wang X**, Shen C, Yang J, Yang X, Qin S, Zeng H, Wu X, Tang S, Zeng W. Alpha-Fetoprotein as a Predictive Marker for Patients with Hepatitis B-Related Acute-on-Chronic Liver Failure. *Can J Gastroenterol Hepatol* 2018; **2018**: 1232785 [PMID: 29854714 DOI: 10.1155/2018/1232785]

8 **Huang GQ**, Xie YY, Zhu PW, Wang XD, Lin Z, Wang Y, Ye JP, Wang YM, Chen YX, Jin XZ, Van Poucke S, Chen YP, Zheng MH. Stratified alpha-fetoprotein pattern accurately predicts mortality in patients with acute-on-chronic hepatitis B liver failure. *Expert Rev Gastroenterol Hepatol* 2018; **12**: 295-302 [PMID: 29300103 DOI: 10.1080/17474124.2018.1424540]

9 **Malhi H**, Kaufman RJ. Endoplasmic reticulum stress in liver disease. *J Hepatol* 2011; **54**: 795-809 [PMID: 21145844 DOI: 10.1016/j.jhep.2010.11.005]

10 **Zhong W**, Wang X, Rao Z, Pan X, Sun Y, Jiang T, Wang P, Zhou H. Aging aggravated liver ischemia and reperfusion injury by promoting hepatocyte necroptosis in an endoplasmic reticulum stress-dependent manner. *Ann Transl Med* 2020; **8**: 869 [PMID: 32793713 DOI: 10.21037/atm-20-2822]

11 **Hetz C**. The unfolded protein response: controlling cell fate decisions under ER stress and beyond. *Nat Rev Mol Cell Biol* 2012; **13**: 89-102 [PMID: 22251901 DOI: 10.1038/nrm3270]

12 **Jäger R**, Bertrand MJ, Gorman AM, Vandenabeele P, Samali A. The unfolded protein response at the crossroads of cellular life and death during endoplasmic reticulum stress. *Biol Cell* 2012; **104**: 259-270 [PMID: 22268789 DOI: 10.1111/boc.201100055]

13 **Zhao XC**, Livingston MJ, Liang XL, Dong Z. Cell Apoptosis and Autophagy in Renal Fibrosis. *Adv Exp Med Biol* 2019; **1165**: 557-584 [PMID: 31399985 DOI: 10.1007/978-981-13-8871-2_28]

14 **Grootjans S**, Vanden Berghe T, Vandenabeele P. Initiation and execution mechanisms of necroptosis: an overview. *Cell Death Differ* 2017; **24**: 1184-1195 [PMID: 28498367 DOI: 10.1038/cdd.2017.65]

15 **Chen H**, Chen GM, Liu YJ, Rao JX, Zhou SZ, Chen S, Chen PT, Yang FW, Cheng QJ, He YH. Alpha-fetoprotein/endoplasmic reticulum stress signaling mitigates injury in hepatoma cells. *Neoplasma* 2021; **68**: 983-993 [PMID: 34374292 DOI: 10.4149/neo_2021_210205N180]

16 **Chinese Society of Infectious Diseases**; Chinese Medical Association; Chinese Society of Hepatology, Chinese Medical Association. The guidelines of prevention and treatment for chronic hepatitis B (2019 version). *Zhonghua Gan Zang Bing*

Za Zhi 2019; **27**: 938-961 [PMID: 31941257 DOI: 10.3760/cma.j.issn.1007-3418.2019.12.007]

17 **Simmonds RC**. Bioethics and Animal Use in Programs of Research, Teaching, and Testing. In: Weichbrod RH, Thompson GAH, Norton JN, editors. Management of Animal Care and Use Programs in Research, Education, and Testing. Boca Raton (FL), 2018: 35-62

18 **Chen G**, Yang X, He Y, Tang Y, Tian R, Huang W, Chen H, Yang F, Li Y, Lin S. Inhibiting alpha subunit of eukaryotic initiation factor 2 dephosphorylation protects injured hepatocytes and reduces hepatocyte proliferation in acute liver injury. *Croat Med J* 2019; **60**: 532-544 [PMID: 31894919 DOI: 10.3325/cmj.2019.60.532]

19 **Tian RD**, Chen YQ, He YH, Tang YJ, Chen GM, Yang FW, Li Y, Huang WG, Chen H, Liu X, Lin SD. Phosphorylation of eIF2α mitigates endoplasmic reticulum stress and hepatocyte necroptosis in acute liver injury. *Ann Hepatol* 2020; **19**: 79-87 [PMID: 31548168 DOI: 10.1016/j.aohep.2019.05.008]

20 **Knodell RG**, Ishak KG, Black WC, Chen TS, Craig R, Kaplowitz N, Kiernan TW, Wollman J. Formulation and application of a numerical scoring system for assessing histological activity in asymptomatic chronic active hepatitis. *Hepatology* 1981; **1**: 431-435 [PMID: 7308988 DOI: 10.1002/hep.1840010511]

21 **Huang H**, Zheng XL, Zheng JS, Pan J, Pu XY. Rapid analysis of alpha-fetoprotein by chemiluminescence microfluidic immunoassay system based on super-paramagnetic microbeads. *Biomed Microdevices* 2009; **11**: 213-216 [PMID: 18923903 DOI: 10.1007/s10544-008-9226-z]

22 **Lippi G**, Dipalo M, Musa R, Avanzini P, Ferrarini C, Pattini A, Aloe R. Evaluation of the analytical performances of the novel Beckman Coulter AU5800. *Clin Biochem* 2012; **45**: 502-504 [PMID: 22296728 DOI: 10.1016/j.clinbiochem.2012.01.015]

23 **Kakisaka K**, Kataoka K, Onodera M, Suzuki A, Endo K, Tatemichi Y, Kuroda H, Ishida K, Takikawa Y. Alpha-fetoprotein: A biomarker for the recruitment of progenitor cells in the liver in patients with acute liver injury or failure. *Hepatol Res* 2015; **45**: E12-E20 [PMID: 25376981 DOI: 10.1111/hepr.12448]

24 **Yang N**, Li Z, Yan M, Xiao W, Zhang W, Long Y, Cheng Y, Ming K, Xu B. Evaluation of Serum Alpha-Fetoprotein Level in Chronic Hepatitis C Patients. *Clin Lab* 2019; **65** [PMID: 30775893 DOI: 10.7754/Clin.Lab.2018.180607]

25 **Zhang H**, Cao D, Zhou L, Zhang Y, Guo X, Li H, Chen Y, Spear BT, Wu JW, Xie Z, Zhang WJ. ZBTB20 is a sequence-specific transcriptional repressor of alpha-fetoprotein gene. *Sci Rep* 2015; **5**: 11979 [PMID: 26173901 DOI: 10.1038/srep11979]

26 **Lee K**. [Regulation of human alpha-fetoprotein gene by C/EBPalpha]. *Hokkaido Igaku Zasshi* 2004; **79**: 377-387 [PMID: 15373210]

27 **Jose-Estanyol M**, Danan JL. A liver-specific factor and nuclear factor I bind to the rat alpha-fetoprotein promoter. *J Biol Chem* 1988; **263**: 10865-10871 [PMID: 2455718]

28 **Sakata N**, Kaneko S, Ikeno S, Miura Y, Nakabayashi H, Dong XY, Dong JT, Tamaoki T, Nakano N, Itoh S. TGF- β Signaling Cooperates with AT Motif-Binding Factor-1 for Repression of the α -Fetoprotein Promoter. *J Signal Transduct* 2014; **2014**: 970346 [PMID: 25105025 DOI: 10.1155/2014/970346]

29 **Jeon Y**, Choi YS, Jang ES, Kim JW, Jeong SH. Persistent α-Fetoprotein Elevation in Healthy Adults and Mutational Analysis of α-Fetoprotein Promoter, Enhancer, and Silencer Regions. *Gut Liver* 2017; **11**: 136-141 [PMID: 27609486 DOI: 10.5009/gnl16069]

30 **Bois-Joyeux B**, Danan JL. Members of the CAAT/enhancer-binding protein, hepatocyte nuclear factor-1 and nuclear factor-1 families can differentially modulate the activities of the rat alpha-fetoprotein promoter and enhancer. *Biochem J* 1994; **301** (Pt 1): 49-55 [PMID: 7518671 DOI: 10.1042/bj3010049]

31 **Terentiev AA**, Moldogazieva NT. Structural and functional mapping of alpha-fetoprotein. *Biochemistry (Mosc)* 2006; **71**: 120-132 [PMID: 16489915 DOI: 10.1134/s0006297906020027]

32 **Wang X**, Wang Q. Alpha-Fetoprotein and Hepatocellular Carcinoma Immunity. *Can J Gastroenterol Hepatol* 2018; **2018**: 9049252 [PMID: 29805966 DOI: 10.1155/2018/9049252]

33 **Meng W**, Bai B, Bai Z, Li Y, Yue P, Li X, Qiao L. The immunosuppression role of alpha-fetoprotein in human hepatocellular carcinoma. *Discov Med* 2016; **21**: 489-494 [PMID: 27448785]

34 **Wang S**, Zhu M, Wang Q, Hou Y, Li L, Weng H, Zhao Y, Chen D, Ding H, Guo J, Li M. Alpha-fetoprotein inhibits autophagy to promote malignant behaviour in hepatocellular carcinoma cells by activating PI3K/AKT/mTOR signalling. *Cell Death Dis* 2018; **9**: 1027 [PMID: 30301886 DOI: 10.1038/s41419-018-1036-5]

35 **Li M**, Li H, Li C, Zhou S, Guo L, Liu H, Jiang W, Liu X, Li P, McNutt MA, Li G. Alpha fetoprotein is a novel protein-binding partner for caspase-3 and blocks the apoptotic signaling pathway in human hepatoma cells. *Int J Cancer* 2009; **124**: 2845-2854 [PMID: 19267404 DOI: 10.1002/ijc.24272]

36 **Terentiev AA**, Moldogazieva NT. Alpha-fetoprotein: a renaissance. *Tumour Biol* 2013; **34**: 2075-2091 [PMID: 23765762 DOI: 10.1007/s13277-013-0904-y]

37 **Yang X**, Zhang Y, Zhang L, Mao J. Silencing alpha-fetoprotein expression induces growth arrest and apoptosis in human hepatocellular cancer cell. *Cancer Lett* 2008; **271**: 281-293 [PMID: 18657899 DOI: 10.1016/j.canlet.2008.06.017]

38 **Semenkova LN**, Dudich EI, Dudich IV, Shingarova LN, Korobko VG. Alpha-fetoprotein as a TNF resistance factor for the human hepatocarcinoma cell line HepG2. *Tumour Biol* 1997; **18**: 30-40 [PMID: 8989923 DOI: 10.1159/000218013]

39 **Cavin LG**, Venkatraman M, Factor VM, Kaur S, Schroeder I, Mercurio F, Beg AA, Thorgeirsson SS, Arsura M. Regulation of alpha-fetoprotein by nuclear factor-kappaB protects hepatocytes from tumor necrosis factor-alpha cytotoxicity during fetal liver development and hepatic oncogenesis. *Cancer Res* 2004; **64**: 7030-7038 [PMID: 15466196 DOI: 10.1158/0008-5472.CAN-04-1647]

40 **Huang MY**, Wan DW, Deng J, Guo WJ, Huang Y, Chen H, Xu DL, Jiang ZG, Xue Y, He YH. Downregulation of RIP3 Improves the Protective Effect of ATF an Acute Liver Injury Model. *Biomed Res Int* 2021; **2021**: 8717565 [PMID: 34778458 DOI: 10.1155/2021/8717565]

41 **Mizejewski GJ**. Alpha-fetoprotein structure and function: relevance to isoforms, epitopes, and conformational variants. *Exp Biol Med (Maywood)* 2001; **226**: 377-408 [PMID: 11393167 DOI: 10.1177/153537020122600503]

World Journal of Gastroenterology

Submit a Manuscript: https://www.f6publishing.com

World J Gastroenterol 2022 July 14; 28(26): 3218-3231

DOI: 10.3748/wjg.v28.i26.3218

ISSN 1007-9327 (print) ISSN 2219-2840 (online)

ORIGINAL ARTICLE

Retrospective Cohort Study

Divergent trajectories of lean *vs* obese non-alcoholic steatohepatitis patients from listing to post-transplant: A retrospective cohort study

Fakhar Ali Qazi-Arisar, Raj Uchila, Catherine Chen, Cathy Yang, Shi-Yi Chen, Ravikiran Sindhuvalada Karnam, Amirhossein Azhie, Wei Xu, Zita Galvin, Nazia Selzner, Leslie Lilly, Mamatha Bhat

Specialty type: Gastroenterology and hepatology

Provenance and peer review: Unsolicited article; Externally peer reviewed.

Peer-review model: Single blind

Peer-review report's scientific quality classification

Grade A (Excellent): 0
Grade B (Very good): B
Grade C (Good): C, C
Grade D (Fair): 0
Grade E (Poor): 0

P-Reviewer: Gluvic Z, Serbia; Sibulesky L, United States; Tiejun W, China

Received: February 3, 2022
Peer-review started: February 3, 2022
First decision: April 10, 2022
Revised: April 22, 2022
Accepted: June 15, 2022
Article in press: June 15, 2022
Published online: July 14, 2022

Fakhar Ali Qazi-Arisar, Raj Uchila, Catherine Chen, Cathy Yang, Ravikiran Sindhuvalada Karnam, Amirhossein Azhie, Zita Galvin, Nazia Selzner, Leslie Lilly, Mamatha Bhat, Ajmera Transplant Program, Toronto General Hospital, University Health Network, Toronto M5G 2N2, Ontario, Canada

Fakhar Ali Qazi-Arisar, Raj Uchila, Ravikiran Sindhuvalada Karnam, Zita Galvin, Nazia Selzner, Leslie Lilly, Mamatha Bhat, Division of Gastroenterology and Hepatology, Department of Medicine, University of Toronto, Toronto M5G 2N2, Ontario, Canada

Fakhar Ali Qazi-Arisar, National Institute of Liver and GI Diseases, Dow University of Health Sciences, Karachi 75330, Pakistan

Shi-Yi Chen, Wei Xu, Department of Biostatistics, Princess Margaret Cancer Center, University Health Network, Toronto M5G 2C1, Ontario, Canada

Wei Xu, Division of Biostatistics, Dalla Lana School of Public Health, University of Toronto, Toronto M5G 2C1, Ontario, Canada

Corresponding author: Mamatha Bhat, FRCP (C), MD, PhD, Assistant Professor, Ajmera Transplant Program, Toronto General Hospital, University Health Network, 585 University Ave, 11th Floor, Room 183, Toronto M5G 2N2, Ontario, Canada. mbhat33@gmail.com

Abstract

BACKGROUND

Non-alcoholic steatohepatitis (NASH) cirrhosis is the second most common indication for liver transplantation (LT). The role of body mass index (BMI) on outcomes of NASH cirrhosis has been conflicting.

AIM

To compare the longitudinal trajectories of patients with lean *vs* obese NASH cirrhosis, from listing up to post-transplant, having adjusted their BMI for ascites.

METHODS

We retrospectively reviewed all adult NASH patients listed for LT in our program from 2012 to 2019. Fine-Gray Competing Risk analyses and Cox Proportional-Hazard Models were performed to examine the cumulative incidence of transplant and survival outcomes respectively.

RESULTS
Out of 265 NASH cirrhosis listed patients, 176 were included. Median age was 61.0 years; 46% were females. 111 patients underwent LT. Obese robust patients had better waitlist survival [hazard ratio (HR): 0.12; 95%CI: 0.05–0.29, $P < 0.0001$] with higher instantaneous rate of transplant (HR: 5.71; 95%CI: 1.26–25.9, $P = 0.02$). Lean NASH patients had a substantially higher risk of graft loss within 90 d post-LT (1.2% *vs* 13.8%, $P = 0.032$) and death post-LT (2.4% *vs* 17.2%, $P = 0.029$). 1- 3- and 5-year graft survival was poor for lean NASH (78.6%, 77.3% and 41.7% *vs* 98.6%, 96% and 85% respectively). Overall patient survival post-LT was significantly worse in lean NASH (HR: 0.17; 95%CI: 0.03–0.86, $P = 0.0142$) with 83% lower instantaneous rate of death in obese group.

CONCLUSION
Although lean NASH is considered to be more benign than obese NASH, our study suggests a paradoxical correlation of lean NASH with waitlist outcomes, and graft and patient survival post-LT.

Key Words: Outcomes; Frailty; Waitlist; Liver transplant; Survival

Core Tip: Non-alcoholic steatohepatitis continues to rise as an indication for liver transplantation (LT). In this study, we analyzed our single-center data of adult patients listed for LT between 2012 and 2019 and reported their outcomes on the waitlist as well as post-LT based on their body mass index.

Citation: Qazi-Arisar FA, Uchila R, Chen C, Yang C, Chen SY, Karnam RS, Azhie A, Xu W, Galvin Z, Selzner N, Lilly L, Bhat M. Divergent trajectories of lean *vs* obese non-alcoholic steatohepatitis patients from listing to post-transplant: A retrospective cohort study. *World J Gastroenterol* 2022; 28(26): 3218-3231
URL: https://www.wjgnet.com/1007-9327/full/v28/i26/3218.htm
DOI: https://dx.doi.org/10.3748/wjg.v28.i26.3218

INTRODUCTION

Non-alcoholic steatohepatitis (NASH) cirrhosis is currently the second most common indication for liver transplantation (LT) and is on track to become the leading indication by 2030 in the United States[1,2]. The ability to cure hepatitis C with antivirals and the twin epidemics of diabetes and obesity have fueled the rise of NASH as an indication for LT worldwide.

NASH patients are often older at presentation and have some or all the components of metabolic syndrome such as diabetes, hypertension, dyslipidemia, and obesity. Non-alcoholic fatty liver disease (NAFLD) and NASH have also been described in the absence of obesity[3]. About 25% of all NAFLD patients exhibit this lean phenotype[4]. However, the role of body mass index (BMI) on outcomes of NASH cirrhosis has been conflicting. Several studies have disproved the perception of NAFLD being a 'milder' condition in lean individuals. In fact, lean patients with NASH have been shown to have more severe liver disease, more advanced fibrosis, shorter waitlist survival, and poorer post-transplant graft and patient survival[5-8].

However, these retrospective studies have been limited by their ability to accurately interpret BMI and the paucity of specific details regarding waitlist and post-transplant outcomes such as cardiometabolic disease, recurrent NASH, and graft fibrosis. Previous attempts to correct BMI for ascites have been shown to move at least 20% of patients to a lower BMI group[9]. Therefore, our study's objective is to compare the longitudinal trajectories of patients with lean *vs* obese NASH cirrhosis, from listing up to post-transplant, having adjusted their BMI for ascites.

MATERIALS AND METHODS

The study was approved by the Research Ethics Board of the University Health Network (Toronto, Canada).

Patients

This was a single-centre retrospective study of all NASH cirrhosis patients listed for LT between November 12, 2012, and May 31, 2019, in the Multi-Organ Transplant Program at the University Health

Network in Toronto, Canada. The study's start date was decided as November 13, 2012, as our program transitioned to the model for end stage liver disease (MELD)-Na system for listing on that day. All patients were followed until May 31, 2020, yielding a minimum follow-up of 1 year. In our program, NASH cirrhosis was diagnosed either based on findings of significant steatosis on histopathology (pre-transplant liver biopsy or explant pathology), or the presence of risk factors (diabetes, obesity, and metabolic syndrome) in the absence of significant alcohol consumption and evidence of other etiology on serology or histopathology.

We excluded candidates listed for hepatocellular carcinoma with exception points, all other candidates listed with exception points, patients with fulminant liver failure, NASH concomitant with a secondary etiology of chronic liver disease (such as alcohol, viral, autoimmune hepatitis, or cryptogenic cirrhosis), multiorgan transplants and those relisted for transplantation.

Data collected from the database on each recipient at the time of listing included age, gender, height, weight, BMI, Na MELD, Creatinine, estimated glomerular filtration rate (eGFR), biochemical parameters (bilirubin, albumin, international normalized ratio), frailty using clinical frailty scale, complications of cirrhosis including the severity of ascites and associated comorbidities were collected. The severity of ascites (mild, moderate, or severe) is graded according to what was recorded in the patient's clinical notes as determined either by physical or more often by radiological examination. Duration on the waitlist, intensive care unit (ICU) stay, sepsis, outcomes on the waitlist, reasons for delisting, and cause of death were also collected. Post-transplant data includes the type of transplant, re-hospitalization within 90 d, recurrence of NAFLD and NASH, time to recurrent NAFLD or NASH, metabolic, cardiovascular, and biliary complications, BMI at 1 and 5 years, patient, and graft survival details.

The above data was collected from the Organ Transplant Tracking Registry software, an internal transplant database linked to the electronic medical record of all patients evaluated at the University Health Network.

Our primary outcomes included patient and graft survival at 90 d, 1- 3- and 5 years.

Dry-weight BMI or adjusted BMI

The adjusted BMI was calculated by evaluating the patient's dry weight, which is estimated by post-paracentesis body weight, or weight recorded before fluid retention if available, or by subtracting a percentage of weight based upon the severity of ascites (mild 5%; moderate 10%; severe 15%) as performed in several studies. The dry-weight BMI or adjusted BMI was then calculated by dividing the patient's estimated dry weight (kg) by the square of the patient's height (m) as performed in several studies[10,11]. We categorized the variable of calculated adjusted BMI at listing into two groups: Group 1 comprising of overweight (BMI ≥ 25 and < 30 kg/m^2) or obese group (BMI ≥ 30 kg/m^2) and Group 2 comprising of underweight (< 18.5 kg/m^2) or normal (≥ 18.5 and < 25 kg/m^2) BMI group.

Adjusted BMI was determined for all the listed patients. The cohort of patients was analyzed according to their weight category.

Statistical analysis

A two-sided test with an overall sample size of 153 subjects (51 in the underweight or normal group, and 102 in the overweight or obese group) achieved 80% power at a 0.05 significance level when the estimated hazard ratio (HR) for the overall survival was 0.5 with the null hypothesis of HR = 1. To account for drop-offs, final sample size was increased to 54 and 122. These results assume that the HR was constant throughout the study and that Cox proportional hazards (PH) regression was used to analyze the data.

Descriptive statistics were performed for demographic and clinical variables. Counts and proportions were calculated for categorical variables and the differences between patients with lean *vs* obese NASH were compared using the Chi-squared test or Fisher's exact test. Mean ± SD and median (range) were calculated for continuous variables and the differences between the two groups were compared using two-sample t-tests or Wilcoxon tests, depending on the distribution of the data.

Cumulative incidence of transplant by lean *vs* obese NASH was plotted and group differences were compared using Gray k-sample test and Fine-Gray Competing risk models. Kaplan-Meier plots for waitlist survival and post-transplant survival were also plotted and differences between patients with lean and obese NASH were compared using log-rank tests and Cox PH models. Complete-case analyses were performed on observations with complete sets of data while the data for observations that has one or more missing values were removed.

Sample size was calculated using PASS (Power Analysis and Sample Size Software) 2021. (NCSS, LLC. Kaysville, Utah, United States, ncss.com/software/pass). SAS 9.4 (SAS Institute, Cary NC) was used to perform statistical analyses. Statistical significance was defined as a P value of ≤ 0.05.

RESULTS

Patient characteristics

Out of 265 patients listed for NASH cirrhosis, 176 met the eligibility criteria. The median age was 61 (32–71.4) years; 46% were females. A total of 111 patients underwent LT, 78 deceased donor LT (DDLT), and 33 living donor LT (LDLT). Table 1 describes the pre-LT clinical and laboratory variables.

Impact of ascites on BMI

Correcting for ascites volume resulted in patients moving into a lower BMI classification among all groups except the underweight group (BMI < 18 kg/m^2). The change was larger among patients in the higher BMI groups with 72.2%, 62.9%, and 78.1% of patients moved to a lower BMI group from Obesity classes 3, 2, and 1, respectively as shown in Table 2.

Waitlist parameters and outcomes

Patients in lean NASH group were elderly at time of listing (median age 61.6 years *vs* 60.3 years, P = 0.048), had worse renal functions at end of listing (median eGFR 48 mL/min/1.73 m^2 *vs* 57 mL/min/1.73 m^2, P = 0.017), carried more severe ascites (66.6% *vs* 45%, P = 0.03) and were more paracentesis dependent (72.2% *vs* 52.9%, P = 0.016). Other characteristics such as sex, clinical frailty scale, and frequency of complications were similar between the two groups.

Patients in the overweight/obese group spent a median of 139.5 d on the waitlist which was not dissimilar to the 117 d spent by their counterparts in the lean group. Waitlist events such as episodes of sepsis and ICU stay were similar in the two groups. With regards to waitlist outcomes, a similar number of patients were de-listed or transplanted in both groups. More patients belonging to the lean NASH group compared to the obese group died (31.5% *vs* 20.5%, P = 0.26); however, the difference was not significant. Time to death or delisting was similar in both obese and lean groups (HR: 0.83; 95%CI: 0.46–1.50, P = 0.53). However, when sub-grouped based on BMI and frailty, patients with obese NASH and none/mild frailty had better survival than lean NASH with moderate to severe frailty (HR: 0.12; 95%CI: 0.05–0.29, P < 0.0001) (Figure 1).

With regards to transplant data, a comparable number of patients underwent DDLT and LDLT in both obese and lean groups (DDLT: 69.5% in overweight/obese group and 72.4% in the lean group; P = 0.77). The cumulative incidence of transplant was equal in both groups (HR: 1.33; 95%CI: 0.87–2.05, P = 0.16). However, obese NASH patients with none/mild frailty had a significantly better instantaneous rate of transplant than lean NASH with moderate to severe frailty (HR: 5.71; 95%CI: 1.26–25.9, P = 0.02) (Figure 2). The Median cold ischemia time in obese patients undergoing DDLT was significantly longer than that of lean patients (465 min *vs* 330.5 min, P = 0.024).

Post-transplant outcomes

Compared to listing, the obese group had a significant reduction in BMI 1 year post-transplant (β = -2.08, SE = 0.87, P = 0.006). At 5-year post-transplant, the overweight or obese group's BMI returned to the same level as listing time (β = 1.80, SE = 1.54, P = 0.52). No change in BMI was observed in the underweight or normal group (overall P = 0.3) (Figure 3). There was no difference in post-transplant parameters such as 90-d rehospitalization, biliary complications or recurrence of NASH in lean *vs* obese groups. However, renal function was significantly better in lean NASH patients at 5 years (median creatinine 111 μmol/L *vs* 153.5 μmol/L, P = 0.019) (Table 3).

The graft loss within 90 d post-transplant (1.2% *vs* 13.8%, P = 0.032) and death following transplant (2.4% *vs* 17.2%, P = 0.029) were significantly higher in lean patients compared to obese patients. The 1- 3- and 5-year graft survivals were significantly worse for lean patients 98.6%, 96% and 85% *vs* 78.6%, 77.3% and 41.7% respectively, all P < 0.05) (Table 3). There was a trend toward worse 1- 3- and 5-year patient survival (98.7%, 96% and 90% *vs* 89.7%, 81.8% and 58.3%; P = 0.06, 0.07 and 0.07 respectively). The two groups were analysed to compare patient survival using Kaplan Meier Survival Plots and Cox PH models, which noted a statistically significant difference in overall survival between the two groups (HR: 0.17; 95%CI: 0.03–0.86, P = 0.0142). The instantaneous rate of death in the overweight/obese group was 83% lower than those in the underweight/normal weight group (Figure 4).

DISCUSSION

Our study highlights the paradoxical impact of pretransplant BMI on the survival of NASH patients post-liver transplant, with lean NASH patients demonstrating inferior 90-d, 1- 3- and 5-year graft survival, and overall patient survival.

Lean NAFLD prevalence varies from 12% to 20% depending on the population. The presence of comorbid conditions such as components of metabolic syndrome along with older age increases the morbidity and mortality of NASH cirrhotic patients. However, it is unclear if the same applies to lean NASH. The prevalence of metabolic syndrome is less common in lean NAFLD patients as compared to

Table 1 Pre-liver transplant clinical and laboratory variables

	Total (*n* = 176)	BMI groups after ascites correction		*P* value
		Overweight or obese (*n* = 122)	Underweight or normal (*n* = 54)	
Age at listing, median (range) years	61.0 (32.0–71.4)	60.3 (32.0–71.4)	61.6 (45.2–71.0)	0.048[a]
Age at end of listing, median (range) years	61.0 (32.0–72.0)	61.0 (32.0–71.0)	62.0 (48.0–72.0)	0.09
Female sex, *n* (%)	81 (46.02)	53 (43.44)	28 (51.85)	0.30
Height at listing, median (range) cm	168.0 (148.0–193.0)	168.0 (148.0–188.0)	168.0 (150.0–193.0)	0.23
Weight at listing, median (range) kg	88.3 (39.6–146.5)	94.9 (69.0–146.5)	72.0 (39.6–94.2)	< 0.001[c]
Ascites adjusted weight at listing, median (range) kg	77.4 (33.7–140.0)	85.1 (60.5–140.0)	64.4 (33.7–80.1)	< 0.001[c]
Weight at end of listing, median (range) kg	86.9 (39.6–161.8)	92.9 (50.7–161.8)	73.9 (39.6–94.2)	< 0.001[c]
BMI at listing, median (range) kg/m^2	31.0 (17.6–48.9)	33.7 (25.6–48.9)	25.4 (17.6–30.8)	< 0.001[c]
Ascites adjusted BMI at listing, median (range) kg/m^2	27.4 (15.0–45.3)	29.2 (25.0–45.3)	22.6 (15.0–24.9)	< 0.001[c]
Na MELD (at listing), median (range)	22.0 (10.0–48.0)	21.0 (11.0–48.0)	22.0 (10.0–43.0)	0.34
Na MELD at end of listing, median (range)	23.0 (6.0–45.0)	23.0 (6.0–44.0)	23.0 (10.0–45.0)	0.41
Creatinine at listing, median (range) μmol/L	98.5 (51.0–564.0)	96.5 (55.0–564.0)	103.0 (51.0–399.0)	0.50
Creatinine at end of listing, median (range) μmol/L	112.5 (44.0–719.0)	115.0 (44.0–719.0)	109.0 (49.0–483.0)	0.50
eGFR at listing, median (range) mL/min/1.73 m^2	63.0 (17.0–120.0)	65.5 (18.0–117.0)	56.0 (17.0–120.0)	0.11
eGFR at end of listing, median (range) mL/min/1.73 m^2	52.5 (17.0–116.0)	57.0 (17.0–116.0)	48.0 (20.0–98.0)	0.017[a]
Bilirubin at listing, median (range) μmol/L	49.0 (8.0–955.0)	51.0 (8.0–755.0)	45.5 (14.0–955.0)	0.11
Bilirubin at end of listing, median (range) μmol/L	56.5 (3.0–927.0)	58.0 (8.0–927.0)	50.0 (3.0–802.0)	0.19
INR at listing, median (range)	1.5 (1.1–4.7)	1.5 (1.1–4.7)	1.5 (1.1–3.9)	0.05
INR at end of listing, median (range)	1.7 (1.1–7.6)	1.7 (1.1–7.6)	1.8 (1.1–5.0)	0.46
Na at listing, median (range) mEq/L	134.0 (116.0–147.0)	135.0 (120.0–147.0)	133.0 (116.0–142.0)	0.014[a]
Na at end of listing, median (range) mEq/L	135.0 (116.0–159.0)	135.0 (116.0–159.0)	134.0 (120.0–152.0)	0.10
Albumin at listing, median (range) g/L	30.5 (9.0 – 47.0)	29.5 (20.0–47.0)	31.0 (9.0–42.0)	0.08
Albumin at end of listing, median (range) g/L	30.0 (10.0–54.0)	30.0 (12.0–54.0)	30.0 (10.0–50.0)	0.28
Frailty score (*n* = 159), median (range)	4.0 (2.0–8.0)	4.0 (2.0–8.0)	5.0 (3.0–8.0)	0.25
None to mild, *n* (%)	116 (72.96)	78 (71.56)	38 (76)	0.56
Moderate to severe, *n* (%)	43 (27.04)	31 (28.44)	12 (24)	
Missing, *n* (%)	17 (9.66)	13 (10.66)	4 (7.41)	
Encephalopathy, *n* (%)	141 (80.11)	99 (81.15)	42 (77.78)	0.61
Ascites, *n* (%)	161 (91.48)	109 (089.34)	052 (096.30)	0.15
Degree of ascites, *n* (%)				
None	14 (07.95)	13 (10.66)	1 (1.85)	0.030[a]
Mild	41 (23.30)	30 (24.59)	11 (20.37)	
Moderate	30 (17.05)	24 (019.67)	6 (11.11)	
Severe	91 (51.70)	55 (45.08)	36 (66.67)	
Need for LVP, *n* (%)	103 (58.86)	64 (52.89)	39 (72.22)	0.016[a]

SBP, *n* (%)	46 (26.44)	33 (27.05)	13 (25.00)	0.78
Variceal bleed, *n* (%)	53 (30.11)	34 (27.87)	19 (35.19)	0.33
Hepatorenal syndrome, *n* (%)	48 (27.27)	30 (24.59)	18 (33.33)	0.23
Hypertension, *n* (%)	80 (45.45)	58 (47.54)	22 (40.74)	0.40
Diabetes, *n* (%)	104 (59.09)	68 (55.74)	36 (66.67)	0.17
Hyperlipidemia, *n* (%)	57 (32.39)	35 (28.69)	22 (40.74)	0.12
CKD, *n* (%)	18 (10.23)	12 (9.84)	6 (11.11)	0.80
CAD, *n* (%)	29 (16.48)	22 (18.03)	7 (12.96)	0.40
Time on waiting list, median (range) days	136.0 (1.0–1566.0)	139.5 (1.0–1497.0)	117.0 (1.0–1566.0)	0.42
ICU stay within 90 d before end of listing, *n* (%)	30 (17.05)	21 (17.21)	9 (16.67)	0.93
No of hospitalizations within 90 d before end of listing, median (range), *n* (%)	1.0 (0.0–5.0)	1.0 (0.0–5.0)	1.0 (0.0–5.0)	0.42
< 2	151 (85.80)	105 (86.07)	46 (85.19)	0.88
≥ 2	25 (14.20)	17 (13.93)	8 (14.81)	
Bacteraemia/sepsis within 90 d before end of listing, *n* (%)	19 (11.66)	12 (10.62)	7 (14.00)	0.54
Outcome, *n* (%)				
Active living	1 (0.57)	1 (0.82)	0 (00)	0.26
De-listed	22 (12.50)	14 (11.48)	8 (14.81)	
Died	42 (23.86)	25 (20.49)	17 (31.48)	
Transplanted	111 (63.07)	82 (67.21)	29 (53.70)	
Type of LT received, *n* (%)				
DDLT	78 (70.27)	57 (69.51)	21 (72.41)	0.77
LDLT	33 (29.73)	25 (30.49)	8 (27.59)	

[a]$P < 0.05$.
[c]$P < 0.001$.
BMI: Body mass index; CAD: Coronary artery disease; CKD: Chronic kidney disease; DDLT: Deceased donor liver transplant; eGFR: Estimated glomerular filtration rate; ICU: Intensive care unit; INR: International normalized ratio; LT: Liver transplant; LDLT: Living donor liver transplant; LVP: Large volume paracentesis; MELD: Model for end stage liver disease; Na: Sodium; SBP: Spontaneous bacterial peritonitis.

obese[4,12-14]. A long-term follow-up study showed that biopsy-proven lean NAFLD patients are more likely to develop severe liver disease (F3/F4) than overweight patients[5]. Literature is scant about the outcomes of lean NASH while on the waiting list for LT. A study comprising of 1090 patients revealed shorter cumulative survival in lean NAFLD compared to non-lean NAFLD (log-rank test = 5.6; $P < 0.02$)[6] In a recent study, morbid obesity and diabetes were related to an increased risk of drop out of NASH patients from the waiting list[15].

Frailty, a common complication of cirrhosis, is seen more frequently in NASH cirrhosis patients as compared to other etiologies such as alcoholic liver disease[16]. Frailty has previously been shown to determine a patient's overall health, the number of hospitalizations, length of hospital stay, delisting, and waitlist mortality[17-21]. especially in patients older than 65 years of age[22] independent of portosystemic encephalopathy or ascites[23]. However, the impact of frailty in the NASH cohort was not assessed. In a multicentre study, frailty was associated with a 2-fold higher risk of wait-list mortality among nonobese/class 1 obese patients, while more than 3-fold higher risk of wait-list mortality among class 2 or greater obese liver transplant candidates[24]. However, NASH comprised only 17.5% of their patient population, while BMI was not corrected for ascites which was present in 37.1% of their patients. In a retrospective analysis, a higher frailty score was associated with an increased risk of delisting in NASH patients (HR: 1.46; 95%CI: 1.06–2.03, $P = 0.02$)[16]. In our study, lean NASH patients with frailty had poor survival (HR: 0.12; 95%CI: 0.05–0.29, $P < 0.0001$) with lower instantaneous rate of transplant (HR: 5.71; 95%CI: 1.26–25.9, $P = 0.02$). Therefore, the convergence of frailty with lean NASH led to significantly worse outcomes on the waitlist as well as in the early period post-transplant.

Though lean NAFLD is considered to be benign, the dysfunctional adipose tissue, in particular, visceral adiposity is related with increase cardiometabolic risk in lean NAFLD. Further, alterations in

Table 2 Percentage of patients who changed body mass index groups after ascites correction

Reduction in BMI after ascites correction					Original/uncorrected	Unchanged
Underweight	Normal	Overweight	Obesity 1	Obesity 2		
					Underweight, 2 (1.1%)	2 (100%)
5 (22.73%)					Normal, 22 (12.5%)	17 (77.27%)
	29 (55.77%)				Overweight, 52 (29.55%)	23 (44.23%)
	1 (1.82%)	42 (76.36%)			Obesity 1, 55 (31.25%)	12 (21.82%)
			17 (62.96%)		Obesity 2, 27 (15.34%)	10 (37.04%)
			2 (11.11%)	11 (61.11%)	Obesity 3, 18 (10.23%)	5 (27.78%)
All BMI group had some level of decrease after correction		Especially higher BMI groups have more % reduction			Total (n = 176)	% of unchanged are higher among low BMI groups

BMI: Body mass index.

TM6SF2, a gene conferring susceptibility to NASH and fibrosis, are shown to be increased in lean NAFLD than obese NAFLD patients. However, there is a paucity of data on post-transplant outcomes in lean patients specifically[25]. In the post-transplant setting, a pivotal study looking at the patients on the UNOS database revealed that both short- and long-term survivals were low in patients who were morbidly obese before transplantation, owing to adverse cardiovascular events[26]. However, none of the patients in this study belonged to the NASH group. On the contrary, obesity was noted to paradoxically favour the NASH patients compared to their non-NASH counterparts. A recent study found that lean patients have both poorer graft and patient survival than their obese counterparts[7]. However, they did not adjust the BMI for ascites, whereas elevated BMI might have reflected fluid overload instead of true obesity. There is still much that is not known or understood, and hence it is challenging to explain the underlying molecular mechanisms linking lean NASH with worse outcomes post LT. Nonetheless, our study also confirms the enigmatic effect of obesity in the NASH subset. This study also highlighted the importance of correcting BMI for ascites. Despite correcting BMI for ascites, 69% of NASH patients belong to the overweight/obese group.

NASH has been associated with metabolic syndrome-related complications such as cardiovascular disease and chronic kidney disease (CKD)[27]. Post-transplant the risk of metabolic complications increases further owing to the immunosuppressive medications. Furthermore, calcineurin inhibitors carry direct nephrotoxic effects. In general, obese NAFLD patients appear to have a higher risk of developing CKD than non-obese[28]. In post-LT patients, obesity has been identified as a risk for post-operative severe acute kidney injury[29] as well as renal disease progression needing a kidney transplant after LT[30]. We further augmented this data by showing that median creatinine in our obese patients was significantly higher than in lean patients at 5 years (153.5 μmol/L *vs* 111 μmol/L, P = 0.019). The incidence of diabetes and hypertension were numerically higher in the obese group at 1 and 5 years, however, this difference was statistically insignificant. Further, the incidence of cardiovascular events was also not significantly different among the two groups. Further expansion of follow-up to 10 years might show a statistically meaningful difference. However, this analysis was not possible in the current study. Given the selection criteria with the start of the study from November 2012, none of the patients has achieved the 10-year benchmark yet.

This study has been limited by its retrospective design, smaller sample size, and lack of a comparison group from a non-NASH subset. We also acknowledge the limitation of missing data given the retrospective design, transfer of care to other local centres post-transplant, and a limited number of patients achieving the 5-year benchmark. The results of this study should be interpreted cautiously as it does not suggest the listing of all morbidly obese NASH cirrhotic patients for liver transplant. Nonetheless, under current practice, outcomes of carefully selected NASH patients with higher BMI are better than their lean counterparts. This conundrum could have been explained by improvement in patient selection protocols, post-transplant critical care support, and immunosuppressive treatment. Future larger studies would be required to validate the generalizability of our findings. Moreover, there is need of identifying the factors such as genetic variants, and body fat distribution/visceral adiposity, which can play role in this paradox.

CONCLUSION

Lean NASH is associated with adverse outcomes on the waiting list as well as early post-transplant, in

Table 3 Post transplant outcomes

	Total (n = 111)	BMI after ascites correction		P value
		Overweight or obese (n = 82)	Underweight or normal (n = 29)	
Biliary stricture, n (%)	22 (19.8)	16 (19.5)	6 (20.7)	0.97
Biliary leak, n (%)	10 (9)	7 (8.5)	3 (10.3)	1.0
Hepatic artery thrombosis, n (%)	2 (1.8)	0 (0)	2 (6.9)	0.07
90-d re-hospitalization (n = 103), n (%)	23 (22.3)	17 (22.6)	6 (21.4)	0.89
Recurrent NAFLD, n (%)	57 (51.4)	44 (53.7)	13 (44.8)	0.59
Time to recurrent NAFLD, median (range) days	568 (13–2135)	489 (13–1821)	757 (80–2135)	0.21
Recurrent NASH, n (%)	7 (6.3)	5 (6.1)	2 (6.9)	1.0
Time to recurrent NASH, median (range) days	812 (363–1119)	802 (363–1119)	957.5 (812–1103)	0.28
BMI at 1 yr (n = 83), median (range) kg/m^2	30.3 (19.2–44.0)	31.7 (23.2–44.0)	26.1 (19.2–34.2)	< 0.001[c]
BMI at 5 yr (n = 17), median (range) kg/m^2	33.9 (20.3–47.9)	35.1 (26.6 – 47.9)	27.0 (20.3–31.5)	0.004[b]
Creatinine at 1 yr (n = 70), median (range) μmol/L	114.0 (54.0–279.0)	117.5 (63.0–279.0)	106.0 (54.0–178.0)	0.21
Creatinine at 5 yr (n = 19), median (range) μmol/L	143.0 (67.0-257.0)	153.5 (78.0–257.0)	111.0 (67.0–127.0)	0.019[a]
Diabetes at 1 yr (n = 82), n (%)	36 (43.9)	27 (45.8)	9 (39.1)	0.59
Diabetes at 5 yr (n = 20), n (%)	10 (50)	8 (53.3)	2 (40)	0.72
Hypertension at 1 yr (n = 83), n (%)	44 (53)	33 (55)	11 (47.8)	0.56
Hypertension at 5 yr (n = 20), n (%)	12 (60)	10 (66.7)	2 (40)	0.35
Cardiovascular events post LT, n (%)	22 (19.8)	14 (17)	8 (27.6)	0.45
Fibroscan Elastography (n = 48), median (range) kPa	6.4 (2.3–21.8)	6.8 (3.5–21.8)	4.8 (2.3–14.5)	0.011[a]
Fibroscan CAP (n = 48), median (range) dB/m	286.5 (181.0–400.0)	298.0 (198.0–400.0)	283.5 (181.0–400.0)	0.26
Graft loss within 90 d post LT, n (%)	5 (4.5)	1 (1.2)	4 (13.8)	0.032[a]
Graft survival post LT 1 yr (n = 101), n (%)	94 (93.1)	72 (98.6)	22 (78.6)	0.002[b]
Graft survival post LT 3 yr (n = 72), n (%)	65 (90.3)	48 (96)	17 (77.3)	0.025[a]
Graft survival post LT 5 yr (n = 32), n (%)	22 (68.8)	17 (85)	5 (41.7)	0.018[a]
Deaths post LT, n (%)	7 (6.3)	2 (2.4)	5 (17.2)	0.029[a]
Time to death post LT (n = 7), median (range) days	224 (13–1176)	192.5 (20–365)	224 (13–1176)	0.42
Death within 90 d post-LT, n (%)	2 (1.8)	1 (1.2)	1 (3.4)	0.38
Patient survival at 1 yr (n = 108), n (%)	104 (96.3)	78 (98.7)	26 (89.7)	0.06
Patient survival at 3 yr (n = 97), n (%)	66 (91.7)	48 (96)	18 (81.8)	0.07
Patient survival at 5 yr (n = 32), n (%)	25 (78.1)	18 (90)	7 (58.3)	0.07

[a]P < 0.05.
[b]P < 0.01.
[c]P < 0.001.
BMI: Body mass index; CAP: Controlled attenuation parameter; LT: Liver transplant; NAFLD: Non-alcoholic fatty liver disease; NASH: Non-alcoholic steatohepatitis.

conjunction with often comorbid frailty. Our study emphasizes the need to actively support the nutritional and physical functional status of lean NASH patients on the waiting list. Post-transplant, all NASH patients should have active lifestyle counselling regarding a healthy diet and regular exercise to improve long-term cardiometabolic outcomes.

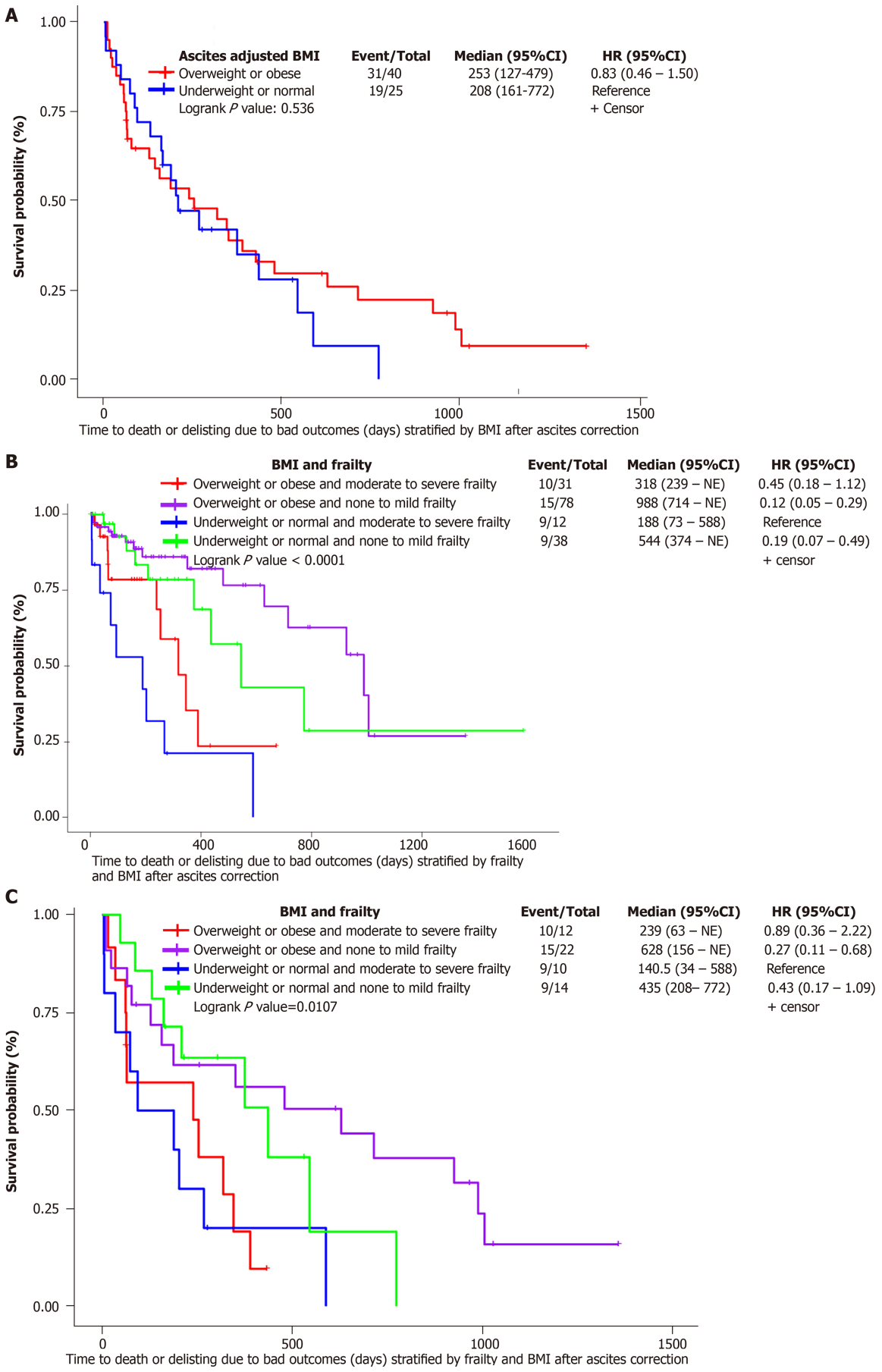

DOI: 10.3748/wjg.v28.i26.3218

Figure 1 Kaplan-Meier–overall survival: Time to delisting or death on waitlist. A: Ascites adjusted body mass index (BMI) groups (non-transplanted

patients only); B: Ascites adjusted BMI and frailty (full cohort); C: Ascites adjusted BMI and frailty (non-transplanted patients only). HR: Hazard ratio; BMI: Body mass index.

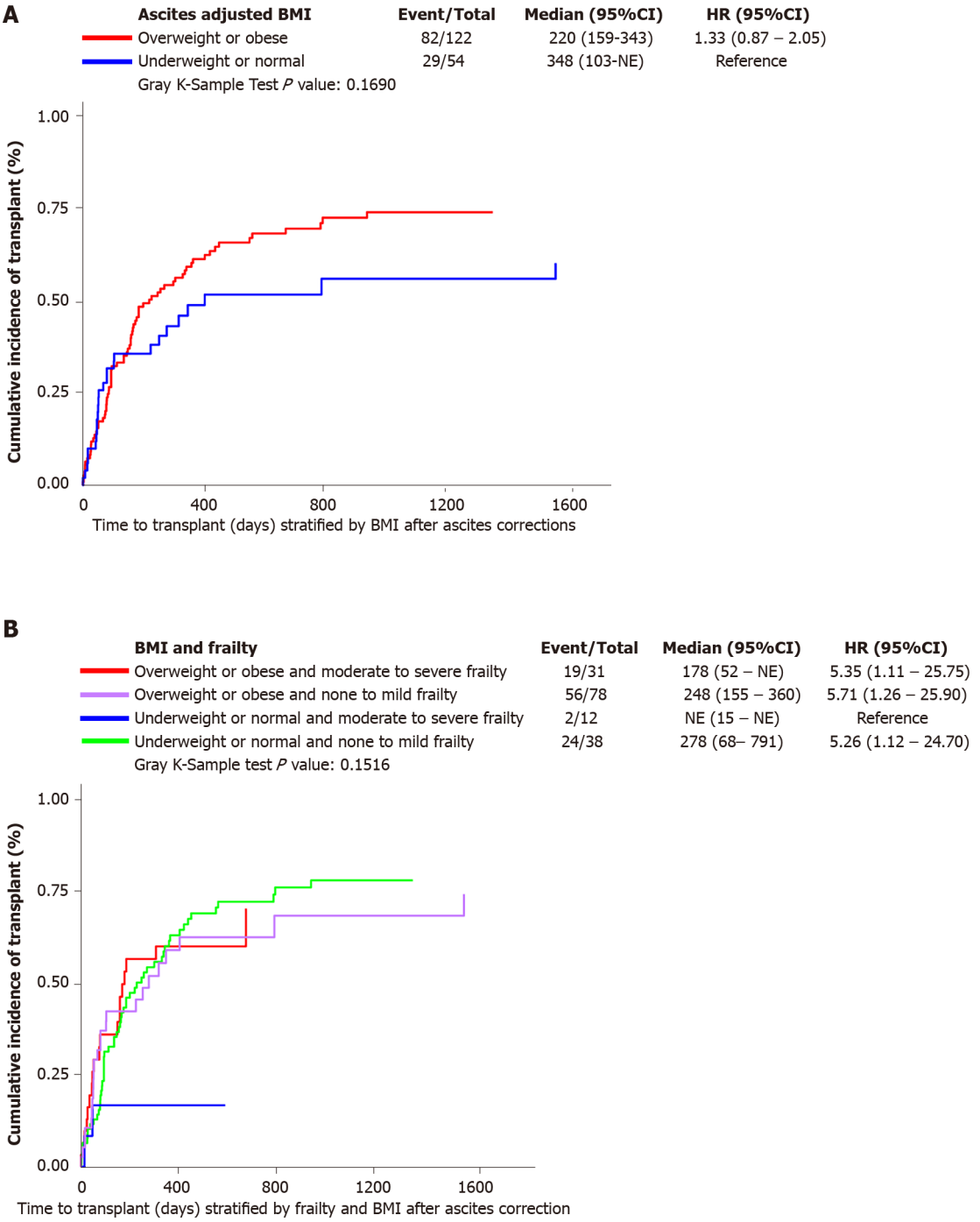

DOI: 10.3748/wjg.v28.i26.3218

Figure 2 Competing risk analysis for time to transplant. A: Ascites adjusted body mass index (BMI) groups; B: Ascites adjusted BMI and frailty. HR: Hazard ratio; BMI: Body mass index.

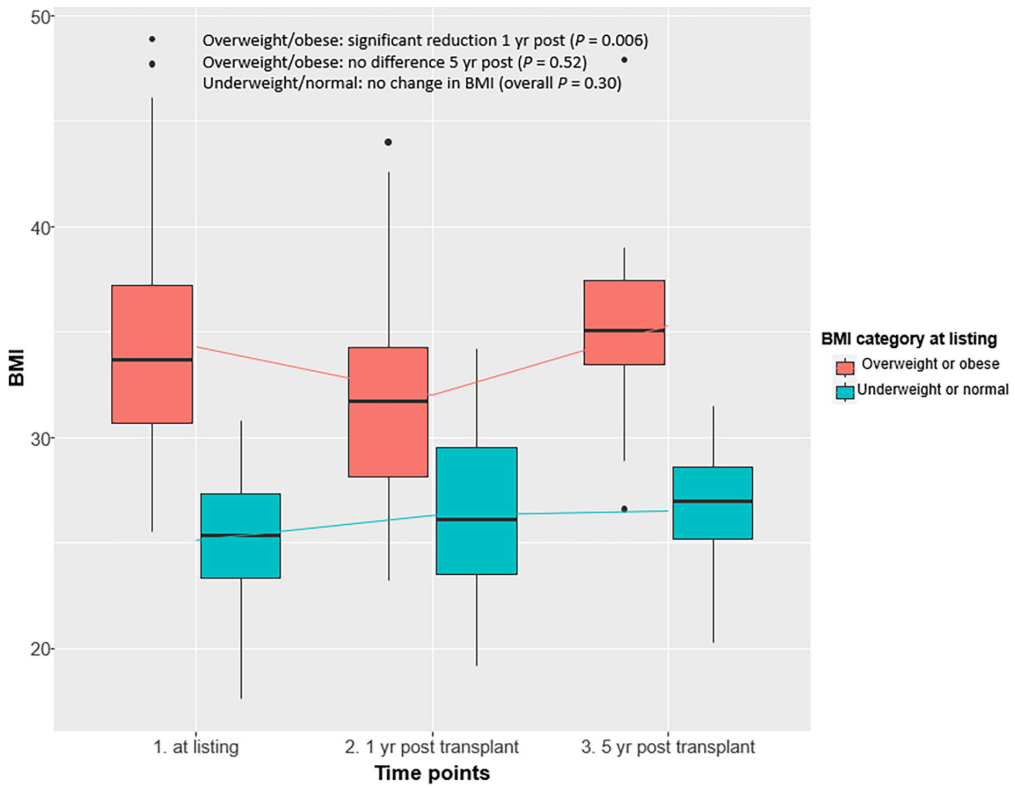

DOI: 10.3748/wjg.v28.i26.3218

Figure 3 Change in body mass index from time of listing to post liver transplant at 1 and 5 yr. BMI: Body mass index.

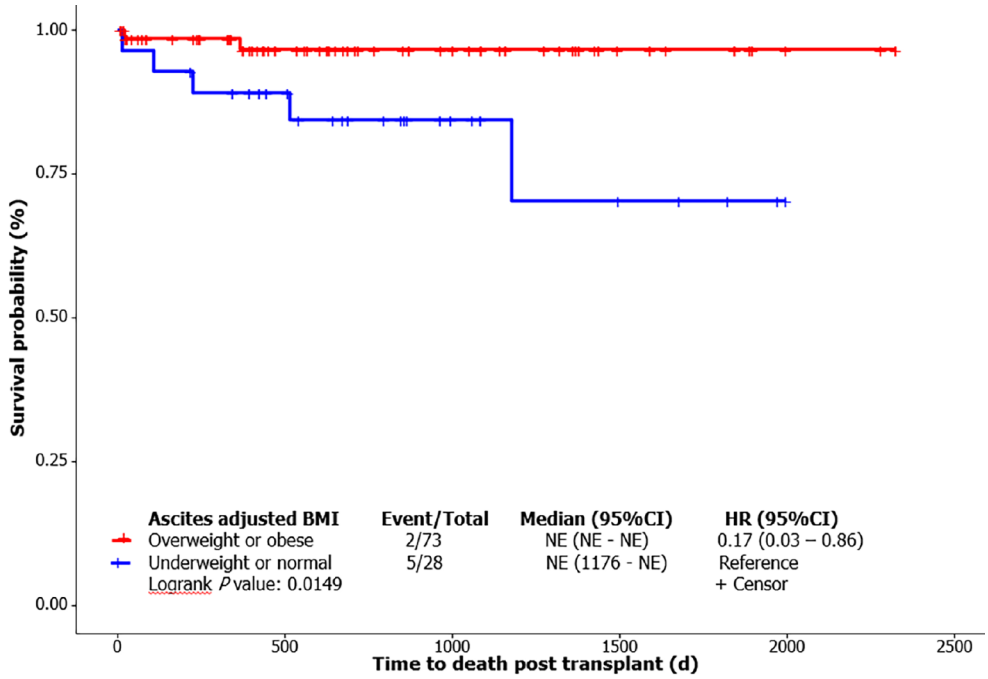

Survival estimations (95%CI)	Overweight or obese	Underweight or normal	*P* value
1 yr	96.7% (92.2% - 100%)	89.1% (78.3% - 100%)	0.13
5 yr	96.7% (92.2% - 100%)	70.4% (47.4% - 100%)	0.01

DOI: 10.3748/wjg.v28.i26.3218

Figure 4 Kaplan-Meier–overall survival: Time to death post liver transplant stratified by ascites adjusted body mass index groups. Lower panel shows the 1- and 5-yr survival estimates. HR: Hazard ratio; BMI: Body mass index.

ARTICLE HIGHLIGHTS

Research background

Non-alcoholic steatohepatitis (NASH) cirrhosis is the second leading indication for liver transplantation (LT). There is a conflicted role of body mass index (BMI) on outcomes of NASH cirrhosis while on waitlist and post liver transplant.

Research motivation

There are few reports on the waitlist and post liver transplant outcomes of lean *vs* obese NASH patients, and the impact of ascites adjusted BMI have not been fully clarified.

Research objectives

The objective of this study was to compare the longitudinal trajectories of patients with lean *vs* obese NASH cirrhosis, from listing up to post-transplant, having adjusted their BMI for ascites.

Research methods

A retrospective analysis of all adult NASH patients listed for LT at the University Health Network, Toronto between November 2012 and May 2019 was performed. We summarized the clinical characteristics of patients with lean and obese NASH. Competing risk analyses and Cox Proportional Hazard models were used to assess the cumulative incidence of transplant and survival outcomes.

Research results

Out of 265 patients listed for NASH cirrhosis, 176 were included. The median age was 61 (32–71.4) years; 46% were females. 111 patients underwent LT. Lean NASH patients were elderly at time of listing (median age 61.6 years *vs* 60.3 years, P = 0.048), worse renal functions at end of listing (median estimated glomerular filtration 48 mL/min/1.73 m^2 *vs* 57 mL/min/1.73 m^2, P = 0.017), carried more severe ascites (66.6% *vs* 45%, P = 0.03) and were more paracentesis dependent (72.2% *vs* 52.9%, P = 0.016). Obese robust patients had better waitlist survival [hazard ratio (HR): 0.12; 95%CI: 0.05–0.29, P < 0.0001] with higher instantaneous rate of transplant (HR: 5.71; 95%CI: 1.26–25.9, P = 0.02). Lean NASH patients had a substantially higher risk of graft loss within 90 d post-LT (1.2% *vs* 13.8%, P = 0.032) and death post-LT (2.4% *vs* 17.2%, P = 0.029). 1- 3- and 5-year graft survival was poor for lean NASH (78.6%, 77.3% and 41.7% *vs* 98.6%, 96% and 85% respectively). Overall patient survival post-LT was significantly worse in lean NASH (HR: 0.17; 95%CI: 0.03–0.86, P = 0.0142) with 83% lower instantaneous rate of death in obese group. Post-transplant renal function was significantly better in lean NASH patients at 5 years (median creatinine 111 μmol/L *vs* 153.5 μmol/L, P = 0.019).

Research conclusions

Although lean NASH was thought to be more benign than obese NASH, our study suggests a paradoxical correlation of lean NASH with waitlist outcomes, and graft and patient survival post-LT, in conjunction with often comorbid frailty.

Research perspectives

To understand the underlying molecular mechanisms linking lean NASH with worse outcomes, there is need of identifying the factors such as genetic variants, body fat distribution/visceral adiposity, which can play role in this paradox.

FOOTNOTES

Author contributions: Qazi-Arisar FA and Uchila R given their equal contribution in the manuscript; Bhat M was the guarantor and designed the study; Qazi-Arisar FA, Uchila R, Chen C, Yang C, Chen SY, Karnam RS and Azhie A participated in the acquisition, analysis, and interpretation of the data, and drafted the initial manuscript; Qazi-Arisar FA, Xu W, Galvin Z, Selzner N, Lilly L and Bhat M revised the article critically for important intellectual content.

Institutional review board statement: The study was reviewed and approved by the Research Ethics board of the University Health Network (Toronto, Canada).

Informed consent statement: Given retrospective nature of study from chart review, written informed consent was not required.

Conflict-of-interest statement: Dr. Bhat reports other from Novo Nordisk, other from Ipsen, grants from Paladin, grants from Natera, grants from Oncoustics, grants from MedoAI, grants from Lallemand, personal fees from Novartis, personal fees from Lupin, outside the submitted work.

Data sharing statement: No additional data are available.

STROBE statement: The authors have read the STROBE Statement—checklist of items, and the manuscript was prepared and revised according to the STROBE Statement—checklist of items.

Country/Territory of origin: Canada

ORCID number: Mamatha Bhat 0000-0003-1960-8449.

Corresponding Author's Membership in Professional Societies: American Association for the Study of Liver Diseases.

S-Editor: Fan JR
L-Editor: A
P-Editor: Yu HG

REFERENCES

1 **Parikh ND**, Marrero WJ, Wang J, Steuer J, Tapper EB, Konerman M, Singal AG, Hutton DW, Byon E, Lavieri MS. Projected increase in obesity and non-alcoholic-steatohepatitis-related liver transplantation waitlist additions in the United States. *Hepatology* 2019; **70**: 487-495 [PMID: 28833326 DOI: 10.1002/hep.29473]

2 **Vernon G**, Baranova A, Younossi ZM. Systematic review: the epidemiology and natural history of non-alcoholic fatty liver disease and non-alcoholic steatohepatitis in adults. *Aliment Pharmacol Ther* 2011; **34**: 274-285 [PMID: 21623852 DOI: 10.1111/j.1365-2036.2011.04724.x]

3 **Non-alcoholic Fatty Liver Disease Study Group**, Lonardo A, Bellentani S, Argo CK, Ballestri S, Byrne CD, Caldwell SH, Cortez-Pinto H, Grieco A, Machado MV, Miele L, Targher G. Epidemiological modifiers of non-alcoholic fatty liver disease: Focus on high-risk groups. *Dig Liver Dis* 2015; **47**: 997-1006 [PMID: 26454786 DOI: 10.1016/j.dld.2015.08.004]

4 **Young S**, Tariq R, Provenza J, Satapathy SK, Faisal K, Choudhry A, Friedman SL, Singal AK. Prevalence and Profile of Nonalcoholic Fatty Liver Disease in Lean Adults: Systematic Review and Meta-Analysis. *Hepatol Commun* 2020; **4**: 953-972 [PMID: 32626829 DOI: 10.1002/hep4.1519]

5 **Hagström H**, Nasr P, Ekstedt M, Hammar U, Stål P, Hultcrantz R, Kechagias S. Risk for development of severe liver disease in lean patients with nonalcoholic fatty liver disease: A long-term follow-up study. *Hepatol Commun* 2018; **2**: 48-57 [PMID: 29404512 DOI: 10.1002/hep4.1124]

6 **Cruz ACD**, Bugianesi E, George J, Day CP, Liaquat H, Charatcharoenwitthaya P, Mills PR, Dam-Larsen S, Bjornsson ES, Haflidadottir S, Adams LA, Bendtsen F, Angulo P. Characteristics and Long-Term Prognosis of Lean Patients With Nonalcoholic Fatty Liver Disease. *Gastroenterology* 2014; **146**: S-909 [DOI: 10.1016/s0016-5085(14)63307-2]

7 **Satapathy SK**, Jiang Y, Agbim U, Wu C, Bernstein DE, Teperman LW, Kedia SK, Aithal GP, Bhamidimarri KR, Duseja A, Maiwall R, Maliakkal B, Jalal P, Patel K, Puri P, Ravinuthala R, Wong VW, Abdelmalek MF, Ahmed A, Thuluvath PJ, Singal AK; Global NAFLD Consortium. Posttransplant Outcome of Lean Compared With Obese Nonalcoholic Steatohepatitis in the United States: The Obesity Paradox. *Liver Transpl* 2020; **26**: 68-79 [PMID: 31665561 DOI: 10.1002/lt.25672]

8 **Wang Q**, You H, Ou X, Zhao X, Sun Y, Wang M, Wang P, Wang Y, Duan W, Wang X, Wu S, Kong Y, Saxena R, Gouw ASH, Jia J. Non-obese histologically confirmed NASH patients with abnormal liver biochemistry have more advanced fibrosis. *Hepatol Int* 2019; **13**: 766-776 [PMID: 31559605 DOI: 10.1007/s12072-019-09982-z]

9 **Leonard J**, Heimbach JK, Malinchoc M, Watt K, Charlton M. The impact of obesity on long-term outcomes in liver transplant recipients-results of the NIDDK liver transplant database. *Am J Transplant* 2008; **8**: 667-672 [PMID: 18294163 DOI: 10.1111/j.1600-6143.2007.02100.x]

10 **European Association for the Study of the Liver**. EASL Clinical Practice Guidelines on nutrition in chronic liver disease. *J Hepatol* 2019; **70**: 172-193 [PMID: 30144956 DOI: 10.1016/j.jhep.2018.06.024]

11 **Tandon P**, Low G, Mourtzakis M, Zenith L, Myers RP, Abraldes JG, Shaheen AA, Qamar H, Mansoor N, Carbonneau M, Ismond K, Mann S, Alaboudy A, Ma M. A Model to Identify Sarcopenia in Patients With Cirrhosis. *Clin Gastroenterol Hepatol* 2016; **14**: 1473-1480.e3 [PMID: 27189915 DOI: 10.1016/j.cgh.2016.04.040]

12 **Fracanzani AL**, Petta S, Lombardi R, Pisano G, Russello M, Consonni D, Di Marco V, Cammà C, Mensi L, Dongiovanni P, Valenti L, Craxì A, Fargion S. Liver and Cardiovascular Damage in Patients With Lean Nonalcoholic Fatty Liver Disease, and Association With Visceral Obesity. *Clin Gastroenterol Hepatol* 2017; **15**: 1604-1611.e1 [PMID: 28554682 DOI: 10.1016/j.cgh.2017.04.045]

13 **Akyuz U**, Yesil A, Yilmaz Y. Characterization of lean patients with nonalcoholic fatty liver disease: potential role of high hemoglobin levels. *Scand J Gastroenterol* 2015; **50**: 341-346 [PMID: 25540973 DOI: 10.3109/00365521.2014.983160]

14 **Margariti A**, Deutsch M, Manolakopoulos S, Tiniakos D, Papatheodoridis GV. The severity of histologic liver lesions is independent of body mass index in patients with nonalcoholic fatty liver disease. *J Clin Gastroenterol* 2013; **47**: 280-286

[PMID: 23391869 DOI: 10.1097/MCG.0b013e31826be328]

15 **Kardashian AA**, Dodge JL, Roberts J, Brandman D. Weighing the risks: Morbid obesity and diabetes are associated with increased risk of death on the liver transplant waiting list. *Liver Int* 2018; **38**: 553-563 [PMID: 28727287 DOI: 10.1111/liv.13523]

16 **Bhanji RA**, Narayanan P, Moynagh MR, Takahashi N, Angirekula M, Kennedy CC, Mara KC, Dierkhising RA, Watt KD. Differing Impact of Sarcopenia and Frailty in Nonalcoholic Steatohepatitis and Alcoholic Liver Disease. *Liver Transpl* 2019; **25**: 14-24 [PMID: 30257063 DOI: 10.1002/lt.25346]

17 **Dolgin NH**, Smith AJ, Harrington SG, Movahedi B, Martins PNA, Bozorgzadeh A. Association Between Sarcopenia and Functional Status in Liver Transplant Patients. *Exp Clin Transplant* 2019; **17**: 653-664 [PMID: 30295589 DOI: 10.6002/ect.2018.0018]

18 **Kahn J**, Wagner D, Homfeld N, Müller H, Kniepeiss D, Schemmer P. Both sarcopenia and frailty determine suitability of patients for liver transplantation-A systematic review and meta-analysis of the literature. *Clin Transplant* 2018; **32**: e13226 [PMID: 29478305 DOI: 10.1111/ctr.13226]

19 **Van Jacobs AC**. Frailty Assessment in Patients with Liver Cirrhosis. *Clin Liver Dis (Hoboken)* 2019; **14**: 121-125 [PMID: 31632663 DOI: 10.1002/cld.825]

20 **Lai JC**, Feng S, Terrault NA, Lizaola B, Hayssen H, Covinsky K. Frailty predicts waitlist mortality in liver transplant candidates. *Am J Transplant* 2014; **14**: 1870-1879 [PMID: 24935609 DOI: 10.1111/ajt.12762]

21 **Lai JC**, Dodge JL, Sen S, Covinsky K, Feng S. Functional decline in patients with cirrhosis awaiting liver transplantation: Results from the functional assessment in liver transplantation (FrAILT) study. *Hepatology* 2016; **63**: 574-580 [PMID: 26517301 DOI: 10.1002/hep.28316]

22 **Wang CW**, Covinsky KE, Feng S, Hayssen H, Segev DL, Lai JC. Functional impairment in older liver transplantation candidates: From the functional assessment in liver transplantation study. *Liver Transpl* 2015; **21**: 1465-1470 [PMID: 26359787 DOI: 10.1002/lt.24334]

23 **Lai JC**, Rahimi RS, Verna EC, Kappus MR, Dunn MA, McAdams-DeMarco M, Haugen CE, Volk ML, Duarte-Rojo A, Ganger DR, O'Leary JG, Dodge JL, Ladner D, Segev DL. Frailty Associated With Waitlist Mortality Independent of Ascites and Hepatic Encephalopathy in a Multicenter Study. *Gastroenterology* 2019; **156**: 1675-1682 [PMID: 30668935 DOI: 10.1053/j.gastro.2019.01.028]

24 **Haugen CE**, McAdams-DeMarco M, Verna EC, Rahimi RS, Kappus MR, Dunn MA, Volk ML, Gurakar A, Duarte-Rojo A, Ganger DR, O'Leary JG, Ladner D, Garonzik-Wang J, Segev DL, Lai JC. Association Between Liver Transplant Wait-list Mortality and Frailty Based on Body Mass Index. *JAMA Surg* 2019; **154**: 1103-1109 [PMID: 31509169 DOI: 10.1001/jamasurg.2019.2845]

25 **VanWagner LB**, Armstrong MJ. Lean NAFLD: A not so benign condition? *Hepatol Commun* 2018; **2**: 5-8 [PMID: 29404505 DOI: 10.1002/hep4.1143]

26 **Nair S**, Verma S, Thuluvath PJ. Obesity and its effect on survival in patients undergoing orthotopic liver transplantation in the United States. *Hepatology* 2002; **35**: 105-109 [PMID: 11786965 DOI: 10.1053/jhep.2002.30318]

27 **Kovalic AJ**, Cholankeril G, Satapathy SK. Nonalcoholic fatty liver disease and alcoholic liver disease: metabolic diseases with systemic manifestations. *Transl Gastroenterol Hepatol* 2019; **4**: 65 [PMID: 31620647 DOI: 10.21037/tgh.2019.08.09]

28 **Chon YE**, Kim HJ, Choi YB, Hwang SG, Rim KS, Kim MN, Lee JH, Ha Y, Lee MJ. Decrease in waist-to-hip ratio reduced the development of chronic kidney disease in non-obese non-alcoholic fatty liver disease. *Sci Rep* 2020; **10**: 8996 [PMID: 32488147 DOI: 10.1038/s41598-020-65940-y]

29 **Zhou J**, Lyu L, Zhu L, Liang Y, Dong H, Chu H. Association of overweight with postoperative acute kidney injury among patients receiving orthotopic liver transplantation: an observational cohort study. *BMC Nephrol* 2020; **21**: 223 [PMID: 32527305 DOI: 10.1186/s12882-020-01871-0]

30 **Locke JE**, Shelton B, Orandi B, Olthoff K, Pomfret E, Forde KA, Sawinski D, Gray M, Ascher N. Obesity is a risk factor for progression to kidney transplant waitlisting after liver transplantation. *Clin Transplant* 2021; **35**: e14317 [PMID: 33866616 DOI: 10.1111/ctr.14317]

World Journal of Gastroenterology

Submit a Manuscript: https://www.f6publishing.com

World J Gastroenterol 2022 July 14; 28(26): 3232-3242

DOI: 10.3748/wjg.v28.i26.3232

ISSN 1007-9327 (print) ISSN 2219-2840 (online)

ORIGINAL ARTICLE

Retrospective Study

Tumor-feeding artery diameter reduction is associated with improved short-term effect of hepatic arterial infusion chemotherapy plus lenvatinib treatment

De-Di Wu, Xiao-Feng He, Chen Tian, Peng Peng, Chuan-Li Chen, Xue-Han Liu, Hua-Jin Pang

Specialty type: Gastroenterology and hepatology

Provenance and peer review: Unsolicited article; Externally peer reviewed.

Peer-review model: Single blind

Peer-review report's scientific quality classification

Grade A (Excellent): 0
Grade B (Very good): B
Grade C (Good): C
Grade D (Fair): 0
Grade E (Poor): 0

P-Reviewer: Dilek ON, Turkey; Tsoulfas G, Greece

Received: January 22, 2022
Peer-review started: January 22, 2022
First decision: March 8, 2022
Revised: March 17, 2022
Accepted: June 18, 2022
Article in press: June 18, 2022
Published online: July 14, 2022

De-Di Wu, Xiao-Feng He, Chen Tian, Peng Peng, Hua-Jin Pang, Division of Vascular and Interventional Radiology, Department of General Surgery, Nanfang Hospital, Southern Medical University, Guangzhou 510515, Guangdong Province, China

Chuan-Li Chen, Medical Imaging Center, Nanfang Hospital, Southern Medical University, Guangzhou 510515, Guangdong Province, China

Xue-Han Liu, Department of Statistics, Huazhong University of Science and Technology, Wuhan 430000, Hubei Province, China

Corresponding author: Hua-Jin Pang, PhD, Associate Chief Physician, Associate Professor, Division of Vascular and Interventional Radiology, Department of General Surgery, Nanfang Hospital, Southern Medical University, No. 1838 North Baiyun Avenue, Guangzhou 510515, Guangdong Province, China. nfyyphj@163.com

Abstract

BACKGROUND

Recently, hepatic arterial infusion chemotherapy (HAIC) plus lenvatinib has been frequently used to treat unresectable hepatocellular carcinoma (uHCC) in China. In the clinic, the hepatic arteries of some patients shrink significantly during this treatment, leading to improved short-term efficacy.

AIM

To investigate the relationship between the shrinkage of hepatic arteries and the short-term effect of HAIC plus lenvatinib treatment.

METHODS

Sixty-seven participants with uHCC were enrolled in this retrospective study. The patients received HAIC every 3 wk, followed by oral lenvatinib after the first HAIC course. Hepatic artery diameters were measured on CT before treatment and after 1 and 2 mo of treatment. Meanwhile, the changes in tumor capillaries were also examined on pathological specimens before and after 1 mo of treatment. The antitumor response after 1, 3, and 6 mo of treatment was assessed using the modified Response Evaluation Criteria in Solid Tumors (mRECIST). The relationship between the changes in vessel diameters and the short-term effect of the combination treatment was evaluated by receiver-operating characteristic and

logistic regression analyses.

RESULTS

The hepatic artery diameters were all significantly decreased after 1 and 2 mo of treatment (P < 0.001), but there was no difference in the vessel diameters between 1 and 2 mo (P > 0.05). The microvessel density in the tumor lesions decreased significantly after 1 mo of combination treatment (P < 0.001). According to mRECIST, 46, 41, and 24 patients had complete or partial responses after 1, 3, and 6 mo of treatment, respectively, whereas 21, 21, and 32 patients had a stable or progressive disease at these times, respectively. Shrinkage of the tumor-feeding artery was significantly associated with the tumor response after 1, 3, and 6 mo of treatment (P < 0.001, P = 0.004, and P = 0.023, respectively); however, changes in other hepatic arteries were not significantly associated with the tumor response. Furthermore, shrinkage of the tumor-feeding artery was an independent factor for treatment efficacy (P = 0.001, P = 0.001, and P = 0.002 and 1, 3, and 6 mo, respectively).

CONCLUSION

The hepatic arteries shrank rapidly after treatment with HAIC plus lenvatinib, and shrinkage of the tumor-feeding artery diameter was closely related to improved short-term efficacy.

Key Words: Hepatocellular carcinoma; Hepatic arterial infusion chemotherapy; Lenvatinib; Short-term effect; Hepatic artery; Vessel diameter

Core Tip: In this study, it was observed for the first time that the hepatic arteries shrank rapidly after hepatic arterial infusion chemotherapy plus lenvatinib therapy, and the close relationship between shrinkage of the tumor-feeding artery and improved short-term effect in patients with unresectable hepatocellular carcinoma was also confirmed. These findings would be of great significance to physicians for evaluating the effectiveness of this combination therapy earlier in the course of treatment and altering the treatment plan as needed.

Citation: Wu DD, He XF, Tian C, Peng P, Chen CL, Liu XH, Pang HJ. Tumor-feeding artery diameter reduction is associated with improved short-term effect of hepatic arterial infusion chemotherapy plus lenvatinib treatment. *World J Gastroenterol* 2022; 28(26): 3232-3242

URL: https://www.wjgnet.com/1007-9327/full/v28/i26/3232.htm

DOI: https://dx.doi.org/10.3748/wjg.v28.i26.3232

INTRODUCTION

Hepatocellular carcinoma (HCC) is one of the most common malignant tumors, with 850000 new cases reported per year worldwide[1,2]. In total, 70%-80% of patients with HCC in China are ineligible for surgical resection at the time of onset[3]. Recently, hepatic arterial infusion chemotherapy (HAIC) has been increasingly used to treat patients with unresectable HCC (uHCC) in Asian countries[4,5]. HAIC is recommended as a major treatment option in patients with intermediate and advanced HCC by current Japanese and Chinese guidelines[6].

Lenvatinib is an oral multi-target tyrosine kinase inhibitor (TKI) with antiangiogenic effects. Previous studies demonstrated the survival benefit of lenvatinib plus HAIC *vs* lenvatinib alone in patients with advanced HCC[7]. This combination therapy often requires 6-8 cycles, and early assessment of the antitumor response appears essential for both patients and physicians[8].

Recently, a clinical study demonstrated that the diameters of hepatic arteries are significantly reduced after TKI therapy[9]. Since the early imaging response is often associated with survival benefits, it should be clarified whether the changes in hepatic vessel diameters are related to the efficacy of HAIC combined with lenvatinib. As a result, we conducted a retrospective study of patients with uHCC treated with HAIC plus lenvatinib. The aim of this study was to: (1) Explore the changes in hepatic arteries after combination treatment; and (2) Determine the relationship between the hepatic artery changes and early therapeutic effects.

MATERIALS AND METHODS

Patient eligibility

This was a single-center, retrospective analysis of data from 67 patients with uHCC treated at our institution from January 2019 to October 2020. Approval for the study was obtained from the local ethics committee on human research. The HCC diagnosis was based on the findings of pathological, imaging, and clinical assessments using the European Association for the Study of the Liver criteria[10]. Eligible patients were those aged 18 years or older with uHCC (including patients with large/multifocal HCC and/or with vascular invasion and extrahepatic spread) who received HAIC plus lenvatinib as an initial treatment. Patients who underwent transcatheter arterial chemoembolization or received other TKIs before combination therapy were excluded. Enrolled patients who discontinued treatment during the follow-up period were also excluded.

Treatments

HAIC was repeated at an interval of 3 wk in enrolled patients in our hospital. A catheter was initially advanced into the celiac or superior mesenteric artery for digital subtraction angiography from the femoral artery; then, a microcatheter was left in the tumor-feeding artery (TFA) for subsequent treatment.

The patients received the following regimen for HAIC through the indwelling microcatheter connected to an artery infusion pump in the ward: oxaliplatin 85 mg/m^2 administered intraarterially for 2 h, leucovorin 400 mg/m^2 administered intraarterially for 1 h, and 5FU 400 mg/m^2 intra-arterial bolus injection on day 1, followed by 5FU 2400 mg/m^2 continuous arterial infusion for 46 h. Three days after the first HAIC course, patients began to take lenvatinib (Eisai, Tokyo, Japan) orally at the recommended doses of 12 mg/day for patients weighing ≥ 60 kg and 8 mg/day for patients weighing < 60 kg[11]. Dose adjustment or termination of lenvatinib therapy was allowed when drug-related adverse events (AEs) occurred. Discontinuation of the combination treatment was also allowed for potentially fatal AEs, clinical tumor progression, or the need for conversion therapy.

Evaluations and measurement

Therapeutic responses after 1, 3, and 6 mo of combination treatment were assessed according to the modified Response Evaluation Criteria in Solid Tumors using CT (Philips Brilliance iCT; Philips Medical Systems, Best, the Netherlands) images. Treatment responders were defined as patients with a complete response (CR) or partial response (PR). Non-responders were defined as patients with stable disease (SD) or progressive disease (PD). AEs were assessed using the Common Terminology Criteria for Adverse Events (CTCAE) version 5.0[12].

Epigastric enhanced CT Digital Imaging and Communication of Medicine (DICOM) data were collected before treatment and after 1 and 2 mo of treatment and introduced into an image post-processing workstation (Philips IntelliSpace Portal; Koninklijke Philips N.V., Eindhoven, the Netherlands) for three-dimensional reconstruction. On the image post-processing workstation, multiplanar reconstruction images centered on the contrast-enhanced hepatic arteries and the centerline (CLL) of the blood vessels were generated by the software to straighten the curved arteries. The trunk or the thickest branch of the TFA was selected as the object of measurement. The CLL was adjusted manually to measure the largest diameter of the arteries. The diameters of the opening of the common hepatic artery (CHA), proper hepatic artery (PHA), left hepatic artery (LHA), right hepatic artery (RHA), and TFA were further measured by manually drawing the region of interest (Figure 1)[13]. The change in vessel diameters was defined and calculated using the following formula: $\Delta_{artery} = (D_{post} - \Delta_{pre}) / \Delta_{pre}$ (Δ_{artery}: The rate of change in the diameter of CHA, PHA, LHA, RHA, or TFA; D_{pre}: The vessel diameter before combination treatment; D_{post}: The vessel diameter after combination treatment).

Both the measurement of artery diameters and the evaluation of therapeutic efficacy were individually conducted by two physicians with experience in gastroenterological diagnostics, and differences were resolved by a more experienced physician.

Immunohistochemistry

Tumor angiogenesis was evaluated by measuring microvessel density (MVD) after staining using an anti-CD34 antibody. Punch biopsy samples were obtained from tumor lesions before and 1 mo after the start of HAIC plus lenvatinib therapy. The tumor samples were fixed in 10% formalin and embedded in paraffin. After routine laboratory procedures, immunohistochemistry was performed to detect the expression of CD34 (endothelial cell marker) through the avidin–biotin–peroxidase complex[14,15]. MVD was measured at × 100 magnification in five regions of interest using a light microscope. All endothelial cells, including individual cells and grouped cells, were counted as a single vessel if they were separated from the surrounding tumor and other connective tissues[16].

Statistical analysis

Statistical analyses were performed using IBM SPSS Statistics 26.0. The measurement data were presented as the mean ± SD, and $P < 0.05$ indicated statistical significance. Considering the loss to

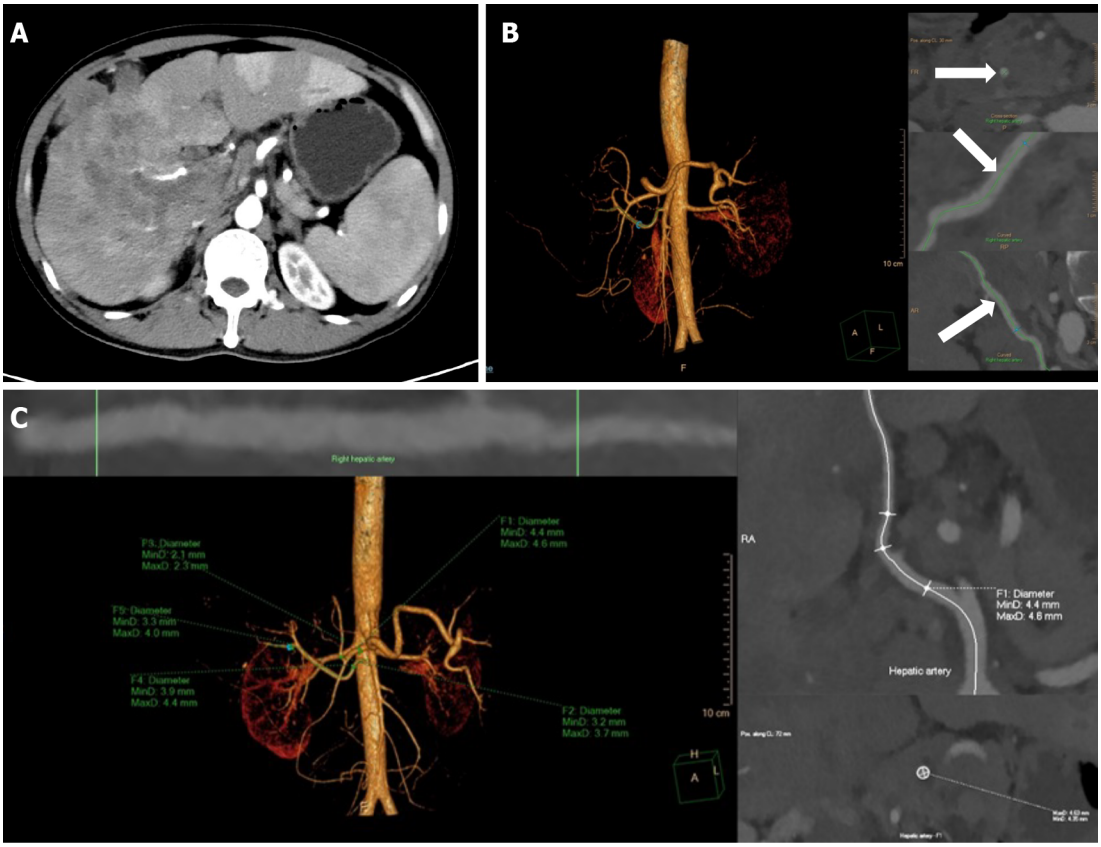

DOI: 10.3748/wjg.v28.i26.3232

Figure 1 Reconstruction and measurement of the hepatic arteries. A: The thickest branch of tumor-feeding arteries generated from the right hepatic artery; B: Three-dimensional reconstruction of hepatic arteries in an image post-processing workstation and the adjustment of center line (arrows) on multiple layers; C: The hepatic artery diameters are measured automatically by drawing the region of interest. F1-5, the opening of the common hepatic artery, the proper hepatic artery, the left hepatic artery, the right hepatic artery and the tumor-feeding artery.

follow-up, the changes in the artery diameters were compared using the mixed linear model for repeated measured data, and follow-up pairwise comparison was conducted among the three periods. The independent-samples *t*-test was used to analyze the changes in MVD. Receiver-operating characteristic (ROC) analysis was used to evaluate the changes in the diameter of all hepatic arteries to differentiate between responders and non-responders and identify the cutoff values. The cutoff was calculated for any factors that were statistically significant in the ROC analysis, which were candidates for univariate and multivariable logistic regression analyses with baseline data.

RESULTS

Participant characteristics

During the study period, patients meeting the inclusion criteria were followed up for 6 mo after the start of the combination treatment. The study population was predominantly male (59/67, 88.1%), and most of the enrolled patients were infected with hepatitis B virus (53/67, 79.1%). In total, 45 (67.2%) patients were estimated to have Child–Pugh stage A liver function, and 22 (32.8%) patients were categorized as Child–Pugh stage B. Portal vein tumor thrombosis was diagnosed in 44 (65.7%) patients, hepatic vein tumor thrombus in 17 (25.4%) patients, and extrahepatic spread occurred in 13 (19.4%) patients. The characteristics of the patients are summarized in Table 1.

Treatment-related AEs

There were no treatment-related deaths in our study. According to CTCAE, grade 1-2 events were observed in 37 patients (55.2%) and grade 3 events in 2 (3.0%) patients, whereas no grade ≥ 4 AEs occurred. The most common grade 1-2 events were abdominal pain (17/67, 25.4%), fever (8/67, 11.9%), and transient nausea and vomiting (8/67, 11.9%). The grade 3 events were liver dysfunction and decreased leukocyte counts, both of which normalized after treatment.

Table 1 The baseline characteristics of patients

Characteristics	*n* (%)
Age	
≤ 60	52 (77.6)
> 60	15 (22.4)
Gender	
Male	59 (88.1)
Female	8 (11.9)
ECOG PS	
0	52 (77.6)
1	15 (22.4)
HBsAg	
Positive	53 (79.1)
Negative	14 (20.9)
Child-Pugh Class	
Class A	45 (67.2)
Class B	22 (32.8)
Tumor size, cm	
≤ 10	43 (64.2)
> 10	24 (35.8)
No. of intrahepatic tumors	
≤ 3	32 (47.8)
> 3	35 (52.2)
Baseline AFP level, ng/mL	
≤ 400	29 (43.3)
> 400	38 (56.7)
PVTT	
Absent	23 (34.3)
Present	44 (65.7)
HVTT	
Absent	50 (74.6)
Present	17 (25.4)
Metastasis	
Absent	54 (80.6)
Present	13 (19.4)

ECOG PS: Eastern Cooperative Oncology Group performance status; HBsAg: Hepatitis B surface antigen; AFP: Alfa-fetoprotein; PVTT: Portal vein tumor thrombus; HVTT: Hepatic vein tumor thrombus.

Efficacy

Five patients missed the 3-mo imaging evaluation, and 11 patients missed the 6-mo evaluation because of loss to follow-up. In total, 46, 41, and 24 patients were classified as responders (CR + PR) after 1, 3, and 6 mo of treatment, respectively, whereas the numbers of non-responders (SD + PD) at these time points were 21, 21, and 32, respectively. The overall response rates (ORR) in this study at 1, 3, and 6 mo were 68.7%, 66.1%, and 42.9%, respectively. Eight patients received downstaging therapy within 1 year after treatment, of which six patients underwent hepatectomy and the other two patients underwent radiofrequency ablation.

Artery diameters

Vessel diameters were measured in all patients before treatment and after 1 mo of treatment, whereas six patients missed the 2-month measurement. After 1 and 2 mo of treatment, all vessel diameters had gradually decreased compared with the baseline ($P < 0.001$), but the difference in vessel diameters between 1 and 2 mo was not significant ($P > 0.05$, Figure 2). According to the ROC analysis, the change in the TFA diameter was significantly different between the responders and non-responders at 1, 3, and 6 mo ($P < 0.001$, $P = 0.004$, and $P = 0.023$, respectively), and the corresponding cutoff values were -0.169, -0.169, and -0.264, respectively. Meanwhile, there were no significant differences in the diameters of other hepatic arteries between the groups (Table 2). Considering the unclear clinical meaning of continuous changes in vessel diameters, the change in the TFA diameter was classified as reduced or unchanged based on the cutoff values.

The results of the univariate and multivariable logistic regression analyses of tumor response are listed in Table 3. According to the multivariable analysis, the change in the TFA diameter was an independent factor for the efficacy of HAIC plus lenvatinib after 1 [odds ratio (OR) = 0.12; 95% confidence interval (CI): 0.03-0.43; $P = 0.001$], 3 (OR = 0.06; 95%CI: 0.01-0.29; $P = 0.001$), and 6 mo (OR = 0.14; 95%CI: 0.04-0.47; $P = 0.002$) of treatment. Other independent factors included the alpha-fetoprotein level (OR = 0.17; 95%CI: 0.04-0.73; $P = 0.018$) at 1 mo and tumor size (OR = 7.65; 95%CI: 1.36-42.88; $P = 0.021$) at 3 mo.

MVD

The MVD of tumor lesions after the administration of lenvatinib was robustly smaller than that before treatment, suggesting that angiogenesis was strongly suppressed by lenvatinib ($P < 0.001$, Figure 3).

DISCUSSION

In the present study, significant shrinkage of hepatic arteries was observed in patients with uHCC after 1 mo of HAIC plus lenvatinib therapy for the first time. We also confirmed that the morphological change in the TFA was closely related to the tumor response after 1, 3, and 6 mo of combination treatment, and this change was an independent factor for improved short-term therapeutic efficacy. These findings would be of great significance to physicians for evaluating the effectiveness of this combination therapy earlier in the course of treatment and altering the treatment plan as needed.

Hepatic arteries were shown to be markedly thin following TKI treatment, and Chen *et al*[17] attributed these morphological changes to the anti-angiogenic effect of targeted drugs. Notably, lenvatinib more effectively suppresses angiogenesis and inhibits tumor growth than sorafenib by targeting both vascular endothelial growth factor (VEGF) and fibroblast growth factor[18,19]. In our study, shrinkage of hepatic vessels was observed early after the start of HAIC plus lenvatinib therapy, and the powerful antiangiogenic effect of lenvatinib was proven by the decrease in the MVD of the tumor lesions. Meanwhile, anti-VEGF therapies can reverse vessel abnormalities and improve the tumor microenvironment[20]. The decline in local tumor perfusion secondary to the decrease in tumor capillaries and the "normalization hypothesis" may be the main reasons for the conspicuous reduction of hepatic arteries with the combination regimen.

The efficiency of HAIC combined with lenvatinib for intermediate and advanced HCC has been confirmed in previous studies[21,22]. In this study, the ORR reached 68.7%, 66.1%, and 42.9% at 1, 3, and 6 mo, and conversion therapy was achieved in eight patients, which further verified the effectiveness of the combination therapy. Thus, it was necessary to explore the mechanism of action of this combination therapy. A reduction in hepatic artery diameters was observed in most patients in the present study. Kuorda *et al*[23] also reported that local tumor perfusion declined significantly after oral lenvatinib administration. These findings illustrated that lenvatinib reduces the tumor blood supply after combination therapy. Meanwhile, HAIC has the advantage of achieving high local concentrations in the tumor during arterial infusion[24]. According to the pharmacokinetic characteristics of the intra-arterial infusion[25], a decrease in tumor blood flow can increase the dose of the drug in the target organ, thus enhancing the antitumor effect of HAIC. Furthermore, the normalization and improved functionality of tumor vessels including reduced hypoxia, reduced vascular leakage, and improved vascular permeability can improve the delivery of local chemotherapeutic drugs in tumors[26,27]. The increased drug accumulation in the target organ often results in improved therapeutic efficacy. Since the combined therapy could improve the therapeutic effect, it may also expand the scope of HAIC, which is limited to patients with HCC and multinodule lesions or vascular invasion.

In clinical practice, HAIC often requires 6-8 courses. Moreover, repetitive and inefficient treatment is harmful to patients with uHCC. Therefore, early evaluation of the treatment response is of great significance. In this study, we found that the reduction in the TFA diameter after combination therapy was an independent factor for improved therapeutic efficacy within 6 mo. The morphological change in the TFA is easy to observe during HAIC, and it can help in estimating the early therapeutic effect. Since an improved short-term effect often results in a good prognosis, the observation on thinning of the TFA is significant and more practical for patients with uHCC who are receiving HAIC plus lenvatinib.

Table 2 Receiver-operating characteristic analysis for antitumor response

Δ_{artery}	1 mo			3 mo			6 mo		
	Responder	Non-responder	*P* value	Responder	Non-responder	*P* value	Responder	Non-responder	*P* value
CHA	- (0.17 ± 0.17)	- (0.14 ± 0.18)	0.25	- (0.15 ± 0.16)	- (0.18 ± 0.19)	1.00	- (0.18 ± 0.16)	- (0.15 ± 0.18)	0.51
PHA	- (0.21 ± 0.14)	- (0.13 ± 0.25)	0.15	- (0.20 ± 0.15)	- (0.16 ± 0.20)	0.35	- (0.16 ± 0.16)	- (0.22 ± 0.17)	0.30
LHA	- (0.27 ± 0.17)	- (0.21 ± 0.28)	0.59	(0.28 ± 0.18)	(0.20 ± 0.27)	0.43	- (0.22 ± 0.24)	- (0.30 ± 0.17)	0.18
RHA	- (0.22 ± 0.17)	- (0.16 ± 0.23)	0.26	- (0.20 ± 0.19)	- (0.22 ± 0.20)	0.58	- (0.16 ± 0.23)	- (0.24 ± 0.17)	0.44
TFA	- (0.33 ± 0.20)	- (0.16 ± 0.19)	< 0.001	- (0.32 ± 0.19)	- (0.18 ± 0.22)	0.004	- (0.36 ± 0.16)	- (0.25± 0.23)	0.023

Δ_{artery}: The rate of change in vessel diameters of hepatic arteries; CHA: Common hepatic artery; PHA: Proper hepatic artery; LHA: Left hepatic artery; RHA: Right hepatic artery; TFA: Tumor-feeding artery.

Table 3 Univariate and multivariate logistic regression analysis for efficacy of treatment with hepatic arterial infusion chemotherapy plus lenvatinib

	1 mo			3 mo			6 mo		
	Univariate	Multivariate		Univariate	Multivariate		Univariate	Multivariate	
	P1 value	*P2* value	OR (95%CI)	*P1* value	*P2* value	OR (95%CI)	*P1* value	*P2* value	OR (95%CI)
TFA (reduced/basically unchanged)	< 0.001	0.001	0.12 (0.03-0.43)	< 0.001	0.001	0.06 (0.01-0.29)	0.002	0.002	0.14 (0.04-0.47)
Sex (male/female)	0.680	-	-	0.349	-	-	0.892	-	-
Age (≤ 60/> 60)	0.850	-	-	0.868	-	-	0.573	-	-
ECOG (0/1)	0.412	-	-	0.147	-	-	0.365	-	-
HBsAg (positive/negative)	0.122	-	-	0.113	-	-	0.784	-	-
AFP, ng/mL (≤ 400/> 400)	0.003	0.018	0.17 (0.04-0.73)	0.089	0.546	-	0.040	0.122	-
Child-Pugh (A/B)	0.384	-	-	0.897	-	-	0.869	-	-
Tumor size, cm (≤ 10/> 10)	0.166	-	-	0.053	0.021	7.65 (1.36-42.88)	0.625	-	-
Tumor number (≤ 3/> 3)	0.609	-	-	0.533	-	-	0.280	-	-
PVTT (absent/present)	0.220	-	-	0.169	-	-	0.577	-	-
HVTT (absent/present)	0.842	-	-	0.455	-	-	1.000	-	-
Metastasis (absent/present)	0.960	-	-	0.694	-	-	0.615	-	-

Any factors that were statistically significant at $P < 0.10$ in the univariate logistic regression analysis were candidates for entry into the multivariate logistic regression analysis. TFA: The tumor-feeding artery; ECOG PS: Eastern Cooperative Oncology Group performance status; HBsAg: Hepatitis B surface antigen; AFP: Alfa-fetoprotein; PVTT: Portal vein tumor thrombus; HVTT: Hepatic vein tumor thrombus; OR: Odds ratio; CI: Confidence interval.

The present study had some limitations. This was a single-center retrospective study, and the sample size was small.

CONCLUSION

In conclusion, lenvatinib can reduce the diameters of hepatic arteries and thus enhance the effect of HAIC. Shrinkage of the TFA after HAIC plus lenvatinib therapy was linked to improved short-term outcomes in patients with uHCC.

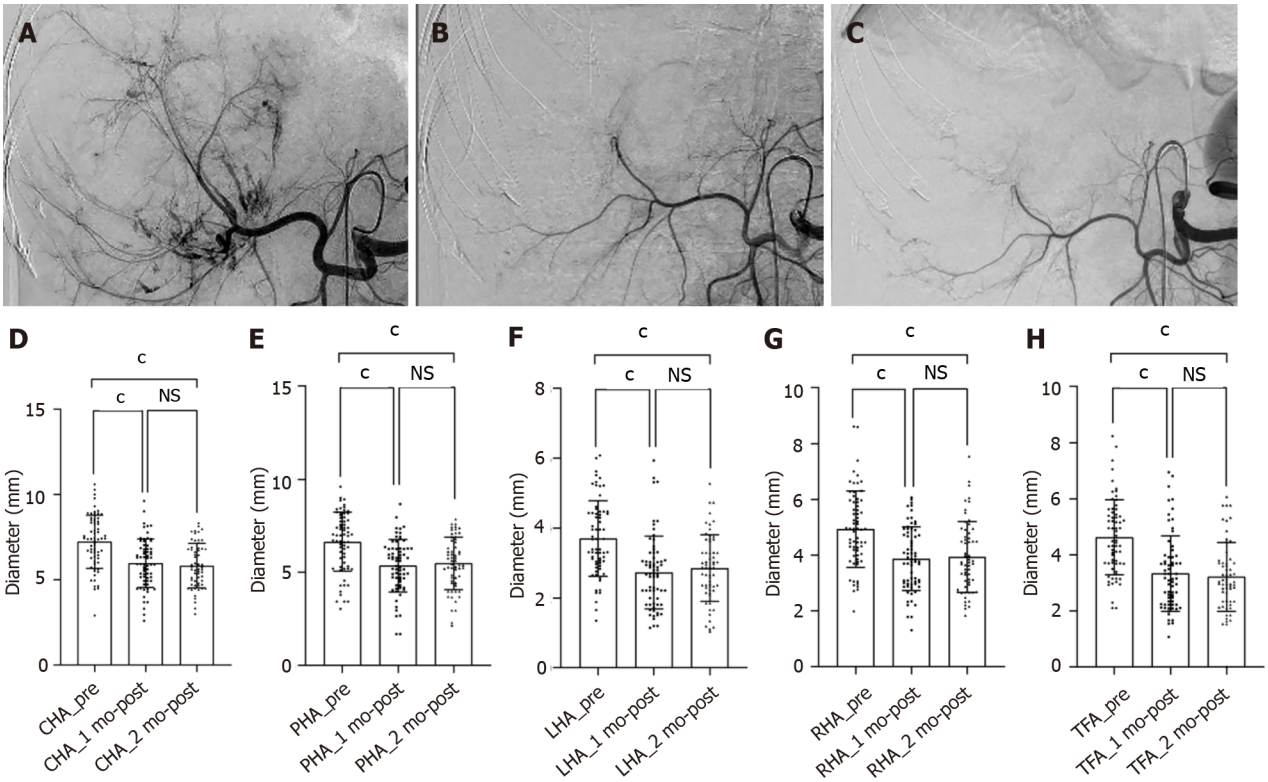

DOI: 10.3748/wjg.v28.i26.3232

Figure 2 Shrinkage of the hepatic artery diameters in patient with unresectable hepatocellular carcinoma after treatment with hepatic arterial infusion chemotherapy plus lenvatinib. A-C: Digital subtraction angiography performed before treatment (A), after 1 (B) and 2 (C) mo of treatment; D-H: Bars represent the vessel diameters before treatment, at 1 and 2 mo after treatment. *P*-values are calculated using the mixed linear model for repeated measured data. $^{c}P < 0.001$. NS: Not significant ($P > 0.05$); CHA: Common hepatic artery; PHA: Proper hepatic artery; LHA: Left hepatic artery; RHA: Right hepatic artery; TFA: Tumor-feeding artery.

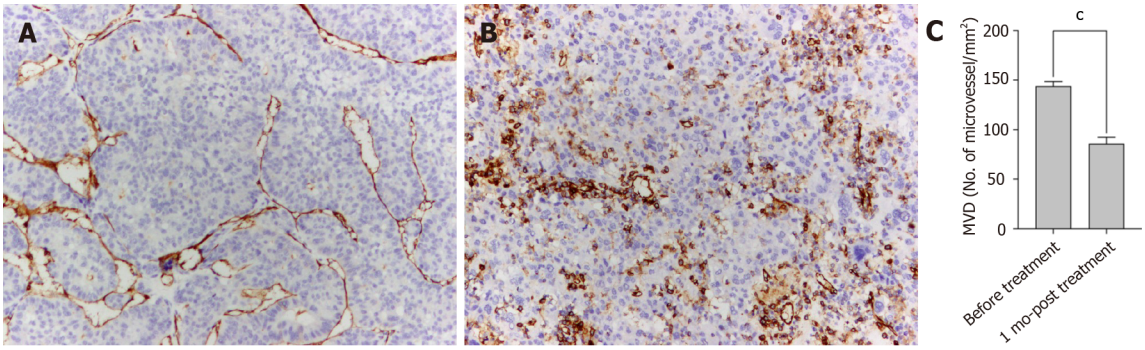

DOI: 10.3748/wjg.v28.i26.3232

Figure 3 Anti-angiogenic activities of lenvatinib in tumor lesions. A and B: The microvessels in the tumor lesion collected before (A) and after 1 mo (B) of treatment with lenvatinib are stained with anti-CD34 antibody (× 100); C: Bars represent the microvessel density that decreased sharply after administration of lenvatinib. Data are presented as means ± SD. $^{c}P < 0.001$ *vs* before treatment. MVD: Micro-vessel density.

ARTICLE HIGHLIGHTS

Research background

Combination of hepatic arterial infusion chemotherapy (HAIC) and lenvatinib has been frequently used to treat unresectable hepatocellular carcinoma (uHCC) in China.

Research motivation

Shrinkage of hepatic arteries after the combination therapy is a common phenomenon and may early reflect the antitumor response, the relationship between which needs further exploration.

Research objectives
To investigate the relationship between hepatic artery diameters reduction and the short-term efficacy of HAIC plus lenvatinib.

Research methods
Sixty-seven patients with uHCC receiving HAIC plus lenvatinib were analyzed retrospectively. The modified Response Evaluation Criteria in Solid Tumors was used to assess the antitumor response after 1, 3, and 6 mo of treatment. The measurement of hepatic artery diameters before treatment and after 1 and 2 mo of treatment were conducted in a computed tomography image post-processing workstation. Meanwhile, the changes in tumor capillaries were also examined on pathological specimens before and after 1 mo of treatment.

Research results
All the hepatic artery diameters and the microvessel density in the tumor lesions were significantly decreased after the combination treatment (all $P < 0.001$). Shrinkage of the tumor-feeding artery (TFA) was significantly associated with the antitumor response after 1, 3, and 6 mo of treatment ($P < 0.001$, $P = 0.004$, and $P = 0.023$, respectively) and an independent factor for treatment efficacy ($P = 0.001$, $P = 0.001$, and $P = 0.002$ and 1, 3, and 6 mo, respectively).

Research conclusions
The retrospective study demonstrated that the shrinkage of the TFA diameter was closely related to improved short-term efficacy of treatment with HAIC plus lenvatinib for the first time.

Research perspectives
We believe the findings in this paper will be of interest to the researchers in uHCC. Further, prospective randomized multicenter trials are needed to confirm the relationship between the morphological change in TFA and the early therapeutic effect of uHCC treatment.

ACKNOWLEDGEMENTS

All authors are grateful to Dr. Fan XY for assisting with the reconstruction of the CT images.

FOOTNOTES

Author contributions: Wu DD and Pang HJ designed this study; Wu DD, Tian C, and Chen CL performed the reconstruction and measurement; Wu DD, Liu XH, and Pang HJ analyzed the data; Peng P collected the clinical data; Wu DD wrote the paper; He XF and Pang HJ made critical revisions to the paper; all authors approved the publication of the paper.

Institutional review board statement: The research was conducted in accordance with the 1975 Declaration of Helsinki and approved by the medical ethics committee of Nanfang Hospital, Southern Medical University.

Informed consent statement: The requirement for informed consent was waived owing to the retrospective nature of the study.

Conflict-of-interest statement: There was no conflict of interest to disclose.

Data sharing statement: No additional data are available.

Country/Territory of origin: China

ORCID number: De-Di Wu 0000-0001-8409-9770; Xiao-Feng He 0000-0001-8255-1874; Chen Tian 0000-0003-4260-290X; Peng Peng 0000-0001-9864-0580; Chuan-Li Chen 0000-0001-7610-5966; Xue-Han Liu 0000-0002-8966-7172; Hua-Jin Pang 0000-0001-7367-5701.

S-Editor: Yan JP
L-Editor: A

P-Editor: Yan JP

REFERENCES

1 **Torre LA**, Bray F, Siegel RL, Ferlay J, Lortet-Tieulent J, Jemal A. Global cancer statistics, 2012. *CA Cancer J Clin* 2015; **65**: 87-108 [PMID: 25651787 DOI: 10.3322/caac.21262]

2 **Llovet JM**, Zucman-Rossi J, Pikarsky E, Sangro B, Schwartz M, Sherman M, Gores G. Hepatocellular carcinoma. *Nat Rev Dis Primers* 2016; **2**: 16018 [PMID: 27158749 DOI: 10.1038/nrdp.2016.18]

3 **European Association for the Study of the Liver**. Corrigendum to "EASL Clinical Practice Guidelines: Management of hepatocellular carcinoma" [J Hepatol 69 (2018) 182-236]. *J Hepatol* 2019; **70**: 817 [PMID: 30739718 DOI: 10.1016/j.jhep.2019.01.020]

4 **Kudo M**, Trevisani F, Abou-Alfa GK, Rimassa L. Hepatocellular Carcinoma: Therapeutic Guidelines and Medical Treatment. *Liver Cancer* 2016; **6**: 16-26 [PMID: 27995084 DOI: 10.1159/000449343]

5 **Ikeda M**, Morizane C, Ueno M, Okusaka T, Ishii H, Furuse J. Chemotherapy for hepatocellular carcinoma: current status and future perspectives. *Jpn J Clin Oncol* 2018; **48**: 103-114 [PMID: 29253194 DOI: 10.1093/jjco/hyx180]

6 **Kudo M**, Matsui O, Izumi N, Iijima H, Kadoya M, Imai Y, Okusaka T, Miyayama S, Tsuchiya K, Ueshima K, Hiraoka A, Ikeda M, Ogasawara S, Yamashita T, Minami T, Yamakado K; Liver Cancer Study Group of Japan. JSH Consensus-Based Clinical Practice Guidelines for the Management of Hepatocellular Carcinoma: 2014 Update by the Liver Cancer Study Group of Japan. *Liver Cancer* 2014; **3**: 458-468 [PMID: 26280007 DOI: 10.1159/000343875]

7 **He MK**, Liang RB, Zhao Y, Xu YJ, Chen HW, Zhou YM, Lai ZC, Xu L, Wei W, Zhang YJ, Chen MS, Guo RP, Li QJ, Shi M. Lenvatinib, toripalimab, plus hepatic arterial infusion chemotherapy *versus* lenvatinib alone for advanced hepatocellular carcinoma. *Ther Adv Med Oncol* 2021; **13**: 17588359211002720 [PMID: 33854567 DOI: 10.1177/17588359211002720]

8 **Obi S**, Sato S, Kawai T. Current Status of Hepatic Arterial Infusion Chemotherapy. *Liver Cancer* 2015; **4**: 188-199 [PMID: 26674592 DOI: 10.1159/000367746]

9 **Matsuda N**, Imai N, Kuzuya T, Yamamoto K, Ito T, Ishizu Y, Honda T, Ishigami M, Fujishiro M. Progression After Molecular Targeted Agents: Hepatic Arterial Changes and Transarterial Chemoembolization in Hepatocellular Carcinoma. *In Vivo* 2021; **35**: 1185-1189 [PMID: 33622919 DOI: 10.21873/invivo.12367]

10 **Jiang H**, Liu X, Chen J, Wei Y, Lee JM, Cao L, Wu Y, Duan T, Li X, Ma L, Song B. Man or machine? *Cancer Imaging* 2019; **19**: 84 [PMID: 31806050 DOI: 10.1186/s40644-019-0266-9]

11 **Okusaka T**, Ikeda K, Kudo M, Finn R, Qin S, Han KH, Cheng AL, Piscaglia F, Kobayashi M, Sung M, Chen M, Wyrwicz L, Yoon JH, Ren Z, Mody K, Dutcus C, Tamai T, Ren M, Hayato S, Kumada H. Safety and efficacy of lenvatinib by starting dose based on body weight in patients with unresectable hepatocellular carcinoma in REFLECT. *J Gastroenterol* 2021; **56**: 570-580 [PMID: 33948712 DOI: 10.1007/s00535-021-01785-0]

12 **Freites-Martinez A**, Santana N, Arias-Santiago S, Viera A. Using the Common Terminology Criteria for Adverse Events (CTCAE - Version 5.0) to Evaluate the Severity of Adverse Events of Anticancer Therapies. *Actas Dermosifiliogr (Engl Ed)* 2021; **112**: 90-92 [PMID: 32891586 DOI: 10.1016/j.ad.2019.05.009]

13 **Pang H**, Chen Y, He X, Tan X, Wang J, Yao Q, Liu X. Twelve-Month Computed Tomography Follow-Up after Thoracic Endovascular Repair for Acute Complicated Aortic Dissection. *Ann Vasc Surg* 2021; **71**: 444-450 [PMID: 32891743 DOI: 10.1016/j.avsg.2020.08.125]

14 **Matsuki M**, Adachi Y, Ozawa Y, Kimura T, Hoshi T, Okamoto K, Tohyama O, Mitsuhashi K, Yamaguchi A, Matsui J, Funahashi Y. Targeting of tumor growth and angiogenesis underlies the enhanced antitumor activity of lenvatinib in combination with everolimus. *Cancer Sci* 2017; **108**: 763-771 [PMID: 28107584 DOI: 10.1111/cas.13169]

15 **Matsuki M**, Hoshi T, Yamamoto Y, Ikemori-Kawada M, Minoshima Y, Funahashi Y, Matsui J. Lenvatinib inhibits angiogenesis and tumor fibroblast growth factor signaling pathways in human hepatocellular carcinoma models. *Cancer Med* 2018; **7**: 2641-2653 [PMID: 29733511 DOI: 10.1002/cam4.1517]

16 **Mohamed A**, Chenna A, Abdelfatah M, Sanjay J, Mohammad MK, Saber I, Kauh J, Elhammali B, Kaseb A. Microvessel density analysis in patients with viral hepatitis-related hepatocellular carcinoma. *J Gastrointest Cancer* 2015; **46**: 104-108 [PMID: 25645584 DOI: 10.1007/s12029-015-9684-5]

17 **Chen L**, Zheng Y, Zhang H, Pan H, Liu Q, Zhou X, Wei W, Liu Y, Zhen M, Wang J, Zhou J, Zhao Y. Comparative analysis of tumor-associated vascular changes following TACE alone or in combination with sorafenib treatment in HCC: A retrospective study. *Oncol Lett* 2018; **16**: 3690-3698 [PMID: 30127979 DOI: 10.3892/ol.2018.9055]

18 **Yamamoto Y**, Matsui J, Matsushima T, Obaishi H, Miyazaki K, Nakamura K, Tohyama O, Semba T, Yamaguchi A, Hoshi SS, Mimura F, Haneda T, Fukuda Y, Kamata JI, Takahashi K, Matsukura M, Wakabayashi T, Asada M, Nomoto KI, Watanabe T, Dezso Z, Yoshimatsu K, Funahashi Y, Tsuruoka A. Lenvatinib, an angiogenesis inhibitor targeting VEGFR/FGFR, shows broad antitumor activity in human tumor xenograft models associated with microvessel density and pericyte coverage. *Vasc Cell* 2014; **6**: 18 [PMID: 25197551 DOI: 10.1186/2045-824X-6-18]

19 **Perera S**, Kelly D, O'Kane GM. Non-immunotherapy options for the first-line management of hepatocellular carcinoma: exploring the evolving role of sorafenib and lenvatinib in advanced disease. *Curr Oncol* 2020; **27**: S165-S172 [PMID: 33343210 DOI: 10.3747/co.27.7159]

20 **Liu K**, Zhang X, Xu W, Chen J, Yu J, Gamble JR, McCaughan GW. Targeting the vasculature in hepatocellular carcinoma treatment: Starving *vs* normalizing blood supply. *Clin Transl Gastroenterol* 2017; **8**: e98 [PMID: 28617447 DOI: 10.1038/ctg.2017.28]

21 **Shimose S**, Iwamoto H, Tanaka M, Niizeki T, Shirono T, Noda Y, Kamachi N, Okamura S, Nakano M, Suga H, Yamaguchi T, Kawaguchi T, Kuromatsu R, Noguchi K, Koga H, Torimura T. Alternating Lenvatinib and Trans-Arterial Therapy Prolongs Overall Survival in Patients with Inter-Mediate Stage HepatoCellular Carcinoma: A Propensity Score Matching Study. *Cancers (Basel)* 2021; **13** [PMID: 33466496 DOI: 10.3390/cancers13010160]

22 **Mai QC**, Mo ZQ, Shi F, Chen XM. Lenvatinib plus hepatic arterial infusion of modified FOLFOX regime in patients with advanced hepatocellular carcinoma. *J Clin Oncol* 2020; **38** [DOI: 10.1200/jco.2020.38.15_suppl.e16603]

23 **Kuorda H**, Abe T, Fujiwara Y, Okamoto T, Yonezawa M, Sato H, Endo K, Oikawa T, Sawara K, Takikawa Y. Change in arterial tumor perfusion is an early biomarker of lenvatinib efficacy in patients with unresectable hepatocellular carcinoma. *World J Gastroenterol* 2019; **25**: 2365-2372 [PMID: 31148907 DOI: 10.3748/wjg.v25.i19.2365]

24 **Kondo Y**, Fukuda R. [Cutting Edge of Hepatic Artery Infusion Chemotherapy for Hepatocellular Carcinoma]. *Gan To Kagaku Ryoho* 2020; **47**: 1-5 [PMID: 32381852]

25 **Chen HS**, Gross JF. Intra-arterial infusion of anticancer drugs: theoretic aspects of drug delivery and review of responses. *Cancer Treat Rep* 1980; **64**: 31-40 [PMID: 6155210 DOI: 10.1016/0304-3835(80)90154-8]

26 **Jain RK**. Normalizing tumor vasculature with anti-angiogenic therapy: a new paradigm for combination therapy. *Nat Med* 2001; **7**: 987-989 [PMID: 11533692 DOI: 10.1038/nm0901-987]

27 **Willett CG**, Boucher Y, di Tomaso E, Duda DG, Munn LL, Tong RT, Chung DC, Sahani DV, Kalva SP, Kozin SV, Mino M, Cohen KS, Scadden DT, Hartford AC, Fischman AJ, Clark JW, Ryan DP, Zhu AX, Blaszkowsky LS, Chen HX, Shellito PC, Lauwers GY, Jain RK. Direct evidence that the VEGF-specific antibody bevacizumab has antivascular effects in human rectal cancer. *Nat Med* 2004; **10**: 145-147 [PMID: 14745444 DOI: 10.1038/nm988]

World Journal of Gastroenterology

Submit a Manuscript: https://www.f6publishing.com

World J Gastroenterol 2022 July 14; 28(26): 3243-3257

DOI: 10.3748/wjg.v28.i26.3243

ISSN 1007-9327 (print) ISSN 2219-2840 (online)

ORIGINAL ARTICLE

Observational Study

Impact of sodium glucose cotransporter-2 inhibitors on liver steatosis/fibrosis/inflammation and redox balance in non-alcoholic fatty liver disease

Francesco Bellanti, Aurelio Lo Buglio, Michał Dobrakowski, Aleksandra Kasperczyk, Sławomir Kasperczyk, Palok Aich, Shivaram P Singh, Gaetano Serviddio, Gianluigi Vendemiale

Specialty type: Gastroenterology and hepatology

Provenance and peer review: Invited article; Externally peer reviewed.

Peer-review model: Single blind

Peer-review report's scientific quality classification

Grade A (Excellent): 0
Grade B (Very good): B
Grade C (Good): C
Grade D (Fair): 0
Grade E (Poor): 0

P-Reviewer: Boscá L , Spain; Zhao XK, China

Received: January 10, 2022
Peer-review started: January 10, 2022
First decision: March 8, 2022
Revised: March 18, 2022
Accepted: June 18, 2022
Article in press: June 18, 2022
Published online: July 14, 2022

Francesco Bellanti, Aurelio Lo Buglio, Gaetano Serviddio, Gianluigi Vendemiale, Department of Medical and Surgical Sciences, University of Foggia, Foggia 71122, Italy

Michał Dobrakowski, Aleksandra Kasperczyk, Sławomir Kasperczyk, Department of Biochemistry, Medical University of Silesia in Katowice, Zabrze 41-808, Poland

Palok Aich, School of Biological Sciences, National Institute of Science Education and Research, Khurdha 752050, India

Shivaram P Singh, Department of Gastroenterology, SCB Medical College, Cuttack 753007, India

Corresponding author: Francesco Bellanti, MD, PhD, Associate Professor, Department of Medical and Surgical Sciences, University of Foggia, viale Pinto, 1, Foggia 71122, Italy. francesco.bellanti@unifg.it

Abstract

BACKGROUND

Sodium glucose cotransporter-2 inhibitors (SGLT2-I) are the most recently approved drugs for type 2 diabetes (T2D). Recent clinical trials of these compounds reported beneficial cardiovascular (CV) and renal outcomes. A major cause of vascular dysfunction and CV disease in diabetes is hyperglycemia associated with inflammation and oxidative stress. Pre-clinical studies demonstrated that SGLT2-I reduce glucotoxicity and promote anti-inflammatory effects by lowering oxidative stress.

AIM

To investigate the effects of SGLT2-I on markers of oxidative stress, inflammation, liver steatosis, and fibrosis in patients of T2D with non-alcoholic fatty liver disease (NAFLD).

METHODS

We referred fifty-two consecutive outpatients treated with metformin monotherapy and exhibiting poor glycemic control to our centre. We introduced the outpatients to an SGLT2-I (dapagliflozin, empagliflozin, or canagliflozin; n = 26)

or a different hypoglycemic drug [other glucose-lowering drugs (OTHER), n = 26]. We evaluated circulating interleukins and serum hydroxynonenal (HNE)- or malondialdehyde (MDA)-protein adducts, fatty liver index (FLI), NAFLD fibrosis score, aspartate aminotransferase (AST)/alanine aminotransferase (ALT) ratio, AST-to-platelet-ratio index (APRI), and fibrosis-4 on the day before (T0) and following treatment for six months (T1). We also performed transient elastography at T0 and T1.

RESULTS

Add-on therapy resulted in improved glycemic control and reduced fasting blood glucose in both groups. Of note, following treatment for six months, a reduction of FLI and APRI, as well as of the FibroScan result, was reported in patients treated with SGLT2-I, but not in the OTHER group; furthermore, in the SGLT2-I group, we reported lower circulating levels of interleukin (IL)-1β, IL-6, tumor necrosis factor, vascular endothelial growth factor, and monocyte chemoattractant protein-1, and higher levels of IL-4 and IL-10. We did not observe any modification in circulating interleukins in the OTHER group. Finally, serum HNE- and MDA-protein adducts decreased significantly in SGLT2-I rather than OTHER patients and correlated with liver steatosis and fibrosis scores.

CONCLUSION

The present data indicate that treatment with SGLT2-I in patients with T2D and NAFLD is associated with improvement of liver steatosis and fibrosis markers and circulating pro-inflammatory and redox status, more than optimizing glycemic control.

Key Words: Sodium glucose cotransporter-2 inhibitors; Non-alcoholic fatty liver disease; Oxidative stress; Type 2 diabetes; Liver fibrosis; Inflammation

Core Tip: Non-alcoholic fatty liver disease (NAFLD) is the most common hepatic disorder, and it is often associated with type 2 diabetes mellitus (T2DM). Diabetic patients often suffer from advanced NAFLD and are keen on progressing toward severe fibrosis and end-stage liver disease. There is no approved treatment for NAFLD, but new drug classes introduced to treat T2DM can exert favorable effects beyond glucose control. This pilot study demonstrates that treatment with sodium glucose cotransporter-2 inhibitors in patients with T2DM and NAFLD is associated with improving liver steatosis and fibrosis markers and circulating pro-inflammatory and redox status.

Citation: Bellanti F, Lo Buglio A, Dobrakowski M, Kasperczyk A, Kasperczyk S, Aich P, Singh SP, Serviddio G, Vendemiale G. Impact of sodium glucose cotransporter-2 inhibitors on liver steatosis/fibrosis/inflammation and redox balance in non-alcoholic fatty liver disease. *World J Gastroenterol* 2022; 28(26): 3243-3257
URL: https://www.wjgnet.com/1007-9327/full/v28/i26/3243.htm
DOI: https://dx.doi.org/10.3748/wjg.v28.i26.3243

INTRODUCTION

Patients affected by type 2 diabetes mellitus (T2DM) present with an increased risk of cardiovascular (CV) disease, which is associated with a high mortality rate and low quality of life[1,2]. T2DM is strongly associated with non-alcoholic fatty liver disease (NAFLD), whose prevalence in diabetic patients is over 60%[3,4]. NAFLD is the most common chronic liver disease, characterized by a broad spectrum of hepatic disorders, ranging from simple steatosis to steatohepatitis (non-alcoholic steatohepatitis), fibrosis, and cirrhosis[5]. The co-existence of NAFLD and T2DM pushes the progression of liver damage, increasing the risk of advanced fibrosis[6]. Besides, NAFLD is an independent risk factor of CV disease. Patients with T2DM and NAFLD present a higher CV risk than diabetic patients without NAFLD, suggesting that these conditions share common pathophysiological mechanisms, including low-grade systemic inflammation and oxidative stress[7].

Studies using new classes of antidiabetic drugs, such as sodium-glucose co-transporter-2 inhibitors (SGLT2-I) and glucagon-like peptide-1 receptor agonists (GLP1-RA), demonstrated definite CV advantage in patients with T2D[8]. Several clinical trials suggest that both classes also ameliorate liver steatosis and inflammation, potentially reversing fibrosis in NAFLD[9]. The currently approved SGLT2-I are dapagliflozin, canagliflozin, empagliflozin, and ertugliflozin, which increase urinary glucose

excretion and improve glycemic control independent of insulin. Furthermore, these drugs reduce body weight, visceral adiposity, blood pressure, and arterial stiffness[10]. Real-world CVD-REAL and CVD-REAL 2 studies have demonstrated that the benefits of SGLT2-I on CV outcomes observed in clinical trials may be attributed to a class effect and may be extended to a broad range of patients[11,12]. Despite clinical evidence on the efficacy of SGLT2-I in both the reduction of CV events and the improvement of hepatic damage in NAFLD, human mechanistic trials remain elusive.

Pre-clinical studies demonstrated that dapagliflozin, empagliflozin, and canagliflozin attenuate inflammation in apolipoprotein E knockout mice[13-15], reduce oxidative stress and improve mitochondrial function through direct pleiotropic and epigenetic effects[16,17]. Furthermore, these compounds may also exert antifibrotic effects in diabetic and non-diabetic cardiopathy or nephropathy [18-20]. Such results strongly encourage clinical studies to clarify the impact of SGLT2-I on systemic inflammation, oxidative stress, and liver fibrosis in diabetic patients with NAFLD. Thus, the present investigation was aimed to evaluate the effects of SGLT2-I addition to metformin on circulating markers of inflammation and oxidative protein damage in patients affected by uncontrolled T2DM and NAFLD and compare these outcomes with other glucose-lowering drugs (OTHER).

MATERIALS AND METHODS

Study design

We collected and analyzed data from 204 patients affected by T2DM who underwent outpatient consultation between June 2017 and June 2018 at the University Internal Medicine clinic of the "Policlinico Riuniti" in Foggia (Italy). We designed the investigation as an observational pilot study considering the problematic setting, the limited scale, and the multiple outcome parameters. Patients aged > 18 years old who were: (1) Diagnosed with NAFLD; and (2) Presented with glycated hemoglobin equal to or greater than 7% after at least three months of treatment with metformin monotherapy at the maximal tolerated dosage were assessed for eligibility. NAFLD was suspected on previous ultrasound imaging and/or altered liver function tests[21]. We did not consider subjects diagnosed with viral or autoimmune hepatitis, atherosclerotic CV disease, chronic inflammatory disorders, or those diagnosed with active cancer for the study. Further exclusion criteria were alcohol consumption > 20 g/d (women) or > 30 g/d (men), anemia, severe hepatic failure, glomerular filtration rate < 60 mg/min/m^2, use of drugs affecting redox balance, use of anti-inflammatory medications or corticosteroids during the observational period, use of medications associated with fatty liver (amiodarone, tamoxifen, sodium valproate, methotrexate), current smoker status, and prescription of a glucagon-like peptide-1 agonist (Supplementary Figure 1).

52 patients were finally referred to a combination therapy; of these, 26 patients were treated with an SGLT2-I, while 26 patients were treated with OTHER. The combination therapy was not randomized, and the second compound was chosen according to the standard of medical care in diabetes - 2017, considering the clinical characteristics of patients to maximize therapeutic advantages and minimize risks and side effects[22]. Compliance and adverse events were assessed by a verbal questionnaire. The frequency and distribution of the different compounds prescribed are reported in the Supplementary Table 1. For the study purposes, patients enrolled were assessed at baseline (T0) and after six months (T1). Our Institutional Review Board approved the study at the Policlinico Riuniti in Foggia (reference number 2325/2018) and performed it according to the Declaration of Helsinki. All patients gave written informed consent.

Laboratory measurements

Blood samples were obtained from a brachial vein between 8:00 and 9:00 AM, after an overnight fast, and immediately processed. Standard laboratory measurements included glycated hemoglobin A1c (HbA1c), fasting serum glucose, serum triglycerides, serum aspartate aminotransferase (AST), alanine aminotransferase (ALT) and gamma-glutamyl transpeptidase (gamma-GT) activities, platelet count, and serum albumin. The concentrations of serum cytokines and growth factors, including several interleukins (IL), such as IL-1α, IL-1β, IL-2, IL-4, IL-6, IL-8, IL-10, tumor necrosis factor (TNF), interferon-γ (IFN-γ), monocyte chemoattractant protein-1 (MCP-1), epidermal growth factor (EGF), and vascular endothelial growth factor (VEGF), were measured using the EV 3513 cytokine biochip array and competitive chemiluminescence immunoassays (Randox Laboratories Ltd, Crumlin, United Kingdom), according to the manufacturer's instructions, using the Randox Evidence Investigator[23]. As previously reported, serum fluorescent adducts formed between peroxidation-derived aldehydes [hydroxynonenal (HNE) and malondialdehyde (MDA)] and proteins were measured by spectrofluorimetry[24].

Non-invasive markers of liver steatosis and fibrosis

Patients were assessed at baseline and after six months of treatment for the following parameters: Fatty liver index (FLI), calculated according to the formula e^y / (1 + e^y) × 100, where "y" = 0.953 × ln(triglycerides, mg/dL) + 0.139 × body mass index (BMI), kg/m^2 + 0.718 × ln (gamma-GT, U/L) + 0.053 × waist circumference, cm - 15.745[25]; AST-to-platelet ratio index (APRI), calculated according to the formula

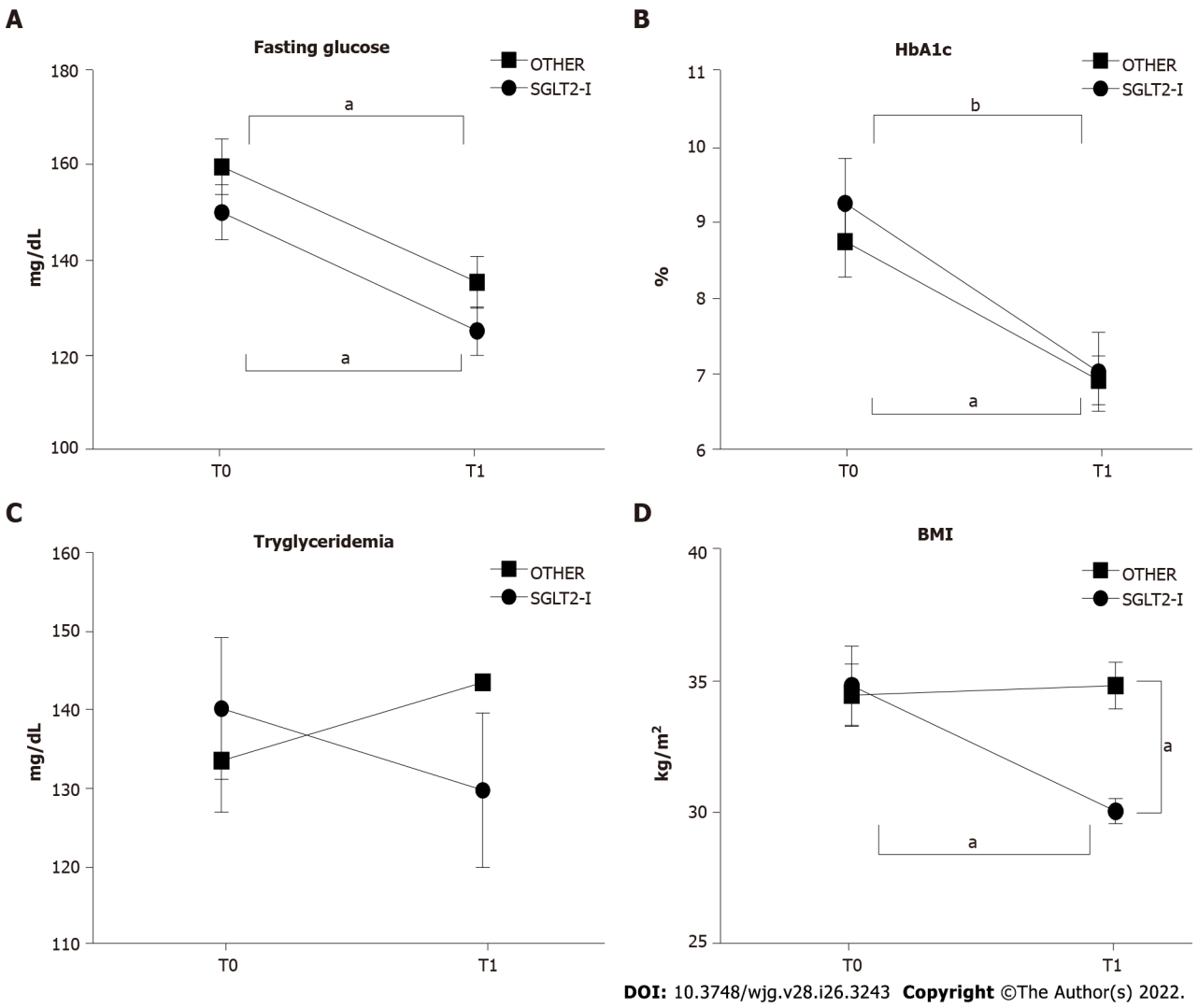

DOI: 10.3748/wjg.v28.i26.3243

Figure 1 Glycemic control and body weight in patients enrolled in the study and included in groups treated with the sodium-glucose co-transporter-2 inhibitors or other glucose-lowering drugs before (T0) and after 1 wk of treatment (T1). A: Serum fasting glucose; B: Serum hemoglobin A1c; C: Serum triglycerides; D: Body mass index in patients observed in the study, grouped according to the assigned treatment. Data in the graphs are represented as mean ± SEM. Two-way analysis of variance and Tukey assessed statistical differences as post hoc test. $^{a}P < 0.05$, $^{b}P < 0.001$. HbA1c: Hemoglobin A1c; SGLT2-I: Sodium-glucose co-transporter-2 inhibitor; OTHER: Other glucose lowering drug; BMI: Body mass index.

AST, IU/L/AST upper limit of normal, IU/L/platelets, 10^9/L[26]; NAFLD fibrosis score, calculated according to the formula - 1.675 + 0.037 × age, years + 0.094 × BMI, kg/m^2 + 1.13 × impaired fasting glucose or diabetes (yes = 1, no = 0) + 0.99 × AST/ALT ratio - 0.013 × platelets, 10^9/L - 0.66 × albumin, g/dL[27]. The cut-off values chosen to categorize fibrosis grades F0-F2 or F3-F4 were < -1.455 and > 0.675, respectively; fibrosis-4 (FIB-4), calculated according to the formula (age, years × AST, IU/L)/(platelets, 10^9/L × rad ALT, IU/L)[28]. The cut-off values chosen to categorize fibrosis grades F0-F1 or F3-F4 were < -1.30 and > 2.67, respectively; AST/ALT ratio, whose cut-off value > 0.8 is associated with advanced disease[29].

Transient elastography

Transient elastography (TE) was performed by a Fibroscan (Echosense, Paris) on supine patients with the right arm elevated. The probe tip was put on the intercostal space at the level of the right liver lobe. The Fibroscan probe contains an ultrasound transducer and a mechanical device that provides a controlled vibrating external shot on the body surface to generate shear waves. TE measures liver stiffness (LS) in 1 cm cylindric volume (width: 25-65 mm, M probe; 35-75 mm, XL probe) below the skin surface. Criteria for a valid examination were as follows: (1) At least 10 valid measurements; (2) A success rate [(valid + invalid measurements)/total measurements] > 70%; and (3) An interquartile range < 30% of the median value. Measurements were expressed as KPa[30].

Statistical analysis

Data were expressed as count and percentages for categorical variables and as mean ± SDM for

Table 1 Baseline characteristics of patients observed in the study (*n* = 52) and included in groups treated with the sodium-glucose co-transporter-2 inhibitors or other glucose lowering drugs

Variable	SGLT2-I (*n* = 26)	OTHER (*n* = 26)	*P* value
Age (yr)	60.6 ± 6.78	63.4 ± 10.4	0.246
Sex (male/female)	15/11	15/11	1.000
BMI (kg/m^2)	34.8 ± 7.7	34.5 ± 5.9	0.875
No comorbidities, *n* (%)	2 (7.7)	2 (7.7)	1.000
Dyslipidemia, *n* (%)	13 (50.0)	15 (57.7)	0.578
Hypertension, *n* (%)	10 (38.5)	15 (57.7)	0.165
Chronic heart failure, *n* (%)	8 (30.8)	3 (11.5)	0.089
Chronic kidney disease, *n* (%)	9 (34.6)	4 (15.4)	0.109
AST (U/L)	48.5 ± 26.6	54.7 ± 13.3	0.293
ALT (U/L)	49.6 ± 39.2	65.0 ± 18.7	0.077
Gamma-GT (U/L)	151.3 ± 87.2	179.2 ± 56.9	0.178
Tryglycerides (mg/dL)	140.2 ± 45.9	133.5 ± 33.2	0.549
Fasting glucose (mg/dL)	150.1 ± 45.9	159.7 ± 49.8	0.473
HbA1c (%)	9.24 ± 3.01	8.73 ± 2.31	0.496
Creatininemia (mg/dL)	1.01 ± 0.44	0.88 ± 0.32	0.229
eGFR (mL/min/1.73 m^2)	61.4 ± 38.9	73.2 ± 24.6	0.197
Albuminemia (g/dL)	3.91 ± 0.44	4.08 ± 0.47	0.184
Platelets (*n*, × 10^3/mm^3)	175.7 ± 113.1	179.7 ± 76.7	0.882

BMI: Body mass index; AST: Aspartate aminotransferase; ALT: Alanine aminotransferase; Gamma-GT: Gamma-glutamyl transpeptidase; HbA1c: Hemoglobin A1c; eGFR: Epidermal growth factor receptor; SGLT2-I: Sodium-glucose co-transporter-2 inhibitor; OTHER: Other glucose lowering drug.

quantitative variables. Gaussian distribution of the samples was evaluated by Kolgomorov-Smirnov test. The significance of differences between the 2 treatment groups (SGLT2-I *vs* OTHER) at baseline was assessed by student's *t*-test (continuous variables) or in contingency tables by Pearson's Chi-squared test and Fisher's exact test (categorical variables). The significance of differences between the 2 treatment groups between the beginning (T0) and the end of the observational period (T1) was assessed by the two-way analysis of variance to test the main effects of time and treatment as a between-subject factor; the interaction time × treatment was studied, and a Tukey test was applied as post hoc test for multiple comparisons. The correlation analysis between changes in non-invasive markers of hepatic steatosis and fibrosis with fasting serum glucose or HbA1c, serum interleukins, or serum HNE- and MDA-protein adducts was performed using Pearson correlation test followed by linear regression. All tests were 2-sided, and $P < 0.05$ were considered statistically significant. Statistical analysis was performed with the Statistical Package for Social Sciences version 23.0 (SPSS, Inc., Chicago, IL) and Graph-Pad Prism 6.0 for Windows (GraphPad Software, Inc., San Diego, CA).

RESULTS

Baseline characteristics of the subjects included in the SGLT2-I or the OTHER group are represented in Table 1. The two groups were comparable in terms of clinical and biochemical features. No side effects in both groups were reported. After six months of treatment, a lowering effect on both fasting serum glucose (time factor: $F_{(1, 100)} = 16.04$, $P < 0.0001$) and HbA1c (time factor: $F_{(1, 100)} = 14.83$, $P < 0.0001$) was observed, with a significant reduction from T0 to T1 in both groups (Figures 1A and B). No significant variations were reported as regards serum triglycerides after 6 mo of treatment (Figure 1C). Interestingly, we observed an impact of time, treatment and interaction on body mass index (time factor: $F_{(1, 100)} = 4.146$, $P = 0.0444$; treatment factor: $F_{(1, 100)} = 4.169$, $P = 0.0438$; interaction factor: $F_{(1, 100)} = 5.650$, $P = 0.0194$), and the post hoc analysis resulted in significant differences between the two treatment groups at T1, and between T0 and T1 in the SGLT2-I group (Figure 1D). These data suggest that 6 mo of add-on treatment to metformin improves glycemic control compared to baseline; nevertheless, this improvement is not related to a particular drug class. Furthermore, a beneficial impact on weight loss is

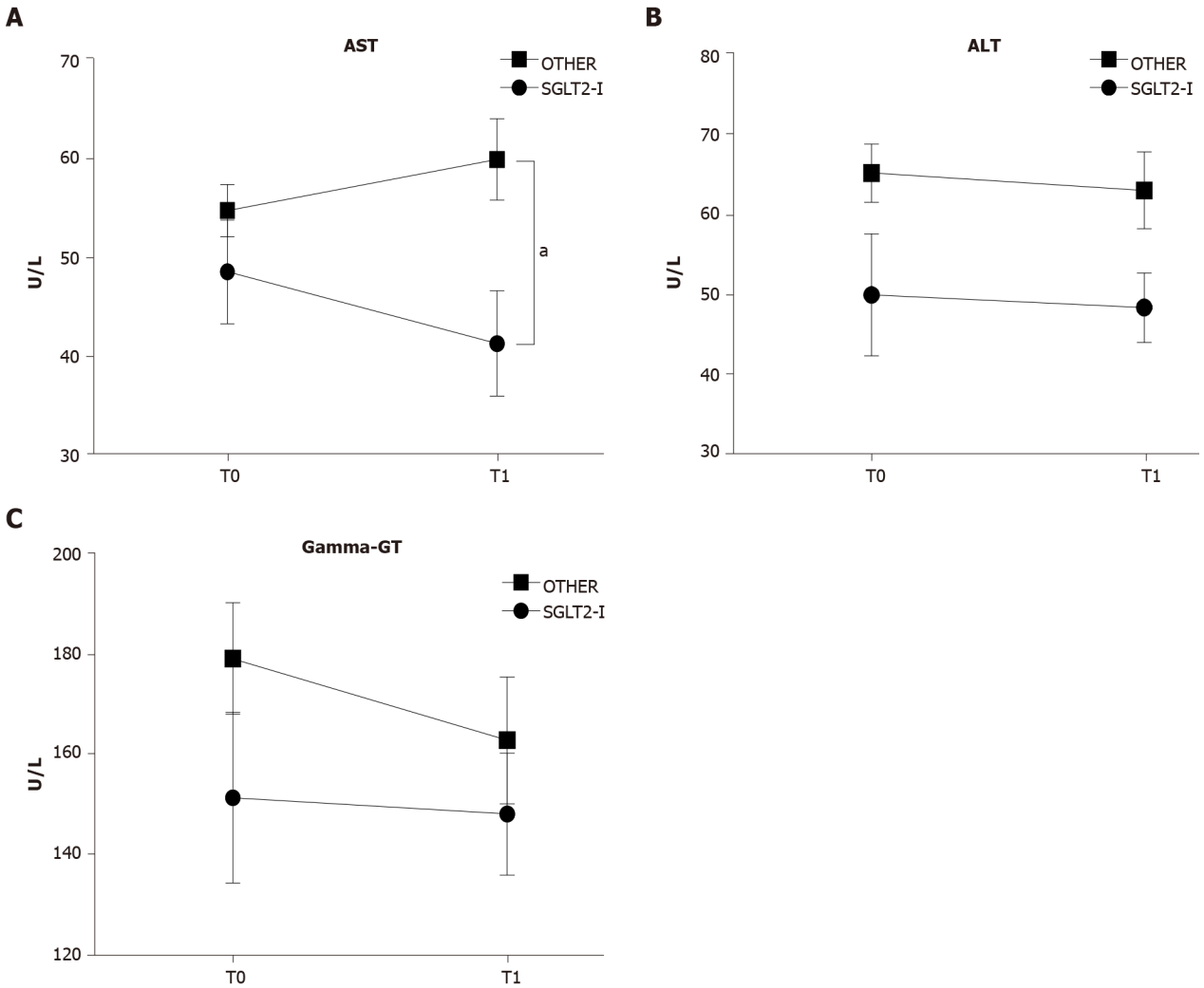

DOI: 10.3748/wjg.v28.i26.3243

Figure 2 Serum liver enzyme activities in patients enrolled in the study and included in groups treated with the sodium-glucose co-transporter-2 inhibitors or other glucose-lowering drugs before (T0) and after 1 wk of treatment (T1). A: Serum aspartate aminotransferase; B: Serum alanine aminotransferase; C: Serum gamma-glutamyl transpeptidase activities in patients observed in the study, grouped according to the assigned treatment. Data in the graphs are represented as mean ± SEM. Two-way analysis of variance and Tukey assessed statistical differences as posthoc test. $^{a}P < 0.05$. AST: Aspartate aminotransferase; ALT: Alanine aminotransferase; Gamma-GT: Gamma-glutamyl transpeptidase; SGLT2-I: Sodium-glucose co-transporter-2 inhibitor; OTHER: Other glucose lowering drug.

exerted by SGLT2-I but not by other glucose-lowering agents.

Effect of different add-on therapies on liver function tests and non-invasive markers of hepatic steatosis/fibrosis

We then compared the impact of combined treatment with SGLT2-I *vs* OTHER on circulating liver enzymes. The effect of treatment was significant for serum AST level ($F_{(1, 100)} = 7.703$, $P = 0.0066$), and the post hoc analysis showed lower values in SGLT2-I rather than the OTHER group at T1 (Figure 2A). No significant variations were reported for serum ALT and gamma-GT activities (Figures 2B and C). Non-invasive liver steatosis and fibrosis markers were further evaluated at baseline and after 6 mo of therapy in both groups. We observed the effect of both time and treatment on FLI (time factor: $F_{(1, 100)} = 8.279$, $P = 0.0049$ and treatment factor: $F_{(1, 100)} = 5.113$, $P = 0.0259$), but after 6 mo it decreased only in the SGLT2-I group - and not in OTHER patients - with respect to baseline (Figure 3A). A significant effect of treatment was also observed for the APRI ($F_{(1, 100)} = 5.309$, $P = 0.0233$), with a lower value in SGLT2-I rather than OTHER group at T1 (Figure 3B). The proportion of patients affected by a fibrotic form of liver disease according to NAFLD fibrosis score, FIB-4, and AST/ALT ratio reduced significantly after 6 mo of therapy in the SGLT2-I group rather than in the OTHER group (Table 2). Finally, we observed a significant effect of time ($F_{(1, 100)} = 7.996$, $P = 0.0057$) and interaction ($F_{(1, 100)} = 4.772$, $P = 0.0313$) on hepatic elastometry, and LS in patients treated with SGLT2-I for six months was lower with respect to baseline and to the OTHER group (Figure 3C).

Table 2 Non-invasive markers of hepatic fibrosis in patients observed in the study (*n* = 52) and included in groups treated with the sodium-glucose co-transporter-2 inhibitors or other glucose lowering drugs at baseline (T0) and after 6 mo of therapy (T1)

		T0	T1	*P* value
NAFLD fibrosis score (F3/4), *n* (%)	SGLT2-I (*n* = 26)	9 (34.6)	4 (15.4)	0.042
	OTHER (*n* = 26)	7 (26.9)	7 (26.9)	
FIB-4 (F3/4), *n* (%)	SGLT2-I (*n* = 26)	11 (42.3)	6 (23.1)	0.036
	OTHER (*n* = 26)	7 (26.9)	7 (26.9)	
AST/ALT ≥ 0.8, *n* (%)	SGLT2-I (*n* = 26)	15 (57.7)	6 (23.1)	0.001
	OTHER (*n* = 26)	10 (38.5)	11 (42.3)	

NAFLD: Non-alcoholic fatty liver disease; FIB-4: Fibrosis-4; AST: Aspartate aminotransferase; ALT: Alanine aminotransferase; SGLT2-I: Sodium-glucose co-transporter-2 inhibitor; OTHER: Other glucose lowering drug.

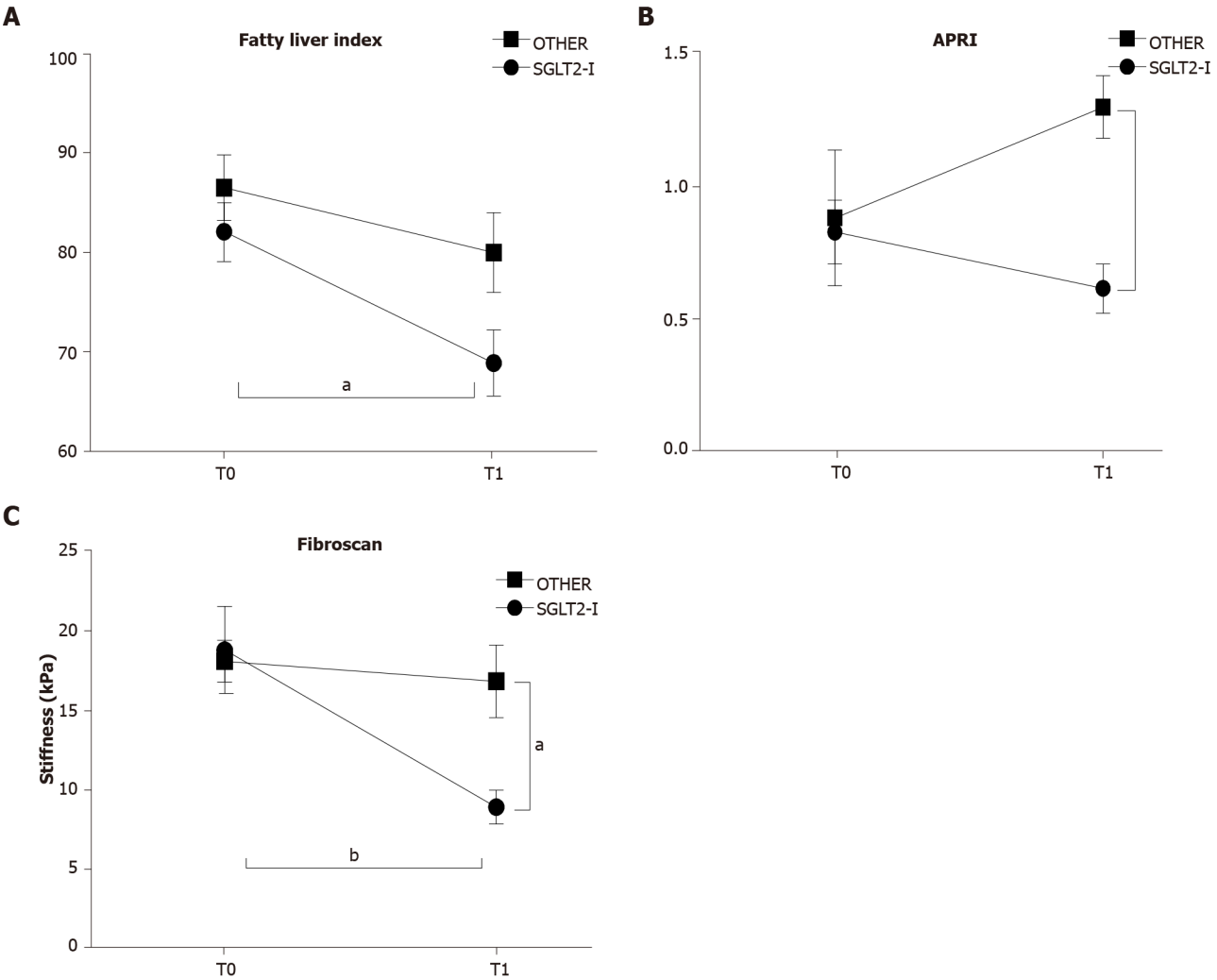

DOI: 10.3748/wjg.v28.i26.3243

Figure 3 Non-invasive markers of liver steatosis and fibrosis in patients enrolled in the study and included in groups treated with the sodium-glucose co-transporter-2 inhibitors or other glucose glucose-lowering before (T0) and after 1 wk of treatment (T1). A: Fatty liver index; B: Aspartate aminotransferase-to-platelet ratio index; C: Hepatic elastometry in patients observed in the study grouped according to the assigned treatment. Data in the graphs are represented as mean ± SEM. Two-way analysis of variance and Tukey assessed statistical differences as posthoc test. $^{a}P < 0.05$, $^{b}P < 0.01$. SGLT2-I: Sodium-glucose co-transporter-2 inhibitor; OTHER: Other glucose lowering drug; APRI: Aspartate aminotransferase-to-platelet ratio index.

Effect of different add-on therapies on circulating markers of inflammation and oxidative stress

We further analyzed markers of systemic inflammation, such as circulating interleukins and growth factors. Table 3 summarizes the results related to serum levels of 12 different cytokines and growth

Table 3 Circulating interleukin levels in patients enrolled in the study and included in groups treated with the sodium-glucose co-transporter-2 inhibitors or other glucose lowering drugs before (T0) and after 1 wk of treatment (T1)

Variable	SGLT2-I (*n* = 26)		OTHER (*n* = 26)		Fisher's test (1, 100)		
	T0	T1	T0	T1	Time	Treatment	Interaction
IL-1α (pg/mL)	1.35 ± 1.64	1.58 ± 1.30	1.44 ± 1.88	1.59 ± 1.56	0.373	0.026	0.016
IL-1β (pg/mL)	9.90 ± 2.39	7.31 ± 3.51[e]	8.84 ± 2.54	9.15 ± 2.42	4.455[a]	0.521	7.207[b]
IL-2 (U/mL)	≤ 0.5	≤ 0.5	≤ 0.5	≤ 0.5	-	-	-
IL-4 (pg/mL)	5.39 ± 4.20	8.54 ± 3.51[d]	4.89 ± 3.54	5.94 ± 3.66	8.207[b]	4.471[a]	2.052
IL-6 (pg/mL)	9.41 ± 4.21	6.92 ± 1.98	11.4 ± 5.41	13.7 ± 9.01[h]	0.007	15.4[c]	4.516[a]
IL-8 (pg/mL)	428 ± 216	409 ± 271	412 ± 296	449 ± 204	0.338	0.060	0.327
IL-10 (pg/mL)	1.33 ± 1.02	2.31 ± 1.12[e]	1.29 ± 1.06	1.32 ± 1.04[g]	5.894[a]	6.130[a]	5.214[a]
TNF (pg/mL)	6.82 ± 3.02	4.61 ± 2.01[d]	7.94 ± 3.14	7.81 ± 3.56[g]	3.989[a]	13.59[c]	3.151
VEGF (pg/mL)	262 ± 162	142 ± 109[d]	244 ± 201	268 ± 147[f]	2.393	3.029	5.384[a]
IFN-γ (pg/mL)	0.53 ± 0.23	0.57 ± 0.57	0.50 ± 0.39	0.61 ± 0.44	0.809	0.004	0.176
MCP-1 (pg/mL)	411 ± 168	291 ± 156	389 ± 154	414 ± 184[f]	2.131	2.408	4.964[a]
EGF (pg/mL)	25.7 ± 13.7	22.2 ± 12.1	24.9 ± 20.1	23.6 ± 18.6	0.553	0.009	0.116

[a]$P < 0.05$.
[b]$P < 0.01$.
[c]$P < 0.001$.
[d]$P < 0.05$ *vs* sodium-glucose co-transporter-2 inhibitor T0.
[e]$P < 0.01$ *vs* sodium-glucose co-transporter-2 inhibitor T0.
[f]$P < 0.05$ *vs* sodium-glucose co-transporter-2 inhibitor T1.
[g]$P < 0.01$ *vs* sodium-glucose co-transporter-2 inhibitor T1.
[h]$P < 0.001$ *vs* sodium-glucose co-transporter-2 inhibitor T1.
Data are expressed as mean ± SD. Statistical differences were assessed by two-way analysis of variance. VEGF: Vascular endothelial growth factor; MCP-1: Monocyte chemoattractant protein-1; EGF: Epidermal growth factor; SGLT2-I: Sodium-glucose co-transporter-2 inhibitor; OTHER: Other glucose lowering drug; IL: Interleukin; TNF: Tumor necrosis factor; IFN: Interferon.

factors evaluated at baseline (T0) and after 6 mo of therapy (T1) in both treatment groups. We could not observe any significant impact of time, treatment, or interaction on IL-1α, IL-2, IL-8, IFN-γ, and EGF. On the contrary, the time effect was observed for IL-1β, IL-4, IL-10, and TNF; the treatment effect was reported for IL-4, IL-6, IL-10, and TNF; the interaction effect was described for IL-1β, IL-6, IL-10, VEGF, and MCP-1. According to the post-hoc analysis, SGLT2-I patients at T1 showed: (1) Lower values of the pro-inflammatory cytokines IL-1β and TNF, and VEGF than T0; (2) Lower values of the pro-inflammatory cytokines IL-6 and TNF, VEGF, and MCP-1 than OTHER patients at T1; and (3) Higher values of the anti-inflammatory cytokines IL-4 and IL-10 as compared to SGLT2-I at T0 and OTHER at T1.

We evaluated systemic oxidative stress markers changes by measuring serum HNE- and MDA-protein adducts. A significant effect of treatment and interaction was observed for both HNE-protein adducts (treatment factor: $F_{(1, 100)} = 7.924$, $P = 0.0059$; interaction factor: $F_{(1, 100)} = 4.820$, $P = 0.0305$) and MDA-protein adducts (treatment factor: $F_{(1, 100)} = 10.17$, $P = 0.0019$; interaction factor: $F_{(1, 100)} = 5.844$, $P = 0.0174$). The post hoc analysis showed that, after 6 mo of therapy, circulating markers of oxidative stress were lower in the SGLT2-I group rather than OTHER patients; furthermore, HNE-protein adducts were significantly reduced from T0 to T1 in SGLT2-I patients (Figures 4A and B).

Reduction of liver steatosis and fibrosis markers is associated with decreased circulating oxidative stress in patients treated with SGLT2-I

We then focused on patients treated with SGLT2-I. We performed a Pearson's correlation analysis on non-invasive markers of hepatic steatosis and fibrosis, circulating parameters of glucose metabolism, inflammation, and oxidative stress after 6 mo of therapy. Of note, the FLI, the APRI, and LS showed: (1) A positive bivariate relationship with pro-inflammatory cytokines (IL-1β, IL6, TNF); and (2) A negative correlation with the anti-inflammatory cytokines (IL-4 and IL-10). Interestingly, all the non-invasive liver steatosis and fibrosis markers were strongly related to HNE- and MDA-protein adducts (Supplementary Table 2).

To verify whether the improvement of non-invasive markers of liver steatosis and fibrosis reported in patients treated with SGLT2-I after 6 mo of therapy was associated with the observed reduction of serum HNE- and MDA-protein adducts, a linear regression analysis on T1-T0 difference values was

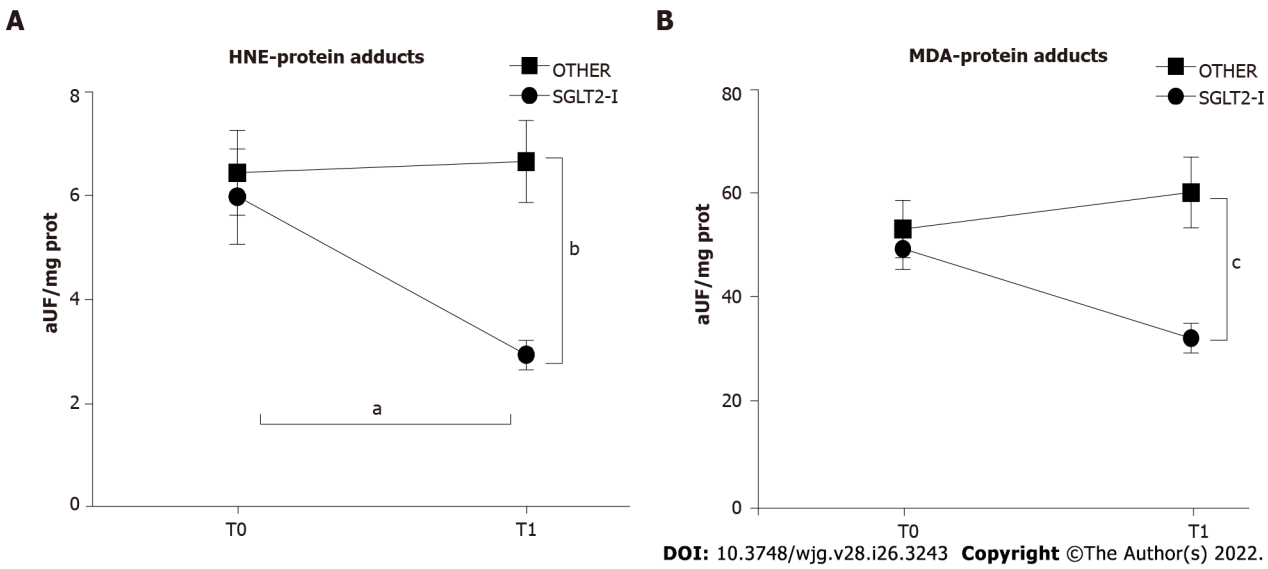

Figure 4 Circulating markers of oxidative stress in patients enrolled in the study and included in groups treated with the sodium-glucose co-transporter-2 inhibitors or other glucose-lowering drugs before (T0) and after 1 wk of treatment (T1). Data in the graphs are represented as mean ± SEM. Two-way analysis of variance and Tukey assessed statistical differences as a post hoc test. $^{a}P < 0.05$, $^{b}P < 0.01$, $^{c}P < 0.001$. HNE: Hydroxynonenal; MDA: Malondialdehyde; SGLT2-I: Sodium-glucose co-transporter-2 inhibitor; OTHER: Other glucose lowering drug.

performed. Further, SGLT2-I treatment related alterations in both markers of circulating oxidative stress were directly related to variations in FLI, APRI, and LS (Figures 5A-C).

DISCUSSION

The present study demonstrates that the addition of an SGLT2-I - as compared to dipeptidyl peptidase-4 inhibitors (DPP4-I) or pioglitazone - to metformin monotherapy exerts a positive impact on systemic inflammation and circulating oxidative stress in patients with T2DM and NAFLD. It is associated with favorable changes in the non-invasive hepatic steatosis and fibrosis markers. The incidence of T2DM is exponentially increasing worldwide[31]. T2DM often presents associated with NAFLD since insulin resistance accounts for the alteration of lipid homeostasis, favoring hepatic fat accumulation by induction of lipogenesis and inhibition of very-low-density lipoprotein secretion[32,33]. Furthermore, hyperglycemia in diabetic patients worsens insulin resistance through mechanisms induced by glucose toxicity[34]. In addition, the efficacy of several antidiabetic drugs is lost during the time, leading to the progression of T2DM, which could worsen NAFLD[35]. There are currently no approved therapies for the treatment for NAFLD. Several compounds tested in phase 2 and phase 3 clinical trials target metabolic stress as a critical factor for the initiation and progression of hepatic injury. Data on the effects of antidiabetic drugs in NAFLD are limited although pioglitazone and GLP1-RA have demonstrated some protective effects[36]. SGLT2-I are molecules with direct action on the kidney, reduce the reabsorption of filtered glucose and significantly decrease blood glucose levels both in fasting and post-prandial conditions, with consequent decline of glucose toxicity and improvement of insulin resistance [37]. Moreover, these drugs may interfere with several mechanisms involved in the progression of T2DM, such as dysfunction or apoptosis of pancreatic β-cells[38].

Clinical studies testing the efficacy of SGLT2-I on NAFLD demonstrated that this class of drugs reduces both hepatic steatosis, as evaluated by several imaging techniques, and serum liver enzymes [39]. Our study confirms these observations since we report that the addition of SGLT2-I to metformin reduces both the FLI and serum AST after 6 mo; this effect is not observed when pioglitazone or DPP4-I are added to metformin. Furthermore, our data show that six months of therapy with an SGLT2-I are associated with reducing hepatic fibrosis - which occurs mainly in NAFLD patients with higher fibrosis grade - as suggested by decrease in NAFLD fibrosis score, FIB-4, as well as LS measured by TE. These results are comparable to the reported outcome in a similar study, suggesting that SGLT2-I are superior to other oral hypoglycemic agents in reducing hepatic steatosis and fibrosis[40].

Among other glucose-lowering agents, pioglitazone and GLP1-RA were demonstrated to reduce hepatic steatosis, inflammation, and fibrosis[41,42]. We designed this study by excluding patients treated with GLP1-RA, even though 38.5% of patients of the OTHER group were treated with pioglitazone added to metformin. Despite this subgroup of patients in the comparison group, SGLT2-I improved non-invasive liver steatosis and fibrosis markers. A previous randomized trial compared the SGLT2-I ipragliflozin against pioglitazone, showing that both treatments were equivalent in reducing

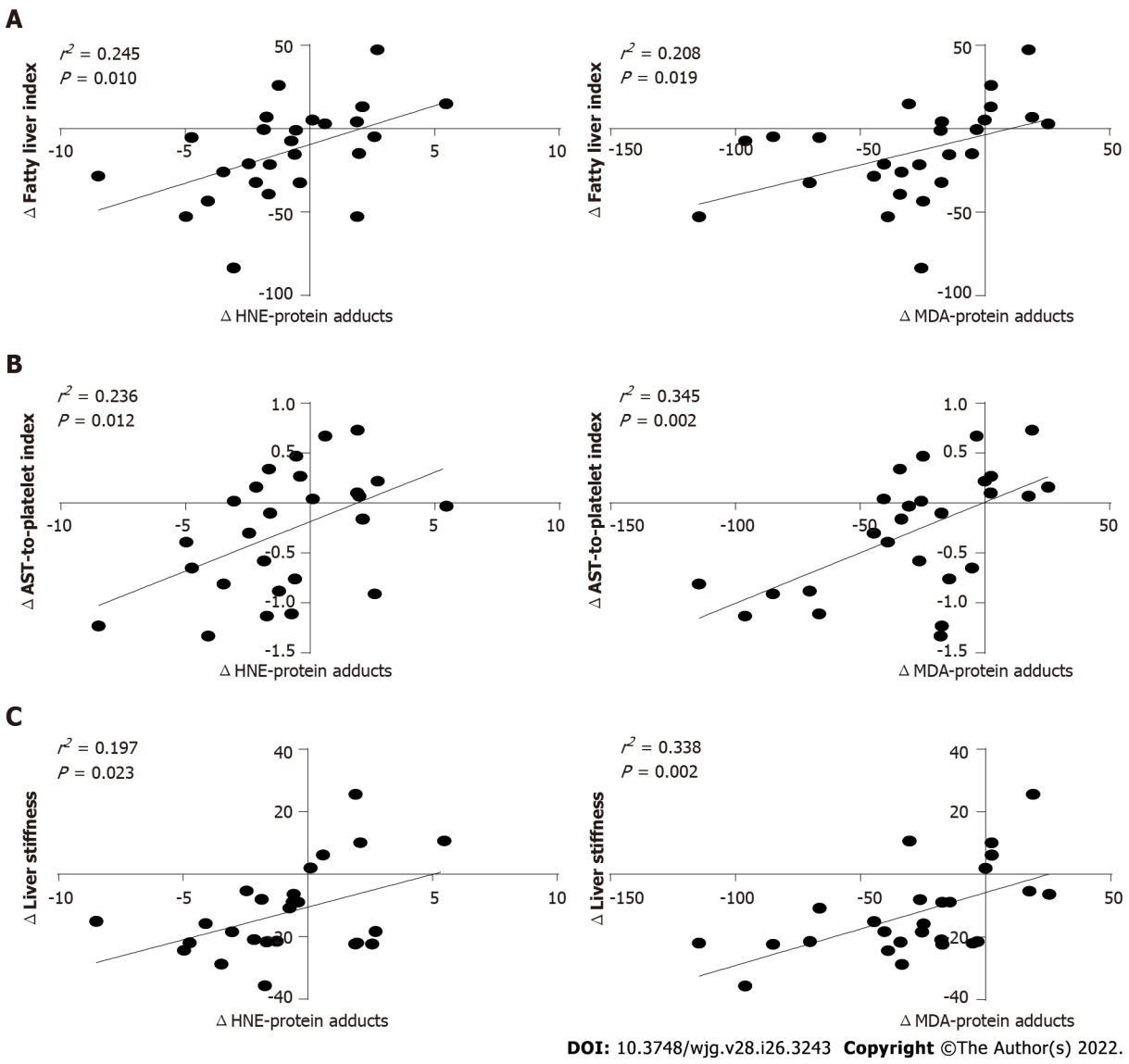

DOI: 10.3748/wjg.v28.i26.3243

Figure 5 Linear regression analysis between the variation of circulating oxidative stress parameters and non-invasive markers of hepatic steatosis or fibrosis in patients treated with the sodium-glucose co-transporter-2 inhibitors. Data in the graphs represent scatterplots of hydroxynonenal- or malondialdehyde-protein adducts A: Fatty liver index; B: Aspartate aminotransferase-to-platelet ratio index; C: Liver stiffness. HNE: Hydroxynonenal; AST: Aspartate aminotransferase; MDA: Malondialdehyd.

liver fat infiltration and serum aminotransferase levels, even though ipragliflozin effected a reduction in body weight and abdominal fat area[43]. However, it is worth noting that more than one-third of patients included in our study showed a high grade of steatosis and fibrosis as assessed by non-invasive markers. In contrast, previous studies using pioglitazone enrolled patients with milder hepatic injury. More than potentially explaining differences between the present results and those of different studies, our results suggest that SGLT2-I treatment would be more beneficial in T2DM patients with advanced NAFLD.

Mechanisms explaining the benefits of SGLT2-I therapy in T2DM and NAFLD are primarily undefined, but the results of this study lead to several speculations. Even though SGLT2-I significantly controls blood glucose, an improvement in glucose metabolism was described in all patients treated with additional drugs. However, other studies could not demonstrate that amelioration of NAFLD after SGLT2-I treatment was dependent on improved circulating glucose concentration[44-46]. Weight loss induced by non-pharmacological interventions such as diet, exercise, or bariatric surgery, may ameliorate liver damage in NAFLD[47]. SGLT2-I decreases body weight and fat mass, reducing hepatic steatosis and serum liver enzymes[48]. Our data show that SGLT2-I effectively promoted weight loss after 6 mo of therapy in patients with T2DM and NAFLD. However, there was no relationship between BMI reduction and the improvement of non-invasive markers of hepatic steatosis and fibrosis.

Besides, previous studies have also shown improved liver function tests, and steatosis irrespective of weight loss in patients affected by T2DM and NAFLD treated with SGLT2-I[49,50]. The evidence so far indicated that SGLT2-I would induce different beneficial mechanisms than glucose control and weight

loss in NAFLD. The present results further revealed that SGLT2-I - and not pioglitazone or DPP4-I - favorably modulate circulating cytokines, switching from pro-inflammatory to anti-inflammatory patterns, and reducing systemic markers of oxidative stress. These results are further buttressed by pre-clinical studies providing proving2-I inhibits pro-inflammatory cytokine secretion and reduces oxidative stress[16,51,52]. Our study clearly demonstrates a significant association between improving hepatic steatosis/fibrosis markers and reducing circulating oxidative stress in patients treated with SGLT2-I for 6 mo. On the other hand, we could not find any relationship between changes in circulating cytokines and reduction of liver injury markers. Reactive oxygen species (ROS) and reactive nitrogen species (RNS) represent physiological products of cellular metabolism, which are normally counteracted by endogenous antioxidants. When ROS/RNS production overwhelms the antioxidant defense, oxidative stress occurs with consequent injury of macromolecules such as nucleic acids (DNA oxidation), lipids (lipoperoxidation), and proteins, which in turn leads to an impairment of normal cellular functions[53]. Oxidative stress promotes the generation of HNE and MDA, lipid peroxidation products which are able to generate adducts with cellular and circulating proteins, which may be used as systemic markers of injury. Oxidative stress is considered one of the main determinants of NAFLD pathogenesis and progression[54]. For the first time, our study provides evidence that the reduction of circulating oxidative stress induced by SGLT2-I is related to improved markers of hepatic damage in T2DM patients with NAFLD, suggesting a potential protective mechanism by this drug class. Studies to define how SGLT2-I modulate molecular pathways that impact redox balance need to be designed.

This study suffers from the following limitations: (1) It was not designed as a randomized placebo-controlled trial since the type of combined treatment was decided according to a patient-centered approach (of note, the newest Standards of Medical Care in Diabetes were not available at the time of enrolment); (2) Patients treated with GLP-1 agonists were not included; (3) Since this study was performed at a single-center, it may have presented some bias, resulting in slightly larger intervention effects than multicenter studies; (4) Our small pilot study was not designed to determine the impact of single compounds; and (5) Liver histology was not performed to evaluate steatosis, inflammation, and fibrosis.

CONCLUSION

In conclusion, treatment with SGLT2-I in T2DM patients affected by NAFLD is associated with a rapid improvement of non-invasive markers of hepatic steatosis and fibrosis, providing insights into the mechanisms by which such class of antidiabetic drugs may reduce liver damage in humans. More extensive randomized controlled trials are encouraged to confirm these preliminary observations, and fundamental studies are needed to define the molecular mechanisms underlying the effects of SGLT2-I in NAFLD.

ARTICLE HIGHLIGHTS

Research background

Clinical trials of sodium glucose cotransporter-2 inhibitors (SGLT2-I), recently approved drugs for type 2 diabetes (T2D), reported beneficial cardiovascular (CV) and renal outcomes.

Research motivation

Inflammation and oxidative stress are major causes of vascular dysfunction and CV disease in diabetes and pre-clinical studies demonstrated that SGLT2-I promote anti-inflammatory effects by lowering oxidative stress.

Research objectives

To investigate the effects of SGLT2-I on markers of oxidative stress, inflammation, liver steatosis, and fibrosis in patients of T2D with non-alcoholic fatty liver disease (NAFLD).

Research methods

Observational prospective study enrolling 52 consecutive outpatients treated with metformin monotherapy and exhibiting poor glycemic control, which were introduced to an SGLT2-I (n = 26) or a different hypoglycemic drug (n = 26). Circulating interleukins and serum hydroxynonenal (HNE)- or malondialdehyde (MDA)-protein adducts, fatty liver index (FLI), NAFLD fibrosis score, aspartate aminotransferase (AST)/alanine aminotransferase (ALT) ratio ratio, AST-to-platelet-ratio index (APRI), and fibrosis-4, as well as transient elastography (FibroScan) on the day before (T0) and following treatment for six months (T1) were evaluated.

Research results

With respect to other hypoglycemic drugs, treatment with SGLT2-I resulted in a reduction of FLI and APRI, as well as of the FibroScan result, as well as lower circulating levels of interleukins (IL)-1β, IL-6, tumor necrosis factor, vascular endothelial growth factor, and monocyte chemoattractant protein-1, higher levels of IL-4 and IL-10, decreased serum HNE- and MDA-protein adducts. Markers of circulating oxidative stress correlated with liver steatosis and fibrosis scores.

Research conclusions

This study indicates that, more than optimizing glucose control, treatment with SGLT2-I in patients with T2D and NAFLD is associated with improvement of liver steatosis and fibrosis markers and circulating pro-inflammatory and redox status.

Research perspectives

This study encourages extensive randomized controlled trials to confirm these preliminary observations, and basic investigations to define the molecular mechanisms underlying the effects of SGLT2-I in NAFLD.

FOOTNOTES

Author contributions: Bellanti F and Vendemiale G designed and coordinated the study; Bellanti, F, Lo Buglio A, Dobrakowsky M, and Kasperczyk A performed the experiments, acquired and analyzed data; Bellanti F, Lo Buglio A, Dobrakowsky M, Kasperczyk A, Kasperczyk S, Serviddio G, Singh SP, Aich P, and Vendemiale G interpreted the data; Bellanti F wrote the manuscript; Kasperczyk S, Serviddio G, Singh SP, Aich P, and Vendemiale G supervised the manuscript; and all authors approved the final version of the article.

Institutional review board statement: The study was reviewed and approved by the Institutional Review Board at the University of Foggia.

Informed consent statement: All study participants, or their legal guardian, provided informed written consent prior to study enrollment.

Conflict-of-interest statement: All the authors report no relevant conflicts of interest for this article.

Data sharing statement: No additional data are available.

STROBE statement: The Authors have read the STROBE statement - checklist of items, and the manuscript was prepared and revised according to the STROBE statement - checklist of items.

Country/Territory of origin: Italy

ORCID number: Francesco Bellanti 0000-0002-8196-7373; Aurelio Lo Buglio 0000-0003-1569-3658; Michał Dobrakowski 0000-0001-8399-7624; Aleksandra Kasperczyk 0000-0002-2035-0388; Sławomir Kasperczyk 0000-0001-8974-5786; Palok Aich 0000-0003-4927-7812; Shivaram P Singh 0000-0002-8197-2674; Gaetano Serviddio 0000-0002-6424-7841; Gianluigi Vendemiale 0000-0002-7951-0219.

S-Editor: Wang JJ
L-Editor: A
P-Editor: Wang JJ

REFERENCES

1 **Redekop WK**, Koopmanschap MA, Stolk RP, Rutten GE, Wolffenbuttel BH, Niessen LW. Health-related quality of life and treatment satisfaction in Dutch patients with type 2 diabetes. *Diabetes Care* 2002; **25**: 458-463 [PMID: 11874930 DOI: 10.2337/diacare.25.3.458]

2 **Rao Kondapally Seshasai S**, Kaptoge S, Thompson A, Di Angelantonio E, Gao P, Sarwar N, Whincup PH, Mukamal KJ, Gillum RF, Holme I, Njølstad I, Fletcher A, Nilsson P, Lewington S, Collins R, Gudnason V, Thompson SG, Sattar N, Selvin E, Hu FB, Danesh J; Emerging Risk Factors Collaboration. Diabetes mellitus, fasting glucose, and risk of cause-specific death. *N Engl J Med* 2011; **364**: 829-841 [PMID: 21366474 DOI: 10.1056/NEJMoa1008862]

3 **Younossi ZM**, Loomba R, Rinella ME, Bugianesi E, Marchesini G, Neuschwander-Tetri BA, Serfaty L, Negro F, Caldwell SH, Ratziu V, Corey KE, Friedman SL, Abdelmalek MF, Harrison SA, Sanyal AJ, Lavine JE, Mathurin P, Charlton MR, Chalasani NP, Anstee QM, Kowdley KV, George J, Goodman ZD, Lindor K. Current and future therapeutic regimens for nonalcoholic fatty liver disease and nonalcoholic steatohepatitis. *Hepatology* 2018; **68**: 361-371 [PMID: 29222911 DOI: 10.1002/hep.29724]

4 **Younossi Z**, Tacke F, Arrese M, Chander Sharma B, Mostafa I, Bugianesi E, Wai-Sun Wong V, Yilmaz Y, George J, Fan J, Vos MB. Global Perspectives on Nonalcoholic Fatty Liver Disease and Nonalcoholic Steatohepatitis. *Hepatology* 2019; **69**: 2672-2682 [PMID: 30179269 DOI: 10.1002/hep.30251]

5 **Hardy T**, Oakley F, Anstee QM, Day CP. Nonalcoholic Fatty Liver Disease: Pathogenesis and Disease Spectrum. *Annu Rev Pathol* 2016; **11**: 451-496 [PMID: 26980160 DOI: 10.1146/annurev-pathol-012615-044224]

6 **Younossi Z**, Anstee QM, Marietti M, Hardy T, Henry L, Eslam M, George J, Bugianesi E. Global burden of NAFLD and NASH: trends, predictions, risk factors and prevention. *Nat Rev Gastroenterol Hepatol* 2018; **15**: 11-20 [PMID: 28930295 DOI: 10.1038/nrgastro.2017.109]

7 **Caussy C**, Aubin A, Loomba R. The Relationship Between Type 2 Diabetes, NAFLD, and Cardiovascular Risk. *Curr Diab Rep* 2021; **21**: 15 [PMID: 33742318 DOI: 10.1007/s11892-021-01383-7]

8 **Sajja AP**, Dey AK, Guha A, Elnabawi Y, Joshi AA, Kalra A. SGLT-2 Inhibitors and GLP-1 Agonists: First-Line Therapy for Diabetes With Established Cardiovascular Disease. *J Cardiovasc Pharmacol Ther* 2019; **24**: 422-427 [PMID: 31064213 DOI: 10.1177/1074248419838511]

9 **Dougherty JA**, Guirguis E, Thornby KA. A Systematic Review of Newer Antidiabetic Agents in the Treatment of Nonalcoholic Fatty Liver Disease. *Ann Pharmacother* 2021; **55**: 65-79 [PMID: 32571083 DOI: 10.1177/1060028020935105]

10 **Wu JH**, Foote C, Blomster J, Toyama T, Perkovic V, Sundström J, Neal B. Effects of sodium-glucose cotransporter-2 inhibitors on cardiovascular events, death, and major safety outcomes in adults with type 2 diabetes: a systematic review and meta-analysis. *Lancet Diabetes Endocrinol* 2016; **4**: 411-419 [PMID: 27009625 DOI: 10.1016/S2213-8587(16)00052-8]

11 **Kosiborod M**, Cavender MA, Fu AZ, Wilding JP, Khunti K, Holl RW, Norhammar A, Birkeland KI, Jørgensen ME, Thuresson M, Arya N, Bodegård J, Hammar N, Fenici P; CVD-REAL Investigators and Study Group*. Lower Risk of Heart Failure and Death in Patients Initiated on Sodium-Glucose Cotransporter-2 Inhibitors Versus Other Glucose-Lowering Drugs: The CVD-REAL Study (Comparative Effectiveness of Cardiovascular Outcomes in New Users of Sodium-Glucose Cotransporter-2 Inhibitors). *Circulation* 2017; **136**: 249-259 [PMID: 28522450 DOI: 10.1161/CIRCULATIONAHA.117.029190]

12 **Kosiborod M**, Lam CSP, Kohsaka S, Kim DJ, Karasik A, Shaw J, Tangri N, Goh SY, Thuresson M, Chen H, Surmont F, Hammar N, Fenici P; CVD-REAL Investigators and Study Group. Cardiovascular Events Associated With SGLT-2 Inhibitors Versus Other Glucose-Lowering Drugs: The CVD-REAL 2 Study. *J Am Coll Cardiol* 2018; **71**: 2628-2639 [PMID: 29540325 DOI: 10.1016/j.jacc.2018.03.009]

13 **Leng W**, Ouyang X, Lei X, Wu M, Chen L, Wu Q, Deng W, Liang Z. The SGLT-2 Inhibitor Dapagliflozin Has a Therapeutic Effect on Atherosclerosis in Diabetic ApoE$^{-/-}$ Mice. *Mediators Inflamm* 2016; **2016**: 6305735 [PMID: 28104929 DOI: 10.1155/2016/6305735]

14 **Han JH**, Oh TJ, Lee G, Maeng HJ, Lee DH, Kim KM, Choi SH, Jang HC, Lee HS, Park KS, Kim YB, Lim S. The beneficial effects of empagliflozin, an SGLT2 inhibitor, on atherosclerosis in ApoE $^{-/-}$ mice fed a western diet. *Diabetologia* 2017; **60**: 364-376 [PMID: 27866224 DOI: 10.1007/s00125-016-4158-2]

15 **Nasiri-Ansari N**, Dimitriadis GK, Agrogiannis G, Perrea D, Kostakis ID, Kaltsas G, Papavassiliou AG, Randeva HS, Kassi E. Canagliflozin attenuates the progression of atherosclerosis and inflammation process in APOE knockout mice. *Cardiovasc Diabetol* 2018; **17**: 106 [PMID: 30049285 DOI: 10.1186/s12933-018-0749-1]

16 **Steven S**, Oelze M, Hanf A, Kröller-Schön S, Kashani F, Roohani S, Welschof P, Kopp M, Gödtel-Armbrust U, Xia N, Li H, Schulz E, Lackner KJ, Wojnowski L, Bottari SP, Wenzel P, Mayoux E, Münzel T, Daiber A. The SGLT2 inhibitor empagliflozin improves the primary diabetic complications in ZDF rats. *Redox Biol* 2017; **13**: 370-385 [PMID: 28667906 DOI: 10.1016/j.redox.2017.06.009]

17 **Lahnwong S**, Chattipakorn SC, Chattipakorn N. Potential mechanisms responsible for cardioprotective effects of sodium-glucose co-transporter 2 inhibitors. *Cardiovasc Diabetol* 2018; **17**: 101 [PMID: 29991346 DOI: 10.1186/s12933-018-0745-5]

18 **Das NA**, Carpenter AJ, Belenchia A, Aroor AR, Noda M, Siebenlist U, Chandrasekar B, DeMarco VG. Empagliflozin reduces high glucose-induced oxidative stress and miR-21-dependent TRAF3IP2 induction and RECK suppression, and inhibits human renal proximal tubular epithelial cell migration and epithelial-to-mesenchymal transition. *Cell Signal* 2020; **68**: 109506 [PMID: 31862399 DOI: 10.1016/j.cellsig.2019.109506]

19 **Quagliariello V**, De Laurentiis M, Rea D, Barbieri A, Monti MG, Carbone A, Paccone A, Altucci L, Conte M, Canale ML, Botti G, Maurea N. The SGLT-2 inhibitor empagliflozin improves myocardial strain, reduces cardiac fibrosis and pro-inflammatory cytokines in non-diabetic mice treated with doxorubicin. *Cardiovasc Diabetol* 2021; **20**: 150 [PMID: 34301253 DOI: 10.1186/s12933-021-01346-y]

20 **Zeng S**, Delic D, Chu C, Xiong Y, Luo T, Chen X, Gaballa MMS, Xue Y, Cao Y, Hasan AA, Stadermann K, Frankenreiter S, Yin L, Krämer BK, Klein T, Hocher B. Antifibrotic effects of low dose SGLT2 Inhibition with empagliflozin in comparison to Ang II receptor blockade with telmisartan in 5/6 nephrectomised rats on high salt diet. *Biomed Pharmacother* 2022; **146**: 112606 [PMID: 34968924 DOI: 10.1016/j.biopha.2021.112606]

21 **European Association for the Study of the Liver (EASL)**; European Association for the Study of Diabetes (EASD); European Association for the Study of Obesity (EASO). EASL-EASD-EASO Clinical Practice Guidelines for the management of non-alcoholic fatty liver disease. *J Hepatol* 2016; **64**: 1388-1402 [PMID: 27062661 DOI: 10.1016/j.jhep.2015.11.004]

22 Standards of Medical Care in Diabetes-2017: Summary of Revisions. *Diabetes Care* 2017; **40**: S4-S5 [PMID: 27979887 DOI: 10.2337/dc17-S003]

23 **Molloy RM**, Mc Connell RI, Lamont JV, FitzGerald SP. Automation of biochip array technology for quality results. *Clin Chem Lab Med* 2005; **43**: 1303-1313 [PMID: 16309365 DOI: 10.1515/CCLM.2005.224]

24 **Bellanti F**, Romano AD, Lo Buglio A, Castriotta V, Guglielmi G, Greco A, Serviddio G, Vendemiale G. Oxidative stress is increased in sarcopenia and associated with cardiovascular disease risk in sarcopenic obesity. *Maturitas* 2018; **109**: 6-12 [PMID: 29452783 DOI: 10.1016/j.maturitas.2017.12.002]

25 **Koehler EM**, Schouten JN, Hansen BE, Hofman A, Stricker BH, Janssen HL. External validation of the fatty liver index for identifying nonalcoholic fatty liver disease in a population-based study. *Clin Gastroenterol Hepatol* 2013; **11**: 1201-1204 [PMID: 23353640 DOI: 10.1016/j.cgh.2012.12.031]

26 **Tapper EB**. The aspartate aminotransferase-to-platelet ratio and the evaluation of non-alcoholic fatty liver disease. *Gastroenterol Rep (Oxf)* 2014; **2**: 326-327 [PMID: 25371483 DOI: 10.1093/gastro/gou080]

27 **Angulo P**, Hui JM, Marchesini G, Bugianesi E, George J, Farrell GC, Enders F, Saksena S, Burt AD, Bida JP, Lindor K, Sanderson SO, Lenzi M, Adams LA, Kench J, Therneau TM, Day CP. The NAFLD fibrosis score: a noninvasive system that identifies liver fibrosis in patients with NAFLD. *Hepatology* 2007; **45**: 846-854 [PMID: 17393509 DOI: 10.1002/hep.21496]

28 **Shah AG**, Lydecker A, Murray K, Tetri BN, Contos MJ, Sanyal AJ; Nash Clinical Research Network. Comparison of noninvasive markers of fibrosis in patients with nonalcoholic fatty liver disease. *Clin Gastroenterol Hepatol* 2009; **7**: 1104-1112 [PMID: 19523535 DOI: 10.1016/j.cgh.2009.05.033]

29 **McPherson S**, Stewart SF, Henderson E, Burt AD, Day CP. Simple non-invasive fibrosis scoring systems can reliably exclude advanced fibrosis in patients with non-alcoholic fatty liver disease. *Gut* 2010; **59**: 1265-1269 [PMID: 20801772 DOI: 10.1136/gut.2010.216077]

30 **Wong VW**, Vergniol J, Wong GL, Foucher J, Chan HL, Le Bail B, Choi PC, Kowo M, Chan AW, Merrouche W, Sung JJ, de Lédinghen V. Diagnosis of fibrosis and cirrhosis using liver stiffness measurement in nonalcoholic fatty liver disease. *Hepatology* 2010; **51**: 454-462 [PMID: 20101745 DOI: 10.1002/hep.23312]

31 **Chatterjee S**, Khunti K, Davies MJ. Type 2 diabetes. *Lancet* 2017; **389**: 2239-2251 [PMID: 28190580 DOI: 10.1016/S0140-6736(17)30058-2]

32 **Poulsen MK**, Nellemann B, Stødkilde-Jørgensen H, Pedersen SB, Grønbæk H, Nielsen S. Impaired Insulin Suppression of VLDL-Triglyceride Kinetics in Nonalcoholic Fatty Liver Disease. *J Clin Endocrinol Metab* 2016; **101**: 1637-1646 [PMID: 26829441 DOI: 10.1210/jc.2015-3476]

33 **Smith GI**, Shankaran M, Yoshino M, Schweitzer GG, Chondronikola M, Beals JW, Okunade AL, Patterson BW, Nyangau E, Field T, Sirlin CB, Talukdar S, Hellerstein MK, Klein S. Insulin resistance drives hepatic de novo lipogenesis in nonalcoholic fatty liver disease. *J Clin Invest* 2020; **130**: 1453-1460 [PMID: 31805015 DOI: 10.1172/JCI134165]

34 **Luo W**, Ai L, Wang BF, Zhou Y. High glucose inhibits myogenesis and induces insulin resistance by down-regulating AKT signaling. *Biomed Pharmacother* 2019; **120**: 109498 [PMID: 31634780 DOI: 10.1016/j.biopha.2019.109498]

35 **Evans JL**, Goldfine ID. Aging and insulin resistance: just say iNOS. *Diabetes* 2013; **62**: 346-348 [PMID: 23349542 DOI: 10.2337/db12-1239]

36 **Snyder HS**, Sakaan SA, March KL, Siddique O, Cholankeril R, Cummings CD, Gadiparthi C, Satapathy SK, Ahmed A, Cholankeril G. Non-alcoholic Fatty Liver Disease: A Review of Anti-diabetic Pharmacologic Therapies. *J Clin Transl Hepatol* 2018; **6**: 168-174 [PMID: 29951362 DOI: 10.14218/JCTH.2017.00050]

37 **Chao EC**. SGLT-2 Inhibitors: A New Mechanism for Glycemic Control. *Clin Diabetes* 2014; **32**: 4-11 [PMID: 26246672 DOI: 10.2337/diaclin.32.1.4]

38 **Terami N**, Ogawa D, Tachibana H, Hatanaka T, Wada J, Nakatsuka A, Eguchi J, Horiguchi CS, Nishii N, Yamada H, Takei K, Makino H. Long-term treatment with the sodium glucose cotransporter 2 inhibitor, dapagliflozin, ameliorates glucose homeostasis and diabetic nephropathy in db/db mice. *PLoS One* 2014; **9**: e100777 [PMID: 24960177 DOI: 10.1371/journal.pone.0100777]

39 **Scheen AJ**. Effect of sodium-glucose cotransporter type 2 inhibitors on liver fat in patients with type 2 diabetes: hepatic beyond cardiovascular and renal protection? *Ann Transl Med* 2018; **6**: S68 [PMID: 30613643 DOI: 10.21037/atm.2018.10.39]

40 **Arai T**, Atsukawa M, Tsubota A, Mikami S, Ono H, Kawano T, Yoshida Y, Tanabe T, Okubo T, Hayama K, Nakagawa-Iwashita A, Itokawa N, Kondo C, Kaneko K, Emoto N, Nagao M, Inagaki K, Fukuda I, Sugihara H, Iwakiri K. Effect of sodium-glucose cotransporter 2 inhibitor in patients with non-alcoholic fatty liver disease and type 2 diabetes mellitus: a propensity score-matched analysis of real-world data. *Ther Adv Endocrinol Metab* 2021; **12**: 20420188211000243 [PMID: 33815743 DOI: 10.1177/20420188211000243]

41 **Musso G**, Cassader M, Paschetta E, Gambino R. Thiazolidinediones and Advanced Liver Fibrosis in Nonalcoholic Steatohepatitis: A Meta-analysis. *JAMA Intern Med* 2017; **177**: 633-640 [PMID: 28241279 DOI: 10.1001/jamainternmed.2016.9607]

42 **Lv X**, Dong Y, Hu L, Lu F, Zhou C, Qin S. Glucagon-like peptide-1 receptor agonists (GLP-1 RAs) for the management of nonalcoholic fatty liver disease (NAFLD): A systematic review. *Endocrinol Diabetes Metab* 2020; **3**: e00163 [PMID: 32704576 DOI: 10.1002/edm2.163]

43 **Ito D**, Shimizu S, Inoue K, Saito D, Yanagisawa M, Inukai K, Akiyama Y, Morimoto Y, Noda M, Shimada A. Comparison of Ipragliflozin and Pioglitazone Effects on Nonalcoholic Fatty Liver Disease in Patients With Type 2 Diabetes: A Randomized, 24-Week, Open-Label, Active-Controlled Trial. *Diabetes Care* 2017; **40**: 1364-1372 [PMID: 28751548 DOI: 10.2337/dc17-0518]

44 **Cefalu WT**, Leiter LA, Yoon KH, Arias P, Niskanen L, Xie J, Balis DA, Canovatchel W, Meininger G. Efficacy and safety of canagliflozin *vs* glimepiride in patients with type 2 diabetes inadequately controlled with metformin (CANTATA-SU): 52 wk results from a randomised, double-blind, phase 3 non-inferiority trial. *Lancet* 2013; **382**: 941-950 [PMID: 23850055 DOI: 10.1016/S0140-6736(13)60683-2]

45 **Kuchay MS**, Krishan S, Mishra SK, Farooqui KJ, Singh MK, Wasir JS, Bansal B, Kaur P, Jevalikar G, Gill HK, Choudhary NS, Mithal A. Effect of Empagliflozin on Liver Fat in Patients With Type 2 Diabetes and Nonalcoholic Fatty Liver Disease: A Randomized Controlled Trial (E-LIFT Trial). *Diabetes Care* 2018; **41**: 1801-1808 [PMID: 29895557

DOI: 10.2337/dc18-0165]

46 **Lee PCH**, Gu Y, Yeung MY, Fong CHY, Woo YC, Chow WS, Tan K, Lam KSL. Dapagliflozin and Empagliflozin Ameliorate Hepatic Dysfunction Among Chinese Subjects with Diabetes in Part Through Glycemic Improvement: A Single-Center, Retrospective, Observational Study. *Diabetes Ther* 2018; **9**: 285-295 [PMID: 29322486 DOI: 10.1007/s13300-017-0355-3]

47 **Hannah WN Jr**, Harrison SA. Effect of Weight Loss, Diet, Exercise, and Bariatric Surgery on Nonalcoholic Fatty Liver Disease. *Clin Liver Dis* 2016; **20**: 339-350 [PMID: 27063273 DOI: 10.1016/j.cld.2015.10.008]

48 **Koutoukidis DA**, Koshiaris C, Henry JA, Noreik M, Morris E, Manoharan I, Tudor K, Bodenham E, Dunnigan A, Jebb SA, Aveyard P. The effect of the magnitude of weight loss on non-alcoholic fatty liver disease: A systematic review and meta-analysis. *Metabolism* 2021; **115**: 154455 [PMID: 33259835 DOI: 10.1016/j.metabol.2020.154455]

49 **Komiya C**, Tsuchiya K, Shiba K, Miyachi Y, Furuke S, Shimazu N, Yamaguchi S, Kanno K, Ogawa Y. Ipragliflozin Improves Hepatic Steatosis in Obese Mice and Liver Dysfunction in Type 2 Diabetic Patients Irrespective of Body Weight Reduction. *PLoS One* 2016; **11**: e0151511 [PMID: 26977813 DOI: 10.1371/journal.pone.0151511]

50 **Sattar N**, Fitchett D, Hantel S, George JT, Zinman B. Empagliflozin is associated with improvements in liver enzymes potentially consistent with reductions in liver fat: results from randomised trials including the EMPA-REG OUTCOME® trial. *Diabetologia* 2018; **61**: 2155-2163 [PMID: 30066148 DOI: 10.1007/s00125-018-4702-3]

51 **Mancini SJ**, Boyd D, Katwan OJ, Strembitska A, Almabrouk TA, Kennedy S, Palmer TM, Salt IP. Canagliflozin inhibits interleukin-1β-stimulated cytokine and chemokine secretion in vascular endothelial cells by AMP-activated protein kinase-dependent and -independent mechanisms. *Sci Rep* 2018; **8**: 5276 [PMID: 29588466 DOI: 10.1038/s41598-018-23420-4]

52 **Lee DM**, Battson ML, Jarrell DK, Hou S, Ecton KE, Weir TL, Gentile CL. SGLT2 inhibition *via* dapagliflozin improves generalized vascular dysfunction and alters the gut microbiota in type 2 diabetic mice. *Cardiovasc Diabetol* 2018; **17**: 62 [PMID: 29703207 DOI: 10.1186/s12933-018-0708-x]

53 **Sies H**. Oxidative stress: a concept in redox biology and medicine. *Redox Biol* 2015; **4**: 180-183 [PMID: 25588755 DOI: 10.1016/j.redox.2015.01.002]

54 **Chen Z**, Tian R, She Z, Cai J, Li H. Role of oxidative stress in the pathogenesis of nonalcoholic fatty liver disease. *Free Radic Biol Med* 2020; **152**: 116-141 [PMID: 32156524 DOI: 10.1016/j.freeradbiomed.2020.02.025]

World Journal of Gastroenterology

Submit a Manuscript: https://www.f6publishing.com

World J Gastroenterol 2022 July 14; 28(26): 3258-3273

DOI: 10.3748/wjg.v28.i26.3258

ISSN 1007-9327 (print) ISSN 2219-2840 (online)

SYSTEMATIC REVIEWS

Endoscopic techniques for diagnosis and treatment of gastro-entero-pancreatic neuroendocrine neoplasms: Where we are

Roberta Elisa Rossi, Alessandra Elvevi, Camilla Gallo, Andrea Palermo, Pietro Invernizzi, Sara Massironi

Specialty type: Gastroenterology and hepatology

Provenance and peer review: Invited article; Externally peer reviewed.

Peer-review model: Single blind

Peer-review report's scientific quality classification

Grade A (Excellent): A
Grade B (Very good): B
Grade C (Good): 0
Grade D (Fair): 0
Grade E (Poor): 0

P-Reviewer: Batyrbekov K, Kazakhstan; Poddymova AV, Russia

Received: October 27, 2021
Peer-review started: October 27, 2021
First decision: December 27, 2021
Revised: January 4, 2022
Accepted: April 15, 2022
Article in press: April 15, 2022
Published online: July 14, 2022

Roberta Elisa Rossi, HPB Surgery, Hepatology and Liver Transplantation, ENETS Center of Excellence, Fondazione IRCCS Istituto Nazionale Tumori (INT, National Cancer Institute), Milan 20133, Italy

Alessandra Elvevi, Camilla Gallo, Andrea Palermo, Pietro Invernizzi, Sara Massironi, Division of Gastroenterology and Center for Autoimmune Liver Diseases, Department of Medicine and Surgery, University of Milano-Bicocca, Monza 20900, Italy

Corresponding author: Roberta Elisa Rossi, MD, PhD, Doctor, HPB Surgery, Hepatology and Liver Transplantation, ENETS Center of Excellence, Fondazione IRCCS Istituto Nazionale Tumori (INT, National Cancer Institute), Via G. Venezian 1, Milan 20133, Italy. robertaelisa.rossi@gmail.com

Abstract

BACKGROUND

The correct localization of the primary tumor site and a complete histological diagnosis represent the milestones for the proper management of gastro-entero-pancreatic neuroendocrine neoplasms (GEP-NENs).

AIM

To analyze current evidence on the role of endoscopy in the diagnosis/treatment of GEP-NENs.

METHODS

An extensive bibliographical search was performed in PubMed to identify guidelines and primary literature (retrospective and prospective studies, systematic reviews, case series) published in the last 15 years, using both medical subject heading (MeSH) terms and free-language keywords: gastro-entero-pancreatic neuroendocrine neoplasms; endoscopy; ultrasound endoscopy; capsule endoscopy; double-balloon enteroscopy; diagnosis; therapy; staging.

RESULTS

In the diagnostic setting, endoscopic ultrasonography (EUS) represents the diagnostic gold standard for pancreatic NENs and the technique of choice for the locoregional staging of gastric, duodenal and rectal NENs. The diagnosis of small bowel NENs (sbNENs) has been improved with the advent of video capsule endoscopy and double-balloon enteroscopy, which allow for direct visualization of the entire small bowel; however, data regarding the efficacy/safety of these techniques in the detection of sbNENs are scanty and often inconclusive. From a

therapeutic point of view, endoscopic removal is the treatment of choice for the majority of gastric NENs (type 1/2), for well-differentiated localized nonmetastatic duodenal NENs < 1 cm, confined to the submucosa layer and for < 10 mm, stage T1–T2, rectal NENs. EUS-guided pancreatic locoregional ablative treatments have been proposed in recent studies with promising results in order to control symptoms or reduce tumor burden in selected patients.

CONCLUSION

Standard axial endoscopy and EUS still play a pivotal role in several GEP-NENs. Advanced techniques for increasing the rate of R0 resection should be reserved for high-volume referral centers.

Key Words: Gastro-entero-pancreatic neuroendocrine neoplasms; Endoscopy; Ultrasound endoscopy; Capsule endoscopy; Double-balloon enteroscopy; Diagnosis; Therapy; Staging

Core tip: Standard axial endoscopy and endoscopic ultrasonography (EUS) play a pivotal role in gastro-entero-pancreatic neuroendocrine neoplasms (GEP-NENs). Upper/lower gastrointestinal endoscopy is essential for the detection of gastrointestinal NENs. EUS represents the diagnostic gold standard for pancreatic NENs and the technique of choice for the locoregional staging of gastric, duodenal and rectal NENs. The diagnosis of small bowel NENs has been improved with the advent of capsule endoscopy and double-balloon enteroscopy, however, their use is limited in clinical practice. In selected localized GEP-NENs, endoscopic therapy is appropriate with radical intent. The multidisciplinary management and the referral to high-volume tertiary centers remain fundamental.

Citation: Rossi RE, Elvevi A, Gallo C, Palermo A, Invernizzi P, Massironi S. Endoscopic techniques for diagnosis and treatment of gastro-entero-pancreatic neuroendocrine neoplasms: Where we are. *World J Gastroenterol* 2022; 28(26): 3258-3273

URL: https://www.wjgnet.com/1007-9327/full/v28/i26/3258.htm

DOI: https://dx.doi.org/10.3748/wjg.v28.i26.3258

INTRODUCTION

Gastro-entero-pancreatic neuroendocrine neoplasms (GEP-NENs) represent heterogeneous and rare tumors, whose incidence has been progressively increased in the last decades[1]. The prognosis of these neoplasms is widely variable depending on several factors including the site of the primary tumor, the grading as assessed by the specific WHO classification, and the stage as classified in a specific TNM system[2]. It is therefore clear that the correct localization of the primary tumor site, as well as a complete histologic diagnosis, represent the milestones for the proper management and the prognosis of these tumors[3-5].

In this scenario, despite advances in radiological and metabolic imaging, standard axial endoscopy and endoscopic ultrasonography (EUS) still play a pivotal role in several GEP-NENs. Upper gastrointestinal (GI) endoscopy is essential for the detection and characterization of esophageal, gastric, and duodenal NENs. Ileocolonoscopy allows the assessing and diagnosing of rectal, colonic and rarely distal ileal lesions. Small bowel NENs have proven difficult to diagnose, given their nonspecific presentation and poor accessibility of the distal small bowel to common endoscopic techniques. The diagnosis of small bowel NENs (sbNENs) has been largely improved with the advent of video capsule endoscopy (CE) in 2000 and double-balloon enteroscopy (DBE), the most promising device-assisted enteroscopy (DAE) system, in 2001, which allow for direct visualization of the entire Sb[6]. Finally, EUS is the modality of choice for both diagnosing pancreatic NENs and for the locoregional staging of several NENs, including gastric, duodenal, pancreatic and rectal NENs; of note, in the setting of pancreatic NENs (panNENs), it has demonstrated higher accuracy in tumor detection than other imaging modalities[7].

The present review is aimed at analyzing current evidence on the role of endoscopy in the management of GEP-NENs, with a specific focus on CE and DBE for sbNENs and EUS for the diagnosis and staging of panNENs and other NENs. Furthermore, we summarized available evidence on the role of endoscopy in the radical treatment of selected GEP-NENs.

MATERIALS AND METHODS

An extensive bibliographical search was performed in PubMed to identify guidelines and primary literature (retrospective and prospective studies, systematic reviews, case series) published in the last 15 years, using both medical subject heading (MeSH) terms and free-language keywords: gastro-entero-pancreatic neuroendocrine neoplasms; endoscopy; ultrasound endoscopy; capsule endoscopy; double-balloon enteroscopy; diagnosis; therapy; staging. The reference lists from the studies returned by the electronic search were manually searched to identify further relevant reports. The reference lists from all available review articles, primary studies, and proceedings of major meetings were also considered. Articles published as abstracts were included, whereas non-English language papers were excluded.

RESULTS

A total of 448 records were reviewed and 84 were defined as fulfilling the criteria for final consideration. Figure 1 presents the flow chart showing the process of study selection.

DIAGNOSIS

Ultrasound endoscopy (EUS)

EUS represents the diagnostic gold standard for panNENs and the technique of choice for the locoregional staging of gastric, duodenal and rectal NENs. According to the latest European Neuroendocrine Tumor Society (ENETS) Consensus guidelines, EUS proved to be the most accurate diagnostic technique in panNENs detection, leading to an up-to-94% sensitivity[8]; PanNENs usually appear rounded and homogeneously hypoechoic at EUS examination (Figure 2). EUS sensitivity in detecting panNENs is even higher than noninvasive computed tomography (CT)-scan or magnetic resonance imaging (MRI) pancreatic lesion detection rate[9]. EUS is also extremely accurate in locating the lesions, even very small ones, within the pancreatic parenchyma, and it can describe the distance between the lesion and the main pancreatic duct, which represents an independent predictor of aggressive tumor behavior and of developing pancreatic fistulas[10]. EUS overall complication rate is about 1%–2%, higher for pancreatic cysts rather than for solid masses[11].

Advanced EUS techniques allow to study specific morphological and histological details of the detected lesions that may be helpful in the differential diagnosis of panNENs and in the choice of the corresponding best-suited treatment[7]. Contrast-enhanced harmonic EUS (CH-EUS) allows real-time visualization of parenchymal perfusion and, thus, helps in distinguishing hypovascular carcinomas from hypervascular less aggressive lesions. It consists of harmonic detectors that register microbubbles produced by contrast agents administrated intravenously; this method allows the identification of microvessels even with slow blood flow[12]. As demonstrated for nonfunctioning panNENs, the CH-EUS vascular pattern of neuroendocrine lesions represents an indirect reliable surrogate predictor of their aggressiveness and, thus, of their prognosis; a statistically significant positive correlation was, in fact, proven between the inhomogeneous sonographic pattern of the lesions and their Ki67 proliferative index, which in turn represents the most reliable independent predictor of malignancy. Sonographic heterogeneity at CH-EUS, and especially hypoenhancement in the early arterial phase, corresponds to lower intratumoral microvascular density and to a greater degree of fibrosis on pathological specimens, which were demonstrated to be typical features of tumor aggressiveness on a par with tumor grading [13]. According to a Japanese retrospective study[14], hypoenhancement at CH-EUS proved to be a reliable predictor of tumor aggressiveness and poor prognosis also for G1 and G2 panNENs, with sensitivity, specificity, positive predictive value, negative predictive value and accuracy of 94.7%, 100%, 100%, 96.6% and 97.9%, respectively.

EUS-fine needle aspiration (FNA) is another diagnostic advanced EUS technique, which represents the gold standard least invasive option to obtain the histological identification of a suspected pancreatic neoplasm or peripancreatic lymph nodes, with a sensitivity ranging between 80% and 90% and a specificity of nearly 96%[15] (Figure 3). It is also the operative technique of choice to aspirate the contents of cystic lesions for serological analysis and for the tumor marker dosage, which might help in the differential diagnosis of pancreatic cystic lesions. It can be performed with different diameter needles, mainly depending on the type and site of the lesion, its consistency, and echogenicity. There are several techniques described, which make different use of the suction: some of them suggest not to apply any suction due to the high risk of contaminating the specimen with blood (especially in case of highly vascularized lesions), some others apply wet or dry negative-pressure suction to guarantee sufficient material for histological diagnosis, and others again proposed a slow-pull fanning technique to ensure at the same time a greater collection of pathological cells and a low blood contamination risk [16]; to date, even if still no consensus has been reached on the optimal strategy, overall FNA–EUS sampling adequacy rates up to 94%[17,18] and its diagnostic sensitivity proved to be significantly higher

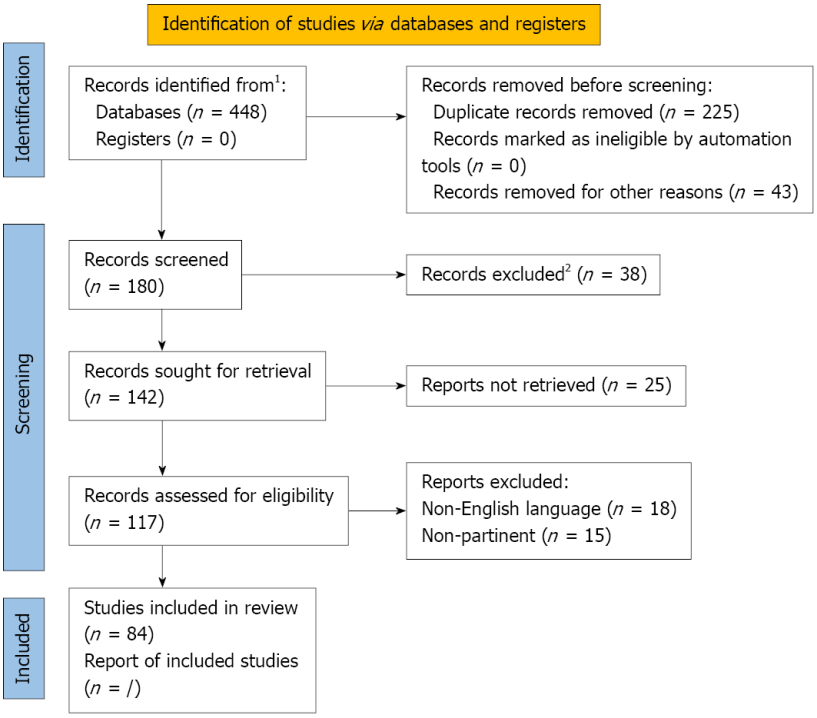

DOI: 10.3748/wjg.v28.i26.3258

Figure 1 The flow chart showing the process of study selection.

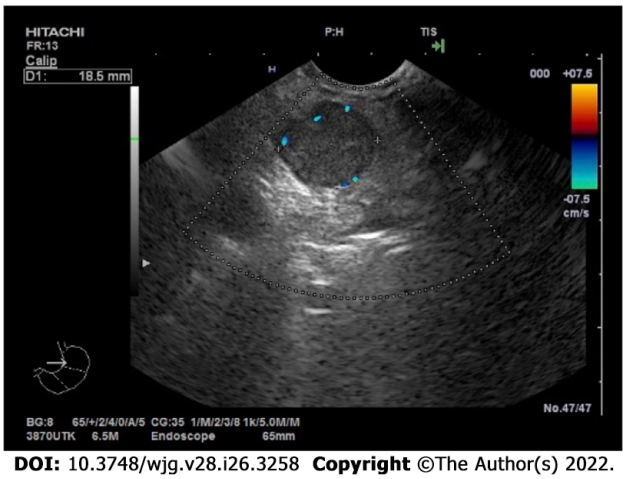

DOI: 10.3748/wjg.v28.i26.3258

Figure 2 Endoscopic appearance at endoscopic ultrasound of a pancreatic neuroendocrine neoplasm with marginal vascularization.

than CT and/or MRI specifically in case of solid, cystic and combined solid-cystic panNENs (84% *vs* 42%, 70% *vs* 10% and 81% *vs* 36% respectively)[19].

The Ki-67 index histological expression of the suspected pancreatic lesion plays a fundamental role in defining the aggressiveness of the tumor, together with its radiological aspect, its localization and distance from the pancreatic duct, and its CH-EUS vascular behavior. Therefore, the Ki-67 index also drives the choice of the best-suited therapeutic approach. Data about the concordance rate between EUS–FNA and surgical specimens in terms of G1, G2 or G3 panNEN and G3 pan-neuroendocrine carcinoma differentiation based on the Ki-67 index are discordant, ranging from a 78% of accordance rate (k-statistic: 0.65)[10], to a relatively significant discrepancy, especially for G2 lesions[20]. This discordance may be first attributed to the fact that endoscopic sampling of large lesions > 20 mm, often included in the studies available to date, may not be representative of the area with the highest concentration of malignant cells and, thus, that the measured Ki-67 index might be not indicative of the most proliferative area of the neoplasm. There is a strong necessity for further studies that subclassify more accurately the included lesions depending on their size.

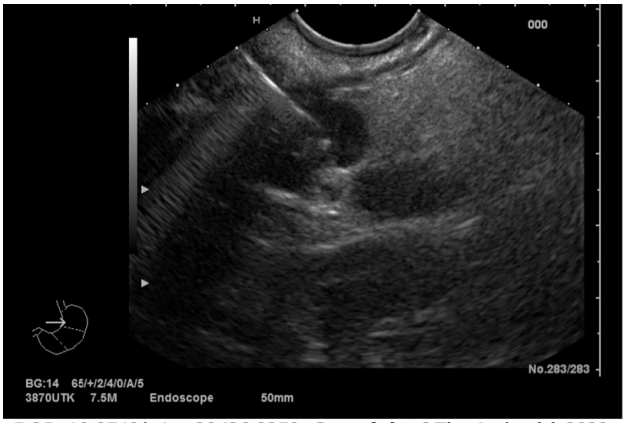

DOI: 10.3748/wjg.v28.i26.3258

Figure 3 Endoscopic appearance at endoscopic ultrasound of a pancreatic neuroendocrine neoplasm located at the tail of the pancreas during fine needle aspiration/biopsy procedure.

New EUS needle acquisition techniques (*i.e.*, 19/22/25- G ProCoreTM needle, Cook Endoscopy, Winston-Salem, NC, USA; 19-G fine-needle biopsy, Cook Endoscopy Inc., Limerick, Ireland; Acquire® Endoscopic Ultrasound Fine Needle Biopsy (FNB) Device 22/25-G, Boston Scientific, Natick, MA, USA; SharkCoreTM, Covidien, Dublin, Ireland) have been proposed to overcome the rare cases of EUS–FNA inadequate tissue sampling; these devices are designed to maximize tissue capture and minimize bleeding and tissue fragmentation and some of them are thought to provide both cytological and histological sampling[21]. However, further studies are needed to validate these approaches in the specific setting of NENs.

EUS real-time elastography (EUS–RTE) allows not only a qualitative but also a quantitative assessment of the elasticity of the suspected pancreatic lesion compared to the one of the normal surrounding pancreatic parenchyma. Based on the evidence of higher tissue stiffness in the case of malignant lesions when compared to the normal parenchyma[22], some authors have proposed different quantitative elastography cutoffs to stratify the risk of malignancy. Havre *et al*[23] observed a EUS–RTE sensitivity of 67% and specificity of 71% in detecting pancreatic malignant lesions with a strain ratio cutoff of 4.4. Iglesias-García *et al*[24] showed an EUS–RTE sensitivity of 100% and specificity of 88% in differentiating specifically pancreatic adenocarcinomas from panNENs with a 26.6 strain ratio cutoff value. Even if, according to the European Federation of Societies for Ultrasound in Medicine and Biology (EFSUMB) guidelines, EUS–RTE cannot yet replace the histo-cytopathological diagnosis of carcinoma[25], this technique may facilitate the differentiation from benign to malignant pancreatic lesions.

Another advanced technique in EUS that can drive in the diagnostic orientation is represented by the needle-based confocal laser endomicroscopy, which allows the real-time direct *in vivo* visualization of the histological aspect of the GI mucosa overlying pancreatic NENs, which is traditionally described as clusters of compact cells on a dark background surrounded by numerous small and irregular vessels and fibrotic areas[26]. Giovannini *et al*[27], observed a negative predictive value of 100% for the characterization of pancreatic NENs in EUS needle-based confocal laser endomicroscopy; therefore supporting the concept that it cannot be considered as an alternative to the histological diagnosis, but that it may help to rule out malignancy.

Further applications of EUS in panNENs is represented by the preoperative EUS-guided fine-needle tattooing and EUS-guided fiducial implantation, which may help surgeons find little pancreatic lesions during laparoscopic surgery, limiting the laparoscopic resection to the lesion itself, sparing the normal surrounding parenchyma, and reducing the operating time[28].

As regards GI-NENs, EUS mainly plays a diagnostic and staging role; its sensitivity in detecting GI-NENs is up to 94%[29]; they usually appear as submucosal rounded, hypoechoic, well-demarcated lesions and can be detected when smaller than 10 mm, especially rectal NENs thanks to the growing sensibility to colorectal carcinoma screening. According to the ENETS most recent guidelines, in case of the endoscopic identification of a GI lesion that is compatible with a GI-NEN, EUS is recommended in case of lesions > 10 mm in order to study the depth of the lesion, to stage the hypothetical presence of locoregional lymph nodes and, thus, to drive the choice of the most appropriate endoscopic or surgical treatment[30]. Less than 10 mm GI-NENs, in fact, have a low risk of both lymphatic invasion and distant metastases, which is reported to be 1%–2%[31]. GI-NENs measuring 10–19 mm at their first endoscopic diagnosis deserve more accurate EUS evaluation because of the reported higher incidence rate of lymph node invasion or distant metastases, leading up to 5%–15%[32]. If the GI-NEN is limited to the submucosa and does not invade the muscularis mucosae (which corresponds to a T1 lesion), regardless of its lateral spreading, a simple *en bloc* endoscopic resection treatment has proved to be effective in

guaranteeing a radical resection and a very limited recurrence rate during the follow-up[33], otherwise, a surgical approach is suggested. T2 or N+ stage lesions should be accurately studied with total body imaging such as 68-Ga-DOTATATE positron emission tomography (PET) and a CT scan in order to plan the best therapeutic approach.

Capsule Endoscopy (CE) and Double-balloon enteroscopy (DBE)

The small intestine is the most common NEN site in humans. Historically, sbNENs have proved difficult to diagnose because of both the lack of specific symptoms at presentation and the poor accessibility of the distal small bowel[34]. Conventional radiology (both CT and MRI either in the standard technique or in combination with enteroclysis) are often not accurate enough in the detection of sbNENs [35], whereas PET/CT with 68Ga-DOTA peptides remains the most sensitive modality in the detection of well-differentiated NENs, although it does not allow to get a histological diagnosis and might not be fully accurate in the anatomical location of the primary tumor being, for instance, unable to differentiate between intestinal and mesenteric localization[36]. Furthermore, in the case of metastatic disease, the detection of the primary tumor is recommended in both resectable and non resectable diseases. However, in up to 10% of the cases after the discovery of liver or lymph node metastases, the primary tumor site remains unknown despite an extensive workup[35].

With the advent of CE and DBE the diagnosis of sbNENs has improved, even if data regarding the efficacy and safety of these techniques in the detection of sbNENs are scanty and mainly based on small retrospective series, given the rarity of the disease and the still-limited use of these techniques in routine clinical practice. Most of the available studies are focused on small bowel tumors in general and only a small percentage of included patients displayed an sbNEN[37-39]. In a study comparing CT, enteroclysis, nuclear imaging, and CE of the small bowel[34], CE showed a high diagnostic yield (45%) in identifying primary tumors. Of note, in 12 of 20 patients (60%), CE showed small-intestinal lesions that were then confirmed histologically as NEN in six of seven patients who underwent surgery.

When considering the few studies specifically focused on NENs, the results came back to be inconclusive. In a retrospective study by Frilling *et al*[40], including 390 patients with metastatic NENs of whom 11 with unknown primary tumor, CE identified lesions suggestive of small bowel primary in 8/10 patients in whom it was successful, and these tumors were all histologically confirmed. In a recent prospective study[41], the diagnostic yield of CE was reported to be limited. In 24 patients with a histological diagnosis of metastatic NEN of unknown origin, CE, which was preferred to DBE as less invasive and less expensive, was requested before explorative laparotomy and its diagnostic yield was compared to the surgical exploration. CE identified a primary sbNEN in 11 subjects. However, diagnosis of sbNEN was confirmed only in five (41%) cases after surgical and ultrasound exploration were performed. The high number of false-positive results could have been related to small bowel contractions, extrinsic compression, lymph stasis, or submucosal lesion of another type.

Although CE is less invasive, DBE is necessary for determining the precise location, number of tumors, and pathological diagnosis; it can be carried out through the oral (antegrade) or the anal (retrograde) route and with a combined oral and anal approach[42]. Bellutti *et al*[43], in a study involving 12 consecutive patients with suspected sbNEN or with liver NEN metastases, who underwent DBE, found a diagnostic yield of DBE for primary tumor of 33%. In a case series by Scherubl *et al*[44], five consecutive patients with metastatic midgut carcinoids underwent DBE and an NEN of the ileum was detected in four of the five patients; the histopathological evaluation of their biopsy specimens confirmed the diagnosis revealing well-differentiated NENs. Conversely, conventional radiological imaging did not visualize any of the primary tumors.

In our recent prospective study[45], we reported sensitivity and specificity of 60% and 100%, respectively for DBE in detecting sbNEN in six patients with unknown primary, showing that DBE is a safe and effective procedure in diagnosing sbNENs. We suggested that when a sbNEN is suspected, DBE should be taken into account as an accurate diagnostic tool in order both to collect biopsies for final diagnosis and to make tattoos before surgery; of note, DBE should be preferred over CE in the presurgical setting given the high specificity. Considering the limited available data, further studies are needed to better define the actual role of CE and DBE in the diagnosis of sbNENs.

TREATMENT

Gastric NENs

Gastric NENs (gNENs) are usually subclassified into three types, according to their pathophysiology and behavior[29,46]. Type I tumors correspond to the majority of gNENs (~80%) and are associated with autoimmune atrophic gastritis. Histologically, type I gNENs are composed of enterochromaffin-like cells. The diagnosis is made by upper digestive endoscopy with biopsy. The majority of type I gNENs present as small, multiple tumors, located in the gastric body or fundus, and limited to the mucosal or submucosal layers of the stomach wall[46,47]. Since the risk of metastasis is < 5% in type I gNENs, a conservative approach based on endoscopic follow-up with lesion resection is advised for this kind of tumor. The treatment of choice for type I gNENs is endoscopic resection for lesions > 0.5 cm and

endoscopic surveillance for lesions < 0.5 cm[46,48,49]. This approach has been shown to be safe and effective in a prospective series of 33 type I gNENs, with no significant procedure-related complications, no development of metastases, and a 100% long-term survival rate[50].

The ENETS guidelines[29] suggest performing EUS in case of lesions > 1 cm. Staging EUS is frequently performed to confirm the appropriateness of endoscopic resection, which applies to lesions not infiltrating beyond the muscularis propria[7]. For lesions > 1 cm, EUS is excellent for determining the exact tumor size and for excluding infiltration of the type I gNENs into the muscularis propria (T2) or enlarged regional lymph nodes[47,51].

Type II gNENs correspond to 5%–10% of gNENs; they usually develop when multiple endocrine neoplasia type 1 is present and are often associated with Zollinger–Ellison syndrome[46,48]. Like type I gNENs, type II gNENs originate from enterochromaffin-like cells. They are small, multiple, and relatively benign tumors, even though about 10%–30% of patients present as metastatic at the diagnosis [52]. For type II gNENs local excision is recommended, preferentially by endoscopy; as well as for type I gNENs, EUS plays a pivotal role in determining the tumor size, lymph node involvement, and depth of invasion; endoscopic treatment is again reserved for lesions not infiltrating beyond the muscularis propria, without lymph node involvement[7,53].

Type III gastric NENs are usually larger sporadic tumors with an infiltrative and metastatic tendency and account for 15% of all gNENs. They are generally characterized by being single lesions, > 1 cm and with a greater likelihood of evolving to regional and systemic metastases, as more than half of patients with type III gNENs are metastatic at diagnosis, mainly to the liver[46,48]. From a therapeutic point of view, surgery is the standard treatment, *i.e.*, total or subtotal gastrectomy together with lymphadenectomy, as recommended in gastric adenocarcinoma. For patients with any surgical contraindication, endoscopic resection may be an alternative, but the risk of regional lymph node spread remains high [46]. Of note, in selected cases of small (< 1 cm) type III G1/G2 (Ki-67 < 5%) gNENs fully resected (R0) by endoscopy with no risk factors for metastatic disease, endoscopic resection might be sufficient[54]. As for other gNENs, EUS is a useful tool for locoregional staging, particularly to stage the disease by assessing the presence of regional lymph node involvement.

Conventional polypectomy with a snare for flat mucosal lesions should be avoided because complete resection is often not achieved. Early gNENs are generally removed by endoscopic mucosal resection (EMR) or endoscopic submucosal dissection (ESD)[47,54]. In EMR, snare resection is preceded by the submucosal injection of saline in order to raise the tumor and cut into the submucosa below the tumor [47]. ESD is preferred over EMR in case of suspicion of limited submucosal invasion or a tumor > 2 cm [55]. After submucosal injection of saline, the submucosa is dissected with specific knives in order to achieve endoscopic *en bloc* resection of the whole neoplasm.

The resected specimen has to be carefully evaluated regarding grade, angioinvasion, and infiltration of the deep resection margin. In case of angioinvasion, histological infiltration of the muscularis propria (T2), or grade G2/G3, radicalization with surgery with lymph node dissection is the therapy of choice in localized neuroendocrine disease[47].

Duodenal NENs

Duodenal NENs (dNENs) are rare, usually small well-differentiated tumors in most of the cases; however, according to a recent multicenter retrospective study[56], dNENs' prognosis may be highly variable as these tumors can be metastatic in up to 50% of the cases at the time of first diagnosis and can develop metastases thereafter. Upper GI endoscopy with biopsy is necessary for dNEN diagnosis and EUS should be performed to assess the local extent of tumor depth.

In view of this heterogeneous behavior, surgical resection has been suggested as the preferred treatment modality over endoscopic treatment, and surgery is generally recommended for ampullary dNENs and lesions > 2 cm in size[38]. Endoscopic resection is the treatment of choice for well-differentiated localized nonmetastatic tumors with a diameter < 1 cm and confined to the submucosa layer and the rationale for preferring the endoscopic treatment for tumors < 1 cm relies on the fact that they seem to have a low rate of nodal disease[57]. In this setting, there is no current evidence to prefer an endoscopic approach over another as prospective studies comparing the available techniques (*i.e.*, ESD *vs* EMR) are lacking.

However, there is still controversy regarding the management of tumors between 1 and 2 cm, which is mainly based on the tumor location and the presence of nodal involvement on imaging. According to some authors, > 10% of patients with dNENs < 1 cm in size develop lymph node metastases, thus suggesting the need for a radical surgical approach for all dNENs despite the size of the primary tumor [58-60]. Another issue to be taken into account is the high risk of conventional and functional imaging of understaging mainly due to the presence of nodal and distant micrometastases[60]. These results represent a sign of warning for conservative approaches including endoscopy, suggesting as a possible strategy, the inclusion of EUS in the preoperative phase, although prospective studies are necessary to draw solid conclusions.

In summary, all considered, endoscopic resection either EMR or ESD should be reserved for dNENs < 10 mm, limited to the submucosal layer without evidence of lymph node or distant metastases, whereas surgery might be advised for dNENs > 10 mm with evidence of muscular layer invasion or nodal involvement. EUS should be encouraged for all dNENs in order to plan the best therapeutic approach.

Rectal NENs

Endoscopic treatment for rectal NENs (rNENs) is indicated if there is no evidence of invasion beyond submucosa and presence of locoregional disease since it aims to achieve a complete oncological resection[61].

The ENETS guidelines[30] suggest that well-differentiated (G1/G2) rNENs that are < 10 mm in stage T1 and T2 and rNENs between 10 and 20 mm in stage T1 without lymph node metastasis should be removed endoscopically. On the contrary, surgical resection is indicated in cases of G3 rNENs, 10–19 mm with muscolaris propria invasion (stage T2) and for tumors > 20 mm and/or in presence of lymph node metastases.

Endoscopic techniques for treating rNENs include standard polypectomy, EMR, modified EMR, ESD, and endoscopic full-thickness resection (EFTR). Standard polypectomy does not offer an adequate and complete resection of the lesion; therefore, it is not indicated in rNEN treatment[62]. Of note, a large number of rNENs is still removed by an improper method, such as routine snare polypectomy, during colorectal cancer screening making management more complex and putting patients at risk of metastatic spread[63].

EMR is largely used in the resection of small and superficial neoplasia confined to the mucosa and submucosal layer, but its application in rNENs is still debated since modified EMR and ESD are superior in terms of *en bloc* resection rate and histological complete resection rate (defined as *en bloc* resection with no margin involved)[64,65].

Recently, Park *et al*[66] observed that when EMR is performed underwater, the histological complete resection rate of NENs < 10 mm is similar to that for ESD (86.1% *vs* 86.1%, respectively) but with a shorter procedure time (5.8 ± 2.9 *vs* 26.6 ±13.4 min, respectively).

EMR performed with a dual-channel endoscope allows deeper resection compared to conventional EMR by lifting the lesion with forceps. Lee *et al*[67] observed that dual-channel EMR reaches a complete histological resection rate similar to that of ESD for rNENs < 16 mm (86.3 *vs* 88.4 %, respectively), but with a shorter procedure time (9.75 ± 7.11 *vs* 22.38 ± 7.56 min, respectively) and fewer complications.

Modified EMR techniques include the use of special devices that allow better resection of the tumor. EMR after circumferential precutting (EMR-P) is performed by lifting the submucosal with saline injection, precutting using the tip of the snare or special endoknife and resecting the tumor with a snare. Cap-assisted EMR (EMR-C) is performed by lifting the mucosa with saline injection, suctioning the lesion with a transparent cap fitted to the scope and then removing it with a snare looped along the ridge of the cap. EMR with a ligation device (EMR-L) is conducted by lifting the lesion with saline injection, deploying an elastic band around its base, and resecting with a snare. Histological complete resection rate for EMR-P is superior to EMR and no difference was found between EMR-P and the other modified EMR techniques, even if it required a longer procedure time[68]. Park *et al*[69] demonstrated that EMR-C is a safe and effective technique for rNENs, with a histological complete resection rate even better than that of ESD (92.3% *vs* 78.4%, respectively).

EMR-L is only applicable for tumors of < 10 mm due to the short diameter of the caps fitted to colonoscopes, but it is significantly superior to EMR in terms of complete resection of rNENs (93.3% *vs* 65.5%, respectively), regardless of the tumor location[70]. Histological complete resection rate is similar between EMR-C and EMR-L. However, Lee *et al*[71] demonstrated that EMR-L might be preferable for achieving a higher rate of *en bloc* resection (100% *vs* 92.9%, respectively), but this could be due to the fact that the band thickness used in EMR-L is larger than the snare thickness of EMR-C.

ESD is an interventional procedure suitable for *en bloc* resection of slightly invasive GI lesions. After injection of the submucosal with a viscous solution, an endoknife is used to incise the mucosa surrounding the lesion and to dissect it from the submucosal layer. ESD is an effective technique to treat rectal lesions, even if it is associated with a high risk of complications and a long procedure time. As it concerns rNENs, ESD has been demonstrated to be superior to EMR in terms of histological complete resection rate, but there are no significant differences between ESD and modified EMR[70].

Niimi *et al*[72] observed that ESD is associated with a longer procedure time and hospitalization period compared with EMR-L, with a similar complete resection rate. In order to reduce procedure time, Wang *et al*[73] proposed a hybrid ESD, in which the mucosal incision is performed with a polypectomy snare instead of an endoknife. This technique showed a similar *en bloc* resection rate (99.2% *vs* 98.2) and complete resection rate (94.1% *vs* 90.9%) to ESD but with a shorter procedure time (13.2 ± 8.3 *vs* 18.1 ± 9.7 min).

EFTR is a technique mainly used in lesions that are difficult to resect and its application in rNENs has recently been proposed. A full-thickness resection device is fitted over the scope and, after placement of a modified over-the-scope-clip, allows a single step EFTR (Figure 4).

Meier *et al*[74] collected data on 40 EFTRs in rNENs and observed that resection was macroscopically and histologically complete in all cases without major events, but prospective comparative studies between different resection techniques are still missing.

To conclude, rNENs < 10 mm should be treated endoscopically, and EMR-L should be considered as the first-line treatment; ESD can be used as second-line therapy when EMR-L is not applicable. EFTR can be an effective and safe technique in lesions that are difficult to treat. Treatment of rNENs with a size of 10-19 mm should be chosen after assessing the stage and the grade of differentiation.

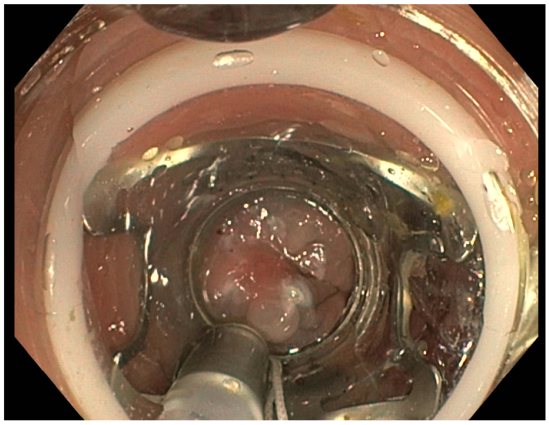

DOI: 10.3748/wjg.v28.i26.3258

Figure 4 Over-the-scope clipping system for endoscopic full-thickness resection of a rectal neuroendocrine neoplasm.

pancreatic NENs

In recent years there has been a great development of EUS techniques, not only used as diagnostic, but also as therapeutic tools. These methods find application in the management of panNENs, given the direct approach to the pancreas through the echoendoscope. The incidentally discovered small panNENs, mainly nonfunctional, represent a therapeutic challenge because surgery could be very complex in the face of neoplasms with indolent biological behavior, and active surveillance may represent an option for G1 or low G2 neoplasms, asymptomatic, mainly localized in the head of the pancreas, without radiological signs suspicious for malignancy[8,75]. In this setting, however, EUS-guided pancreatic locoregional ablative treatments, using either ethanol injection or radiofrequency ablation, have been proposed in recent studies with promising results in order to control symptoms or reduce tumor burden in selected patients[76]. The thermoablative techniques are the most used, mainly the radiofrequency methods. EUS-guided radiofrequency ablation (RFA) is reported to be a potentially effective and safe treatment for Pan-NENs[77].

Several RFA devices for EUS-guided applications are currently available. The Habib EUS-guided RFA probe (EndoHPB, EMcision UK, London, UK) is a 1 Fr (0.33 mm), monopolar catheter, which can be inserted through a regular 19- or 22-gauge FNA needle and connected to a standard radiofrequency generator. The other systems are needle-electrodes, and the most commonly used in literature is the one from Taewoong Medical (EUSRA, Taewoong Medical Co. Ltd., Gimpo-si, Geyonggi-do, South Korea), an 18- or 19-gauge needle with a long electrode lacking insulation over the terminal tip, connected to a dedicated RF current source, and an inner cooling system that circulates chilled saline inside the needle to avoid tissue charring. Under the EUS guide, the needle is inserted into the target lesion that is being treated by using high-frequency alternating current, and the energy release is applied when the needle tip of the electrode is within the lesion, while maintaining a distance of at least 2 mm from the pancreatic and bile ducts and vessels, to avoid injury or duct strictures. A recent systematic literature review explored the feasibility, effectiveness, and safety of EUS–RFA in the treatment of panNENs[94]: 12 articles describing 61 patients and 73 panNENs were analyzed and the overall effectiveness of EUS–RFA resulted in 96% (75%–100%) without any difference between functional and nonfunctional panNENs and without relevant side effects (mild adverse events, AEs 13.7%)[78-81].

The same conclusions were also confirmed by a further systematic review which included 14 studies with a total of 158 patients with solid pancreatic tumors[82]. However, even if the results of these studies are encouraging, especially for nonfunctioning panNENs and insulinomas < 2 cm, EUS–RFA is a recent technique and long-term data are thus lacking[82]. Larger studies with longer follow-up are needed to evaluate the long-term effectiveness of EUS–RFA. The specific setting of patients and the actual indication for the radiofrequency has not been standardized.

As concerned EUS-guided ethanol injection for small panNENs, this option has been proposed and studied for the treatment of patients with small panNENs not suitable for surgery or who refused surgical approach. Using pure ethanol or ethanol–lipiodol emulsion, the complete ablation rate has been reported to be ~50% up to 80% by performing more sessions[83].

In view of these results, a study protocol for a multicenter prospective study has been published[84] and the results will become available in due time.

Finally, possible future intriguing perspectives can be represented by the application, also in panNENs, of the novel techniques of locoregional delivery of drugs, such as LOcal Drug EluteR [LODER(TM)] which is a novel biodegradable polymeric matrix that shields drugs. panNENs may be considered as a possible future field of application of locoregional radiotherapy by using fiducial markers implantation, similarly to other pancreatic cancers.

Table 1 Available endoscopic treatment options for gastro-entero-pancreatic neuroendocrine neoplasms

Primary site	Tumor characteristics	Endoscopic management
Stomach	Type I < 5 mm	Surveillance
	Type I ≥ 5 mm	Resection (EMR, ESD)
	Type II	
	Type III	Resection (EMR, ESD)[1]
	G1-G2	
	< 10 mm	
Duodenum	< 10 mm[2]	Resection (EMR, ESD)
	G1	
	No muscularis mucosae invasion	
	No periampullary	
Pancreas	≤ 20 mm	Surveillance; EUS-guided RFA; EUS-guided ethanol injection
	G1-low G2	
	Non-functioning	
	No bile/pancreatic duct compression	
	Functioning tumors, not suitable for surgery	EUS-guided ethanol injection
	The patient refuses the surgical approach	
Rectum	< 10 mm[3]	Resection (EMR, mEMR, ESD, EFTR)
	G1-G2	
	No muscularis mucosae invasion	

[1]Endoscopic resection of type III gastric NENs can be considered curative only in case of histological complete resection.
[2]There is still controversy regarding the management of duodenal NENs between 10 and 20 mm.
[3]Treatment of rectal NENs with a size of 10–19 mm should be chosen after assessing the stage and the grade of differentiation.
G: Grading according to WHO classification; EMR: Endoscopic mucosal resection; mEMR: Modified endoscopic mucosal resection; ESD: Endoscopic submucosal dissection; EFTR: Endoscopic full-thickness resection; EUS: Endoscopic ultrasound.

DISCUSSION

The incidence of GEP-NENs has hugely increased over the last decades mainly due to better disease knowledge and to an improvement in diagnostic techniques, including endoscopy. Standard axial endoscopy and EUS still play a pivotal role in several GEP-NENs. Upper GI endoscopy is essential for the detection and characterization of esophageal, gastric and duodenal NENs. EUS represents the diagnostic gold standard for panNENs and the technique of choice for the locoregional staging of gastric, duodenal and rectal NENs. Ileocolonoscopy allows the assessing and diagnosing of rectal, colonic and rarely distal ileal lesions. However, the diagnosis of sbNENs has been largely improved with the advent of CE and DBE, although data regarding the safety and efficacy of these techniques in the neuroendocrine setting are still scanty and their use is still limited in clinical practice. In terms of treatment, in selected localized GI-NENs with the absence of features associated with lymph node metastases, endoscopic therapy is generally an appropriate treatment with radical intent. In highly selected G1 or low G2 small neoplasms without radiological signs suspicious for malignancy EUS-guided pancreatic locoregional ablative treatments, using either ethanol injection or radiofrequency ablation, have been proposed in recent studies with promising results in order to control symptoms or reduce tumor burden. Table 1 summarizes available endoscopic treatment options for GEP-NENs.

CONCLUSION

In summary, endoscopy plays a key role for diagnosis and treatment of GEP-NENs. In selected localized GEP-NENs, endoscopic therapy is appropriate with radical intent. Advanced resection techniques aimed at increasing the rate of R0 resection should be reserved to high-volume referral centers. The multidisciplinary management remains the gold standard to offer the patient the best therapeutic

approach.

ARTICLE HIGHLIGHTS

Research background

The prognosis of gastro-entero-pancreatic neuroendocrine neoplasms (GEP-NENs) is widely variable depending on several factors including the site of the primary tumor, the grading, and the stage. The correct localization of the primary tumor site, as well as a complete histologic diagnosis, represent the milestones for the proper management and the prognosis of these tumors. Standard axial endoscopy and endoscopic ultrasonography (EUS) still play a pivotal role in several GEP-NENs.

Research motivation

The incidence of GEP-NENs has hugely increased over the last decades; given the well-known heterogeneity of these tumors and the lack of large prospective studies, there is an urgent need to standardize their management.

Research objectives

To analyze current evidence on the role of endoscopy in the management of GEP-NENs (both diagnosis and potential treatment). A specific focus will be reserved to capsule endoscopy, double-balloon enteroscopy and ultrasound endoscopy.

Research methods

An extensive bibliographical search was performed in PubMed to identify guidelines and primary literature (retrospective and prospective studies, systematic reviews, case series) published in the last 15 years, using both medical subject heading (MeSH) terms and free-language keywords: gastro-entero-pancreatic neuroendocrine neoplasms; endoscopy; ultrasound endoscopy; capsule endoscopy; double-balloon enteroscopy; diagnosis; therapy; staging.

Research results

EUS represents the diagnostic gold standard for pancreatic NENs (panNENs) and the technique of choice for the locoregional staging of gastric, duodenal and rectal NENs. EUS proved to be the most accurate diagnostic technique in panNEN detection. EUS–fine needle aspiration is a diagnostic advanced EUS technique, which represents the gold standard least invasive option to obtain the histological identification of a suspected pancreatic neoplasm or peripancreatic lymph node. The diagnosis of small bowel NENs (sbNENs) has been improved with the advent of capsule endoscopy (CE) and double-balloon enteroscopy (DBE), even if data regarding the efficacy and safety of these techniques in the detection of sbNENs are scanty and mainly based on small retrospective series, given the rarity of the disease and the still-limited use of these techniques in routine clinical practice. In selected localized gastrointestinal NENs with the absence of features associated with lymph node metastases, endoscopic therapy is generally an appropriate treatment with radical intent. In highly selected G1 or low G2 small neoplasms without radiological signs suspicious for malignancy EUS-guided pancreatic locoregional ablative treatments, using either ethanol injection or radiofrequency ablation, have been proposed in recent studies with promising results in order to control symptoms or reduce tumor burden.

Research conclusions

Endoscopy plays a key role in GEP-NENs for both the diagnosis and the treatment. In selected localized GEP-NENs, endoscopic therapy is appropriate with radical intent. The multidisciplinary management and the referral to high-volume tertiary centers remain fundamental.

Research perspectives

Further studies are needed: (1) To better define the actual role of CE and DBE in the diagnosis of sbNENs; and (2) To better analyze the possible role of endoscopic confocal laser endomicroscopy in the diagnosis of panNENs and radiofrequency ablation as a potential treatment. Possible future intriguing perspectives can be represented by the application, also in panNENs, of the novel techniques of locoregional delivery of drugs.

FOOTNOTES

Author contributions: Rossi RE designed the research; Rossi RE, Elvevi A, Gallo C, Palermo A, and Massironi S performed the literature search and wrote the first draft of the paper; Rossi RE, Invernizzi P and Massironi S

reviewed for important intellectual content; Rossi RE and Massironi S wrote the final version of the paper; all the authors approved it.

Conflict-of-interest statement: None.

PRISMA 2009 Checklist statement: The authors have read the PRISMA 2009 Checklist, and the manuscript was prepared and revised according to the PRISMA 2009 Checklist.

Country/Territory of origin: Italy

ORCID number: Roberta Elisa Rossi 0000-0003-4208-4372; Alessandra Elvevi 0000-0001-9841-2051; Camilla Gallo 0000-0002-7598-7220; Andrea Palermo 0000-0001-8057-9398; Pietro Invernizzi 0000-0003-3262-1998; Sara Massironi 0000-0003-3214-8192.

S-Editor: Wu YXJ
L-Editor: Kerr C
P-Editor: Wu YXJ

REFERENCES

1 **Dasari A**, Shen C, Halperin D, Zhao B, Zhou S, Xu Y, Shih T, Yao JC. Trends in the Incidence, Prevalence, and Survival Outcomes in Patients With Neuroendocrine Tumors in the United States. *JAMA Oncol* 2017; **3**: 1335-1342 [PMID: 28448665 DOI: 10.1001/jamaoncol.2017.0589]

2 **Rindi G**, Bordi C, La Rosa S, Solcia E, Delle Fave G; Gruppo Italiano Patologi Apparato Digerente (GIPAD); Società Italiana di Anatomia Patologica e Citopatologia Diagnostica/International Academy of Pathology, Italian division (SIAPEC/IAP). Gastroenteropancreatic (neuro)endocrine neoplasms: the histology report. *Dig Liver Dis* 2011; **43** Suppl 4: S356-S360 [PMID: 21459341 DOI: 10.1016/S1590-8658(11)60591-4]

3 **Rindi G**, Falconi M, Klersy C, Albarello L, Boninsegna L, Buchler MW, Capella C, Caplin M, Couvelard A, Doglioni C, Delle Fave G, Fischer L, Fusai G, de Herder WW, Jann H, Komminoth P, de Krijger RR, La Rosa S, Luong TV, Pape U, Perren A, Ruszniewski P, Scarpa A, Schmitt A, Solcia E, Wiedenmann B. TNM staging of neoplasms of the endocrine pancreas: results from a large international cohort study. *J Natl Cancer Inst* 2012; **104**: 764-777 [PMID: 22525418 DOI: 10.1093/jnci/djs208]

4 **Boninsegna L**, Panzuto F, Partelli S, Capelli P, Delle Fave G, Bettini R, Pederzoli P, Scarpa A, Falconi M. Malignant pancreatic neuroendocrine tumour: lymph node ratio and Ki67 are predictors of recurrence after curative resections. *Eur J Cancer* 2012; **48**: 1608-1615 [PMID: 22129889 DOI: 10.1016/j.ejca.2011.10.030]

5 **Panzuto F**, Boninsegna L, Fazio N, Campana D, Pia Brizzi M, Capurso G, Scarpa A, De Braud F, Dogliotti L, Tomassetti P, Delle Fave G, Falconi M. Metastatic and locally advanced pancreatic endocrine carcinomas: analysis of factors associated with disease progression. *J Clin Oncol* 2011; **29**: 2372-2377 [PMID: 21555696 DOI: 10.1200/JCO.2010.33.0688]

6 **Rossi RE**, Conte D, Elli L, Branchi F, Massironi S. Endoscopic techniques to detect small-bowel neuroendocrine tumors: A literature review. *United European Gastroenterol J* 2017; **5**: 5-12 [PMID: 28405316 DOI: 10.1177/2050640616658220]

7 **Zilli A**, Arcidiacono PG, Conte D, Massironi S. Clinical impact of endoscopic ultrasonography on the management of neuroendocrine tumors: lights and shadows. *Dig Liver Dis* 2018; **50**: 6-14 [PMID: 29102525 DOI: 10.1016/j.dld.2017.10.007]

8 **Falconi M**, Eriksson B, Kaltsas G, Bartsch DK, Capdevila J, Caplin M, Kos-Kudla B, Kwekkeboom D, Rindi G, Klöppel G, Reed N, Kianmanesh R, Jensen RT; Vienna Consensus Conference participants. ENETS Consensus Guidelines Update for the Management of Patients with Functional Pancreatic Neuroendocrine Tumors and Non-Functional Pancreatic Neuroendocrine Tumors. *Neuroendocrinology* 2016; **103**: 153-171 [PMID: 26742109 DOI: 10.1159/000443171]

9 **Manta R**, Nardi E, Pagano N, Ricci C, Sica M, Castellani D, Bertani H, Piccoli M, Mullineris B, Tringali A, Marini F, Germani U, Villanacci V, Casadei R, Mutignani M, Conigliaro R, Bassotti G, Zullo A. Pre-operative Diagnosis of Pancreatic Neuroendocrine Tumors with Endoscopic Ultrasonography and Computed Tomography in a Large Series. *J Gastrointestin Liver Dis* 2016; **25**: 317-321 [PMID: 27689195 DOI: 10.15403/jgld.2014.1121.253.ned]

10 **Fujimori N**, Osoegawa T, Lee L, Tachibana Y, Aso A, Kubo H, Kawabe K, Igarashi H, Nakamura K, Oda Y, Ito T. Efficacy of endoscopic ultrasonography and endoscopic ultrasonography-guided fine-needle aspiration for the diagnosis and grading of pancreatic neuroendocrine tumors. *Scand J Gastroenterol* 2016; **51**: 245-252 [PMID: 26513346 DOI: 10.3109/00365521.2015.1083050]

11 **Atiq M**, Bhutani MS, Bektas M, Lee JE, Gong Y, Tamm EP, Shah CP, Ross WA, Yao J, Raju GS, Wang X, Lee JH. EUS-FNA for pancreatic neuroendocrine tumors: a tertiary cancer center experience. *Dig Dis Sci* 2012; **57**: 791-800 [PMID: 21964743 DOI: 10.1007/s10620-011-1912-7]

12 **Dietrich CF**, Ignee A, Braden B, Barreiros AP, Ott M, Hocke M. Improved differentiation of pancreatic tumors using contrast-enhanced endoscopic ultrasound. *Clin Gastroenterol Hepatol* 2008; **6**: 590-597.e1 [PMID: 18455699 DOI:

10.1016/j.cgh.2008.02.030]
13 **Malagò R**, D'Onofrio M, Zamboni GA, Faccioli N, Falconi M, Boninsegna L, Mucelli RP. Contrast-enhanced sonography of nonfunctioning pancreatic neuroendocrine tumors. *AJR Am J Roentgenol* 2009; **192**: 424-430 [PMID: 19155405 DOI: 10.2214/AJR.07.4043]
14 **Ishikawa R**, Kamata K, Hara A, Tanaka H, Okamoto A, Yamazaki T, Nakai A, Omoto S, 4inaga K, Yamao K, Takenaka M, Minami Y, Watanabe T, Chiba Y, Chikugo T, Matsumoto I, Takeyama Y, Matsukubo Y, Hyodo T, Kudo M. Utility of contrast-enhanced harmonic endoscopic ultrasonography for predicting the prognosis of pancreatic neuroendocrine neoplasms. *Dig Endosc* 2021; **33**: 829-839 [PMID: 33020955 DOI: 10.1111/den.13862]
15 **Leiman G**. My approach to pancreatic fine needle aspiration. *J Clin Pathol* 2007; **60**: 43-49 [PMID: 16698956 DOI: 10.1136/jcp.2005.034959]
16 **Matsubayashi H**, Matsui T, Yabuuchi Y, Imai K, Tanaka M, Kakushima N, Sasaki K, Ono H. Endoscopic ultrasonography guided-fine needle aspiration for the diagnosis of solid pancreaticobiliary lesions: Clinical aspects to improve the diagnosis. *World J Gastroenterol* 2016; **22**: 628-640 [PMID: 26811612 DOI: 10.3748/wjg.v22.i2.628]
17 **Chen S**, Lin J, Wang X, Wu HH, Cramer H. EUS-guided FNA cytology of pancreatic neuroendocrine tumour (PanNET): a retrospective study of 132 cases over an 18-year period in a single institution. *Cytopathology* 2014; **25**: 396-403 [PMID: 24635775 DOI: 10.1111/cyt.12137]
18 **Gornals J**, Varas M, Catalá I, Maisterra S, Pons C, Bargalló D, Serrano T, Fabregat J. Definitive diagnosis of neuroendocrine tumors using fine-needle aspiration-puncture guided by endoscopic ultrasonography. *Rev Esp Enferm Dig* 2011; **103**: 123-128 [PMID: 21434714 DOI: 10.4321/s1130-01082011000300003]
19 **Mitra V**, Nayar MK, Leeds JS, Wadehra V, Haugk B, Scott J, Charnley RM, Oppong KW. Diagnostic performance of endoscopic ultrasound (EUS)/endoscopic ultrasound--fine needle aspiration (EUS-FNA) cytology in solid and cystic pancreatic neuroendocrine tumours. *J Gastrointestin Liver Dis* 2015; **24**: 69-75 [PMID: 25822436 DOI: 10.15403/jgld.2014.1121.vmi]
20 **Weynand B**, Borbath I, Bernard V, Sempoux C, Gigot JF, Hubert C, Lannoy V, Deprez PH, Jouret-Mourin A. Pancreatic neuroendocrine tumour grading on endoscopic ultrasound-guided fine needle aspiration: high reproducibility and inter-observer agreement of the Ki-67 labelling index. *Cytopathology* 2014; **25**: 389-395 [PMID: 24750272 DOI: 10.1111/cyt.12111]
21 **Delconte G**, Cavalcoli F, Magarotto A, Centonze G, Bezzio C, Cattaneo L, Rausa E, Kelly ME, Bonitta G, Milione M, Enzo M. Does ProCore Fine-Needle Biopsy Really Improve the Clinical Outcome of Endoscopic Ultrasound-Guided Sampling of Pancreatic Masses? *Dig Dis* 2022; **40**: 78-84 [PMID: 33780932 DOI: 10.1159/000516177]
22 **Dietrich CF**, Săftoiu A, Jenssen C. Real time elastography endoscopic ultrasound (RTE-EUS), a comprehensive review. *Eur J Radiol* 2014; **83**: 405-414 [PMID: 23643030 DOI: 10.1016/j.ejrad.2013.03.023]
23 **Havre RF**, Ødegaard S, Gilja OH, Nesje LB. Characterization of solid focal pancreatic lesions using endoscopic ultrasonography with real-time elastography. *Scand J Gastroenterol* 2014; **49**: 742-751 [PMID: 24713038 DOI: 10.3109/00365521.2014.905627]
24 **Iglesias-Garcia J**, Larino-Noia J, Abdulkader I, Forteza J, Dominguez-Munoz JE. Quantitative endoscopic ultrasound elastography: an accurate method for the differentiation of solid pancreatic masses. *Gastroenterology* 2010; **139**: 1172-1180 [PMID: 20600020 DOI: 10.1053/j.gastro.2010.06.059]
25 **Cosgrove D**, Piscaglia F, Bamber J, Bojunga J, Correas JM, Gilja OH, Klauser AS, Sporea I, Calliada F, Cantisani V, D'Onofrio M, Drakonaki EE, Fink M, Friedrich-Rust M, Fromageau J, Havre RF, Jenssen C, Ohlinger R, Săftoiu A, Schaefer F, Dietrich CF; EFSUMB. EFSUMB guidelines and recommendations on the clinical use of ultrasound elastography. Part 2: Clinical applications. *Ultraschall Med* 2013; **34**: 238-253 [PMID: 23605169 DOI: 10.1055/s-0033-1335375]
26 **Napoleon B**, Lemaistre AI, Pujol B, Caillol F, Lucidarme D, Bourdariat R, Morellon-Mialhe B, Fumex F, Lefort C, Lepilliez V, Palazzo L, Monges G, Poizat F, Giovannini M. In vivo characterization of pancreatic cystic lesions by needle-based confocal laser endomicroscopy (nCLE): proposition of a comprehensive nCLE classification confirmed by an external retrospective evaluation. *Surg Endosc* 2016; **30**: 2603-2612 [PMID: 26428198 DOI: 10.1007/s00464-015-4510-5]
27 French comment on article: Endoscopic ultrasound-guided needle-based confocal laser endomicroscopy in solid pancreatic masses. *Endoscopy* 2016; **48**: 961 [PMID: 27669477 DOI: 10.1055/s-0042-116197]
28 **Varas MJ**, Gornals JB, Pons C, Espinós JC, Abad R, Lorente FJ, Bargalló D. Usefulness of endoscopic ultrasonography (EUS) for selecting carcinoid tumors as candidates to endoscopic resection. *Rev Esp Enferm Dig* 2010; **102**: 577-582 [PMID: 21039065 DOI: 10.4321/s1130-01082010001000002]
29 **Delle Fave G**, O'Toole D, Sundin A, Taal B, Ferolla P, Ramage JK, Ferone D, Ito T, Weber W, Zheng-Pei Z, De Herder WW, Pascher A, Ruszniewski P; Vienna Consensus Conference participants. ENETS Consensus Guidelines Update for Gastroduodenal Neuroendocrine Neoplasms. *Neuroendocrinology* 2016; **103**: 119-124 [PMID: 26784901 DOI: 10.1159/000443168]
30 **Ramage JK**, De Herder WW, Delle Fave G, Ferolla P, Ferone D, Ito T, Ruszniewski P, Sundin A, Weber W, Zheng-Pei Z, Taal B, Pascher A; Vienna Consensus Conference participants. ENETS Consensus Guidelines Update for Colorectal Neuroendocrine Neoplasms. *Neuroendocrinology* 2016; **103**: 139-143 [PMID: 26730835 DOI: 10.1159/000443166]
31 **Cangemi DJ**, Patel MK, Gomez V, Cangemi JR, Stark ME, Lukens FJ. Small bowel tumors discovered during double-balloon enteroscopy: analysis of a large prospectively collected single-center database. *J Clin Gastroenterol* 2013; **47**: 769-772 [PMID: 23426457 DOI: 10.1097/MCG.0b013e318281a44e]
32 **Bader TR**, Semelka RC, Chiu VC, Armao DM, Woosley JT. MRI of carcinoid tumors: spectrum of appearances in the gastrointestinal tract and liver. *J Magn Reson Imaging* 2001; **14**: 261-269 [PMID: 11536403 DOI: 10.1002/jmri.1182]
33 **Frilling A**, Sotiropoulos GC, Radtke A, Malago M, Bockisch A, Kuehl H, Li J, Broelsch CE. The impact of 68Ga-DOTATOC positron emission tomography/computed tomography on the multimodal management of patients with neuroendocrine tumors. *Ann Surg* 2010; **252**: 850-856 [PMID: 21037441 DOI: 10.1097/SLA.0b013e3181fd37e8]
34 **van Tuyl SA**, van Noorden JT, Timmer R, Stolk MF, Kuipers EJ, Taal BG. Detection of small-bowel neuroendocrine tumors by video capsule endoscopy. *Gastrointest Endosc* 2006; **64**: 66-72 [PMID: 16813805 DOI:

10.1016/j.gie.2006.01.054]
35 **Prasad V**, Ambrosini V, Hommann M, Hoersch D, Fanti S, Baum RP. Detection of unknown primary neuroendocrine tumours (CUP-NET) using (68)Ga-DOTA-NOC receptor PET/CT. *Eur J Nucl Med Mol Imaging* 2010; **37**: 67-77 [PMID: 19618183 DOI: 10.1007/s00259-009-1205-y]
36 **Sharma P**, Arora S, Mukherjee A, Pal S, Sahni P, Garg P, Khadgawat R, Thulkar S, Bal C, Kumar R. Predictive value of 68Ga-DOTANOC PET/CT in patients with suspicion of neuroendocrine tumors: is its routine use justified? *Clin Nucl Med* 2014; **39**: 37-43 [PMID: 24152621 DOI: 10.1097/RLU.0000000000000257]
37 **Cobrin GM**, Pittman RH, Lewis BS. Increased diagnostic yield of small bowel tumors with capsule endoscopy. *Cancer* 2006; **107**: 22-27 [PMID: 16736516 DOI: 10.1002/cncr.21975]
38 **McEwen BS**. Protective and damaging effects of stress mediators. *N Engl J Med* 1998; **338**: 171-179 [PMID: 9428819 DOI: 10.1056/NEJM199801153380307]
39 **Sidhu R**, McAlindon ME. The use of capsule endoscopy for the investigation of small bowel tumors: experience from a United Kingdom single center. *Dig Dis Sci* 2011; **56**: 2763 [PMID: 21750932 DOI: 10.1007/s10620-011-1813-9]
40 **Frilling A**, Smith G, Clift AK, Martin J. Capsule endoscopy to detect primary tumour site in metastatic neuroendocrine tumours. *Dig Liver Dis* 2014; **46**: 1038-1042 [PMID: 25086997 DOI: 10.1016/j.dld.2014.07.004]
41 **Furnari M**, Buda A, Delconte G, Citterio D, Voiosu T, Ballardini G, Cavallaro F, Savarino E, Mazzaferro V, Meroni E. The role of wireless capsule endoscopy (WCE) in the detection of occult primary neuroendocrine tumors. *J Gastrointestin Liver Dis* 2017; **26**: 151-156 [PMID: 28617885 DOI: 10.15403/jgld.2014.1121.262.wce]
42 **Tominaga K**, Kamimura K, Yokoyama J, Terai S. Usefulness of Capsule Endoscopy and Double-balloon Enteroscopy for the Diagnosis of Multiple Carcinoid Tumors in the Small Intestine: Case Reports and a Literature Review. *Intern Med* 2019; **58**: 655-659 [PMID: 30333421 DOI: 10.2169/internalmedicine.1700-18]
43 **Bellutti M**, Fry LC, Schmitt J, Seemann M, Klose S, Malfertheiner P, Mönkemüller K. Detection of neuroendocrine tumors of the small bowel by double balloon enteroscopy. *Dig Dis Sci* 2009; **54**: 1050-1058 [PMID: 18770038 DOI: 10.1007/s10620-008-0456-y]
44 **Scherübl H**, Faiss S, Tschöpe R, Zeitz M. Double-balloon enteroscopy for the detection of midgut carcinoids. *Gastrointest Endosc* 2005; **62**: 994; author reply 994-994; author reply 995 [PMID: 16301062 DOI: 10.1016/j.gie.2005.08.012]
45 **Rossi RE**, Elli L, Branchi F, Conte D, Massironi S. Double-Balloon Enteroscopy in Detecting Small-Bowel Neuroendocrine Neoplasms: A Single-Center Prospective Study. *Digestion* 2021; **102**: 722-730 [PMID: 33361694 DOI: 10.1159/000511850]
46 **Roberto GA**, Rodrigues CMB, Peixoto RD, Younes RN. Gastric neuroendocrine tumor: A practical literature review. *World J Gastrointest Oncol* 2020; **12**: 850-856 [PMID: 32879663 DOI: 10.4251/wjgo.v12.i8.850]
47 **Scherübl H**, Cadiot G. Early Gastroenteropancreatic Neuroendocrine Tumors: Endoscopic Therapy and Surveillance. *Visc Med* 2017; **33**: 332-338 [PMID: 29177161 DOI: 10.1159/000459404]
48 **Putzer D**, Schullian P, Jaschke W, Bale R. NEN: Advancement in Diagnosis and Minimally Invasive Therapy. *Rofo* 2020; **192**: 422-430 [PMID: 31747704 DOI: 10.1055/a-1030-4631]
49 **Panzuto F**, Massironi S, Partelli S, Campana D, Rinzivillo M, Invernizzi P, Andreasi V, Lamberti G, Falconi M. Gastro-entero-pancreatic neuroendocrine neoplasia: The rules for non-operative management. *Surg Oncol* 2020; **35**: 141-148 [PMID: 32877883 DOI: 10.1016/j.suronc.2020.08.015]
50 **Merola E**, Sbrozzi-Vanni A, Panzuto F, D'Ambra G, Di Giulio E, Pilozzi E, Capurso G, Lahner E, Bordi C, Annibale B, Delle Fave G. Type I gastric carcinoids: a prospective study on endoscopic management and recurrence rate. *Neuroendocrinology* 2012; **95**: 207-213 [PMID: 21811050 DOI: 10.1159/000329043]
51 **Manfredi S**, Walter T, Baudin E, Coriat R, Ruszniewski P, Lecomte T, Laurenty AP, Goichot B, Rohmer V, Roquin G, Cojocarasu OZ, Lombard-Bohas C, Lepage C, Morcet J, Cadiot G. Management of gastric neuro-endocrine tumours in a large French national cohort (GTE). *Endocrine* 2017; **57**: 504-511 [PMID: 28664309 DOI: 10.1007/s12020-017-1355-9]
52 **Kwon YH**, Jeon SW, Kim GH, Kim JI, Chung IK, Jee SR, Kim HU, Seo GS, Baik GH, Choi KD, Moon JS. Long-term follow up of endoscopic resection for type 3 gastric NET. *World J Gastroenterol* 2013; **19**: 8703-8708 [PMID: 24379589 DOI: 10.3748/wjg.v19.i46.8703]
53 **Scherübl H**, Jensen RT, Cadiot G, Stölzel U, Klöppel G. Management of early gastrointestinal neuroendocrine neoplasms. *World J Gastrointest Endosc* 2011; **3**: 133-139 [PMID: 21860682 DOI: 10.4253/wjge.v3.i7.133]
54 **Pimentel-Nunes P**, Dinis-Ribeiro M, Ponchon T, Repici A, Vieth M, De Ceglie A, Amato A, Berr F, Bhandari P, Bialek A, Conio M, Haringsma J, Langner C, Meisner S, Messmann H, Morino M, Neuhaus H, Piessevaux H, Rugge M, Saunders BP, Robaszkiewicz M, Seewald S, Kashin S, Dumonceau JM, Hassan C, Deprez PH. Endoscopic submucosal dissection: European Society of Gastrointestinal Endoscopy (ESGE) Guideline. *Endoscopy* 2015; **47**: 829-854 [PMID: 26317585 DOI: 10.1055/s-0034-1392882]
55 **Massironi S**, Campana D, Partelli S, Panzuto F, Rossi RE, Faggiano A, Brighi N, Falconi M, Rinzivillo M, Delle Fave G, Colao AM, Conte D. Heterogeneity of Duodenal Neuroendocrine Tumors: An Italian Multi-center Experience. *Ann Surg Oncol* 2018; **25**: 3200-3206 [PMID: 30054824 DOI: 10.1245/s10434-018-6673-5]
56 **Kim GH**, Kim JI, Jeon SW, Moon JS, Chung IK, Jee SR, Kim HU, Seo GS, Baik GH, Lee YC; Korean College of Helicobacter and Upper Gastrointestinal Research. Endoscopic resection for duodenal carcinoid tumors: a multicenter, retrospective study. *J Gastroenterol Hepatol* 2014; **29**: 318-324 [PMID: 24117946 DOI: 10.1111/jgh.12390]
57 **Untch BR**, Bonner KP, Roggin KK, Reidy-Lagunes D, Klimstra DS, Schattner MA, Fong Y, Allen PJ, D'Angelica MI, DeMatteo RP, Jarnagin WR, Kingham TP, Tang LH. Pathologic grade and tumor size are associated with recurrence-free survival in patients with duodenal neuroendocrine tumors. *J Gastrointest Surg* 2014; **18**: 457-62; discussion 462 [PMID: 24448999 DOI: 10.1007/s11605-014-2456-x]
58 **Gamboa AC**, Liu Y, Lee RM, Zaidi MY, Staley CA, Kooby DA, Winer JH, Shah MM, Russell MC, Cardona K, Maithel SK. Duodenal neuroendocrine tumors: Somewhere between the pancreas and small bowel? *J Surg Oncol* 2019; **120**: 1293-1301 [PMID: 31621090 DOI: 10.1002/jso.25731]
59 **Hatta W**, Koike T, Iijima K, Asanuma K, Asano N, Musha H, Inomata Y, Sano T, Endo H, Ikehata A, Horii T, Ohyauchi

M, Yokosawa S, Kasajima A, Fujishima F, Sasano H, Nakaya N, Nakamura T, Shimosegawa T. The Risk Factors for Metastasis in Non-Ampullary Duodenal Neuroendocrine Tumors Measuring 20 mm or Less in Diameter. *Digestion* 2017; **95**: 201-209 [PMID: 28315861 DOI: 10.1159/000459619]

60 **Rossi RE**, Milanetto AC, Andreasi V, Campana D, Coppa J, Nappo G, Rinzivillo M, Invernizzi P, Modica R, David A, Partelli S, Lamberti G, Mazzaferro V, Zerbi A, Panzuto F, Pasquali C, Falconi M, Massironi S; ItaNet (Italian Association for Neuroendocrine Tumours) study group. Risk of preoperative understaging of duodenal neuroendocrine neoplasms: a plea for caution in the treatment strategy. *J Endocrinol Invest* 2021; **44**: 2227-2234 [PMID: 33651317 DOI: 10.1007/s40618-021-01528-1]

61 **Basuroy R**, Haji A, Ramage JK, Quaglia A, Srirajaskanthan R. Review article: the investigation and management of rectal neuroendocrine tumours. *Aliment Pharmacol Ther* 2016; **44**: 332-345 [PMID: 27302838 DOI: 10.1111/apt.13697]

62 **Son HJ**, Sohn DK, Hong CW, Han KS, Kim BC, Park JW, Choi HS, Chang HJ, Oh JH. Factors associated with complete local excision of small rectal carcinoid tumor. *Int J Colorectal Dis* 2013; **28**: 57-61 [PMID: 22821140 DOI: 10.1007/s00384-012-1538-z]

63 **Dąbkowski K**, Szczepkowski M, Kos-Kudła B, Starzynska T. Endoscopic management of rectal neuroendocrine tumours. How to avoid a mistake and what to do when one is made? *Endokrynol Pol* 2020; **71**: 343-349 [PMID: 32852049 DOI: 10.5603/EP.a2020.0045]

64 **He L**, Deng T, Luo H. Efficacy and safety of endoscopic resection therapies for rectal carcinoid tumors: a meta-analysis. *Yonsei Med J* 2015; **56**: 72-81 [PMID: 25510749 DOI: 10.3349/ymj.2015.56.1.72]

65 **Zhou X**, Xie H, Xie L, Li J, Cao W, Fu W. Endoscopic resection therapies for rectal neuroendocrine tumors: a systematic review and meta-analysis. *J Gastroenterol Hepatol* 2014; **29**: 259-268 [PMID: 24118068 DOI: 10.1111/jgh.12395]

66 **Park SS**, Han KS, Kim B, Chang Kim B, Hong CW, Sohn DK, Chang HJ. Comparison of underwater endoscopic mucosal resection and endoscopic submucosal dissection of rectal neuroendocrine tumors (with videos). *Gastrointest Endosc* 2020; **91**: 1164-1171.e2 [PMID: 31904380 DOI: 10.1016/j.gie.2019.12.039]

67 **Lee WH**, Kim SW, Lim CH, Kim JS, Cho YK, Lee IS, Choi MG, Choi KY. Efficacy of endoscopic mucosal resection using a dual-channel endoscope compared with endoscopic submucosal dissection in the treatment of rectal neuroendocrine tumors. *Surg Endosc* 2013; **27**: 4313-4318 [PMID: 23807754 DOI: 10.1007/s00464-013-3050-0]

68 **Lee HS**, Moon HS, Kwon IS, Park JH, Kim JS, Kang SH, Lee ES, Kim SH, Sung JK, Lee BS, Jeong HY. Comparison of conventional and modified endoscopic mucosal resection methods for the treatment of rectal neuroendocrine tumors. *Surg Endosc* 2021; **35**: 6055-6065 [PMID: 33094828 DOI: 10.1007/s00464-020-08097-z]

69 **Park SB**, Kim HW, Kang DH, Choi CW, Kim SJ, Nam HS. Advantage of endoscopic mucosal resection with a cap for rectal neuroendocrine tumors. *World J Gastroenterol* 2015; **21**: 9387-9393 [PMID: 26309365 DOI: 10.3748/wjg.v21.i31.9387]

70 **Kim HH**, Park SJ, Lee SH, Park HU, Song CS, Park MI, Moon W. Efficacy of endoscopic submucosal resection with a ligation device for removing small rectal carcinoid tumor compared with endoscopic mucosal resection: analysis of 100 cases. *Dig Endosc* 2012; **24**: 159-163 [PMID: 22507089 DOI: 10.1111/j.1443-1661.2011.01190.x]

71 **Lee J**, Park YE, Choi JH, Heo NY, Park J, Park SH, Moon YS, Nam KH, Kim TO. Comparison between cap-assisted and ligation-assisted endoscopic mucosal resection for rectal neuroendocrine tumors. *Ann Gastroenterol* 2020; **33**: 385-390 [PMID: 32624659 DOI: 10.20524/aog.2020.0485]

72 **Niimi K**, Goto O, Fujishiro M, Kodashima S, Ono S, Mochizuki S, Asada-Hirayama I, Konno-Shimizu M, Mikami-Matsuda R, Minatsuki C, Yamamichi N, Koike K. Endoscopic mucosal resection with a ligation device or endoscopic submucosal dissection for rectal carcinoid tumors: an analysis of 24 consecutive cases. *Dig Endosc* 2012; **24**: 443-447 [PMID: 23078437 DOI: 10.1111/j.1443-1661.2012.01303.x]

73 **Wang XY**, Chai NL, Linghu EQ, Li HK, Zhai YQ, Feng XX, Zhang WG, Zou JL, Li LS, Xiang JY. Efficacy and safety of hybrid endoscopic submucosal dissection compared with endoscopic submucosal dissection for rectal neuroendocrine tumors and risk factors associated with incomplete endoscopic resection. *Ann Transl Med* 2020; **8**: 368 [PMID: 32355812 DOI: 10.21037/atm.2020.02.25]

74 **Meier B**, Albrecht H, Wiedbrauck T, Schmidt A, Caca K. Full-thickness resection of neuroendocrine tumors in the rectum. *Endoscopy* 2020; **52**: 68-72 [PMID: 31614372 DOI: 10.1055/a-1008-9077]

75 **Partelli S**, Ramage JK, Massironi S, Zerbi A, Kim HB, Niccoli P, Panzuto F, Landoni L, Tomazic A, Ibrahim T, Kaltsas G, Bertani E, Sauvanet A, Segelov E, Caplin M, Coppa J, Armstrong T, Weickert MO, Butturini G, Staettner S, Boesch F, Cives M, Moulton CA, He J, Selberherr A, Twito O, Castaldi A, De Angelis CG, Gaujoux S, Almeamar H, Frilling A, Vigia E, Wilson C, Muffatti F, Srirajaskanthan R, Invernizzi P, Lania A, Kwon W, Ewald J, Rinzivillo M, Nessi C, Smid LM, Gardini A, Tsoli M, Picardi EE, Hentic O, Croagh D, Toumpanakis C, Citterio D, Ramsey E, Mosterman B, Regi P, Gasteiger S, Rossi RE, Smiroldo V, Jang JY, Falconi M. Management of Asymptomatic Sporadic Nonfunctioning Pancreatic Neuroendocrine Neoplasms (ASPEN) ≤2 cm: Study Protocol for a Prospective Observational Study. *Front Med (Lausanne)* 2020; **7**: 598438 [PMID: 33425946 DOI: 10.3389/fmed.2020.598438]

76 **Melita G**, Pallio S, Tortora A, Crinò SF, Macrì A, Dionigi G. Diagnostic and Interventional Role of Endoscopic Ultrasonography for the Management of Pancreatic Neuroendocrine Neoplasms. *J Clin Med* 2021; **10** [PMID: 34203922 DOI: 10.3390/jcm10122638]

77 **Imperatore N**, de Nucci G, Mandelli ED, de Leone A, Zito FP, Lombardi G, Manes G. Endoscopic ultrasound-guided radiofrequency ablation of pancreatic neuroendocrine tumors: a systematic review of the literature. *Endosc Int Open* 2020; **8**: E1759-E1764 [PMID: 33269308 DOI: 10.1055/a-1261-9605]

78 **Rossi S**, Viera FT, Ghittoni G, Cobianchi L, Rosa LL, Siciliani L, Bortolotto C, Veronese L, Vercelli A, Gallotti A, Ravetta V. Radiofrequency ablation of pancreatic neuroendocrine tumors: a pilot study of feasibility, efficacy, and safety. *Pancreas* 2014; **43**: 938-945 [PMID: 24717825 DOI: 10.1097/MPA.0000000000000133]

79 **Pai M**, Habib N, Senturk H, Lakhtakia S, Reddy N, Cicinnati VR, Kaba I, Beckebaum S, Drymousis P, Kahaleh M, Brugge W. Endoscopic ultrasound guided radiofrequency ablation, for pancreatic cystic neoplasms and neuroendocrine tumors. *World J Gastrointest Surg* 2015; **7**: 52-59 [PMID: 25914783 DOI: 10.4240/wjgs.v7.i4.52]

80 **Oleinikov K**, Dancour A, Epshtein J, Benson A, Mazeh H, Tal I, Matalon S, Benbassat CA, Livovsky DM, Goldin E,

Gross DJ, Jacob H, Grozinsky-Glasberg S. Endoscopic Ultrasound-Guided Radiofrequency Ablation: A New Therapeutic Approach for Pancreatic Neuroendocrine Tumors. *J Clin Endocrinol Metab* 2019; **104**: 2637-2647 [PMID: 31102458 DOI: 10.1210/jc.2019-00282]

81 **de Nucci G**, Imperatore N, Mandelli ED, di Nuovo F, d'Urbano C, Manes G. Endoscopic ultrasound-guided radiofrequency ablation of pancreatic neuroendocrine tumors: a case series. *Endosc Int Open* 2020; **8**: E1754-E1758 [PMID: 33269307 DOI: 10.1055/a-1261-9359]

82 **Zhang L**, Tan S, Huang S, Zhong C, Lü M, Peng Y, Tang X. The safety and efficacy of endoscopic ultrasound-guided ablation therapy for solid pancreatic tumors: a systematic review. *Scand J Gastroenterol* 2020; **55**: 1121-1131 [PMID: 32730715 DOI: 10.1080/00365521.2020.1797870]

83 **Park DH**, Choi JH, Oh D, Lee SS, Seo DW, Lee SK, Kim MH. Endoscopic ultrasonography-guided ethanol ablation for small pancreatic neuroendocrine tumors: results of a pilot study. *Clin Endosc* 2015; **48**: 158-164 [PMID: 25844345 DOI: 10.5946/ce.2015.48.2.158]

84 **Matsumoto K**, Kato H, Kitano M, Hara K, Kuwatani M, Ashida R, Takenaka M, Yamazaki T, Sakurai J, Yoshida M, Okada H. Study protocol for endoscopic ultrasonography-guided ethanol injection therapy for patients with pancreatic neuroendocrine neoplasm: a multicentre prospective study. *BMJ Open* 2021; **11**: e046505 [PMID: 34253667 DOI: 10.1136/bmjopen-2020-046505]

World Journal of Gastroenterology

Submit a Manuscript: https://www.f6publishing.com

World J Gastroenterol 2022 July 14; 28(26): 3274-3278

DOI: 10.3748/wjg.v28.i26.3274

ISSN 1007-9327 (print) ISSN 2219-2840 (online)

LETTER TO THE EDITOR

Intestinal inflammation and the microbiota: Beyond diversity

Gabriela Gama Freire Alberca, Naiane Samira Souza Cardoso, Rosa Liliana Solis-Castro, Viviane Nakano, Ricardo Wesley Alberca

Specialty type: Gastroenterology and hepatology

Provenance and peer review: Invited article; Externally peer reviewed.

Peer-review model: Single blind

Peer-review report's scientific quality classification
Grade A (Excellent): 0
Grade B (Very good): B, B, B, B
Grade C (Good): C
Grade D (Fair): 0
Grade E (Poor): 0

P-Reviewer: Carannante F, Italy; Gao W, China; Suzuki T, Japan; Xu PF, United States; Zhao G, China

Received: August 6, 2021
Peer-review started: August 6, 2021
First decision: September 4, 2021
Revised: September 5, 2021
Accepted: June 23, 2022
Article in press: June 23, 2022
Published online: July 14, 2022

Gabriela Gama Freire Alberca, Naiane Samira Souza Cardoso, Viviane Nakano, Department of Microbiology, Institute of Biomedical Sciences, University of São Paulo, São Paulo 05508-000, Brazil

Rosa Liliana Solis-Castro, Departamento Académico de Biología Bioquímica, Facultad de Ciencias de la Salud, Universidad Nacional de Tumbes, Pampa Grande 24000, Tumbes, Peru

Ricardo Wesley Alberca, Laboratorio de Dermatologia e Imunodeficiencias, Departamento de Dermatologia, Faculdade de Medicina FMUSP, Universidade de São Paulo, São Paulo 01246-903, Brazil

Corresponding author: Ricardo Wesley Alberca, PhD, Academic Research, Research Fellow, Laboratorio de Dermatologia e Imunodeficiencias, Departamento de Dermatologia, Faculdade de Medicina FMUSP, Universidade de São Paulo, 455-Cerqueira César, São Paulo 01246-903, Brazil. ricardowesley@gmail.com

Abstract

The recent manuscript entitled "Relationship between clinical features and intestinal microbiota in Chinese patients with ulcerative colitis" reported a difference in the intestinal microbiota of patients with ulcerative colitis according to the severity of the colitis. The influence of the intestinal microbiota on the development and progress of gastrointestinal disorders is well established. Besides the diversity in the microbiome, the presence of virulence factors and toxins by commensal bacteria may affect an extensive variety of cellular processes, contributing to the induction of a proinflammatory environment.

Key Words: Inflammation; Microbiota; Toxins; Intestinal; Ulcerative; Colitis; Cancer

Core Tip: The manuscript entitled "Relationship between clinical features and intestinal microbiota in Chinese patients with ulcerative colitis" and previous investigations have identified alterations in the intestinal microbiome of patients with inflammatory bowel disease, ulcerative colitis, and colorectal cancer. The microbiota composition impacts the development of inflammatory disorders. Nevertheless, investigations should focus on identifying alterations not only on the diversity of the microbiota but the presence of the toxin-producing bacteria. Further investigations should investigate alterations in the microbiota composition and the production of toxins by commensal bacteria such as *Escherichia coli*, *Clostridium perfringens*, and *Bacteroides fragilis*.

Citation: Alberca GGF, Cardoso NSS, Solis-Castro RL, Nakano V, Alberca RW. Intestinal inflammation and the microbiota: Beyond diversity. *World J Gastroenterol* 2022; 28(26): 3274-3278
URL: https://www.wjgnet.com/1007-9327/full/v28/i26/3274.htm
DOI: https://dx.doi.org/10.3748/wjg.v28.i26.3274

TO THE EDITOR

We read with great interest the manuscript entitled "Relationship between clinical features and intestinal microbiota in Chinese patients with ulcerative colitis" published by He *et al*[1] in the World Journal Gastroenterology. He *et al*[1] performed an investigation on the microbiota composition on the fecal and mucosa samples from patients with ulcerative colitis. Their work reinforces the importance of the microbiota on the inflammatory process and gastrointestinal disorders. Importantly, the manuscript provided information on the composition of the gastrointestinal microbiota of patients with ulcerative colitis of various severity and patients without ulcerative colitis[1]. We would like to raise a few considerations regarding the microbiota and gastrointestinal inflammatory disorders.

The microbiota is an ecosystem in constant regulation, influenced by the diet, antibiotics, sanitary conditions, environmental stimulus, and the host's immune system[2]. The gastrointestinal tract is the largest reservoir of bacteria in the human body and shapes both the local and systemic immune responses[3-5]. The microbiome influences the maturation and development of the host's immune system[6], regulating the development of food tolerance, response to inflammation, infections, vaccination, and metabolism[7,8]. Importantly, the microbiota directly influences the development of the inflammatory process independent of dietary intake[9], and abrupt alterations in the microbiota composition can result in an inflammatory insult[10]. He *et al*[1] identified an increase in *Escherichia* and *Shigella* in patients with ulcerative colitis in comparison to patients without ulcerative colitis[1]. *Escherichia* and *Shigella* has been implicated in a reduction in the response to anticoagulation therapy and could impact the treatment of patients with gastrointestinal disorders and under anticoagulation therapy such as coronavirus disease 2019 patients[11-14].

Shiga toxin-producing *Shigella* species and *Escherichia coli* are considered pathogenic, associated with diarrhea and colitis[15]. These toxins can induce the activation of the NOD-like receptor protein 3 inflammasome, inducing the production of interleukin (IL)-1β and IL-18 and cellular death by pyroptosis[16]. The virulence of Shiga-toxin-producing *Escherichia coli* can lead to diarrheal sicknesses and death[17,18]. Shiga-toxins can be encapsulated within microvesicles and influence the inflammatory response in other organs, such as the kidneys[19]. Shiga toxin-producing *Escherichia coli* (O26:H11 strain 97-3250 and O145:H28 strain 4865/96) induces a greater production of chemokines and cytokines, such as IL-8 and IL-1β, in comparison to *Escherichia coli* (O9:H4 strain HS)[20].

The complex symbiotic interaction between the microbiota and the host is mediated by an equilibrium in the tolerance and inflammatory response to microbial products in the gut[6]. He *et al*[1] did not identify an increase in other strains in patients with ulcerative colitis. Nevertheless, in addition to the microbiota composition, certain commensal bacteria, such as *Clostridium perfringens* and *Bacteroides fragilis*, can express a wide range of toxins and metabolic compounds to induce inflammation [21-23]. *Clostridium perfringens* is a gram-positive anaerobic bacteria, commonly in the environment and is part of the resident microbiota but can become virulent by the expression of toxin genes[24,25]. *Clostridium perfringens* can produce over 20 toxins including alpha (α), beta (β), epsilon (e), enterotoxins, and hydrolytic enzymes[26-29]. These toxins can damage and kill intestinal cells, disturb the epithelial barrier, and induce proinflammatory and propathogenic milieu[26,30,31].

The alpha toxin produced by *Clostridium perfringens* is a zinc-dependent metalloenzyme, is able to rupture the plasma membrane of the host's cells[25,32], induces an immature profile in the host's innate immune response (neutrophils), and is involved in the formation of myonecrosis in animals, including humans[33,34]. The β toxin is a pore-forming toxin associated with hemorrhagic diarrhea[35]. *Clostridium perfringens* with the expression of α and β toxins is associated with necrotic enteritis in animals and humans[36-38]. The e toxin is also pore-forming and is involved in intestinal and neurological diseases in humans[39-43].

In addition, *Clostridium perfringens* is able to produce several other toxins such as enterotoxins[44-46], NetB[47,48], and TpeL[49,50], which can induce inflammatory responses, biofilm formation, and chronically disrupt the intestinal epithelium[44,47,50]. *Bacteroides fragilis,* another resident bacteria, can produce a zinc-dependent metalloprotease called fragilisyn[51]. Fragilisyn-producing *Bacteroides fragilis* are named *Enterotoxigenic Bacteroides Fragilis* (ETBF)[52]. ETBF toxin is coded by the *bft* gene and is highly correlated with diarrhea in humans[53,54]. ETBF can cleave E-cadherin in the epithelial cells, allowing bacterial translocation[55,56]. ETBF induces an IL-17-mediated immune response with the infiltration of lymphocytes and neutrophils and damages the DNA *via* the formation of microadenoma [4,53,54]. In addition, the inflammatory process may be mediated by several bacteria. For example, in the "driver-passenger" model, the colonization by one bacteria may facilitate the expansion and proinflammatory action of another microorganism[55].

A recent manuscript by Avril and DePaolo[56], identified that the co-colonization of ETBF and *Escherichia coli* strains, harboring the pks island, promotes the development of intestinal cancer. ETBF promotes the degradation of the intestinal mucus and induction of IL-17-mediated inflammation by the host's immune cells. This process enables the adherence of *Escherichia coli* to the intestinal wall, releases colibactin, and promotes cancer development[56]. Therefore, quantitative analyses are important to characterize the composition of the microbiota in several diseases and aid in the design of possible interventions to modulate the immune response of the host in microbiota-mediated inflammatory disorders[1]. Nevertheless, due to the potential pathobiont role of several resident bacteria, investigations on toxin-producing bacteria are crucial for an overall interpretation of the role of the microbiota on gastrointestinal disorders.

FOOTNOTES

Author contributions: All authors wrote and reviewed the manuscript.

Conflict-of-interest statement: All the authors report no relevant conflicts of interest for this article.

Country/Territory of origin: Brazil

ORCID number: Gabriela Gama Freire Alberca 0000-0002-3467-5562; Naiane Samira Souza Cardoso 0000-0002-3305-6567; Rosa Liliana Solis-Castro 0000-0002-1813-8644; Viviane Nakano 0000-0002-7005-3701; Ricardo Wesley Alberca 0000-0002-3602-3306.

S-Editor: Wang JJ
L-Editor: Filipodia
P-Editor: Wang JJ

REFERENCES

1 **He XX**, Li YH, Yan PG, Meng XC, Chen CY, Li KM, Li JN. Relationship between clinical features and intestinal microbiota in Chinese patients with ulcerative colitis. *World J Gastroenterol* 2021; **27**: 4722-4737 [PMID: 34366632 DOI: 10.3748/wjg.v27.i28.4722]

2 **Voreades N**, Kozil A, Weir TL. Diet and the development of the human intestinal microbiome. *Front Microbiol* 2014; **5**: 494 [PMID: 25295033 DOI: 10.3389/fmicb.2014.00494]

3 **Jandhyala SM**, Talukdar R, Subramanyam C, Vuyyuru H, Sasikala M, Nageshwar Reddy D. Role of the normal gut microbiota. *World J Gastroenterol* 2015; **21**: 8787-8803 [PMID: 26269668 DOI: 10.3748/wjg.v21.i29.8787]

4 **Lucas C**, Barnich N, Nguyen HTT. Microbiota, Inflammation and Colorectal Cancer. *Int J Mol Sci* 2017; **18** [PMID: 28632155 DOI: 10.3390/ijms18061310]

5 **Chiu CY**, Chan YL, Tsai MH, Wang CJ, Chiang MH, Chiu CC. Gut microbial dysbiosis is associated with allergen-specific IgE responses in young children with airway allergies. *World Allergy Organ J* 2019; **12**: 100021 [PMID: 30937143 DOI: 10.1016/j.waojou.2019.100021]

6 **Pandiyan P**, Bhaskaran N, Zou M, Schneider E, Jayaraman S, Huehn J. Microbiome Dependent Regulation of T_{regs} and Th17 Cells in Mucosa. *Front Immunol* 2019; **10**: 426 [PMID: 30906299 DOI: 10.3389/fimmu.2019.00426]

7 **Round JL**, Mazmanian SK. The gut microbiota shapes intestinal immune responses during health and disease. *Nat Rev Immunol* 2009; **9**: 313-323 [PMID: 19343057 DOI: 10.1038/nri2515]

8 **Fonseca DM**, Hand TW, Han SJ, Gerner MY, Glatman Zaretsky A, Byrd AL, Harrison OJ, Ortiz AM, Quinones M, Trinchieri G, Brenchley JM, Brodsky IE, Germain RN, Randolph GJ, Belkaid Y. Microbiota-Dependent Sequelae of Acute

Infection Compromise Tissue-Specific Immunity. *Cell* 2015; **163**: 354-366 [PMID: 26451485 DOI: 10.1016/j.cell.2015.08.030]

9 **Battson ML**, Lee DM, Li Puma LC, Ecton KE, Thomas KN, Febvre HP, Chicco AJ, Weir TL, Gentile CL. Gut microbiota regulates cardiac ischemic tolerance and aortic stiffness in obesity. *Am J Physiol Heart Circ Physiol* 2019; **317**: H1210-H1220 [PMID: 31559829 DOI: 10.1152/ajpheart.00346.2019]

10 **Saltzman ET**, Palacios T, Thomsen M, Vitetta L. Intestinal Microbiome Shifts, Dysbiosis, Inflammation, and Non-alcoholic Fatty Liver Disease. *Front Microbiol* 2018; **9**: 61 [PMID: 29441049 DOI: 10.3389/fmicb.2018.00061]

11 **Wang L**, Liu L, Liu X, Xiang M, Zhou L, Huang C, Shen Z, Miao L. The gut microbes, Enterococcus and Escherichia-Shigella, affect the responses of heart valve replacement patients to the anticoagulant warfarin. *Pharmacol Res* 2020; **159**: 104979 [PMID: 32505835 DOI: 10.1016/j.phrs.2020.104979]

12 **Gu S**, Chen Y, Wu Z, Gao H, Lv L, Guo F, Zhang X, Luo R, Huang C, Lu H, Zheng B, Zhang J, Yan R, Zhang H, Jiang H, Xu Q, Guo J, Gong Y, Tang L, Li L. Alterations of the Gut Microbiota in Patients With Coronavirus Disease 2019 or H1N1 Influenza. *Clin Infect Dis* 2020; **71**: 2669-2678 [PMID: 32497191 DOI: 10.1093/cid/ciaa709]

13 **Alberca GGF**, Solis-Castro RL, Solis-Castro ME, Alberca RW. Coronavirus disease-2019 and the intestinal tract: An overview. *World J Gastroenterol* 2021; **27**: 1255-1266 [PMID: 33833480 DOI: 10.3748/wjg.v27.i13.1255]

14 **Giannis D**, Ziogas IA, Gianni P. Coagulation disorders in coronavirus infected patients: COVID-19, SARS-CoV-1, MERS-CoV and lessons from the past. *J Clin Virol* 2020; **127**: 104362 [PMID: 32305883 DOI: 10.1016/j.jcv.2020.104362]

15 **Wang X**, Sun J, Wan L, Yang X, Lin H, Zhang Y, He X, Zhong H, Guan K, Min M, Sun Z, Wang B, Dong M, Wei C. The *Shigella* Type III Secretion Effector IpaH4.5 Targets NLRP3 to Activate Inflammasome Signaling. *Front Cell Infect Microbiol* 2020; **10**: 511798 [PMID: 33117724 DOI: 10.3389/fcimb.2020.511798]

16 **Hauser JR**, Atitkar RR, Petro CD, Lindsey RL, Strockbine N, O'Brien AD, Melton-Celsa AR. The Virulence of *Escherichia coli* O157:H7 Isolates in Mice Depends on Shiga Toxin Type 2a (Stx2a)-Induction and High Levels of Stx2a in Stool. *Front Cell Infect Microbiol* 2020; **10**: 62 [PMID: 32175286 DOI: 10.3389/fcimb.2020.00062]

17 **Harrison LM**, Lacher DW, Mammel MK, Leonard SR. Comparative Transcriptomics of Shiga Toxin-Producing and Commensal *Escherichia coli* and Cytokine Responses in Colonic Epithelial Cell Culture Infections. *Front Cell Infect Microbiol* 2020; **10**: 575630 [PMID: 33194815 DOI: 10.3389/fcimb.2020.575630]

18 **Huycke MM**, Gaskins HR. Commensal bacteria, redox stress, and colorectal cancer: mechanisms and models. *Exp Biol Med (Maywood)* 2004; **229**: 586-597 [PMID: 15229352 DOI: 10.1177/153537020422900702]

19 **Blacher E**, Levy M, Tatirovsky E, Elinav E. Microbiome-Modulated Metabolites at the Interface of Host Immunity. *J Immunol* 2017; **198**: 572-580 [PMID: 28069752 DOI: 10.4049/jimmunol.1601247]

20 **Louis P**, Hold GL, Flint HJ. The gut microbiota, bacterial metabolites and colorectal cancer. *Nat Rev Microbiol* 2014; **12**: 661-672 [PMID: 25198138 DOI: 10.1038/nrmicro3344]

21 **Uzal FA**, Vidal JE, McClane BA, Gurjar AA. *Clostridium Perfringens* Toxins Involved in Mammalian Veterinary Diseases. *Open Toxinology J* 2010; **2**: 24-42 [PMID: 24511335]

22 **Kiu R**, Hall LJ. An update on the human and animal enteric pathogen Clostridium perfringens. *Emerg Microbes Infect* 2018; **7**: 141 [PMID: 30082713 DOI: 10.1038/s41426-018-0144-8]

23 **Revitt-Mills SA**, Rood JI, Adams V. Clostridium perfringens extracellular toxins and enzymes: 20 and counting. *Microbiol Aust* 2015; **36** [DOI: 10.1071/MA15039]

24 **Liu F**, Li J, Guan Y, Lou Y, Chen H, Xu M, Deng D, Chen J, Ni B, Zhao L, Li H, Sang H, Cai X. Dysbiosis of the Gut Microbiome is associated with Tumor Biomarkers in Lung Cancer. *Int J Biol Sci* 2019; **15**: 2381-2392 [PMID: 31595156 DOI: 10.7150/ijbs.35980]

25 **Rood JI**, Adams V, Lacey J, Lyras D, McClane BA, Melville SB, Moore RJ, Popoff MR, Sarker MR, Songer JG, Uzal FA, Van Immerseel F. Expansion of the Clostridium perfringens toxin-based typing scheme. *Anaerobe* 2018; **53**: 5-10 [PMID: 29866424 DOI: 10.1016/j.anaerobe.2018.04.011]

26 **Hotze EM**, Tweten RK. Membrane assembly of the cholesterol-dependent cytolysin pore complex. *Biochim Biophys Acta* 2012; **1818**: 1028-1038 [PMID: 21835159 DOI: 10.1016/j.bbamem.2011.07.036]

27 **Schwabe RF**, Jobin C. The microbiome and cancer. *Nat Rev Cancer* 2013; **13**: 800-812 [PMID: 24132111 DOI: 10.1038/nrc3610]

28 **Jewell SA**, Titball RW, Huyet J, Naylor CE, Basak AK, Gologan P, Winlove CP, Petrov PG. Clostridium perfringensα-toxin interaction with red cells and model membranes. *Soft Matter* 2015; **11**: 7748-7761 [PMID: 26303814 DOI: 10.1039/c5sm00876j]

29 **Junior CAO**, Silva ROS, Lobato FCF, Navarro MA, Uzal FA. Gas gangrene in mammals: a review. *J Vet Diagn Invest* 2020; **32**: 175-183 [PMID: 32081096 DOI: 10.1177/1040638720905830]

30 **Takehara M**, Takagishi T, Seike S, Ohtani K, Kobayashi K, Miyamoto K, Shimizu T, Nagahama M. Clostridium perfringens α-Toxin Impairs Innate Immunity *via* Inhibition of Neutrophil Differentiation. *Sci Rep* 2016; **6**: 28192 [PMID: 27306065 DOI: 10.1038/srep28192]

31 **Hunter SE**, Brown JE, Oyston PC, Sakurai J, Titball RW. Molecular genetic analysis of beta-toxin of Clostridium perfringens reveals sequence homology with alpha-toxin, gamma-toxin, and leukocidin of Staphylococcus aureus. *Infect Immun* 1993; **61**: 3958-3965 [PMID: 8359918 DOI: 10.1128/iai.61.9.3958-3965.1993]

32 **Matsuda T**, Okada Y, Inagi E, Tanabe Y, Shimizu Y, Nagashima K, Sakurai J, Nagahama M, Tanaka S. Enteritis necroticans 'pigbel' in a Japanese diabetic adult. *Pathol Int* 2007; **57**: 622-626 [PMID: 17685936 DOI: 10.1111/j.1440-1827.2007.02149.x]

33 **Posthaus H**, Kittl S, Tarek B, Bruggisser J. *Clostridium perfringens* type C necrotic enteritis in pigs: diagnosis, pathogenesis, and prevention. *J Vet Diagn Invest* 2020; **32**: 203-212 [PMID: 31955664 DOI: 10.1177/1040638719900180]

34 **Thiel A**, Mogel H, Bruggisser J, Baumann A, Wyder M, Stoffel MH, Summerfield A, Posthaus H. Effect of Clostridium perfringens β-Toxin on Platelets. *Toxins (Basel)* 2017; **9** [PMID: 29064418 DOI: 10.3390/toxins9100336]

35 **Wagley S**, Bokori-Brown M, Morcrette H, Malaspina A, D'Arcy C, Gnanapavan S, Lewis N, Popoff MR, Raciborska D, Nicholas R, Turner B, Titball RW. Evidence of Clostridium perfringens epsilon toxin associated with multiple sclerosis.

Mult Scler 2019; **25**: 653-660 [PMID: 29681209 DOI: 10.1177/1352458518767327]

36 **Savva CG**, Clark AR, Naylor CE, Popoff MR, Moss DS, Basak AK, Titball RW, Bokori-Brown M. The pore structure of Clostridium perfringens epsilon toxin. *Nat Commun* 2019; **10**: 2641 [PMID: 31201325 DOI: 10.1038/s41467-019-10645-8]

37 **Popoff MR**. Epsilon toxin: a fascinating pore-forming toxin. *FEBS J* 2011; **278**: 4602-4615 [PMID: 21535407 DOI: 10.1111/j.1742-4658.2011.08145.x]

38 **Freedman JC**, McClane BA, Uzal FA. New insights into Clostridium perfringens epsilon toxin activation and action on the brain during enterotoxemia. *Anaerobe* 2016; **41**: 27-31 [PMID: 27321761 DOI: 10.1016/j.anaerobe.2016.06.006]

39 **Harkness JM**, Li J, McClane BA. Identification of a lambda toxin-negative Clostridium perfringens strain that processes and activates epsilon prototoxin intracellularly. *Anaerobe* 2012; **18**: 546-552 [PMID: 22982043 DOI: 10.1016/j.anaerobe.2012.09.001]

40 **Freedman JC**, Shrestha A, McClane BA. Clostridium perfringens Enterotoxin: Action, Genetics, and Translational Applications. *Toxins (Basel)* 2016; **8** [PMID: 26999202 DOI: 10.3390/toxins8030073]

41 **Grass JE**, Gould LH, Mahon BE. Epidemiology of foodborne disease outbreaks caused by Clostridium perfringens, United States, 1998-2010. *Foodborne Pathog Dis* 2013; **10**: 131-136 [PMID: 23379281 DOI: 10.1089/fpd.2012.1316]

42 **Li J**, Miyamoto K, Sayeed S, McClane BA. Organization of the cpe locus in CPE-positive clostridium perfringens type C and D isolates. *PLoS One* 2010; **5**: e10932 [PMID: 20532170 DOI: 10.1371/journal.pone.0010932]

43 **Rood JI**, Keyburn AL, Moore RJ. NetB and necrotic enteritis: the hole movable story. *Avian Pathol* 2016; **45**: 295-301 [PMID: 27009522 DOI: 10.1080/03079457.2016.1158781]

44 **Keyburn AL**, Bannam TL, Moore RJ, Rood JI. NetB, a pore-forming toxin from necrotic enteritis strains of Clostridium perfringens. *Toxins (Basel)* 2010; **2**: 1913-1927 [PMID: 22069665 DOI: 10.3390/toxins2071913]

45 **Chen J**, McClane BA. Characterization of Clostridium perfringens TpeL toxin gene carriage, production, cytotoxic contributions, and trypsin sensitivity. *Infect Immun* 2015; **83**: 2369-2381 [PMID: 25824828 DOI: 10.1128/IAI.03136-14]

46 **Schorch B**, Heni H, Zahaf NI, Brummer T, Mione M, Schmidt G, Papatheodorou P, Aktories K. Targeting oncogenic Ras by the *Clostridium perfringens* toxin TpeL. *Oncotarget* 2018; **9**: 16489-16500 [PMID: 29662661 DOI: 10.18632/oncotarget.24740]

47 **Pierce JV**, Bernstein HD. Genomic Diversity of Enterotoxigenic Strains of Bacteroides fragilis. *PLoS One* 2016; **11**: e0158171 [PMID: 27348220 DOI: 10.1371/journal.pone.0158171]

48 **Shah N**, Osmon D, Tande AJ, Steckelberg J, Sierra R, Walker R, Berbari EF. Clinical and Microbiological Characteristics of *Bacteroides* Prosthetic Joint Infections. *J Bone Jt Infect* 2017; **2**: 122-126 [PMID: 28540148 DOI: 10.7150/jbji.17129]

49 **Zhang G**, Svenungsson B, Kärnell A, Weintraub A. Prevalence of enterotoxigenic Bacteroides fragilis in adult patients with diarrhea and healthy controls. *Clin Infect Dis* 1999; **29**: 590-594 [PMID: 10530453 DOI: 10.1086/598639]

50 **Sears CL**. Enterotoxigenic Bacteroides fragilis: a rogue among symbiotes. *Clin Microbiol Rev* 2009; **22**: 349-369, Table of Contents [PMID: 19366918 DOI: 10.1128/CMR.00053-08]

51 **Wu S**, Rhee KJ, Zhang M, Franco A, Sears CL. Bacteroides fragilis toxin stimulates intestinal epithelial cell shedding and gamma-secretase-dependent E-cadherin cleavage. *J Cell Sci* 2007; **120**: 1944-1952 [PMID: 17504810 DOI: 10.1242/jcs.03455]

52 **Deng H**, Li Z, Tan Y, Guo Z, Liu Y, Wang Y, Yuan Y, Yang R, Bi Y, Bai Y, Zhi F. A novel strain of Bacteroides fragilis enhances phagocytosis and polarises M1 macrophages. *Sci Rep* 2016; **6**: 29401 [PMID: 27381366 DOI: 10.1038/srep29401]

53 **DeStefano Shields CE**, Van Meerbeke SW, Housseau F, Wang H, Huso DL, Casero RA Jr, O'Hagan HM, Sears CL. Reduction of Murine Colon Tumorigenesis Driven by Enterotoxigenic Bacteroides fragilis Using Cefoxitin Treatment. *J Infect Dis* 2016; **214**: 122-129 [PMID: 26908749 DOI: 10.1093/infdis/jiw069]

54 **Chung L**, Thiele Orberg E, Geis AL, Chan JL, Fu K, DeStefano Shields CE, Dejea CM, Fathi P, Chen J, Finard BB, Tam AJ, McAllister F, Fan H, Wu X, Ganguly S, Lebid A, Metz P, Van Meerbeke SW, Huso DL, Wick EC, Pardoll DM, Wan F, Wu S, Sears CL, Housseau F. Bacteroides fragilis Toxin Coordinates a Pro-carcinogenic Inflammatory Cascade *via* Targeting of Colonic Epithelial Cells. *Cell Host Microbe* 2018; **23**: 203-214.e5 [PMID: 29398651 DOI: 10.1016/j.chom.2018.01.007]

55 **Tjalsma H**, Boleij A, Marchesi JR, Dutilh BE. A bacterial driver-passenger model for colorectal cancer: beyond the usual suspects. *Nat Rev Microbiol* 2012; **10**: 575-582 [PMID: 22728587 DOI: 10.1038/nrmicro2819]

56 **Avril M**, DePaolo RW. "Driver-passenger" bacteria and their metabolites in the pathogenesis of colorectal cancer. *Gut Microbes* 2021; **13**: 1941710 [PMID: 34225577 DOI: 10.1080/19490976.2021.1941710]

World Journal of Gastroenterology

Submit a Manuscript: https://www.f6publishing.com

World J Gastroenterol 2022 July 14; 28(26): 3279-3281

DOI: 10.3748/wjg.v28.i26.3279

ISSN 1007-9327 (print) ISSN 2219-2840 (online)

LETTER TO THE EDITOR

Intestinal virome: An important research direction for alcoholic and nonalcoholic liver diseases

Yan Li, Wen-Cheng Liu, Bing Chang

Specialty type: Gastroenterology and hepatology

Provenance and peer review: Unsolicited article; Externally peer reviewed.

Peer-review model: Single blind

Peer-review report's scientific quality classification

Grade A (Excellent): A
Grade B (Very good): B
Grade C (Good): 0
Grade D (Fair): 0
Grade E (Poor): 0

P-Reviewer: AbdEl-Wahab EW, Ghoneim S

Received: November 3, 2021
Peer-review started: November 3, 2021
First decision: November 29, 2021
Revised: December 7, 2021
Accepted: June 13, 2022
Article in press: June 13, 2022
Published online: July 14, 2022

Yan Li, Wen-Cheng Liu, Bing Chang, Department of Gastroenterology, The First Affiliated Hospital of China Medical University, Shenyang 110001, Liaoning Province, China

Corresponding author: Bing Chang, MD, Associate Professor, Department of Gastroenterology, The First Affiliated Hospital of China Medical University, No. 155 Nanjing North Street, Heping District, Shenyang 110001, Liaoning Province, China. cb000216@163.com

Abstract

In recent years, the interaction between the gut microflora and liver diseases has attracted much attention. The intestinal microflora is composed of bacteria, archaea, fungi and viruses. There are few studies on the intestinal virome, and whether it has a causal relationship with bacterial changes in the gut is still unclear. However, it is undeniable that the intestinal virome is also a very important portion of the blueprint for the development of liver diseases and the diagnosis and therapeutic modalities in the future.

Key Words: Alcoholic fatty liver disease; Nonalcoholic fatty liver disease; Fatty liver disease; Gut microbiome; Intestinal virome

Core Tip: As of the study of the gut microflora expands, the interaction between the intestinal virome and liver diseases has been gradually revealed. In this letter to the editor, we discuss the changes in the intestinal virome in patients with alcoholic liver disease and nonalcoholic liver disease, and provide suggestions for developing future diagnosis and treatment methods.

Citation: Li Y, Liu WC, Chang B. Intestinal virome: An important research direction for alcoholic and nonalcoholic liver diseases. *World J Gastroenterol* 2022; 28(26): 3279-3281
URL: https://www.wjgnet.com/1007-9327/full/v28/i26/3279.htm
DOI: https://dx.doi.org/10.3748/wjg.v28.i26.3279

TO THE EDITOR

We have carefully studied the reviews recently written by Sharma *et al*[1], titled "Significance of gut microbiota in alcoholic and nonalcoholic fatty liver diseases". The authors elaborated the intestinal microecological changes in both alcoholic and nonalcoholic liver diseases, and the important effects of intestinal microorganisms on the development of fatty liver diseases. These findings could provide new ideas for the future diagnosis and treatment of fatty liver disease.

In addition to bacteria, archaea and a small amount of fungi, viruses are also an indispensable part of the intestinal microflora in human[2] . In 2020, a multicenter observational study on the enteroviruses from 89 patients with alcoholic hepatitis, 36 patients with alcohol use disorder and 17 patients without alcohol use disorder was concluded[3]. The results showed that in stool samples from patients with alcoholic liver disease, bacterial and fungal diversity decreased and virus diversity increased, which mainly manifested as a large increase in the number of *Myoviridae*, *Lactobacillus* phages, *Streptococcus* phages, *Podoviridae*, *Geobacillus* phages, *Escherichia* phages, and *Herpesviridae*[3]. This trend was positively correlated with the severity of the disease. The changes in the intestinal microecology of people with alcohol use disorder are mainly characterized by an increase in *Parvoviridae* and *Lactococcus* phages[3]. Another study of the intestinal virome in patients with nonalcoholic fatty liver disease (NAFLD) showed that the average relative abundance and viral diversity of phages in patients with NAFLD and severe hepatic fibrosis were significantly lower than those in patients with NAFLD and no or mild hepatic fibrosis[4]. Hence viruses also have positive implications in the diagnosis, severity classification, treatment and prognosis of alcoholic and nonalcoholic liver diseases. However, as an easily neglected part of gut microecology, the impact of viruses was not mentioned in Sharma *et al*[1]'s article.

Bacteria and fungi in the gut microflora have large individual variability and are susceptible to various factors such as age, drugs[5], environment[6], and diet[7]. Likewise, the same is true for viruses. A shotgun metagenome sequencing analysis of DNA viruses in fecal samples from cynomolgus monkeys of different ages showed that the abundance of DNA viruses was inversely proportional to age; that is, the DNA virus group in fecal samples of elderly individuals decreased significantly[8]. However, Lang *et al*[4] found that after the use of proton pump inhibitors, enteroviruses in the feces of patients with nonalcoholic liver disease were also changed. In addition, in high-fat diet-fed mice, the structural composition and β-diversity of enteroviruses were changed. There was a significant decrease in the expression of *Siphoviridae* and a significant increase in the expression of the eukaryotic viruses *Phycodnavridae* and *Mimivirdae*, and these changes were accompanied by changes in intestinal bacteria [9]. Therefore, considering the original proposal that gut microorganisms should be included in future liver disease diagnosis and treatment, we suggest that in addition to performing a horizontal comparison and finding representative biological markers, it is indispensable to have a methodological design and vertical comparison. However, the effects of confounding factors should also be considered, and individualized diagnosis and treatment plans should be developed for different patients.

ACKNOWLEDGEMENTS

We would like to thank the Department of Gastroenterology of the First Affiliated Hospital of China Medical University for technical assistance.

FOOTNOTES

Author contributions: Li Y and Liu WC wrote this manuscript; Li Y and Chang B revised this manuscript; and all the authors contributed to the writing of this manuscript.

Conflict-of-interest statement: All the authors report no relevant conflicts of interest for this article.

Country/Territory of origin: China

ORCID number: Yan Li 0000-0002-1749-0283; Wen-Cheng Liu 0000-0002-7721-6892; Bing Chang 0000-0003-1965-5827.

S-Editor: Antwi SO, United States S-Editor
L-Editor: A

P-Editor: Wang JJ

REFERENCES

1 **Sharma SP**, Suk KT, Kim DJ. Significance of gut microbiota in alcoholic and non-alcoholic fatty liver diseases. *World J Gastroenterol* 2021; **27**: 6161-6179 [PMID: 34712025 DOI: 10.3748/wjg.v27.i37.6161]

2 **Whon TW**, Shin NR, Kim JY, Roh SW. Omics in gut microbiome analysis. *J Microbiol* 2021; **59**: 292-297 [PMID: 33624266 DOI: 10.1007/s12275-021-1004-0]

3 **Jiang L**, Lang S, Duan Y, Zhang X, Gao B, Chopyk J, Schwanemann LK, Ventura-Cots M, Bataller R, Bosques-Padilla F, Verna EC, Abraldes JG, Brown RS Jr, Vargas V, Altamirano J, Caballería J, Shawcross DL, Ho SB, Louvet A, Lucey MR, Mathurin P, Garcia-Tsao G, Kisseleva T, Brenner DA, Tu XM, Stärkel P, Pride D, Fouts DE, Schnabl B. Intestinal Virome in Patients With Alcoholic Hepatitis. *Hepatology* 2020; **72**: 2182-2196 [PMID: 32654263 DOI: 10.1002/hep.31459]

4 **Lang S**, Demir M, Martin A, Jiang L, Zhang X, Duan Y, Gao B, Wisplinghoff H, Kasper P, Roderburg C, Tacke F, Steffen HM, Goeser T, Abraldes JG, Tu XM, Loomba R, Stärkel P, Pride D, Fouts DE, Schnabl B. Intestinal Virome Signature Associated With Severity of Nonalcoholic Fatty Liver Disease. *Gastroenterology* 2020; **159**: 1839-1852 [PMID: 32652145 DOI: 10.1053/j.gastro.2020.07.005]

5 **Fasullo M**, Rau P, Liu DQ, Holzwanger E, Mathew JP, Guilarte-Walker Y, Szabo G. Proton pump inhibitors increase the severity of hepatic encephalopathy in cirrhotic patients. *World J Hepatol* 2019; **11**: 522-530 [PMID: 31293720 DOI: 10.4254/wjh.v11.i6.522]

6 **Ng KM**, Aranda-Díaz A, Tropini C, Frankel MR, Van Treuren W, O'Loughlin CT, Merrill BD, Yu FB, Pruss KM, Oliveira RA, Higginbottom SK, Neff NF, Fischbach MA, Xavier KB, Sonnenburg JL, Huang KC. Recovery of the Gut Microbiota after Antibiotics Depends on Host Diet, Community Context, and Environmental Reservoirs. *Cell Host Microbe* 2019; **26**: 650-665.e4 [PMID: 31726029 DOI: 10.1016/j.chom.2019.10.011]

7 **González Olmo BM**, Butler MJ, Barrientos RM. Evolution of the Human Diet and Its Impact on Gut Microbiota, Immune Responses, and Brain Health. *Nutrients* 2021; **13** [PMID: 33435203 DOI: 10.3390/nu13010196]

8 **Tan X**, Chai T, Duan J, Wu J, Zhang H, Li Y, Huang Y, Hu X, Zheng P, Song J, Ji P, Jin X, Xie P. Dynamic changes occur in the DNA gut virome of female cynomolgus macaques during aging. *Microbiologyopen* 2021; **10**: e1186 [PMID: 33970533 DOI: 10.1002/mbo3.1186]

9 **Schulfer A**, Santiago-Rodriguez TM, Ly M, Borin JM, Chopyk J, Blaser MJ, Pride DT. Fecal Viral Community Responses to High-Fat Diet in Mice. *mSphere* 2020; **5** [PMID: 32102942 DOI: 10.1128/msphere.00833-19]

Published by **Baishideng Publishing Group Inc**
7041 Koll Center Parkway, Suite 160, Pleasanton, CA 94566, USA
Telephone: +1-925-3991568
E-mail: bpgoffice@wjgnet.com
Help Desk: https://www.f6publishing.com/helpdesk
https://www.wjgnet.com